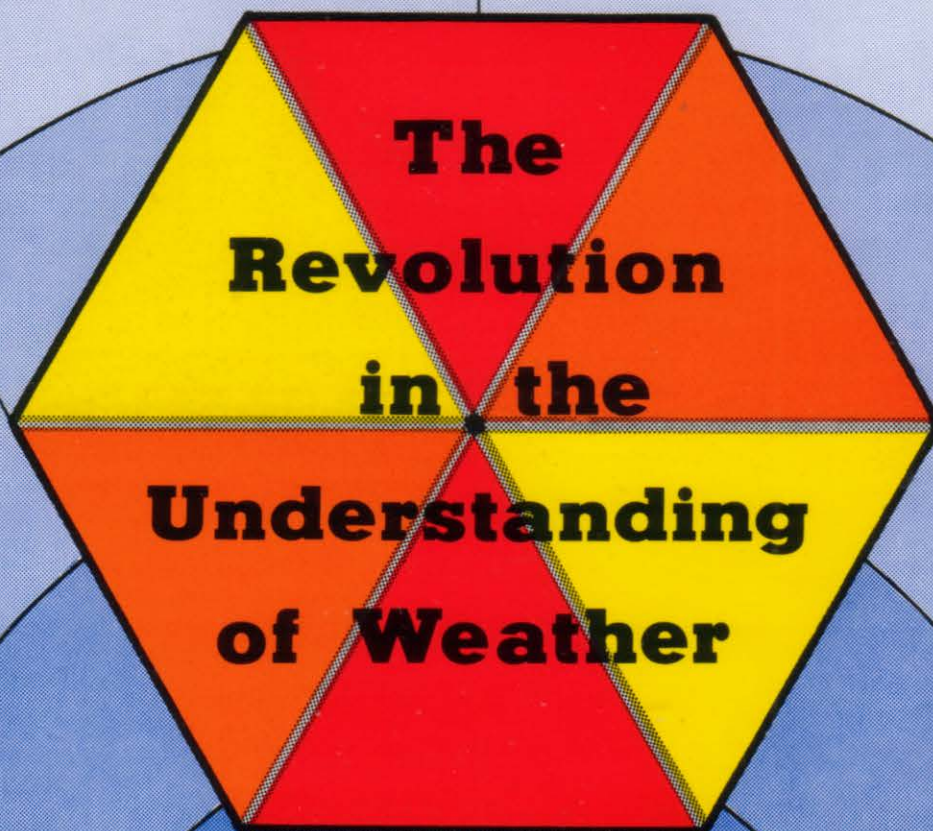


SINGER'S LOCK



PART 1

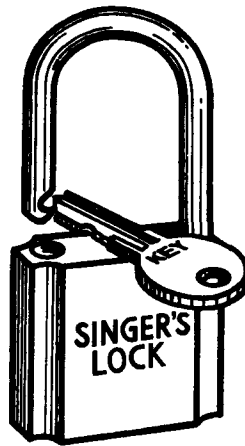
The Revolution in the Understanding of Weather

SINGER'S LOCK:

The Revolution in the Understanding of Weather

Part I

by Oscar Singer



with 190 illustrated charts
drawn by *Daniel Bender*

Copyright © 1983 by Oscar Singer

All rights reserved, including the copyright of translations into any language. No part of this publication may be reproduced or transmitted in any form or by any means, electronic or mechanical, including photocopy, recording, or any information storage and retrieval system without the written permission of the author.

First Printing

Printed in the United States of America

Library of Congress Catalog Card Number 83-90086

ISBN 0-9610922-0-3

**SINGER PRESS
P.O. Box 63302
Los Angeles, California 90063
Tel. (213) 263-2640**

Acknowledgment

I am especially indebted to Daniel Bender whose help was invaluable as I worked on the manuscript. He shared in every detail of my map constructions, was ruthless in criticism if anything was not clear, and tireless in the detection of error. His line-by-line review of the complete final manuscript and his overall help with all phases of the final product (drafting of the figures, typesetting, camera work, and the actual printing) was essential. All of this might not have been possible without the heart-warming support of his immediate family.

I would like to thank Raphael Castro whose help in 1967 made it possible for me to lay some of the foundations that led to this book.

A personal debt of appreciation is owed to Alan Hagge of Olympic Sales Company in Pasadena, whose skill in programming was invaluable in creating a computer print-out of the relationships between the points shown in the Radial Charts.

A note of thanks is owed to Christina Rose for her drawing of the lock and key logo.

Finally, acknowledgement is made to the following employees of Postal Instant Press in Arcadia—Jim Blacklock, Judy Crine, Frank Huber, Juanita Hughes, Gloria Renter, Janie Richter, Kim Service, Guy Simone, Alex Westfall—who assisted in furnishing certain materials to aid in the printing of this book.

While I acknowledge the help of these generous persons. I must reserve to myself the responsibility for any errors of whatever nature that might be hiding in some of these pages. The authorship of any such bloopers must be considered as mine alone.

TABLE OF CONTENTS

PREFACE	ix-xv
CHAPTER 1 Introduction.....	1-3
CHAPTER 2 Some Geometry	4-11
Some Differences Between Plane and Spherical Geometry	4
General Definitions	5
Angles on a Sphere.....	7
Distances Between Points on the Surface of a Sphere	9
Definition of Polygons on a Sphere	9
Spherical Triangles	10
CHAPTER 3 The Polar Stereographic Map.....	12-27
Construction of the Polar Stereographic Map	13
What is a Straight Line on the Polar Stereographic Map?	15
The Nature of Pattern Distortions Created by the Polar Stereographic Map.....	17
The Irregular Appearance of the Projection of the Centers of Circles.....	21
All Circles on the Earth's Surface Project as Circles on the Map	22
The Value of the Angle Between any two Arcs on the Surface of a Sphere is Exactly Reproduced on the Polar Stereographic Map	26
CHAPTER 4 Organization in Space	28-49
Space and Some of its Features	28
Space Filling Patterns on a Two-Dimensional Surface	34
Principles of Closest Packing of Spheres	41
Examples and Experiments in Closest Packing of Spheres	44
Angles of the Hexagon	48

CHAPTER 5 Organized Patterns of Movement in Space	50-57
General	50
The Principle of Similitude	50
Kepler's Laws	51
Wolf's Law	52
Rings and Spokes of Saturn	53
Roche's Law	53
Laws of the Atom	54
CHAPTER 6 Waves	58-65
General	58
Equilibrium	59
Oscillations and Resonance	59
Harmonic Movement	60
Fourier Analysis	61
Wave Pulses	63
Interference	63
CHAPTER 7 Symmetry	66-81
Definition of Symmetry	66
Classes of Symmetry	67
Types of Symmetry Operations	68
Symmetry Along a Straight Line	71
Dilation Symmetry	71
Symmetry in a Network of Points	71
Equivalent Symmetry Points	76
Symmetry of Averages	76
How Many Points Will be Crossed by any Straight Line in a Regular Network?	77
Symmetry and Equilibrium	79
CHAPTER 8 The Problem of Plateau	82-90
The Conic Sections	82
Surfaces of Revolution	84
Collapse of Cylindrical Structures	86
The Splash of a Drop	89
The Center of a Structure is Related to its Shape	89
CHAPTER 9 The Chladni Figures and Wavenumbers	91-95
Two Modes of Vibration	92
Some Differences Between the Hemispheric Cap of Air and Chladni Plates	94

CHAPTER 10 Quantum Units and Angular Numbers	96-106
Everything is Packaged in Quantum Units	96
Some Factors Determining the Quantum Sized Vortex on a Surface Weather Map	97
“Diffraction Grating” for Finding the Quantum Vortex and also for Exposing Simple Geometric Configurations	99
Construction of the Weather Tool	102
Other Possible Weather Tools	103
CHAPTER 11 General Explanation of the charts	107-114
Why December 7, 1950 was Chosen for Analysis	107
Why June 6, 1944 was Chosen	108
Some Rules Followed in the Drawing of the Charts	108
The Identification Chart	109
Some Unusual Aspects of the Charts	111
Some Simple Definitions of Simple Weather Terms	111
What is the Center of a Low or High and How is it to be Determined?	112
Two Types of Chart Analysis: Circumferential and Radial	114
CHAPTER 12 The Circumferential Charts	115-168
Some Rules Followed in Drawing the Circumferential Charts	115
CHAPTER 13 The Radial Charts	169-319
CHAPTER 14 June 6, 1944	320-322
CHAPTER 15 Some Firsts in Meteorology	323-325
CHAPTER 16 Problems Following Discoveries	326-330
About the Author	331
About the Assistant	331
REFERENCES	332
INDEX	333-336

Preface

The aim of this book and the books that are to follow, is to give a new revolutionary understanding as to how the weather works over the entire surface of the Earth. This revolutionary understanding can be applied equally to all the planets of this solar system and all other planets throughout the Universe that have an atmosphere.

You will find the theoretical explanations to be a revolution in their applications to weather maps. You will also find that these same theoretical explanations are “old hat”, and are being used and have been used for centuries in many fields of scientific endeavor.

This book stands on two legs. The first leg is the empirical evidence as shown by the series of weather maps in the later chapters. The empirical evidence shown by these charts is sufficient to stand alone in a book without any theoretical explanation. Yet, inevitably, the questions would come pouring in: Why? How did you draw these charts? How did you find the patterns? The second leg is the theoretical explanation as to what is happening. These explanations are a revelation in the understanding of weather and are sufficient to stand alone, likewise, in a book without any empirical evidence to back them up. Nevertheless, questions would also come pouring in as to “Where are some examples that show an application of these theories?”

The examples analyzing a weather map are all mine and they have never been seen or described heretofore. The theoretical explanation of the complex maneuvers that the air makes over the Earth or a hemisphere could hardly be my discovery alone. The explanation is basically a combination of material drawn together from numerous other published sources, and a summary of the experiences in many fields. I owe a debt to all these unnamed contributors, since the theory

behind this material is based upon their works.

I define *Singer's Lock* as the summation of all the procedures used to make a forecast of any high, low, or other feature on a weather map. The forecast period is for 24 hours exactly. The same procedures could be used on this 24 hour forecast to extend the forecast period to 48 hours, exactly, and so on, to 72 hours, etc. The word *lock* is used because every high and low "locks" into an exact position with "bull's eye" accuracy for a forecast covering a period of 24 hours. The error in the forecast is theoretically zero. In practice there is an error due to surveying or locating the exact centers of the highs and lows. Any errors in locating the positions of the centers will inevitably be transferred into an error in the forecast. These procedures apply to all levels of the atmosphere, from the surface of the Earth, to the point where weather is not significant.

It obviously is a gigantic task to assemble and analyze all the data to make this type of forecast for the entire world, or as a minimum for a hemisphere of the Earth. It is likewise a gigantic task to even explain and prove out this procedure, especially since it represents a clean break with the present forecasting procedures used in every country in the world. To solve this dilemma, I decided to make an analysis of a single weather map at a fixed moment in time. I had solved the dynamical principles of the movement of all highs and lows with the use of *Singer's Lock*. Some of these dynamical principles should be evident on the surface map at any given moment in time. There is an advantage in beginning the explanation of *Singer's Lock* with a single map at a fixed time. We do not have the necessity of comparing a given low center for one day with its new position on the next day. There could be some confusion as to the exact center on both days, since the low in the new position 24 hours later will have changed in many ways. By sticking with a single day at a fixed time, we have the situation where nothing moves, which makes it easier to prove certain conclusions.

In summation, the intent of this book is to establish some of the great natural laws of the Universe that can be used on a surface weather map at any given moment in time, especially since that moment in time is frozen on the map. It will be easier to prove the dynamics of movement of weather systems, once the principles have been grasped on a weather map fixed in time.

Preface

In succeeding books I will go into the totally new empirical and theoretical proofs for the movement of all highs and lows, the exact forces that control the movements of hurricanes, the new mathematical descriptions dealing with frontal systems, the changes of shape or curvature of all features on a weather map, and some heretofore unknown causes of deepening or intensification and filling or weakening of highs and lows. This sounds like a big order to fill, but you will find that one step at a time will whittle it down to something that can be digested rather easily.

All of the preceding is not intended to give the impression that everything that is known about the weather today, prior to this book, is faulty. All of descriptive meteorology that describes all types of weather phenomena, the shapes of individual storms, etc., still holds. The forecasting rules, Rossby waves, the numerical computer procedures, etc., have an element of truth in them, but they see the truth only vaguely, since the rules are not exact physical laws that calculate exactly what is happening, as is evident from the faulty forecasts that we may get from time to time. Likewise, the statistics of meteorology are still true except that statistics and probability are usually used where the causes are not known.

There are three general ways that information is handled by the human mind: by the words of language, by the letters and symbols of mathematics, and by pictures or diagrams. The advantage of a chart or picture is that the information it gives is easy to follow or check, it is simpler than words, it clarifies difficulties, it helps the mind make a permanent record for remembering and for further analysis. Because of this power of a chart, you can jump immediately to **Chapters 12 and 13** where the charts are located and you will find them interesting and understandable. Nevertheless, you will need the words (and Figures) of the first part of the book to get a better appreciation of what the charts and pictures mean. In addition, you will find the simple mathematical statement establishing the main rules for constructing the charts, as given in **Chapter 9**, to be satisfying and refreshing. The mathematical formulas of course state in a concise and compact manner the generalization made by the words. You will find that everything in this book is aimed at explaining the number, order, and position of weather patterns. I have done this in accordance with the instructions of the ancient Pythagoreans who first said that all material things can

be described by: number (a numeral by which a thing is designated when it is part of a series), order (the shape, form, or arrangement of things), and lastly, position (the way in which a thing is placed relative to other things). The understanding of number, order, and position exposes symmetry patterns. Symmetry patterns, of course, permeate almost every physical phenomenon in the Universe.

This book is written at a level that hopefully can be understood by the average person, with perhaps a high school education. Some of the hard mathematical formulas that creep in at various points, as in the chapter on the polar stereographic map, are not necessary for an understanding of the charts at the end of the book. Whatever mathematics does occur is not beyond the reach of a first or second year college level. Do not let this relatively elementary and simple approach to the explanation of *Singer's Lock* fool you. What you will be reading in this book is the leading or cutting edge of weather research. This book is also written for every meteorologist in the world, for no meteorologist has ever seen anything like it. That this is true can be seen from a few isolated excerpts from the history of my attempts to get something published:

1. From an unpublished paper by *Dr. J. E. Pournelle*, Science Writer, dated 18 April 1976.

"The extraordinary thing is that it does seem to work. Why a moving storm should stop as if influenced by the position of a previous storm is beyond my comprehension: but in case after case Singer demonstrated it to me. I even took some charts at random from Singer's stack—he had them all for a five year period—and worked it myself, and I got the same result. . . .

Now there are some obvious problems with Singer's theories. . . . he gave examples of the "Lock" operating on storms moving north-south, . . . Now such lines on that projection are not great circles; in fact, they have no meaning at all. . . .

So. Singer is almost certainly wrong in at least part of his theoretical justification for his formula. . . ."

2. Letter from *Dr. Chester Newton*, Editor of the *Monthly Weather Review*, of the American Meteorological Society, dated 27 September 1976.

"Two reviewers comment that the lines for the Lock are drawn on a polar stereographic projection. As discussed

by referee C, this means that the same line on other projections will not be straight, and that this disqualifies the Lock as a physical law."

The following are excerpts from the reviewers referred to above:

Referee C, 27 September 1976.

"As the author states, the rules apply only on a polar stereographic projection. They would be broken on Lambert conformal or Mercator projections, for instance. Thus the rules are utterly lacking in a physical basis despite the attempt of the author to invoke physical arguments. Physical laws must remain invariant under coordinate transformations. Mother nature can hardly be expected to reserve her laws for one or another of our humanly devised coordinate systems. . . ."

Referee B, 27 September 1976.

"It is always pleasant to see a paper in which interest is taken in forecasting. The present article is concerned with prediction of the 24-hr motion of cyclones on the surface map, no doubt a matter in which improvements over the computer and official forecasts are often possible. Singer's simple requirement of using only the surface hemisphere chart for his prediction provides for a means of acquiring a large back file quickly and carry out forecasts of "operational research".

The relationships which author believes to have found probably result in part from the properties of the base map used (polar stereographic) and in part from what may be the Fujiwhara description of rotation of centers.

3. Letter from *Dr. Daniel Lufkin*, Deputy Director, Office of Meteorological and Hydrological Services, 5 October 1977. I had requested help from *Richard A. Frank*, Administrator of the National Oceanic and Atmospheric Administration (NOAA)—Dr. Lufkin spoke for NOAA and the National Weather Service.

- a. "First, I want to go on the record as agreeing with you that Referee C's remarks about the use of the polar stereographic projection were entirely mistaken. The characteristic of the polar stereographic projection is precisely that it preserves great-circle angular relationships. If Singer's Lock works on a polar stereographic map, it will work on the globe. Referee C made a mistake that should have been corrected. . . ."

Dr. Lufkin, 6 December 1977

- b. "I'm afraid I've got a problem for you on the question of map projections: I had agreed with you that the conformal property of the polar stereographic projection implied that angular relationships were conserved across the entire globe. I have found though that that statement is true only for small regions . . . I must confess that I thought you were right—on the question of projection, at least,—but now I don't see any way out of the referee's objection. . . ."

Dr. Lufkin, again, 27 January 1978.

- c. "I'm glad to hear that you have gone ahead on the explanation of the polar stereographic projection as it it pertains to your method. Since the angle at which two great circles intersect is going to be rather hard to evaluate if you can't treat great circles as straight lines on the map, I'm curious to see how this complication can be handled within the framework of your previous development.

Your remark that most meteorologists don't understand the properties of the polar projection is well taken. Because the angular relationships involved in your work are so far removed from the considerations of scale that meteorologists have been concerned with, my advice is for you to be fairly thorough in the development of the discussion in your paper. In essence, you'll have to show that there is some factor in the angular lock phenomenon that compensates for the variation in the angle with latitude. Good luck, because I can't imagine what it could be. . . ."

So if you are just beginning to study weather, you will find yourself on a relatively equal footing with top professional meteorologists with regard to what you see in the charts in this book.

I have been asked many times, "What is the formula for Singer's Lock?" When you read what follows, you will see the complex of formulas and principles needed to establish the beginning steps. To go deeper into *Singer's Lock* requires additional principles and complexes of formulas. It would be ludicrous to expect that one simple formula could describe the huge number of activities, changing from moment to moment, throughout the Earth's atmosphere. Fortunately, I have an immense amount of empirical and theoretical proofs for my

Preface

breakthrough in weather. I did expose some useful pieces of information to some of the leading research meteorologists in the **National Weather Service**, but it only represented a drop in the bucket.

I made my initial breakthrough in 1966. I have since then analyzed over 25 years (September through March) of Historical Weather Maps in assembling the thousands of little steps leading to what you see in this book, and what lies ahead. All the work over the years was done at my own expense and entertainment. The actual preparation of this book took me over 2½ years, with the faithful assistance of Daniel Bender in the many chores that it takes to assemble a book of this nature. This was done, all at my own expense in time and money, and the same can be said of Daniel's efforts. I mention this for those who wonder as to why I stopped where I did. This whole book can only be considered as an opener, or down payment, if you please, in cold cash, that what I have is of a value that can not be ignored.

It is an interesting sidelight, that *Dr. George Fischbeck*, the local TV weatherman (*Eyewitness News*, Ch. 7. KABC Los Angeles) mentioned to me in 1976 that the best way to establish something new is to first prove its value to some trustworthy individual—it turned out that Daniel Bender met these specifications.

This book is a breakthrough to a golden era for all those who are now in the weather profession and all those who hope to enter the profession and its related fields. The discovery of the transistor led to an explosion in electronic discovery, and those individuals experienced in vacuum tube technology may have feared for their jobs. True, vacuum tubes do not hold the primacy today that they did prior to the transistor era, but the field of electronics is greater than ever, and the former vacuum tube experts have more work than before—the same will be true for meteorologists.

Oscar Singer

Los Angeles, California

1 February 1983

Chapter 1

Introduction

Two major advances have been made in the understanding of weather processes in this century. The first was the emphasis on the importance of frontal systems by *J. Bjerknes* (1) in 1922; the second was the advent of weather satellite information in the 1960's. Using fronts gave a global unity to weather forecasting; while the satellite pictures gave a global unity to the understanding of what was happening over the globe at the time the photograph was taken. The satellites do not give a forecast, but they do give a correct picture so that the forecaster has the right information. With the right information and a lot of work, a weather forecast can be made. There have been many relatively smaller discoveries, partly explaining tornadoes, hurricanes, lightning, rain drops, etc. All of these developments have led to a weather forecast capability that is far better than pure chance, but still (disappointingly) not full reliable.

What do we have to do to make a successful weather forecast? There are three major steps that must be completed:

1. An accurate weather map must be drawn to show the weather conditions at the time the forecast is being prepared. Fortunately, this step is quite reliable, thanks to the *National Weather Service*, especially since the availability of satellite weather photos. So, this first step is not a serious problem at the present time.
2. A forecast map must be prepared showing the high pressure centers, the low pressure centers, and the patterns of the isobars or winds, at a given time in the future. This time can be 24 hours, 48 hours, one week, or as desired. This second step of the forecast procedure is the most difficult and is the cause of most poor forecasts. Here, precisely, is where the explanation given by *Singer's Lock* is of immense value.

3. The consequences of the second step must be correctly forecast. A decision must be made as to how strong the wind might be, how high or low the temperature, how much rain, how much cloud cover, and when all this might happen. This third step is an entirely different ball-game, and errors can be made, even if the positions of the lows and highs are predicted accurately. The author makes no claim of any special expertise in forecasting these consequences.

Part of the reason for some unhappy weather forecasts has been the lack of a unified hemispheric explanation of how each individual low and high sends out an *interference* that disturbs other lows and highs in the hemisphere. It is obvious that every movement of every low and high must be counterbalanced somewhere else on the Earth by an equivalent movement (since the total mass of air over the globe is almost constant for practical purposes). There have been attempts made to give a unified hemispheric explanation to weather patterns, but these have been statistical in nature. Many studies have shown, that on the *average*, certain weather patterns are likely to occur over a hemisphere. Statistics, while useful and valuable for many purposes, have been given so much prominence (especially since the advent of the computer) that the physics as to what is really happening is obscured. There are a surfeit of studies in the meteorological literature showing a spectral analysis of patterns for a whole week, a whole month, a whole year, etc.—but not a single analysis has ever been made, showing the relationships between all highs and lows over the hemisphere at a given moment in time.

Let us analyze why a unified hemispheric (or global) explanation of how “the weather really works” has been shrouded in mystery for so long. There are a cluster of “mini-problems” that have to be solved before we can even come to grips with the actual movement of storm centers. These “mini-problems” are both scientific and political in nature. At this point we will only consider the scientific problems, and leave the last chapter of the book to touch on some of the political problems.

Let us divide the scientific problems into three parts.

1. What forces cause the movements of all highs and lows over a hemisphere?
2. What is known about the geometry of a sphere? The surface of the spherical Earth is the play-ground of the forces mentioned in 1. above. We may have a hard time understanding how these forces behave if we don't understand the

three-dimensional nature and mathematics of a sphere.

3. Do we understand what using a flat weather map of a round world does to our neat little formulas about a sphere, and the forces that act on the surface of a sphere? The *polar stereographic* map (used by all weather services) is the best possible flat map to be used for weather analysis and forecasting. Nevertheless, any way that you may look at it, or hold it, you will not actually see a round sphere. How could you hope to recognize any useful hemispheric patterns with a goofy map?

In the following pages we will take a good look at some important geometric principles of a sphere, and then we'll take a hard look at the polar stereographic map. This will set the stage for understanding the various configurations that are present on every single weather map. It will be possible to use and understand the various patterns (that will be shown later in the book) without knowing the geometric principles of a sphere or even how the map works. Lack of this mathematical knowledge, however, will leave you wondering and guessing how some of the results occurred on a flat map of a round world.

If you hang on through the earlier parts of this book, you will find the later parts more interesting. Even if you're an experienced mathematician, this "simple" geometry may have certain twists to it that you may not have noticed previously, or at any rate, you may not have seen any direct connection with meteorology, heretofore.

Chapter 2

Some Geometry

This chapter explores the geometry of shapes on a sphere. This information is of course available in any book on spherical geometry (in much greater detail), but is not properly discussed in books on meteorology. I am including some of the principles so that you won't have to go to another text for this information unless you so desire. The terms used in this chapter are helpful in understanding the configurations shown in the later chapters, since we are looking at, and measuring angles and circular arcs on a flat map, while we are actually describing what is happening on the surface of a sphere. Nevertheless, you will be able to enjoy and understand the charts in the last sections of this book even if you decide to skip this chapter. You can come back to this chapter later on if you feel the need for a deeper perspective.

Spherical geometry may be a fringe area in meteorology, but it is used extensively in sailing, astronomy, surveying, and in other areas of science. Since lows and highs also sail about on the surface of the Earth, we will take a closer look at some of the theorems and definitions of this branch of mathematics. And since we live continuously in a three-dimensional world, many of the properties and relationships of lines and planes in space are quite familiar.

Some Differences Between Plane and Spherical Geometry

1. The *spherical surface* is used as the basis for spherical geometry, while the *plane* is used as the basis for plane geometry.
2. Two points do not necessarily determine a single line. For example, the North and South poles lie on an infinite number of *great circles*, as can be seen on any three-

dimensional globe of the Earth. The same is true for the end points of any diameter on a sphere.

3. A line on the surface of a sphere can not have an infinite length as in a plane, but has a maximum finite length. If the radius of the sphere is considered as being equal to 1, then the greatest possible distance on the surface between any two points is half of the circumference of $2\pi r$, and is equal to π when $r = 1$.
4. Given three points on a line around a sphere, we can not say that only one of the three points is in the middle between the other two points. Each point, in turn, can be considered as lying between the other two.
5. A perpendicular to a line on a sphere from another point on the sphere, always exists (as in a plane), but is not necessarily the only perpendicular. As an example, any line joining a pole to any point on the equator is perpendicular to the equator.

General Definitions

A spherical surface is a *curved surface* on which every point is at an equal distance from the center of the sphere, and a line joining any point on the surface with the center is a **radius**.

When a plane intersects or cuts a sphere, the intersection at the surface of the sphere is always a circle. When the plane intersecting the sphere passes through the center of the sphere, the intersection at the surface is called a **great circle**; if the plane does not pass through the center, its intersection with the surface is called a **small circle**. For example, the equator and the longitudinal lines (or meridians) on the Earth are great circles, while the parallels of latitude are small circles, except for the equator.

An **arc** of any circle is measured in degrees, minutes, and seconds by the angle (alpha), *subtended* at its center. See **Figure 2-1**.

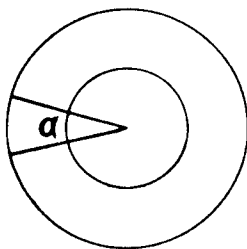


Figure 2-1. The angle α (alpha) cuts off an arc of greater length on the larger circle (as compared with the smaller circle), but the angle is the same for both arcs.

The angle formed in space when two planes intersect is called a **dihedral angle**, as shown in **Figure 2-2**. The line of intersection (EF)

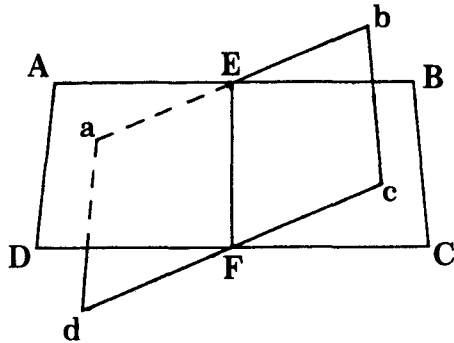


Figure 2-2. Four angles are formed when two planes intersect. The values of the dihedral angles can be represented by: DFd, dFC, CFc, and cFD.

between the two planes is called the **edge**, and each of the planes is called a **face**. To find the magnitude of a dihedral angle (see **Figure 2-3**), we

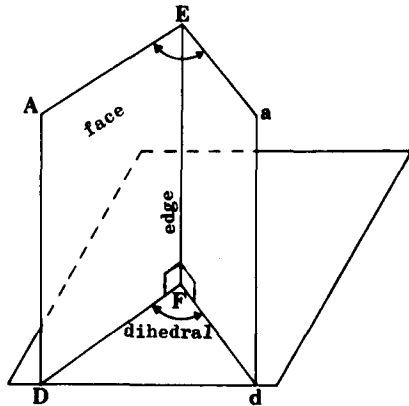


Figure 2-3. Here is a view of a dihedral angle, formed when two planes intersect.

pass a plane which is perpendicular to the edge. This plane will intersect the faces of the dihedral angle in straight lines and will thereby form a plane angle (DFd) in the plane of intersection. The **magnitude of the dihedral angle** is equal to the plane angle, (DFd).

A line (or plane) that is perpendicular to the radius of a circle (or sphere) at the outer surface, is called a **tangent line** (or a plane in three-dimensions). See **Figure 2-4**.

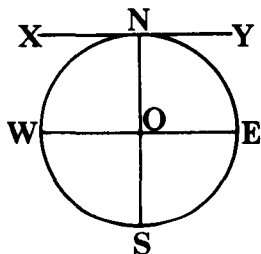


Figure 2-4. The line XNY is tangent to circle NESW with a radius ON.

Angles on a Sphere

Figure 2-5 shows three great circles intersecting to form the **spherical triangle ABC**. This surface triangle forms a spherical pyramid **OABC** when the vertexes are joined to the center **O** by radial lines. Side **AB** of the spherical triangle is measured by the plane angle **BOA**; side **AC** is measured by the plane angle **COA**; and side **BC** is measured by the plane angle **BOC**. The sides are measured as angular degrees. The *sum of the sides* of a spherical triangle is less than 360° , since the angles are measured around the vertex at **O**.

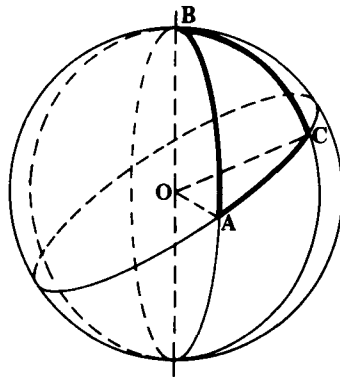


Figure 2-5. A spherical triangle on the surface of a sphere is part of a spherical pyramid formed by **OABC**.

The angle at **A** is measured by the dihedral angle formed by the intersecting faces **BOA** and **COA**, the angle at **B** is measured by the dihedral angle formed by the intersecting faces **AOB** and **COB**, and the angle at **C** is measured by the intersecting faces of **AOC** and **BOC**. The sum of the **dihedral angles** of a spherical triangle is greater than 180° and less than 540° .

How do we determine the angle between two great circles (or parts of great circles) of a sphere? There are three general approaches:

First, we draw a tangent line to each great circle at the points where they cross each other. The plane angle formed by these two tangent lines is called the **spherical angle**. In Figure 2-6, the line **CD** is drawn tangent

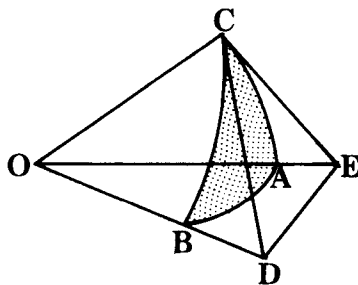


Figure 2-6. Two tangent lines to an angle of a spherical pyramid form a tangent plane **CDE**.

to the arc BC while CE is the line tangent to the arc CA. The plane angle formed by points DCE is the magnitude of the spherical angle BCA.

Second, each great circle can be considered to be lying in a plane. Therefore, two different great circles can be considered as two different planes intersecting each other at a dihedral angle. This dihedral angle is also the spherical angle between the two great circles.

Third, we can consider the point of crossing or vertex of two great circles as a pole. For any point P, chosen as a pole, we can draw another great circle, which is called the equator (GABH in Figure 2-7) for that point on that sphere. In Figure 2-7, we have the arcs of two great circles, PAP' and PBP' both intersecting at P and P'. The spherical angle at the intersection P (or P') is equal to the plane angle AOB which lies in the plane of the equatorial circle GABH. Every equatorial circle can be divided into 360° . Therefore, the planes of the two great circles cut off the arc AB, which gives the measure of the spherical angle in degrees, on this equatorial circle. PAP' and PBP', together, form a lune which is the part of the surface of a sphere that is bounded by two semicircles of two great circles. For a spherical angle of 180° , the lune becomes half of a sphere or a hemisphere.

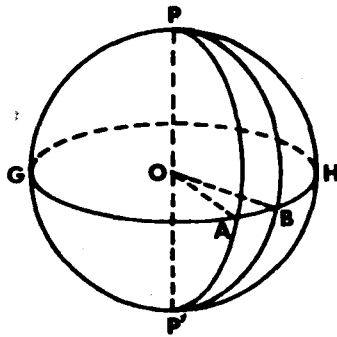


Figure 2-7. Two great circle arcs, PAP' and PBP', meeting at P and P'.

All great circles that go through a point, meet again at a point known as the antipodal point. The crossings are also called polar points or vertexes. These antipodal points are opposite, since there is one at each end of the diameter of the sphere. Through two antipodal points an infinite number of great circles can be drawn.

Since we are also concerned with the patterns of small circles in *Singer's Lock*, it is necessary to define the angle which is formed when two small circles or when a small and great circle cross. These crossings can't be called spherical angles according to the definition above. Therefore, since I have not come across an official name for this type of angle, I

will call this crossing of arcs an **arc angle**, to distinguish it from spherical angles.

Distances Between Points on the Surface of a Sphere

The shortest path between two points on the surface of a sphere is an arc of a great circle. We must also consider the path of a small circle, which is not the shortest distance between two points, but is rather a path of constant curvature. There are an infinite number of small circle paths that can be taken between any two points. There can also be an infinite number of irregular or zig-zag paths, but they are not significant for our purposes. Lastly, the shortest distance between two points on a sphere in three-dimensional space (if we burrow beneath the surface of the sphere) is a **chord**, which is just a straight line connecting the two points.

Definition of Polygons on a Sphere

That part of the surface of a sphere enclosed by three or more arcs of great circles is called a **spherical polygon**. See Figure 2-8. The enclosing arcs are the **sides** of the polygon, and the vertexes of the spherical angles are the **vertexes** of the polygon. A spherical polygon with three sides is called a **spherical triangle**. The angle formed at the center of the sphere by these sides is called a **trihedral angle**. A **polyhedral angle** is a general term for a similar angle formed by three or more sides coming into the center of the sphere. The sides of a spherical polygon are measured in degrees in the same way as a spherical angle, because the sides of a spherical polygon are always arcs of great circles—all great circles on the same sphere have the same size and length.

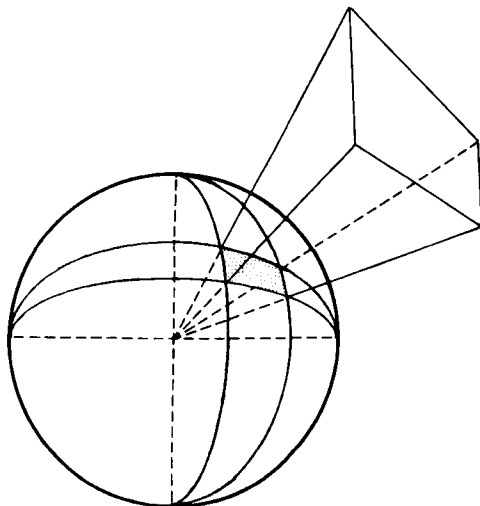


Figure 2-8. A spherical rectangle, on the surface of a sphere, is shown extended into space to help visualize its shape.

An **arc polygon** will be formed when a part of the surface of a sphere is enclosed by three or more arcs, and at least one of these three arcs is part of a small circle.

Spherical Triangles

Three mutually perpendicular planes passed through the center of a sphere, cut the surface of the sphere into eight spherical triangles, as shown in Figure 2-9. Now consider only one of the eight spherical tri-

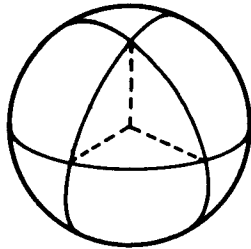


Figure 2-9. Eight equal spherical triangles on a sphere.

angles; you will see that each corner of the triangle is 90° . Since there are three corners to a spherical triangle, the total of all the angles is three times 90° , or 270° . This is an example of the general rule that the sum of the angles of a spherical triangle is always something greater than 180° , but always less than 540° . Also, the amount by which the sum of the angles of a spherical triangle exceeds 180° is called the **spherical excess of the triangle**. The area of a spherical triangle is given by

$$(2-1) \quad A = \frac{\pi r^2 E}{180}$$

where A is the area, E is the spherical excess measured in degrees, and r is the radius of the sphere. The larger the area of the spherical triangle, the greater the amount of spherical excess, as can be seen in Figure 2-10.

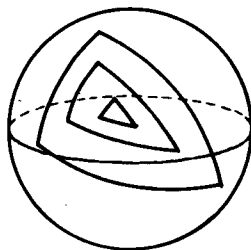


Figure 2-10. Spherical triangles of increasing size on the surface of a sphere.

With an approximate diameter of 8,000 miles, we find that the Earth's surface is about 200 million square miles. The icosahedral pattern, shown in Figure 2-11, will give twenty equilateral triangles, which is the largest number that can be drawn on a spherical surface like the Earth. Each one of these twenty equilateral spherical triangles can be subdivided equally into six right triangles by bisectors, which are perpendicular to the side opposite each angle. See Figure 2-11.

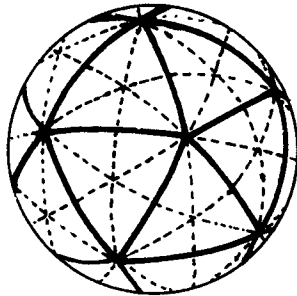


Figure 2-11. An icosahedral pattern with the 20 equilateral triangles, each sub-divided into 6 right triangles.

The angles formed by the triangle in Figure 2-12 (which is one of the 120 triangles generated by an icosahedral pattern) has exactly 6 degrees of spherical excess, since the total of the three angles is 186° . The area of one of these triangles on the Earth, is approximately, 1,666,666 square miles.

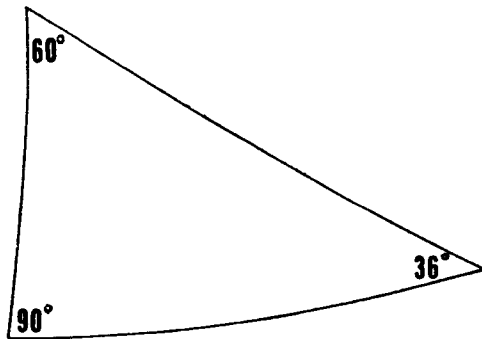


Figure 2-12. The angles formed by one of the 120 triangles generated by an icosahedral pattern.

Chapter 3

The Polar Stereographic Map

This chapter explains what the polar stereographic map is, how it works, and how it can be used to our advantage, since it is the most widely used map in weather analysis and forecasting. A more extensive and detailed explanation can be found in other books. Skipping the equations in this chapter will not interfere with your understanding of the following chapters. Mathematical equations are quite often used as the proof that certain facts or conclusions are true. You can still accept the conclusions as being true, even if you don't know or understand the mathematics involved. I have added the mathematics for those who want the exact proofs. If you have studied the equivalent of high school geometry, the mathematics in this section should not be too difficult. The explanation I offer is perhaps easier to understand than any book on the polar stereographic map that I have been able to find. It is, nevertheless, precise and lays the foundation for meteorologists (and everybody else) as to some of the mathematics behind the charts in the latter part of the book. There is nothing new in my explanation of the map, but I have developed specific tools to aid in the use of the weather map that are indeed new to the field of meteorology.

Every map maker knows that there are all types of projections to show a spherical Earth on a flat piece of paper. But since no projection on paper can be completely right for all purposes, different ones are used for many different purposes. Some flat maps reproduce shapes, others are accurate for angles, directions, equal area comparisons, others for small areas, etc. With these known facts, a straight line or angle on one type of flat map doesn't have the same meaning as on another type. A straight line on one type of map can be compared with a straight line on another type of map by the means of transformation formulas.

The Polar Stereographic Map

Polar stereographic maps are used (among other reasons) because:

- a. A circle on a sphere is reproduced exactly as a circle on the map.
- b. All lines of latitude and longitude cross at 90° angles everywhere on the map in the same manner as they do on the surface of the Earth.
- c. It is the best map available to show an area as large as a hemisphere.

Construction of the Polar Stereographic Map

In the polar stereographic projection, a point of light is placed at the South Pole and a tangent plane is placed at the North Pole, which is the plane upon which the projection is made. To get a better understanding, see Figure 3-1. The point of light at the South Pole of the sphere is called the **center of projection**.

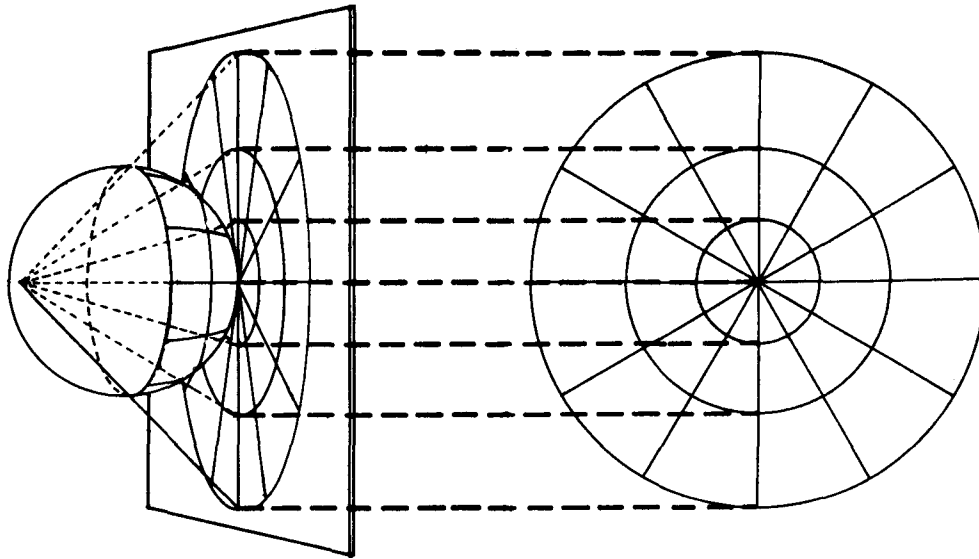


Figure 3-1. Light projected from the south pole onto a flat transparent screen, which is tangent to the north pole, shows lines of longitude (which are great circles) as straight lines; while the circles of latitude (which are small circles except for the equator) show as perfect circles.

In Figure 3-2, NESW represents the plane of a meridian, where N is the North Pole, S the South Pole, and EOW is a line joining two opposite points, E and W on the Equator, where O is the center of the sphere. If we divide arc NE into 9 equal parts, each part in the figure would represent 10° of latitude. Arc NE is of course 90° . All points on the sphere

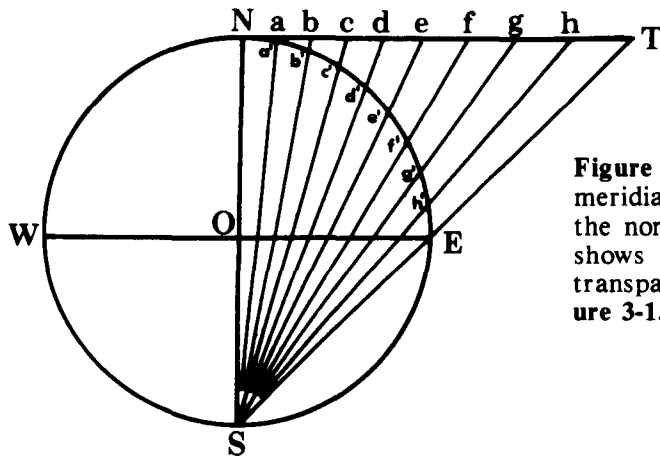


Figure 3-2. The plane of any meridian (NESW) goes through the north and south poles, and shows the trace (NT) of the transparent plane shown in **Figure 3-1**.

with a distance of 10° from the North Pole will lie on a circle with a radius N_a . The circle is on the tangent plane, with N as its center. Those points lying 20° from the North Pole will lie on a circle with a radius N_b , and so on.

The plane of projection could be placed at any latitude below the North Pole, but it must always be above the center of projection at the South Pole. The latitude at which the plane is drawn is called the **standard latitude**. A plane at the equator is known as a **primitive plane** or **equatorial plane**.

There are three things that determine the size of the map: the size of the globe used to construct the map, the standard latitude, and the **scale**.

The scale can be defined as a relation between a given distance on the ground and the corresponding distance on the map. The scale could also be defined as a ratio equal to the distance between two points on the map, divided by the distance between the same two points on the Earth. Remember, the scale represents distance only, not area. Consider the triangle in **Figure 3-3**, where side ab is $\frac{1}{2}$ of side AB , but the area of triangle abc is not $\frac{1}{2}$ of triangle ABC . The historical weather maps used in this book have a scale of $1/30,000,000$ or 1 inch on the map is equal to 30,000,000 inches on the surface of the Earth. It is important to note here that the scale is exact only at the latitude where the plane was

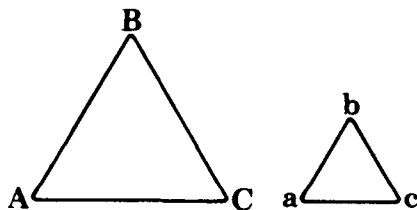


Figure 3-3. Doubling the length of the sides of a triangle, more than doubles the area.

The Polar Stereographic Map

placed, when the projection was made. On the historical weather maps, the scale is accurate at 60° north latitude. The choice of 60° north was made to give smaller average absolute departures of scale over the most important working area of the map. However, to prove certain mathematical relationships on the map, it is easier to assume the plane to be at the North Pole or the Equator, since the results obtained will apply regardless of the standard latitude that may be used.

As can be seen from Figure 3-4, the size of the actual stereographic map is partially determined by the standard latitude used when making the projection. If the plane is large enough, the entire sphere could be shadowed upon it, except for the South Pole, which would be a line at infinity.

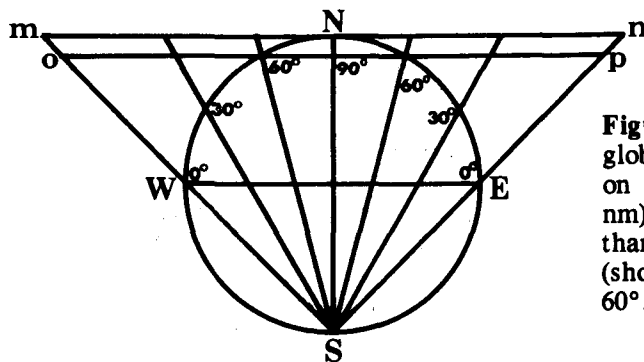


Figure 3-4. For a given sized globe, we see that a projection on a plane (shown by the line nm) at the north pole is larger than the projection on the plane (shown by the line op) at latitude 60° .

What is a Straight Line on the Polar Stereographic Map?

Every straight line on the polar stereographic map is actually part of a circle on the sphere. This is true because any circle that goes through the South Pole will project as a straight line. To understand this better, consider the following: when a straight pencil (used to represent a line) is placed between the source of light at the South Pole and the tangent plane, a shadow of a straight line will be projected on the plane; except when the pencil is parallel to the light rays, and then you'll see only a point projected. In geometry, a point and a straight line can lie on only one plane; in this case the light at the South Pole is considered to be the point, and the pencil is the straight line. This plane will always cut out a circle (which looks like a straight line on the map) on the sphere. The arc of any circle north of the Equator is the only part which will show, since the Equator is usually the outer boundary of most weather maps. All great circles that touch the South Pole will project as lines of longitude, just like AEC in Figure 3-5. Every other straight line on the map (or off

the map), regardless of length, orientation, or distance apart can be considered as physically representing the projection of an arc of a small circle (on the Earth's surface) that touches the South Pole—for example: HI and FG in Figure 3-5.

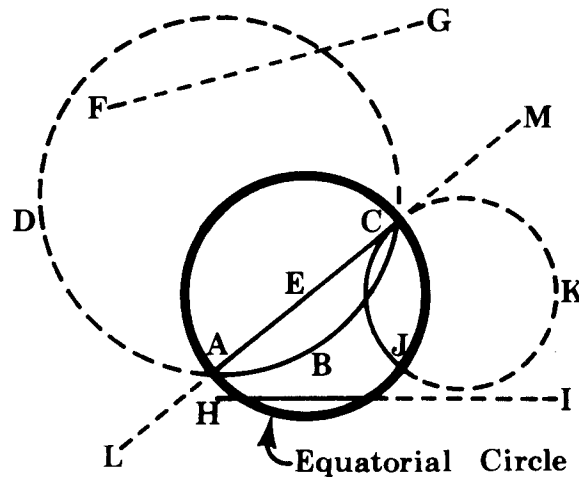


Figure 3-5. The polar stereographic map usually ends at the equator. The circle drawn with a thick line represents the equatorial circle of a polar stereographic map. Here we see how *parts* of some of the small circles and great circles would look if part of the southern hemisphere were to be shown on the map by extending the map plane past the equatorial circle.

a. FG represents a part of a small circle that passes through the point of projection, but the circle is entirely below the equator and is shown as a dashed line.

b. HI represents part of a small circle that passes through the point of projection, with part of the circle above the equator and part of the circle below the equator (shown as a dashed line).

c. LM represents a great circle passing through the projection point, which makes it a meridian, but the extension of the meridian below the equator is shown as a dashed line.

d. CJK shows a small circle that does not pass through the projection point. The part of the circle below the equator is shown as a dashed line.

e. DABC shows a great circle that does not pass through the projection point; the part of the circle below the equator is shown as a dashed line.

When two straight lines intersect on the flat map, regardless of length, they can be considered as the intersection of the arcs of two different circles on the surface of the sphere. The plane angle of intersection measured on the map will be an exact measure of the angle of intersection between these two circles. This is also true for lines that do not even cross in the boundaries of the map, as can be seen in Figure 3-6.

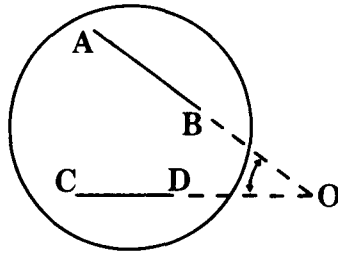


Figure 3-6. It is sometimes necessary to extend the line off the map past the Equatorial circle to measure the angle between two straight lines (provided they are not parallel). The two lines, AB and CD, meet at O to give the angle AOC.

Straight lines on the polar stereographic map can be interpreted in three different ways:

1. When we go a distance of 5° latitude (300 nautical miles) from any point on the Earth's surface we are actually moving along a curved arc. From a practical standpoint, this curved arc is usually considered as a straight line (in a plane) as long as the distance is 5° or less; therefore, the angle between two straight lines that fall within a radius of 5° on the flat map is the same as the angle on the Earth's surface, with only a slight inaccuracy that is tolerable in weather analysis.
2. Straight lines on a flat map can be considered as projections of arcs of circles on a sphere, where the circle goes through the point of projection (the South Pole).
3. The two points at the end of a straight line on the map can be considered as the ends of a projected chord of the sphere.

Stereographic maps are used not only in weather, but in many other fields. They are used for mapping crystal faces in crystallography, and the mapping of geological structures in the field of geology. They have used straight lines on their maps for over a century. This is the first time that attention has been focused on the characteristics of a straight line on a polar stereographic map in meteorology. The significance of straight lines will be seen in the analysis we will make of weather patterns later on in the text.

The Nature of Pattern Distortions Created by the Polar Stereographic Map

What is the actual distortion of measurements on the polar stereographic map? To find the amount of distortion at any latitude, we must first find the actual radius of that latitude from the Earth's north-south axis, and then compare this with the radius as measured on the map. To derive the formula for the actual radius, see Figure 3-7, where nb is the radius of the latitude, and NB is the projected radius. Let ϕ be the

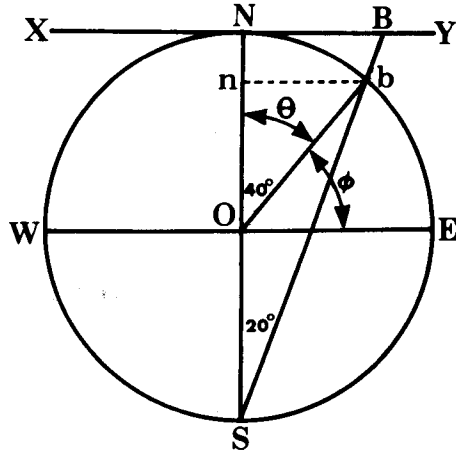


Figure 3-7. S is the point of projection, N is the north pole, line XY is in the plane of projection, and the latitude ϕ is 50°N . The projected radius from the north-south axis, NB, is longer than the actual radius, nb. This difference in length increases as you go to lower latitudes, and decreases as you go to higher latitudes.

latitude for any point on the Earth. Then, θ is the angle of the co-latitude. Co-latitude is defined as being equal to 90° minus the latitude ϕ . Let XY represent the plane which is tangent to the North Pole at N. b is any point on the meridian NESW at latitude ϕ , where the co-latitude is θ , or angle bON. By simple geometry, the angle bON equals two times angle bSN. NO equals R — the radius of the Earth.

Since $bSN = BSN$ then,

$$\begin{aligned}
 \text{(3-1)} \quad & NB = 2R \tan \text{angle } BSN \text{ or } 2R \tan \frac{1}{2}\theta \\
 & \theta = 90^\circ - \phi \\
 & NB = 2R \tan(45 - \frac{1}{2}\phi)
 \end{aligned}$$

Referring to Figure 3-2, the radius at the points a, b, c, . . . T, can be found similarly. The projection of the latitude circles on the polar stereographic map is made by drawing circles with radii Na, Nb, Nc, . . . Nt. a, b, c, . . . T, are $10^\circ, 20^\circ, 30^\circ, \dots 90^\circ$, distant from the North Pole so as to correspond to latitudes of $80^\circ, 70^\circ, 60^\circ, \dots 0^\circ$, while the angles NSa, NSb, NSc, . . . NST, are $5^\circ, 10^\circ, 15^\circ, \dots 45^\circ$, respectively.

We get Table I by substituting different values of latitude in Equation 3-1. The length of the radius for different latitudes of the projection in terms of the radius of the Earth is shown in Column E of Table I below, the length of the actual radius on the Earth for the different parallels is shown in Column D.

Now let's look at some of the distortions created by the map. On the Earth, the circumference of a circle of latitude at ϕ is $2\pi R \cos \phi$. On the projection, the circumference of this same circle becomes $4\pi R \tan(45 - \frac{1}{2}\phi)$. The error in scale of the circles can thus be obtained by their ratio:

$$(3-2) \quad \% \text{ Error} = \left[\frac{(2 \tan(45 - \frac{1}{2} \phi) - \cos \phi)}{\cos \phi} \right] \times 100$$

TABLE I

A Latitude	B (45 - ½ φ)	C tan(45 - ½ φ)	D Radius (actual)	E Radius (projection)
90°	0°	.0000	.000R	.000R
80°	5°	.0875	.174R	.175R
70°	10°	.1763	.342R	.353R
60°	15°	.2679	.500R	.536R
50°	20°	.3640	.643R	.728R
40°	25°	.4663	.766R	.933R
30°	30°	.5774	.866R	1.155R
20°	35°	.7002	.938R	1.400R
10°	40°	.8391	.985R	1.678R
0°	45°	1.0000	1.000R	2.000R

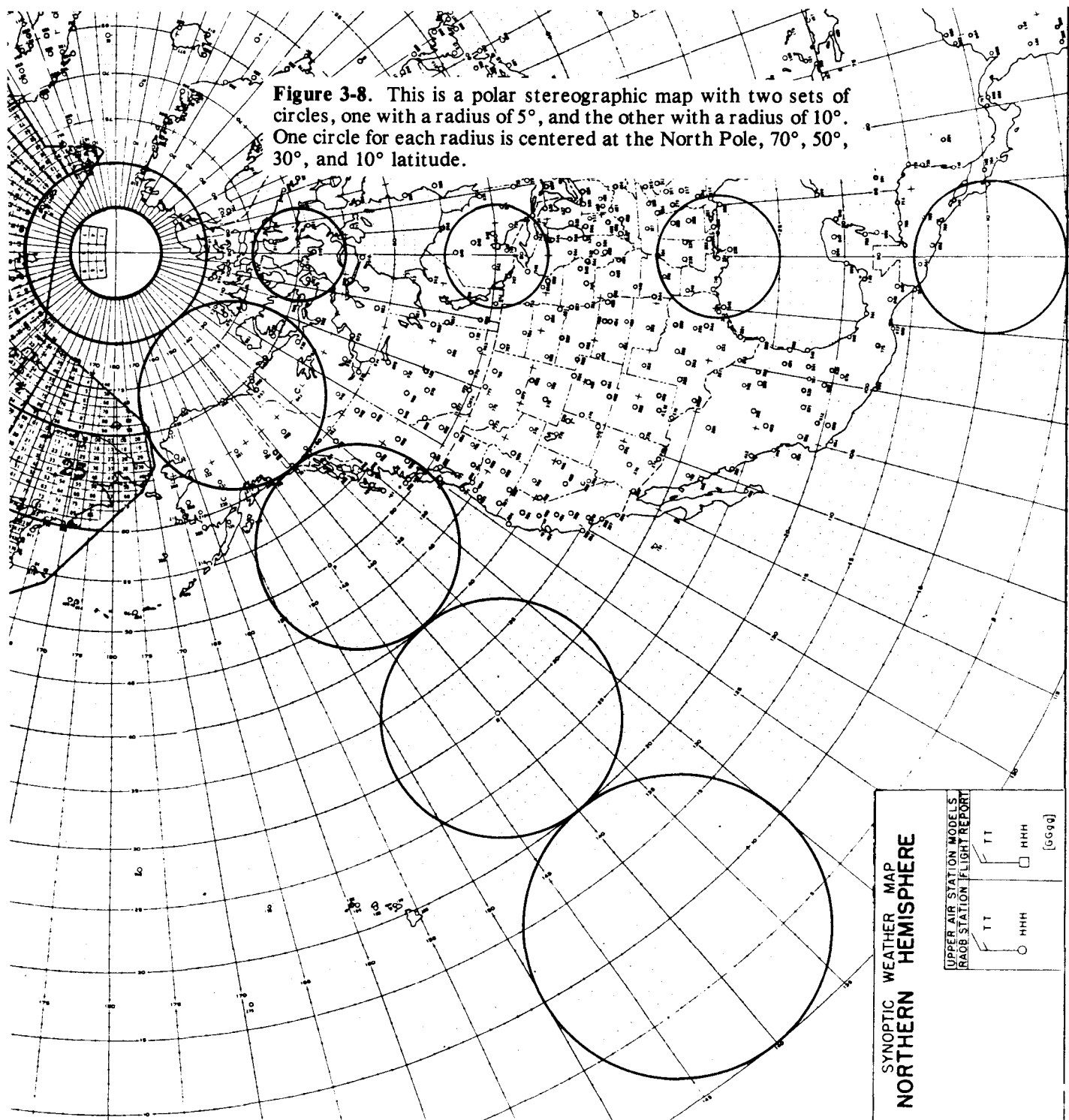
Substituting the values from Table I into Equation 3-2, we get the percentage of error for the 9 circles of latitude and the North Pole, as in Table II below. Column B gives the percentage of error for a projection on a tangent plane at the North Pole. Column C gives the percentage of error for a tangent plane at 60° north latitude. This is of course the standard latitude used in the construction of most weather maps. Column C was obtained by subtracting 7.18% from the values in Column B.

TABLE II

A Latitude	B Tangent at N. Pole	C Tangent at 60°N. Lat.
90°	0.00%	-7.18%
80°	0.76%	-6.42%
70°	3.11%	-4.07%
60°	7.18%	0.00%
50°	13.25%	6.07%
40°	21.74%	14.56%
30°	33.33%	26.15%
20°	49.03%	41.85%
10°	70.41%	63.23%
0°	100.00%	92.80%

The stereographic map possesses the important property that shape is preserved at a point, since every point is stretched equally in all directions like any point on the surface of a rubber balloon. If a face is painted on a round rubber balloon, we will see the same face when the balloon is blown up, but larger in size. The point at the tip of the nose (and all other points) is stretched equally in all directions. We still have

the tip of a nose in the larger blown up version, but the tip occupies more area. Figure 3-8 has been drawn to give a clearer visual picture of this type of distortion on the weather maps used as examples in this book.



The Polar Stereographic Map

On the surface of the Earth, all circles of equal radius are perfect circles, and each one covers the same area. Obviously, Figure 3-8, seems to contradict this fact. The error in this figure is created by the map projection, and the amount of error in the size of the circles can be calculated with the aid of Equation 3-2, as has been done in Table II.

The Irregular Appearance of the Projection of the Centers of Circles

The drawing of Figure 3-8 requires the proof of two separate facts: First, does any circle on the surface of the Earth project as a perfect circle on the map; and second, does the center of the circle on the Earth become the center of the circle on the flat map? Surprisingly, circles on the Earth always show up as circles, parts of circles, or straight lines, on the flat map, but the centers do not match up. What follows is the standard proofs for these conclusions.

In Figure 3-9, the small circle diameter xy projects into XY and the small circle's center c into C ; since the South Pole, S , is the point of projection. P is the middle point between X and Y . We can see that there is a difference between C and P , due to the distortion of length caused by the projection. Therefore, xc and cy will not project as equal lengths, even though they are equal on the surface of the Earth. The true center of the circle lies closer to the North Pole on the polar stereographic map than the center of the projected circle (it lies closer to the South Pole in the Southern Hemisphere).

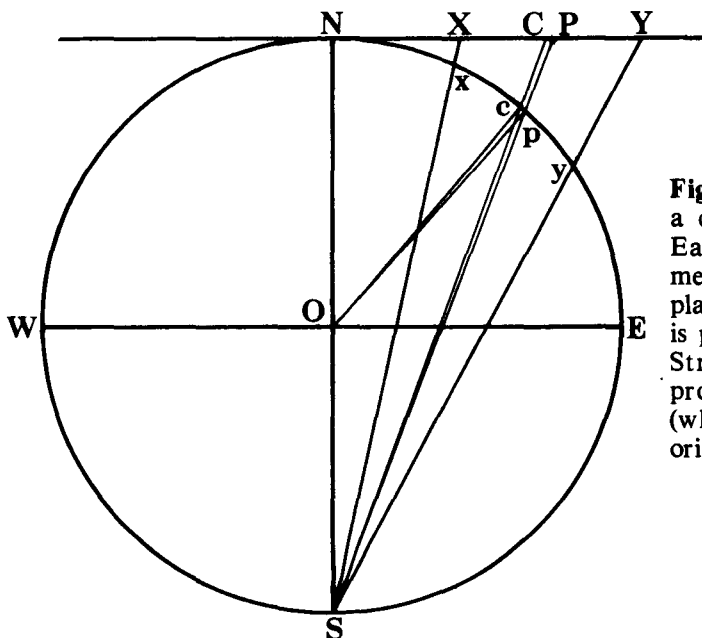


Figure 3-9. The diameter, xy , of a circle on the surface of the Earth, is projected with a diameter of XY , onto the tangent plane. The center of a circle, c , is projected as C on the plane. Strangely, the center of the projected diameter is P , not C (which is the projection of the original center, c).

All Circles on the Earth's Surface Project as Circles on the Map

Now let us prove that all circles on the surface of the Earth show up as circles on the stereographic map. In **Figure 3-10**, let WGEF be the **equatorial circle** (also called the **primitive circle**) of a sphere with N and S as the poles, and with pole S as the point of projection. Let P_1 be any point on the sphere. We will find that a plane through the points of the great circle NP_1GS will intersect the equatorial plane in a straight line GOF. The **polar distance** of a point on the sphere is its angular distance on the surface of the sphere from one of the poles of the equatorial circle. Therefore, the arc NP_1 is the polar distance of P_1 . The magnitude of the angle of NP_1 is determined by the angle NOP_1 . p_1 is the stereographic projection of point P_1 in the equatorial plane, since p_1 is the point in which SP_1 pierces the equatorial plane. Since P_1 was chosen in the Northern Hemisphere, its projection is inside the Equatorial Circle. If P_1 had been chosen as a surface point in the Southern Hemisphere, then the projection point of P_1 would have been outside the Equatorial Circle.

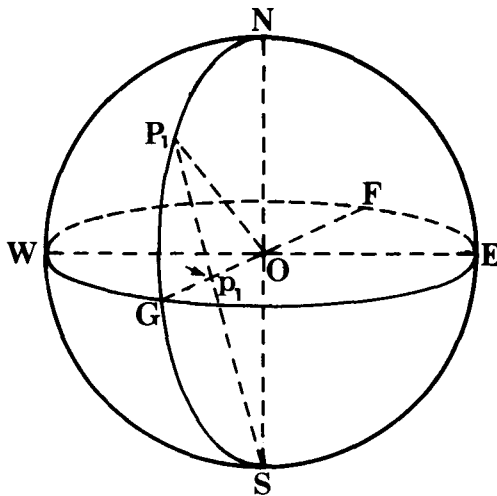


Figure 3-10. See the text for the explanation.

In **Figure 3-11**, WGEF is again the Equatorial plane, with N and S as the poles of the sphere. Let QQ_1R be a small circle on the sphere. The pole P of the small circle is at the end of the radius OP of the sphere. This radius OP is perpendicular to the plane of QQ_1R . The **polar distance** of a circle is the angular distance of any point on its circumference from either one of its two poles (the second pole, which is not shown, is diametrically opposite to pole P). The polar distance of the small circle is PQ, which also equals PR. The **inclination** of a circle is the angle between its own plane and the Equatorial plane. The inclination of the small circle plane

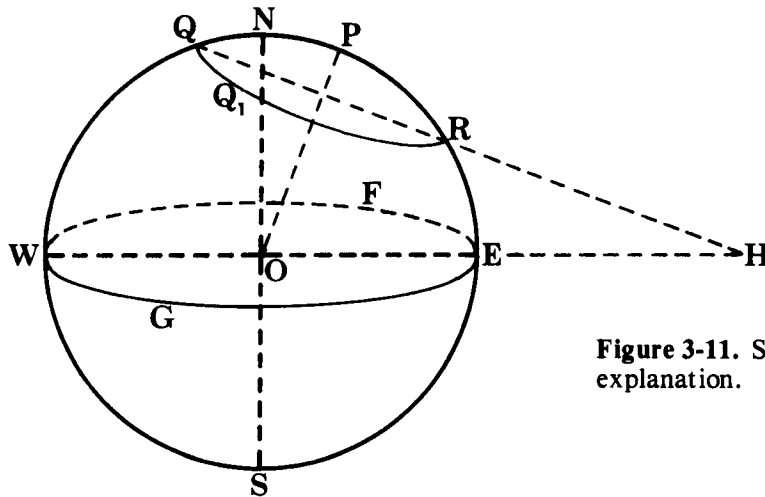


Figure 3-11. See the text for the explanation.

QQ_1R to the Equatorial plane $WGEF$ is the angle RHE , which is also measured by the arc NP . NP , of course, is measured by the angle NOP , which exists between the pole of the equatorial plane and the pole of the small circle. The points N , O , and P lie in a plane, which intersects the Equatorial plane along the line WOE . This line, WOE , is called the **line of measures** of the circle QQ_1R .

In Figure 3-12, we show how the end points Q and R of the small circle (shown in Figure 3-11) project onto the Equatorial plane. We see that R projects as point r , and Q projects as point q , on the line of measures WOE in the Equatorial plane.

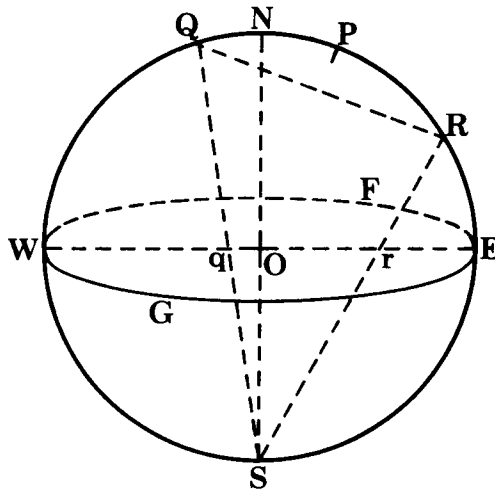


Figure 3-12. See the text for the explanation.

In Figure 3-13, we let P_c be the vertex of a cone tangent to the sphere along the circumference of the small circle QQ_1R , (only the front-half of the circle is shown), with the lines P_cQ and P_cR representing the **extremities** of the cone. The curve qq_1r represents the projection in the equatorial plane of the small circle QQ_1R . By connecting all the points

in the small circle QQ_1R with the center of projection S , we form another cone with SQ and SR at the extremities. P_c as a vertex projects into the equatorial plane as the point p_c .

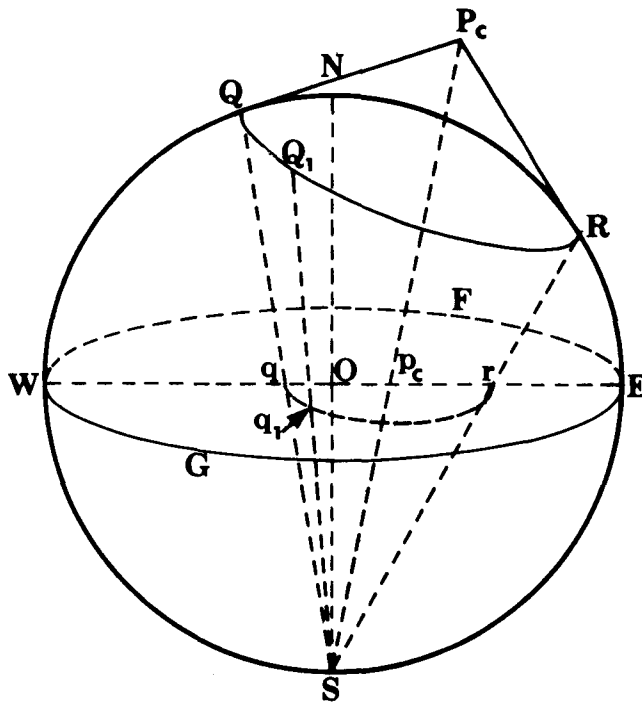


Figure 3-13. See the text for the explanation.

In Figure 3-14, the points S , Q_1 , and P_c lie in a plane. This plane cuts the equatorial circle in the line p_cq_1 which is the projection of the line P_cQ_1 of the cone. We draw a tangent line to the point S that is also in

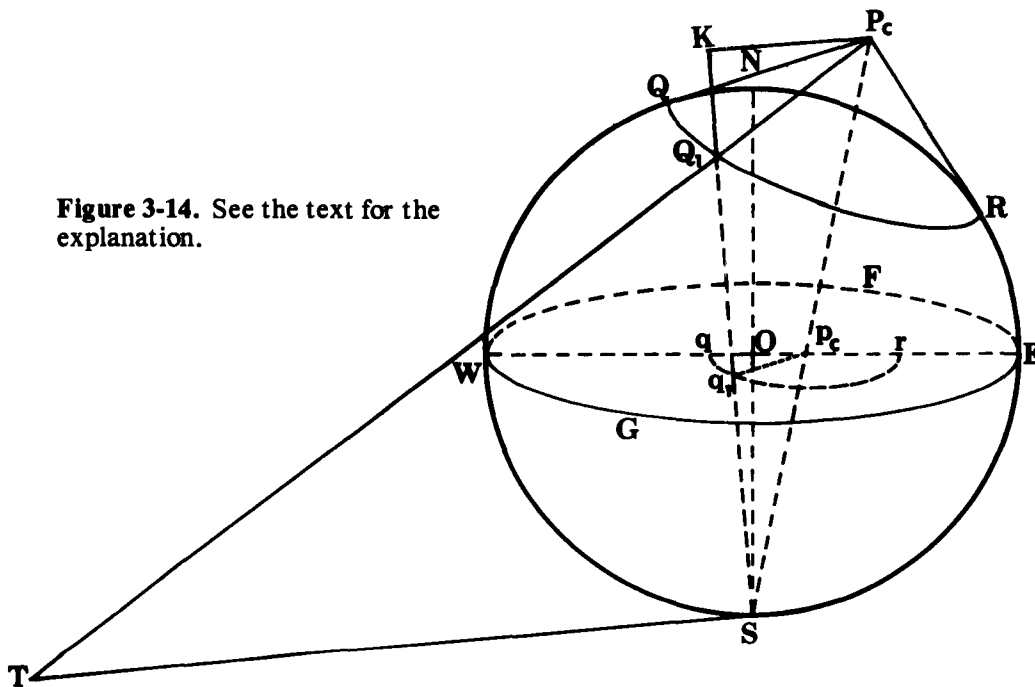


Figure 3-14. See the text for the explanation.

the same plane as SQ_1P_c . We extend the line from P_cQ_1 to the point T where it crosses the tangent line from S. The line SQ_1 is a chord of the sphere since the points S and Q_1 are both on the surface of the sphere. The line ST is parallel to p_cq_1 , since the plane tangent at point S is also parallel to the equatorial plane in which p_cq_1 lies. In this figure, p_cq_1 does not look parallel because the figure is shown in perspective. In an actual three-dimensional sphere the parallelism would be easily seen. We draw P_cK parallel to TS and extend the line Q_1S to where it meets the line from P_c at point K. The points S, T, Q_1 , K, and P_c all lie in the same plane.

In Figure 3-15, we see another view of the plane (STQ₁KP_C) and how it cuts the sphere. Since P_CK and TS are parallel, the *alternate interior angles* TSQ₁ and Q₁KP_C are equal. TS and TQ₁ are tangents from the common point T, so they are equal, and the angle TSQ₁ = angle TQ₁S = angle KQ₁P_C. Therefore P_CK = P_CQ₁. The triangles Sq₁p_C and SKP_C are similar,

$$\frac{P_c q_1}{P_c K} = \frac{P_c q_1}{P_c Q_1} = \frac{P_c S}{P_c S}, \text{ or } P_c q_1 = P_c Q_1 \times \frac{P_c S}{P_c S},$$

which is equal to a constant, since $P_c Q_1$, $p_c S$ and $P_c S$ are all fixed lengths that can not change when we move to different points on the small circle.

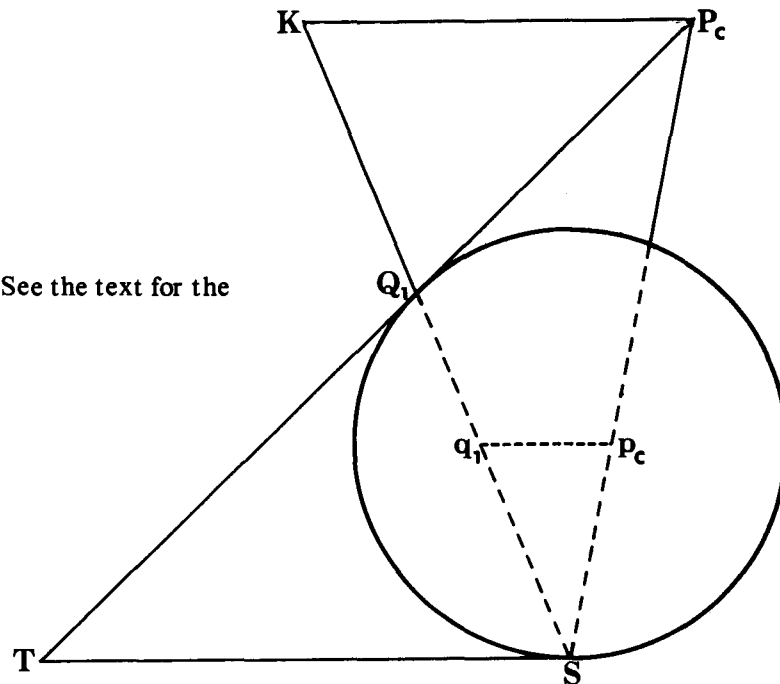
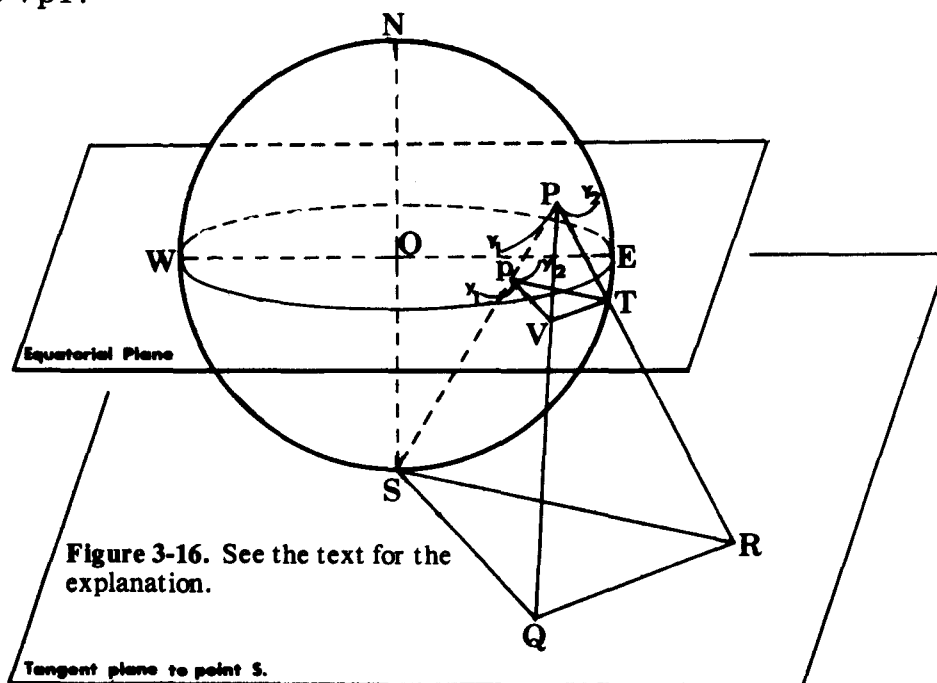


Figure 3-15. See the text for the explanation.

Since $p_c q_1$ is constant, and since the point p_c is fixed; the locus (path) of q_1 (which follows Q_1 , as Q_1 goes around the small circle) is a circle where the center is the projection p_c of the vertex P_c of the tangent cone — which is what we set out to prove.

The Value of the Angle Between any two Arcs on the Surface of a Sphere is Exactly Reproduced on the Polar Stereographic Map

In Figure 3-16, two arcs Y_1 and Y_2 meet at a point P on the sphere. These two arcs project as y_1 and y_2 onto the equatorial plane which is used as the plane of projection. A plane tangent to the projection point S is also parallel to the equatorial plane. In this figure, the tangent lines PV and PT are projected as pV and pT onto the equatorial plane (with the longest parts of the lines outside of the equatorial circle). Now since triangle QSR is in the tangent plane that touches point S , the line QS and RS are tangent to the sphere. Two lines (QS and QP) from point Q are tangent to the sphere at points S and P ; in a similar manner, two lines (RS and RP) from point R are also tangent at points S and P . Therefore, in the two triangles QSR and QPR , we find that QR is common to both triangles, while $QS = QP$, and $RS = RP$ (since any two lines that are tangent to a sphere from a fixed point outside the sphere are always equal in length). Consequently, angle $QSR = \text{angle } QPR = \text{angle } VpT$.



The Polar Stereographic Map

The angle between the two curved arcs that cross on the sphere, Y_1 and Y_2 in **Figure 3-16**, is measured by the angle QPR between their tangent lines, PQ and PR , at the point of intersection of the arcs. Likewise, the angle between the two projected arcs, y_1 and y_2 is the angle VpT between the projected tangents pV and pT . Therefore, when any configuration on the sphere is projected, we find all the angles unchanged in the projection.

Chapter 4

Organization in Space

Space and Some of its Features

In chapters 13 and 14, I show some aspects of an orderly arrangement over a hemisphere of low pressure centers, high pressure centers, and cols (which are points between pressure centers). Therefore, it is appropriate at this time to investigate the subdivisions of space and the mathematical explanation of spatial order. This question of spatial order, or space patterns, is of great importance whether we look at the arrangement of particles in the nucleus, the arrangement of molecules in chemicals, the spiraling of planets, the whirling of galaxies, and, oh yes, the “dance” of highs and lows over any planet with an atmosphere. Space may be an empty nothing, but it does impose irresistible controls over all bodies that dwell in it. These restraints don’t depend on any specific types of forces; they are only determined by geometrical rules.

The first explanation of space started with the *Pythagoreans* (548 B.C. to 490 B.C.). They looked for patterns that could be repeated over and over again on the surface of a plane, and that would fill in that plane completely (like tiles on a floor). They came up with the only regular polygons that could be used for this purpose. Note that a **regular polygon** is a three, or more, sided figure which has equal sides and equal angles. They found that there were only three regular polygons which would fill in a plane; an **equilateral triangle**, a **square**, and a **regular hexagon**. See Figure 4-1. Nevertheless, there are an infinite number of **irregular polygons** that can provide this kind of tiling—a triangle of any shape or any four sided figure will also fill in a plane.

The three-dimensional analog, or resemblance, to a regular polygon is a regular solid. Before we proceed we will add a few definitions so that we don’t get lost in the terminology. A **polyhedron** is a figure or solid

formed by many plane faces. Polyhedrons are named in accordance with the number of plane faces they have. Therefore, polyhedrons of four, five, six, etc., faces are called tetrahedron, pentahedron, hexahedron, etc., respectively.

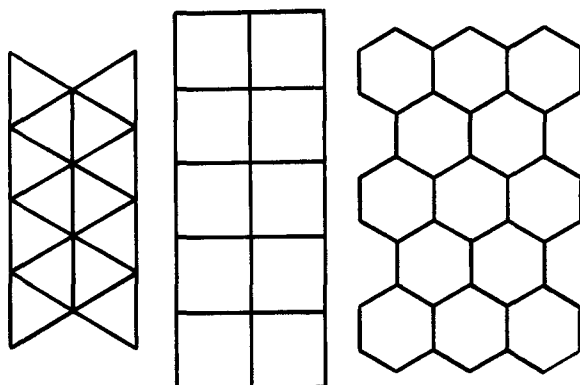


Figure 4-1. The triangle, the square, and the hexagon are the only regular polygons that will fill a plane completely.

If all the faces of a polyhedron are congruent (identical), the solid is called a **regular solid** or **regular polyhedron**. There are only five regular solids possible as shown in Figure 4-2.



Figure 4-2.

The Egyptians discovered the first three regular solids: the **regular tetrahedron**, which has four faces, each face an equilateral triangle, with three faces touching at each vertex; the **regular hexahedron** or **cube**, which has six faces, each face a square, with three faces at each vertex; and the **regular octahedron**, which has eight faces, each one an equilateral triangle, with four faces at each vertex. The Pythagoreans discovered the other two: the **regular dodecahedron**, which has twelve faces, each a regular pentagon, with three faces at each vertex; and the **regular icosahedron**, which has twenty faces, each an equilateral triangle, with five faces at each vertex.

A pattern for making each of the five solids may be formed of cardboard by drawing and cutting out the figures shown by solid lines in Figure 4-3. All you have to do is fold along the dotted lines and tape the free edges together.

Later on we will be looking at the angular relationships between highs and lows on the polar stereographic map. To cast some light on

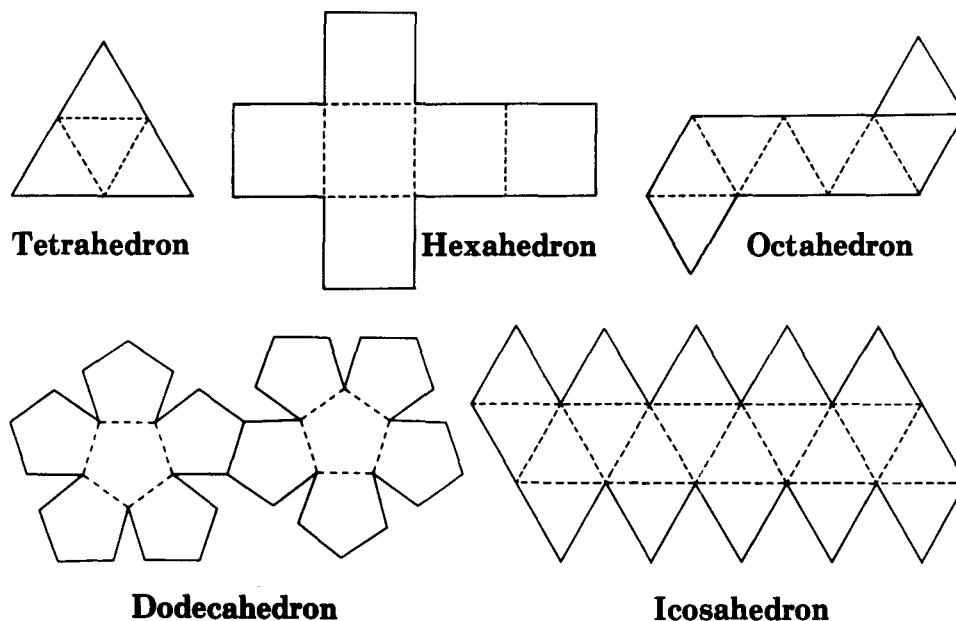


Figure 4-3.

why these relationships exist, we will take a closer look at the regular solids and see why only five are possible. First, we must prove that the sum of the face angles that meet at a vertex of a polyhedron *must always* be less than 360° . To understand why this is so, take a flat piece of paper (crumpled paper doesn't work very well) and mark a point in approximately the center of the paper. Label this point P. Now draw 7 lines of equal radius out from point P; join the ends as shown in Figure 4-4a. You will end up with a group of 7 angles adding up to 360° . Now cut out this 7 sided figure (septagon) and crease along each line. Try to form a polygon by folding along the creases. You'll find that you can't make polyhedral angles whose edges are along the creases. The angles will not fold out of the plane of the paper unless the paper kinks. Now cut out one of the angles, for example, the one whose sides are PA and PG in Figure 4-4b; then bring PA and PG together and tape it to make a polyhedral angle. This shows that the sum of the face angles of a poly-

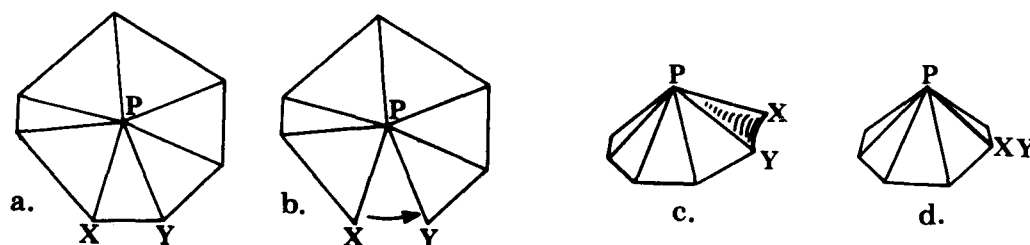


Figure 4-4. See the text for the explanation.

hedral angle must always be less than 360° . To turn a flat piece of paper into a three-dimensional structure, you must always remove a triangular dart. Remember that a flat piece of paper has thickness, and so you are not really cutting out just a flat triangle, but actually a polyhedron.

For a polyhedral or three-dimensional angle to exist, there has to be three or more faces meeting at a vertex. The regular polygon with the least number of sides is the equilateral triangle where every angle is 60° . Only three different polyhedral angles can be formed with only equilateral triangles meeting at the vertex. The first is the **tetrahedron** with three equilateral triangles at each vertex (Figure 4-2a), this give 3 times 60° or 180° around each vertex. The second is the **octahedron** with four equilateral triangles (Figure 4-2c), which gives 4 times 60° or 240° around each vertex. The third and last possible one is the **icosa-hedron** with five equilateral triangles (Figure 4-2e), which gives 5 times 60° or 300° around each vertex.

Each angle of a square has 90° . A cube consists of six squares, where there are three squares at each vertex. Therefore you have a polyhedral angle at each vertex equalling 270° . If you had four squares at each vertex, you would end up with 360° , in other words, a plane, and not a solid.

Each angle of a **regular pentagon** (a 5 sided figure) has 108° . A **dodecahedron** consists of 12 regular pentagons where there are 3 regular pentagons at each vertex. Therefore, you have a polyhedral angle at each vertex equalling 324° .

Each angle of a **regular hexagon** (a 6 sided figure) has 120° . Three such angles would add up to 360° , in other words, a plane. Therefore, a polyhedral angle can not be formed from regular hexagons—so, no regular polyhedron can be formed with hexagons.

The closer the sum of the angles around a vertex add up to 360° (for any polyhedron, regular or otherwise), the closer we come to having a flat surface, which is shown in Figure 4-5. The pointiest regular solid is the tetrahedron with 180° at each vertex; on the other hand, the flattest regular solid is the dodecahedron with 324° at each vertex.



Figure 4-5. The sum of the angles around the vertex at **a.** = 360° (a plane); at **b.** = 300° ; at **c.** = 240° ; at **d.** = 180° .

There appears to be a contradiction here. The sum of the angles around any vertex of a polygon is less than 360° , yet you can stand on the vertex and spin around a complete 360° . This seeming paradox can be resolved relatively easily if you consider a flat plane touching the vertex point. The plane should be perpendicular to the most symmetric axis that passes through the vertex. Now project all the edges of the polygon up into the plane. Imagine yourself standing at the vertex in the plane and looking down on the tetrahedron, you will see the 60° faces sloping down. When you look at the projected edges on the plane, you will note that each of the 3 angles is 120° , not 60° as on the polygon. See Figure 4-6.

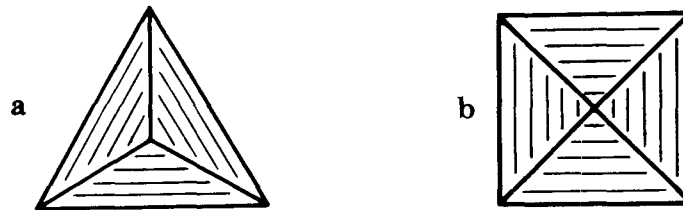


Figure 4-6.

a. The angles at the vertex of a tetrahedron are actually 60° , but they project onto a plane as 120° . Since it is difficult to insert a real tetrahedron on this page, we must do with a flat projection which is drawn showing the angles of 120° . The shading on the drawing is what saves the day by indicating that we are looking at a perspective drawing of a tetrahedron.

b. The angles around the vertex of an octagon are also actually 60° , but project as angles of 90° in a plane.

You might ask, "What does all this have to do with the sphere of the Earth?" Well, the Earth is also a polyhedron, but a round one. The surface of a sphere can be considered as consisting of a *very large* number of vertexes; all joined to each other by straight lines or chords. If you stood at one of the vertexes and looked down, you would find the sum of the angles total to something slightly less than 360° . That the Earth is a polyhedron with an immense number of vertexes is not as strange as it may seem at first, since the Earth, in reality, consists of an immense number of electrons and protons at the atomic level with all of them separated by finite distances.

As a practical matter, let us consider a cluster of actual high and low pressure centers on the surface of the Earth which are separated by great or small distances. Every one of these highs and lows could be joined by straight lines or chords which would represent the chordal distance between their centers. These chords represent the shortest

distance, in absolute space, between two points and actually pass below the surface of the Earth. If you were at the center of one of these highs or lows, you would know that the sum of the angles around that vertex or center would be less than 360° .

This complication can be approached in two different ways. First, these highs and lows are drawn on a flat paper map. Then the chords between the highs and lows are projected onto the flat map. And so the sum of the angles around each high and low on the map now adds up to exactly 360° . The advantage of using a flat map of a round world is that it becomes possible to use straight lines in making certain types of calculations dealing with the surface of the Earth, or for that matter any other sphere. Anytime that you can use straight lines to show relationships on a sphere, you have gained a great simplification in the type of mathematics required. Secondly, the centers of highs and lows surrounding a given high or low could be joined by arcs drawn on the surface of the Earth. Any high or low could be considered as a pole with lines of longitude radiating outwards. Therefore, the sum of the angles around a vertex, using arc curves will add up to exactly 360° (in the same way that the longitude lines add up to 360° around the North Pole).

Let us explore some more of the conditions on the surface of a sphere that are not necessarily obvious. We will analyze the matter of **dimensions or degrees of freedom**. A point inside a cube can move in three mutually perpendicular independent directions (three degrees of freedom) at any given moment. Therefore, space inside a cube is three-dimensional. But a point confined to the *surface* of a cube can move in only two degrees of freedom at any given moment. Likewise, the space inside a sphere is three-dimensional, while the surface of a sphere, even though it is not flat, is two-dimensional (only two degrees of freedom for a moving point at any given moment). On the surface of the Earth, these two degrees of freedom are described by latitude and longitude (which are curved arcs). The fact that the Earth is not a perfect sphere and that it has bumps on it such as mountains does not alter the fact that there can be only two degrees of freedom on a surface.

A tetrahedron can be placed inside a sphere so that all 4 vertexes will lie on the surface of the sphere. The same thing can be done with the 4 remaining regular solids, and of course each vertex will lie on the surface of the sphere. Note that a line joining any two adjacent

vertexes in a regular solid is always an edge of that solid. And so each edge of the regular solid that is inside the sphere becomes a chord of that sphere, since each vertex touches the surface of the sphere.

Let us now project the edges or chords of these regular solids onto the surface of the sphere by using the center of the sphere as the point of projection; this is shown in Figure 4-7. This procedure generates the spherical tetrahedron which is known as the **tetrahedral**; the spherical hexahedron, known as the **hexahedral**; the spherical octahedron, known as an **octahedral**; the spherical icosahedron, known as an **icosahedral**; and last but not least, the spherical dodecahedron, which is known as a **dodecahedron**. The corner angles or polyhedrals in these spherical polyhedrons are much larger than their flat faced friends due to their spherical excess.

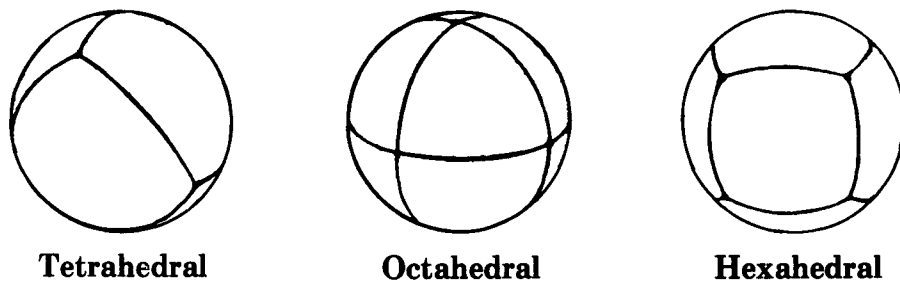


Figure 4-7.

All five of the regular polyhedrons plus some more complicated ones appear in various forms of life. Some examples are shown in Figure 4-8 and 4-9 that were mainly taken from *Art Forms in Nature*, by *Ernst Haeckel* (2).

Likewise, there are a huge variety of crystal forms of inorganic or non-living matter that take the shape of three of the regular polyhedrons (tetrahedron, hexahedron, and the octahedron). The icosahedron and the dodecahedron do not occur in crystal form. It has been proven mathematically that these two forms can not occur due to the fact that crystals are built up from individual particles (atoms) or *quantum units* that can not be further subdivided in a crystal form. You would need some fractional parts of atoms to build an icosahedron or dodecahedron.

Space Filling Patterns on a Two-Dimensional Surface

We will now take a more detailed look at space-filling patterns, regular and irregular. These types of patterns have been called tiles,

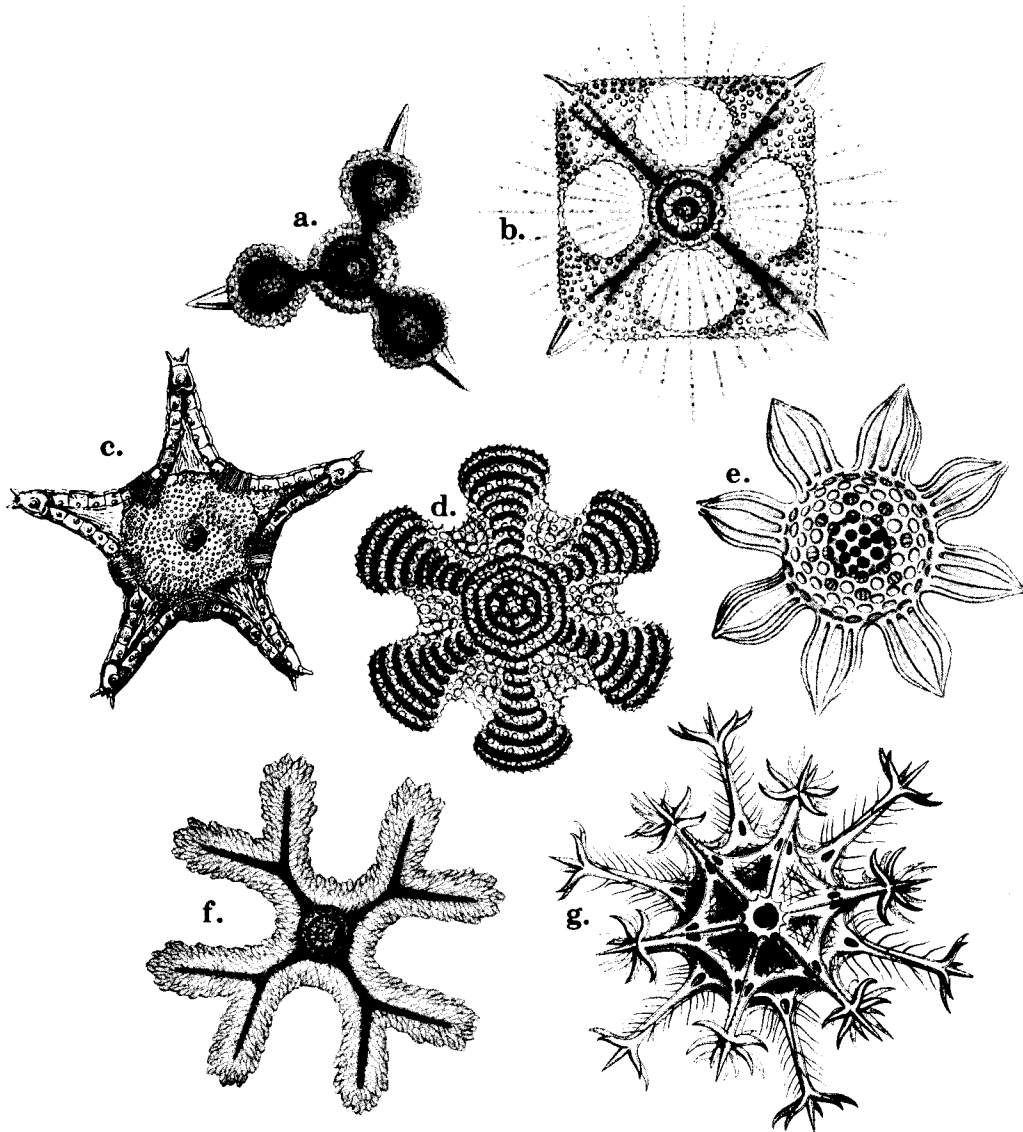


Figure 4-8. Various species of *Radiolaria* (a type of marine Protozoa, except for c., which is a *Blue China Starfish*): a. Triangular (3); b. Square (4); c. Pentagonal (5); d. Hexagonal (6); e. Octagonal (8); f. Octagonal (8); g. Dodecagonal (12).

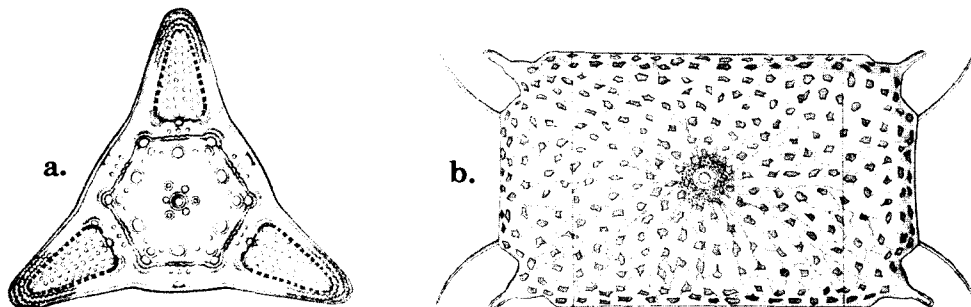


Figure 4-9. Various species of *diatoms* (a type of unicellular plant). a. Triangular with internal hexagons. b. Rectangular.

lattices, and tessellations. **Regular tessellations** (the ones discovered by the Pythagoreans) are those configurations made of regular polygons of one kind only. These are the patterns of squares, triangles, and hexagons that we have pictured in **Figure 4-1**. In **semi-regular tessellations**, the pattern is the same at every vertex, but more than one type of polygon appears in each configuration. It has been proven that there are only 8 of these types possible; these are shown in **Figure 4-10**. Thus, in 4-10a, there are 2 triangles and 2 hexagons at each vertex; in 4-10b, there are 4 triangles and 1 hexagon at each vertex; etc. In **demi-regular tessellations**, we still use regular polygons, but the pattern in which they are used is different for different vertexes. It has been proven that there are only 14 demi-regular configurations possible. They are shown in **Figure 4-11**.

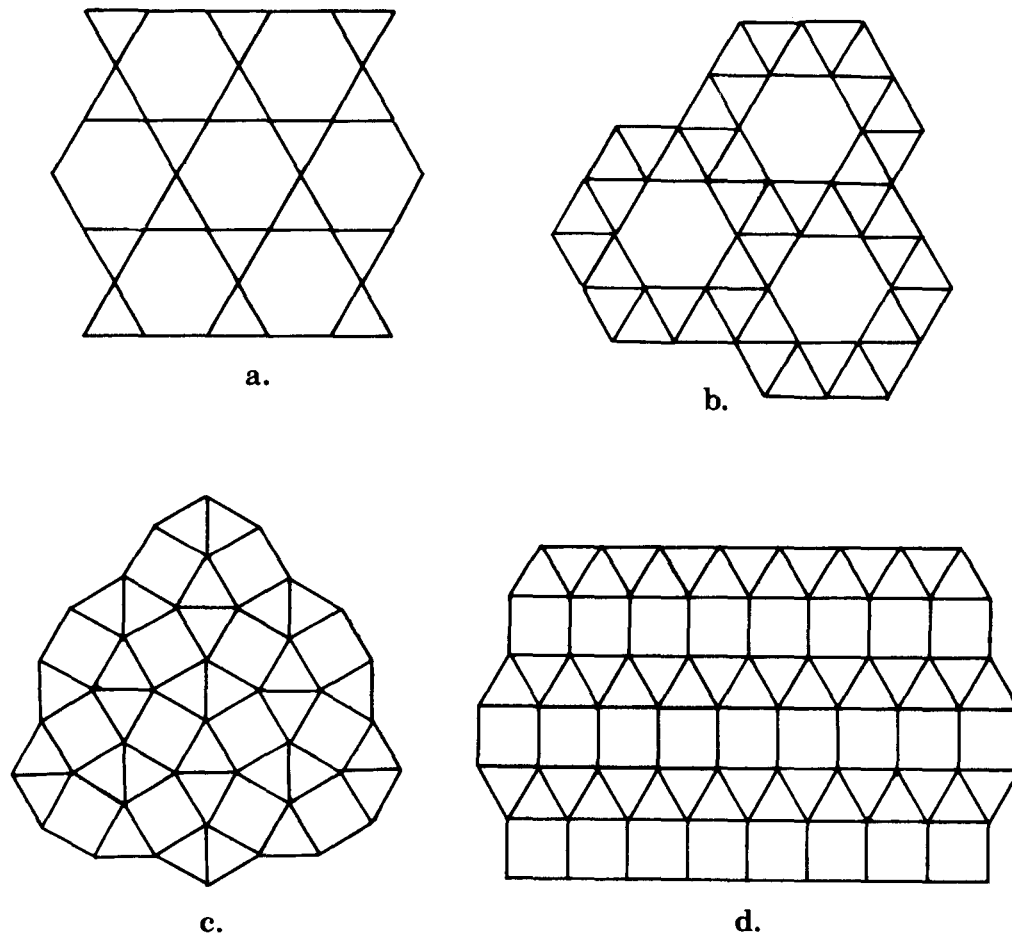
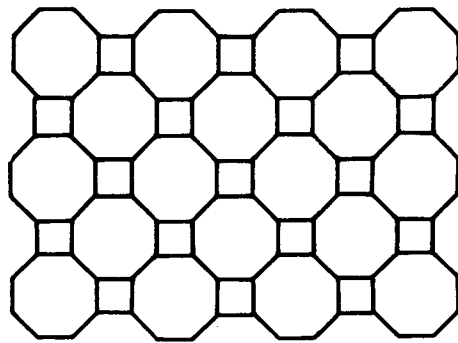
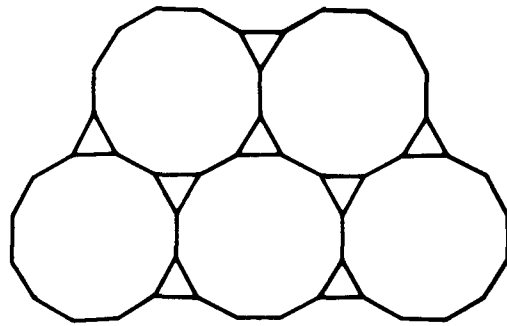


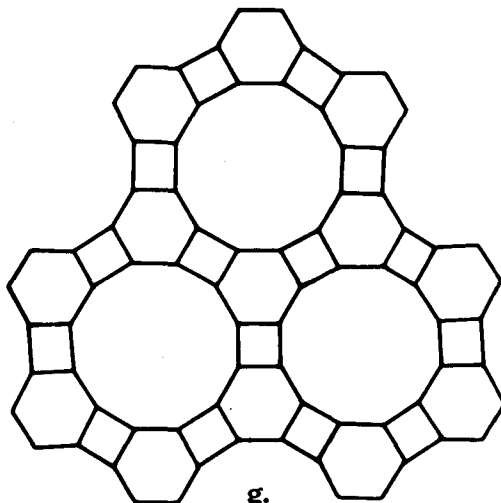
Figure 4-10. There are only 8 semi-regular patterns possible.



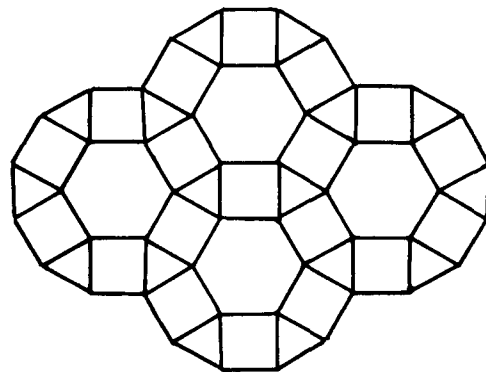
e.



f.



g.



h.

Figure 4-10. Continued.

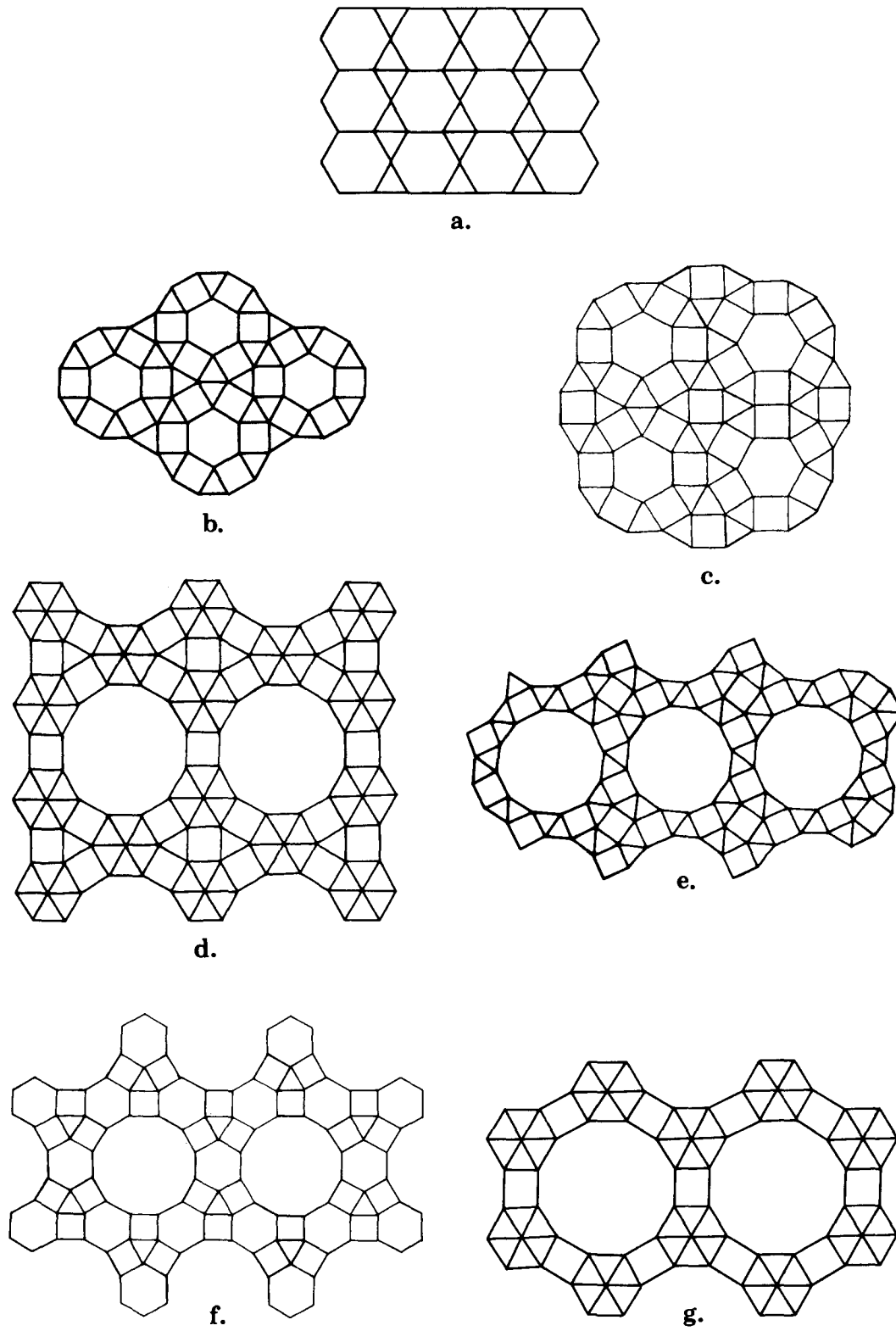


Figure 4-11. There are only 14 demi-regular patterns possible.

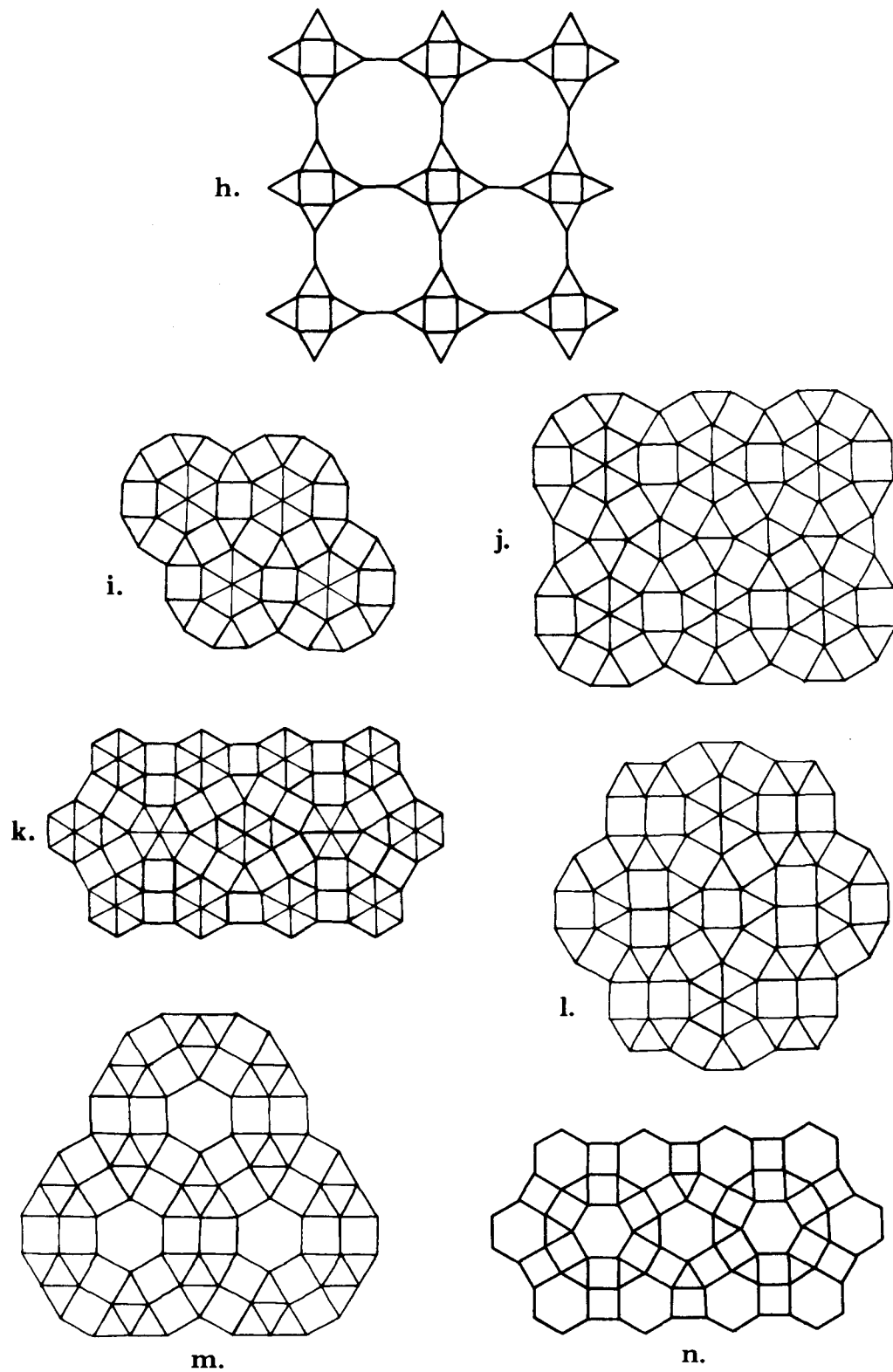


Figure 4-11. Continued.

It is also possible for the vertexes of some polygons to lie on the sides of other polygons to form other tessellations which can be seen in Figure 4-12.

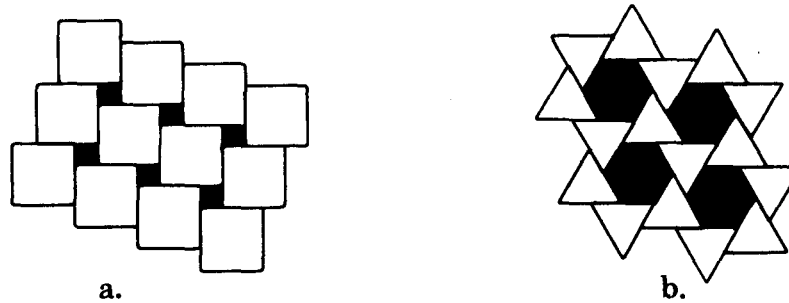


Figure 4-12. Vertexes of these polygons lie on the sides of other polygons.

There are some additional figures that can fill a plane with no gaps or overlaps when they undergo parallel translations. These are the **parallelogons**. They are squares or regular hexagons or configurations that are derived from them by elongations or compressions. See Figure 4-13.

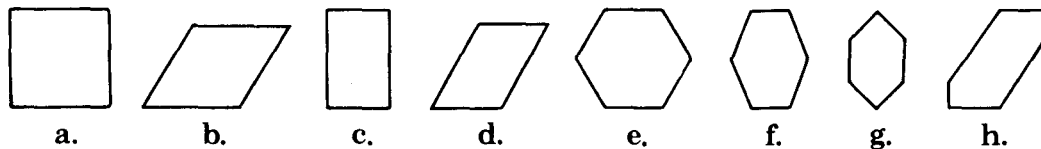


Figure 4-13. Parallelogons: **a.** Square; **b.** Square compressed along one diagonal and elongated along the other; **c.** Square compressed along one side; **d.** Square compressed along one side and then elongated along the diagonals; **e.** Hexagon; **f.** Hexagon elongated along the line bisecting opposite sides; **g.** Hexagon elongated along the line bisecting opposite angles; **h.** Oblique hexagon.

Figure 4-14 is a more detailed version of **Figure 4-13**. Lines of symmetry divide each shape (in **figure 4-14**) into parts which are similar to one another. There are four kinds of lines of symmetry:

1. Lines which join the two middle points of opposite sides.
2. Diagonals that join two opposite vertexes.
3. Lines which join one vertex to the middle point of the opposite side.
4. Odd lines that split the shape into two symmetric parts.

We can draw similar irregular patterns on a surface weather map if we replace all the high and low centers with points and join the points with straight lines.

Organization in Space

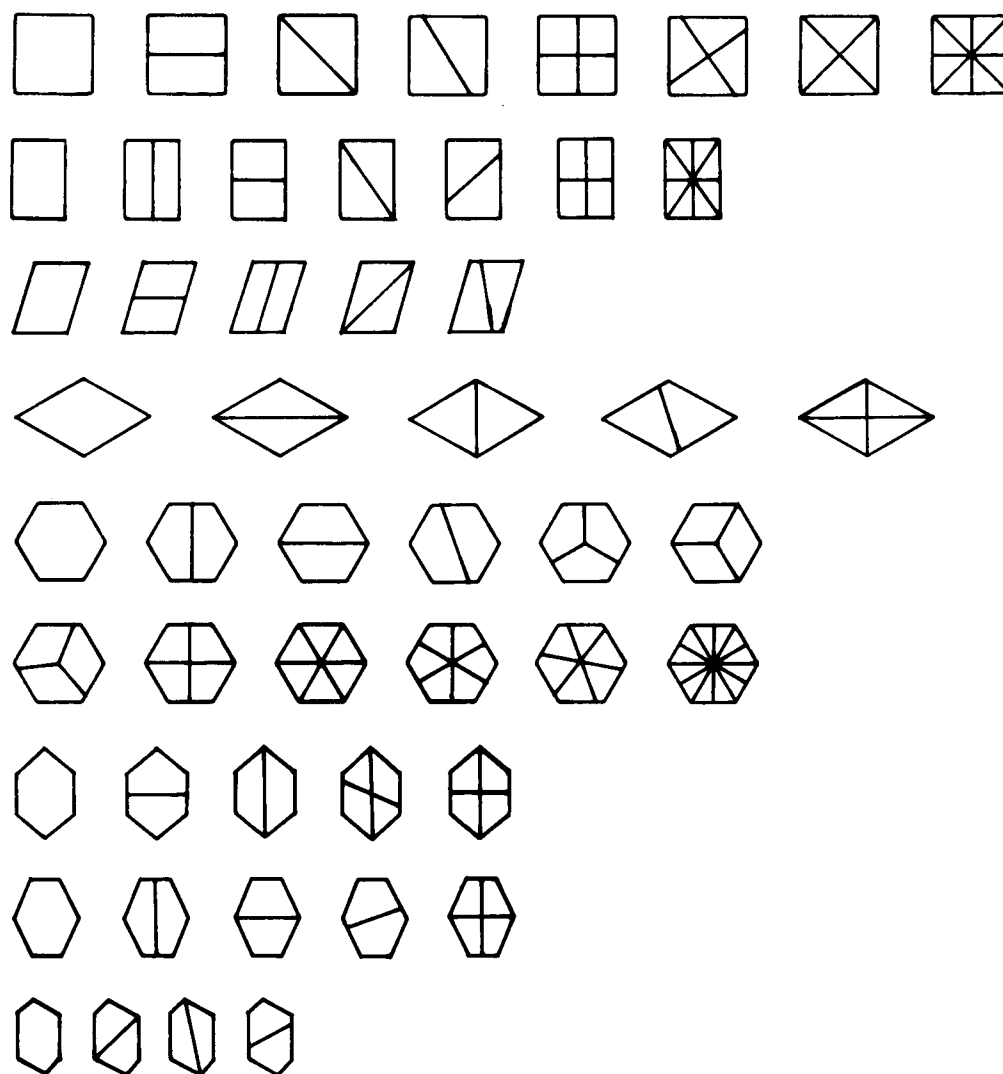


Figure 4-14. Some differing combinations possible with a square and hexagon, subject to compression or elongation. The lines that are drawn inside these figures represent lines of symmetry or reflection.

Principles of Closest Packing of Spheres

The investigations of filling space in a plane with geometric figures eventually led to the investigation of the closest packing of spherical objects in three-dimensions. Understanding the principles of closest packing of spheres led to immense discoveries in many fields of science. In nuclear science it led to a detailed explanation of how the electrons and protons are packed in all the elements of the periodic table. In the field of biology, it led to a better understanding of how cells are related to each other; why various forms of life assume their shapes and forms;

why the honeycomb of a bee is made of hexagonal cells; etc. In physics and chemistry, it has led to an insight into the structure of soap bubbles; foaming of chemicals; etc. There has yet to be a peep on this subject in the field of weather analysis and forecasting. Dear reader, let us now rectify this situation and bring (drag if necessary) meteorology out of the dark ages and into the stream of modern science.

We will now focus on the two-dimensional aspect of closest packing of spheres, since the *spacing* of highs and lows over the surface of the Earth is a two-dimensional phenomenon. We will also study some of the aspects of three-dimensional packing to aid us in the evaluation of the two-dimensional variety of closest packing of spheres.

Spheres of the same size can be piled and packed together in many different ways. If we arrange the spheres or circles in a triangular formation, the number of circles involved will be a triangular number. If we make a square formation, the number of circles will amount to a square number. See Figure 4-15.

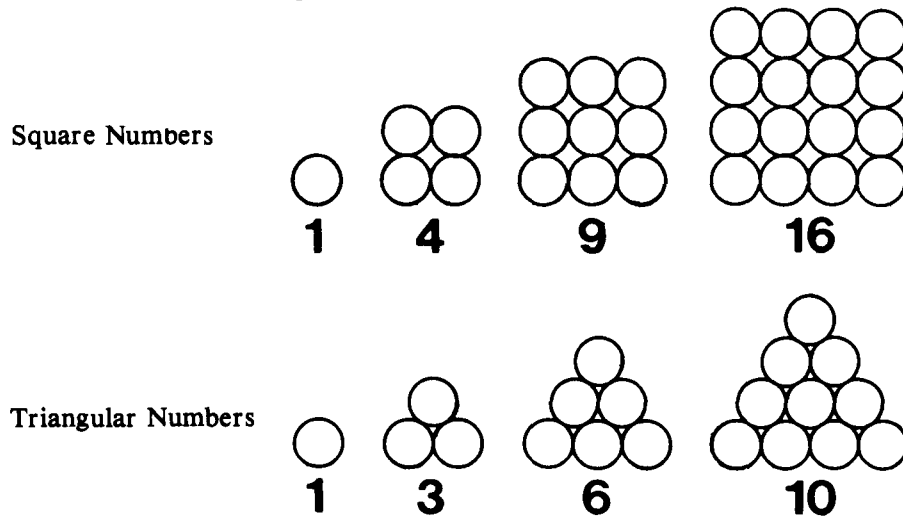


Figure 4-15.

The Pythagoreans were the first to link numbers and shape. They reasoned that the numbers 1, 3, 6, 10, etc., (gotten by taking the sums of 1, $1+2$, $1+2+3$, $1+2+3+4$, etc.), are **triangular numbers**; while the numbers 1, 4, 9, 16, etc. (gotten by taking the products of 1×1 , 2×2 , 3×3 , 4×4 , etc.), are **square numbers**. These are the simplest examples of what the “old timers” called **figurate numbers**. A famous book was written by *Blaise Pascal*, explaining figurate numbers, and although little attention is given them today, they still provide intuitive insights

into many aspects of elementary number theory and geometry. In the measurement of lengths, areas, or volumes, numbers are intimately related to space. In this manner, we find that geometry, which is a study of space, is fused with arithmetic and algebra, which are the study of numbers. We usually think of numbers as being lined up in a straight line with numbers related to each other by a simple relationship such as: *larger than* or *smaller than*. Here we consider numbers as two-dimensional (or three-dimensional when appropriate) entities with each number acting as a part of a geometric structure. In a geometric sense, all vortexes or other points of interest on a weather map could be considered as a structure of geometric numbers. Figure 4-16 shows an

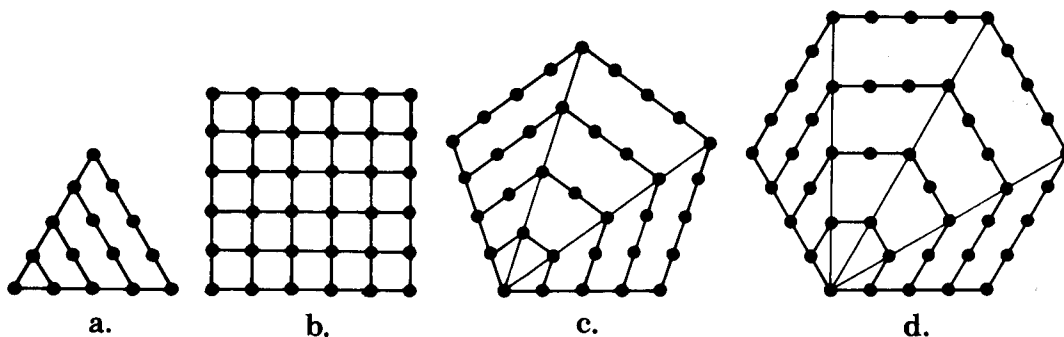


Figure 4-16. Geometric structures built up from points.

arrangement of polygonal arrays of points having 1, 2, or any number of points radiating out from the lower left hand corner. We can count the points in the pentagon of Figure 4-16c, in a similar manner as was done in Figure 4-15, to make the pentagonal series of 1, 5, 12, 22, 35, etc., points. Likewise, in Figure 4-16d we have the hexagonal series of 1, 6, 15, 28, 45, etc., points. We have been using the terms, points and circles (and spheres also), interchangeably, and it should not be confusing if we consider a point as a very small circle.

The figurate numbers are related to each other in various ways. For example, Figure 4-17 shows the fundamental connection of the square with triangular figurate numbers. Figure 4-18 shows the figurate series when the starting number is a nuclear sphere in the center

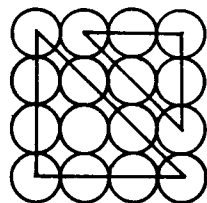


Figure 4-17. A square can be constructed from two triangles.

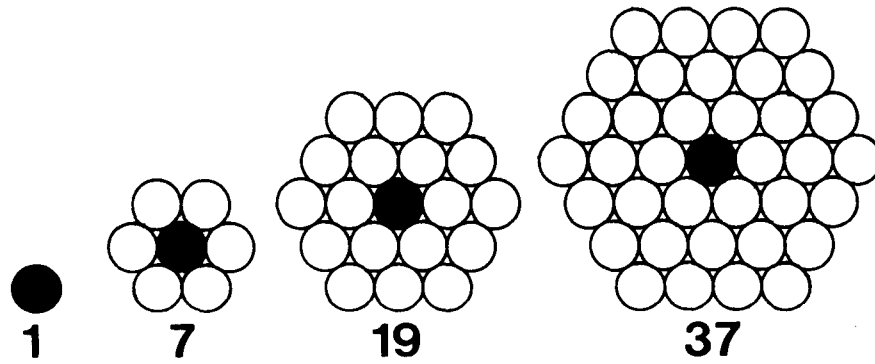


Figure 4-18. Figurate hexagon numbers built around a nuclear sphere.

instead of a corner as in **Figure 4-16**. In this case the series runs 1, 7, 19, 37, etc.

We will now explore another feature of space-filling that was first recognized by *Leonhard Euler* (1707-1783) (3)—that no system of hexagons can *enclose* space no matter if the hexagons are equal or unequal, regular or irregular. Euler showed that a pattern of hexagons may be extended as far as desired over a plane or curved surface as long as it never closes in. On the other hand, 5 hexagons can be arranged around a nuclear pentagon, on the surface of a sphere. An example taken from real life, shown in **Figure 4-19**, where we see a pentagon (which I have shaded) surrounded by hexagons.

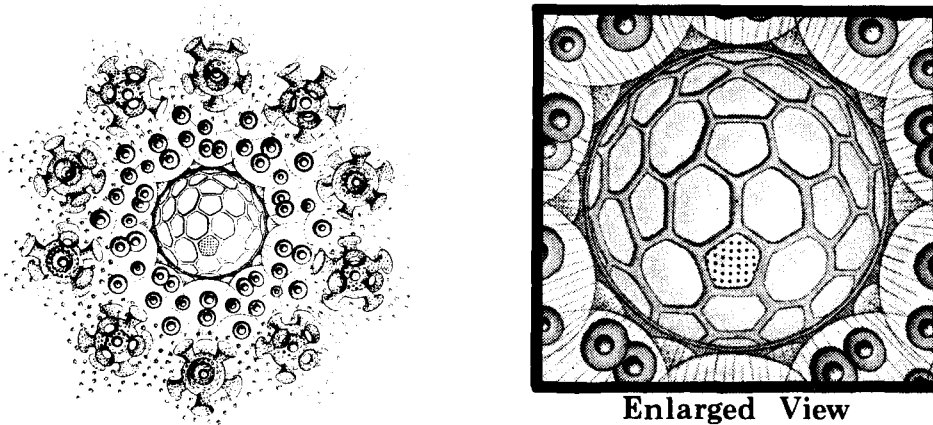


Figure 4-19. *Radiolaria* (a marine Protozoa). We can see a pentagon (indicated by the shading) surrounded by 5 hexagons in the nucleus of this little beast.

Examples and Experiments in Closest Packing of Spheres

We start with four spheres that can come in contact with each other in one of two ways: either as a square formation (**Figure 4-20a**) or as a

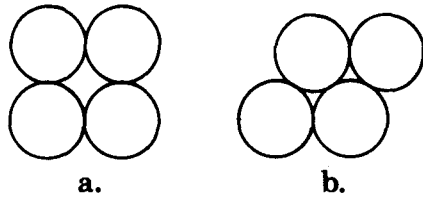


Figure 4-20. The square formation **a.** is unstable. The nested formation **b.** is stable.

nested formation (**Figure 4-20b**). The square formation is unstable and tends to slide into the nested pattern which is the stable one. In embryology, it has been found that a segmenting egg, with 4 or more segments, will take a shape, where only 3 cells are in contact at a vertex—which is the nesting position. The 3 cells meet at angles of 120° . In the example of **Figure 4-21**, we see that an individual cell

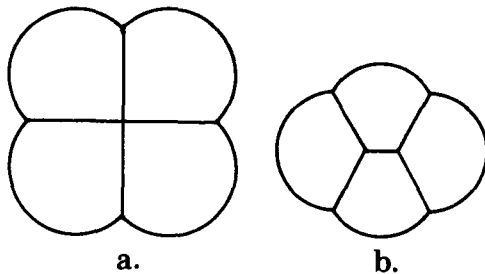


Figure 4-21.

- a.** This arrangement of cells is unstable.
- b.** This is the normal, stable pattern with a polar furrow.

(made of soft material) that would be spherical by itself, forms a flat line of contact with an adjoining spherical cell that presses against it. Conklin (4) in 1897 called the line which joins the two vertexes of triple contact, the **polar furrow**. We see a similar geometric pattern on the skeleton of the *Dictyocha stapedia* in **Figure 4-22**.

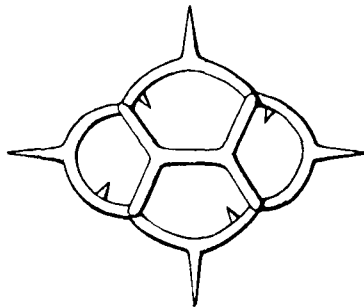


Figure 4-22. A close up view of part of the skeleton of *Dictyocha stapedia*.

In 1727, *Stephen Hales*, an English physiologist wrote about an experiment where he poured peas into a pot to find the closest packing arrangement possible using equal sized spherical objects. The experiment has been repeated many times since in many different forms. The two-dimensional view for closest packing of equal sized spheres is shown in **Figure 4-23**, where we start with a sphere in the center. It is a simple geometrical fact that each of the equal sized circles

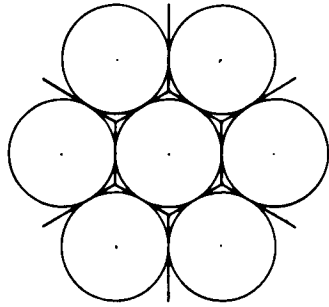


Figure 4-23. Circular shapes can change into hexagonal shapes when subjected to internal and external forces.

is in contact with six others around it. Each circle has 6 points of contact with 6 other circles. Imagine if you will, that a whole system of circular bodies are under a uniform stress of pressure by growth or expansion inside the cellular circles. The 6 points of contact will now become 6 lines of contact between the circles. The equal circular bodies will be converted into equal hexagons, where the angles at the vertexes are 120° .

This hexagonal symmetry of close packing is everywhere you turn. Bees use this method for packing their honey in hexagonal bee cells to form the honeycomb. Each bee busily fills up its cell until the sides of its domain squeeze up against the cells of the 6 other bees surrounding it. See **Figure 4-24**. In the third century, *Pappus* noted that by building hexagonal cells in their honeycombs, the bees made a structure that stores the maximum amount of honey with the minimum use of wax.

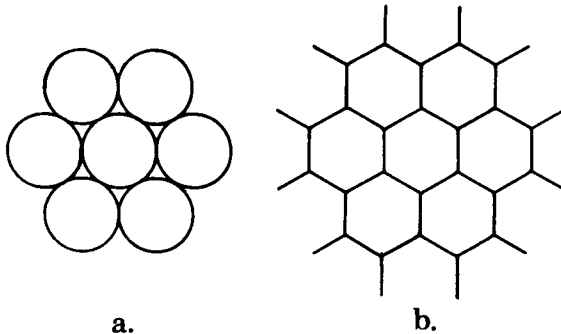


Figure 4-24. The circles in **a.** become honeycomb patterns in **b.** when they press against each other.

Similarly, *Stéphane Leduc* (5) conducted diffusion experiments with different chemicals and liquids to form “artificial tissues” of hexagonal shape, as shown in **Figure 4-25**. All biologists know that these patterns simulate the patterns in organic living tissues. As is well known, these hexagonal patterns also form in various combinations in snow flakes. So now we find these 120° equilateral angles of hexagons in both inorganic and organic arrangements of matter in space.

Another example can be shown with soap bubbles. The solid with the

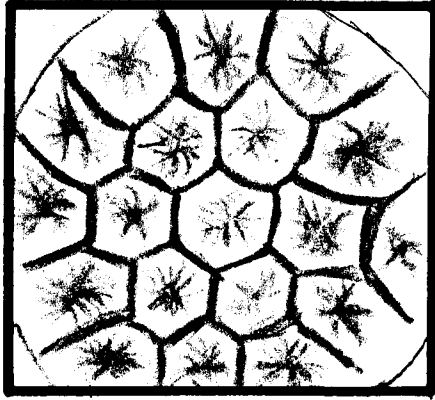


Figure 4-25. *Leduc* created an "artificial tissue" by letting colored drops of common salt solution diffuse into a less dense solution of the same salt.

greatest volume for a given surface area is the sphere. The soap bubble encloses a fixed amount of air which is forced by the tension in the soap film to take the shape that redistributes the enclosed air so that the outside surface of the bubble is as small as possible. This makes the bubble as close as possible to a sphere. Bubbles also collect in the manner of closest packed spheres. Only the outer surface of the outermost bubbles in a cluster of foam retains the spherical surface. Inside a bubble cluster, all the bubble pressures become approximately equal; the points of contact of the individual soap bubbles become lines or plane surfaces of contact to form the familiar hexagonal shapes. See **Figure 4-26**.

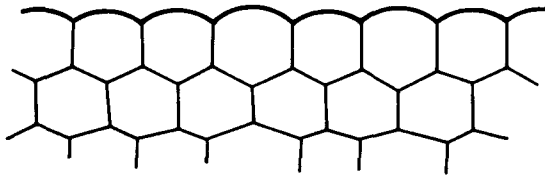


Figure 4-26. A foam with the outer surface of the outer cells rounded, while the inner cell surfaces of contact are flat. This is similar in appearance to the outer layer or epidermis of living skin.

In 1900, *H. Bénard* (6) reported on his experiments with cellular vortexes in a thin layer of liquid, warmed in a copper dish. Little vortexes or cells were formed as he heated the liquid. Whether he started with the liquid in motion or at rest, the geometric patterns formed, would ultimately become uniform and symmetrical. Before a condition of equilibrium was reached, he found mainly hexagonal formations, but 4, 5, or 7 sided cells were also present. The larger cells would tend to grow smaller, while the smaller ones would grow larger or disappear. When 4 cells met in a single corner, they would shift until only 3 cells met in the corner as required for the nesting formation. The sides of the cells would eventually adjust themselves to equal lengths and all the angles would become equal. Lastly all the cells would end up

with a fixed or *quanta* hexagonal size.

The experiment by Bénard was actually preceded by *E. Weber* (7) and has since been demonstrated many times in the laboratory. Weber showed that when a layer of metallic paint mixed with solvent is placed in a dish and allowed to evaporate, a regular pattern of convective motion will start. This is caused by the cooling of the liquid on the top surface by the evaporation of the solvent. This convection causes hexagonal shapes to form when a steady state is reached, as is shown in **Figure 4-27**. The diameter of the hexagonal cells is approximately 3 times their depth; varying the depth of the liquid will vary the diameter of the hexagons.

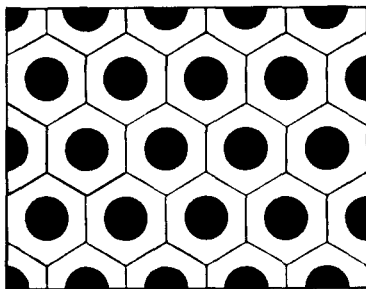


Figure 4-27. An artists conception of hexagonal cells formed in a liquid with regular convection occurring. The white area represents downward motion, while the black area indicates upward motion.

Angles of the Hexagon

It is obvious from all of the preceding information that the hexagon is spread throughout the Universe. Let us take another look at a few of the simple mathematical features of the hexagon. **Figure 4-28a** shows three equal hexagons meeting at point H. We would suspect the presence of hexagonal formations wherever 120° angles occur in any natural phenomenon. **Figure 4-28b** shows that a hexagon is really constructed of 6 equilateral triangles and that a circle can be circumscribed around a hexagon. Any radius, OA, OB, etc., is equal to the length of any chord, such as AB, BC, etc. The circumference of the circle is exactly divided into 6 parts by the 6 chords. All the angles in an equilateral triangle are 60° ; therefore, it should be no surprise to see 60° angles occurring in any natural phenomenon that is infested with hexagons.

Euler said that all geometric patterns consist of three fundamental elements: lines (or trajectories), vertexes (or crossings), and areas (or openings). The triangle is the polygon with the minimum of sides that can enclose an area; which makes it the the fundamental *quanta* or

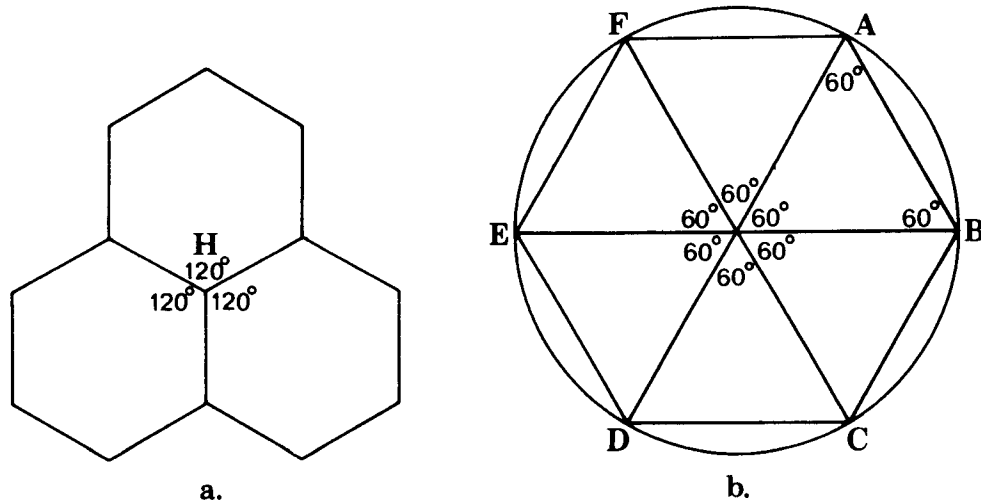


Figure 4-28.

- a. Three hexagons meeting at point H.
- b. A regular hexagon consists of 6 equilateral triangles with any radius equal to any chord of the circle that can be drawn around it.

building block for enclosing area. Even a square is built up by adding two triangles. With energy being injected into a system, as in Bénard's experiment, we find that the average probability is a network of equilateral triangles that cluster in the form of hexagons.

In closing this chapter, it is not unreasonable to say that there is a large amount of statistical evidence (from other fields of science) that indicates there should be some types of similar geometric "weather beasts" in weather patterns.

Chapter 5

Organized Patterns of Movement in Space

General

Everywhere we look, we find an orderly arrangement of matter in the Universe, whether on the atomic level, or that of the galaxies; whether living organic life, or inanimate dead substances. With so many examples all around us in every arena of the Universe, it should seem preposterous that no orderly weather patterns have been found to date. You might ask, "What are the neat patterns in weather?" I asked that question, and began to explore some well known orderly patterns of moving bodies in other fields of science. First, I must say that I discovered the organization in weather systems by using empirical methods—if it works, use it, even if you don't understand why. After that discovery, I began to search for the theoretical foundation of my discoveries. The purpose of this chapter is to show some of the paths by which the theoretical explanations were tracked down.

The examples I use from other areas of science are only a small sampling of the myriad of similar types of examples that can be selected from the whole Universe. My discussion of some of these scientific features is not complete or exhaustive. The examples were chosen merely to illuminate certain well-known and established laws of nature. These general laws of nature also serve as a *statistical* proof of the rules I use for weather patterns. Before we proceed with the examples, it is important to mention the *principle of similitude*.

The Principle of Similitude

The growth, decay, and shape of any structure is determined by the forces acting upon it. The impact of certain forces may be determined by the area of the structure. For example, the wind will push a large

sail on a sailboat with greater force than a small sail. The impact of other forces may be determined by the volume of the structure. An object (made of the same material) floating in the water will have greater buoyancy, the larger it is. In this example, the volume of the structure is the determining factor. We find that in similar figures, the surface increases as the square, and the volume increases as the cube, of the linear dimensions. In the case of the sphere with a radius r , the area in the plane of a great circle is πr^2 ; the area of the surface of the sphere is $4\pi r^2$; and its volume is $4/3\pi r^3$. If the radius of the sphere is doubled, the area of the circle becomes 4 times as large; the surface of the sphere becomes 4 times as large; and the volume becomes 8 times as large. Since volume is closely related to mass or weight, we find that a fish that is doubled in length will weigh 8 times as much.

It was *Galileo* who first described what is known as the **principle of similitude**. He said that some of the forces acting in a system vary with the length, mass, and other factors; other forces vary with the square of these quantities; and still others as the 3rd power of the quantities involved. He also said that if we tried to build ships, palaces, or temples of huge size, that beams and bolts would refuse to hold together; and that a tree or an animal can not grow beyond a certain size and still keep the same shape. They would fall to pieces of their own weight unless: (1) the relative proportions of their parts are changed (which would eventually make them clumsy or inefficient), or (2) they would have to be made of harder and stronger materials.

This principle is mentioned so that we can properly judge phenomena that vary or have a reason to vary when going from a small to a large size. We will now lightly touch on some astronomical and atomic laws that are well known; and then we will try to grasp those features that persist regardless of size to see if the same laws can be applied to the analysis of weather systems.

Kepler's Laws

We start with *Johannes Kepler* (1571-1630) who discovered the three great laws of planetary motion: (1) The orbit of every planet is an ellipse with the Sun at one focus; this defines the shape of the orbit. (2) The straight line joining a planet and the Sun sweeps over equal areas during equal times. Therefore, the speed of a planet increases and decreases as it makes a complete circuit around the Sun. This law is

a consequence of the conservation of angular momentum. See **Figure 5-1**. Finally, (3) the squares of the period of revolution of the planets are proportional to the cubes of their respective mean distances from the Sun. The period is the time required for a planet to complete a round trip on its elliptical pattern. This is often called the **Harmonic Law**.

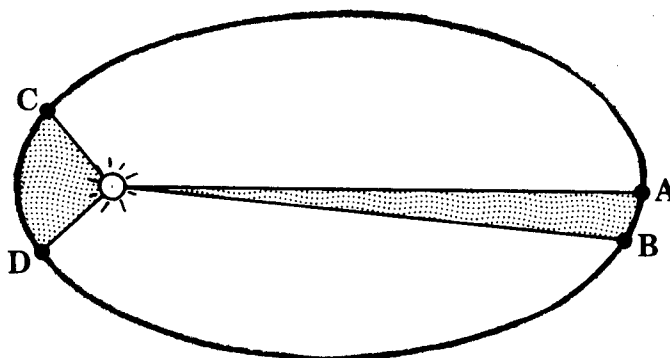


Figure 5-1. According to Kepler's Law of equal areas, it takes a planet the same time to move from C to D, as it does from A to B, since the shaded areas are equal.

Wolf's Law

It has been known for a long time that the distance between the sun and its planets seemed to follow a regular pattern. When these distances are compared, they more or less follow a *law* which was first discovered by *Wolf* in 1741, this was picked up by *Titius* in 1772, and finally popularized by *Bode* in 1778. This law of Wolf (called Bode's Law by some) goes as follows:

Establish the series of numbers beginning with 0, 3, 6, 12, 24, . . . ; where each number is double the value of the number that preceeds it. You will have the following series:

$$\begin{array}{cccccccc} 0 & 3 & 6 & 12 & 24 & 48 & 96 & 192 \\ 0 & 2^0 \times 3 & 2^1 \times 3 & 2^2 \times 3 & 2^3 \times 3 & 2^4 \times 3 & 2^5 \times 3 & 2^6 \times 3 \end{array}$$

If you now add 4 to each of these numbers, you get:

$$4, 7, 10, 16, 52, 100, 196, \dots$$

Now the connection between these numbers is more or less the same as the one between the distance of the Sun and its planets. Taking the Earth's distance at 10, you can calculate the mean distance of every planet in proportion. **Table III** compares Wolf's series of numbers with the relative mean distance between the Sun and the planets. Wolf's

Law does not work for planets past Uranus.

Table III		
Planet	Relative Distance	Wolf's Series
(1) Mercury	3.9	4
(2) Venus	7.2	7
(3) Earth	10.0	10
(4) Mars	15.2	16
(5) Ceres	27.6	28
(asteroids)		
(6) Jupiter	52.0	52
(7) Saturn	95.4	100
(8) Uranus	192.0	196

Is there also a systematic spacing between lows and highs on a weather map? Is there a similar formula?

Rings and Spokes of Saturn

Now another example in the solar system. The rings of Saturn are geometrically perfect, and they lie in the plane of Saturn's equator. They are the flattest known structure in relation to their thinness. The rings consist of many particles. It has been proven that the inner rings move faster than the outer ones; and at speeds made necessary by *Newton's Law of Gravity* and *Kepler's Laws of Motion*.

There are three main sets of rings, with the main controls on the shape and movement of the rings exercised by gravity and centrifugal force. My main interest was to see if there was any similarity in the type of mathematics involved in explaining the rings of Saturn and the movement of storms (in the middle latitudes of a hemisphere) in what seemed to be a ring-like drift around a pole. The Voyager I and II fly-by of Saturn did not alter the fact that the main forces are gravitational and centrifugal; but it did indicate that there are some small additional forces being brought into play to make the rings a little more complex. The discovery of the radial spokes traveling around in the rings of Saturn is intriguing, but geometrically speaking, there should be no surprise—radial spokes are a common occurrence in many types of physical phenomena, in spite of the differences in the kinds of forces involved.

Roche's Law

One more thing before we leave the planets. It has been calculated that if a moon is closer to a planet than a certain distance, tidal forces

will break the moon up into small pieces. Oppositely, if fragments already exist at such a distance where tidal forces are destructive, they will not join together to form a single body. This limit is called the **Roche limit** after the astronomer *E. Roche* who discovered it in 1849. The Roche limit is generally equal to 2.44 times the planet's radius. The rings of Saturn do fall within the Roche limit.

The one common thread in all of these astronomical examples is that there are radial and/or circumferential spacings of some physical quantity as you move out along a radius from any common central object. It shows that (at least on an astronomical scale) that bodies or matter orbiting a central zone can not always take any radial position outward from the center, but are limited to certain fixed positions (or quantum positions). Quantum in the sense that any positions in between the fixed ones are forbidden.

Now let us shrink from the wide astronomical view to the tiny world of the atom.

Laws of the Atom

It is known that the electrons are arranged in systematic rings or shells around the nucleus of an atom. *Niels Bohr* (1885-1962) showed that all three of Kepler's laws for the planets also hold true in the case of the electron circling around the nucleus of the hydrogen atom. In addition, he showed that there was a quantum law, that the electrons can revolve only in certain fixed orbits and in no others. This is a harmonic law similar to the law that limits Saturn's rings to exact size and shape.

Bohr's model of the atom consists of 7 shells or rings. These are quantum rings inasmuch as no electrons can occur in between any two consecutive rings. **Table IV** shows the number of electrons possible for each ring, which is equal to the ring number squared times 2.

The diameter of these rings also follows a rule of squares and is measured in *Angstrom units*, which is the unit of length (equal to one hundred millionth of a centimeter) used to measure light waves. **Table V** gives the diameter, in Angstrom units, of the 7 rings of the hydrogen atom.

The hydrogen atom has only one electron. The ring that the electron occupies depends upon the amount of energy it receives. It will jump from one ring to another when it has the required changes in the

TABLE IV

# of the ring	# of electrons possible	squaring factors
1	2	2×1^2
2	8	2×2^2
3	18	2×3^2
4	32	2×4^2
5	50	2×5^2
6	72	2×6^2
7	98	2×7^2

TABLE V

# of the ring	diameter of ring in Angstrom units	factors of 2
1	1	1^2
2	4	2^2
3	9	3^2
4	16	4^2
5	25	5^2
6	36	6^2
7	49	7^2

amount of energy it receives. The electron never circles in between the rings, but it always jumps the whole distance or not at all. This is in accord with the laws of quantum mechanics for the atom.

With this information, Bohr was able to calculate the speed of the electrons. In the first four rings of the hydrogen atom, he found that the electron moves at 2160 km/sec., 1080 km/sec., 720 km/sec., and 540 km/sec., respectively. These speeds are related in the exact proportion of 12:6:4:3.

It has been found that the velocity of the electron in the hydrogen atom in the first ring is 2.2×10^6 m/sec. and its wavelength is 3.3×10^{-10} meters. Also, the radius of the first ring is 5.3×10^{-11} meters. Since the circumference of a circle is $2\pi r$, we have the circumference of the first ring as follows:

$$2\pi r = 2\pi(5.3 \times 10^{-11} \text{ m}) = 3.3 \times 10^{-10}$$

We come to the conclusion therefore, that the orbit of the electron in a hydrogen atom is equal exactly to one complete electron wave joining to itself around the ring.

To understand this a little better we will look at the vibrations of a ring made of wire. You will see that the number of wavelengths always

fit an integral or whole number of times into the ring's circumference. Each wave connects perfectly with the next one. The **wavenumber** is the number of whole wavelengths that fit into the circumference of a circle. In Figure 5-2, we show only wavenumbers of 1, 2, 3, 4, 5, and 6. If there were no resistive or dissipative effects, these waves would persist indefinitely.



Figure 5-2. The first 6 of the many modes of vibration of a ring of wire.

You will find that you can not fit a fractional number of waves into the ring and still have each wave join the next one smoothly. Fractional wavelengths would set up destructive interference as the waves go around the loop, and the vibrations would die out quickly.

An electron can circle an atomic nucleus only if its orbit is a whole number of electron wavelengths in the circumference. As the electron jumps to a higher ring, we find that the size of the ring increases. The increasing circumference of the higher rings makes it possible for an increasing number of electron wavelengths to fit in. The circumference of the elliptical orbits of the hydrogen atom can likewise only be broken up into whole wavelengths.

The Bohr model is a crude approximation, since the electrons are actually considered to be cloud-like waves over a three-dimensional volume of the atom; what we have been considering is the two-dimensional view.

We see that there are many similar structures, shapes, and rules that apply to the confined space of the atom and to the huge playground of the solar system and the Universe beyond. Rotating high and low pressure centers are somewhere in between these two extremes. The concept of wavenumber has been recognized for a long time in the meteorological literature. There is usually some reference to wavenumber every month in professional journals—but these references are always referring to the average wavenumber on a weather map for a week, a month, or a year; never a precise calculation for a specific weather map for a given moment in time. In addition, the concept of wavenumber has been limited to the measurement of the

number of wave lengths of highs and lows along the circumference of a given latitude circle (or in a range between certain arbitrarily chosen latitude circles). You shall see later that this is an artificial limitation when I introduce the principle of **staggered wavenumber** around a point, in addition to the regular wavenumber as defined around a circle. In **Figure 5-3** we see a *liverwort* showing one ring of 8 short arms or tentacles and a second ring of 8 longer tentacles. We can see that there are two rings, each with a wavenumber of 8. If we join the ends of the tentacles in any one ring with straight lines, we will get 8 equal wavelengths. We can also join the ends of the tentacles alternately to the inner ring with straight lines, we will get 8 equal wavelengths. We can also join the ends of the tentacles alternately to the inner ring and then to the outer ring as shown by the dashed lines to give a staggered wavenumber of 16. In actual weather situations we may find parts of the inner ring missing, or parts of the outer ring missing, as we shall see later on.

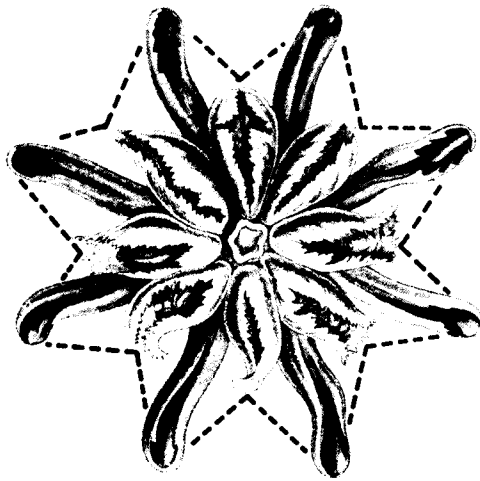


Figure 5-3. A type of *liverwort*, which is related to the mosses, with dashed lines drawn to help calculate the staggered wavenumber.

Chapter 6

Waves

General

We put the camel's nose under the tent when we discussed wavenumber. We may as well put the whole camel into the tent and touch on a few of the well-established features of waves.

The variety of wave phenomena observed in nature is immense, yet there are many features common to all kinds of waves. There are sound waves, water waves, radio waves, seismic waves, gravity waves, Rossby *weather* waves, etc. Any explanation of "how the weather works" on a global basis would inevitably have to involve wave phenomena. There are shelves of books that deal with only one small part of the wave complexities. All we will do is to define a few of the basic wave phenomena and how waves interact with one another. This information is provided for those readers who are not familiar with this subject.

The Universe is full of things that move. These movements can be broken down into two broad types depending on whether the *thing* that moves stays near one place or travels from one place to another. Examples of things that stay near one place are a vibrating violin string, a swinging pendulum, water sloshing back and forth in a bathtub, and the electrons oscillating around an atom. Examples of things that move from one place to another are ocean waves moving towards a beach, the electron rays of a television tube, a light ray from a star reaching your eye. In some cases, both types of movement can occur simultaneously. The ocean waves may be traveling towards the beach, but a ball on the water's surface will only go up and down and forward and backward without traveling to the beach. You can make a wave travel along a stretched rope from one end to the other; the rope

itself vibrates up and down but does not move from its points of attachment.

Equilibrium

Usually, every material object can find at least one position in which it can remain at rest. This position is called a **position of equilibrium**. Any *small* outside disturbance (such as a push, pull, knock, etc.) will make the body move out of the equilibrium position to a new position. When that happens, the forces on the body are no longer evenly balanced and the body experiences a *restoring force* which tends to pull it back to its original position. This restoring force starts by dragging the body back toward its original equilibrium position. In time it reaches this position, but since it is moving with a certain amount of speed, it overshoots the position and travels a certain distance on the other side before stopping. Now it experiences a new force tending to pull it back; again it gives in to this force, picks up speed, overshoots the equilibrium position, and so on, until it stops due to friction or other forces. This kind of motion is called an **oscillation**. When a body moves a *very small* distance, the motion is called a **vibration**. This type of vibratory or oscillatory motion is defined as **simple harmonic motion**.

At this point, I might add that there are certain boundaries or limits to the equilibrium position. A pendulum can be made to swing in larger and larger arcs, always passing through the same center of equilibrium, each trip. A strong enough push, however, will break it completely off its pivot point and force the pendulum to fly off in one direction. This would set up new limits for the equilibrium position of the pendulum; like lying on the floor.

Oscillations and Resonance

A **free** or **natural** oscillation occurs when something is given an initial movement by an external force, and is permitted to oscillate freely without any additional outside force being added after the first push (like the first push of a swing). A body may be kept in motion by regular or periodic impulses delivered by an outside force. In that case, the body is said to be executing **forced oscillations**. When the **frequency** (determined by the properties of the oscillating object) of the forced oscillation is the same as the natural frequency of the oscillating body,

the natural oscillations will reinforce the outside forced oscillation. The **amplitude** is the maximum distance that an oscillating body moves away from the equilibrium position. The amplitude of the forced oscillation increases as the period of the oscillation approaches that of the oscillating system and becomes very large when the two periods coincide. When this occurs, we have a condition which is known as **resonance**. When the forced oscillation has a different frequency from the free oscillation of the body, the received impulses sometimes help and sometimes interfere with the natural oscillations.

Harmonic Movement

It has been shown that the motion of a complicated system having many moving parts can always be considered as being made up of simpler movements, which are called **modes of operation**, all going on at the same time. If a complicated system has a large number of modes we find that each one of its modes still is acting as if it were independent with each individual mode retaining its own properties that are similar to a simple harmonic oscillator.

We can consider that a circular motion performed at a constant speed can be regarded as being made up of two simple harmonic motions in directions at right angles to each other. In **Figure 6-1**, point P moves around circle $XYX'Y'$ with constant speed, like the hand of a clock. At any given position of P, draw a perpendicular PN on to the line XX' , and a perpendicular PM on to the line YY' . Then as P goes around the circle, N moves back and forth along line XX' , at the same time M moves up and down line YY' . Each one of these two points is executing simple harmonic motion.

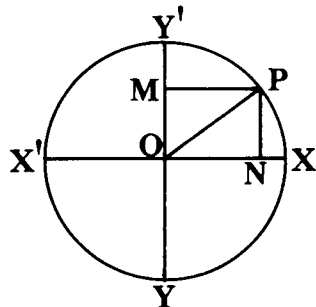


Figure 6-1. Simple harmonic motion around a circle. As point P goes at a constant speed around circle $XYX'Y'$, point M moves up and down, while point N goes back and forth.

It is sometimes convenient to think of the harmonic movement of a point at a uniform velocity around a circle as a **sine wave**. See **Figure 6-2**. As P moves around the circle it creates a harmonic sine wave

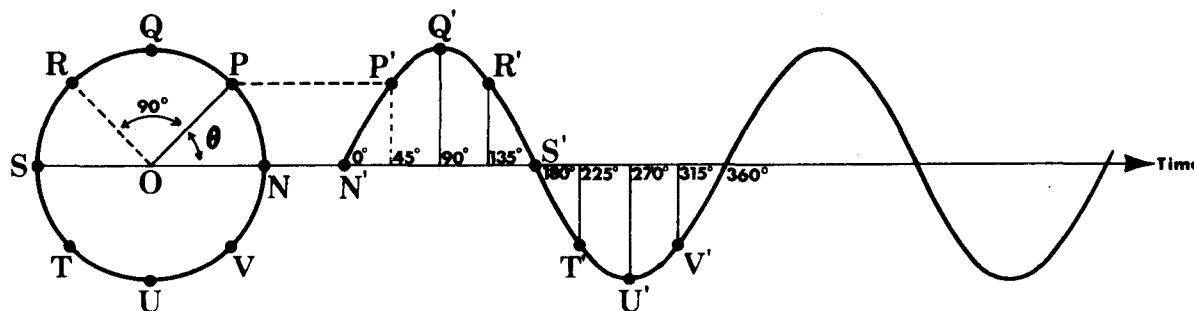


Figure 6-2. A sine wave is created by a moving point around a circle.

(which is shown by the waveform to the right of the circle in the figure) as a function of time. θ (theta), which is called the **phase angle**, is the angle PON, in Figure 6-2. This angle changes continuously as P goes around the circle. When point P starts out at position N, the angle for θ is zero and the time is zero. When point P reaches the position labeled P, the angle is 45° . Since it took some time for the point to reach position P from N, we can consider the size of angle θ as a measure of time; therefore we mark off the X-axis or time axis in degrees. At 45° , point P is a certain distance above the X-axis, and a certain distance from the Y-axis (which lies along OQ); so we draw dashed lines from P to P' and from 45° on the X-axis to P' (which is the point where the two dashed lines cross). The same procedure is followed to locate the points Q', R', S', T', U', V', and N', to generate the sine waveform, which is a harmonic wave since it is generated by harmonic motion, as defined in Figure 6-1.

Fourier Analysis

Anything that repeats itself after a fixed amount of time is called a **periodic time function**. In a periodic wave, one pulse follows another in regular succession. Sound waves, water waves, and light waves are almost always periodic, although in each case a different quantity varies as the wave passes. In general, periodic time functions are not simple waves, but are quite complex. It was shown by *J. B. Fourier* (1768-1830) that any complex periodic time function can be accurately described as the sum of a series of harmonically related waves.

The procedure of breaking up a given periodic wave into simple harmonic components and determining the equation and/or the harmonic waves which represents it, is called **Fourier analysis** or

harmonic analysis. Fourier stated that every curve (wave), no matter what its nature may be, or how it was developed, can be faithfully reproduced by superimposing a sufficient number of simple harmonic curves (waves). **Figure 6-3** is an example of a complex periodic wave with a period of T .

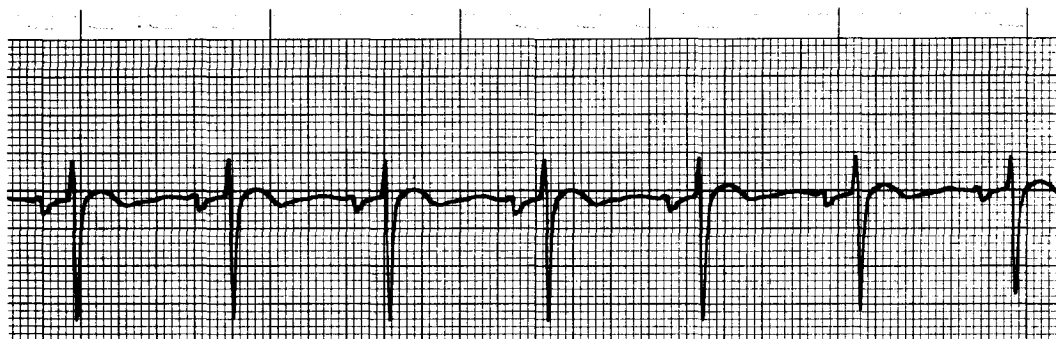


Figure 6-3. A complex wave (electrocardiogram of the heart) with a period equal to T .

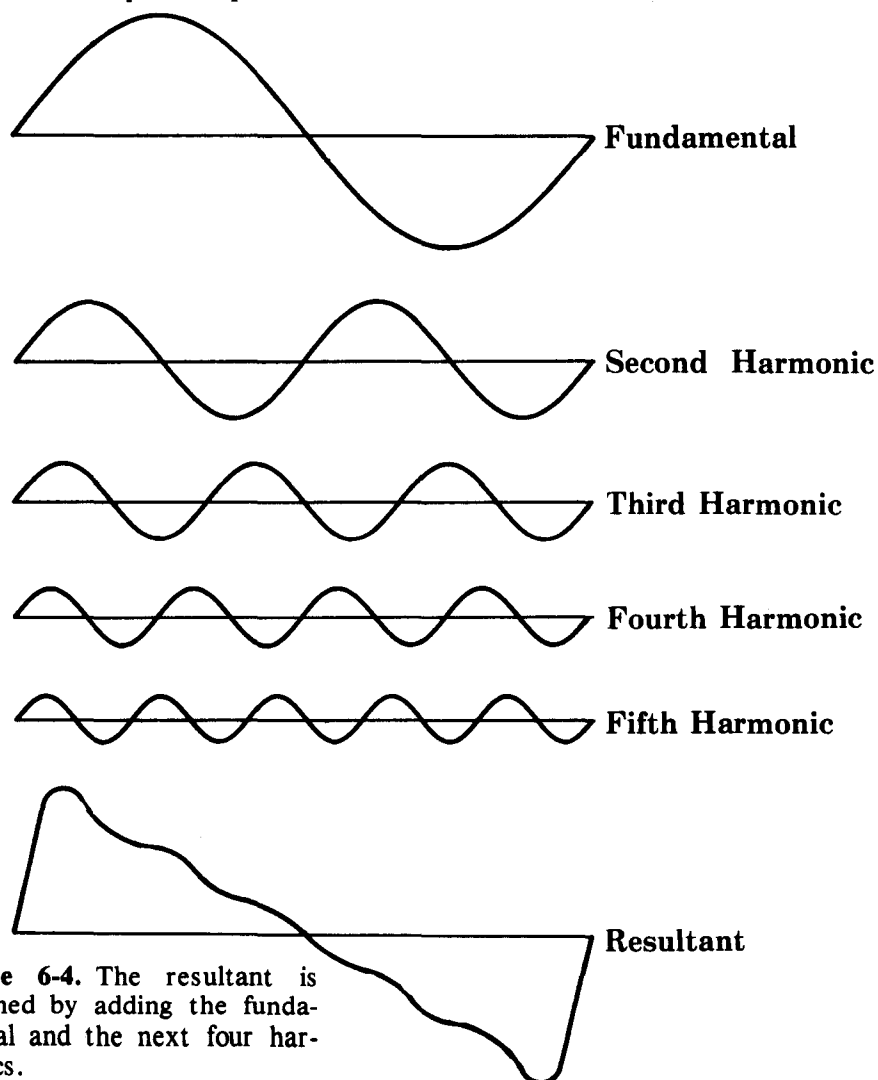


Figure 6-4. The resultant is obtained by adding the fundamental and the next four harmonics.

The components necessary to construct one type of complex wave (of which there are an infinite variety) is shown in **Figure 6-4**. The fundamental wave (or simple fundamental) of a group of waves with different frequencies is that wave with a frequency that is the lowest common denominator of all the other frequencies. Since the fundamental is the **first harmonic**, then the second harmonic is a wave that has twice the frequency of the first harmonic. The **third harmonic** has three times the frequency of the first harmonic, and so on for the fourth, fifth, etc., harmonic.

Wave Pulses

Wave motion can be considered as the transport of energy and momentum from one point in space to another point without the actual transport of matter. In water waves, waves on a rope, or sound waves, the energy and momentum are transported by a disturbance in the medium, which is carried forward because the medium has elastic properties. When a rope is stretched and put under tension and then given a small shake at one end, we find that the string will change shape in a regular manner as shown by **Figure 6-5**. The wave pulse moves to the right; the change in shape of the pulse as it moves along is called **dispersion**.

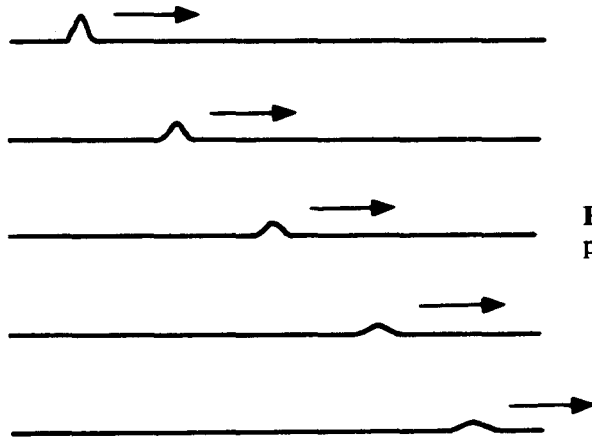


Figure 6-5. Movement of a wave pulse on a rope.

Interference

Interference occurs when two waves meet and combine to form a resultant wave. The fact that two or more waves add algebraically is called the **principle of superposition**. In **Figure 6-6a**, we see a cross-section showing the crossing of a larger and a smaller wave with

constructive interference which gives a resultant wave that is greater than any of the original waves. In Figure 6-6b, we see the crossing of two waves that are similar in size but are opposite in phase (angle), which causes **destructive interference** due to the cancellation of pulses.

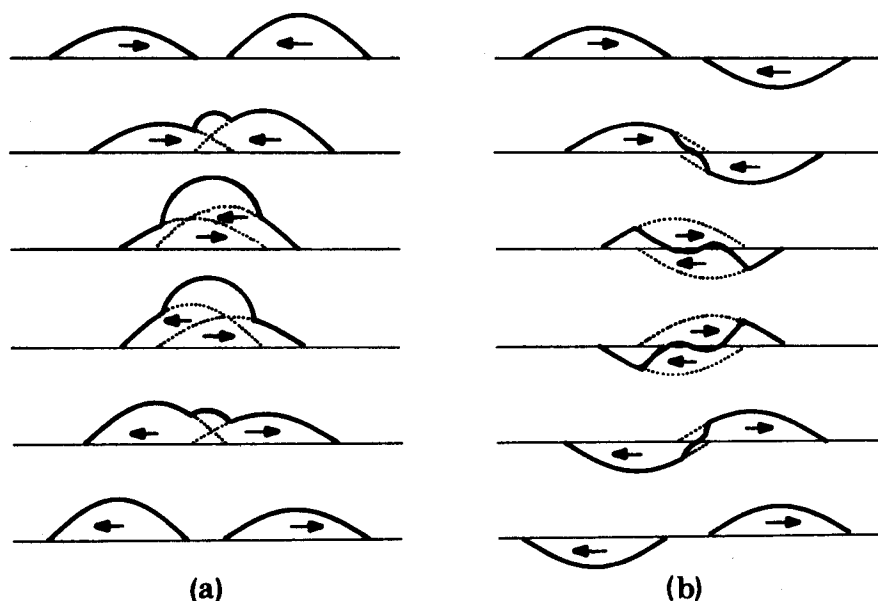


Figure 6-6. The heavy black lines show the resultant waveforms for different types of interfering waves.

When waves are in a confined space, like when we pluck a string whose ends are fixed in place, or in an organ pipe, we will find that reflections bounce off both ends. Therefore, we will have waves traveling in both directions. These waves will add in accordance with the principle of superposition when there is interference. For each string or pipe, there are always certain frequencies where the interference, created by vibrations, causes a stationary pattern which is called a **standing wave**. Figure 6-7 shows standing waves on a rope that

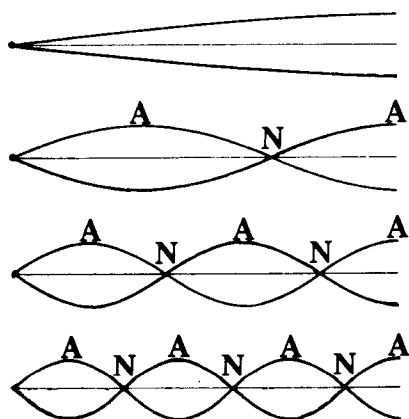


Figure 6-7. Standing waves when a rope is fixed at one end, with a sliding ring attached to a pole, on the other end. The points marked A are antinodes, while those marked N are nodes.

is fixed at one end and is attached to a ring at the other end which is free to slide up and down along a pole. The points marked A, are **antinodes**, where the displacement of the rope varies between its widest limits. The points marked N, are points of zero displacement where the rope does not move at all.

Up to now we have been considering only the type of waveforms that repeat themselves indefinitely or wave forms that occur only once. There is another type of wave that changes with time, which goes on indefinitely, but does not repeat itself periodically. Such waves (or functions), being relatively unpredictable, are called **random time functions**. Traffic noise, the babble of conversation in an auditorium, the noise of construction etc., are all random time functions, since one never knows exactly what the next sound will be.

The spacing of all vortexes and other significant features such as troughs and ridges on a weather map over an entire hemisphere have been falsely considered, by meteorologists, to be of a random nature. Therefore, it is the main purpose of this text to prove that the positioning of vortexes is not random, but is beautifully organized.

Chapter 7

Symmetry

A phenomena that permeates almost every nook and cranny of the Universe (similar to omnipresent waves)—is symmetry. First we will define symmetry and then show some of the most important classes of symmetry.

Definition of Symmetry

Any object is considered as being symmetrical when it consists of geometrically and physically equal parts that are arranged relative to each other in some kind of fixed order. The geometric equality must be a **suitable** equality or a **mirror image** equality. A steel ball and a rubber ball of the same size may be suitably equal, but they are not equal in a physical sense. The right hand is equal to the left hand in all respects, but the right hand can not be made to coincide with the left hand by placing one hand over the other, unless one is reflected in a mirror. The right and left hand have mirror equality. See **Figure 7-1**. A mirror image form of the same symmetry is called **enantiomorphism**.

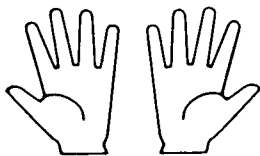


Figure 7-1. Hands are an example of mirror image symmetry.

Another condition of symmetry is that equal parts in any structure must always be arranged in a geometrically regular manner. It must be possible to divide the structure into an equal number of parts without any remaining odd shaped parts left over. In **Figure 7-2**, the scattered triangles become symmetrical as a group only after they have been arranged in an identical manner to form the hexagon.

Symmetry

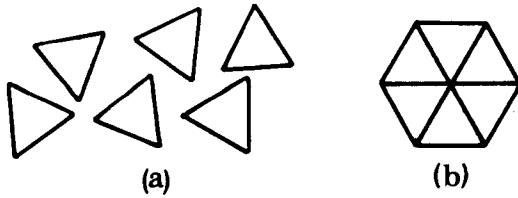


Figure 7-2. The cluster of disorganized triangles in **a.**, become symmetrical when rearranged as in **b.**

Sometimes there can be a combination of different symmetries in one structure. **Figure 7-3** shows an octagon inside a square which is inside a hexagon. Considered as a single unit, the figure is unsymmetrical, but the three figures of which it is composed can be considered as being individually symmetrical.

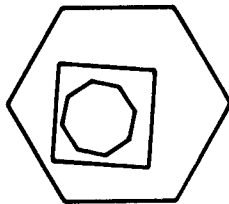


Figure 7-3. Three different symmetrical patterns in one figure.

Classes of Symmetry

According to *A. V. Shubnikov* and *V. A. Koptsik* (8), all symmetries in the Universe can be divided up into as many as 230 different classes. For our purposes, there are three broad geometric classes. The first is the **point**, which is usually associated with the mineral world. The second is the **line**, which is usually associated with the plant domain. The third is the **plane**, which is usually associated with the animal kingdom. See **Figure 7-4**.

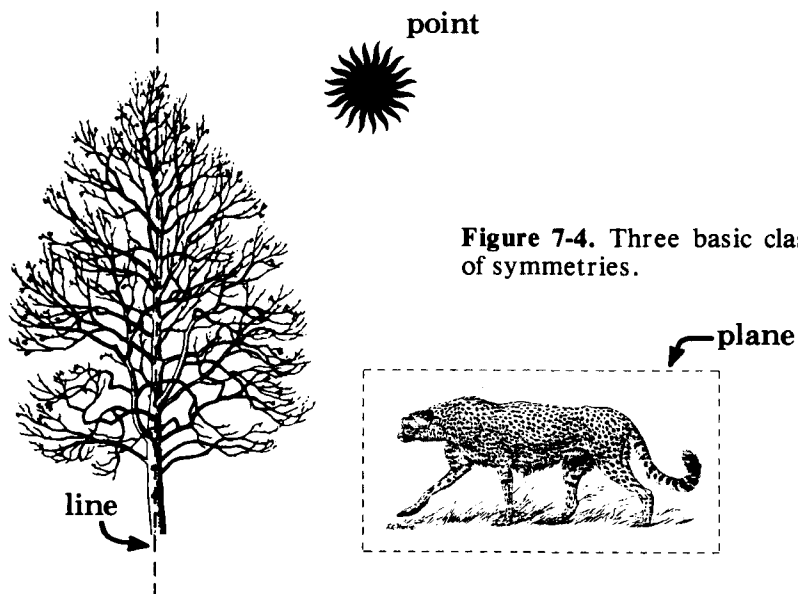


Figure 7-4. Three basic classes of symmetries.

A fundamental mineral form such as a star, a crystal, a soap bubble, etc., tend to be symmetrical around the point at their individual centers. The forces acting on these structures can operate equally in all directions.

Once any form of life attaches itself to the bottom of the sea or to the land (like a tree), a fixed up and down axis is generated. The bottom end with the roots is obviously different from the top end. There is no front or back or left or right for these life forms in either the sea or on the land. They generally take the symmetric form of a cone around the line of the vertical axis. Since the main controlling force is gravity acting along the up and down direction, things tend to spread out equally in all horizontal directions, like the branches of a tree, or water spreading out to form a horizontal surface in a lake, etc.

A moving animal is generally symmetric on either side of the plane that separates the right and left halves of its body. Due to environmental conditions, movements of up and down and forward and backward are all completely different. Moving in a forward direction, without the aid of a compass, can lead to veering to the right or to the left direction with statistically equal frequency—which accounts for the occurrence of bi-lateral symmetry about a plane with things like a right and left hand. In other words, an animal can see a predator (or food), in front, to the left, or to the right, so the animal's body is shaped to meet these directional challenges from the outer world. If a predator sneaks up from behind, he is in trouble and better run fast. . . Many of the man-made structures (like cars, chairs, etc.) have bilateral symmetry to serve man's own bi-lateral symmetry.

Types of Symmetry Operations

Using some of the definitions of crystallography (the science of crystals), we find that the point, the line, and the plane (as pictured in Figure 7-4) are called the **symmetry elements**. Every object possessing at least one symmetry element is symmetrical by definition. A **symmetry operation** is defined as any manipulation that may be performed on an object, after which the object itself appears to be exactly the same. The first symmetry operations we will consider are rotation and reflection.

The sphere is the most perfectly symmetrical figure in three-

dimensions. It can be rotated through any angle around any diameter, which gives it **rotational symmetry**; or it can be reflected in any plane, through the center, which gives it the **symmetry of reflection**.

The circle is the most perfectly symmetrical figure in two-dimensions because it can be rotated around its center through any angle or reflected in any diameter. In three-dimensions, the rotation is around an **axis**, while in two-dimensions, the rotation is around a **point**. Any shape, other than spherical or circular that has rotational symmetry, can be broken up into symmetrical parts. There is always a smallest possible angle in which a pattern can be rotated and where the whole figure appears to be unchanged. For example, if the hexagon in **Figure 7-2b** is rotated around its center by 60° (which is the smallest possible angle), it will look exactly the same after the rotation is completed.

If a pattern can be rotated into 2 positions (half turn), it is called a **two fold** or **diad** rotation. A rotation of 3 positions (one third turn) is called **three fold** or **triad**, and 4 positions (quarter turn) is a **tetrad** . . . the example of the hexagon and its 6 positions is called a **hexad**. There is always a center point or center line in a symmetrical pattern in a plane, as shown in **Figure 7-5**. In performing symmetry operations of rotation or reflection, the center point or line remains fixed.

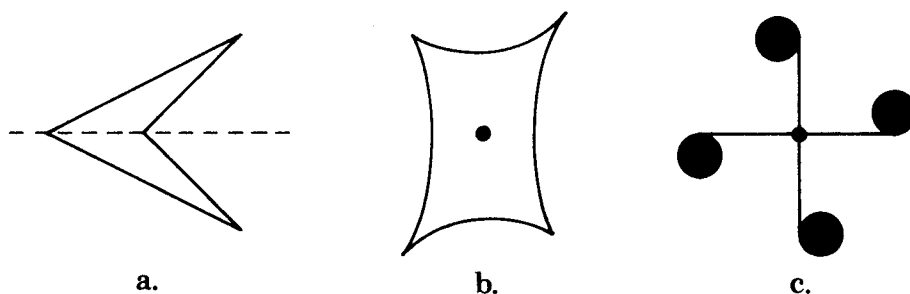


Figure 7-5. a. A plane figure with a center line for rotation or reflection. b. and c. Plane figures with a point as a center of rotation.

There can be a single reflection line as in **Figure 7-5a**, which is the simplest kind. If there is more than one line of reflection, then there must also be a center point of rotation, since every reflection line must pass through the center of the figure. See **Figure 7-6** for multiple axes of reflection.

A face from the front is a good example of symmetry about a line. See **Figure 7-7**. We call the line a **mirror-line**, and the left side of the face is a *mirror image* of the right side. Since a face is

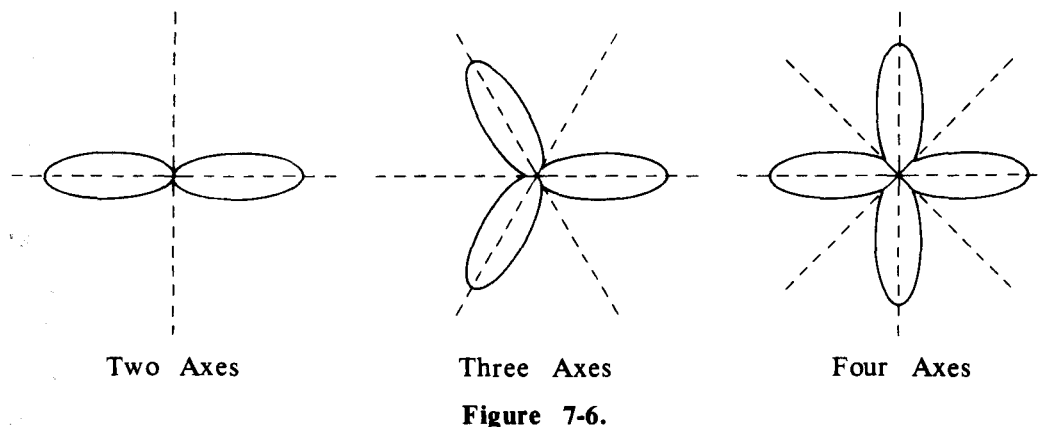


Figure 7-7. The right side of a face is a mirror image of the left side.

three-dimensional, we really have a mirror-plane rather than a mirror-line.

Let us now investigate the symmetry operation of **translation**. Translation, as defined in crystallography, is the moving of a point from one location in an object to some other location in the same object, while the environment around the point remains the same. An example of a structure with translational symmetry is a chain link fence as in Figure 7-8. If you found yourself at point A or B, on any of the squares, everything would look the same in all directions from those two points

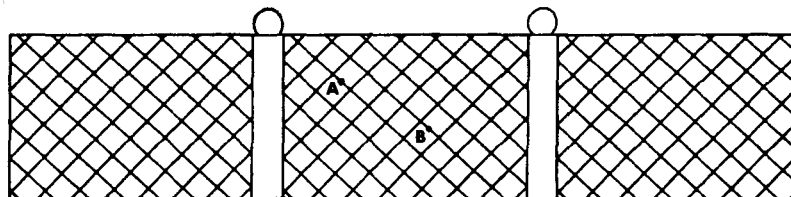


Figure 7-8. A fence showing translational symmetry.

(locations). The operation of moving from point A to point B is called a translation, and the fence has what is known as **translational symmetry**. If we always move a *whole* number of spaces on the fence, everything would appear exactly the same as at point A. However, moving from point A by anything different than a whole number of spaces would result in the fence looking different at that new point. It is possible for a pattern to exhibit a combination of translational and reflectional symmetry simultaneously, as shown in **Figure 7-9**. This kind of symmetry is called **glide reflection**.

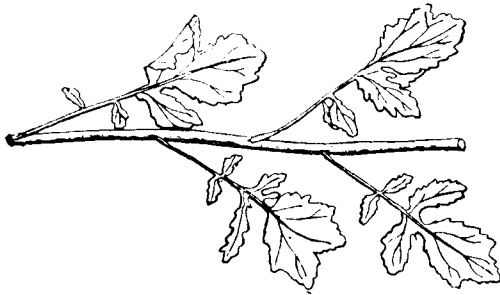


Figure 7-9. Leaf pattern shows glide reflection symmetry.

Symmetry Along a Straight Line

What types of symmetry patterns can be found on both sides along a straight line? According to the laws of symmetry, there are only 7 possible symmetry patterns along a straight line on a plane surface. These are shown in **Figure 7-10**.

Dilation Symmetry

Dilation is the enlargement or reduction of a figure along lines radiating from a central point. See **Figure 7-11** for samples of two-dimensional patterns. There can be dilation along a straight line, as in **Figure 7-12**. There can be dilation with reflection, as in **Figure 7-13**. There can be dilation linked with rotation, as in **Figure 7-14**.

It is impossible to ignore the effect of dilation on any symmetry patterns that can be found on the polar stereographic weather map. In **Figure 3-8**, we can see a built-in dilation, due to the way that the map is constructed.

Symmetry in a Network of Points

Let's turn for a moment to the definition of a crystal. It is a periodic repetition of a group of atoms at equal intervals throughout the volume

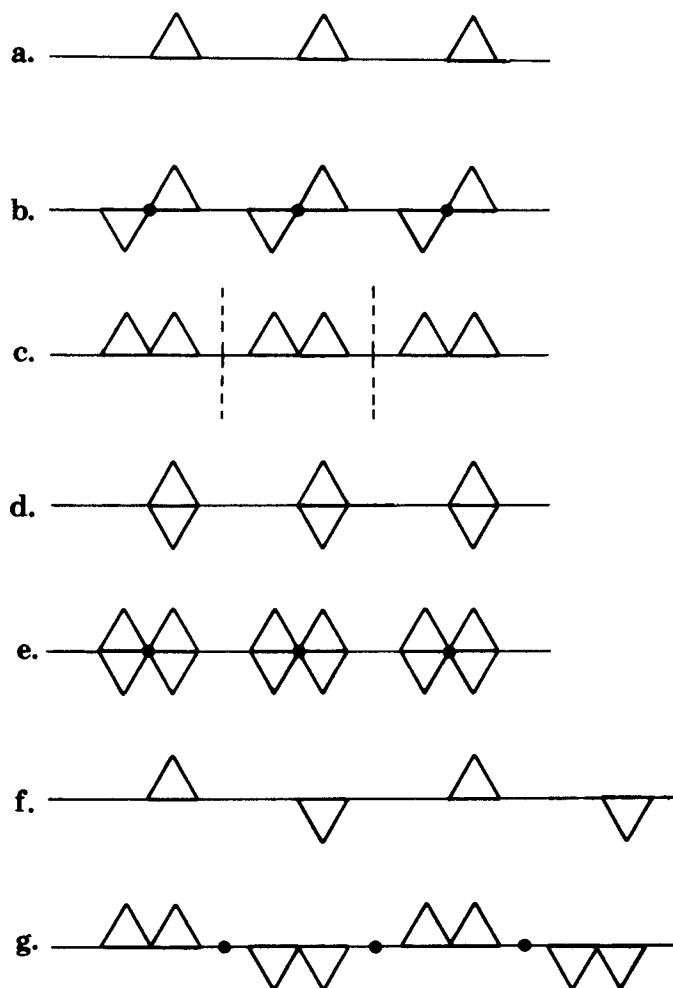


Figure 7-10. The 7 symmetry patterns that are possible along a straight line on a two-dimensional surface.

- a. Translation only—no rotation or reflection.
- b. Half-turn of 180° (with the dot as the center of rotation) will give an identical shape.
- c. Transverse reflection (with the dashed line showing the line of reflection or mirror).
- d. Longitudinal reflection (where the straight line is the line of reflection).
- e. A half-turn combined with both longitudinal and transverse reflection.
- f. Glide (longitudinal translation) and reflection.
- g. Longitudinal glide reflection, combined with transverse reflection and a half-turn around the points in between.

Symmetry

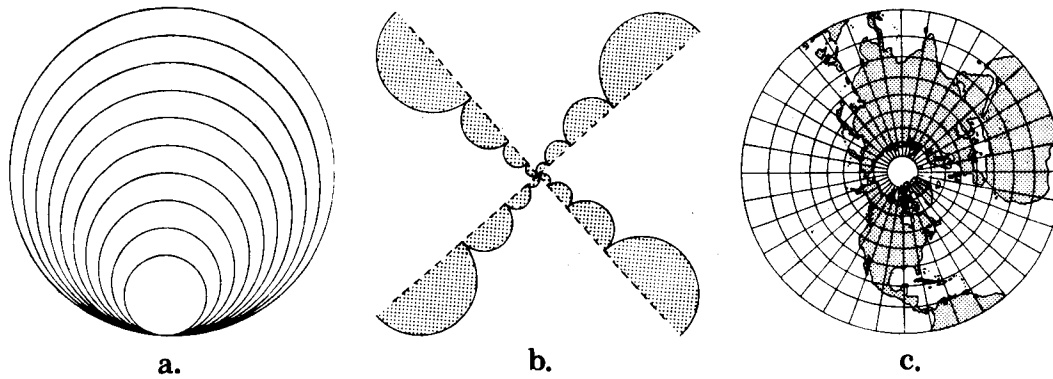


Figure 7-11. Examples of dilation symmetry (c. is the polar stereographic map).

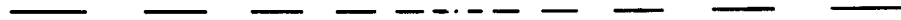


Figure 7-12. Dilation along a line.

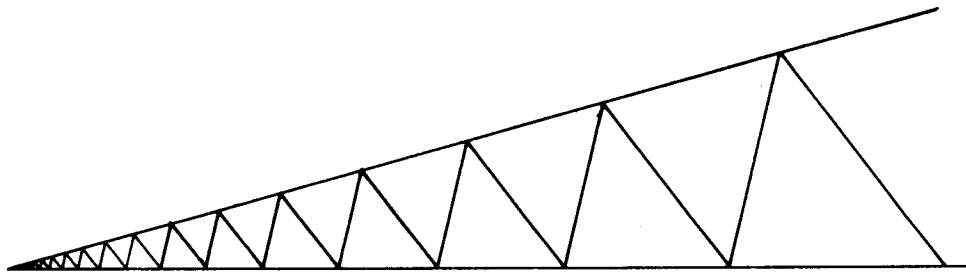


Figure 7-13. Dilation with reflection.

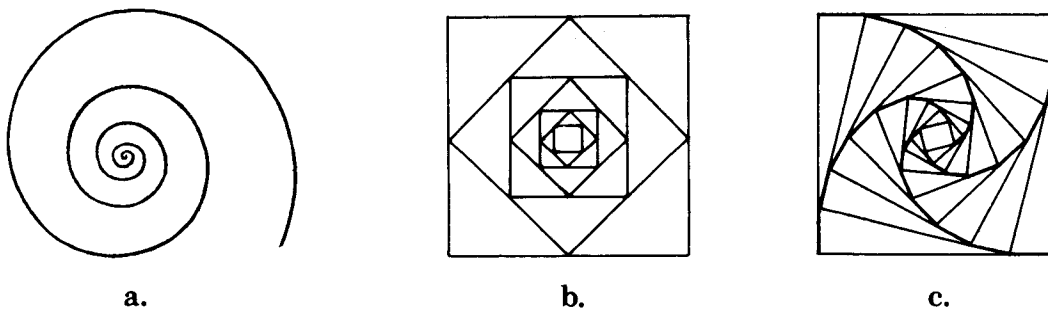


Figure 7-14. Dilation with rotation.

of the sample. As a result, the surroundings of any one of these groups is identical with that of any other group. An arrangement of points in space having the property that each point has identical surroundings of the same orientation is called a lattice.

You may be wondering how this applies to weather patterns. If you were to place a point at every high or low center on a hemispheric map,

you would have a rough network of points. You will find that the principles discovered about crystals have some interesting parallels in patterns on the surface weather maps, as will be shown in the charts later on.

Starting with a square network of points, we find it possible to draw many different networks depending on the method used in connecting the points, and also the total number of points used. See Figure 7-15.

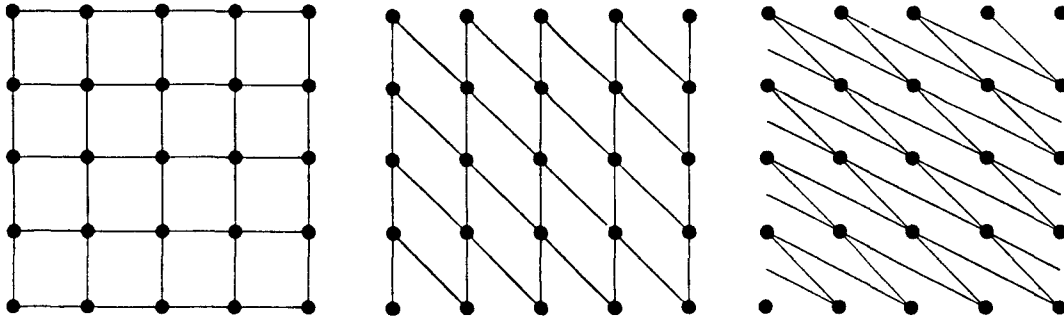


Figure 7-15. The same system of points can give differing networks depending on the method of joining the points.

If the points are connected in such a way that only two straight lines cross at each point, then the area of each parallelogram formed is always the same as the area of one of the squares.

A network of points form what is known as a **wall paper pattern**, which is a design that repeats itself at regular intervals in two directions (for a plane surface). The simplest type is a row of dots repeating themselves in parallel rows to form parallelograms, as in Figure 7-16. This kind of wall paper pattern is called a **net (network)**.

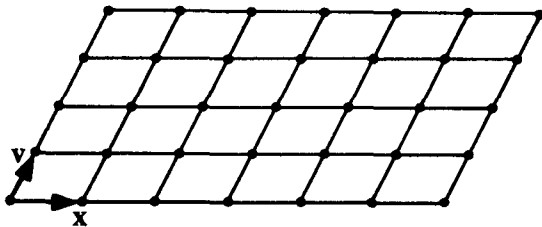


Figure 7-16. Example of one type of net, where leg $x \neq \text{leg } v$.

These type of network patterns are encountered everywhere: in actual wall paper, in carpets, in crystals of course, in the tissues of plants and animals, in honeycombs, etc. In Figure 7-16, the length of the leg of the parallelogram is longer in the X direction than the leg in the V direction. In Figure 7-17, we make the length of the leg in the X direction and in the V direction of the parallelogram equal. This figure has more

Symmetry

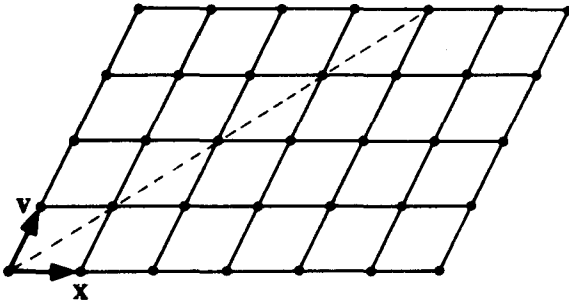


Figure 7-17. Example of a net, where $\text{leg } x = \text{leg } v$.

symmetry elements, since it now includes reflection symmetry; the dashed line represents one of the lines of reflection. Lastly, in Figure 7-18, the angle between leg X and Leg Y is equal to 90° , and the length of leg X equals leg Y. This adds rotational symmetry to the pattern, since we can rotate leg X into leg Y with a 90° rotation for any small square.

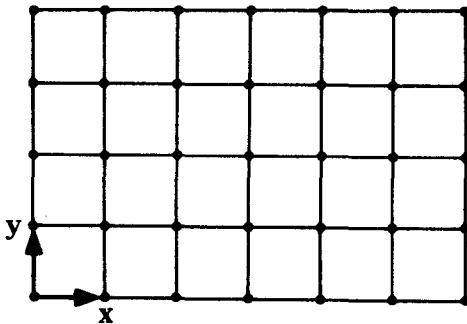


Figure 7-18. Example of a net, where $\text{leg } x = \text{leg } y$, and the angle between them is 90° .

There are only 5 types of parallelogram nets possible, each differing from the other in symmetry. See Figure 7-19. In this figure, we have the individual parallelograms formed by 4 separate points in 7-19a, b, c, and d; while e uses 5 points, with 4 for the corners and one occupying the center. Two of the sides of a parallelogram are indicated as X and Y when the sides meet at right angles, and as X and V when they meet at an angle other than 90° .

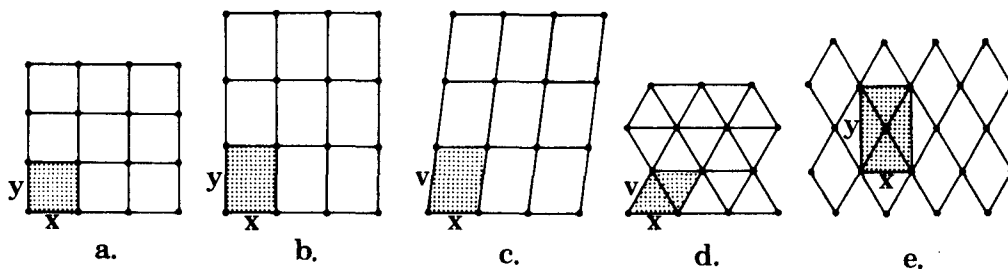


Figure 7-19. The 5 types of parallelogram nets possible.

- Square system where $x = y$.
- Rectangular system where $x \neq y$.
- Oblique parallelogram where $x \neq v$.
- Equilateral triangle system where $x = v$.
- Centered rectangular system where $x \neq y$.

Equivalent Symmetry Points

There is one more aspect of symmetry that we must consider when we look for symmetry patterns on a weather map. As an example, we will take a look at the 4 fold symmetry of a square, as shown in **Figure 7-20**. This symmetry is indicated by the 4 lines going through the

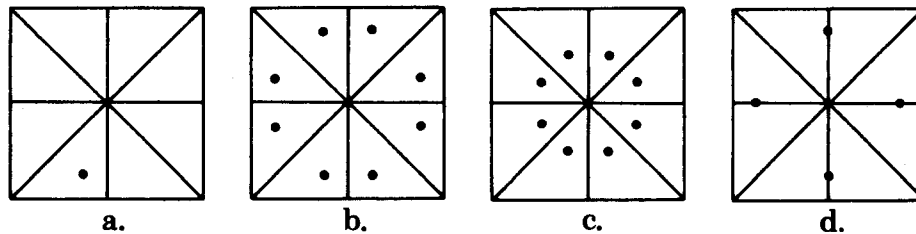


Figure 7-20.

- a. The single dot represents a random point in the square.
- b. Seven additional equivalent points for the point in a.
- c. The equivalent symmetry points when the random point is moved closer to the center.
- d. The eight equivalent points are reduced to four when the random point is moved to a position on one of the symmetry lines.

center. We pick any point in the square that is not on one of the symmetry lines (**Figure 7-20a**). We can see that there are 7 other points that can be spaced in an equivalent or symmetric position (**Figure 7-20b**). If the original point is now moved towards the center (**Figure 7-20 c**), we will find that the similar points will move to the center. All the points will merge into the point at the center when the original point we chose moves into the center. Now if we move the original point towards one of the symmetry lines (**Figure 7-20d**), all the other points similar to the original point will move towards the corresponding symmetry line. In this case, the total number of equivalent points will be cut in half. The same type of analysis can be applied to a triangle as in **Figure 7-21**, and to any other figure with lines of symmetry.

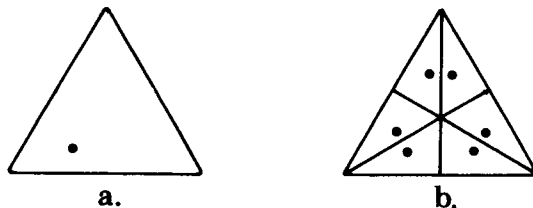


Figure 7-21. a. A random point is chosen in a triangle.
b. The equivalent symmetry points for the point chosen in a.

Symmetry of Averages

In Singer's Lock we are making calculations with a network of points (the centers of highs, lows, and cols). It is a matter of interest to

investigate many aspects of an array of points. In **Figure 7-22a**, we show a square net of points which form a regular figure since each point occupies a similar position with respect to other points. In **Figure 7-22b**, we show a disorderly arrangement of points, but they have the same average density. It can also be considered a regular figure in groups, if it is divided into sections with approximately the same number of points.

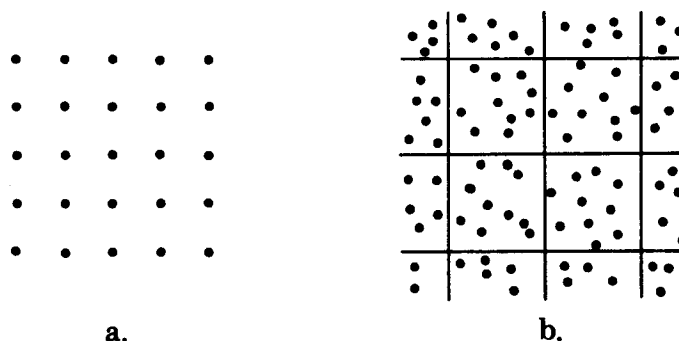


Figure 7-22.

- a. A regular arrangement of points.
- b. This pattern has a regularity since the groups of points inside a given square are comparable in number to the points in any other square.

How Many Points Will be Crossed by any Straight Line in a Regular Network?

Figure 7-23 is a net in a plane where all the points are arranged in a square formation. The net consists of all the points in the XY plane that are whole numbers. Imagine each point in the net as representing a pole sticking vertically out of the plane. If you place yourself at the origin, 0, and look out at the network of poles, you will see some of the poles, while others will be hidden behind a few of the poles that are closest to you. In the figure, the dots indicate only the poles that are visible from the origin at 0. The unmarked points at line crossings represent poles (points) that can not be seen from the origin, because they are behind the ones that can be seen. Every point, whether marked or unmarked, has a coordinate number. For example, the coordinates of the point where $x=3$, and $y=2$, is $(3, 2)$, but we will identify the point as a fraction $2/3$, which is y/x . The interesting feature of identifying each point by a fractional number is that every point that can be seen will have a fraction that can not be reduced to a smaller quantity; for example, for the point at $(12, 10)$, we get a fraction

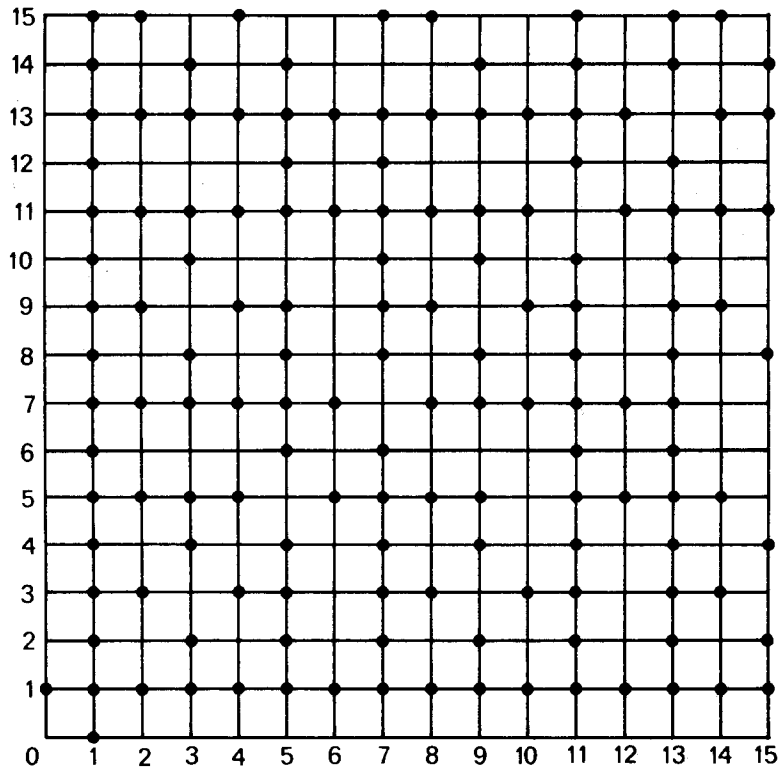


Figure 7-23. A square net, where the dots represent the crossing points that are visible from the origin.

of $10/12$, which can be reduced to $5/6$ (therefore the point at $(12, 10)$ is not visible). The point at $(6, 5)$ has a fraction of $5/6$, which can not be reduced any more, so it is visible. In other words, each point that can not be seen has a fraction that can be reduced to a simpler form using whole numbers only.

Let us now consider the XY plane extended to infinity with a pole or point present at every whole number coordinate out to infinity. Can we tie a rope at the origin and extend it in a straight line out to infinity so that it never touches any other pole? The answer is yes—there is an infinite number of lines or ropes that could be tied to the origin and stretched out to infinity without touching another pole. In fact, there are infinitely more lines that can be drawn that don't touch a pole, than the number of lines that actually touch a pole or point. As a result, if you were to draw a random line in any direction through the lattice, the chance of hitting a point is practically nil. This last statement is true if each point is considered to be infinitely small, and each line infinitely thin. In Figure 7-23 the lines are about $4/10$ of a millimeter, and the dots are roughly $1\frac{1}{2}$ millimeters in diameter.

The network of points in Figure 7-23 is also symmetric in every direction, if the origin from which we look out is placed at the center of any square. In fact, the network is symmetrical in all directions, regardless of where we put the origin. Let us place the origin at random, in any position in between any actual line crossing shown in the figure; looking out from this random origin, we will find a completely different group of points blacked out than if we placed ourselves at one of the regular points of the net. The significant feature is that when we have a symmetrical arrangement of points in space, the points will look symmetrical from any position we may choose, inside or outside the network. The main difference is that the symmetrical pattern will look different from differing positions; but the simplest and most regular symmetry patterns will occur when we use preferred positions like the origin.

Symmetry and Equilibrium

Any situation in the real world is called chaotic when we are in complete ignorance of what is really happening. Any seemingly random or disorderly activity in nature becomes very reasonable and orderly once we understand all the processes involved. The movement of every living and non living thing in a city, a country, or for that matter the Universe, can be accounted for, every second of the day. It is incontestable, that every movement of any storm center or high pressure center on the Earth's surface must be exactly counterbalanced by a very orderly movement of an air mass somewhere else on the globe. There is no such thing as random spacing of highs and lows over the surface of the Earth. Every vortex takes into account what every other vortex on the Earth is doing, before making its own move. Looking at the examples in the chapters with the charts, it almost seems as if the vortexes are in communication with each other—as if they were living entities.

When we look at a weather map of a certain fixed date and time, we can see the instantaneous position of every vortex on the map as it appeared on the Earth. If a vortex decides to change size or direction for some inner reason of its own, a certain amount of time must elapse before this "decision" can be communicated to every other vortex (at the speed of sound). This is in accordance with *Albert Einstein*

emphasizing that events or occurrences between entities are not simultaneous because a certain amount of time must elapse before events can interact with each other.

Every entity in the Universe, when reacting to surrounding entities, tries to reach the "position of equilibrium" or symmetry, which is the simplest arrangement in nature. When outside energy is injected into a system, the entities that were in equilibrium will be forced out into asymmetric (non-symmetric) patterns, and then attempt to swing back again into a symmetric or equilibrious pattern.

There can be what seems to be a "static equilibrium" of a ball resting on the surface of the Earth; or there can be "dynamic equilibrium" of a ball being supported continuously in the air by a high pressure stream of air; or there can be the "simulated equilibrium" of a living cell, which is seldom in equilibrium, since it is continuously absorbing and expending energy.

In the real world, patterns are always oscillating from a position of equilibrium to a position of increasing asymmetry (say positive) on one side, and then back through the equilibrium position, to a position of increasing asymmetry (say negative) on the other side. The symmetric equilibrium position occurs only for a fleeting instant. Any object subjected to varying outside forces will be in an asymmetric phase most of the time. Nevertheless, the asymmetric phase is just as orderly as the symmetric or equilibrium position, but it just doesn't look as neat. The asymmetric position can, of course, be broken down into a group of completely symmetric smaller units. There is no true chaos. When someone states that a situation is chaotic, it is only an admission of ignorance as to what is happening.

The comments of *Gilbert Chesterton* in *Orthodoxy* are appropriate at this time:

"The real trouble with this world of ours, is not that it is an unreasonable world, nor even that it is a reasonable one. The commonest kind of trouble is that it is nearly reasonable, but not quite. . . . It looks just a little more mathematical and regular than it is; its exactitude is obvious, but its inexactitude is hidden; its wildness lies in wait."

As an example, Chesterton has an extraterrestrial examine a human body for the first time. He sees that the right side exactly duplicates

the left with two arms, two legs, two ears, two eyes, two nostrils, and two lobes of the brain. Going a little further, he finds a heart on the left side. He brilliantly calculates that there is another heart on the right side. Unfortunately, he stumbled over that one.

“It is this silent swerving from accuracy by an inch, that is the uncanny element in everything. It seems a sort of secret treason in the Universe . . . Everywhere in things there is this element of the quiet and incalculable.”

Close examination of crystals in the mineral world, and of real honeycombs in the world of bees, shows that they are not accurately regular, geometrically speaking. When the deviations from regularity is small in a crystal, there will still be a high degree of geometric order. It is considered as a crystal with defects. These small defects, however, highlight the importance of understanding imperfection. These defects are common in the crystalline world; they play a critical role in the actual formation of the crystal; and they affect the resulting physical properties of the crystal. Similarly, defects that occur in the symmetry of weather patterns, are signals of change.

Chapter 8

The Problem of Plateau

Another principle that operates throughout the known Universe is that spheres and circular patterns are everywhere. We find them at the atomic level, in raindrops, in the shape of some bacteria, peas, soap bubbles, the Earth, the planets, the orbits of planets, the stars, the shape of galaxies, and even in the shape of highs and lows on the surface of the Earth.

What are the common links between matter, and the space that matter occupies, that leads to the circular or spherical patterns and structures?

One common thread that runs through all phenomena in the Universe is that the sphere has the least surface area for a given volume and is the most suitable structure for restraining internal forces. The exact nature of the forces are immaterial, since they can be nuclear, electrostatic, magnetic, surface tension, elasticity, hydrostatic, centrifugal, convective, gravitational, etc. The type of forces that operate in any given structure are determined partly by the size, amount, and the kind of matter, in a given amount of space. For examples: man is controlled by gravitation; a water beetle by the surface tension on the surface of a pool of water; while bacteria are controlled by the viscosity of the fluid, Brownian movement, and electrostatic charges. The forces controlling high and low pressure centers are usually expressed as pressure differences, centrifugal, gravitational, convective, coriolis forces, etc.

The Conic Sections

The geometrical pattern of a sphere or a circle becomes lost from time to time due to the unbalancing of the forces that would normally lead to a spherical shape. To what new forms do unbalanced spherical patterns

change? They often change to shapes or curves known as **conic sections**, which were discovered in the fourth century B. C., by *Menaechmus*, and more completely investigated by *Apollonius* in the third century B. C. These conic sections are formed by the intersection of a plane and a **right circular cone** (a solid generated by rotating a right triangle around one of the legs of the 90° angle). See Figure 8-1, which shows a double cone.

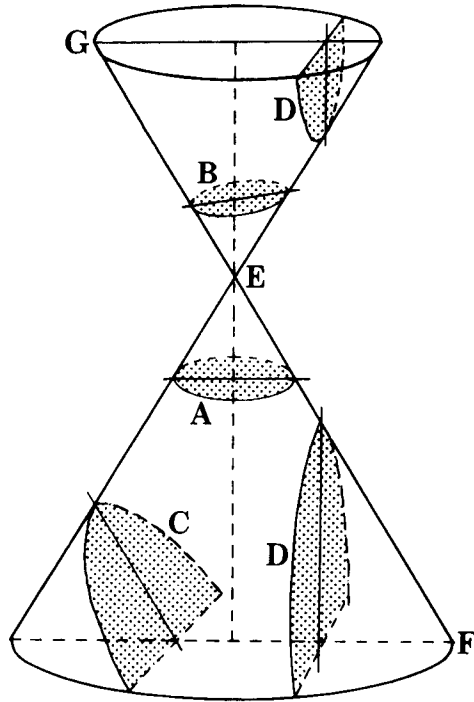


Figure 8-1.
The conic sections:
A circle
B ellipse
C parabola
D hyperbola
E point
FG straight line

If a plane is sliced through the cone in such a way that the plane is perpendicular to the axis of the cone, we get a section of the cone that is a circle (**Figure 8-1 A**). If the plane cuts the circular cone obliquely to the axis, we get a section of the cone that is an ellipse (**Figure 8-1 B**). If the cutting plane is parallel to one of the sides of the circular cone, we get a parabola (**Figure 8-1 C**). If the plane intersects each of the two cones, we get a hyperbola (**Figure 8-1 D**). If the cutting plane is tangent to one of the sides of the circular cone, we get a straight line (**Figure 8-1 EF**). And if the cutting plane is outside the cone, but touches at point E, we get a point (**Figure 8-1 E**).

The mathematics and other details of these shapes are explained in any elementary book on geometry. All we want to establish at this time is that a structure with the shape of any given one of the conic section be transformed into a different kind of conic section under the

imposition of proper deforming forces. For example: a hyperbolic shape can drift into a parabolic shape; a parabolic shape into an elliptical one; an elliptical into a circular, and a circular into a dot; and many other combinations. Are we far afield from the weather map? Of course not! We are laying the groundwork for analyzing the myriad of configurations that highs and lows take on the surface of the Earth.

Surfaces of Revolution

We now come to **Plateau's surfaces of revolution**, which are surfaces of objects that are symmetrical around an axis. They represent examples of other shapes into which conic sections can be transformed. These other shapes, inevitably, are involved in the shapes of various weather phenomena from the size of huge storms to the size of small clouds. These principles were discovered in 1873 by *Joseph Plateau*. He found that there are only 6 types of symmetrical surfaces that can be formed by oil globules or soap bubbles. A bubble can be blown up into a sphere, or shaped into a plane surface, cylinder, unduloid, catenoid, or nodoid. See **Figure 8-2**.

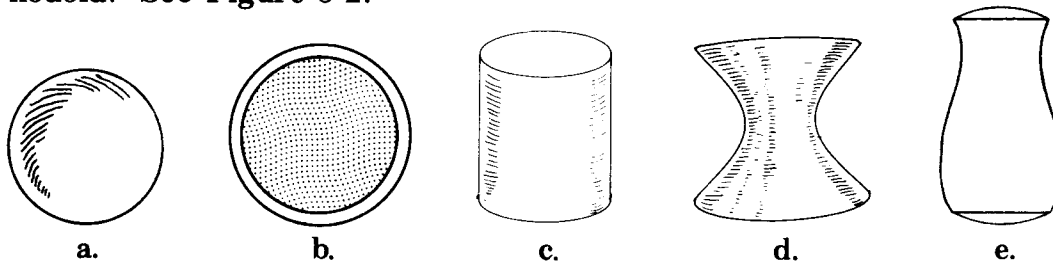


Figure 8-2. Five of the six surfaces of revolution formed by a film of oil or soap. The nodoid is not shown because only sections of it exist in nature.

- a. A soap bubble floating in air forms a sphere.
- b. A ring dipped in a soapy solution will create a plane surface soap film inside the ring.
- c. A soap bubble between two rings can be stretched apart until it takes the shape of a cylinder.
- d. The cylindrical form of the soap bubble is stretched still further to give the shape of a catenoid.
- e. A bubble of oil stretched a proper distance between two rings will cause the lower portion of the cylindrical shape to bulge (due to gravity, surface tension, etc.), thereby forming the unduloid structure.

All these surfaces are related and can easily slip from one to another. The mathematical relationship between them was first shown by *Delaunay* (8) in 1841. He proved that the mathematical curves shown in **Figure 8-3**, which are generated as *roulettes* of the conic sections, can be used to create the shapes of **Figure 8-2**.

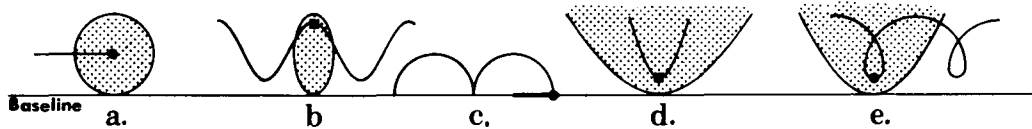


Figure 8-3. Roulettes of five of the conic sections. The conic sections are shaded except for the radius line in c. The dot, in each case, represents the focal point that traces the actual roulette pattern.

- a. Straight line traced by the center of the circle.
- b. Unduloid traced by one focus of an ellipse.
- c. Semi-circle traced by one of the focal points at the end of a straight line.
- d. A catenary traced by the focal point of a parabola.
- e. A nodoid traced by the focal point of a hyperbola.

Take two curves lying in the same plane. Assume one of the curves to be fixed in position (in **Figure 8-3**, the baseline is considered to be the fixed curve). The curve that moves is rolled (no sliding permitted) on the fixed curve. Any point connected with the rolling curve describes a curve called a *roulette*. If we roll a circle, an ellipse, a parabola, a hyperbola, and a short straight line on the baseline, we will get the forms shown in **Figure 8-3**.

If we roll an ellipse on the baseline, either one of its foci will trace a wavy line which is the unduloid—in the figure, we show the curve formed by only one of the foci.

As can be seen in **Figure 8-4**, every ellipse has two axes (one axis passes through the two focal points, with the other axis at right angles to it and passing through the center of the ellipse). We find that the more unequal the length of these axes, the greater will be the swings of the undulation of the roulette. If the two axes are equal, the ellipse becomes a circle. The curve created by the rolling center of a circle is a straight line parallel to the line on which it is rolling. This roulette line, when rotated around the baseline, creates a cylinder. So we can see that the unduloid changes to a cylinder when the ellipse reduces to a

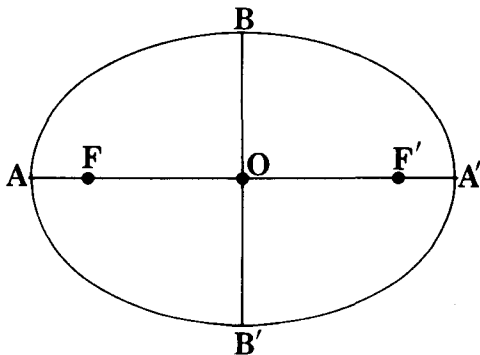


Figure 8-4. An ellipse, where AOA' is called the *major axis*; BOB' is called the *minor axis*; F and F' are the two focal points; and O is the center.

circle. If one axis of the ellipse decreases to zero length but the other axis still has a definite length, then the ellipse is reduced to a straight line with one focus at each end. This generates a roulette of semi-circles. These semi-circles, in turn, rotate around the baseline to create a series of spherical surfaces.

Collapse of Cylindrical Structures

Plateau also proved that a cylinder of liquid is not a structure of stable equilibrium if its length is longer than the circumference (about 3.14 times its diameter). A long cylindrical liquid rod, like in Figure 8-5, if it could be assembled and then left by itself, would immediately collapse into a row of equally sized and equally spaced drops. There is a very simple law that the distance between the centers of the drops is equal to the circumference of the cylinder.



Figure 8-5. A cylinder of liquid can not exist for long if its length is more than approximately 3.14 times its diameter.

In the above example, the cause of collapse would be due, mainly, to surface tension. Surface tension is that property which causes the surface film of all liquids to try and take a form which has the least surface area; in other words, a sphere.

Plateau was able to show by his experiments that any disturbances formed at distances less than the circumference of the cylinder would result in a configuration as in Figure 8-6. The disturbance would affect the curvature of the outside surface in such a way as to make the surface tension push the bulges (shown in the figure) back and pull the hollows outwardly. What if the bulges are farther apart than the circumference of the cylinder? Then the sharper curvature of the skinnier parts will force the liquid in the skinnier part into the parts that are already wider. Thus any such disturbance would cause the bulges to separate still farther, or cause the whole thing to break into drops. Before the break-up occurs, the drops are joined by narrow



Figure 8-6. The liquid cylinder in Figure 8-5 can change to the unduloid shape when it is disturbed.

necks of liquid (**Figure 8-7a**). These narrow necks split themselves up into smaller secondary droplets (**Figure 8-7b**). When dealing with different substances, there will be variations in the actual results obtained. These variations are determined by such things as the viscosity, the inertia of the fluid, etc.

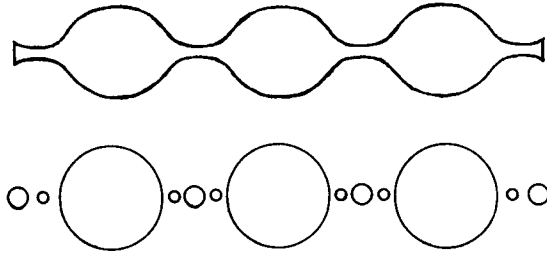


Figure 8-7. Continuation of the break-up of the cylinder of **Figure 8-5**.

Plateau explains the formation of the smaller beads as follows: When contact is nearly broken between two big spheres, there is still a narrow thin neck. The fluid does not flow easily out of this neck into the larger spheres because of internal friction. This thin cylinder now acts like another cylinder, but of smaller circumference. Therefore, it also breaks up when the length becomes greater than the new, smaller circumference. The length is usually such that it breaks at two points. This leaves an end piece attached to each sphere, which is absorbed, and a small sphere in the center. Sometimes the same process of formation of a connecting thread is repeated a second time between the small intermediate bead and the larger sphere. In this case, there are two additional beads of still smaller size on each side of the first small one. This whole process can be observed in a spider web. The thread of a web is formed from a secretion of the spider's glands. It comes out as a semi-fluid cylinder which breaks up into little connected beads which then harden. See **Figure 8-8** for an enlarged view of a strand of spider web.



Figure 8-8. Strand of spider web that has been magnified approximately 200 times.

This process can also be seen in the breaking of a wave against a seashore. As the wave approaches the shoreline, it presents a long, smooth horizontal cylindrical edge. This cylindrical edge breaks up at a given moment into an array of little jets which then subsequently break up into foam. At the same time, we find that the back of the wave which was previously smooth, will have ridges and gullies. The jets are

caused by the breakup of the cylindrical edge, as explained by Plateau, while the ridges between the gullies mark the lines of easier flow determined by the position of the jets. See Figure 8-9.



Figure Figure 8-9. Artist's conception of a breaking wave.

You can take a piece of glass tubing; heat it, and then draw it out. You will form an unduloid portion as in Figure 8-10a. If you blow on the other end, you will form another unduloid of opposite curvature as in Figure 8-10b.



Figure 8-10. A glass tube, where the pattern in a. is produced by pulling the heated glass tube, and b. is produced by blowing into the heated glass.

Wilhelm F. Hofmeister (1824-1877) (9) dipped the long root hairs of a water plant, such as *Trianea*, in a denser fluid containing glycerine. The sap of the cells would diffuse outwards; the protoplasm would separate from the surrounding wall, and then lie loose as a cylinder of protoplasm inside the cell. Soon thereafter, it would show signs of instability and break up into little spherical globules, as shown in Figure 8-11. The narrow surroundings of the spherules prevent them from taking a completely spherical form, giving instead the unduloid pattern trying to separate into spheres. In between, we have the relatively regular beads of smaller size.



Figure 8-11. Break-up pattern of *Trianea*, a water plant, when it is placed in a solution of glycerine.

Spheres, cylinders, and unduloids are the most common shapes among the forms of small single celled organisms—in the processes of growth and decay, they readily transform from one form to another. Figure 8-12 shows some examples.

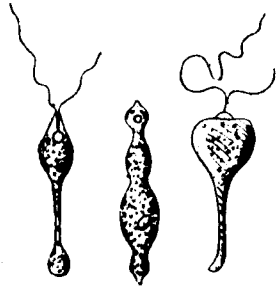


Figure 8-12. Different forms of the flagellate "monad", *Distigma proteus*.

The sphere encloses the greatest volume with the least surface area if there are no outside constraints. On the other hand, some other Plateau configurations are subject to outside constraints, which results in different shapes for the surfaces of minimum area (other than the sphere). These outside constraints may be caused by a pipe which supports a soap bubble; in the case of cells, by partial or complete hardening of the cell walls or surfaces; etc. *Joseph Louis Lagrange* (1736-1813) developed the formula for finding a minimal surface for the boundary of any given closed curve in space. This formula is referred to as the **problem of Plateau**, who solved it with his soap films in 1873.

The Splash of a Drop

This brings us to *A. M. Worthington* (10) and his study of splashes. He points out that what Plateau developed for a straight cylinder of liquid also applies if this straight cylinder is bent into a ring. This ring will break up into a ring of drops.

In another article (11), he showed a series of drawings representing the splash of a drop of mercury 0.15 inch in diameter that fell 3 inches onto a smooth glass plate. **Figure 8-13** is a selection of these drawings that show the progression from a single drop to a final smaller drop in the center surrounded by 12 still smaller drops separated equally from each other at an angle of 30° . The significant feature from the standpoint of weather, is the orderly and systematic angular and circumferential arrangement of the rays (and finally droplets) around the center of the splash.

The Center of a Structure is Related to its Shape

In another area, we find that *Lord Rayleigh* (1842-1919) (12) dealt with the Plateau phenomenon by analyzing its implications on the

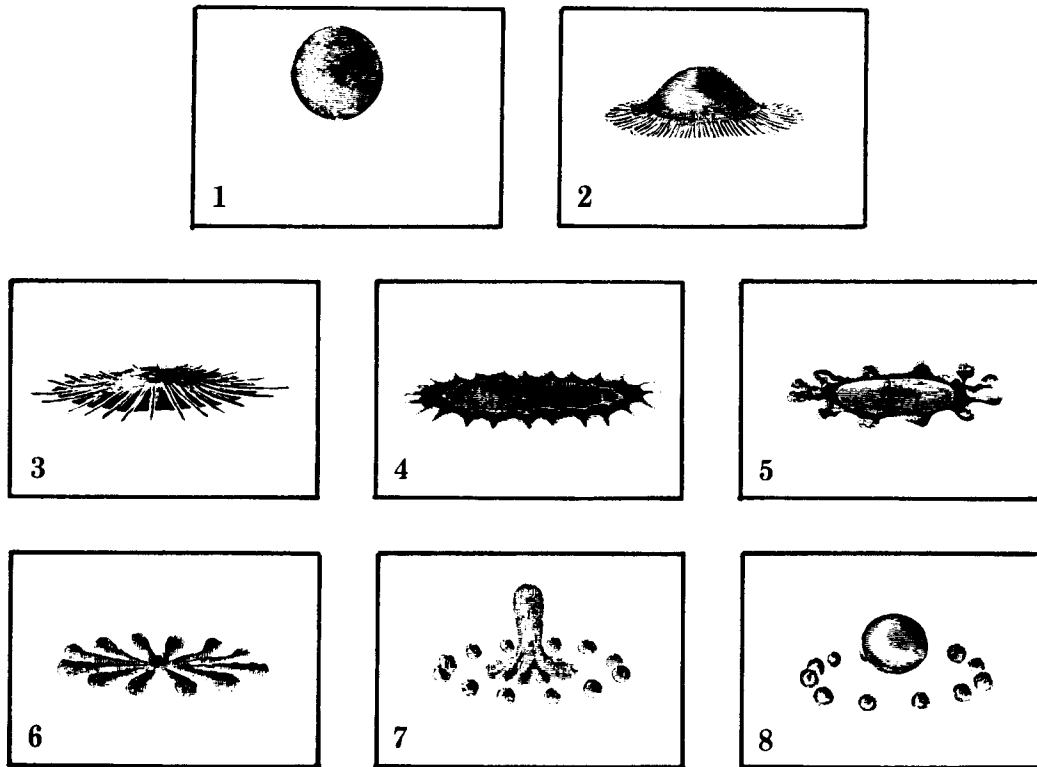


Figure 8-13. A series of time lapse drawings showing the splash of a drop of mercury onto a glass plate.

stability and instability of turbulence. But no one has mentioned how this phenomenon applies to large scale patterns of high and low pressure centers over an entire hemisphere. Of course, there are many different forces involved, but recognizing the conic sections and Plateau's curves are helpful in understanding the shapes of highs and lows as seen on hemispheric weather maps. Locating the exact centers (or focal points) of highs and lows is extremely important, as will be seen in the many charts used to analyze what happened at 1230 GMT, 7 December 1950. Recognizing the type of shape of a vortex is an aid in locating its center. You must keep in mind that the true shape of the Plateau figures on the surface of the Earth are distorted on the polar stereographic map due to the projection.

Chapter 9

The Chladni Figures and Wavenumbers

While investigating the various tones of music, *Ernst Chladni* (1756-1827) made a classic experiment to show the effects of harmonic vibrations. He spread fine sand over a glass or metal plate and set it into vibration with the bow of a violin by scraping the bow along one edge of the plate. The bow would alternately stick and slip in rapid succession on the edge of the plate to create waves of sand (also sound waves). He would hold the plate between his fore finger and thumb; the point where the plate is held is, of course, a node where there can be no movement. The bow sets up waves that move across the plate and then are reflected from the edges. The reflected waves become superimposed on the new waves coming from the bow edge. This results in symmetrical patterns of nodal lines where the plate is not moving. **Figure 9-1** shows square and circular plates that are being held in the center. The type of pattern created depends generally on:

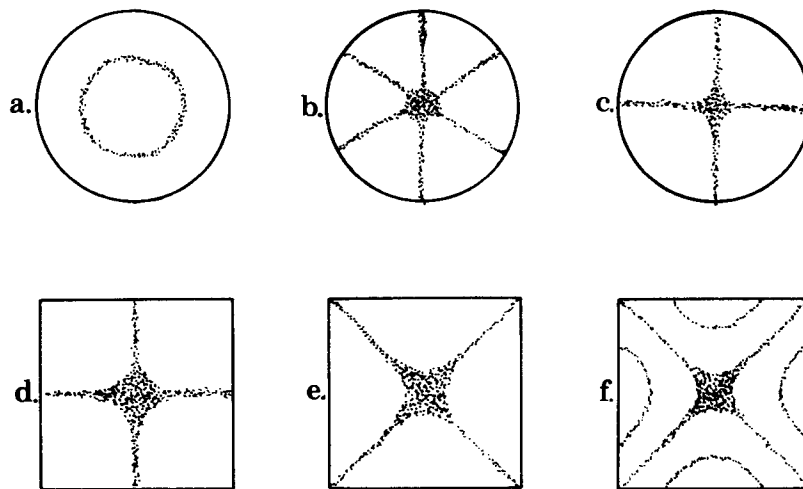


Figure 9-1. Chladni figures showing different vibration patterns for square and circular plates.

the point or points of support and their location; the point where the bow is touched to the plate; the frequency of the vibration which is influenced by the speed the bow is moved; and the properties of the plate itself, such as thickness, volume density, elastic strength, etc.

The symmetry of the Chladni figures is partially determined by the symmetry of the plates chosen. A circular plate can have an infinite number of symmetry lines through the center.

The plate acts like a cymbal or drum and breaks up into vibrating parts separated by the lines which do not move. This is an example of stationary vibration. All the points on one side of a line are moving in opposite direction from the points on the other side of the line (up and down). The sand slides off the moving parts and gathers along the nodal lines.

Two Modes of Vibration

The vibrations of a two-dimensional system can be broken down into two different systematic, types of modes. First, if we consider a circular plate, there can be a set of **nodal diameters** that will give one type of symmetry, as in **Figure 9-2**. In this example, the nodal diameters divide the circular plates into 4, 6, and 8 sectors to give what is known as the **circumferential wavenumber** of 4, 6, 8. Theoretically, the number of diameters can increase to 5, 6, 7, 8, and on to infinity, unless there are restraining forces to prevent a large number of diameters.

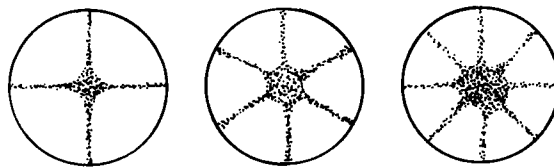


Figure 9-2. Chladni plates with nodal diameters of 2, 3, and 4 which give wavenumbers of 4, 6, and 8 respectively around the circumference. A nodal diameter of 1 does not occur when the edge of the plate is free to move.

Second, there can be a set of **nodal circles**, to give another type of symmetry, as in **Figure 9-3**. Nodal circles divide the circular plate into 2, 3, 4, 5, 6, etc. rings, to give what is the **radial wavenumber** of 2, 3, 4, 5, 6, etc.

We can also have nodal diameters and circles occurring simultaneously as shown in **Figure 9-4**.

The Chladni Figures and Wavenumbers

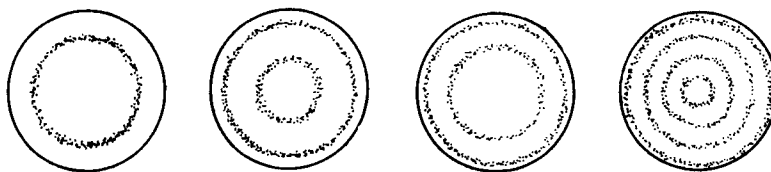


Figure 9-3. Chladni plates with nodal circles only, that divide the plates into 2, 3, 4, and 5 parts.

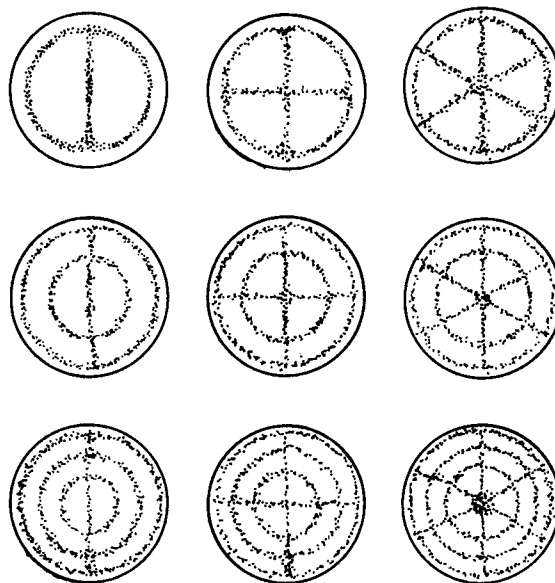


Figure 9-4. Various combinations of circumferential and radial wavenumbers occurring simultaneously.

As a matter of interest, **Figure 9-5** shows a three-dimensional perspective view of some of the patterns of vibration of a clamped circular plate used in telephone receivers and small condenser microphones.

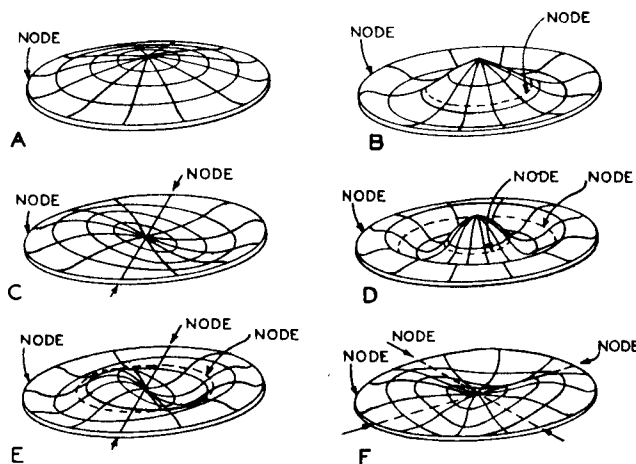


Figure 9-5. Modes of vibration of a clamped circular plate. Courtesy of *Harry F. Olsen*, **Musical Engineering**, McGraw-Hill Book Co., Inc., 1952.

What we see on the Chladni type plates is none other than the same phenomena described by wavenumber earlier in **Figure 5-2**. This time, however, we have two separate wavenumbers operating simultaneously: the circumferential wavenumbers represented by **Figure 9-2**; and the radial wavenumbers (nodal circles) shown by **Figure 9-3**. In addition, the Chladni plates are nothing but another manifestation of Plateau's surfaces of revolution. The different, three-dimensional shapes that form on a flat circular plate behave in a similar manner, even though different forces are involved. In this case however, the plates do not break up into small drops due to the high tensile strength of the materials of which it is constructed.

The phenomena that we associate with weather, such as winds, clouds, precipitation, etc., take place in a relatively thin film of air above the surface of the Earth. This thin film of air resonates in a manner similar to the vibrating Chladni plates. At any given time of the year, there is an equatorial belt insulating some of the weather activity in one hemisphere from the weather activity in the other hemisphere. Therefore, we will analyze only one hemisphere, the Northern hemisphere, due to the Equatorial separation in some of the weather effects, and due to the lack of data, and in order to simplify this first presentation, ever, of the charts shown in the latter part of this book.

Some Differences between the Hemispheric Cap of Air and Chladni Plates

A disturbance set up along the circumference of a circular Chladni plate will propagate automatically to the diametrically opposite side. This serves to prevent odd wavenumbers, since there is always a matching wave for any given wave, due to the stiffness of the metal plate, among other reason.

The thin film of air over the Earth is not a flat, solid plate as in the Chladni experiments. The film of air in which the main weather phenomena take place is hemispherically shaped, immensely flexible or elastic, extremely mobile, and slippery. Therefore, a disturbance along the circumference of a group of geometrically related vortexes will not always propagate or show up as a resonant disturbance on the diametrically opposite side (you will see clusters of vortexes spaced in a circular arc around a central vortex, in the upcoming charts). This

means that odd wavenumbers of the type shown in **Figure 9-6**, are possible in weather phenomena. Nevertheless, there are many times when a disturbance on the circumference of a group of geometrically related vortices will show resonant waves at a diametrically opposite end. This type of situation can be considered as occurring wherever we see three vortices lined up in a straight line. The vortex in the middle can be considered as being the center of the geometrical configuration. We will see a number of these features in my chart series.

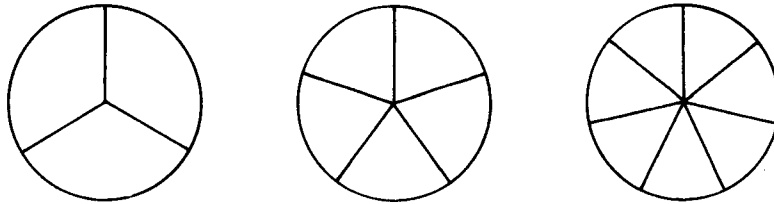


Figure 9-6. Odd wavenumbers of 3, 5, and 7 along the circumference of a circular configuration.

Chapter 10

Quantum Units and Angular Numbers

Everything is Packaged in Quantum Units

Everything in the Universe comes in packages (quantum units), large or small. Everything comes in a fixed range of sizes from one extreme, where it is never found in a smaller size; to the other extreme, where it is never found in a larger size. This applies to eggs, oranges, dogs, cats, men, women, and even stars in the heavens, etc. These larger packages or quantum units, can always be broken up into smaller elementary quantum units. It is useful to enumerate what some of these smaller units are. We will list them like this:

1. The elementary particles, such as the **proton**, **neutron**, and **electron**, are small structural units.
2. The **atom** is the smallest structural unit that matter can be divided into without changing the properties of the matter. The different atoms, of course, are built up of different numbers and combinations of protons, neutrons, and electrons.
3. The **molecule** is the smallest structural unit into which a chemical substance can be subdivided and still have the properties of the substance.
4. The **crystal** occurs when the molecules of any solid material are arranged in a fixed geometric pattern.
5. The energy of an electromagnetic wave (such as a light wave, radio wave, etc.), is quantized into small bundles called **photons**.

So everything is made up of varying numbers of the same type of "bricks", but in varying sizes and varying geometric shapes.

Some Factors that Determine the Size of an Object

The actual size of an object is determined by the forces acting on the object. We find that all living cells, depending on what type they are,

vary little from a certain average size, and no cell can grow larger than a certain absolute magnitude. Some factors that can limit their size are: gravity, surface tension, heat, light, etc. It has also been shown that there is a limit to the amount of cytoplasm that can surround a living nucleus, and that the nucleus itself has a limitation to its size.

One of the factors limiting the size of a human body is the circulatory system, which can keep the body warm or cool only within certain size limitations. Another factor limiting size is the ability of the bones and muscles to support the body weight against the force of gravity. Beyond a certain absolute size, the body would become immobile, or the supporting structure of bones and muscle would collapse.

In a similar manner, the stars are also found to be limited to a certain size range. It is a surprising fact that the mass of stars and even nebulae all fall within the average range of 10^{10} grams of matter per star. Gravitation draws matter in towards the star center, but the radiation outward is an opposite force leading to the disintegration of the star. The two forces approximately balance each other to keep the amount of matter in the average range while the star is in existence.

Some Factors Determining the Quantum Sized Vortex on a Surface Weather Map

In the face of all the evidence throughout the Universe that most things come in packages, large or small, it would be surprising if weather vortexes did not show a minimum size limit and that larger sized highs and lows would be multiples of the minimum or quantum-sized vortex. One of the factors for the limiting quantum size of a high or low would certainly be linked to the depth of the atmospheric layer of air (which varies with the temperature among other reasons). We must keep in mind that the temperature of a column of air (and the subsequent depth of the atmosphere) varies greatly from winter to summer, and from polar regions to the equatorial zone. You may recall from **Chapter 4**, that Bénard found the diameter of the cells to be approximately 3 times their depth, so that if the depth of the liquid varied, the cells diameters also varied.

The surface of the Earth is completely covered every day with highs and lows—the total number must always be a whole, rational number, since there is no such thing as a part of a high or low. The smallest high

or low on a surface hemisphere map (above the equatorial belt at any given point in time could be considered as the elementary quantum unit. Any other high or low on the map would be of a size that is equal to, or 2, 3, 4, 5, etc., times as big as the fundamental vortex. If a map were to be magnified and drawn showing more detail than is shown on the hemispheric map, you would find in many situations, a group of tiny vortexes instead of one single large vortex. The single large vortex that is shown on the map, in this case, is the center around which the other vortexes cluster. Every other vortex center that is stationed in any other location on the Earth will react to the effects of the cluster of vortexes as if it were indeed, a lone vortex with only one center; since the air is generally rising upwards over the whole area of the cluster. So we would find that there would be a whole number of smaller sized quanta units inside the single main vortex—in the same manner as molecules being made up of atoms, and they in turn, being made up of protons, electrons, and neutrons. Smaller sized units (too small to be shown on a hemispheric polar stereographic map) can break the minimum sized units that are actually drawn on the polar stereographic map into 2, 3, 4, 5, etc., parts, exactly, depending on the situation. I do not consider it unreasonable to say that this process of subdividing larger units can be continued right on down to the spacing of clouds.

The concept of a minimum quantum size for vortexes has been very useful to me in my investigations and has been one of the theoretical underpinnings that helped me develop the charts that you will soon be looking at (if you haven't already). I may not have the final explanation in this matter, but many new discoveries have been made, nevertheless, at times, by using partially correct theoretical knowledge. This in turn led to a further advance in the understanding of a given problem. This new advance sometimes altered the original theories on which the advance was made. The concept of quantum-sized vortexes, while useful in explaining some features of the charts, is not vital to the understanding of the charts, which show the spatial arrangement of vortexes (regardless of size).

Some further thoughts on the quantum principle. Oranges can grow from a tiny size to a nice fat, juicy shape. Likewise, a high or low can grow from a tiny disturbance of a few miles (or even smaller), to one

that stretches for thousands of miles. The principle of quantum size, as I visualize it, is that there are preferred sizes for a given vortex. If the vortex is not a quantum size, then it will change very rapidly (by pulses of growth or decay) to the next higher or lower quantum size (which can be 1, 2, 3, etc., times the basic quantum unit). This reminds us of the Chladni plates where the sand slid rapidly to the nodal positions when the plate was vibrated.

“Diffraction Grating” for Finding the Quantum Vortex and also for Exposing Simple Geometric Configurations

Wave numbers can be thought of as wave lengths or wave distances, since we are breaking a circumference up into a certain number of parts when we calculate wave number. Each part of the circumference represents an actual distance. When converting wavenumbers into distances on a polar stereographic map, we express the distance in degrees of latitude. One degree of latitude always represents the same distance of 60 nautical miles anywhere on the map. We don't use degrees of longitude to measure distance, because distance between any two longitude lines varies when going from the pole to the equator.

When we look at the weather map for 7 December 1950, we find that the closest distance between any two vortexes (high or low) is in the range of approximately 3.75 degrees of latitude. Vortex centers #83 and #84 are separated by approximately 3° (see the **Identification map**, pg 109); while #66 is 4.3° from #65, and 4.1° from #67. We see that the vortexes represented by points #65, #66, #67 do not look like closed circular shapes as drawn on the map. There should be no confusion for those readers who have little acquaintance with weather maps, since every high or low of any size, always has a closed circular type of pattern, even though a map may not show all the fine details. A more detailed description of the charts is given in the next chapter. I have found that the 3.75° distance is close to what seems to be the smallest quantum unit of spacing between any two vortex centers in the winter season (since fundamental sizes are likely to vary with changes in temperature).

In 1912, *Max Laue* (1879-1960) came to the conclusion that X-rays were really very short light waves, and the length of the light waves was in the same range as the distance between the atoms in a crystal.

Friedrich and Knipping carried out the experiment which showed that X-rays are waves and crystals are regular arrays of atoms spaced at equal distances apart. They developed a tool that measured the distance between the atoms, which at the same time served to measure the length of the light wave. This tool is the well-known **diffraction grating**, which is a system of close, equidistant, parallel lines ruled on a polished surface. Laue suspected the spacing of the atoms in advance; he said that the wavelength of X-rays would fit neatly into the spaces between the atoms.

Since the closest spacing between any two vortex centers seems to be in the neighborhood of 3.75° , we have a clue as to what wavelength to use for making a tool (similar in principle to the diffraction grating) for analyzing the angular separation between 3 or more vortex centers and the radial spacing between centers. I have found that the use of 1.875° (half of 3.75°) will give greater detail, since half the distance between any two vortex centers can be considered as the radial distance of each of the vortices in the direction of the line joining them. See **Figure 10-1**.

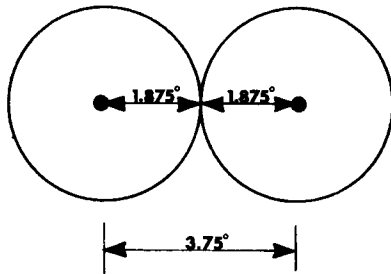


Figure 10-1. Half the distance between two vortex centers will give an indication of the radius of each vortex.

If we divide the 360° circumference of a circle by 1.875° , we get a wavenumber of 192. **Table VI** gives the value in degrees of each of the 192 divisions. We note that the angles of 30° , 60° , and 120° (and their submultiples) occur in this table and also the angles of 45° , 90° , and 180° (and their submultiples). These, of course, are the angles that occur in triangular, square, and hexagonal configurations, as can be seen in **Figures 10-2 through 10-6**. The occurrence of these angles on a weather map would be one of the indications that a regular geometric shape exists.

Figure 10-2 shows three imaginary vortices arranged in a triangular formation. We will find the angles of 60° prevailing between their centers when they are in an equilibrium position with regard to each other.

TABLE VI

01•01.875	33•061.875	65•121.875	097•181.875	129•241.875	161•301.875
02•03.750	34•063.750	66•123.750	098•183.750	130•243.750	162•303.750
03•05.625	35•065.625	67•125.625	099•185.625	131•245.625	163•305.625
04•07.500	36•067.500	68•127.500	100•187.500	132•247.500	164•307.500
05•09.375	37•069.375	69•129.375	101•189.375	133•249.375	165•309.375
06•11.250	38•071.250	70•131.250	102•191.250	134•251.250	166•311.250
07•13.125	39•073.125	71•133.125	103•193.125	135•253.125	167•313.125
08•15.000	40•075.000	72•135.000	104•195.000	136•255.000	168•315.000
09•16.875	41•076.875	73•136.875	105•196.875	137•256.875	169•316.875
10•18.750	42•078.750	74•138.750	106•198.750	138•258.750	170•318.750
11•20.625	43•080.625	75•140.625	107•200.625	139•260.625	171•320.625
12•22.500	44•082.500	76•142.500	108•202.500	140•262.500	172•322.500
13•24.375	45•084.375	77•144.375	109•204.375	141•264.375	173•324.375
14•26.250	46•086.250	78•146.250	110•206.250	142•266.250	174•326.250
15•28.125	47•088.125	79•148.125	111•208.125	143•268.125	175•328.125
16•30.000	48•090.000	80•150.000	112•210.000	144•270.000	176•330.000
17•31.875	49•091.875	81•151.875	113•211.875	145•271.875	177•331.875
18•33.750	50•093.750	82•153.750	114•213.750	146•273.750	178•333.750
19•35.625	51•095.625	83•155.625	115•215.625	147•275.625	179•335.625
20•37.500	52•097.500	84•157.500	116•217.500	148•277.500	180•337.500
21•39.375	53•099.375	85•159.375	117•219.375	149•279.375	181•339.375
22•41.250	54•101.250	86•161.250	118•221.250	150•281.250	182•341.250
23•43.125	55•103.125	87•163.125	119•223.125	151•283.125	183•343.125
24•45.000	56•105.000	88•165.000	120•225.000	152•285.000	184•345.000
25•46.875	57•106.875	89•166.875	121•226.875	153•286.875	185•346.875
26•48.750	58•108.750	90•168.750	122•228.750	154•288.750	186•348.750
27•50.625	59•110.625	91•170.625	123•230.625	155•290.625	187•350.625
28•52.500	60•112.500	92•172.500	124•232.500	156•292.500	188•352.500
29•54.375	61•114.375	93•174.375	125•234.375	157•294.375	189•354.375
30•56.250	62•116.250	94•176.250	126•236.250	158•296.250	190•356.250
31•58.125	63•118.125	95•178.125	127•238.125	159•298.125	191•358.125
32•60.000	64•120.000	96•180.000	128•240.000	160•300.000	192•360.000

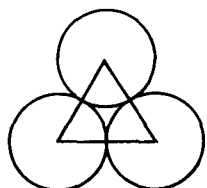


Figure 10-2. Three imaginary vortices (drawn as circles) in a stable equilateral formation.

Next, we will look at angles formed by the centers of four regularly arranged vortices. There are two ways in which four vortices can come together, as shown in Figure 10-3. In Figure 10-3a, we find the angles of 90° and 45° predominating, while in Figure 10-3b, we find the angles of 60° and 120° predominating, which is the stable condition.

If we have a nuclear or central vortex, we find that there are two general arrangements possible, as in Figure 10-4. In 10-4a, we find an extension of the square formation (Figure 10-3a) with the angles of 90°

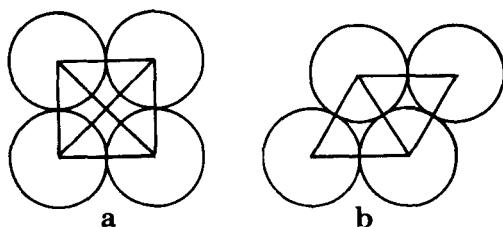


Figure 10-3. Two different regular arrangements of four vortices, drawn as circles, showing the different angles formed between their centers.

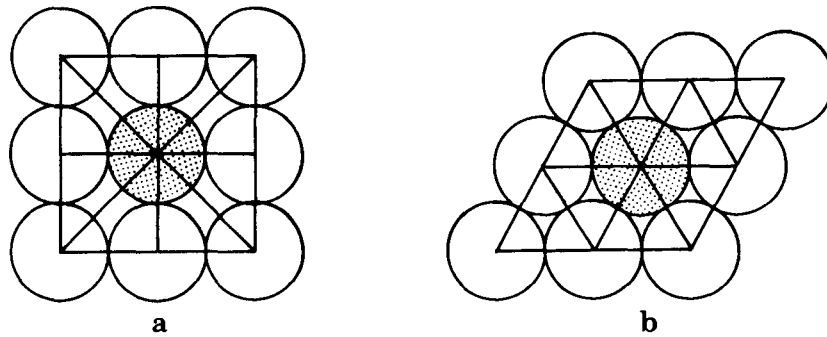


Figure 10-4. The angular relationships for two different regular arrangements of vortices around a central vortex.

and 45° predominating. And in 10-4b, we have the nuclear hexagonal arrangement with the angles of 120° and 60° predominating.

In **Figure 10-5**, we show the arrangement of 5 vortices in a pentagonal form.

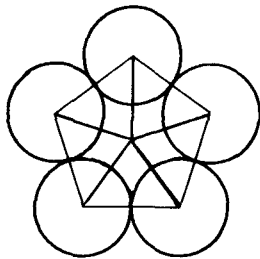


Figure 10-5. In the pentagonal arrangement, we find angles of 72° .

There are many permutations and combinations possible, but I will show one more common configuration in **Figure 10-6**, which shows a variation of 4 vortices in a formation, but with 4 other vortices nesting in the square formation in an outer ring, giving an octagonal array.

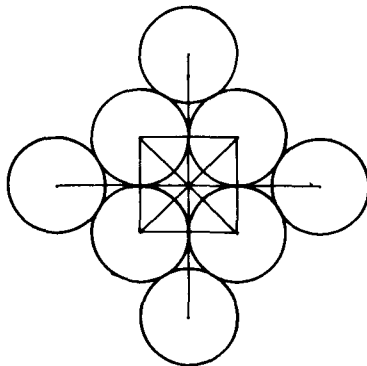


Figure 10-6. Four vortices in a square array, with four others nesting in the square formation in an outer ring, giving an octagonal array.

Construction of the Weather Tool

After this diversion into angular formations, we now turn to the actual construction of a tool that can be used on a weather map. See

Figure 10-7 for a reduced view of the tool, which is a protractor covering the full 360° circle with the unique feature of being divided into sectors that are all equal to 3.75° . The angle of 1.875° has been chosen as the harmonic element to test for resonance. The reason for using the 3.75° spacing, instead of the 1.875° spacing, is that it reduces the clutter of too many lines, especially near the center.

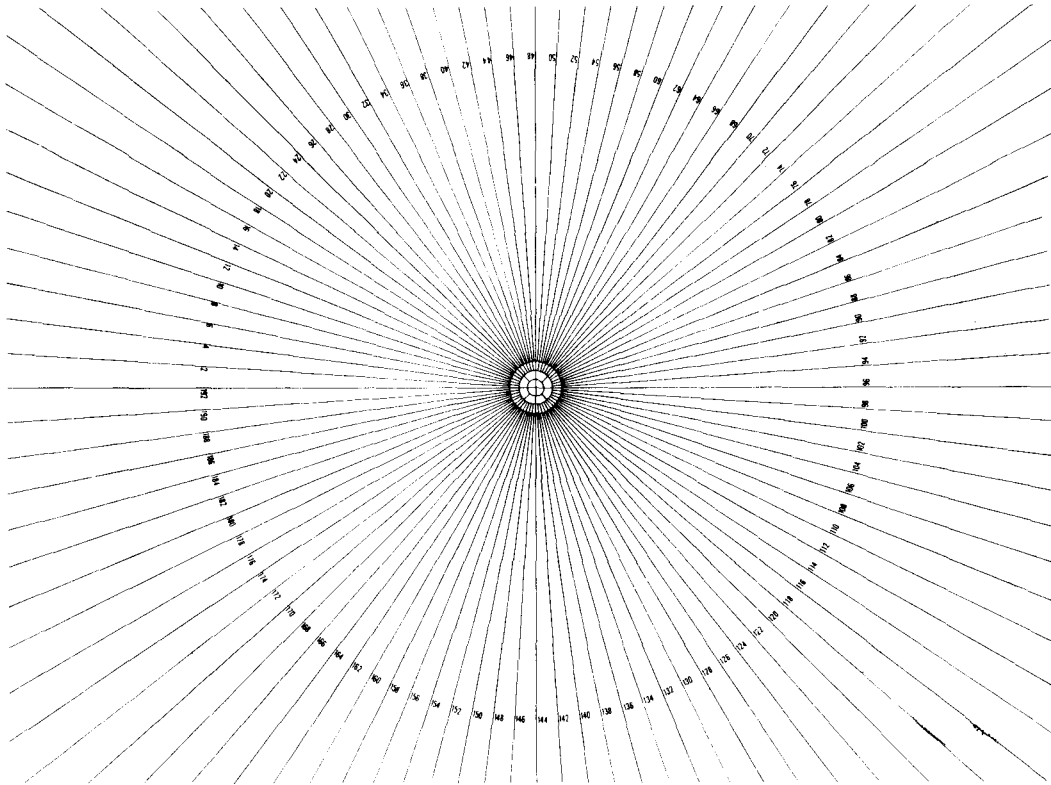


Figure 10-7. A reduced view of the “diffraction” tool used to construct the charts in this book.

This tool, consisting of a transparency, may seem disarmingly simple. The unique feature, as you will shortly see, is that it is a “diffraction grating”, or “tuning fork”, if you please, for the weather map. If I did not introduce this tool, you would find the examples I show in the succeeding pages to be intriguing, but you would be baffled if you attempted to duplicate the results. You would wonder how the accuracy shown could be obtained with the commonly available protractor.

Other Possible Weather Tools

There are other types of “diffraction gratings” that can be constructed for a weather map if we use a different wavelength. If we

use a minimum wavelength of 2.25° , we get a wavenumber of 160. Table VII gives the value in degrees of each of the 160 divisions. In this table, we note the angles of 36° , 72° , 108° and all their submultiples. These are the angles that occur in pentagonal configurations. We also find the angles of 22.5° and 180° etc., which also occur in Table VI.

TABLE VII

01•02.25	33•074.25	65•146.25	097•218.25	129•290.25
02•04.50	34•076.50	66•148.50	098•220.50	130•292.50
03•06.75	35•078.75	67•150.75	099•222.75	131•294.75
04•09.00	36•081.00	68•153.00	100•225.00	132•297.00
05•11.25	37•083.25	69•155.25	101•227.25	133•299.25
06•13.50	38•085.50	70•157.50	102•229.50	134•301.50
07•15.75	39•087.75	71•159.75	103•231.75	135•303.75
08•18.00	40•090.00	72•162.00	104•234.00	136•306.00
09•20.25	41•092.25	73•164.25	105•236.25	137•308.25
10•22.50	42•094.50	74•166.50	106•238.50	138•310.50
11•24.75	43•096.75	75•168.75	107•240.75	139•312.75
12•27.00	44•099.00	76•171.00	108•243.00	140•315.00
13•29.25	45•101.25	77•173.25	109•245.25	141•317.25
14•31.50	46•103.50	78•175.50	110•247.50	142•319.50
15•33.75	47•105.75	79•177.75	111•249.75	143•321.75
16•36.00	48•108.00	80•180.00	112•252.00	144•324.00
17•38.25	49•110.25	81•182.25	113•254.25	145•326.25
18•40.50	50•112.50	82•184.50	114•256.50	146•328.50
19•42.75	51•114.75	83•186.75	115•258.75	147•330.75
20•45.00	52•117.00	84•189.00	116•261.00	148•333.00
21•47.25	53•119.25	85•191.25	117•263.25	149•335.25
22•49.50	54•121.50	86•193.50	118•265.50	150•337.50
23•51.75	55•123.75	87•195.75	119•267.75	151•339.75
24•54.00	56•126.00	88•198.00	120•270.00	152•342.00
25•56.25	57•128.25	89•200.25	121•272.25	153•344.25
26•58.50	58•130.50	90•202.50	122•274.50	154•346.50
27•60.75	59•132.75	91•204.75	123•276.75	155•348.75
28•63.00	60•135.00	92•207.00	124•279.00	156•351.00
29•65.25	61•137.25	93•209.25	125•281.25	157•353.25
30•67.50	62•139.50	94•211.50	126•283.50	158•355.50
31•69.75	63•141.75	95•213.75	127•285.75	159•357.75
32•72.00	64•144.00	96•216.00	128•288.00	160•360.00

If we use still another minimum wavelength of 2.8125° , we get a wavenumber of 128 for 360° . Table VIII gives the value in degrees of each of the 128 divisions. In this table, we find the angles of 45° , 90° , 180° , and their submultiples.

Upon examination, we find that many of the angles in Table VI also appear in Table VII, but more of them appear in Table VIII. The angles of Table VII are the angles associated with the pentagon. While there undoubtedly are some pentagonal formations present to help fill the space on the surface of the hemisphere, they are not as numerous as the common space fillers, such as the hexagon, the equilateral triangle, the square, and their various manifestations and complications.

TABLE VIII

01•02.8125	33•092.8125	65•182.8125	097•272.8125
02•05.6250	34•095.6250	66•185.6250	098•275.6250
03•08.4375	35•098.4375	67•188.4375	099•278.4375
04•11.2500	36•101.2500	68•191.2500	100•281.2500
05•14.0625	37•104.0625	69•194.0625	101•284.0625
06•16.8750	38•106.8750	70•196.8750	102•286.8750
07•19.6875	39•109.6875	71•199.6875	103•289.6875
08•22.5000	40•112.5000	72•202.5000	104•292.5000
09•25.3125	41•115.3125	73•205.3125	105•295.3125
10•28.1250	42•118.1250	74•208.1250	106•298.1250
11•30.9375	43•120.9375	75•210.9375	107•300.9375
12•33.7500	44•123.7500	76•213.7500	108•303.7500
13•36.5625	45•126.5625	77•216.5625	109•306.5625
14•39.3750	46•129.3750	78•219.3750	110•309.3750
15•42.1875	47•132.1875	79•222.1875	111•312.1875
16•45.0000	48•135.0000	80•225.0000	112•315.0000
17•47.8125	49•137.8125	81•227.8125	113•317.8125
18•50.6250	50•140.6250	82•230.6250	114•320.6250
19•53.4375	51•143.4375	83•233.4375	115•323.4375
20•56.2500	52•146.2500	84•236.2500	116•326.2500
21•59.0625	53•149.0625	85•239.0625	117•329.0625
22•61.8750	54•151.8750	86•241.8750	118•331.8750
23•64.6875	55•154.6875	87•244.6875	119•334.6875
24•67.5000	56•157.5000	88•247.5000	120•337.5000
25•70.3125	57•160.3125	89•250.3125	121•340.3125
26•73.1250	58•163.1250	90•253.1250	122•343.1250
27•75.9375	59•165.9375	91•255.9375	123•345.9375
28•78.7500	60•168.7500	92•258.7500	124•348.7500
29•81.5625	61•171.5625	93•261.5625	125•351.5625
30•84.3750	62•174.3750	94•264.3750	126•354.3750
31•87.1875	63•177.1875	95•267.1875	127•357.1875
32•90.0000	64•180.0000	96•270.0000	128•360.0000

We will shortly make an analysis of the weather at 1230 G.M.T. on 7 December 1950, in which we consider 104 disturbances, large and small, occurring in the Northern Hemisphere. There are many smaller or obscure disturbances occurring over the hemisphere that have not been entered or considered, due only to lack of accurate data with which to make calculations. All 104 (and the additional ones that are not analyzed) are like players in a symphony orchestra, each with his or her own instrument. How do we bring order out of the large array of waves that are being generated simultaneously? We use the principles of harmonic analysis—not statistics.

The 1.875° angle is used in two ways: First, as the harmonic element to test for resonance with other vortexes along the radial distance outward from a vortex; and second, along the circumference of any appropriate circular ring. Refer back to Figure 9-4, for a visual picture. The use of the other two harmonic elements shown in Table VII and VIII (or others that may come to mind) would expose formations of interest, but they are not shown to keep this book from becoming too fat

and monstrous. Keep in mind, one of the main purposes of this first book is to establish, beyond any doubt, that there is an undreamt of order in the arrangement of all the features on a surface weather map. Order of a magnitude that no one in the field of meteorology thought was even possible, and would certainly seem difficult to prove with an ordinary surface weather map that was drawn prior to the advent of computers and satellites. The charts I show in this book can only give a glimpse of a few of the "beasts" that almost seem alive as they roam about the surface of the Earth to give us the weather we experience.

Chapter 11

General Explanation of the Charts

Why December 7, 1950 was Chosen for Analysis

The title of this book, perhaps, should have been: “Whatever Happened to the Weather over the Northern Hemisphere at 1230 G.M.T., 7 December 1950?”. I chose that moment in time to show the order and the symmetry of weather patterns. The type of regularity shown is present all the time, continuously, and has been present ever since the Earth has had its atmosphere; and will exist for as long as the Earth cares to remain in one piece with an atmosphere. This regularity also exists on all the planets in the Universe that have an atmosphere.

Nevertheless, the date of December 7, 1950 was chosen for two special reasons. First, and foremost, there were no satellite observations or computer calculations available to draw and interpret the maps of 1950. I wanted to show that uncanny regularity and accuracy of the weather maps was present, even though the skilled analysts who drew the maps, at the time, did not fully appreciate how good they were. Second, a map was chosen with a significant number of highs and lows for which a center could be defined with a minimum of controversy. There are many days in the series of Historical Weather Maps where the centers of the highs and lows are difficult to define. This difficulty may be due to the distorted shapes of some of the weather systems, or the failure of the analysts to identify the pressure centers exactly—they never considered the centers to be that important—this attitude is still held by most present day meteorologists. There are many other days that could have been used quite satisfactorily, instead of December 7, 1950, but I chose it simply because it seemed the best of the first seven days, when I started checking that month.

Why June 6, 1944 was Chosen

I also include a short analysis for 1230 G.M.T., June 6, 1944, the date of the invasion of Europe by the Allied Forces in World War II. The importance of the weather forecast for that day is well known and it has been analyzed and reanalyzed many times over. The analysis that I show has never been made or seen before.

I chose the date of June 6, 1944 to show that the day of December 7, 1950 was not unique, if any of my readers should wonder. In addition, we gain the insight that the principles established for a wintry day in December, are the same in the month of June. I have personally checked every recognizable pressure center for every day of every Historical Weather Map for all the months from August to March, inclusive, for all the years 1940 to 1965. I have found that the same rules illuminated in the examples of this book always apply; you might have to scratch your head occasionally, but everything is always in order.

Some Rules Followed in the Drawing of the Charts

Some general, preliminary information, will help in understanding how the charts for December 7 were constructed. In the **Identification Map** (page 109), a number has been assigned to every high, low and col, that I have chosen to use in the charts. There are additional points on the map that could have been included, but were not for the following reasons:

1. Because their centers are poorly defined.
2. Because of the additional cost in time, labor, and materials to make extra charts and to explain them.
3. Because their use would not alter the major conclusions that are developed by the examples shown.

The order in which the numbers were chosen and the pattern formed by the numbers have no special significance. It was Daniel Bender's suggestion to start the numbers at the top and work down.

In the charts, lows, highs, or cols will usually be referred to, only, by a given number. For example, high number 58 will be referred to simply as #58; low number 76 will be referred to as #76, without designating it as a low; likewise, the col at point number 52 will be referred to as #52.

R MAP
HISPHERE
030 GMT

STATION MODEL
ATIONS SHIP STATIONS

Dsvs
CM PPP
NPP
TTC N NR,
(TTC) h
NAME OR IRAS NO.

Page 109

Register crosses are used in the **Identification Map** to show the actual location of the centers for a given high, low, or col.

Table IX is a listing of the latitude and longitude for each of the 104 points chosen. These numerical values were measured on the master chart used to construct the charts in this book. The register crosses in the **Identification map** were located carefully, but the values indicated in the table take priority for accuracy in all cases. The actual values that were chosen depended on a multitude of factors and principles. It is not possible to present all of the principles used in this first opening book. Nevertheless, I can not lay claim to infallibility as to the locations of the

TABLE IX

#	Lat.	Long.	#	Lat.	Long.	#	Lat.	Long.
1	8.4N	126.7E	36	61.1N	12.7E	71	74.1N	88.0W
2	6.7N	104.5E	37	62.7N	27.1E	72	65.3N	109.1W
3	23.3N	105.3E	38	68.0N	25.5E	73	61.9N	113.0W
4	25.1N	91.7E	39	72.5N	21.8E	74	53.9N	125.4W
5	22.5N	84.3E	40	75.9N	52.8E	75	66.4N	126.2W
6	17.0N	76.8E	41	71.1N	61.5E	76	55.3N	145.2W
7	23.7N	58.5E	42	68.1N	64.7E	77	45.0N	172.0W
8	17.8N	53.9E	43	71.0N	96.2E	78	37.5N	173.5W
9	2.8N	33.4E	44	80.7N	75.0E	79	28.0N	142.1W
10	14.8N	36.9E	45	81.0N	97.0E	80	27.1N	131.1W
11	16.5N	38.9E	46	58.6N	145.2E	81	38.0N	124.2W
12	34.1N	28.0E	47	39.0N	144.2E	82	37.6N	109.9W
13	42.8N	33.4E	48	44.6N	149.7E	83	45.0N	112.8W
14	42.1N	44.8E	49	48.1N	163.2E	84	48.0N	112.4W
15	48.5N	62.1E	50	51.1N	64.5E	85	48.8N	115.6W
16	50.9N	65.7E	51	53.2N	165.3E	86	55.6N	74.7W
17	51.8N	77.7E	52	60.2N	174.1W	87	53.3N	71.0W
18	52.2N	84.3E	53	66.5N	170.0E	88	50.8N	68.3W
19	51.9N	91.6E	54	69.2N	171.3W	89	45.2N	44.4W
20	28.2N	122.9E	55	76.2N	178.0E	90	28.4N	48.0W
21	27.1N	134.9E	56	80.0N	152.8E	91	38.6N	84.1W
22	34.7N	133.3E	57	77.2N	140.0W	92	41.5N	86.1W
23	43.4N	129.4E	58	82.9N	120.5W	93	43.6N	91.0W
24	46.8N	132.0E	59	76.3N	56.2W	94	35.1N	97.4W
25	55.0N	115.0E	60	67.6N	26.8W	95	32.2N	105.2W
26	51.3N	110.3E	61	43.0N	5.8W	96	27.8N	105.9W
27	58.0N	104.5E	62	32.8N	23.2W	97	22.2N	103.3W
28	59.9N	47.0E	63	41.5N	24.9W	98	23.0N	94.9W
29	50.4N	35.3E	64	42.0N	34.0W	99	28.9N	93.8W
30	35.0N	7.1E	65	48.0N	31.4W	100	20.1N	71.3W
31	38.1N	6.9E	66	49.0N	25.1W	101	12.2N	77.8W
32	41.0N	6.9E	67	46.9N	19.8W	102	11.9N	83.9W
33	48.7N	11.7E	68	71.1N	66.3W	103	14.1N	91.1W
34	55.2N	3.0E	69	68.4N	78.0W	104	13.5N	109.5W
35	59.0N	2.5W	70	66.0N	84.8W			

General Explanation of the Charts

centers (especially for the obscure points), and further analysis might lead to slight alterations. Nevertheless, the accuracy of **Table IX** can be seen from the wide range of symmetry patterns developed in the charts. These symmetry patterns could not exist or would be distorted to unrecognizable shapes, if there were any significant errors.

Some Unusual Aspects of the Charts

It may come as a surprise to you that the symmetry patterns shown in the charts are not affected by location in mountainous terrain or in the open sea; that patterns are also not affected by the size, shape, intensity, or distance between the highs and lows that make up the elements of the symmetry patterns. This is not to say that the type of symmetry that occurs has not been caused or influenced by these factors. These symmetry patterns reach out in all directions across the hemisphere, regardless of their cause or causes.

Other features of the weather maps, such as troughs, ridges, and cols are also part of some type of symmetry pattern. As a matter of fact, every change in curvature of the isobars on the surface chart fit precisely into some symmetry pattern—this, however, is not proven in this book.

Some Simple Definitions of Simple Weather Terms

A few definitions are in order for those of you who are not hard-core meteorologists. **Isobars** are lines that are drawn on charts to indicate points of equal barometric pressure along a surface of constant height. This surface can be sea level or any level at any height desired above sea level. The winds usually blow at some relatively small angle with respect to these isobaric lines, so that an isobaric pattern is a general indication of the direction the wind is blowing. A **trough** is a change of curvature in the isobars where the wind that blows along the isobars moves in a counterclockwise direction. A **ridge** is also a change of curvature in the isobars where the wind that blows along the isobars moves in a clockwise direction. A **col** is a point where there is no wind at all between two or more adjacent highs, or between two or more adjacent lows.

What is the Center of a Low or High and how is it to be Determined?

It is extremely important to locate the centers of highs and lows with as great an accuracy as possible, (contrary to current belief by most meteorologists). The charts would have been difficult to construct without having accurate center locations of the pressure centers. When making angular measurements and calculations between three or more pressure centers that are any distance up to 12,000 miles apart, small errors in the location of the centers can be greatly magnified. When the center can be easily located by the shape of the isobars, there is no problem; but in a large number of cases, there *appears* to be no organized center. A large mis-shapen rock composed of minerals with varying density also has no apparent or visible center. Nevertheless, a **center of gravity** can be found, and can be invaluable for making calculations involving force and torque when the rock is moved. Similarly, since force and torque are also involved in the movements of high and low centers; a **center of action** can be located for them, even if there appears to be no organized or visible exact center. In addition, there are some seemingly disorganized pressure centers that are in reality well organized clusters of small centers inside an extended pressure center area. In that case, there are indeed well defined high or low centers, but very small ones.

The more that a vortex departs from a circular shape, the more difficult it may be to locate the center. We know from Plateau's surfaces of revolution that any circular shape subjected to varying forces can change into the other conic surfaces of revolution related to the ellipse, parabola, hyperbola, etc. As an empirical observation, we find that most lows and highs elongate, breakup, and become distorted—generally into an elliptical shape. The parabolic and hyperbolic and other shapes undoubtedly occur, but from a practical or empirical standpoint, any irregular vortex is considered as being elliptically shaped or consisting of several circular and elliptical shapes. Pressure centers #40, #37, and #39 are elliptical in shape, just to name a few on the map.

Changes in the length of either or both the major and minor axis will, of course, change the shape of the ellipse. A question now arises: What is the center of an elliptical high or low? I have found (on the

Historical Weather Maps) that the symbols “L” and “H” (which stand for low or high) stamped somewhere inside a vortex center, are generally quite accurate; and usually identify a point that can be recognized as the center point, equivalent to point O in **Figure 8-4**, or one of the focal points F and F' of the ellipse. The center of a high frequently lies near the center of the crossbar joining the two sides of the letter “H”, while the center of a low is near the junction where the two legs of the letter “L” meet; nevertheless, this is not always the case.

This is all well and good for the internal structure of an elliptical vortex. However, another high or low next to an elliptical vortex may consider either of the two focal points or the central point as being the center of its elliptical neighbor. How an elliptical vortex “looks” to the center of a different but nearby vortex depends somewhat on which of the three centers of the ellipse is closest to the center of the nearby vortex.

The high represented by #17, #18, and #19, and the lows represented by #91, #93, and #103 on the **Identification Map** are examples similar to the collapsing cylinder of Plateau’s liquid cylinders, only here we have air cylinders.

I draw many straight lines on the charts. For all practical purposes, we can be virtually certain that any straight line that crosses an elliptical vortex exactly along the major axis will cross all three possible center points, shown in **Figure 8-4**. Similarly, if the line crosses exactly along the minor axis, we can be reasonably certain of crossing the center of the ellipse. In these examples, we can be fairly certain that the straight line is crossing the center points of the vortex.

You may be wondering as to why I am concentrating on such seemingly minute details as identifying three centers of an elliptical vortex. If you were to ask any practicing meteorologist, he would probably consider it unreasonable to even attempt to identify the exact center, let alone three (or more) centers for any high or low on a weather map. Also, he might feel that the data on the Historical Weather Maps is insufficient and/or not accurate enough to resolve the question of centers in the detail that I am considering. The charts that I show, as you will shortly see, will alleviate these doubts. Of course, it is not possible to identify all the obscure centers on a given weather map,

but it is astonishing how many seemingly irregular centers can be properly identified when using the proper theory and tools.

Two Types of Chart Analysis: Circumferential and Radial

The analysis of what happened on December 7, 1950 is broken down into two major divisions. In the first division, we subject each one of 30 different points on the map to a harmonic analysis that exposes the circumferential patterns; while in the second division, we subject the chosen 30 to a radial analysis. The circumferential patterns are similar to the Chladni plates shown in **Figure 9-2**, where the diametrical lines break up a circumference into different wavenumbers depending on the number of diameters that are created. The radial patterns are similar to **Figure 9-3**, where we encounter different rings as we move out radially from the center of a disturbance.

Chapter 12

The Circumferential Charts

Some Rules Followed in Drawing the Circumferential Charts

In the first division of charts, we find 41 circumferential charts for the 30 highs and lows I have selected for detailed analysis. More than one chart has been drawn for some of the 30 vortexes. Some of the charts have dashed lines, dotted lines, and/or solid lines to indicate various types of symmetry. The particular type of line, whether solid, dashed, or dotted has no special significance. Two or more types of lines on the same chart are used solely to highlight or separate two or more different types of phenomena. The type of line used may change from chart to chart. The charts were drawn over a considerable period of time, during which, Dan and I changed certain drafting techniques. These drafting changes have no effect on the quality of any given chart.

Each chart is labeled with the number of the high or low that is the central or nuclear vortex around which a symmetry pattern is drawn. Since this group of charts show circumferential patterns, we will be looking for patterns with rays that radiate around like the spokes of a bicycle wheel. We will be looking for symmetry in the spacing of the rays from the nuclear vortex. The spacing of the spokes on a wheel can be described by the angular separation between the spokes. The dashed, dotted, or solid lines can be considered as the spokes of a wheel and the angular separation of the spokes or rays is given by a whole number called the **angular number**, which is an exact multiple of 1.875° (see Table VI, page 101). Therefore, the angular separation between any two rays can be described as any number from 1 through 192. The value of this angular number can be read in angular degrees from Table VI.

I will now describe a little detail of this set of charts that could be confusing. The end of a ray starting from a nuclear center does not always terminate at the exact center of the high, low, or col at which it points. Frequently it ends a little to the right or a little to the left of the true position of the chosen point. These lines were drawn with the aid of a transparency of **Figure 10-7**. The transparency was centered over the point to be used as a nucleus, and it was immediately obvious which other points were lying exactly on or very close to any one of the 192 numbered lines. If one of these lines fell slightly to the right or left of a chosen point, then the ray from the nuclear vortex was also drawn slightly to the right or left—exactly as the transparency indicated.

Two or more of the rays are drawn so that they pass through the center of the nuclear vortex. This creates a crossing point which serves as a registration mark for the exact location of the center of the nuclear vortex. The rays that are chosen to pass through the center have no special significance. All the rays were not passed through the center so that they would not obstruct the center under a mass of lines passing through a single point. The lines used to identify the rays are thicker than the lines of the transparency, in order to make the charts easier to use.

I have also entered the great circle distances between the nuclear center and the ends of the rays in each of the first 9 circumferential charts. This radial distance is also given in the same type of numbers as shown in **Table VI**. The circumferential numbers are entered near the center in the angle formed by any two rays radiating out from a nuclear center. The radial numbers, on the other hand, are entered at the ends of the rays.

A little additional clarification is now added to reduce the chance for any misinterpretation of what is being done. The angular numbers near the center of the nucleus represent the angles (when converted to degrees) between any two adjacent straight lines (each of which represents a small circle on the globe). What we will see are symmetry patterns involving arcs or portions of *small circles*. Hereafter, I will use the abbreviation “cu” when referring to the angular number units that can be measured between any two rays when working with circumferential type patterns; i.e. 14 circumferential angular units will be called 14 cu.

The radial distance, however, is given in angular numbers (which can be converted to degrees of latitude) that are a measure of the *great circle* distance between the central vortex and the point at the end of the ray. A line drawn to represent the great circle distance would be slightly curved and could not be represented by the straight line shown as a ray (except when the line passes through a pole). The distance along the straight line of a ray is also slightly larger in value than the great circle distance. Hereafter, I will use the abbreviation “ru” when referring to the units of the radial angular number that represents the radial great circle distance.

In the charts that now follow, I start with points near the center of the map (near the North Pole). The succeeding points are located at lower latitudes. There is no special significance in this order, other than the fact that points near the map center are more completely surrounded by other identifiable points.

You may have been “unnerved” occasionally in the previous chapters by remarks such as: “as will be shown in the charts that follow” or “the charts at the end of the book”—well, congratulations—we will now really investigate “the charts at the end of the book”.

Chart #58

First the obvious symmetry. On one side of the straight line joining #81 and #40, there are two angular numbers of 14 cu that are opposite each other and two angular numbers of 34 cu in the middle. Could you get this pattern by throwing darts at a dart board? Look again; #40 has a radial distance of 11.3 ru, #39 has 12.4 ru, while #81 has 24 ru, which gives a ratio close to 2:1, if we use the average value of #39 and #40. That’s not the end of it; #55 has a radial distance of approximately 6.5 ru, while #60 has 12.7 ru—this is almost 2:1 again.

#60, the other leg of the symmetry pattern involving the angular number 11, has a radial distance of 12.7 ru, which compares closely with #39 at 12.5 ru. We can’t expect everything to be perfectly neat, since we do have a dynamic system that is not in perfect balance or equilibrium.

It must be emphasized that this example was selected to show circumferential symmetry. A simultaneous radial symmetry of any kind is a revelation.

Now, a word about the exact point chosen as the center of #58. It has the shape of two separate ellipses joined together. Here we have a case of multiple centers with the dominating center located at or near the spot where the "H" is marked.

A complete analysis of #58 would require that at least two and probably three centers be chosen around which the various symmetry patterns could be exposed. This type of analysis would give the maximum number of symmetry relations for the conglomerate vortex identified simply by the number 58. The point I chose seemed to give the best overall symmetry.

We will now recall the discussion of Figure 7-23, where the most regular symmetry patterns surrounding any given point will occur when we choose the preferred positions in any system where there is some type of regular spacing of the points. Remember, that any position chosen, even if not a preferred one, will show some type of symmetry, only if the points in the surrounding area have any type of regularity.

Whenever there was any uncertainty as to the location of the center for any given vortex in the charts, the point that was finally chosen, was the point that gave the maximum number of symmetry relationships with the surrounding points. This, of course, was not the only factor considered in locating a center, but nevertheless, a highly important factor.

I chose not to break up #58 into two different sections with different centers, since there are enough other examples to establish the nature of the symmetry pervading the weather map.

If you are not 100% satisfied with my claim of order in the arrangement of all points over a hemisphere (from this first chart), please look at the next chart.

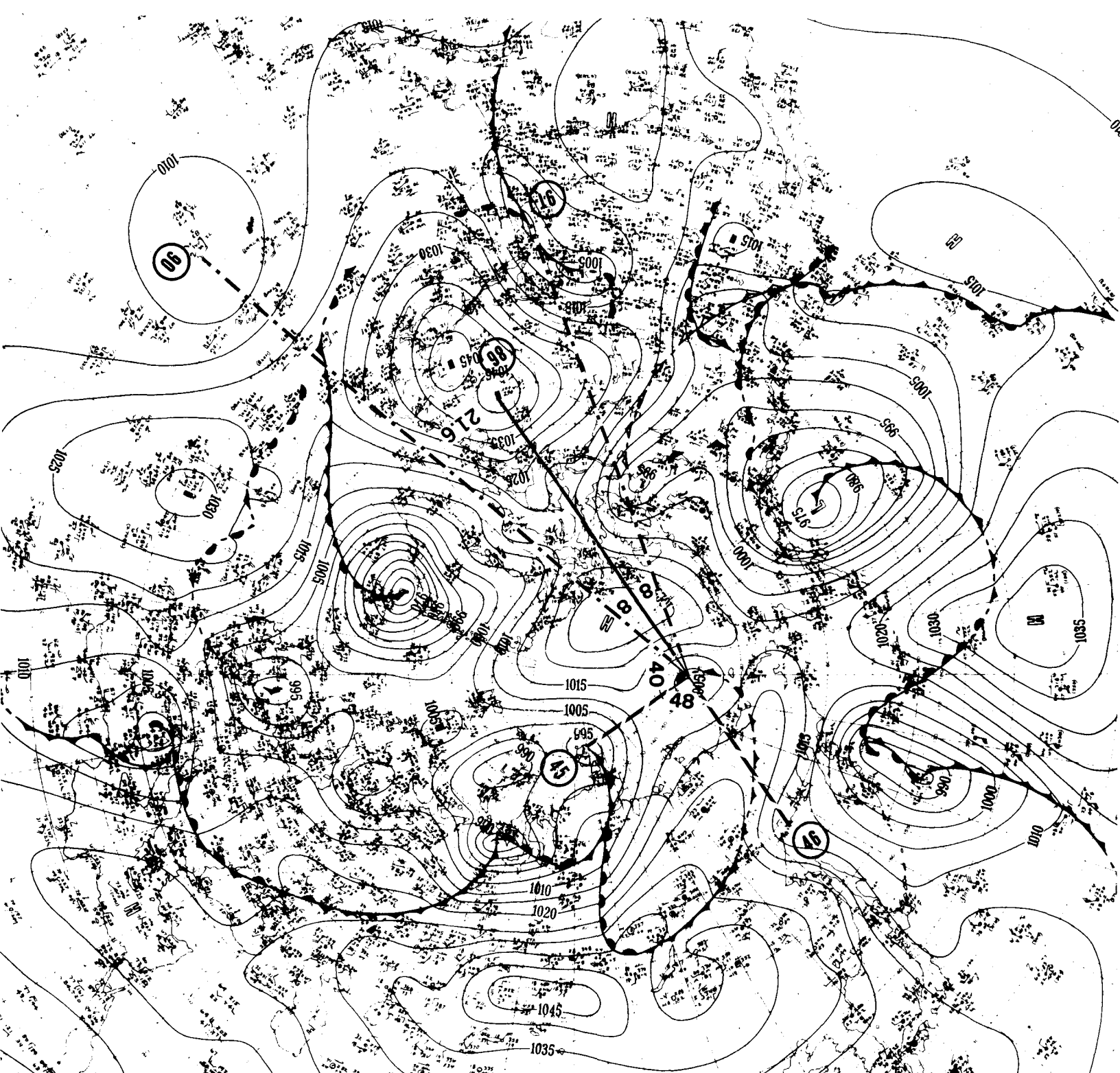
Chart #55 A

In this choice of a symmetry pattern for point #55, we find that 6 is the common factor of the angular numbers of 12, 18, and 36. We find that the circumferential pattern has four 18's, one 36, two 12's balanced by one 24, and a 14 and 22 that add up to 36 to complete the ring of 192 numbers. The solid lines were drawn to three points to show that they are related by the angular numbers of 48, 64, and 80. These translate into 90° , 120° , and 150° which are in the ratio of 3:4:5.

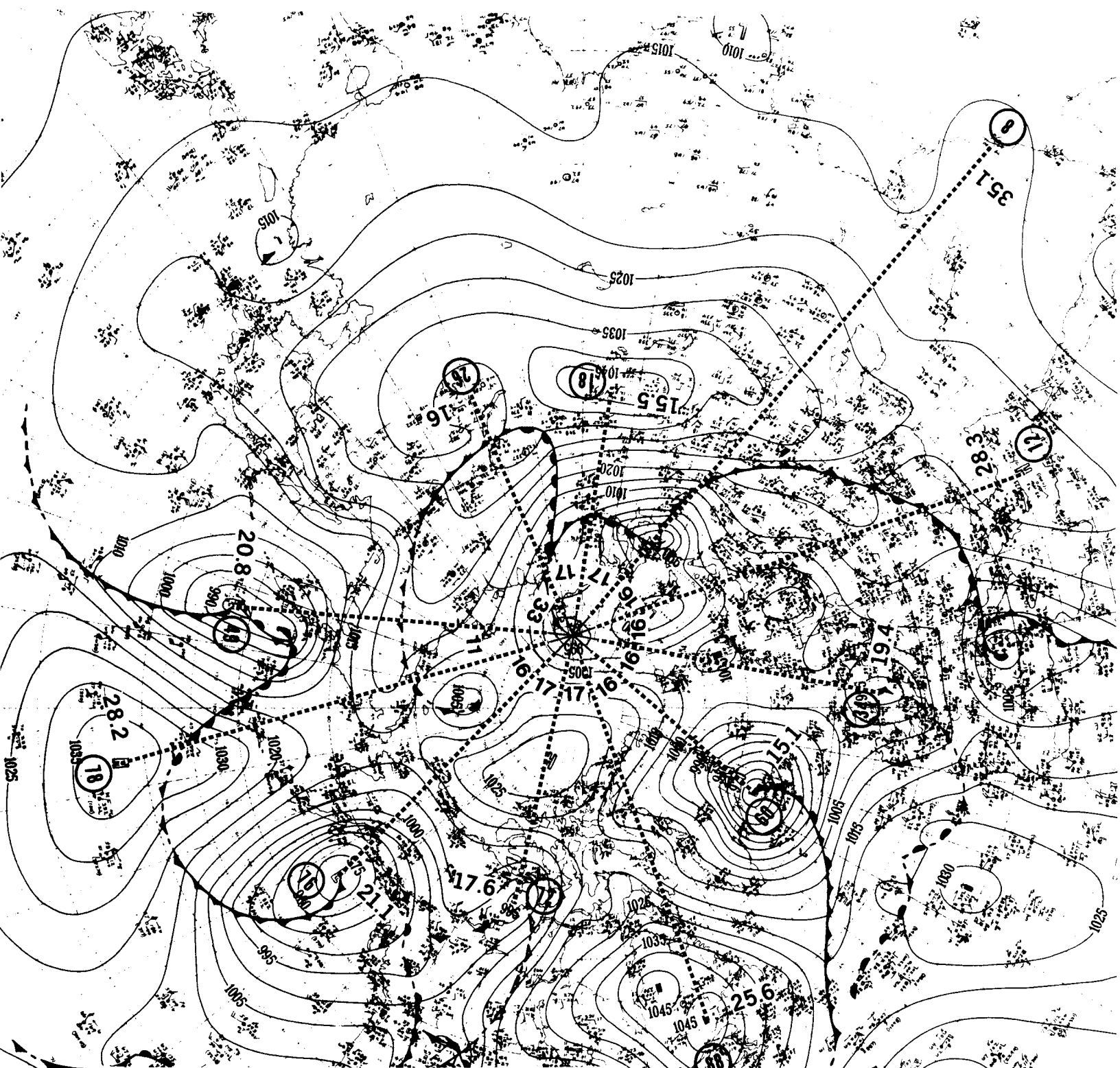
This chart was drawn to show a circumferential symmetry pattern of points around point #55, with no consideration of any kind as to the radial distance of each of these points from the center. But, careful scrutiny will show that point #58 has 6.5 ru, #51 which is opposite has 12.5 ru, while point #76 has 13.3 ru; point #26 has 18.9 ru which is 3 times 6.5 approximately.

Point #46 is a radial distance of 11.2 ru from point #55, while point #86 is a radial distance of 21.6 ru (almost 2 to 1) from point #55. This is on a straight line joining three points. In addition, point #99 is 32.8 ru away, which is almost 3 to 1. Point #45 (8.1 ru) and point #77 (16.8 ru) are nearly 2 to 1. The exact center of the remnant high #77 is approximate but does probably lie along the line drawn from #55 to #77. Point #6 (40.6 ru) is related to point #45 (8.1 ru) in the distance ratio of 5:1.

A symmetrical circumferential pattern is simultaneously locked into simple radial relationships. In legal terms, I rest my case that there is great order in the arrangement of all points of interest on a hemispheric weather map. However, if there are any doubters left at this point kindly take a look at the next chart.



Here we have another symmetry pattern showing the angular number 48 balanced by an angular number sum of $40+8$. An angular number of 48 represents an angle of 90° . What we see is a pattern of rays forming two right angles next to each other, with a spray of two rays spaced at 8 angular units away from one of the legs of one of the right angles. This leg which is the ray to #86, is shown as a solid line.



Here, the symmetries involve cu units of 16 and 17, with four 16's balanced on each side by two 17's each. There is a 33 left over, which is of course 16+17, and magically, the 11 that is needed to complete the sum of 192 cu of circumference, is $\frac{1}{3}$ of 33, for a ratio of 3:1. Very neat!

Just for the sake of curiosity let us analyze a few of the radial distances. #72 (17.6 ru) is nearly opposite #8 (35.1 ru) for a ratio of 2:1. #78 with 28.2 ru is almost opposite #12 with 28.3 ru, for a 1:1 ratio. #60 with 15.1 ru is almost opposite to #26, with 16 ru, and #18 with 15.5 ru, which are close to a 1:1 ratio. #49 with 20.8 ru and #76 with 21.1 ru are virtually equal to 3×7 ; while #78 with 28.2 ru and #12 with 28.3 ru are about 4×7 ; which leaves #8 with 35.1 ru at 5×7 . A mere coincidence?

Chart #45 A
Page 123

Chart #45 B

From the principle of superposition of waves, we know that we can have independent waves occurring simultaneously. Each wave can do its own thing, as if there were no other waves around. In this analysis of point #45, we have extracted another symmetry pattern coexisting around the same point. Here we find that a large portion of the atmosphere of the Northern Hemisphere is resonating at an angular number of 10 around point #45. Of the nineteen points that are linked in this angular mode, we find that the centers of nine of the points at the ends of the rays are not controversial as to location and are very good hits. These nine are #42, #37, #34, #55, #90, #88, #93, #78, and #21. If the other ten points were removed, we would still find an unusual, balanced symmetry pattern, with the separation between rays at 10 cu or a whole number multiple of 10 cu. Not willing to leave it at that, I continued the exploration with good results for the 10 extra points numbered: #5, #61, #67, #66, #63, #84, #80, #50, #46, and #25.

The ray that goes to #63 is not a perfect hit, but is slightly off to one side of the "H". This same ray passes right near #66, which is off by a similar amount, but in the opposite direction. What we have is an example where the ray for this angular number of 10 lies exactly between #63 and #66. This type of symmetry on both sides of a line is quite common and you can find it everywhere that you look on a weather map. This is an example of longitudinal glide reflection of the type shown in Figure 7-9. So it is not unreasonable to consider that this ray, which passes between #63 and #66, can be added as an additional good hit to be added to the original eight.

Points #46 and #25 are poorly defined, but their centers appear to be reasonably located on one of the rays for the angular numbers involving 10 cu. Points #5 and #80 are poor hits for the centers, but they have been entered as a matter of interest. #55 and #84 are very close hits, but not perfect. I must add that most meteorologists would consider such small distances (as are involved in the close but not perfect hits) as being not discernible in any type of measurement they usually make. Any slight variance, however, stands out sharply in the light of the rules of *Singer's Lock*.

You might ask: "How do cols fit into these symmetry patterns?" You will find that cols do indeed fit into the patterns, empirically, as can be

seen in the charts. Point #50 is the col between #49 and #51. Theoretically, there is no difficulty in understanding why. If the centers of highs and lows show an orderly arrangement in space, then the center point in between any two highs or lows must reflect a similar type of symmetry, just from mechanical considerations alone; in the same way as the center point on a bar joining the two bells of a dumb-bell.

Now we come to the fascinating points of #61 and #67. They represent the terminal ends of the symmetry pattern with 10 cu as the fundamental unit. When we go (in an easterly direction) 10 cu, exactly, from #63, we end up a slight distance to the east of the center of #61. I have joined the rays for #61 and #63 with a symbolic coil or spring to illuminate the elastic nature of the termination. Likewise, when we go (in a westerly direction) 10 cu, exactly, from #34, we end up a slight distance to the west of the center of #67. In a similar manner, the rays for #34 and #67 are joined by a symbolic spring.

The symmetry of the way the pattern terminates is an interesting feature. There is an overshoot of two tiny remnant vortexes. The 192 cu of a complete circle should have left a remainder of 2 cu when 192 cu is divided by 10. Instead we have an overlapping at each end to eliminate the need for a remainder of two.

The radial distances are entered without comment at the end of each ray. You can investigate these relationships for your entertainment.

You will recall from the discussion of the Chladni plates in Chapter 9 that the particles of sand slide off moving parts of the plate and gather along nodal lines. In a similar manner, we find that the disturbance (of which #45 is the center) has set the atmosphere into a circumferential oscillation with a spacing of 10 cu between components of the configuration. This oscillation tends to force other vortexes to line up along the nodal positions separated by 10 cu, since vortexes that are not exactly on the nodal line tend to slide towards that line in the same manner as the sand particles on the Chladni plates.

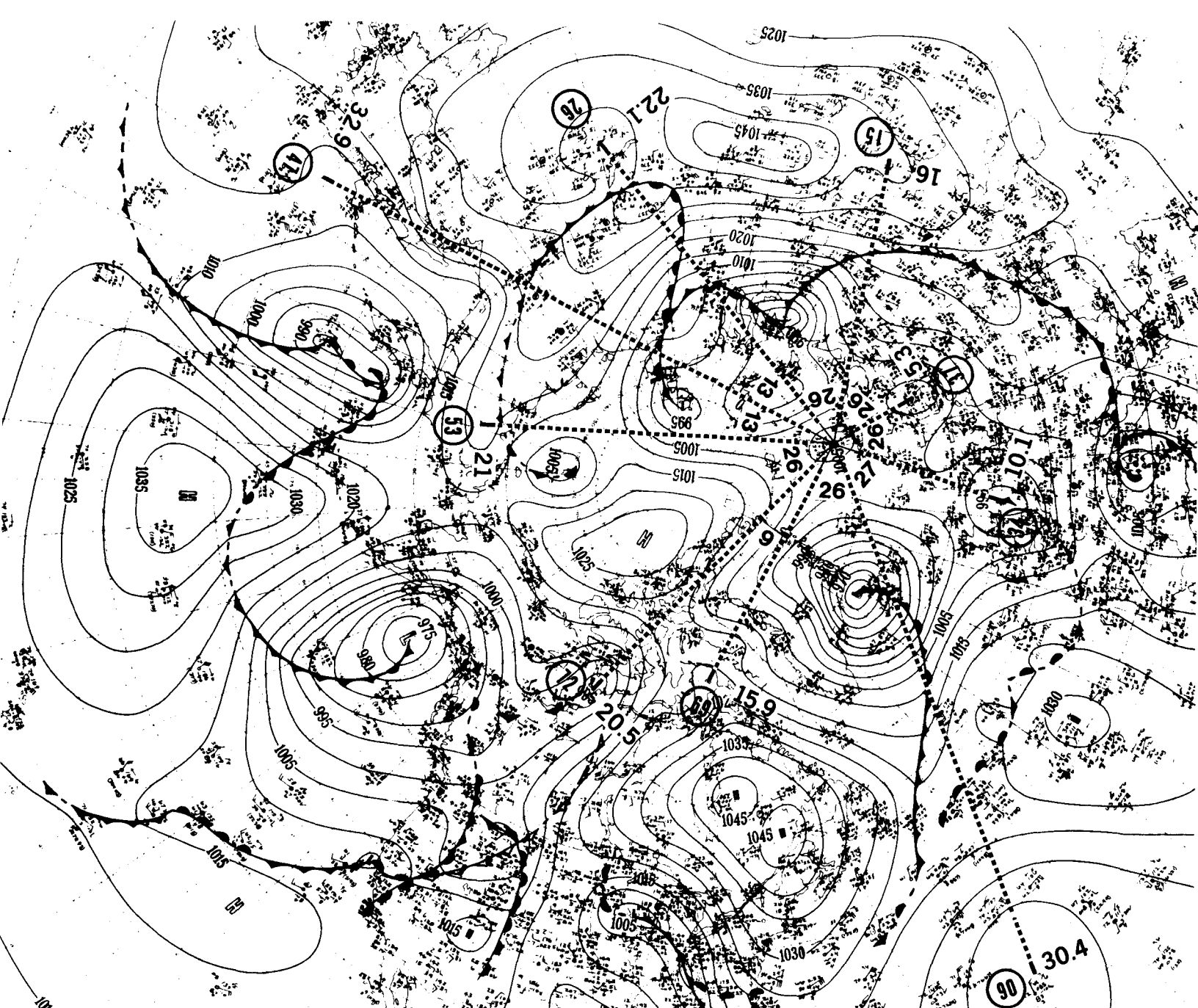
Of course, #45 is not the only disturbance in the hemisphere. There are other centers that are growing or decaying at the same moment in time. The ones that are stronger and are growing will tend to force other vortexes to line up into resonant nodes. The weaker disturbances will tend to lose control of the vortexes in their respective nodes. Whether any given low or high is moving towards any special nodal line, or away from any special nodal line is determined by the resultant of the

forces. The predominantly stronger and growing disturbances will naturally have a stronger influence. In summation, any vortex or col that is near any given line of symmetry will tend to move towards or away from that line in accordance with the well established principles of wave interference. If the conflicting forces are in resonance, the nodal lines will strengthen. If the interference is non-resonant, then the nodal lines will be destroyed.

One other point of interest is to be noted: #34, #88, and #78 are all common to charts #45 A and B. This is one way in which different symmetry patterns are linked to each other through the nuclear #45.

These two symmetry patterns for #45 should prove decisively by themselves that there is an ordered arrangement of all the vortexes over the hemisphere. Just to be on the safe side, however, let's look at the next chart.





In this one, we find the symmetry numbers of 26 cu and 27 cu; there is one 9 cu. I suppose you guessed it already; the ratio of 27 to 9 is 3:1. #37, #34, #90, #69, #72, and #26 are good hits, and the remaining three are okay, but not great.

Now we will explore the radial aspects of these vortexes. #37 (5.3 ru) and #53 (21 ru) give a ratio of 1:4. #37 (5.3 ru) is also in a ratio of 1:3 with #15 (16 ru) and #69 (15.9 ru). #34 (10.1 ru), #72 (20.5 ru), and #90 (30.4 ru) are in a 1:2:3 ratio.

It must be emphasized once again that this pattern of symmetry was generated only as a circumferential pattern. Subsequent investigation revealed the radial symmetry shown above.

Let's look at yet another chart, for those that demand still one more example.

AP
HERE
GMT
MODEL
SHIP
POSITIONS
DMS
W.L.
N.E.

Chart #42

The center for #42 was chosen as the point where the warm and cold fronts meet. The symmetry with 10 cu as the lowest common denominator is obvious. There is one 18 cu and one 4 cu to complete the ring. Only #45, #39, #37, #76, #18, and #90 have the rays going right through their center. These were the points on which the symmetry pattern was set up. The additional points used were added as a matter of interest only, since they represent obscure vortexes and some of the points do not make perfect hits with the ends of the rays. The nuclear vortex in this example does not consider these additional points as being obscure. It is obscure to us, only because we are trying to analyze a map that was drawn without foreknowledge by the ones who drew it, that there were resonant oscillations which could be identified with accurate locations of centers.

In spite of these difficulties, there are also elements of radial symmetry. #40 is 4.6 ru out from the center and this is across from #16, which is 9.2 ru, for a ratio of 1:2. #16 (9.2 ru) and #8 (27.1 ru) are approximately 1:3. #11 (28.9 ru) is almost directly opposite #76 (29 ru).

#40 and #69 are both on a single straight line joining #42, even though the ray from #42 is broken to permit the entry of the numerical data. This is also true for the points of #39 and #90.

There are additional symmetry patterns around #42 that are not shown which you can ferret out on your own. I am only showing some of the major highlights, in the understanding of *Singer's Lock* and all of its ramifications.

I think that you are now 183% convinced that the scattering of highs, lows, and cols over a hemisphere is not a wretched, amorphous arrangement; but is instead, the arrangement of a highly polished diamond with many facets. Nevertheless, I will now toss in 183 more charts as additional proof for the inevitable few remaining hold-outs that need additional arm-twisting to be convinced.

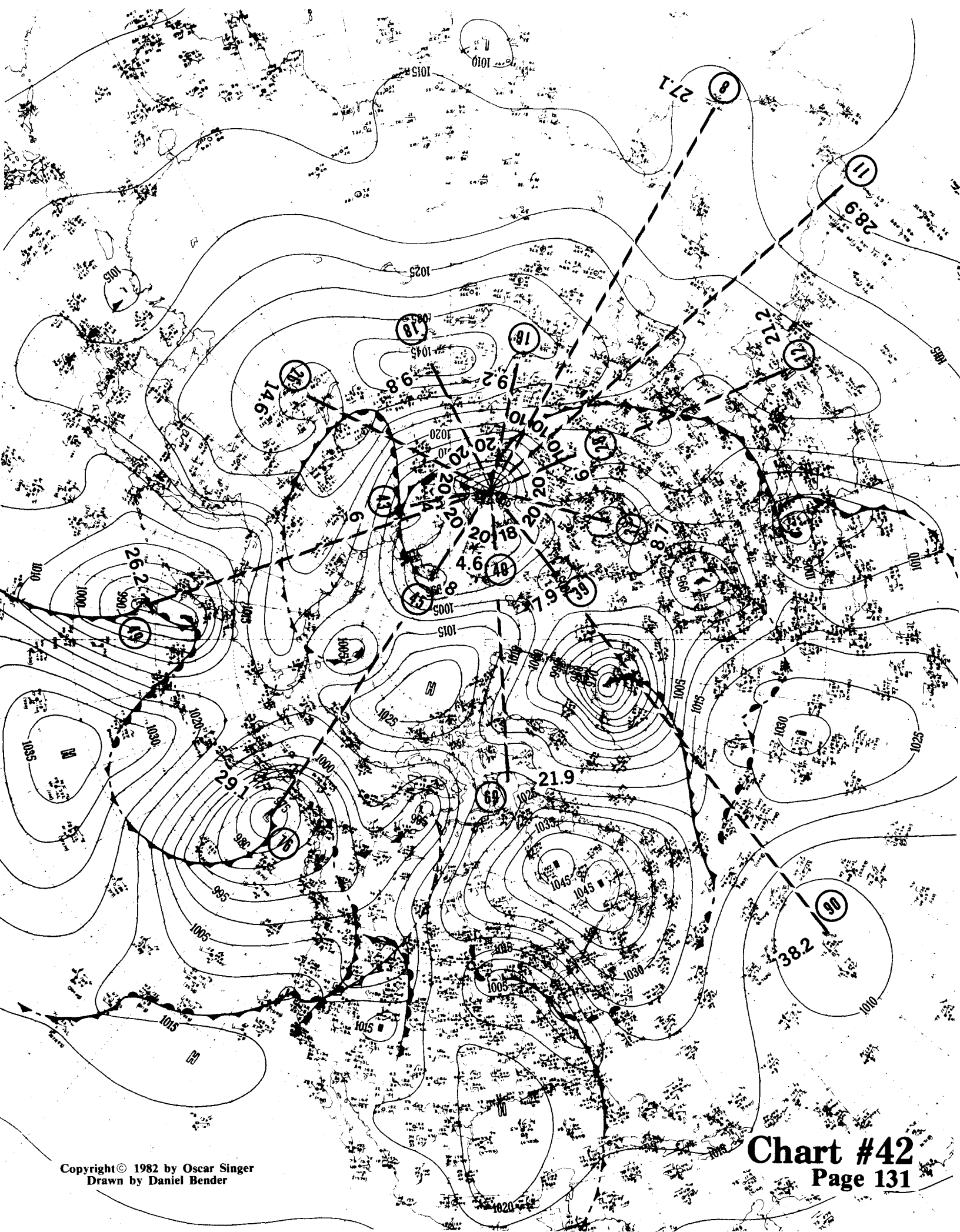


Chart #37

In this example, the rays end on the center of most of the points chosen. Only #8 and #69 are off slightly. The symmetry is not as uniform as in the previous examples, but is still impressive. We find that 15 cu and 14 cu predominate with two 20s side by side; the 7 cu is of course half of 14 cu.

The points creating the three separate 4 cu have radial distances that are fascinating. #88 (25.9 ru) and #8 (25.9 ru) are exactly 1:1; while #86 (25.1 ru) and #7 (23.6 ru) are almost 1:1. This is quite an angular balance in both the circumferential and radial directions, even though #7 and #8 are relatively obscure centers. An additional twist is #60 (11.9 ru) and #7 (23.6 ru), both nearly in a straight line, show a ratio very close to 1:2; while #15 (12.7 ru) is nearly opposite to both #86 (25.1 ru) and #88 (25.9 ru) which gives a very close 1:2 ratio, if we take the average value of #86 and #88. #34 (7.7 ru) and #61 (14.6 ru) are almost in the ratio of 1:2, while on the opposite side we have #42 (8.7 ru) and #18 (16.7 ru) at almost 1:2; and while #18 (16.7 ru) and #30 (16.2 ru) counterbalance each other by nearly 1:1.

#18 (16.7 ru) finds a counterpart in #30 (16.2 ru); while #30 (16.2 ru) and #51 (31.8 ru) are counterparts in the ratio of almost 1:2. In conclusion, #18 (16.7 ru) and #76 (33 ru) are counterparts in the ratio of almost 1:2; while #12 (15.3 ru) and #90 (31.1 ru) are counterparts in the ratio of almost 1:2.

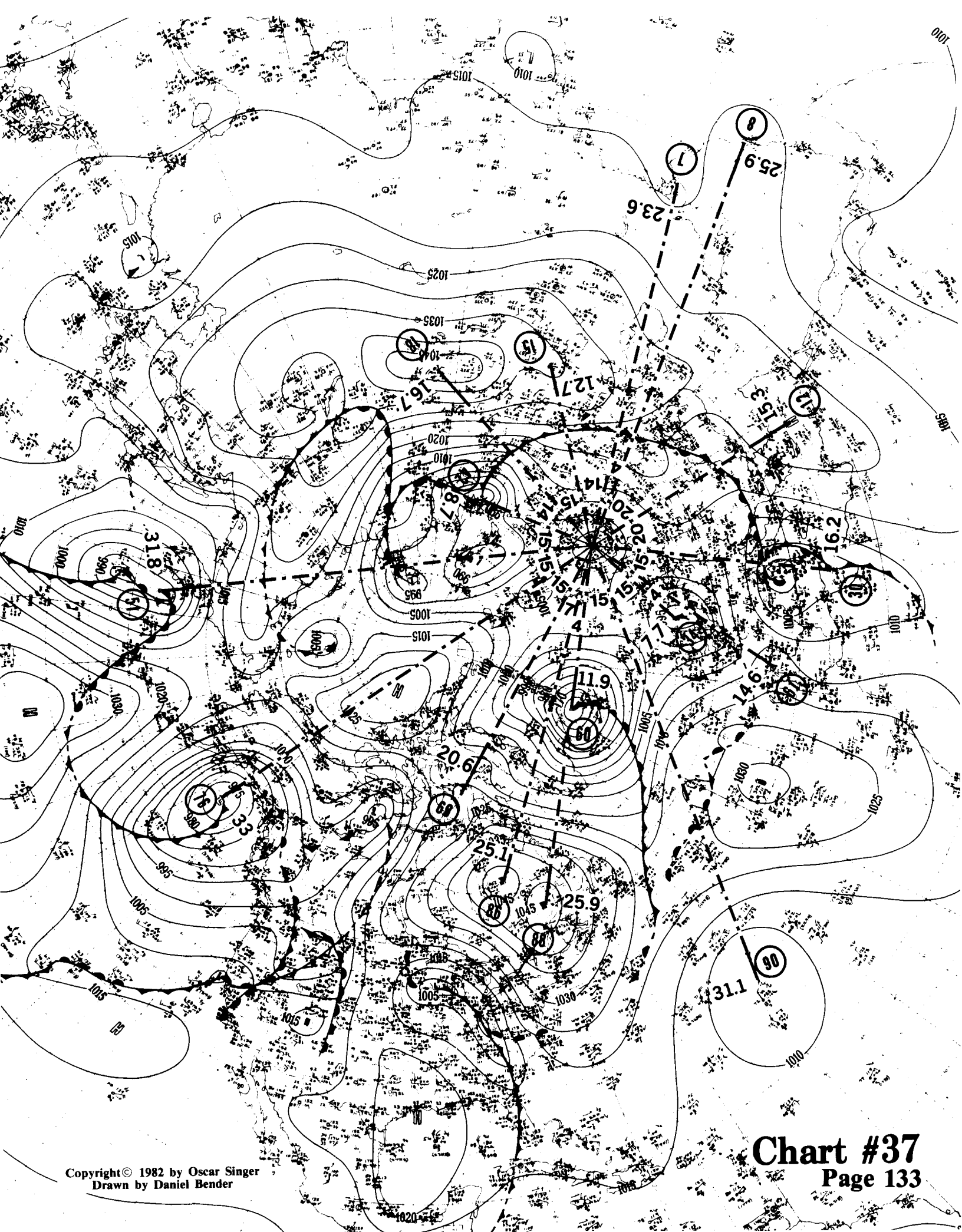


Chart #60

In this example, all the rays hit very close to the center of the selected vortexes. We find that the symmetry pattern is established by the predominating angular number of 11 cu, with 10 cu, 12 cu, and 13 cu also occurring. The angular number of 23 cu is of course composed of an 11 plus a 12; a 6 plus a 7 add up to a 13; and a 6 is one half of a 12. Interestingly enough, we find the two 6 cu are almost symmetrically opposite to each other. I have not shown the radial distances on this chart and in the succeeding charts in this series. After all, this series is concerned with showing circumferential symmetry throughout the entire map. I had added the radial data on the previous charts to spice things up. But enough is enough—for now!

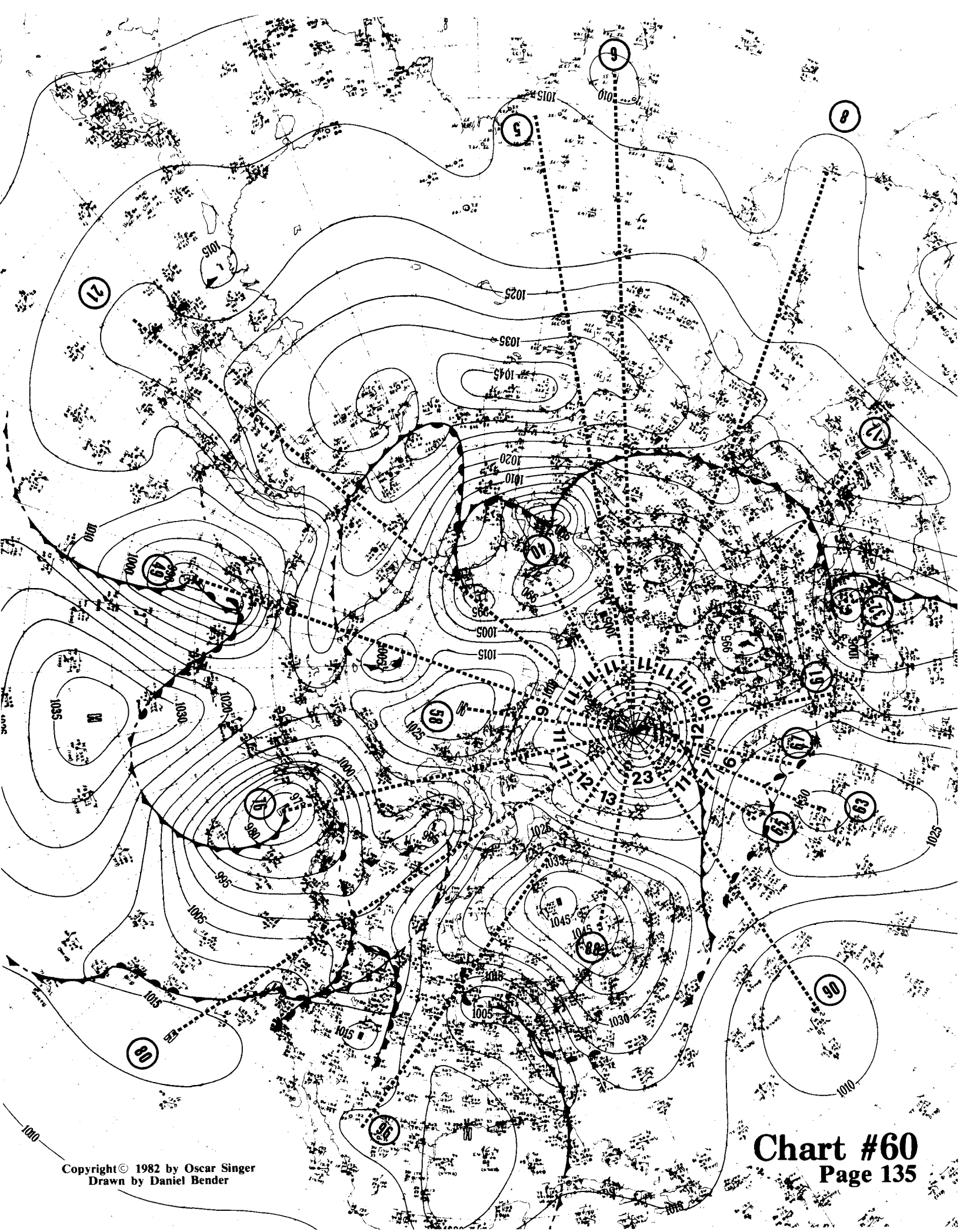
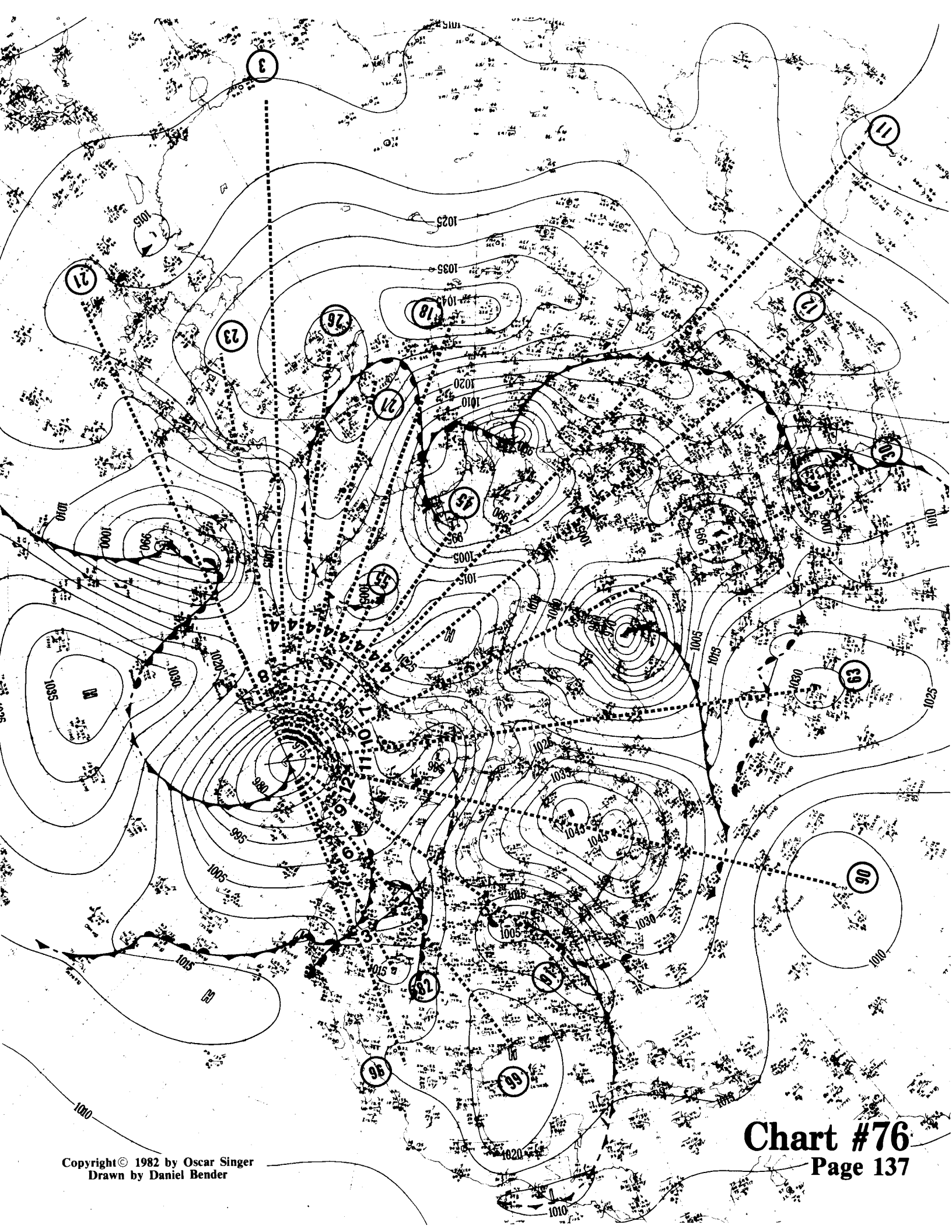
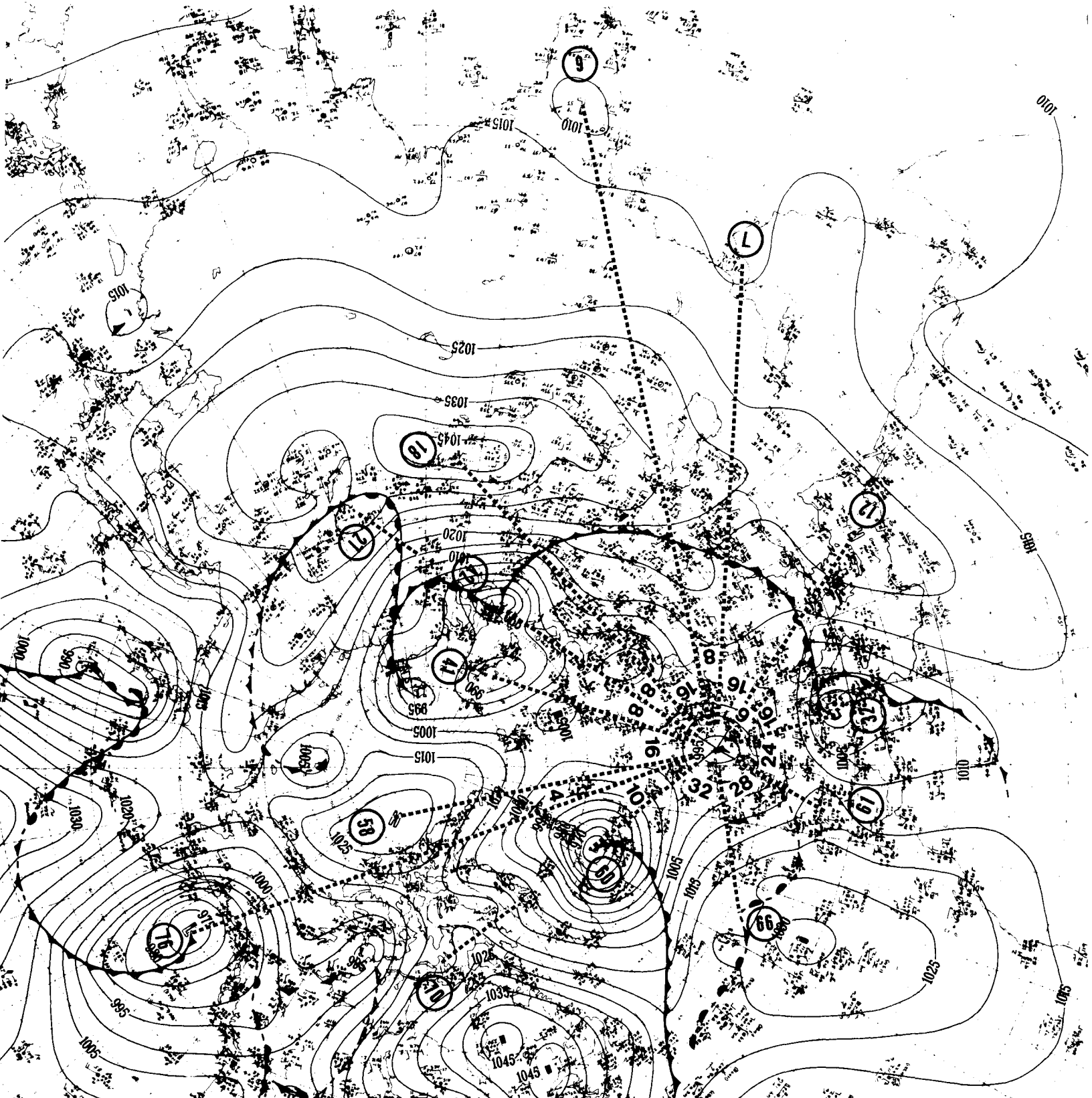


Chart #76

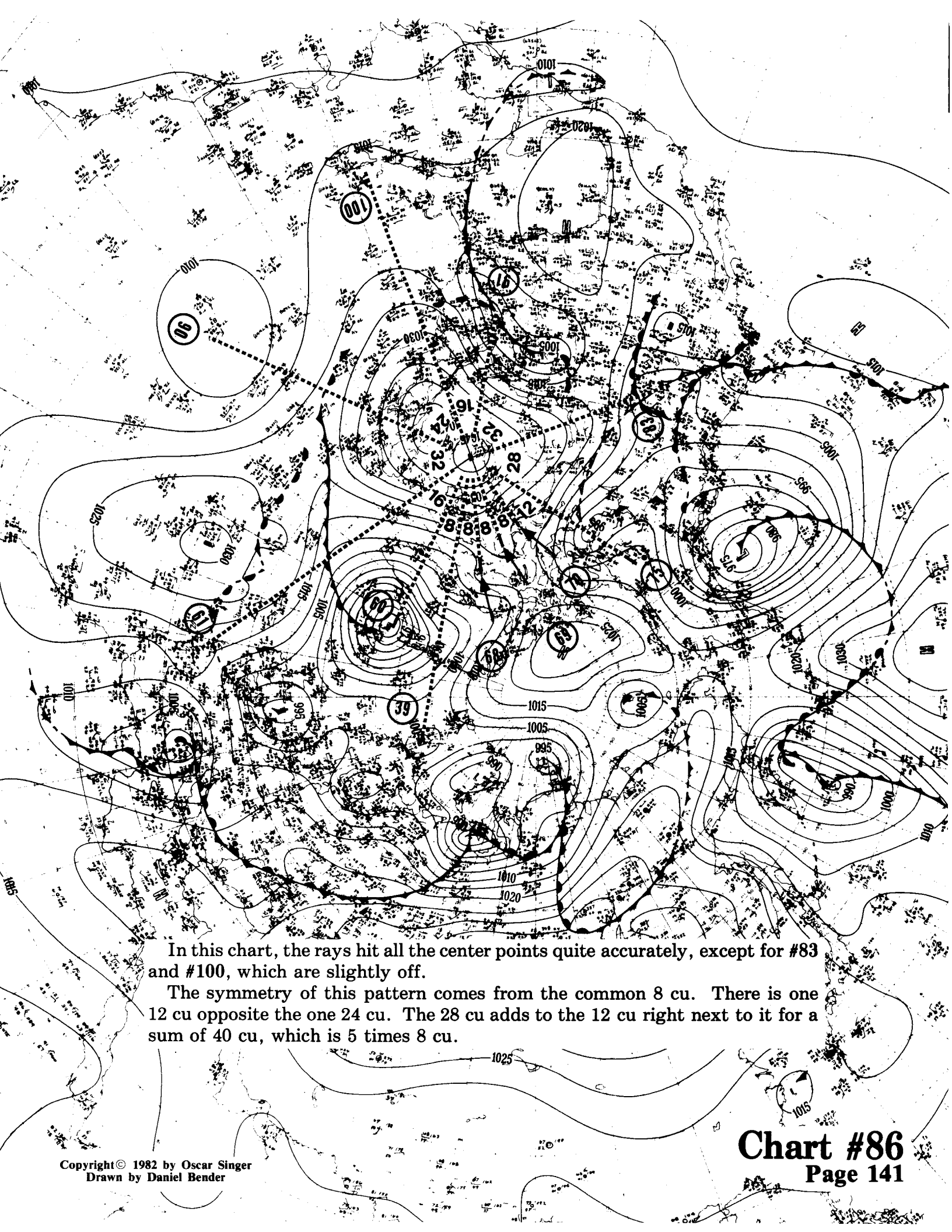
In this chart we find two different symmetry patterns. Starting with #96 and moving in an easterly direction, we find that the angular spacing varies in a systematic manner by going from 3 cu to 6 cu to 9 cu to 12 cu, after which it decreases to 11 cu and 10 cu and then another 11 cu (if you add 7 cu and 4 cu together). The rest of the cycle ends in a symmetrical factor of 4 cu. Points #11 and #3 were drawn in as a matter of curiosity, to show that there is no feature of any kind on the map that is not involved in some symmetry pattern.

The unusual feature of this map is the regular increase by a factor of 3 cu from #96 to #90. This type of uniform increase in spacing is the classical parabolic or step rate of increase in which a quantity varies in a simple additive manner. The cluster or "packet" of vortexes were apparently moving as a group that ran into a braking action. This pattern is just a glimpse into one of the vast arrays of combinations being generated by all the centers of action on the weather map at that moment.





In this chart all the rays end pretty close to centers of the chosen points. The common symmetrical factor for angular measurement in this chart is of course 8 cu. We also find that the one 6 cu and the one 10 cu add up to 16 cu; while the one 28 cu and the one 4 cu add up to 32 cu to balance out the symmetry around the nuclear #34.



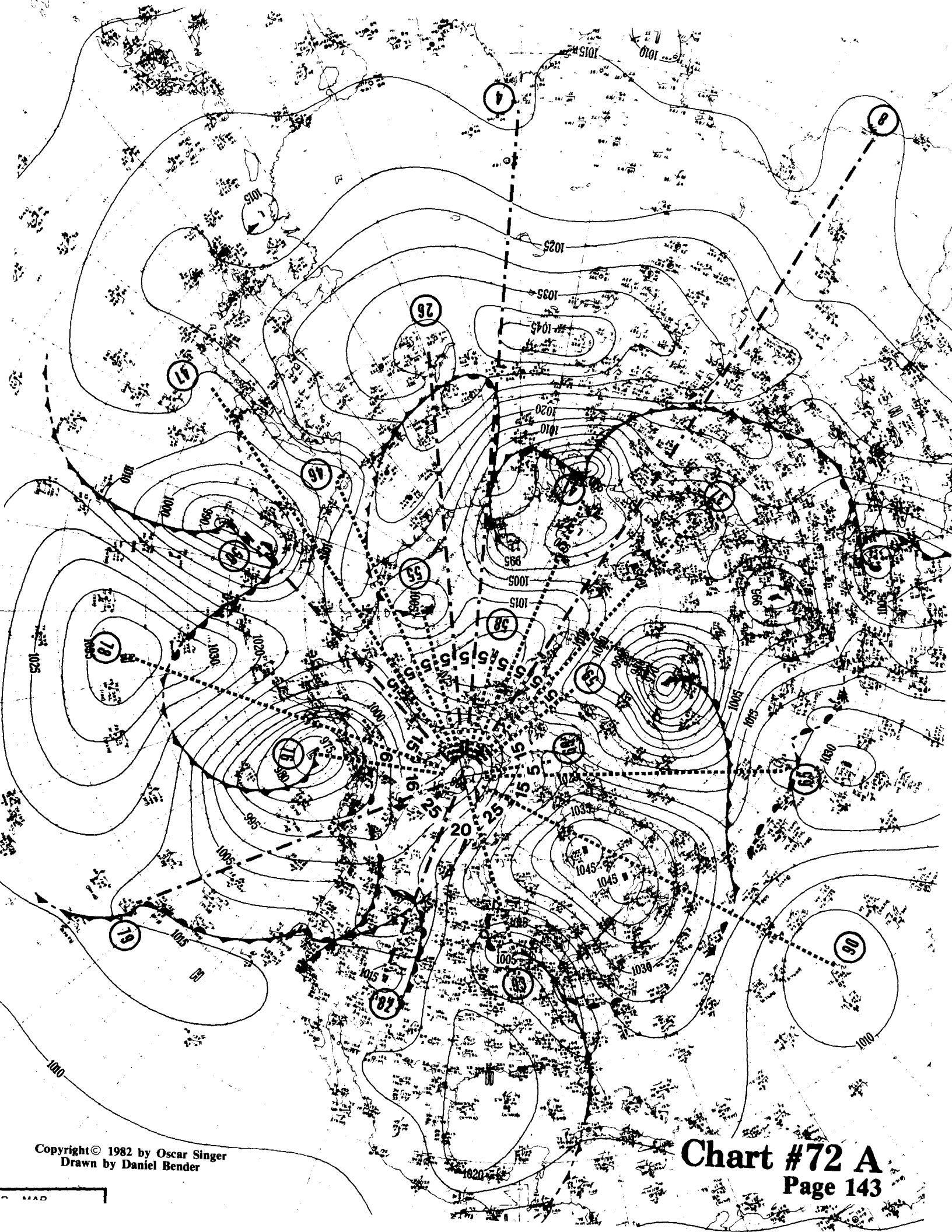
In this chart, the rays hit all the center points quite accurately, except for #83 and #100, which are slightly off.

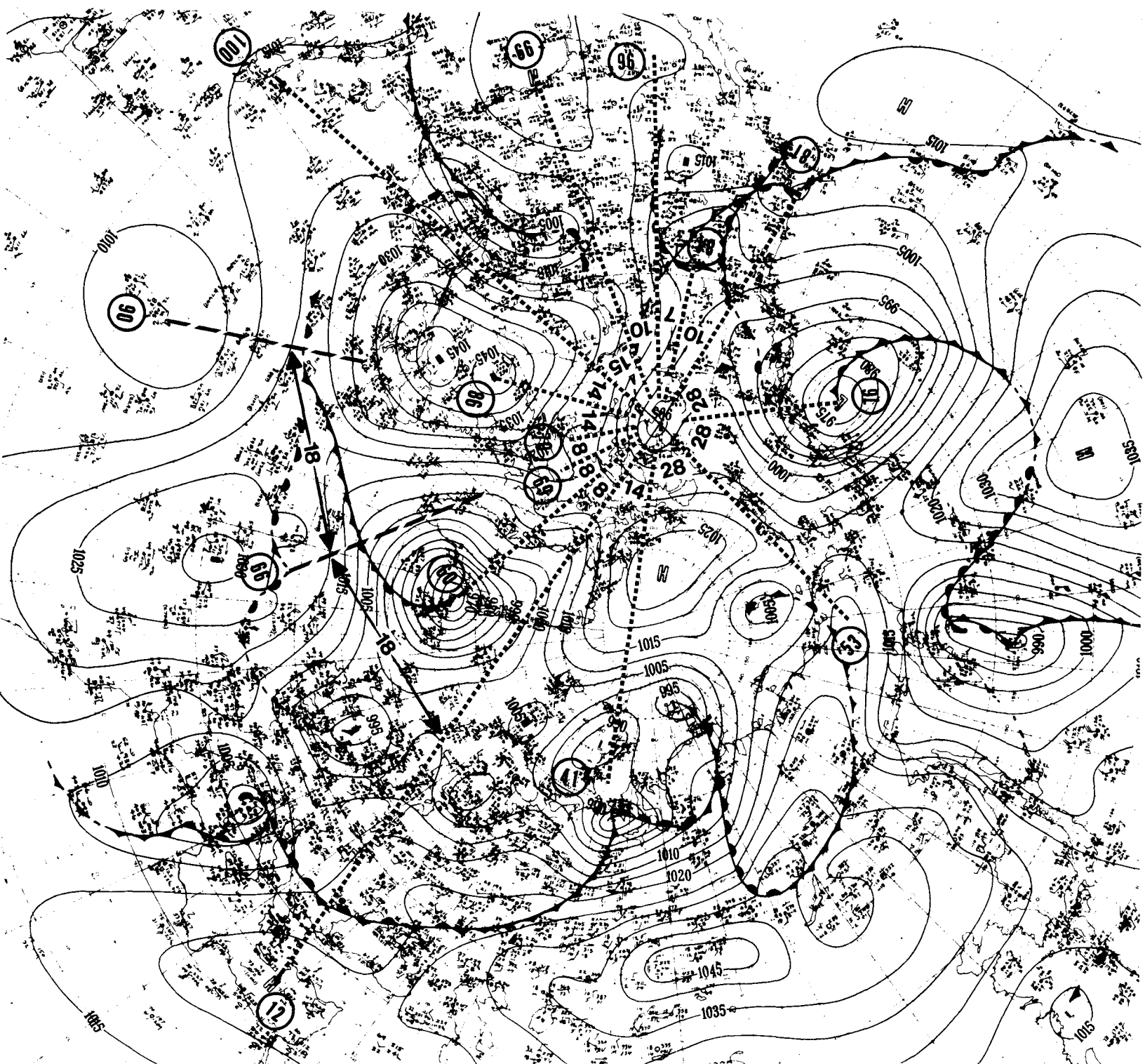
The symmetry of this pattern comes from the common 8 cu. There is one 12 cu opposite the one 24 cu. The 28 cu adds to the 12 cu right next to it for a sum of 40 cu, which is 5 times 8 cu.

Chart #72 A

In this chart, dotted (.....) lines are used for the rays when they terminate exactly at a vortex or col center, while dot-dash (- — -) lines are used when the rays terminate off-center. As usual, the symmetry pattern is established only with those vortexes that are directly at the end of a given ray. The other points that are not perfect hits are entered as a matter of interest.

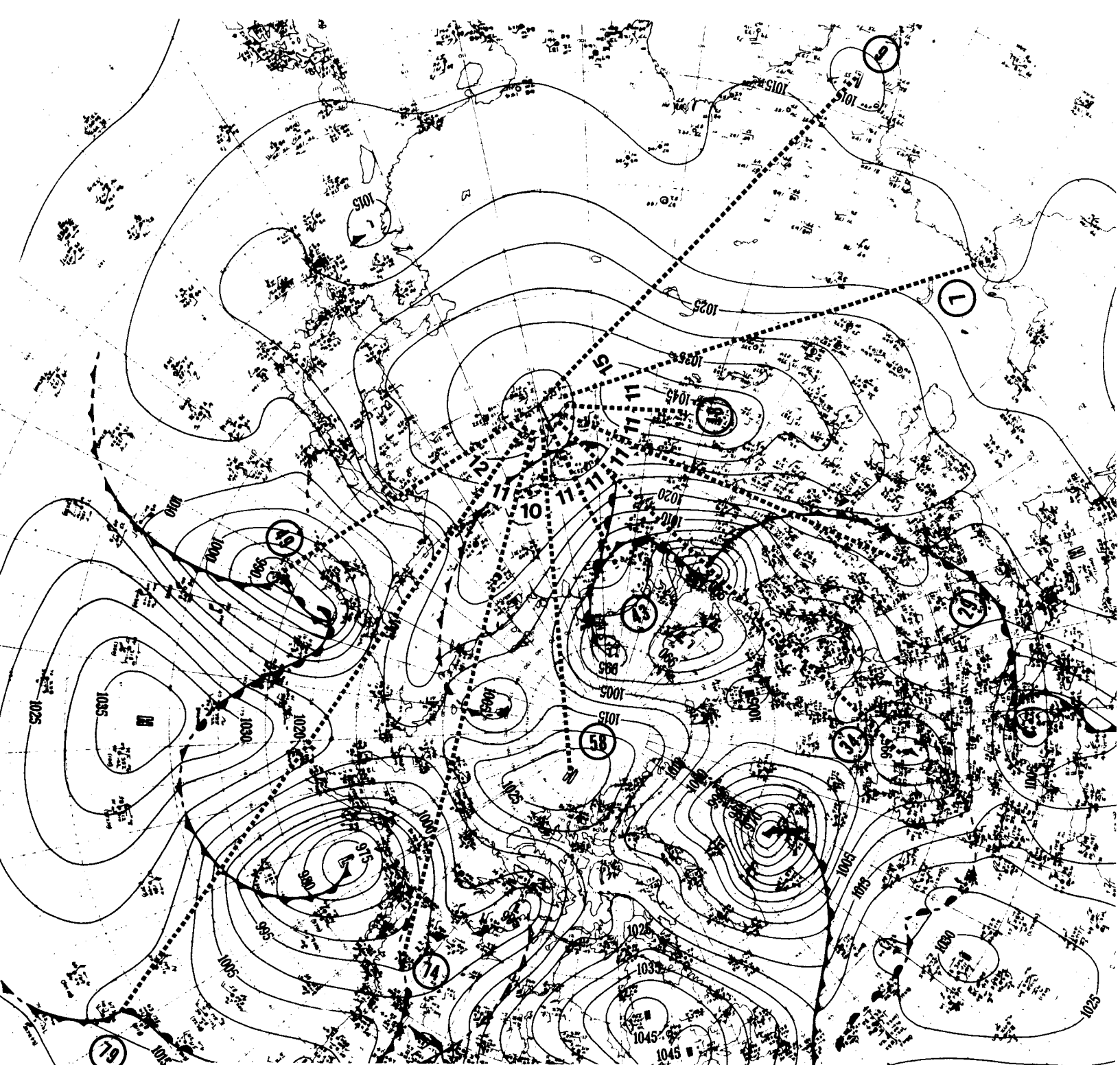
In this example, 5 cu is the symmetry feature that predominates, with one 6 cu and one 16 cu necessary to complete the circle of 192 cu.





Here we have a second symmetry wheel that is operating around the nuclear #72. The following points are common to both symmetry patterns: #90, #76, #69, and #41. This is one mechanism by which one symmetry wheel is linked to another. This pattern shows a cluster of three separate 8 cu; a cluster of three separate 28 cu; three 14 cu; two 10 cu and one 7 cu, that add up to 27 cu; and finally, one 15 cu. 15 cu plus 27 cu equals 14 cu plus 28 cu.

Two heavy dashed rays are drawn, that do not go all the way into the nuclear center, so as to keep the first pattern undisturbed. These heavy dashed rays terminate at #66 and #90. These two points are separated by 18 cu, and there is another 18 cu between #66 and #12. This angular spacing is shown by the two labeled arrows. Here we see a portion of a third symmetry ring.

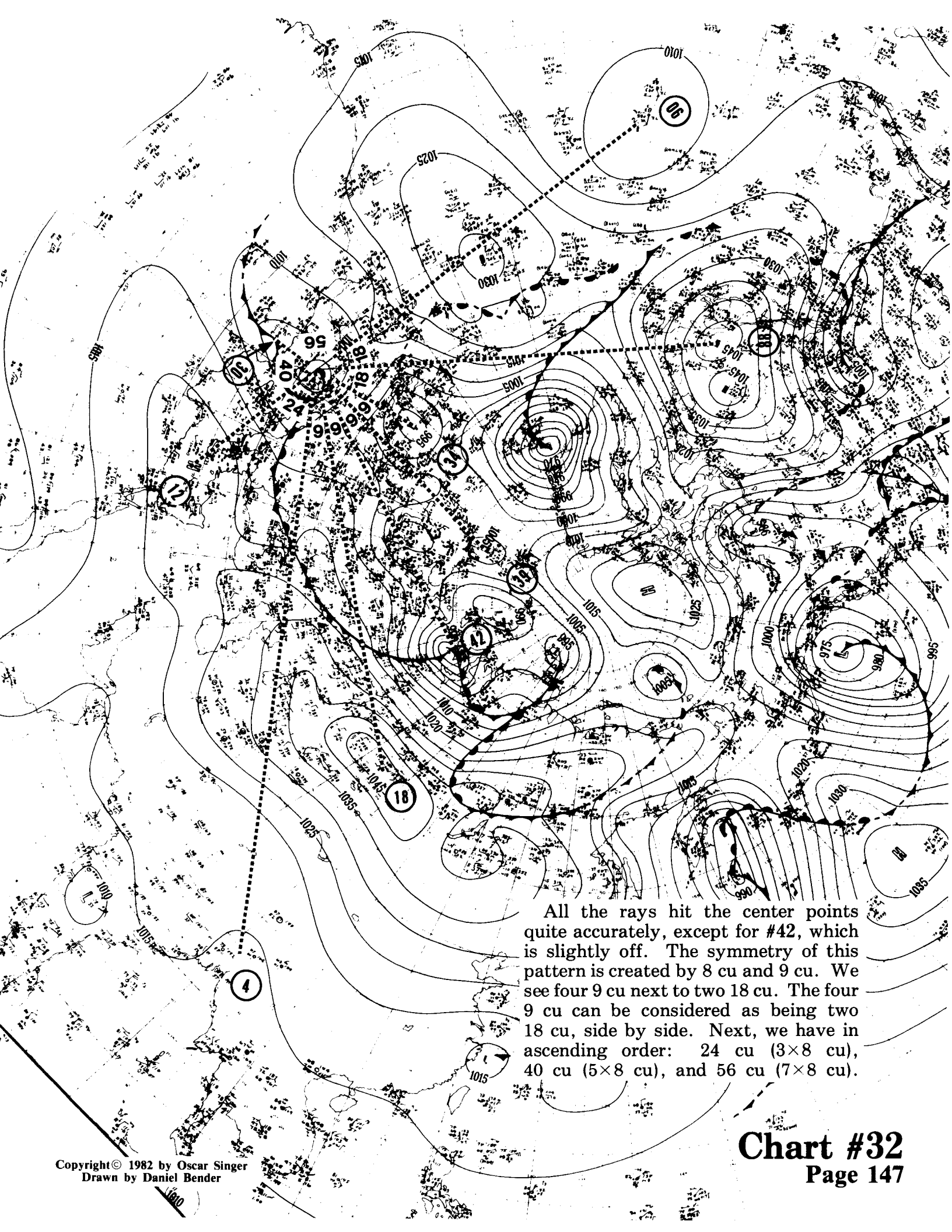


In this case, #6, #18, #29, #58, and #79 are good hits—the rest are so-so. The symmetry in this pattern is based on 11 cu. Inspection will show that the 10 cu is squeezed between two 11 cu, with one 12 cu on the side. The angle between #49 and #79 has increased by 1 cu, to become 12 cu. This angle has taken up the slack created by the 10 cu between #74 and #58.

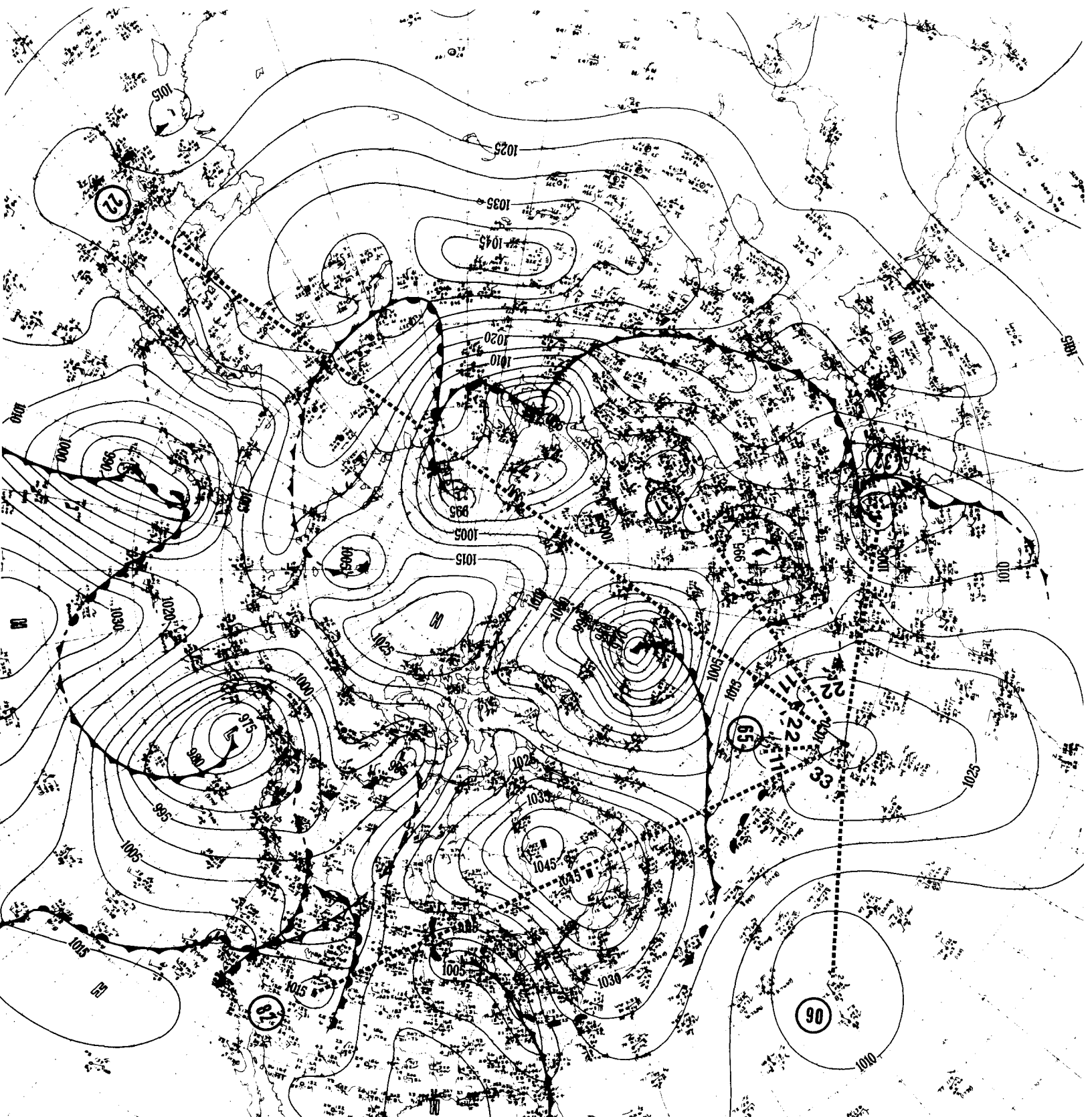
There is one 15 cu between #6 and #7. There is another symmetry pattern coexisting simultaneously with the one shown on this chart. The 15 cu was entered to show how it is hooked to #7, which is in the symmetry pattern involving the 11 cu. The next chart will show how 15 cu is involved in a different pattern.



The rays hit all the center points accurately except for #53, which is off a little. Here we have a central 17 cu, balanced symmetrically on both sides by two 16 cu and two 15 cu, with another 15 cu almost diametrically opposite the 17 cu.



All the rays hit the center points quite accurately, except for #42, which is slightly off. The symmetry of this pattern is created by 8 cu and 9 cu. We see four 9 cu next to two 18 cu. The four 9 cu can be considered as being two 18 cu, side by side. Next, we have in ascending order: 24 cu (3×8 cu), 40 cu (5×8 cu), and 56 cu (7×8 cu).

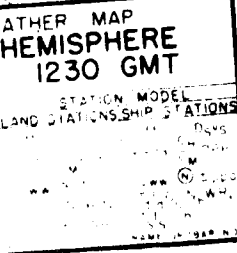


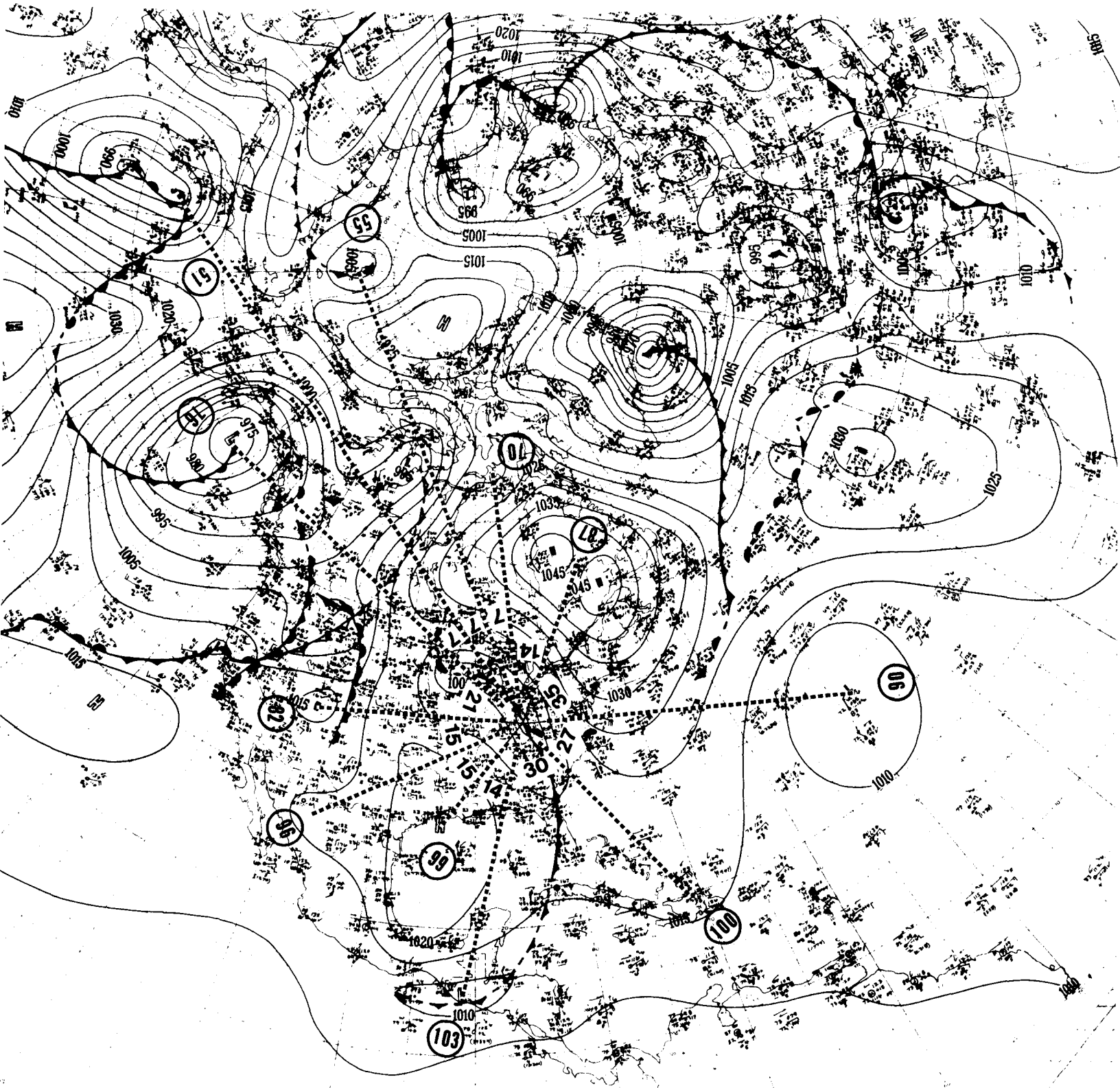
All the rays are hitting the center points accurately. The symmetry of this pattern hinges on 11 cu. The symmetry is neat. We have a 33 cu, followed by 11 cu and then 22 cu, which is repeated twice.

Four separate charts have been prepared for #91 to show at least four different symmetry patterns coexisting around this nuclear vortex. This type of multiple symmetry patterns exist around each of the charts presented up till now. There is no special significance in showing four charts for #91, other to expand your understanding of multiple symmetry.

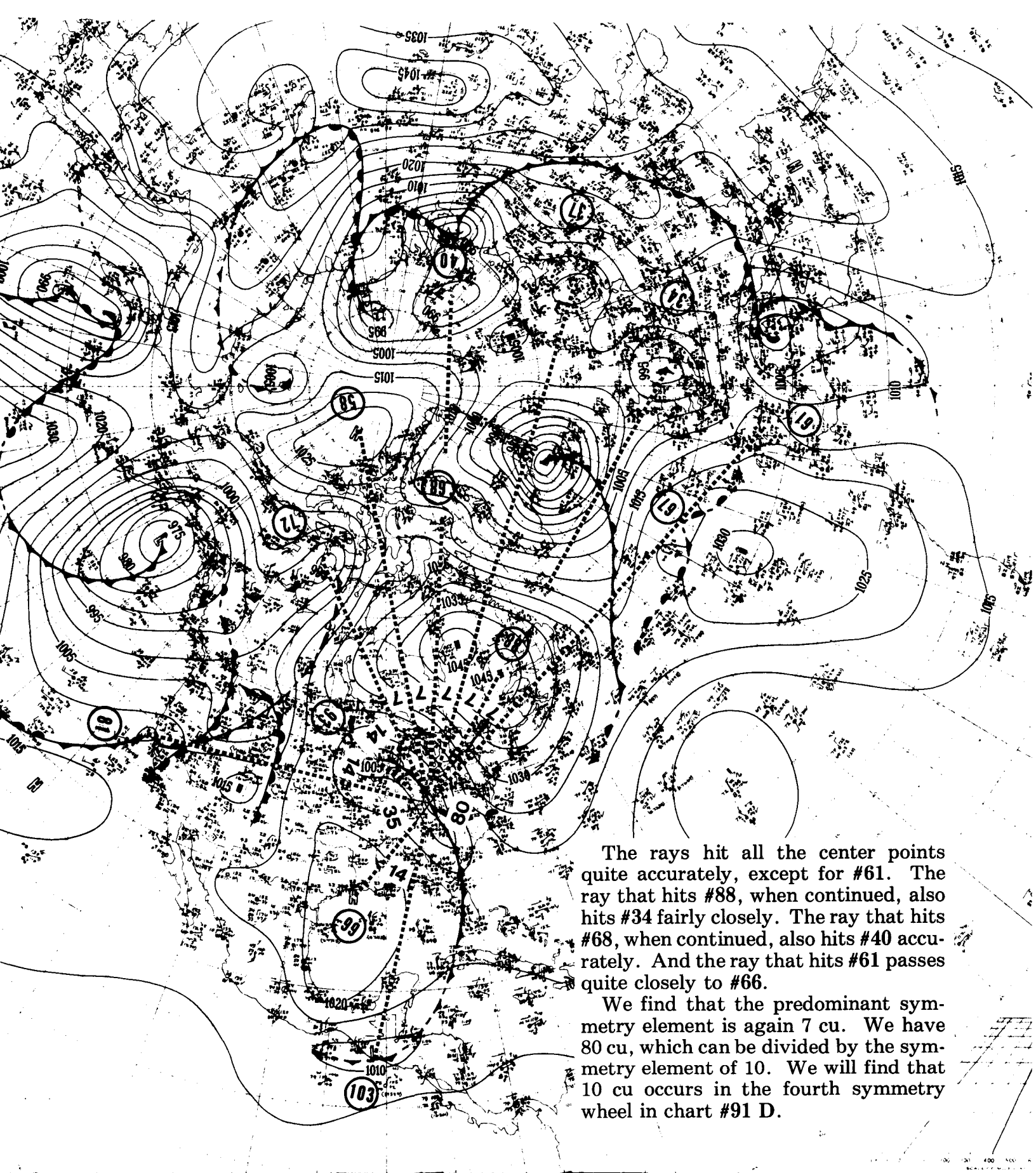
The rays hit all the center points quite accurately, except for #90, which is slightly off, and for #65 and #96, which are poor hits. They have been entered to show what is considered an almost acceptable hit.

The predominant symmetry numbers are 15 cu and 9 cu, both of which are divisible by 3, which is the lowest common denominator. There is one 9 cu, one 18 cu (2×9 cu), and one 27 cu (3×9 cu).



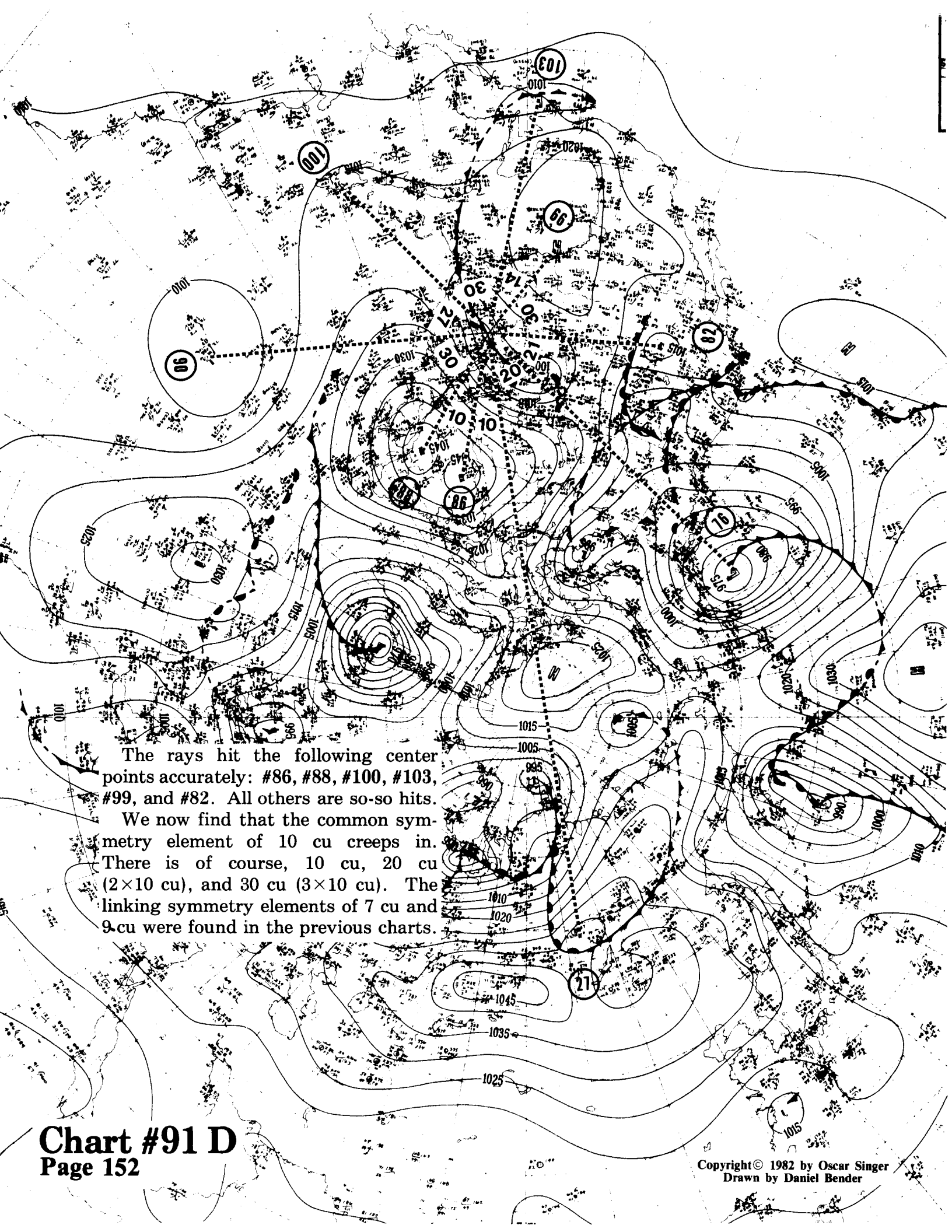


The rays hit all the center points quite accurately, except for #90, #55, #76, #96, and #70, which are slightly off. Here we find the symmetry pattern has added a 7 cu as a symmetry element. The 14 cu was isolated and all by itself in chart #91 A. We now have 7 cu, 14 cu (2×7 cu), 21 (3×7 cu), and 35 (5×7 cu). In addition, we have 15 cu, 30 cu (2×15 cu), and 9 cu represented by 27 cu (3×9 cu). The 15 cu and 9 cu present in a greater frequency in chart #91 A.



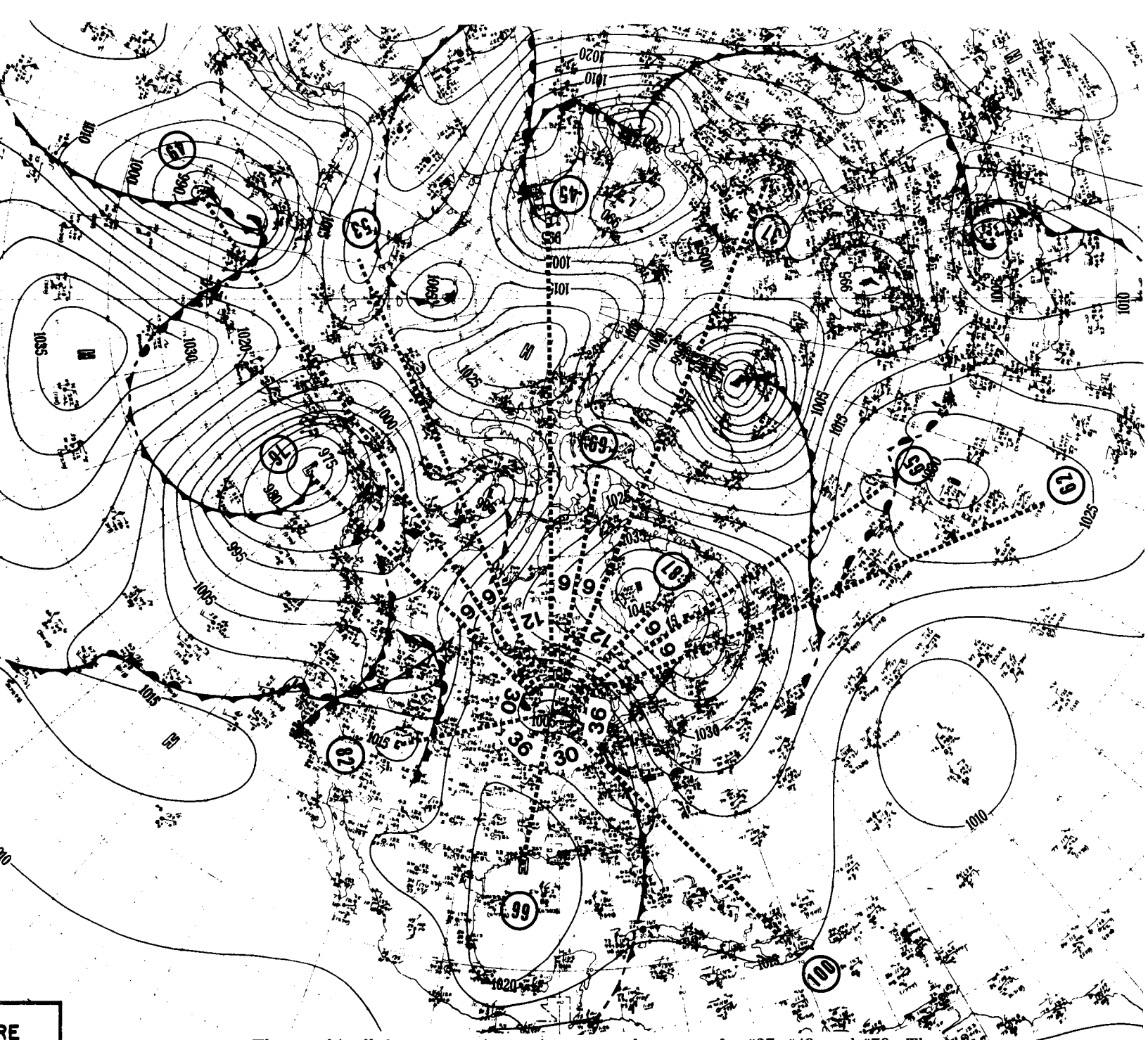
The rays hit all the center points quite accurately, except for #61. The ray that hits #88, when continued, also hits #34 fairly closely. The ray that hits #68, when continued, also hits #40 accurately. And the ray that hits #61 passes quite closely to #66.

We find that the predominant symmetry element is again 7 cu. We have 80 cu, which can be divided by the symmetry element of 10. We will find that 10 cu occurs in the fourth symmetry wheel in chart #91 D.



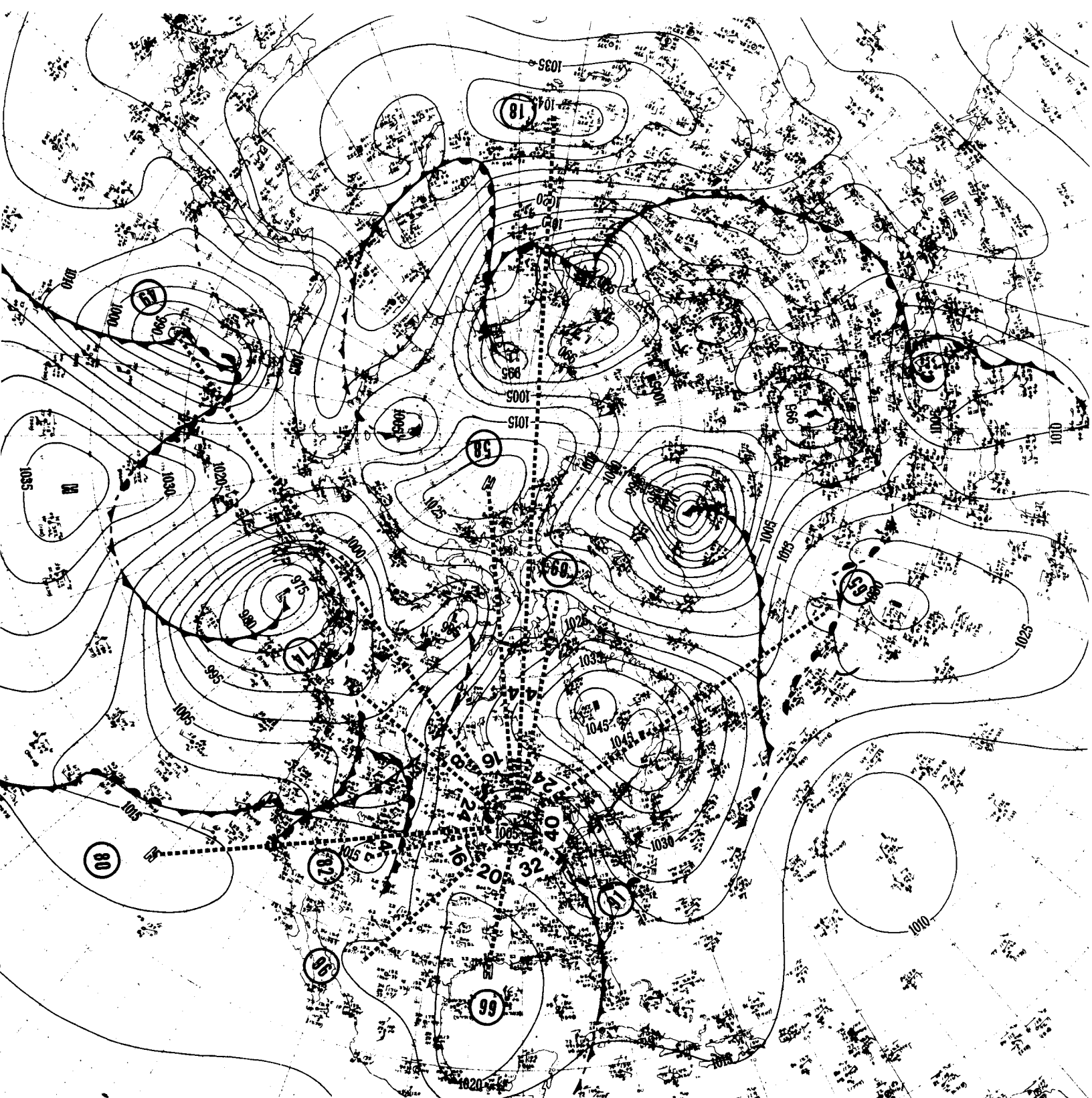
The rays hit the following center points accurately: #86, #88, #100, #103, #99, and #82. All others are so-so hits.

We now find that the common symmetry element of 10 cu creeps in. There is of course, 10 cu, 20 cu (2×10 cu), and 30 cu (3×10 cu). The linking symmetry elements of 7 cu and 9 cu were found in the previous charts.



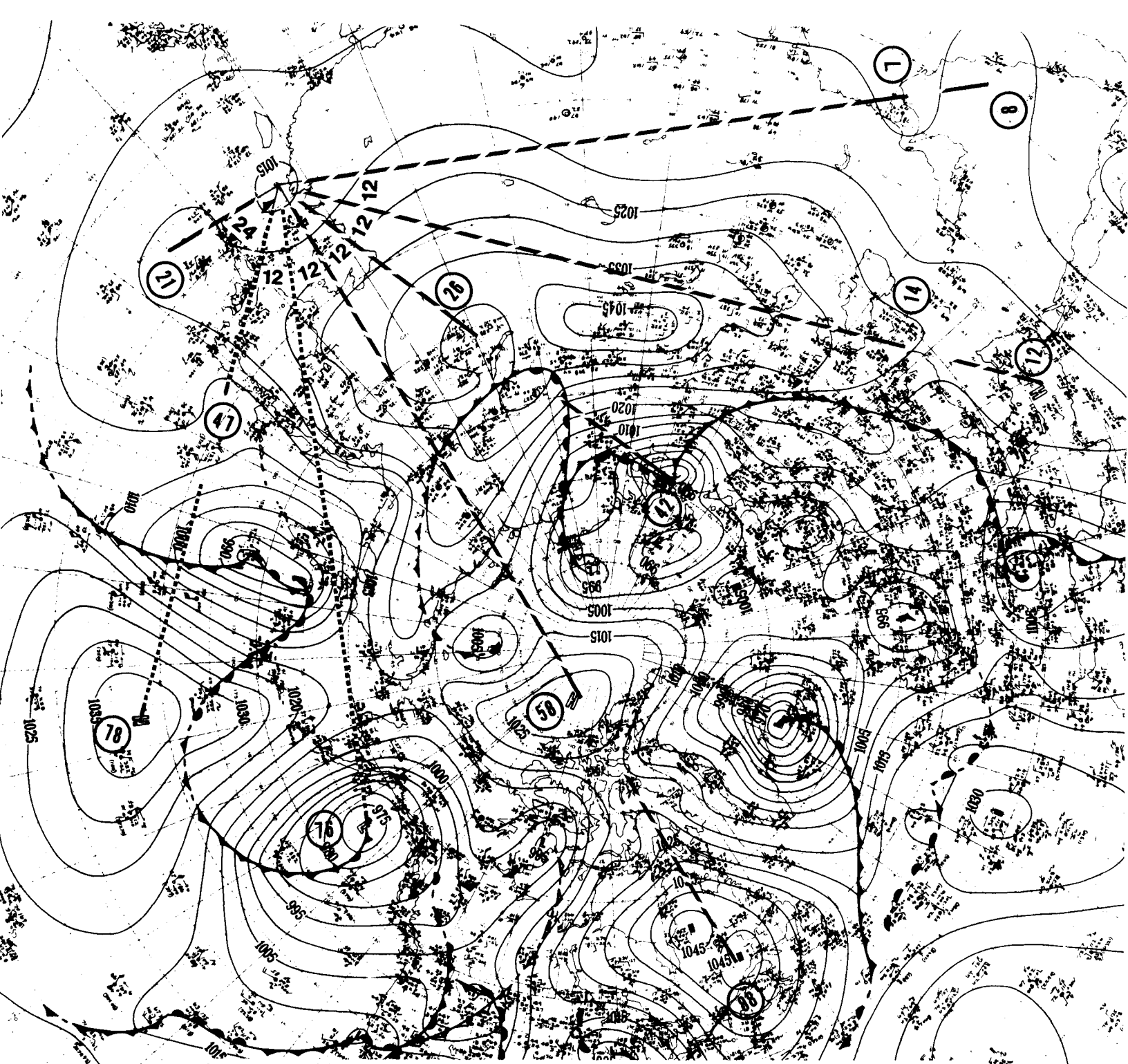
The rays hit all the center points quite accurately, except for #37, #49, and #76. The common symmetry element in this chart is 6 cu. A special feature is the alternating sequence of numbers. There are two 6 cu, with one 12 cu on either side; then there are two 6 cu again, this time on each side of the 12 cu. Then we have 30 cu and 36 cu alternating symmetrically to complete the ring of 192 cu.

Let me reconstruct the manner in which this chart was assembled. First, the hardcore vortexes that set the basis for the chart were identified. They include #99, #82, and #45. Next, the points that looked good were entered, such as #53, #69, #87, #65, and #100. Then a search was made to see if anything fell 6 cu or 12 cu to the left or right of any of these vortexes that had already been entered. This search revealed the approximate vortexes of #76, #49, and #37. The pattern looked so neat and symmetrical at this point, that I looked again to see if there was anything to the south of #65. Sure enough, 6 cu to the south, I entered #62. That point looks like a good location for a second high center, since there is an elliptical bulge to the south of #69. This is in line with the theory discussed earlier with regard to Plateau's drops of oil forming new centers and also with analysis of multiple centers for elliptical shapes. This is one example where this type of symmetry analysis is an aid in identifying where the centers of obscure vortexes may be located.



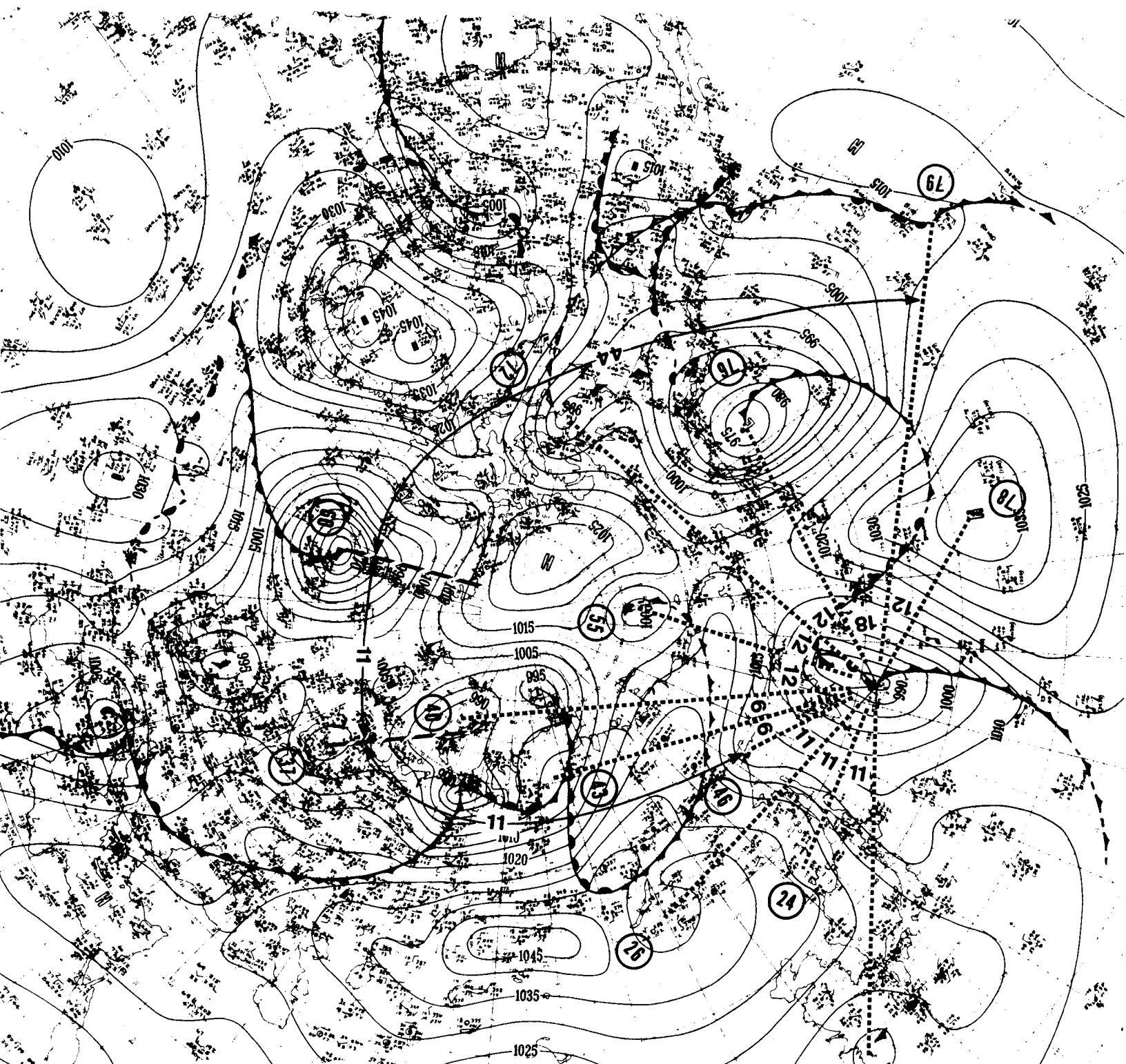
The rays hit all the center points accurately, except for #49 and #96. The ray that goes to #65 passes very close to #88. The center point for the remnant low #74 is considered as being at the tip of the front where the front changes its curvature to a northwesterly direction.

4 cu is the symmetry element for this pattern. All the angular numbers on this chart can be divided into a whole number by 4. There is an additional element of symmetry that is visible if we start with the 16 cu between #49 and #58. On both sides we have 8 cu (4 cu plus 4 cu equals 8 cu). On each side of the 8 cu, we have a 24 cu. On each side of the 24 cu, we have two 40 cu (one 40 cu is 4 cu plus 16 cu plus 20 cu), and finally we have a single 32 cu. A good one.

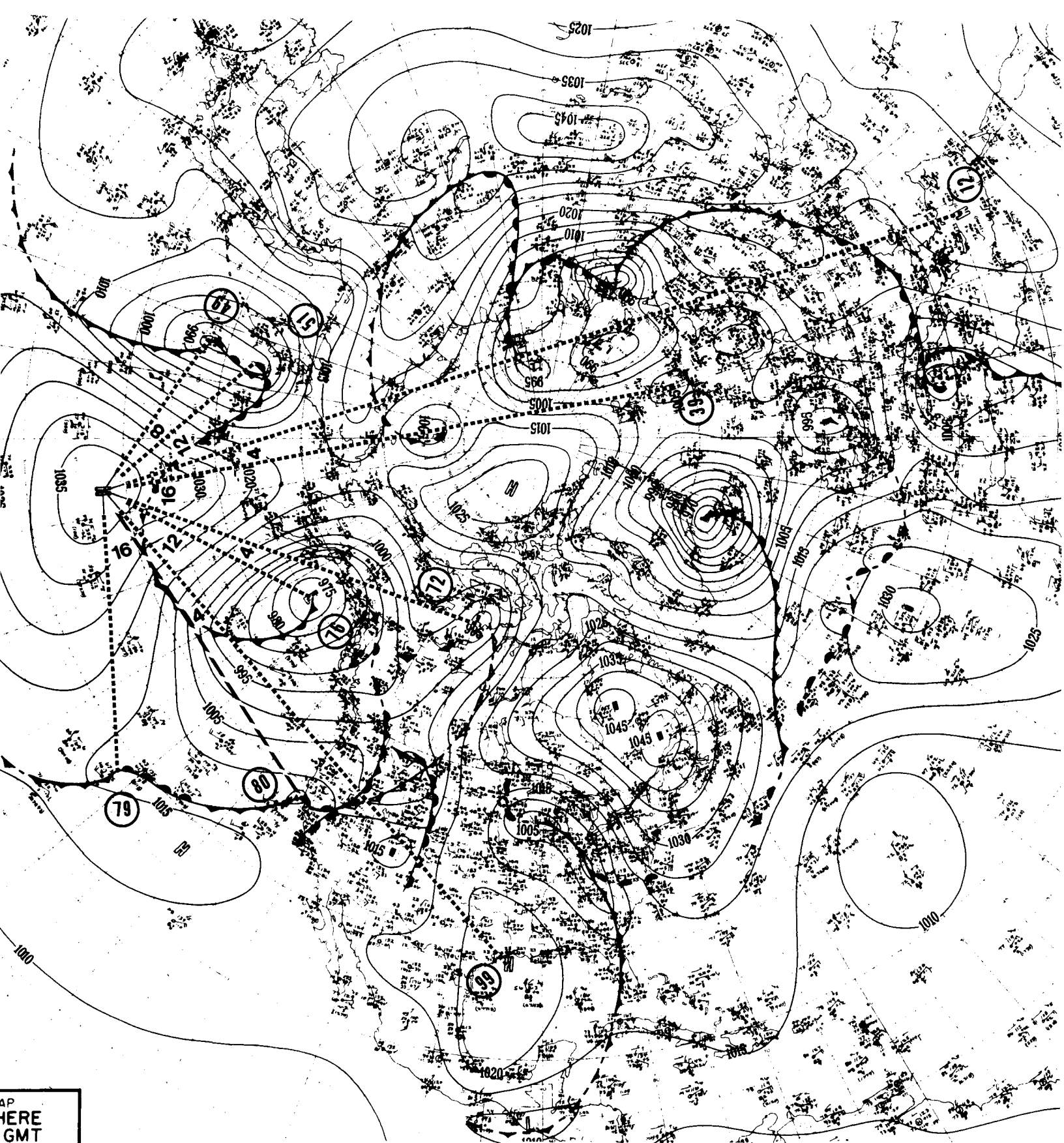


The two rays with the dotted lines hit the center points accurately and set the basis for the 12 cu. The other rays were drawn with dashed lines, since they are not close hits. The dashed and dotted lines will be used in the remainder of the circumferential charts to distinguish between good hits and fair hits.

The approximate points indicated by the dashed lines on this chart seem to detract from its quality, but before you jump to any hasty conclusions, let us take another look at the phenomenon of longitudinal glide reflection. By careful inspection, you will see that #58 and #88 are on opposite sides of the ray line. Likewise, #26 and #42 lie on opposite sides of their common ray. And the same can be said for #12 and the obscure #14, and for the two obscure points #7 and #8. These dashed lines that are approximate hits, really represent average positions between two or more points. This then gives added significance to this symmetry pattern since it also uses some average positions. The preceding charts were examples of simple symmetry, whereas now, I have introduced a clear cut example of complexity which involves glide symmetry. You can now go back to the previous charts and find many other examples of glide reflection which I have not pointed out specifically.

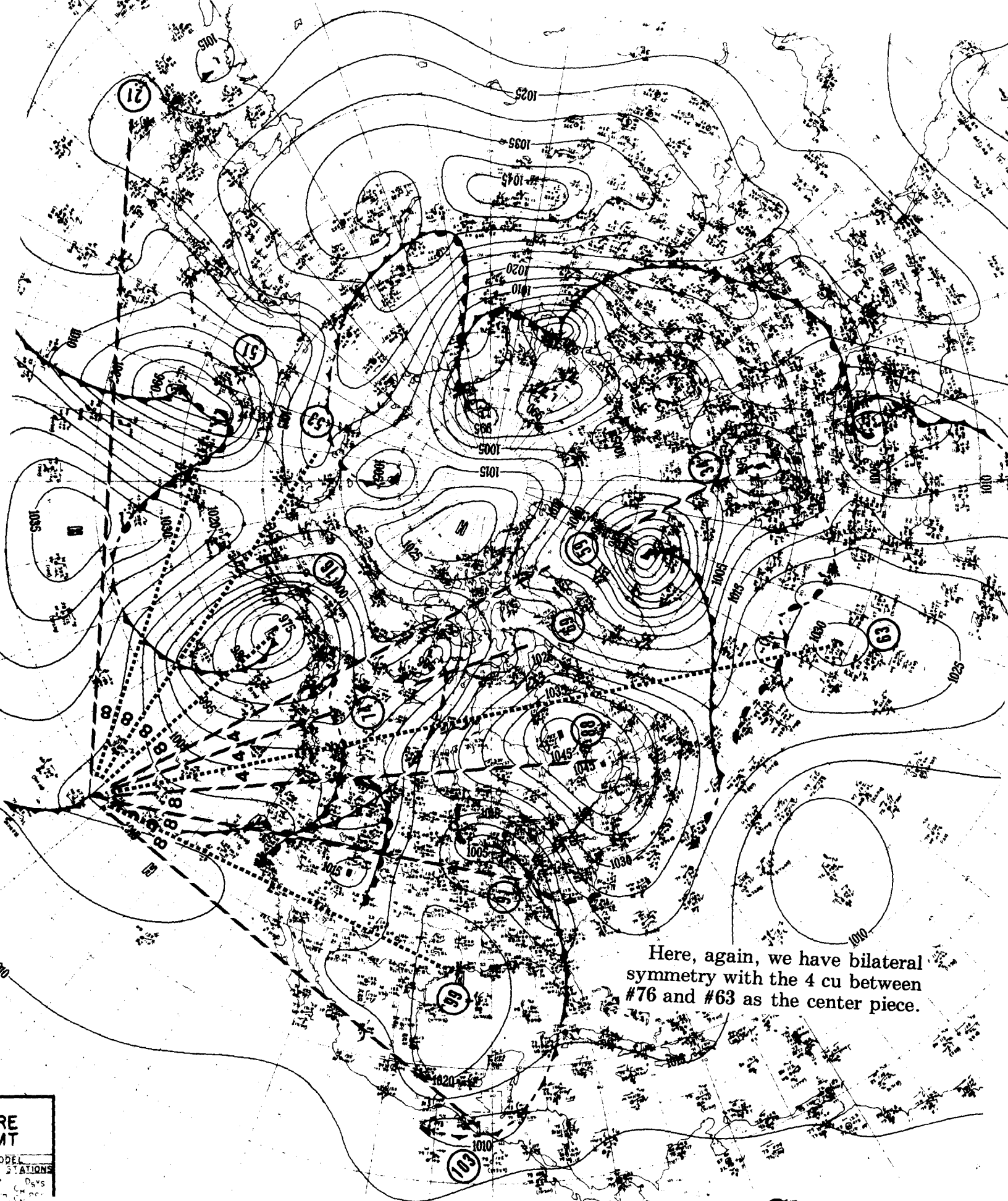


This chart demonstrates two different rings. The inner ring is based on the fundamental units of 11 cu and 6 cu, while 12 cu and 18 cu are multiples of 6 cu. The outer ring, made up of the points #46, #37, #60, and #79, has been drawn to show that it has the fundamental of 11 cu, which is a continuation of 11 cu in the inner ring.



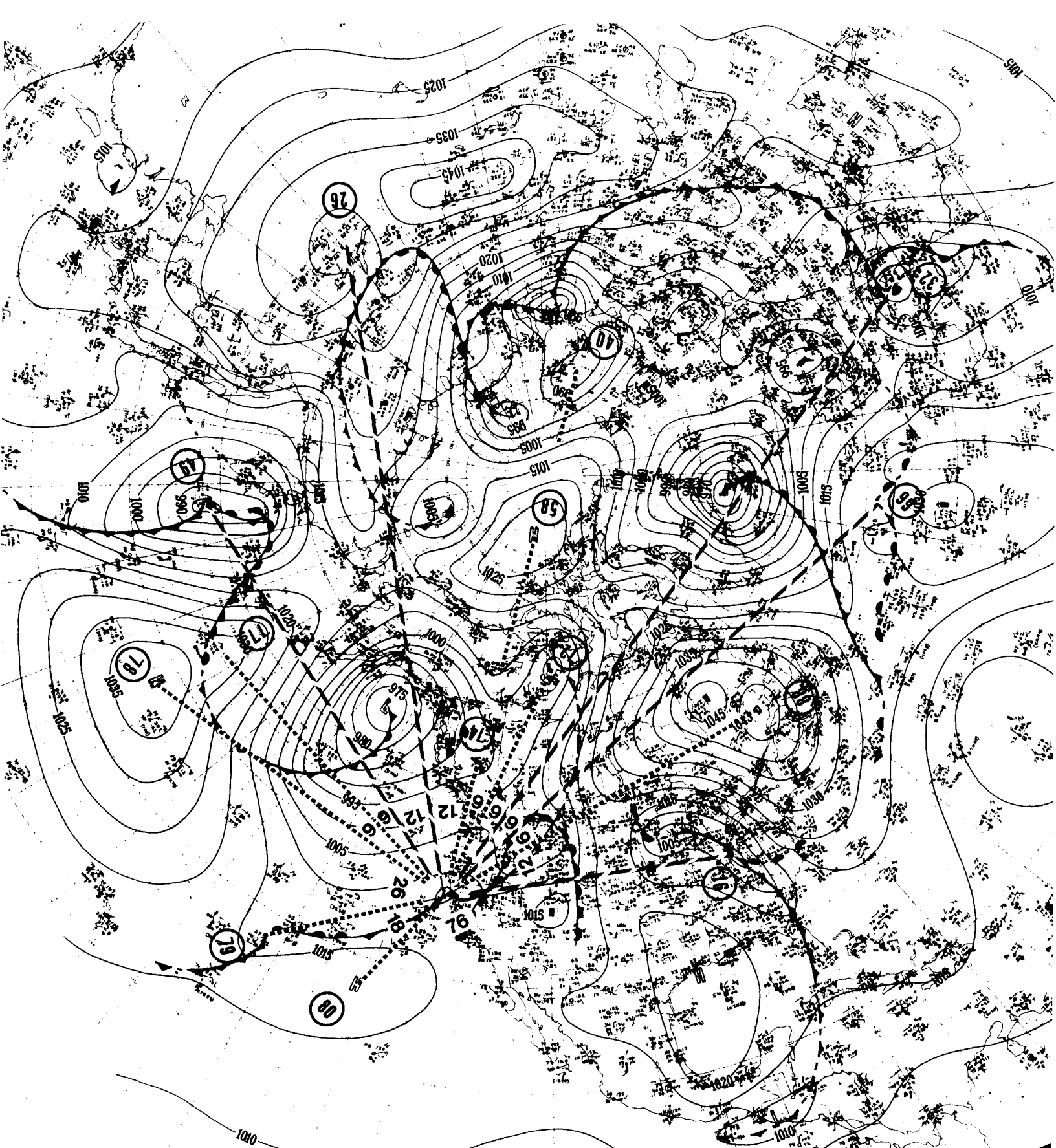
All the angles are divisible by the main symmetry element of 4. There is a balance left and right of bilateral symmetry around the 16 cu between #72 and #39.

AP
HERE
GMT
MODEL
SHIP STATIONS
Days
© 1982
Oscar Singer

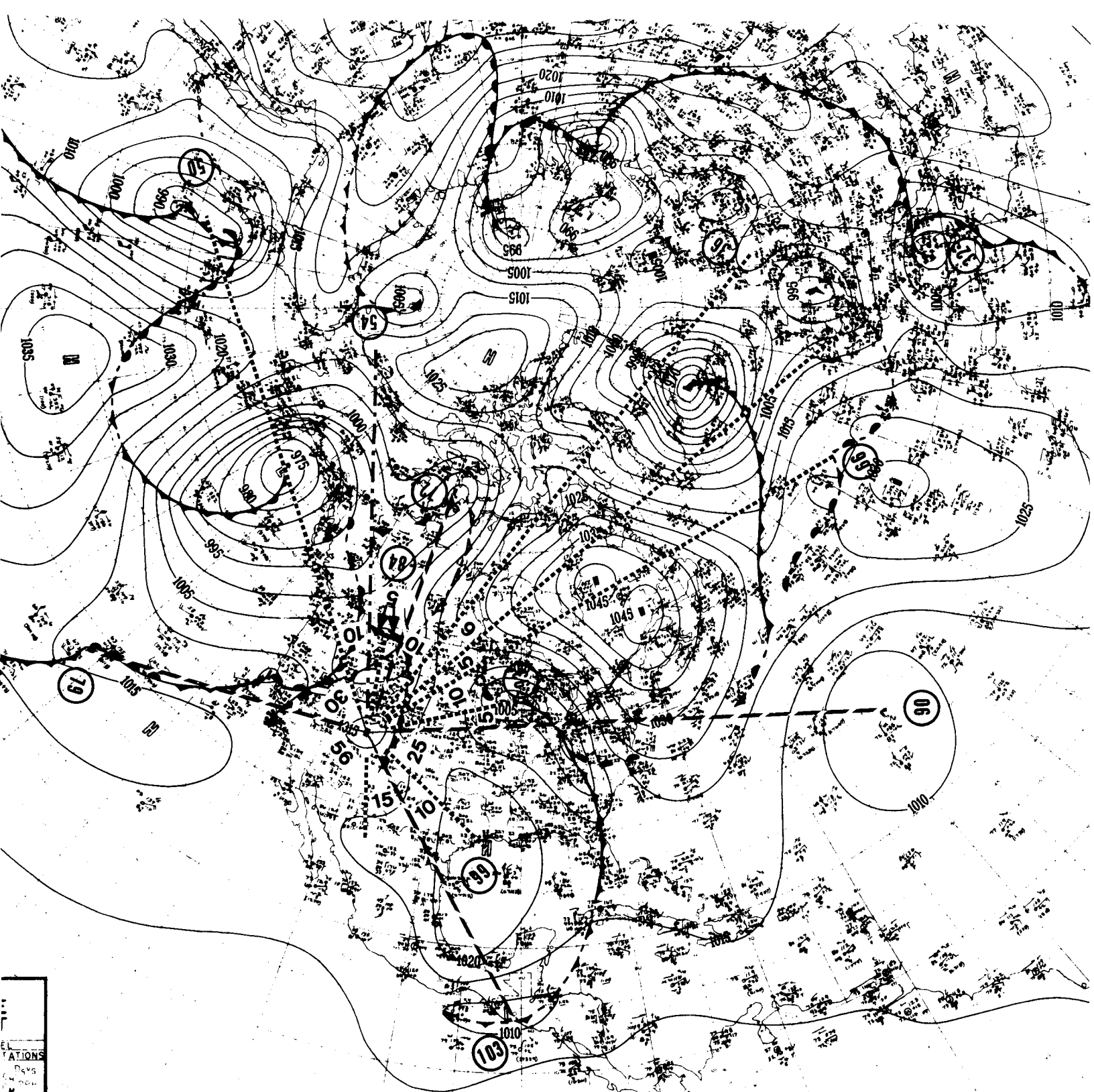


Here, again, we have bilateral symmetry with the 4 cu between #76 and #63 as the center piece.

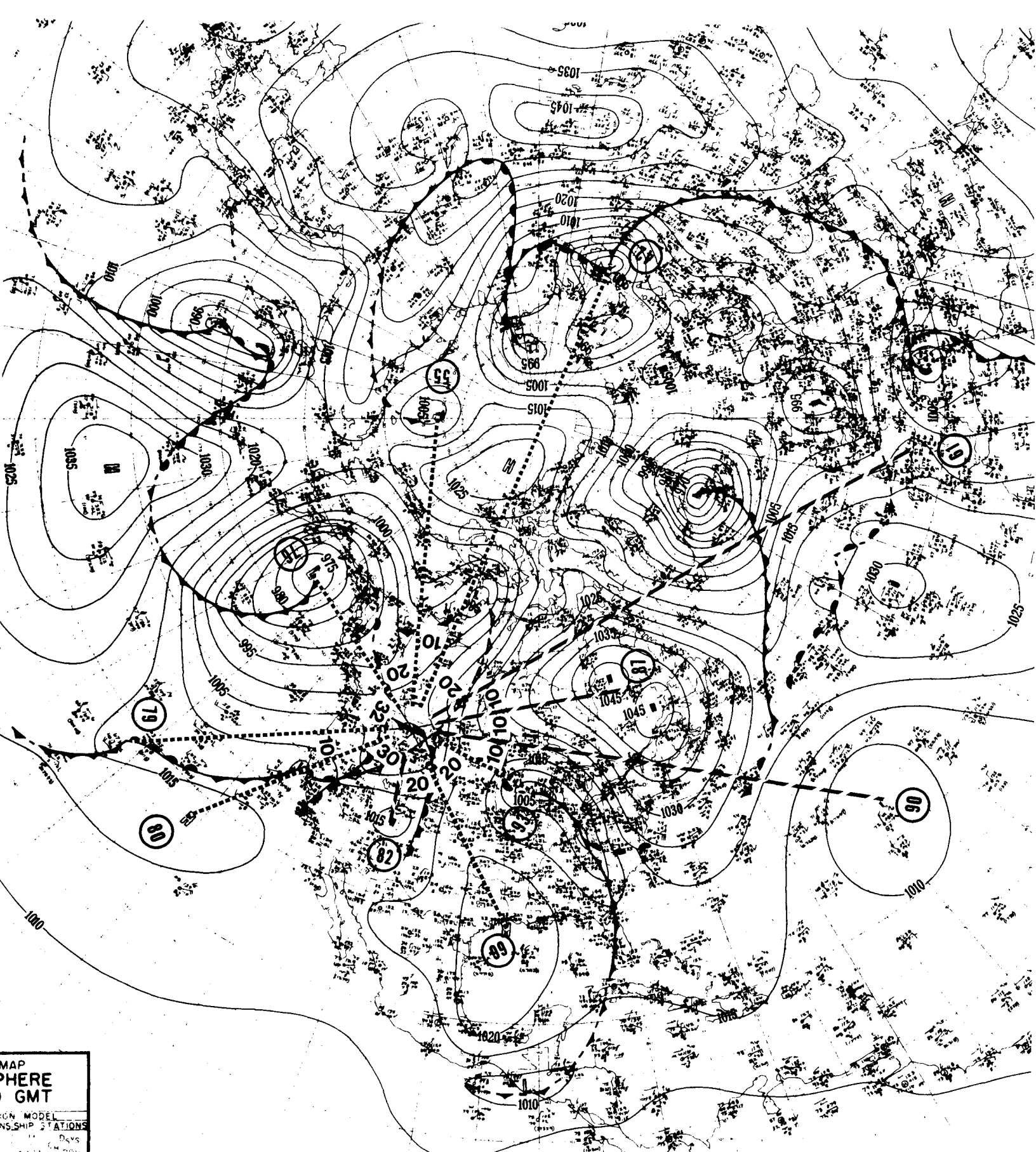
RE
AT
MODEL
STATIONS
Devs
CH



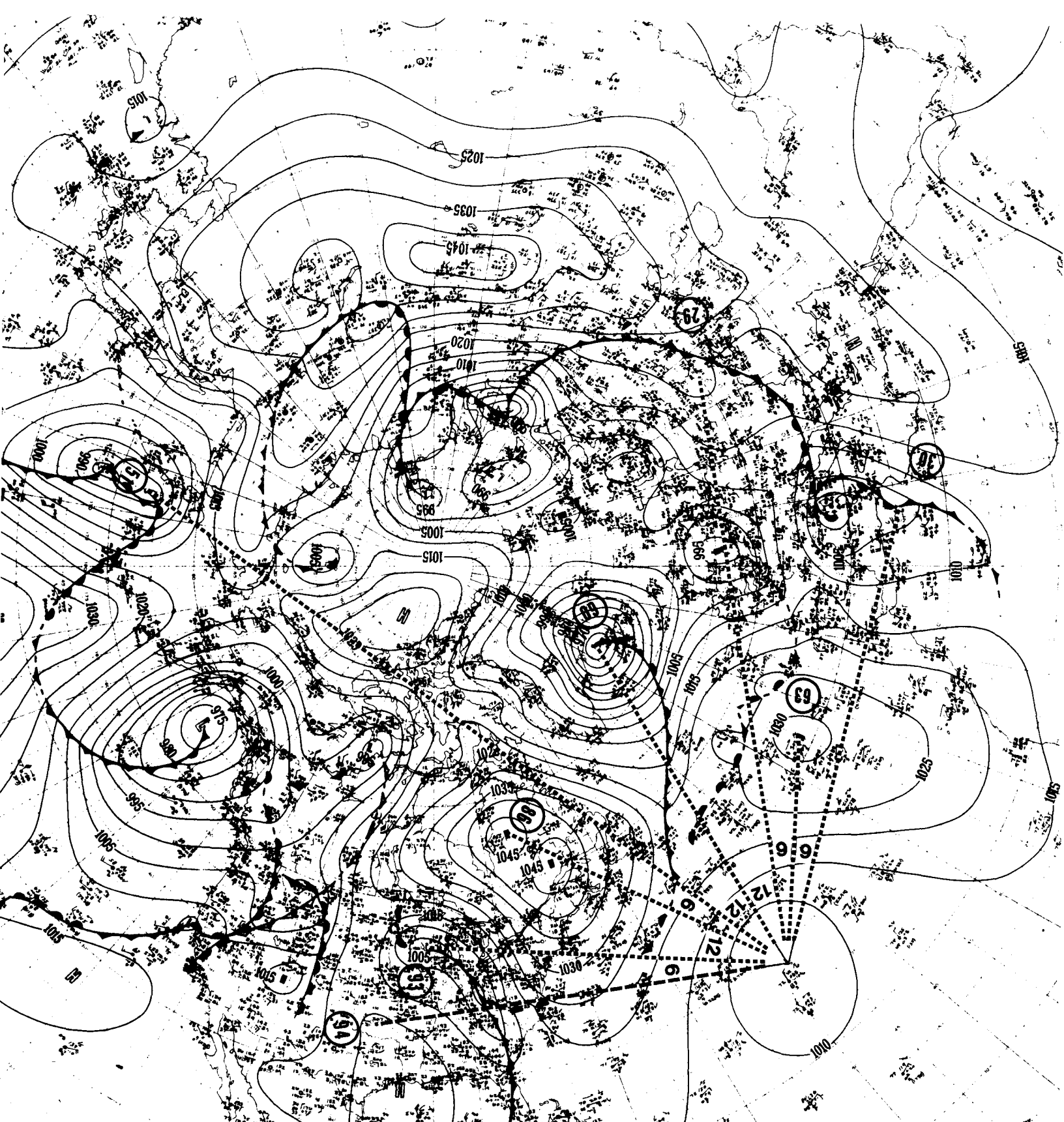
This symmetry pattern is established with 6 cu and its multiples of 12 cu and 18 cu. The sum of the two odd-balls, 26 cu and 76 cu, add up to 102 cu (17×6 cu).



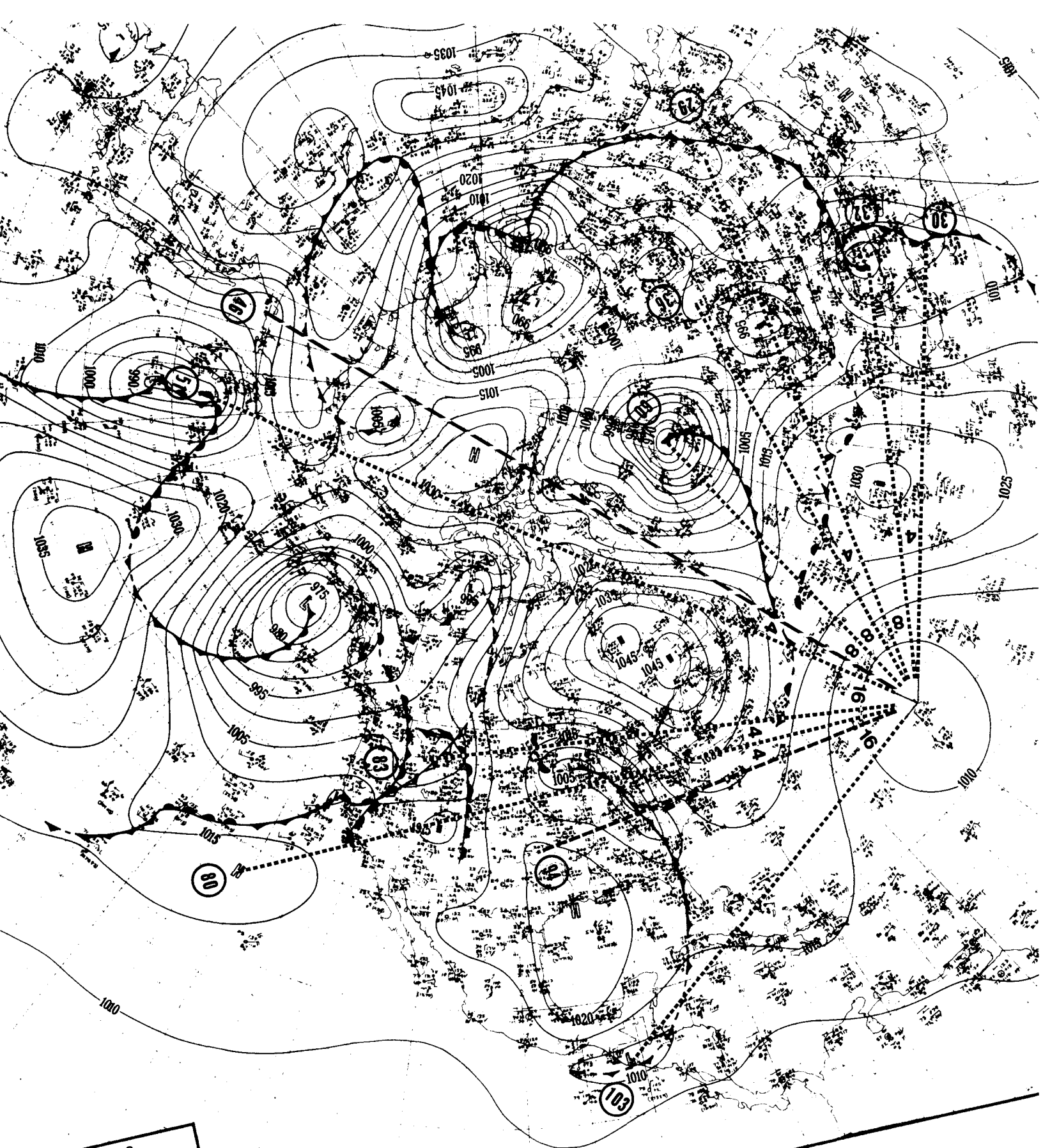
The main symmetry element in this chart is 5 cu and its multiples, with one 6 cu and one 56 cu to complete the ring.



10 cu is the element that brings out this symmetry pattern. One lone 32 cu is necessary to complete the ring.



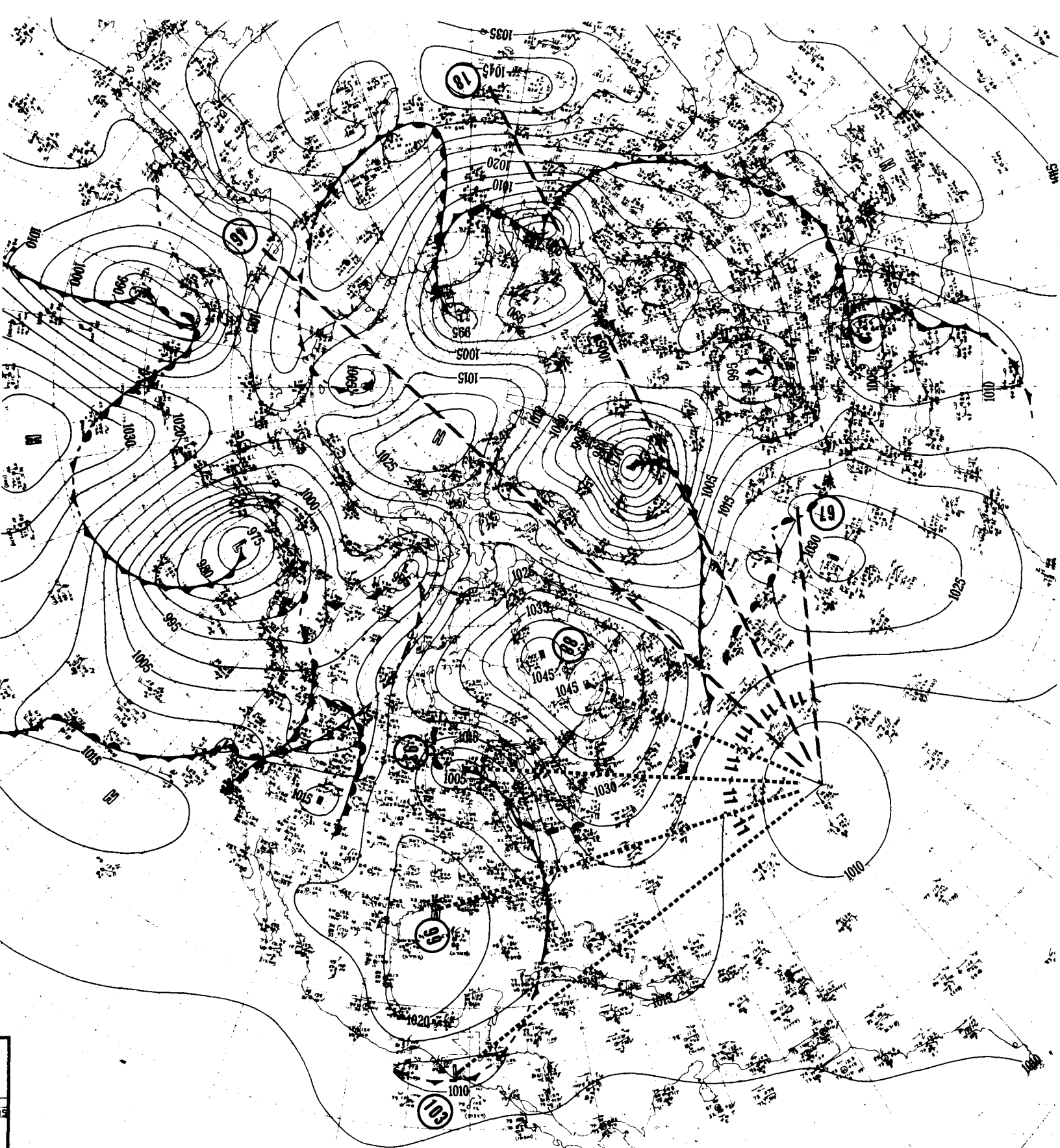
The angular number that imparts symmetry to this pattern is of course 6 cu, with its multiple of 12 cu (2×6 cu). #94 was added as a point of interest to indicate a possible center for the small elliptical projection of #99.



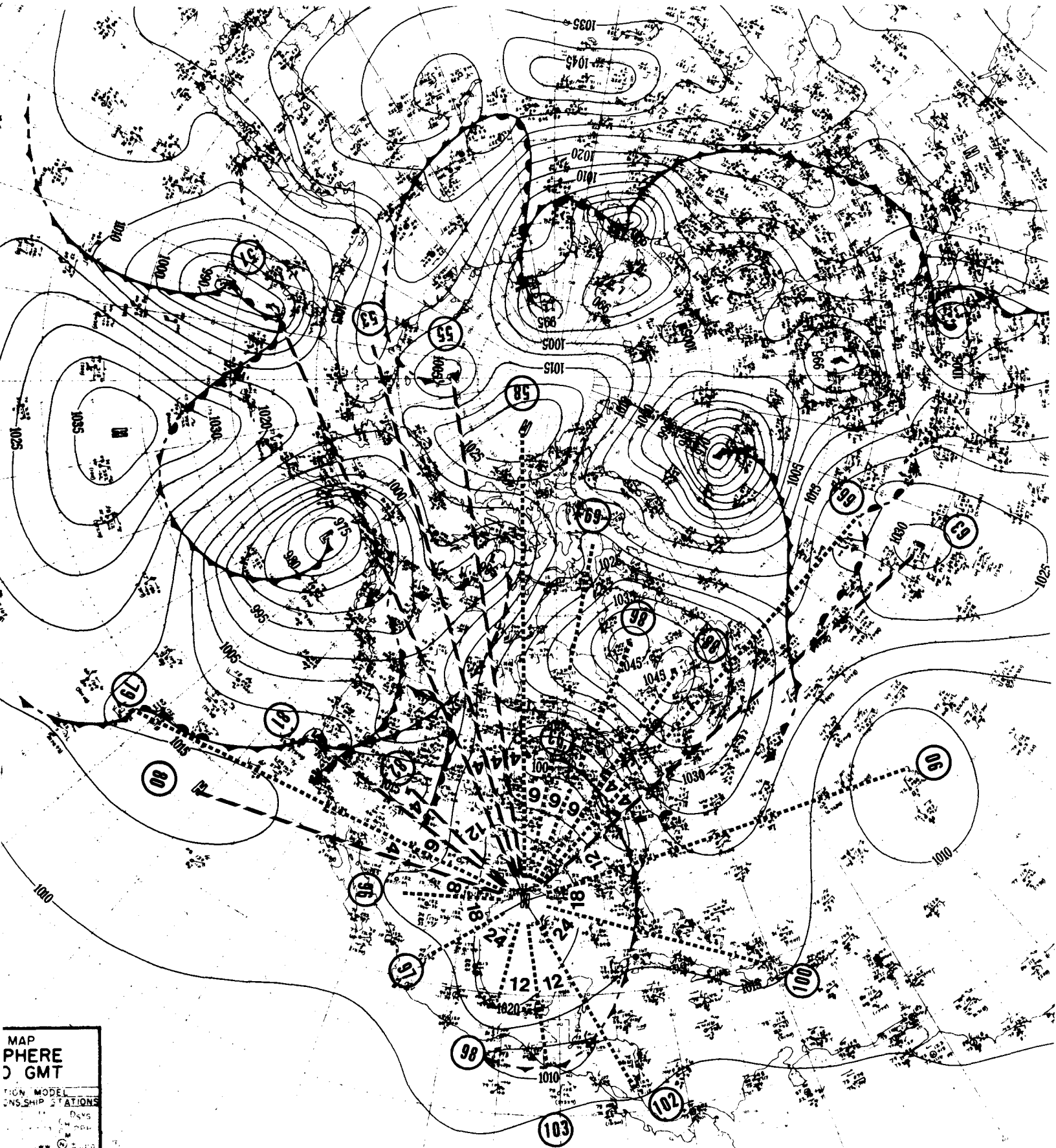
WEATHER MAP
NORTHERN HEMISPHERE
1230 GMT

STATION MODEL
LAND STATIONS SHIP STATIONS

4 cu, with its multiples of 8 cu and 16 cu, gives us this symmetry pattern.

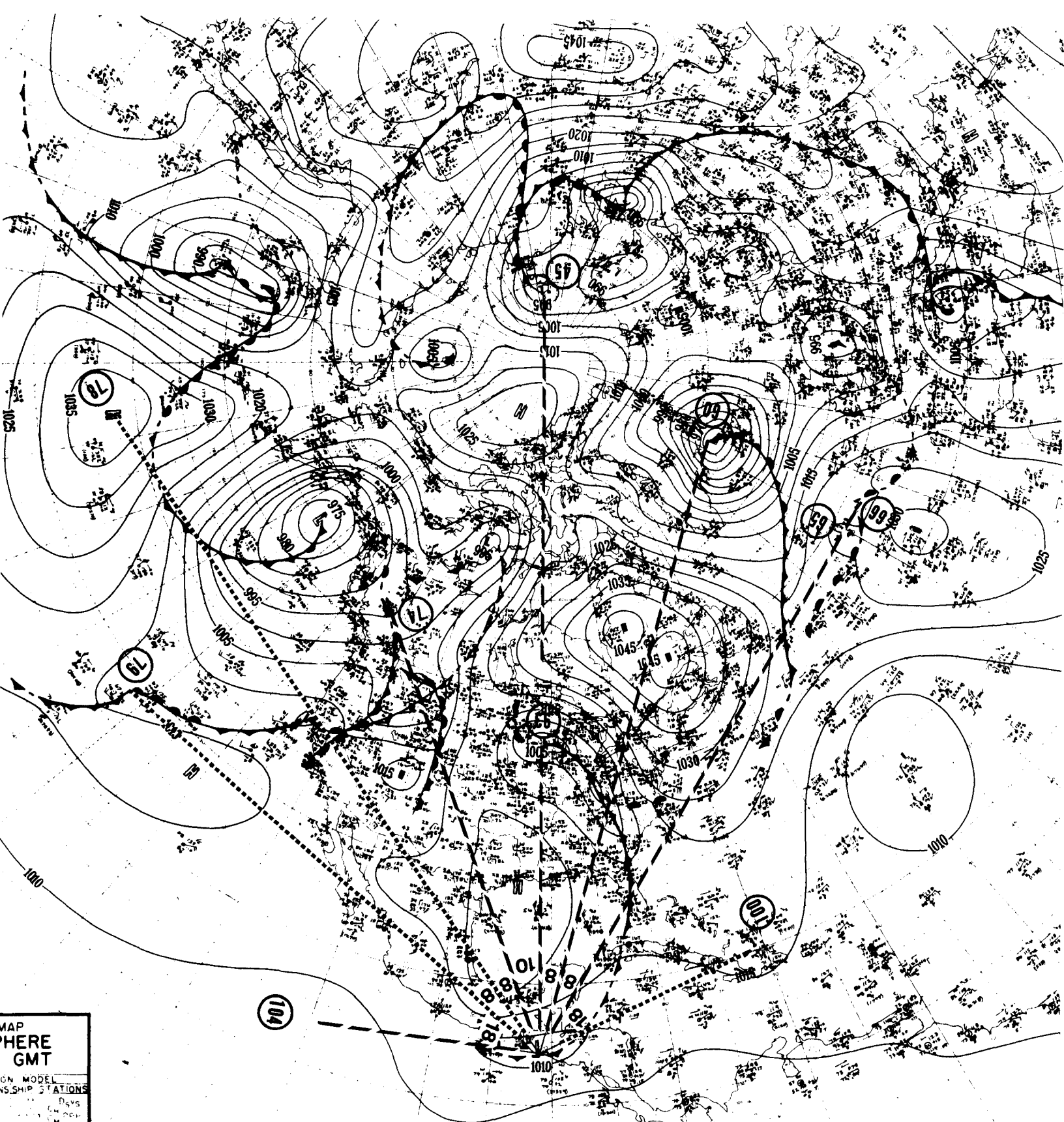


The hard core of this symmetry pattern was set up with #103, #99, #93, and #88—the rest are for interest only. The symmetry pattern is obviously based on 11 cu.



The symmetry pattern is based on 4 cu and 6 cu.

Chart #99
Page 167



This is an example of bi-lateral symmetry with the 10 cu centerpiece being flanked on each side separately by two 8 cu and one 18 cu. #104 is an uncertain position, but it was entered as a possibility.

Chapter 13

The Radial Charts

Radial Spacing, General

This division of the charts is drawn to illustrate the symmetry of the radial spacing of highs, lows, and cols at 1230 G.M.T. on December 7, 1950.

What do you hear when a symphony orchestra plays? You may hear several different tunes or melodies simultaneously; occasionally you may make out an individual instrument, but most of the time you can not make out the individual notes of the individual players. You can subject the entire orchestral music to what is called a harmonic analysis (first developed by Fourier) to separate the various instruments and sounds, or you can simply pluck each player out individually and listen to him or her play the individual melody. Fourier analysis requires some complicated mathematics—whereas listening to the individual player is simple enough for a child to understand. It was necessary to use complicated Fourier analysis to solve some of the principles of *Singer's Lock*, but once the principles were established, the complicated mathematics became redundant. Each of the following charts represents an individual player or note of the symphony of weather incidents occurring simultaneously over the Northern Hemisphere.

The lines that are drawn on the charts are used only to identify the points we are dealing with—nothing else—therefore they are drawn a little thicker and with less care than the lines on the circumferential series of charts. These lines were not used to calculate the distances. The latitude and longitude of each usable high, low, and col was carefully determined and then entered in Table IX. This information was in turn fed to a computer, which calculated the great circle distances between the points I used in the charts. This kept the

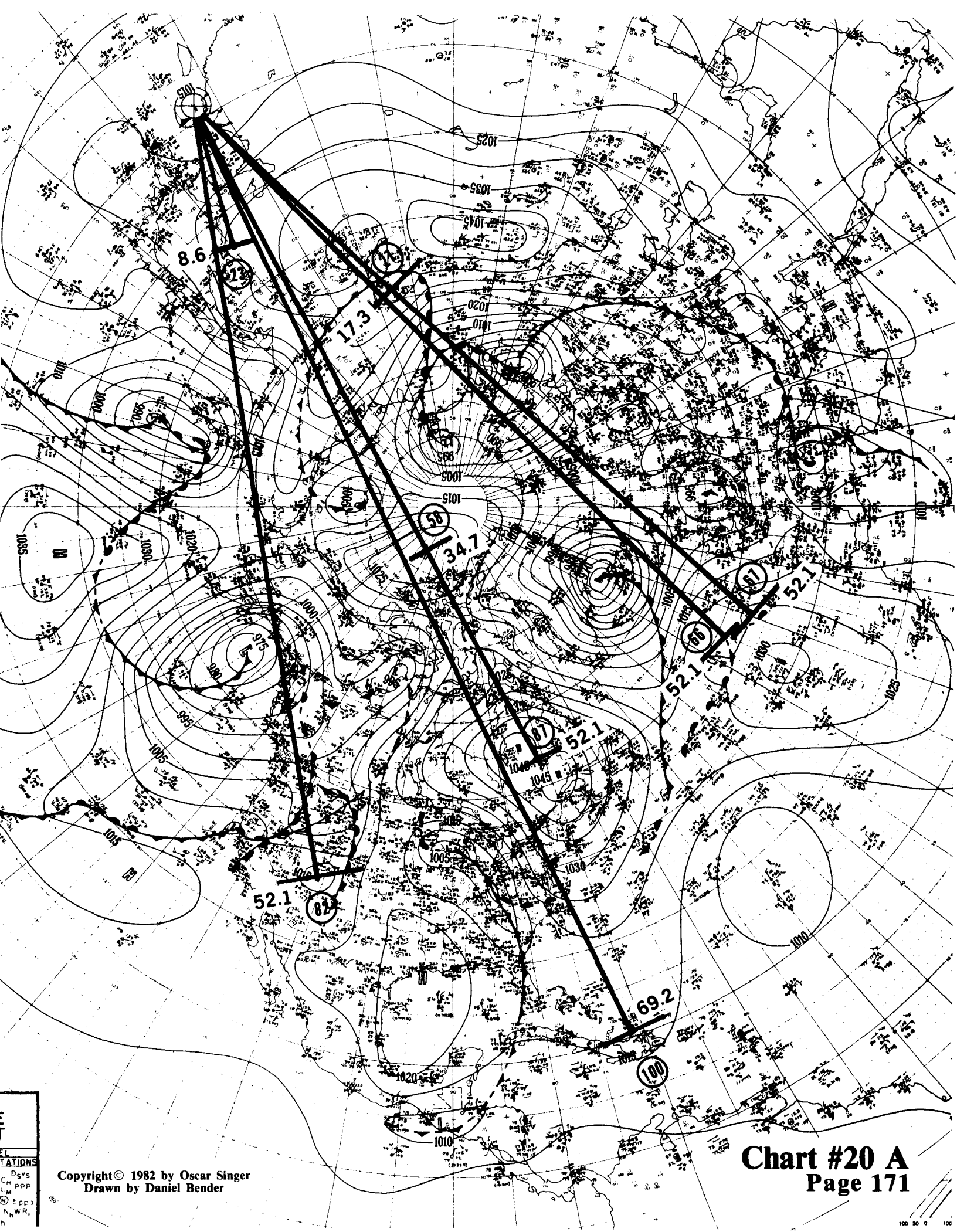
computer busy for 8 hours. These calculated values, expressed in angular numbers, are entered on the map, next to each point where the measurement applies. The other numbers which are circled are used to identify the points being analyzed.

In this set of charts, I am emphasizing the radial spacing, but I will throw in some significant circumferential spacing similar to the first set of charts.

It is desirable to keep in mind that these maps (which are only a small sample of the total that can be drawn) are not just a group of detailed examples of previously unknown facts. These maps represent the proof, for the first time, that there are simple whole number relationships in both a radial and circumferential direction that join all significant features on a weather map, similar to the Chladni Plates shown in Figure 9-4. It may be disappointing to some, that the mathematics of this first part of *Singer's Lock* is as simple as that. The truth is usually simple.

Chart #20 A

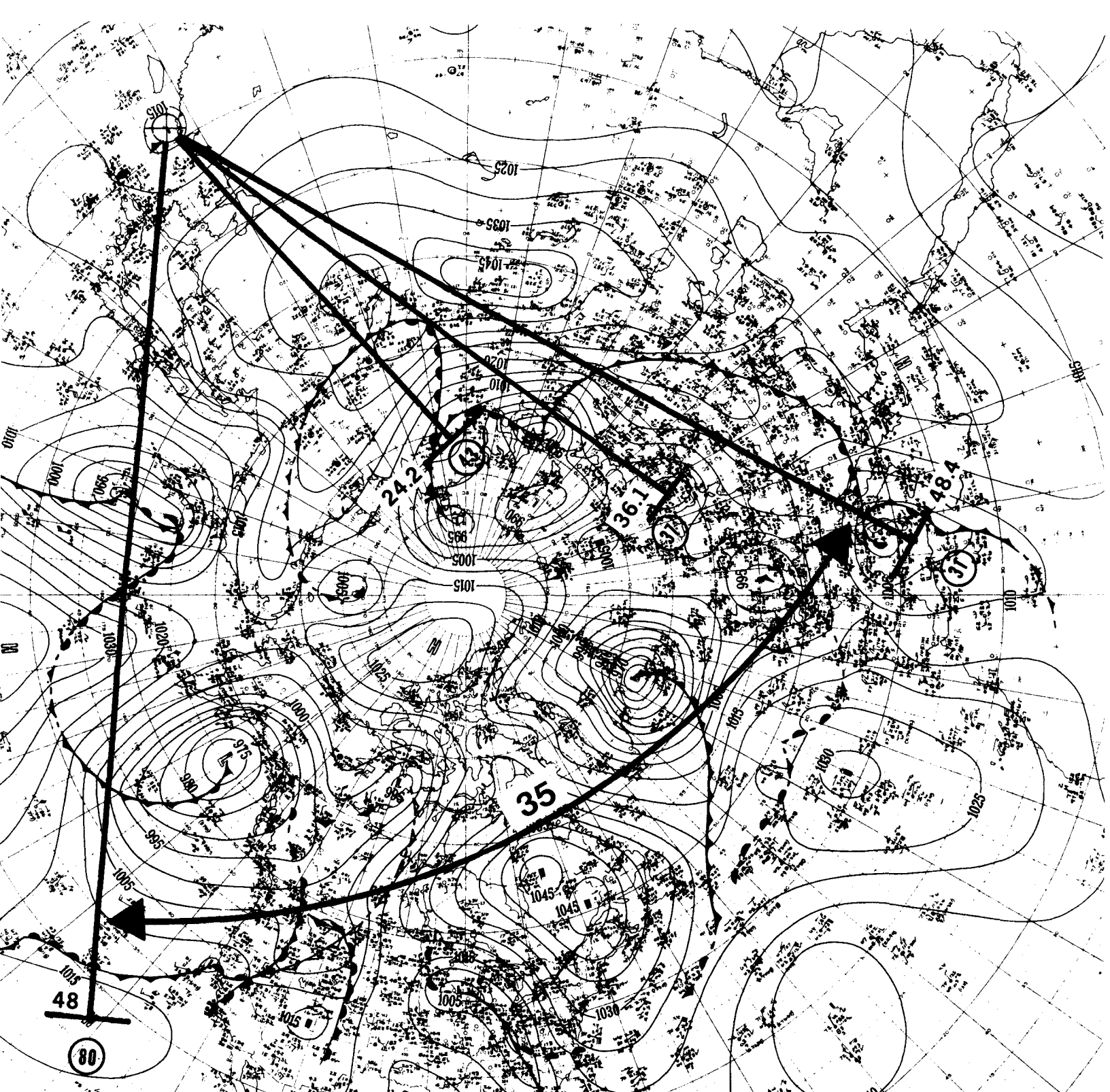
The strong feature on this map is that #27 is 17.3 ru from #20, while #67 is 52.1 ru ($3 \times 17.3 = 51.9$) from #20—all three points (#20, #27, and #67) are roughly on a straight line. Continuing, we find that #58 is 34.7 ru ($2 \times 17.3 = 34.6$), and #87 is 52.1 ru ($3 \times 17.3 = 51.9$)—they are also on a different straight line with #20—in addition, there is a slight offset from the straight line for #100 at 69.2 ru (4×17.3). Lastly, #23 at 8.6 ru, appears to be the *lowest common denominator* (referred to hereafter as LCD) for this group of points since $2 \times 8.6 = 17.2$, which is quite close to 17.3. There is also a symmetry in the angles between the rays of the pattern that seems visually obvious, but we will not go into those additional details for this map.



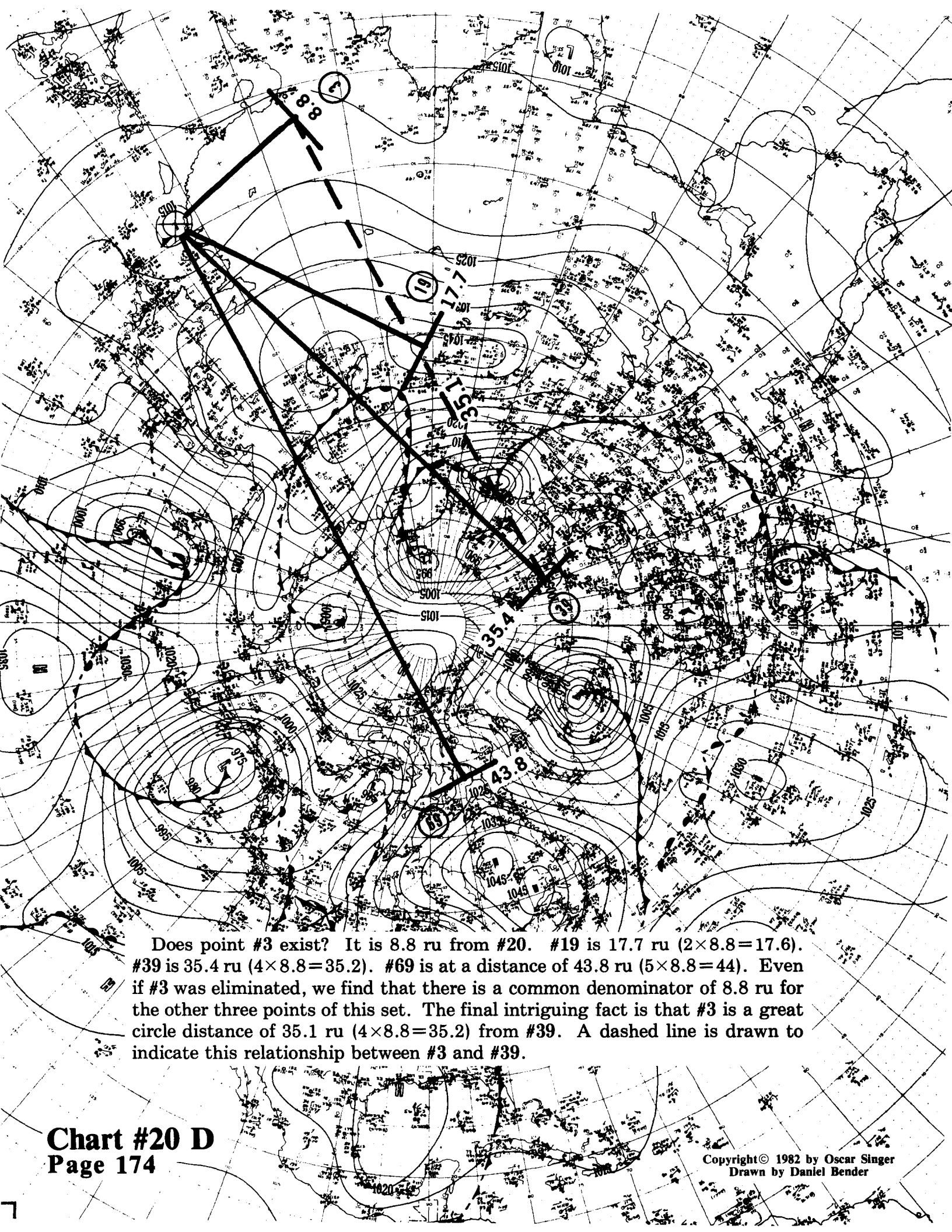
STATIONS
D_{SVS}
C_W PPP
N_W R₁
h

Copyright © 1982 by Oscar Singer
Drawn by Daniel Bender

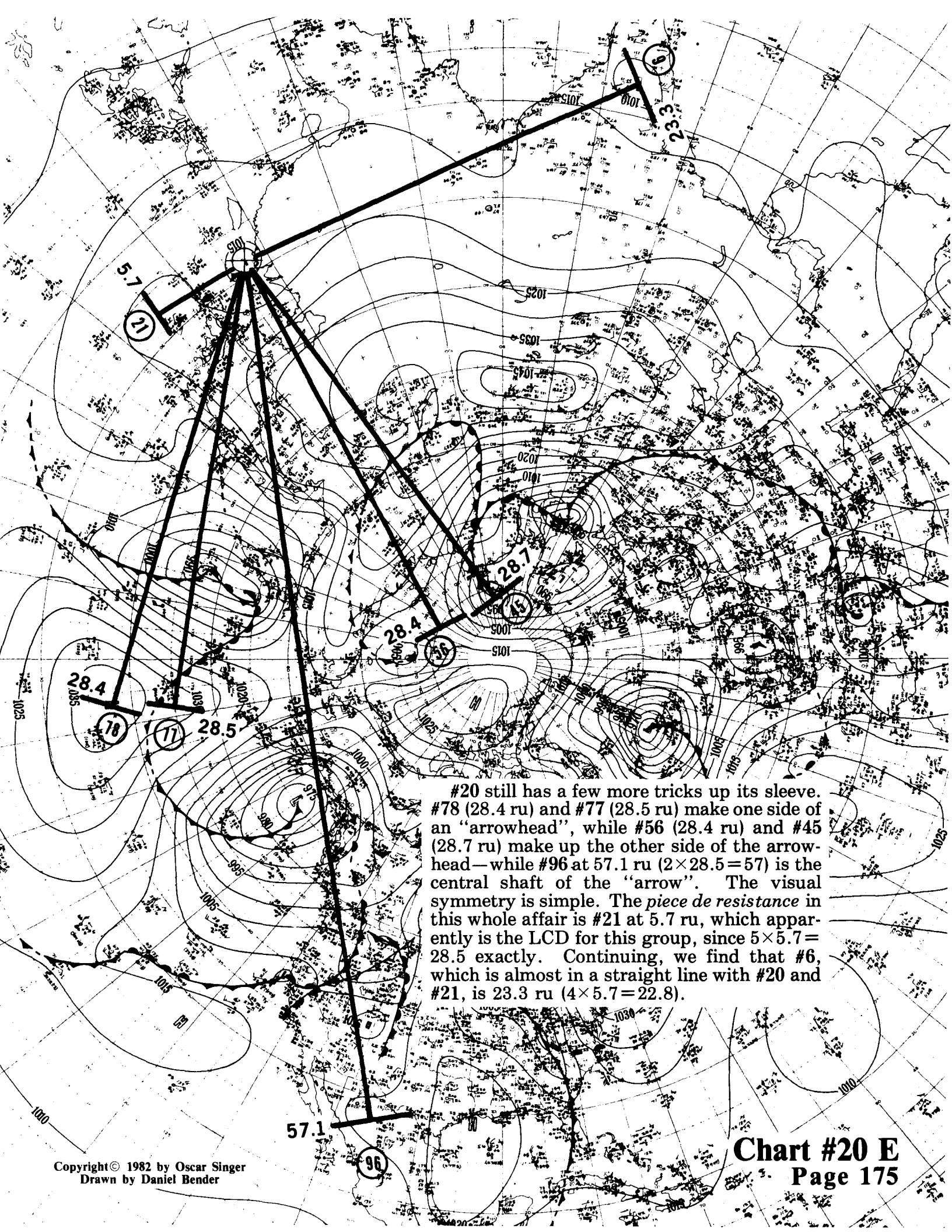
Chart #20 A
Page 171



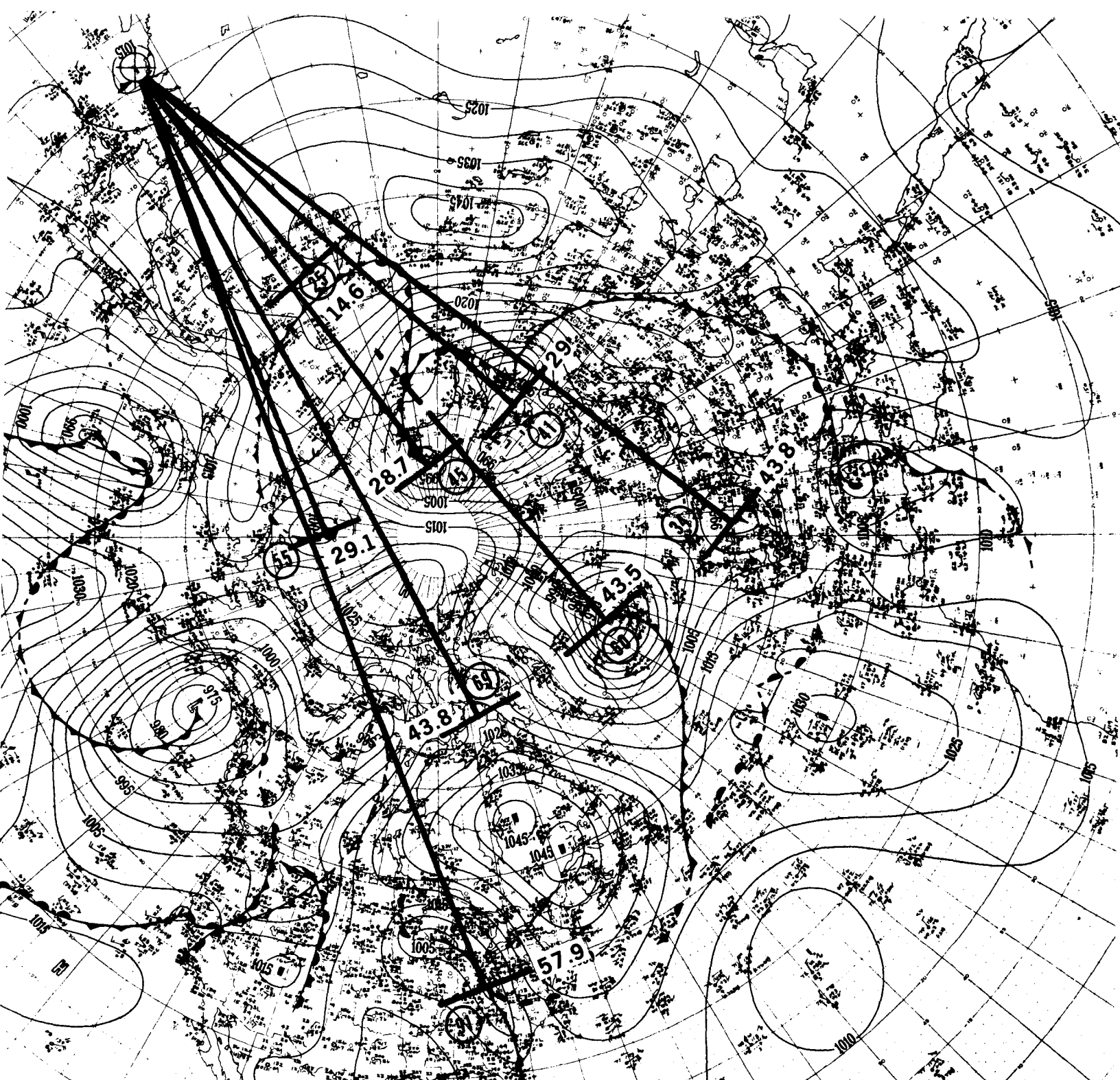
The strong feature on this map is the lining up along an almost straight line of the centers of #43, #37, and #31; all have an LCD of about 12.1 ru, in the ratio of 2:3:4. We find that #80 also has 48 ru, with the added curiosity that the angular measurement between the two rays terminating at #80 and #31 has a value of 35 cu (almost 3×12). In addition, the great circle distance between #80 and #31 is 47.4 ru, which makes an almost perfect equilateral triangle formed by #20, #31, and #80.



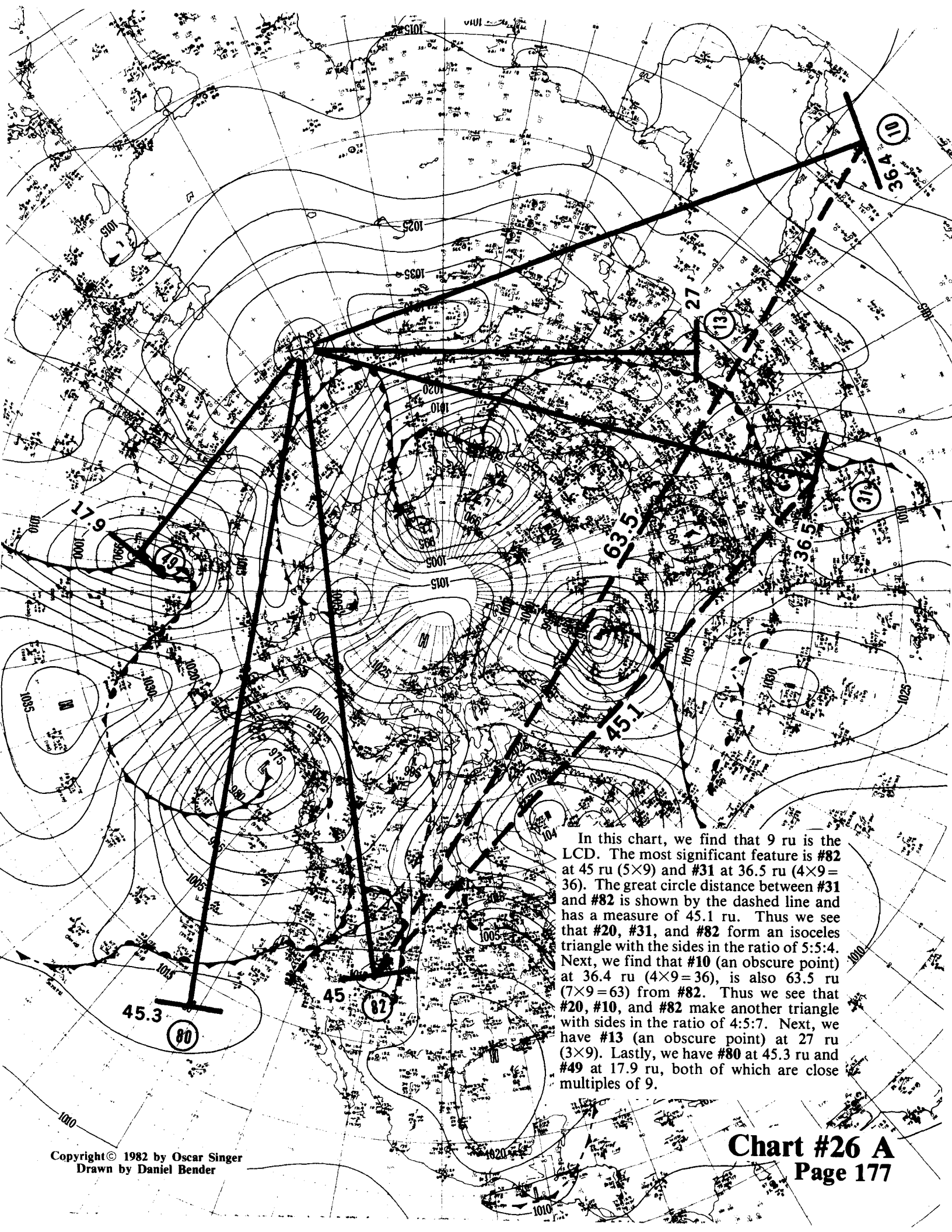
Does point #3 exist? It is 8.8 ru from #20. #19 is 17.7 ru ($2 \times 8.8 = 17.6$). #39 is 35.4 ru ($4 \times 8.8 = 35.2$). #69 is at a distance of 43.8 ru ($5 \times 8.8 = 44$). Even if #3 was eliminated, we find that there is a common denominator of 8.8 ru for the other three points of this set. The final intriguing fact is that #3 is a great circle distance of 35.1 ru ($4 \times 8.8 = 35.2$) from #39. A dashed line is drawn to indicate this relationship between #3 and #39.



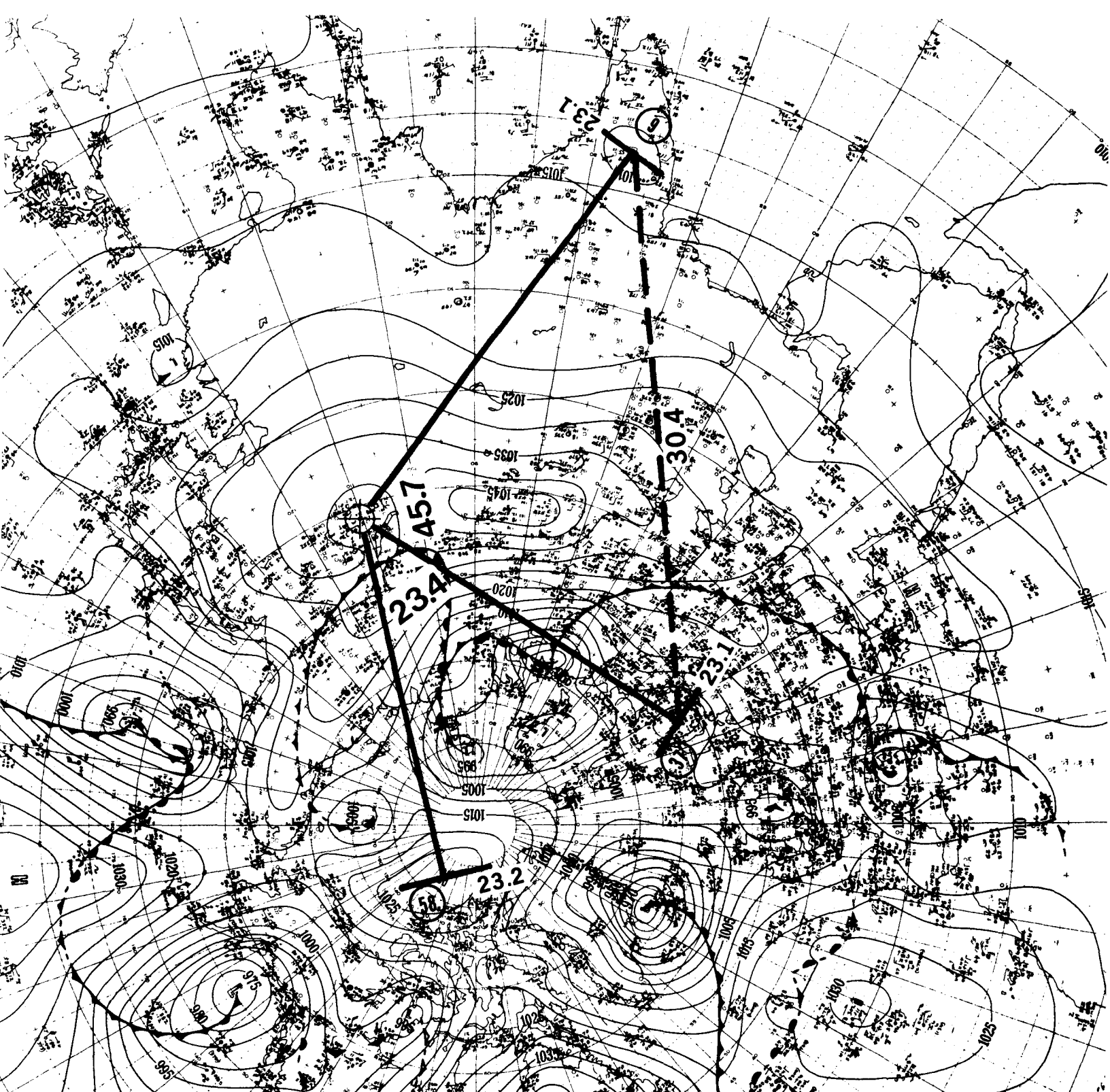
#20 still has a few more tricks up its sleeve. #78 (28.4 ru) and #77 (28.5 ru) make one side of an "arrowhead", while #56 (28.4 ru) and #45 (28.7 ru) make up the other side of the arrowhead—while #96 at 57.1 ru ($2 \times 28.5 = 57$) is the central shaft of the "arrow". The visual symmetry is simple. The *piece de resistance* in this whole affair is #21 at 5.7 ru, which apparently is the LCD for this group, since $5 \times 5.7 = 28.5$ exactly. Continuing, we find that #6, which is almost in a straight line with #20 and #21, is 23.3 ru ($4 \times 5.7 = 22.8$).



Here we start with the obscure #25 at a distance of 14.6 ru. Does this point really exist? Two times 14.6 equals 29.2. #55 at 29.1 ru and #41 at 29 ru are close, with #45 at 28.7 ru, not bad either. Three times 14.6 equals 43.8. Guess what! #69 and #34 are both 43.8 ru exactly with #60 close (in distance) at 43.5 ru. Note that #60 and #45, both nearly in a straight line, are the two that are slightly below the value of the majority. Lastly, we note that #91, which is almost in a straight line with #55, is almost 2:1 ($2 \times 29.1 = 58.2$). Even if #25 did not exist, the symmetry pattern would still be there. Since we can see that the symmetry pattern does indeed exist, then likewise it is easy to conclude that point #25 is real (and accurate).

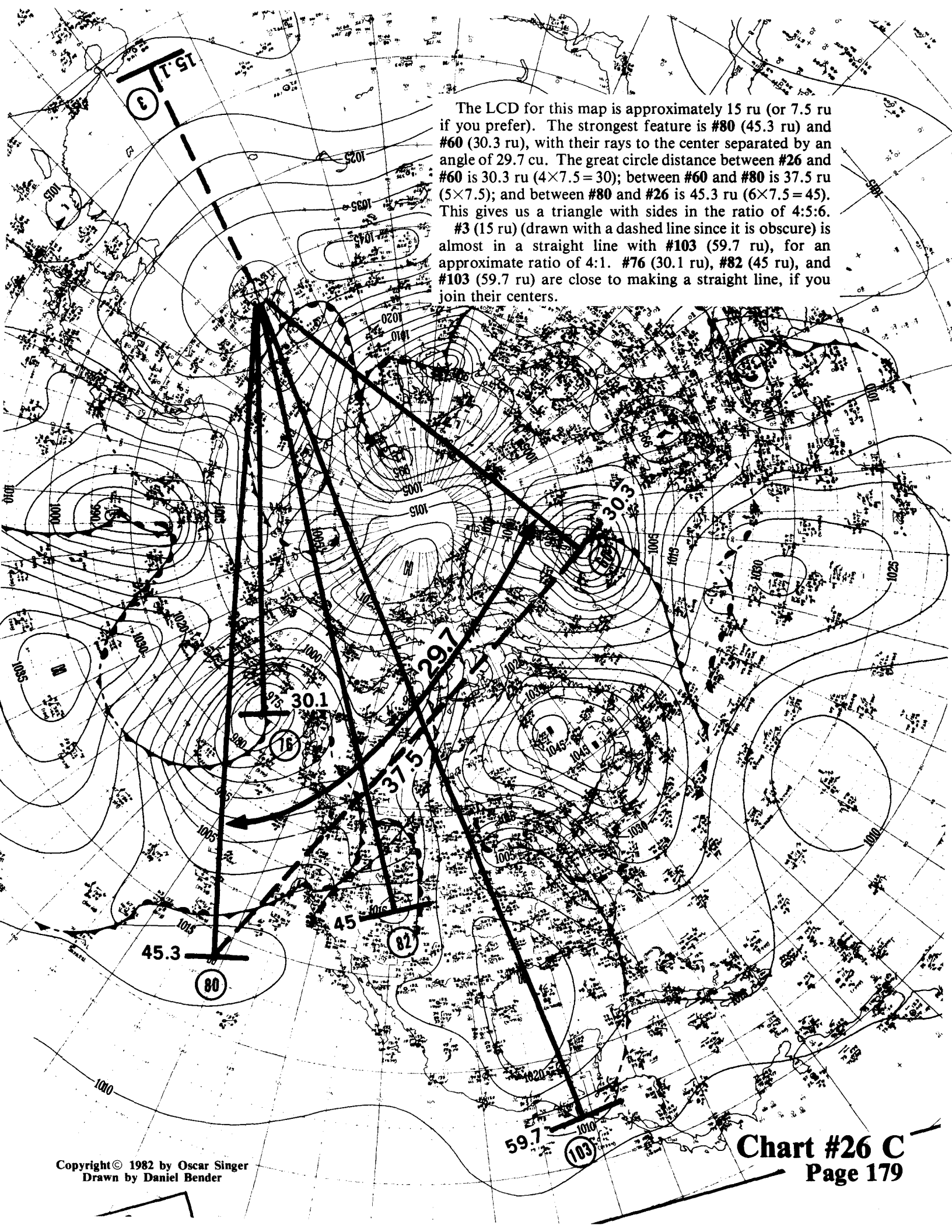


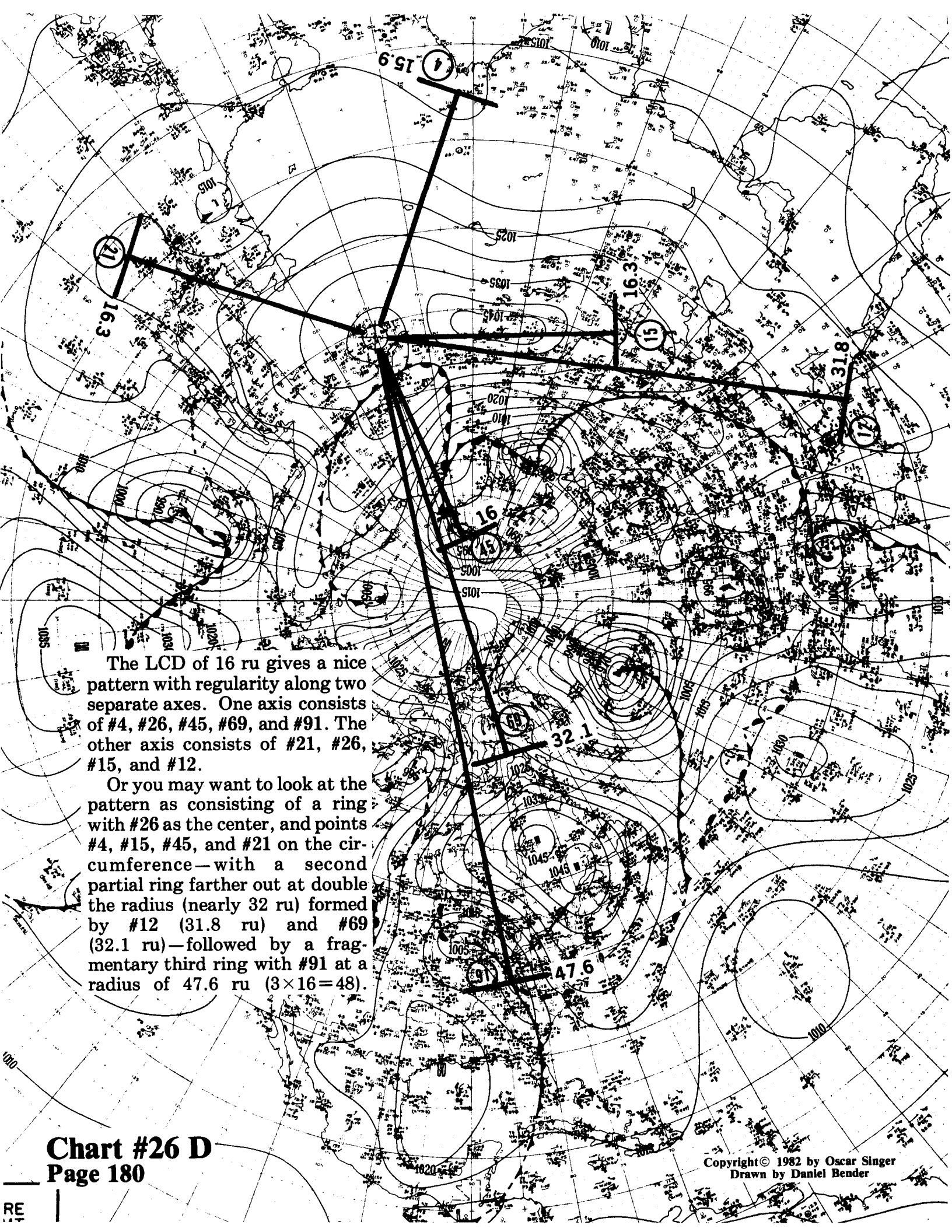
In this chart, we find that 9 ru is the LCD. The most significant feature is #82 at 45 ru (5×9) and #31 at 36.5 ru ($4 \times 9 = 36$). The great circle distance between #31 and #82 is shown by the dashed line and has a measure of 45.1 ru. Thus we see that #20, #31, and #82 form an isosceles triangle with the sides in the ratio of 5:5:4. Next, we find that #10 (an obscure point) at 36.4 ru ($4 \times 9 = 36$), is also 63.5 ru ($7 \times 9 = 63$) from #82. Thus we see that #20, #10, and #82 make another triangle with sides in the ratio of 4:5:7. Next, we have #13 (an obscure point) at 27 ru (3×9). Lastly, we have #80 at 45.3 ru and #49 at 17.9 ru, both of which are close multiples of 9.



This one is a simple gem. #58 is 23.2 ru and #37 is 23.1 ru but from #26. The angle formed by their rays is 23.4 cu. Similarly, the angle formed by the rays of #6 and #37 is 45.7 cu ($2 \times 23.1 = 46$). One last touch, the great circle distance between #6 and #37 is 30.4 ru ($4 \times 7.7 = 30.8$); and since 23.1 ru equals 3×7.7 exactly, we have an isocles triangle with the sides in the ratio of 3:3:4.

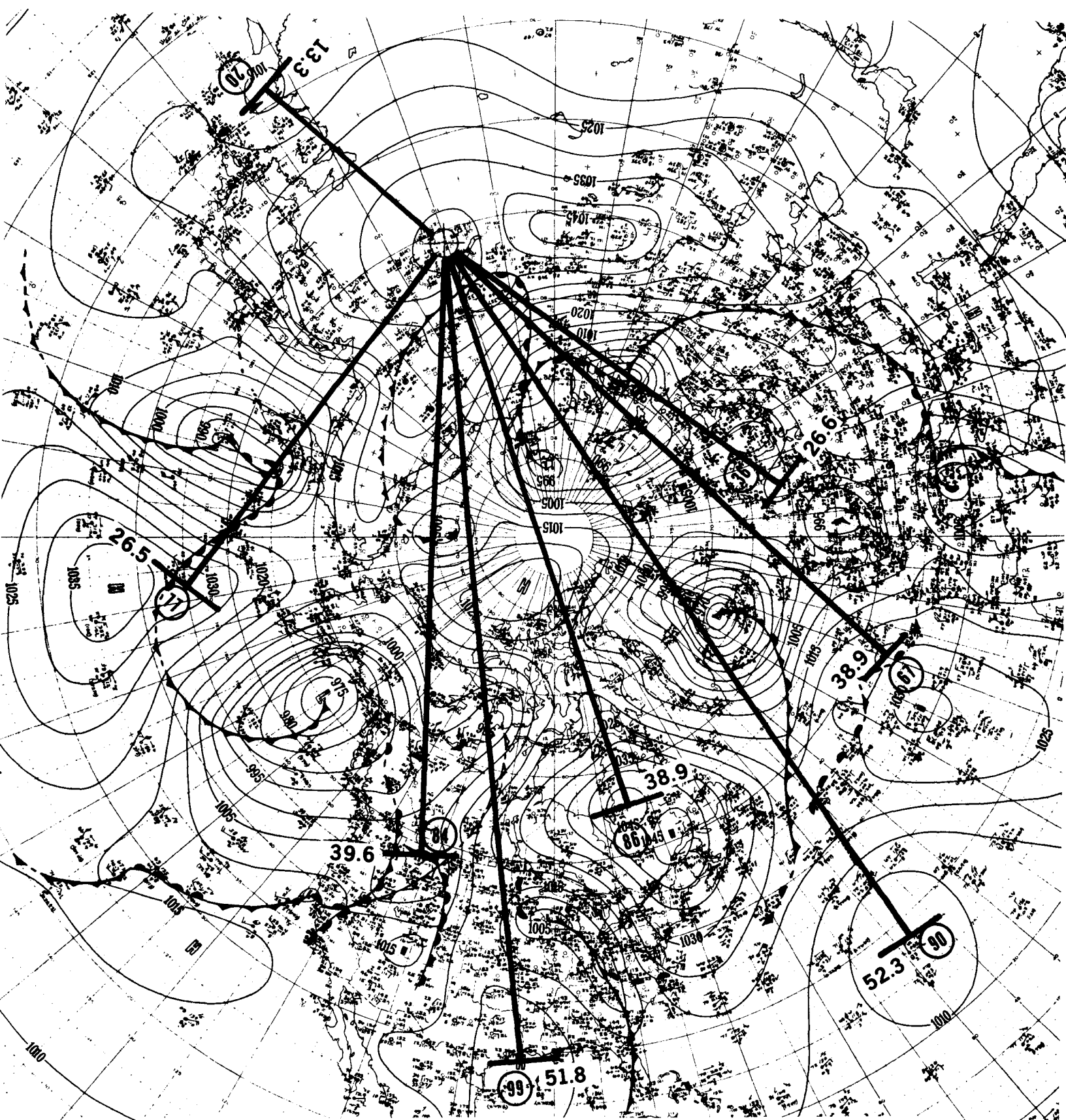
#3 (15 ru) (drawn with a dashed line since it is obscure) is almost in a straight line with **#103** (59.7 ru), for an approximate ratio of 4:1. **#76** (30.1 ru), **#82** (45 ru), and **#103** (59.7 ru) are close to making a straight line, if you join their centers.





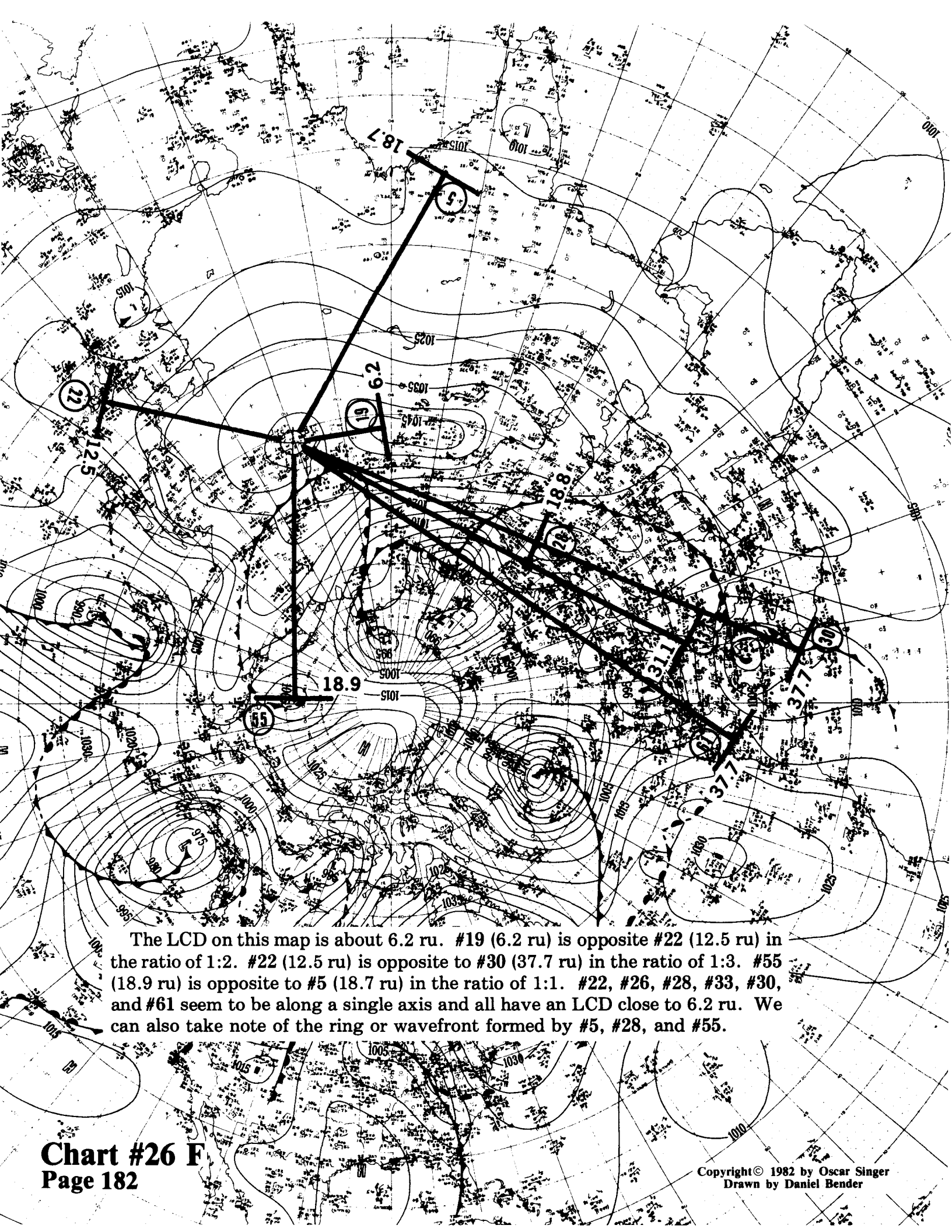
The LCD of 16 ru gives a nice pattern with regularity along two separate axes. One axis consists of #4, #26, #45, #69, and #91. The other axis consists of #21, #26, #15, and #12.

Or you may want to look at the pattern as consisting of a ring with #26 as the center, and points #4, #15, #45, and #21 on the circumference—with a second partial ring farther out at double the radius (nearly 32 ru) formed by #12 (31.8 ru) and #69 (32.1 ru)—followed by a fragmentary third ring with #91 at a radius of 47.6 ru ($3 \times 16 = 48$).

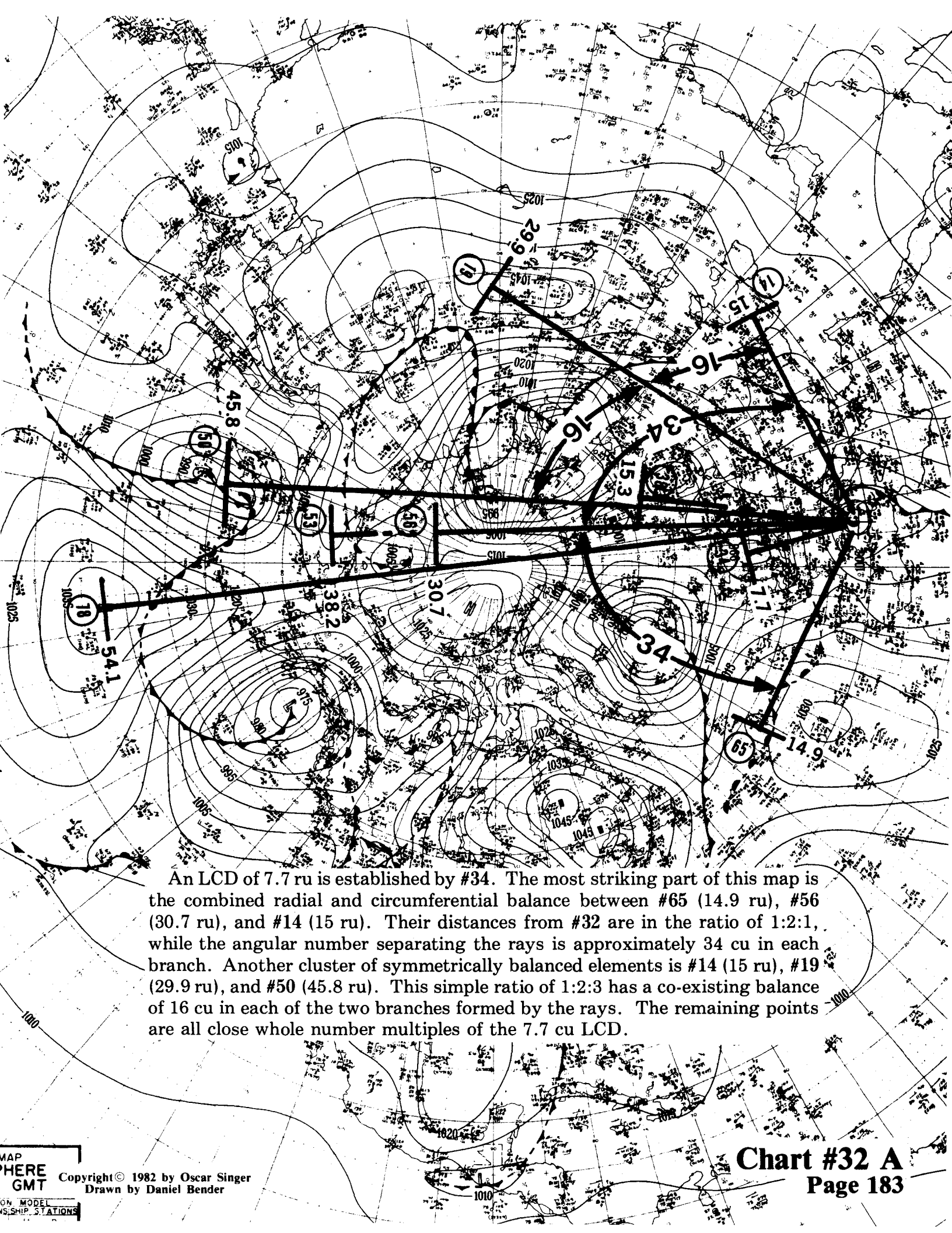


The most straightforward feature on this map is #20 (13.3 ru) on a nearly straight line through #26 and #36 (26.6 ru). The rest of the points can be considered as part of three separate waves or ringlets. The first wave front is #77 (26.5 ru) and #36 (26.6 ru) in the ratio of about 2:1, with the LCD of 13.3 ru. The second wave front consists of #84 (39.6 ru), #86 (38.9 ru), and #67 (38.9 ru) which are in the ratio of about 3:1 to the LCD. The third wave consists of #99 (51.8 ru) and #90 (52.3 ru) which are approximately in the ratio of 4:1.

MAP
WHERE
GMT
ION MODEL
SHIP STATIONS
Dsvs
CH PPP
Copyright © 1982 by Oscar Singer
Drawn by Daniel Bender
NAME OR (BAR NO)



The LCD on this map is about 6.2 ru. #19 (6.2 ru) is opposite #22 (12.5 ru) in the ratio of 1:2. #22 (12.5 ru) is opposite to #30 (37.7 ru) in the ratio of 1:3. #55 (18.9 ru) is opposite to #5 (18.7 ru) in the ratio of 1:1. #22, #26, #28, #33, #30, and #61 seem to be along a single axis and all have an LCD close to 6.2 ru. We can also take note of the ring or wavefront formed by #5, #28, and #55.



An LCD of 7.7 ru is established by #34. The most striking part of this map is the combined radial and circumferential balance between #65 (14.9 ru), #56 (30.7 ru), and #14 (15 ru). Their distances from #32 are in the ratio of 1:2:1, while the angular number separating the rays is approximately 34 cu in each branch. Another cluster of symmetrically balanced elements is #14 (15 ru), #19 (29.9 ru), and #50 (45.8 ru). This simple ratio of 1:2:3 has a co-existing balance of 16 cu in each of the two branches formed by the rays. The remaining points are all close whole number multiples of the 7.7 cu LCD.

Chart #32 B

Here we use an LCD of approximately 12 ru. The stunning feature on this map is the equilateral triangle formed by #32, #81, and #20. We find that the position of the center of each of the three points can be measured with an extreme degree of accuracy because of the small size of the central isobar in each case. The dashed line joining #81 and #20 indicates a great circle distance of 47.4 ru. This compares with the other two sides of 47.4 ru (#20), and 47.6 (#81). We have what is almost a right angled spherical triangle, since an angular number of 48 does equal 90° . These three points are locked into a stable position relative to each other for a fleeting instant at the time of this map.

We are not through with this beauty—the distance between #20 and #9 (also with a well-defined location for the center) is 47.1 ru. Since #9 is 24 ru from #32, we have an isocetes triangle with the sides in the approximate ratio of 2:2:1 as a very neat companion to the first triangle.

We can't quit now, since #9 (24 ru) is counterbalanced in an almost straight line by #97 (47.8 ru) in a nearly perfect 1:2 ratio.

What have we here! Another equilateral triangle? This time, #97, #47 and #32 are locked in close balance, since the dashed line between #97 and #47 indicates a distance of 49.1 ru—not as perfect as the first triangle, but good.

We still can't let go of #97. The distance between #97 and #63 is 35.8 ru; between #97 and #20 is 60.1 ru; and between #97 and #8 is 71.6 ru. All these distances are multiples of the LCD, 12 ru. There are five different distances radiating out from #97 to different members of this cluster of points that have a common LCD of 12 ru—not bad for a point like #97, that most meteorologists might have thought to be of no significance and without merit.

To wrap up this dazzler, we see that #90 at 24.6 ru is almost perfectly counterbalanced in a nearly straight line with #8 at 24.7 ru (with #63 at 12.7 ru acting as an interloper). We see that there is a ring or wavefront involving #90 (24.6 ru), #44 (24.6 ru), #7 (24.6 ru), #8 (24.7 ru), and #9 (24 ru). Lastly, #93 at 36.2 ru and #100 at 36.4 ru form another ringlet. We can't tarry much longer with this chart, since there are other areas of the map to investigate.



Westber Bureau

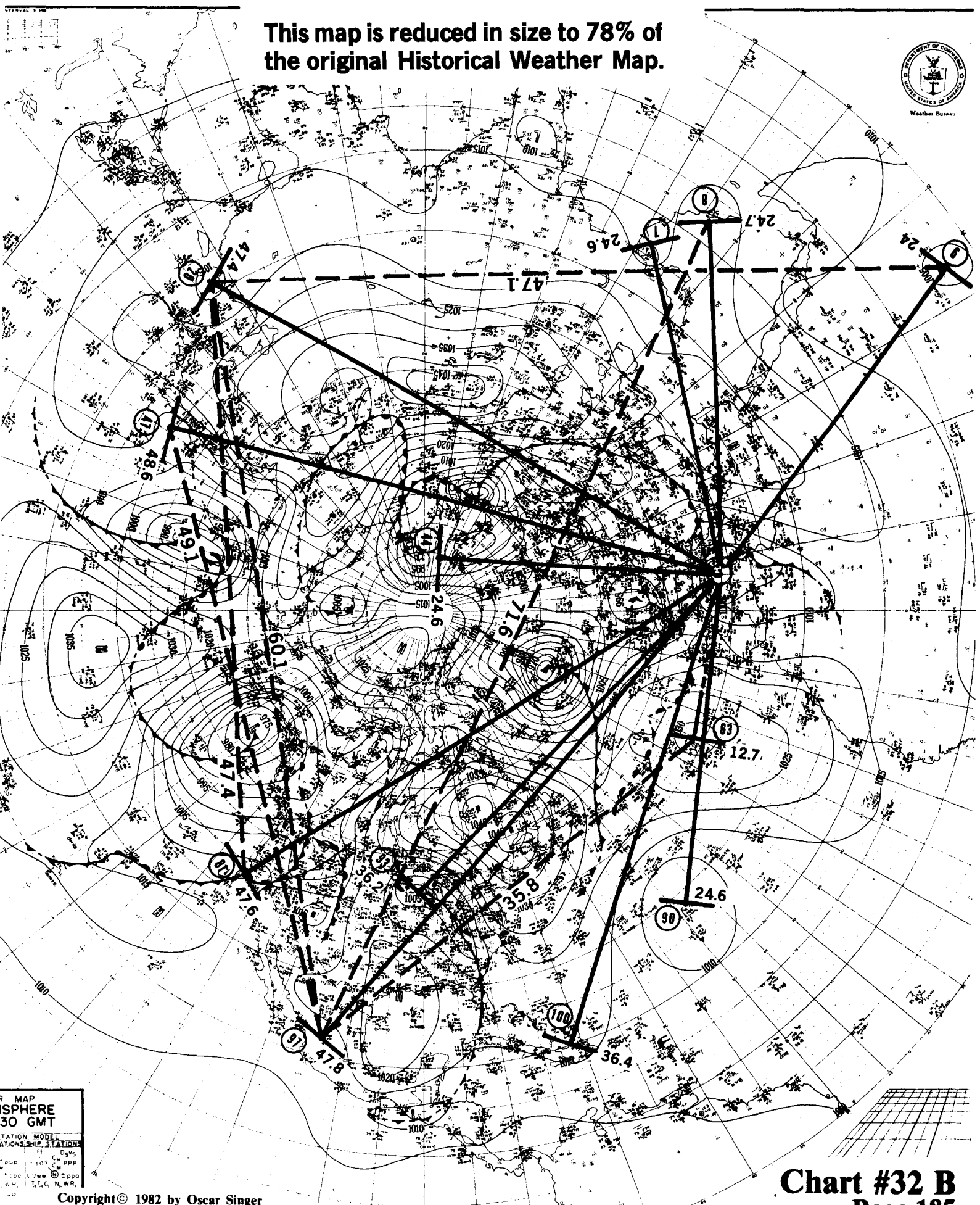
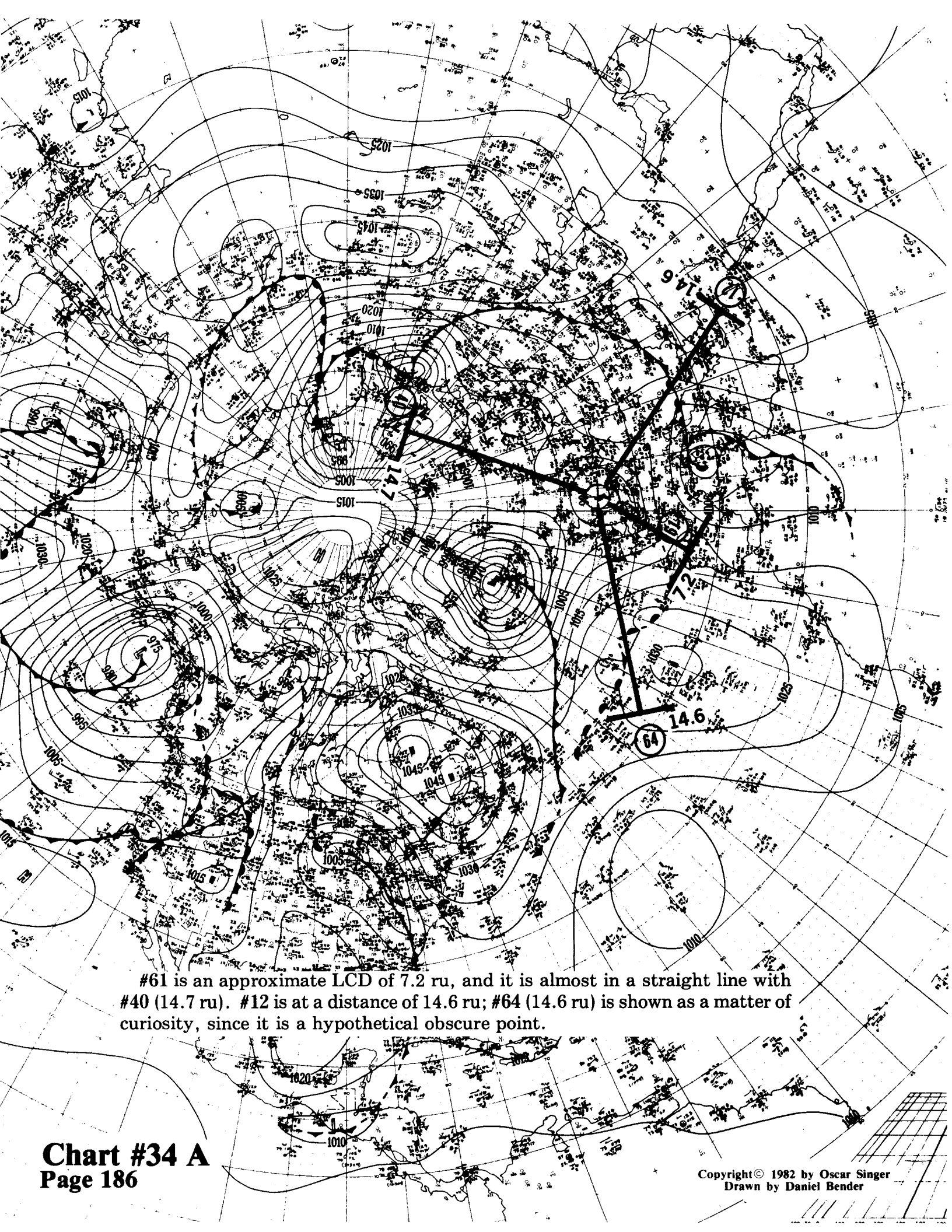
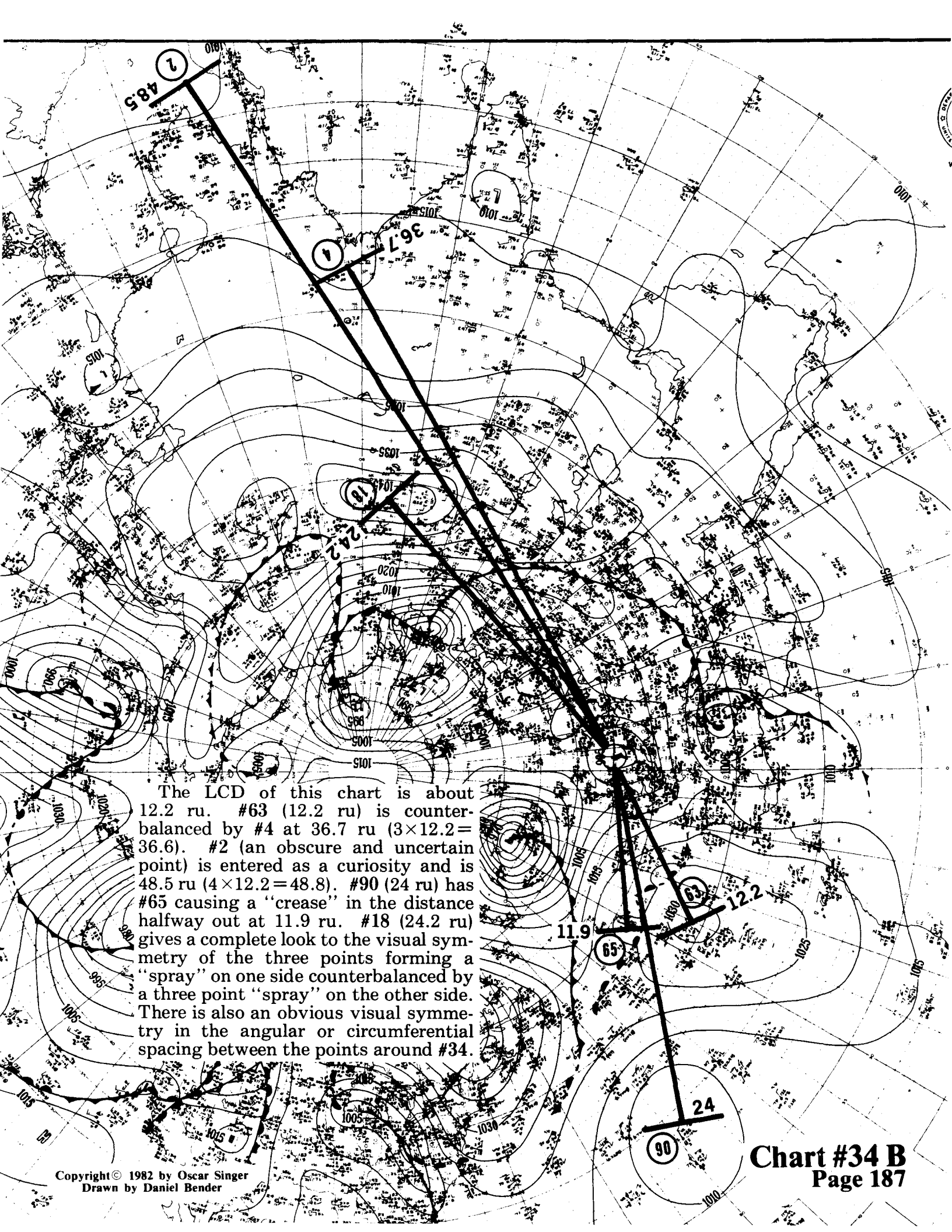


Chart #32 B
Page 185

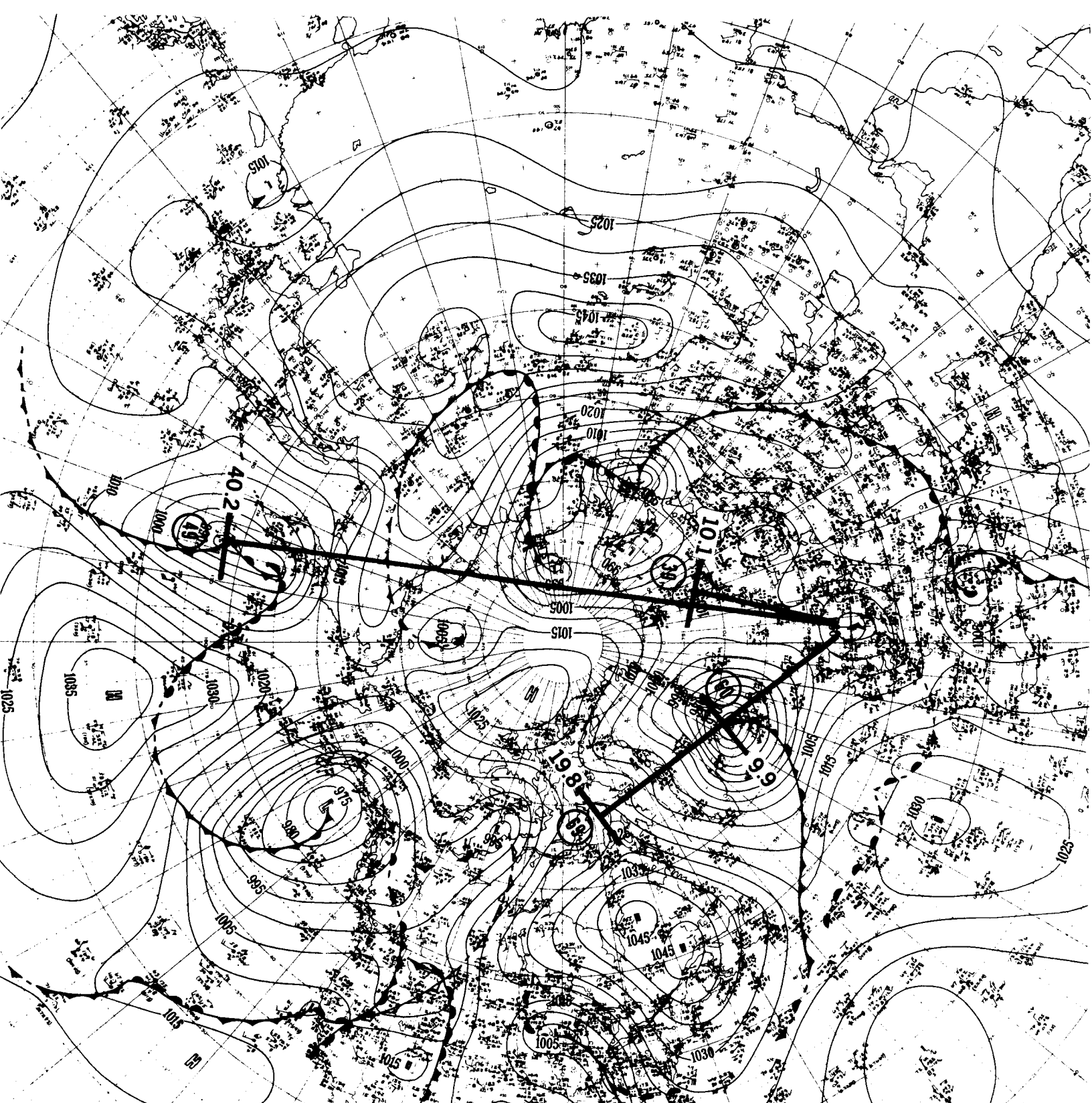


#61 is an approximate LCD of 7.2 ru, and it is almost in a straight line with #40 (14.7 ru). #12 is at a distance of 14.6 ru; #64 (14.6 ru) is shown as a matter of curiosity, since it is a hypothetical obscure point.

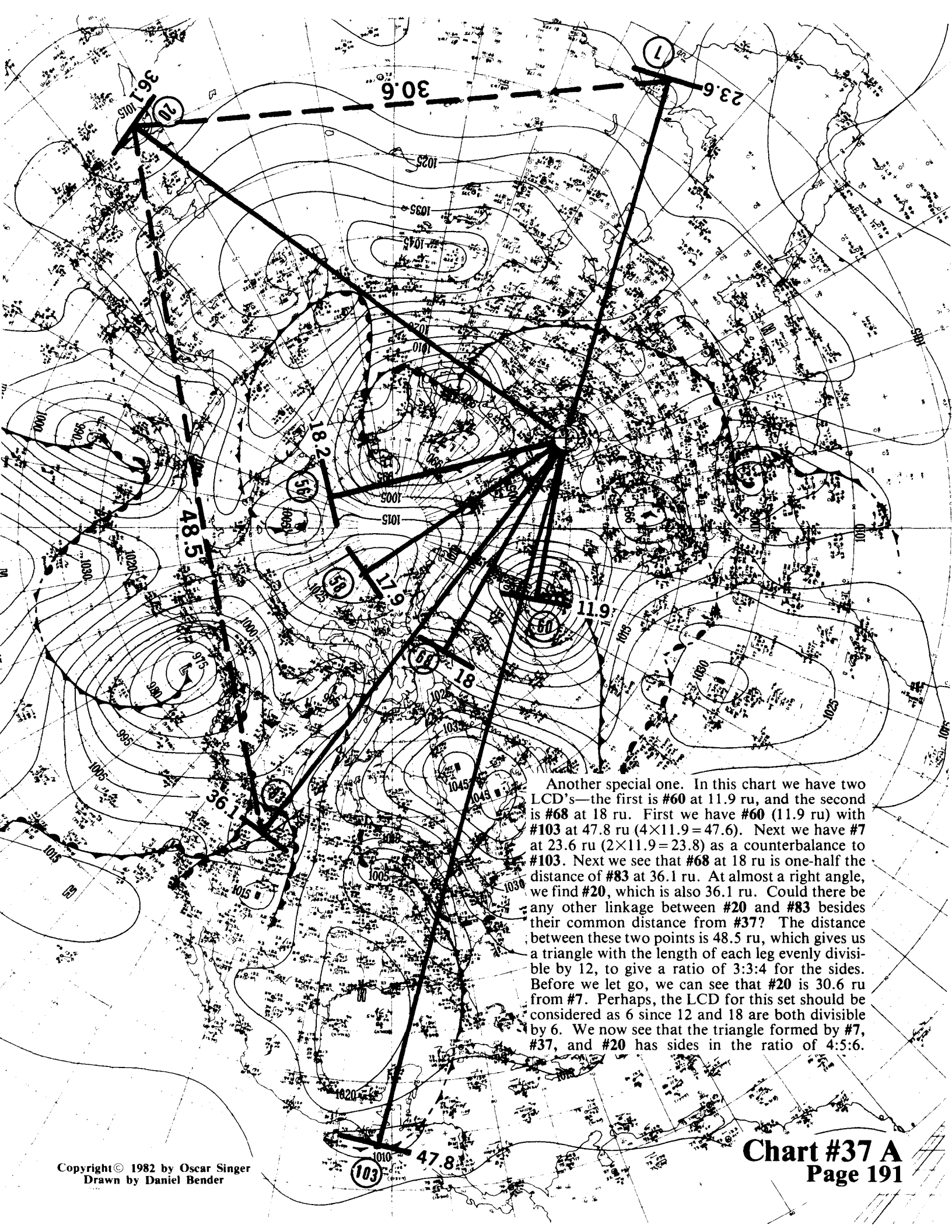


The LCD of this chart is about 12.2 ru. #63 (12.2 ru) is counterbalanced by #4 at 36.7 ru ($3 \times 12.2 = 36.6$). #2 (an obscure and uncertain point) is entered as a curiosity and is 48.5 ru ($4 \times 12.2 = 48.8$). #90 (24 ru) has #65 causing a "crease" in the distance halfway out at 11.9 ru. #18 (24.2 ru) gives a complete look to the visual symmetry of the three points forming a "spray" on one side counterbalanced by a three point "spray" on the other side. There is also an obvious visual symmetry in the angular or circumferential spacing between the points around #34.

#67 (8.8 ru) is balanced very nicely with #38 (8.8 ru). At a little offset, but closely in the same direction moving outwards from #34, we find #44 at 17.6 ru (2×8.8). If we go out in a straight line from #67 through #34, we find #5 at 35.6 ru ($4 \times 8.8 = 35.2$). In a classical pattern, at almost a 90° angle to this straight line we find #76 (35.5 ru), which is approximately 4 times the LCD of 8.8 ru.



The outstanding feature of this chart is #60 (9.9 ru) and #69 (19.8 ru), which are in a straight line and in a perfect 1:2 ratio. As a matter of interest, but not in the same category of accuracy, #39 at 10.1 ru (an obscure and relatively uncertain col) and #49 (40.2 ru) are shown in an approximate ratio of 1:4.

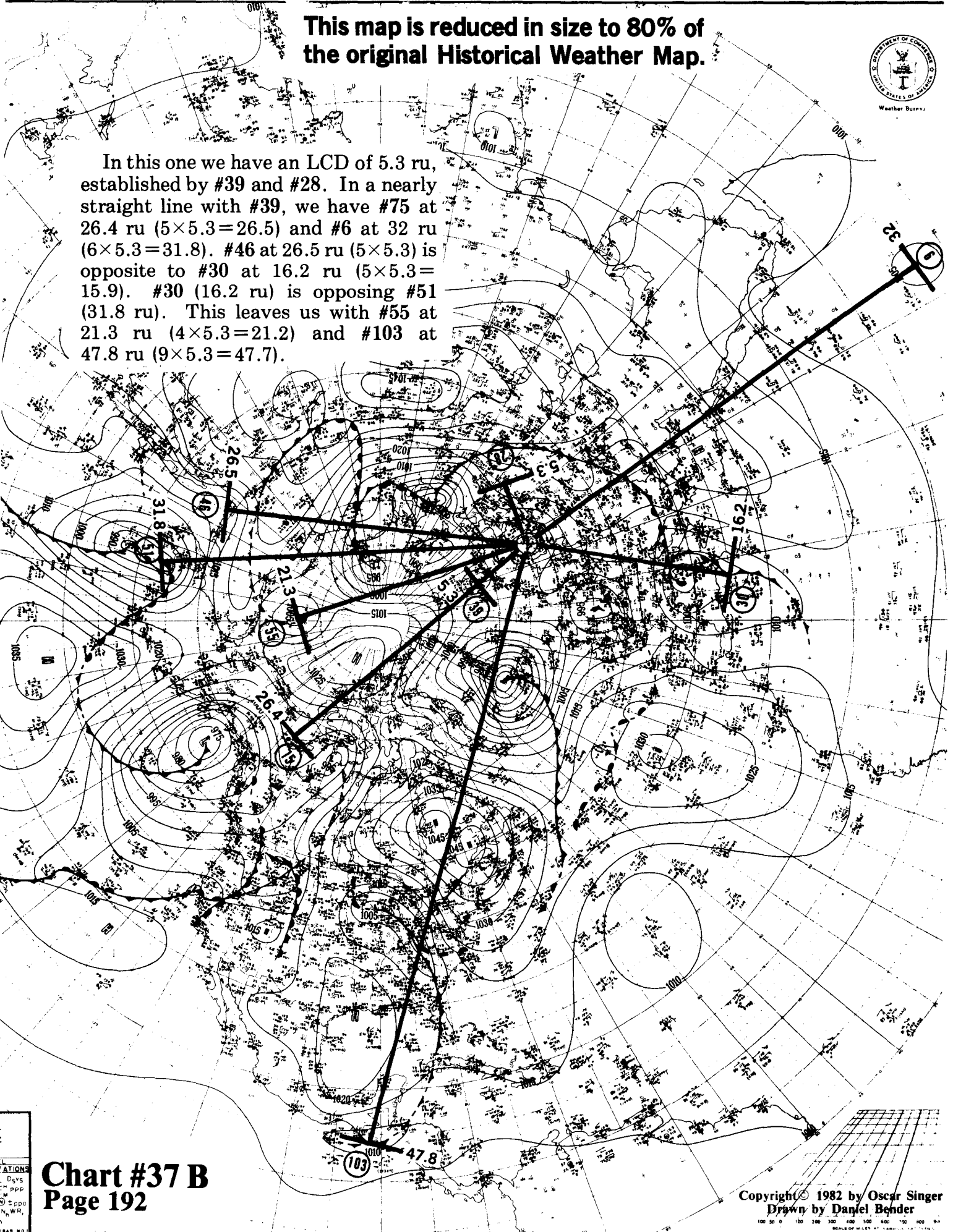


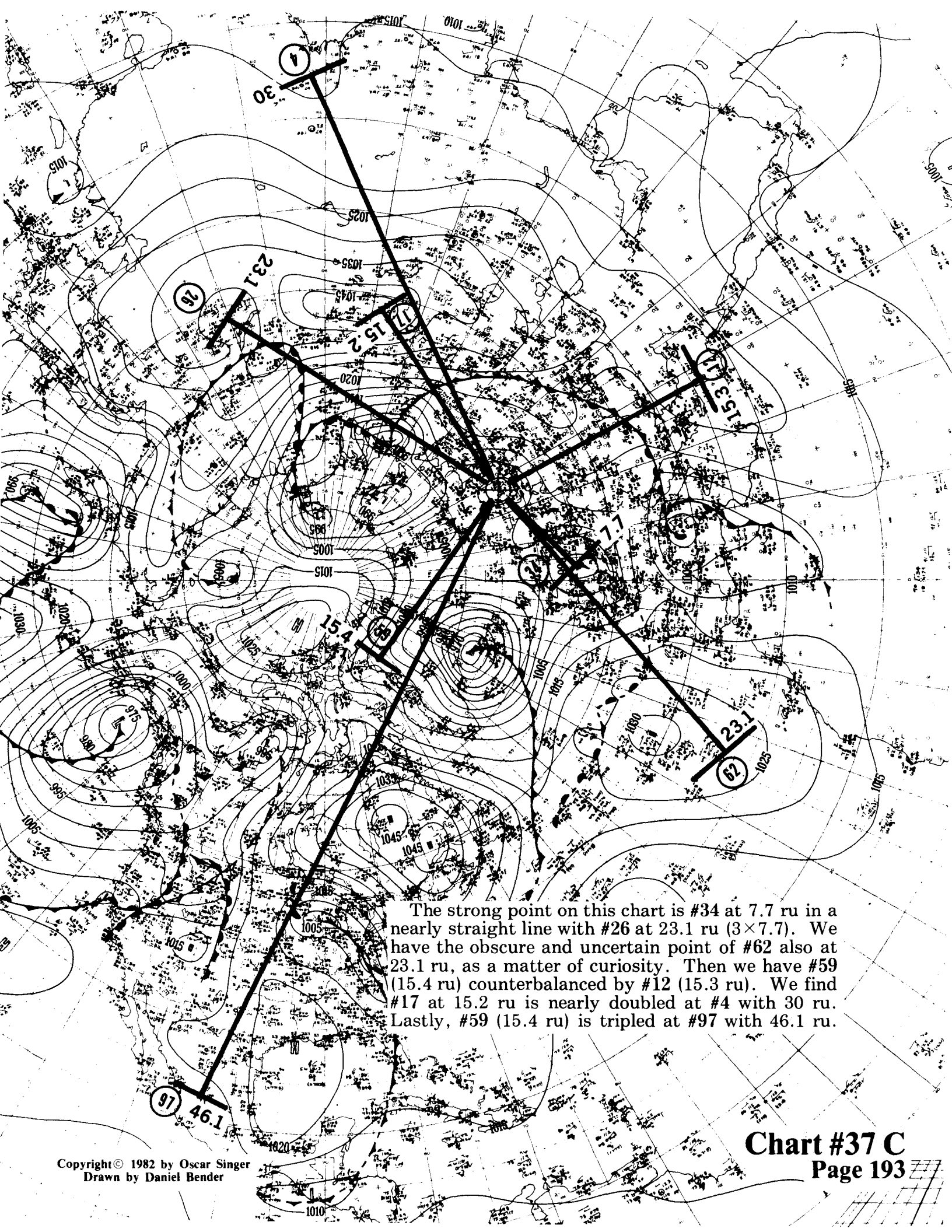
Another special one. In this chart we have two LCD's—the first is #60 at 11.9 ru, and the second is #68 at 18 ru. First we have #60 (11.9 ru) with #103 at 47.8 ru ($4 \times 11.9 = 47.6$). Next we have #7 at 23.6 ru ($2 \times 11.9 = 23.8$) as a counterbalance to #103. Next we see that #68 at 18 ru is one-half the distance of #83 at 36.1 ru. At almost a right angle, we find #20, which is also 36.1 ru. Could there be any other linkage between #20 and #83 besides their common distance from #37? The distance between these two points is 48.5 ru, which gives us a triangle with the length of each leg evenly divisible by 12, to give a ratio of 3:3:4 for the sides. Before we let go, we can see that #20 is 30.6 ru from #7. Perhaps, the LCD for this set should be considered as 6 since 12 and 18 are both divisible by 6. We now see that the triangle formed by #7, #37, and #20 has sides in the ratio of 4:5:6.

This map is reduced in size to 80% of the original Historical Weather Map.

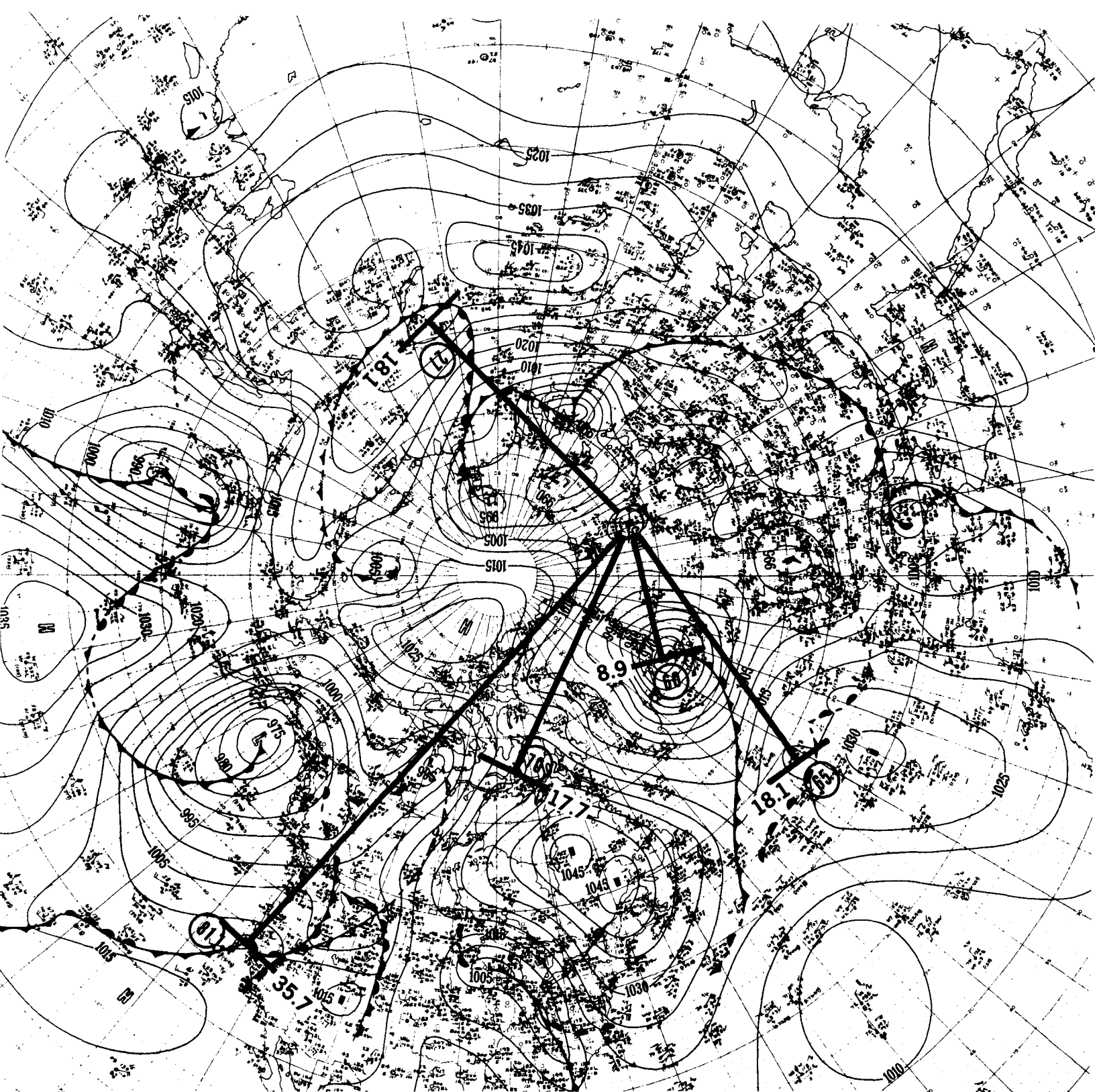


In this one we have an LCD of 5.3 ru, established by #39 and #28. In a nearly straight line with #39, we have #75 at 26.4 ru ($5 \times 5.3 = 26.5$) and #6 at 32 ru ($6 \times 5.3 = 31.8$). #46 at 26.5 ru (5×5.3) is opposite to #30 at 16.2 ru ($5 \times 5.3 = 15.9$). #30 (16.2 ru) is opposing #51 (31.8 ru). This leaves us with #55 at 21.3 ru ($4 \times 5.3 = 21.2$) and #103 at 47.8 ru ($9 \times 5.3 = 47.7$).

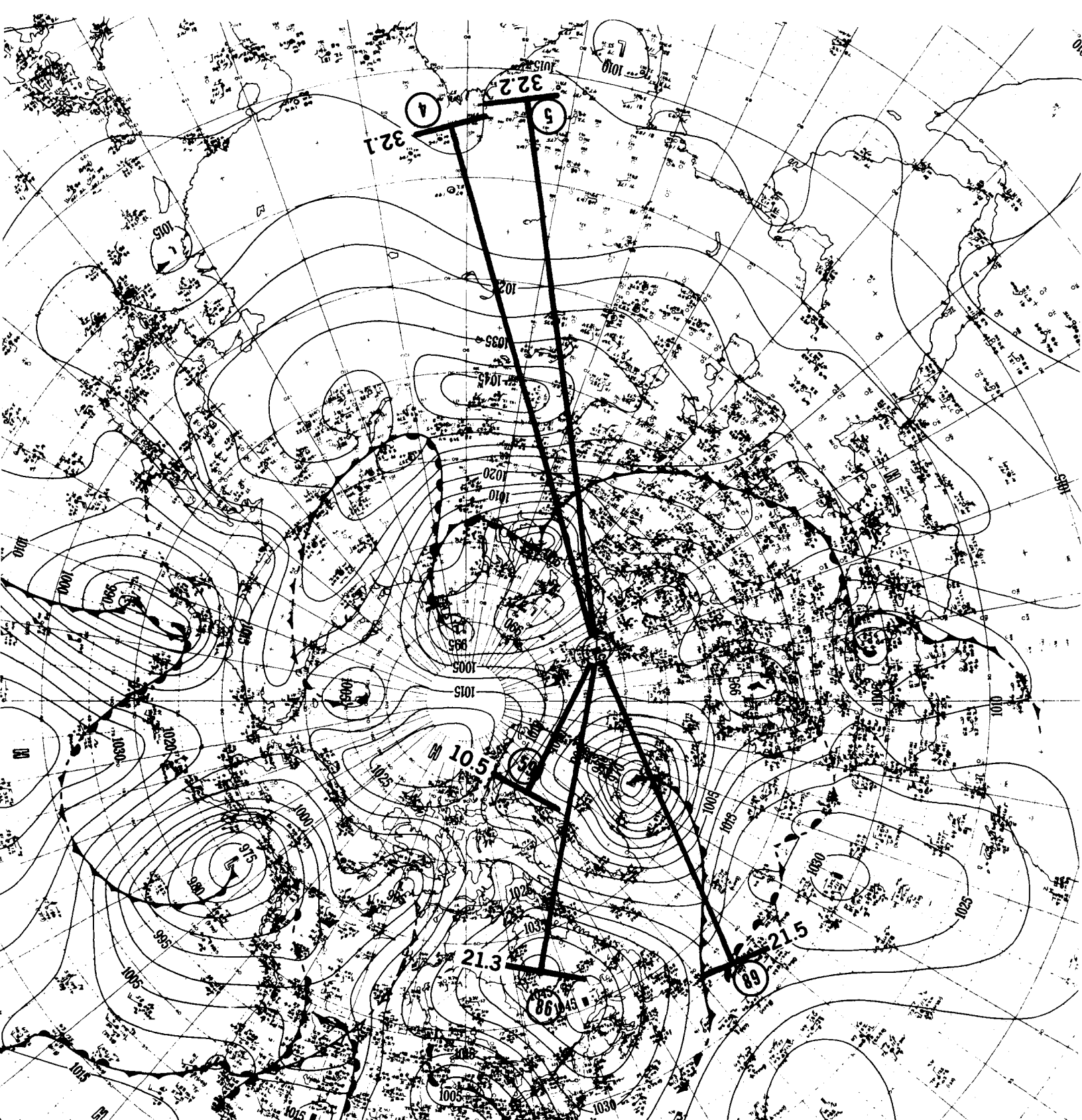




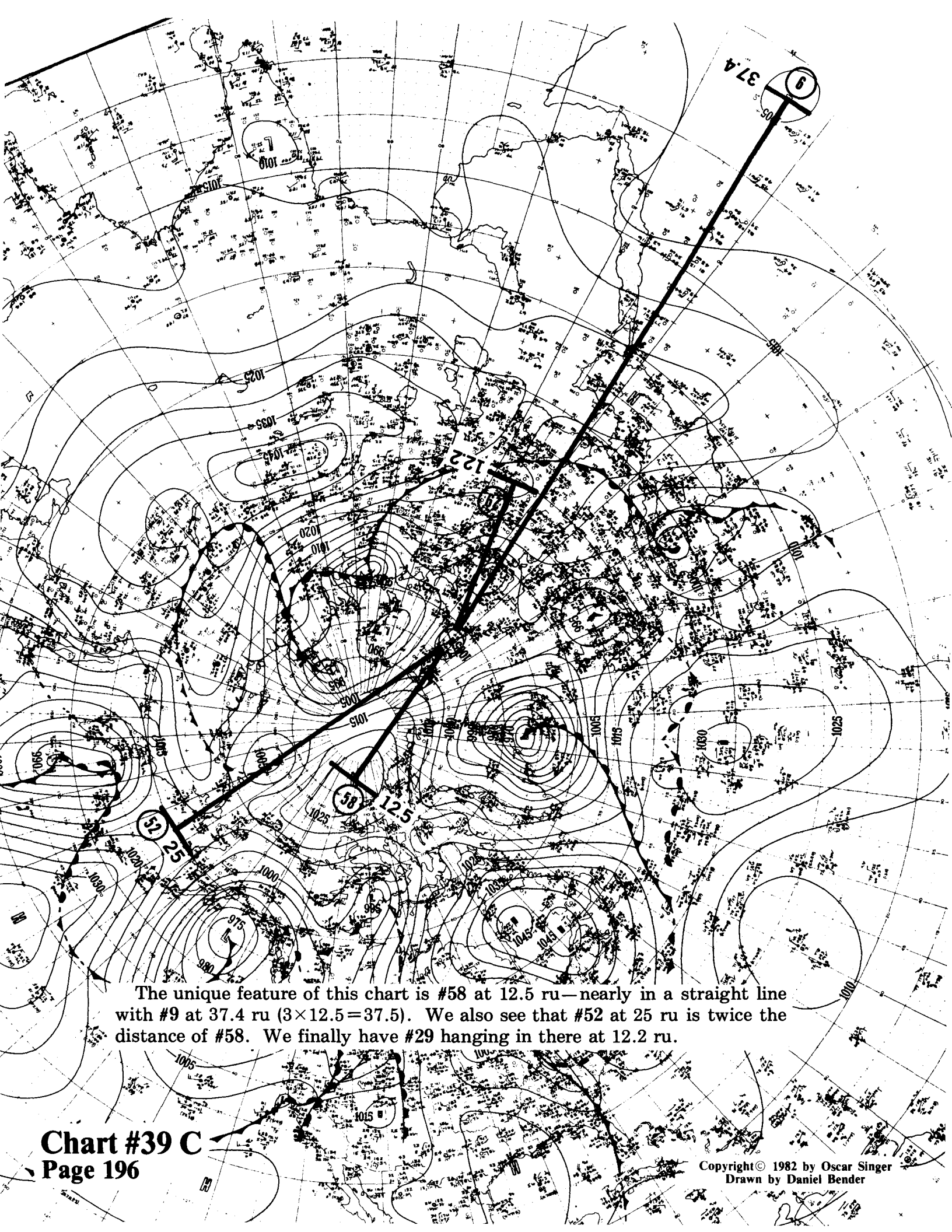
The strong point on this chart is #34 at 7.7 ru in a nearly straight line with #26 at 23.1 ru (3×7.7). We have the obscure and uncertain point of #62 also at 23.1 ru, as a matter of curiosity. Then we have #59 (15.4 ru) counterbalanced by #12 (15.3 ru). We find #17 at 15.2 ru is nearly doubled at #4 with 30 ru. Lastly, #59 (15.4 ru) is tripled at #97 with 46.1 ru.



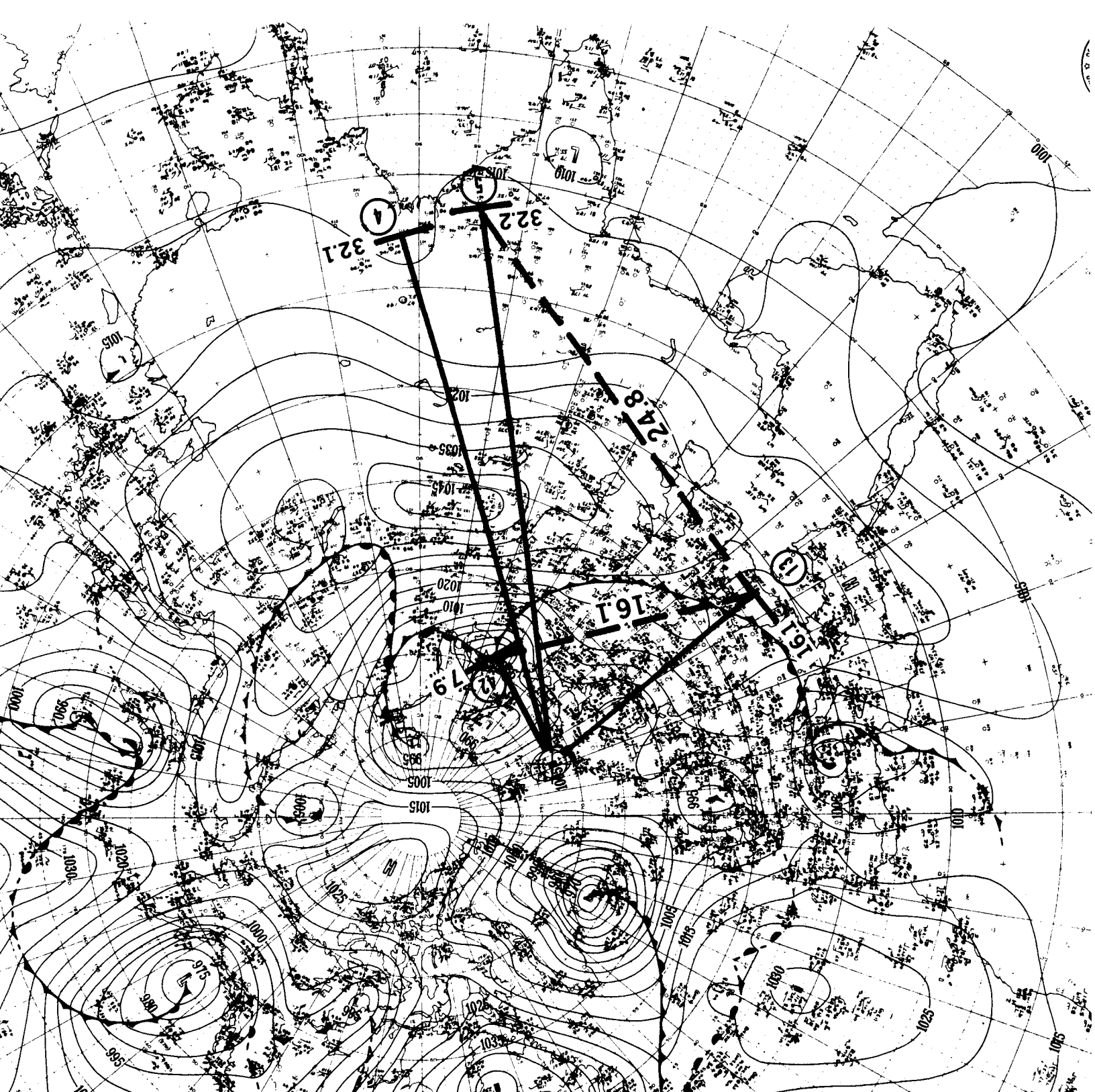
• The first special feature on this chart is the two remnant highs #65 and #27 counterbalancing each other in a nearly straight line with the exact distance of 18.1 ru each. The second special feature is that the centers of #60, #70, and #81 all lie in a nearly straight line with their distances at 8.9 ru, 17.7 ru ($2 \times 8.9 = 17.8$), and 35.7 ru ($4 \times 8.9 = 35.6$).



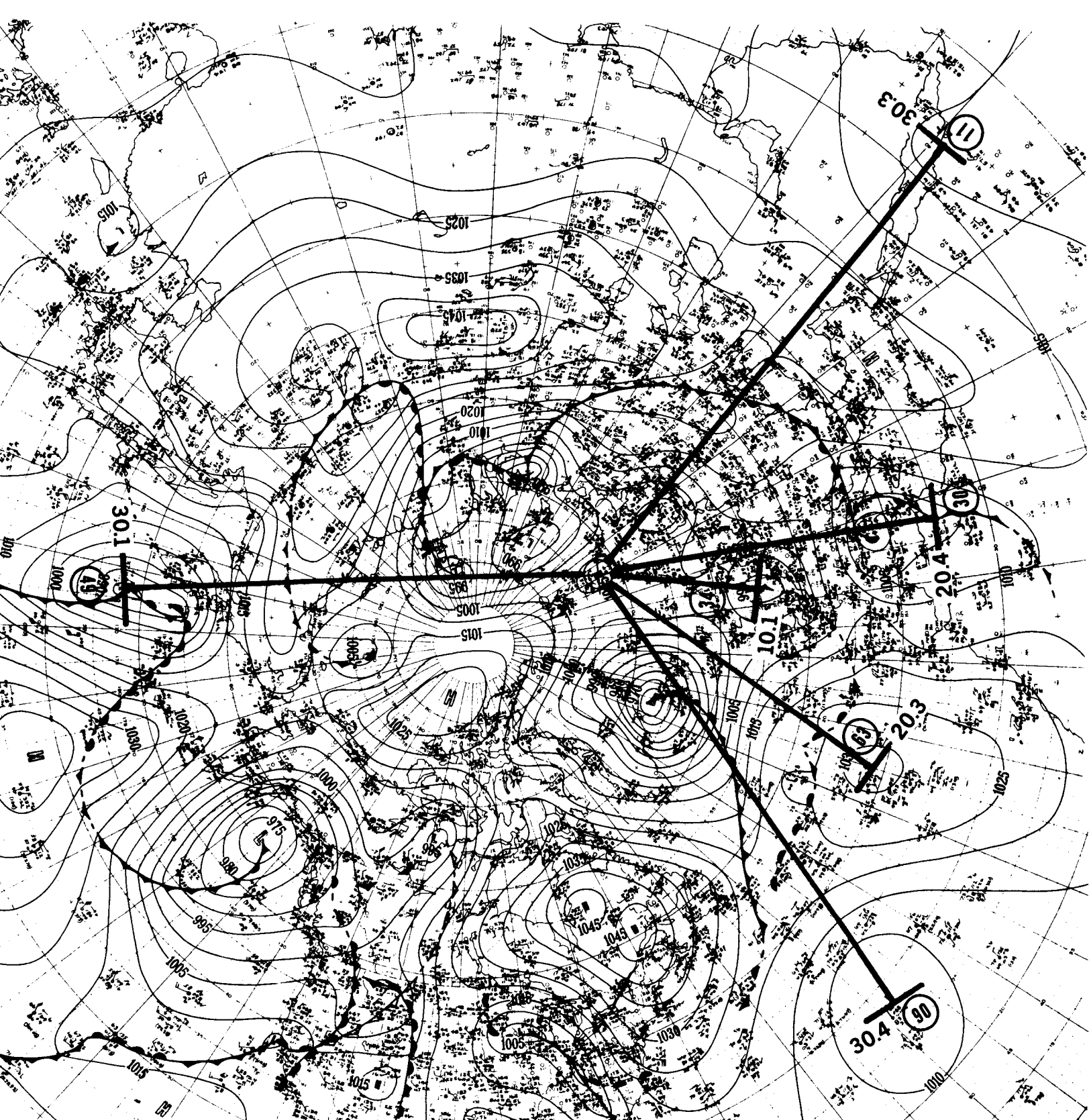
This one has what seems to be an LCD of approximately 10.7 ru. The two points, #86 at 21.3 ru and #89 at 21.5 ru ($2 \times 10.7 = 21.4$), are counterbalanced by #4 (32.1 ru) and #5 at 32.2 ru ($3 \times 10.7 = 32.1$). A very slightly discordant note in this melody is #59 at 10.5 ru, instead of the apparent LCD of 10.7 ru.



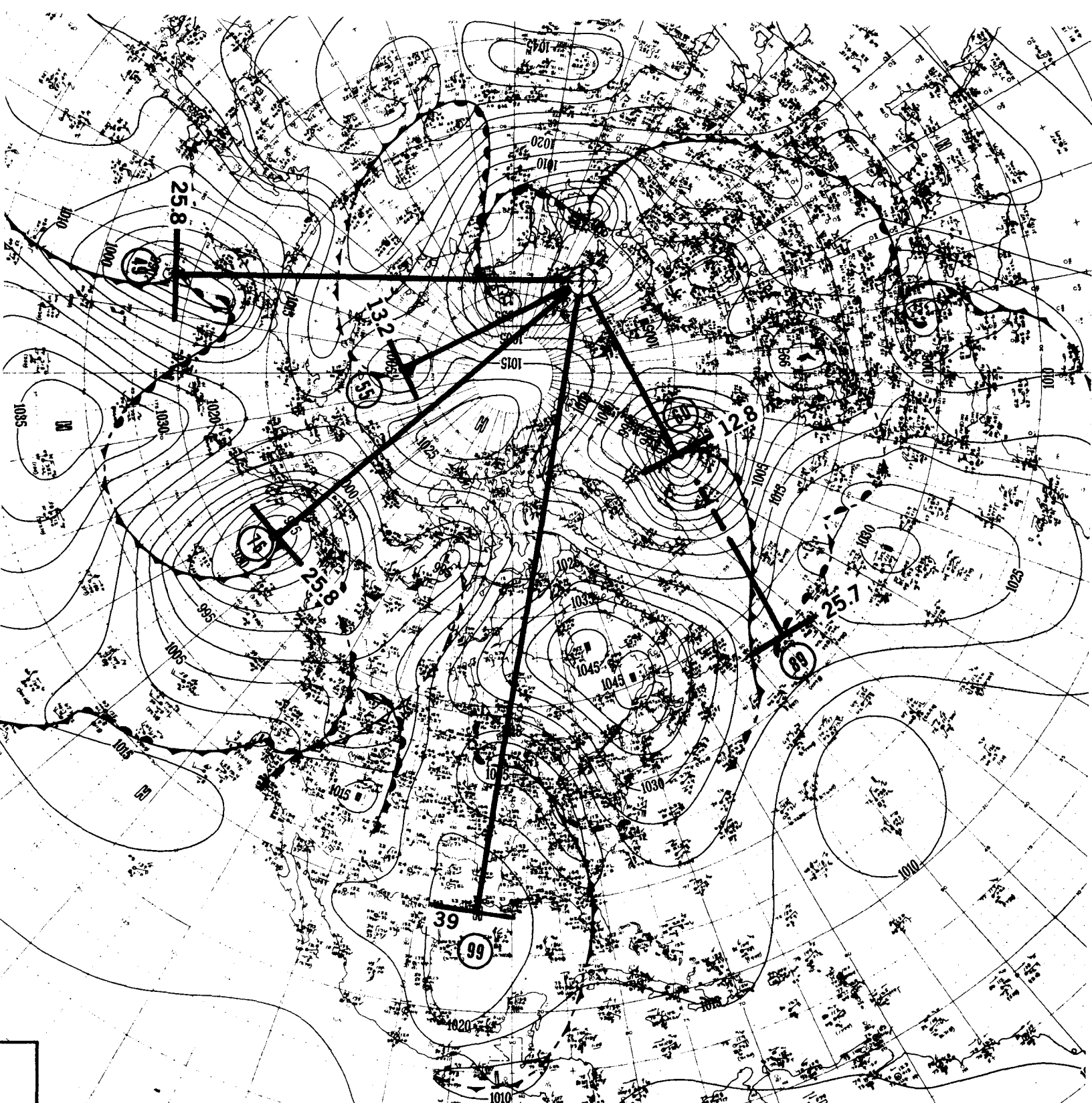
The unique feature of this chart is #58 at 12.5 ru—nearly in a straight line with #9 at 37.4 ru ($3 \times 12.5 = 37.5$). We also see that #52 at 25 ru is twice the distance of #58. We finally have #29 hanging in there at 12.2 ru.



This chart is for general interest only since we are using #4, #5, and #13 (three obscure points). The LCD is approximately 8 ru. The triangle formed by #39, #42, and #13 has three sides in the ratio of 7.9:16.1:16.7 which is approximately 1:2:2. The triangle formed by #39, #5, and #13 has three sides in the ratio of 16.1:24.8:32.2, which is closely 2:3:4.

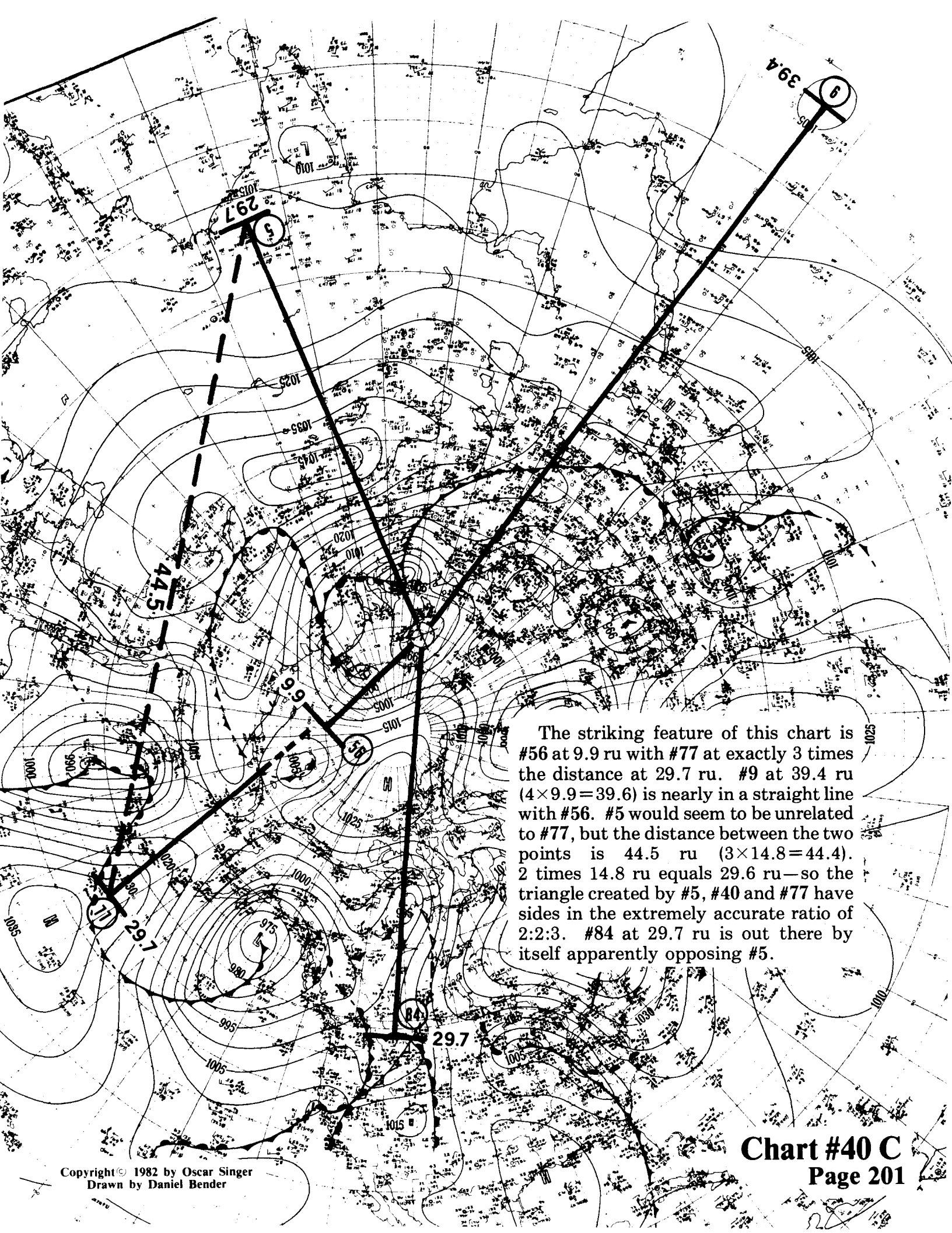


This pattern, with an approximate LCD of 10.1 ru, looks like a rake, with a handle represented by the ray to #49. #30 and #65 are in the 20 ru range, and #11, #90, and #49 are in the 30 ru range. Perhaps #11 should be left out in the view of its obscure and indefinite location, but it was entered for completeness.

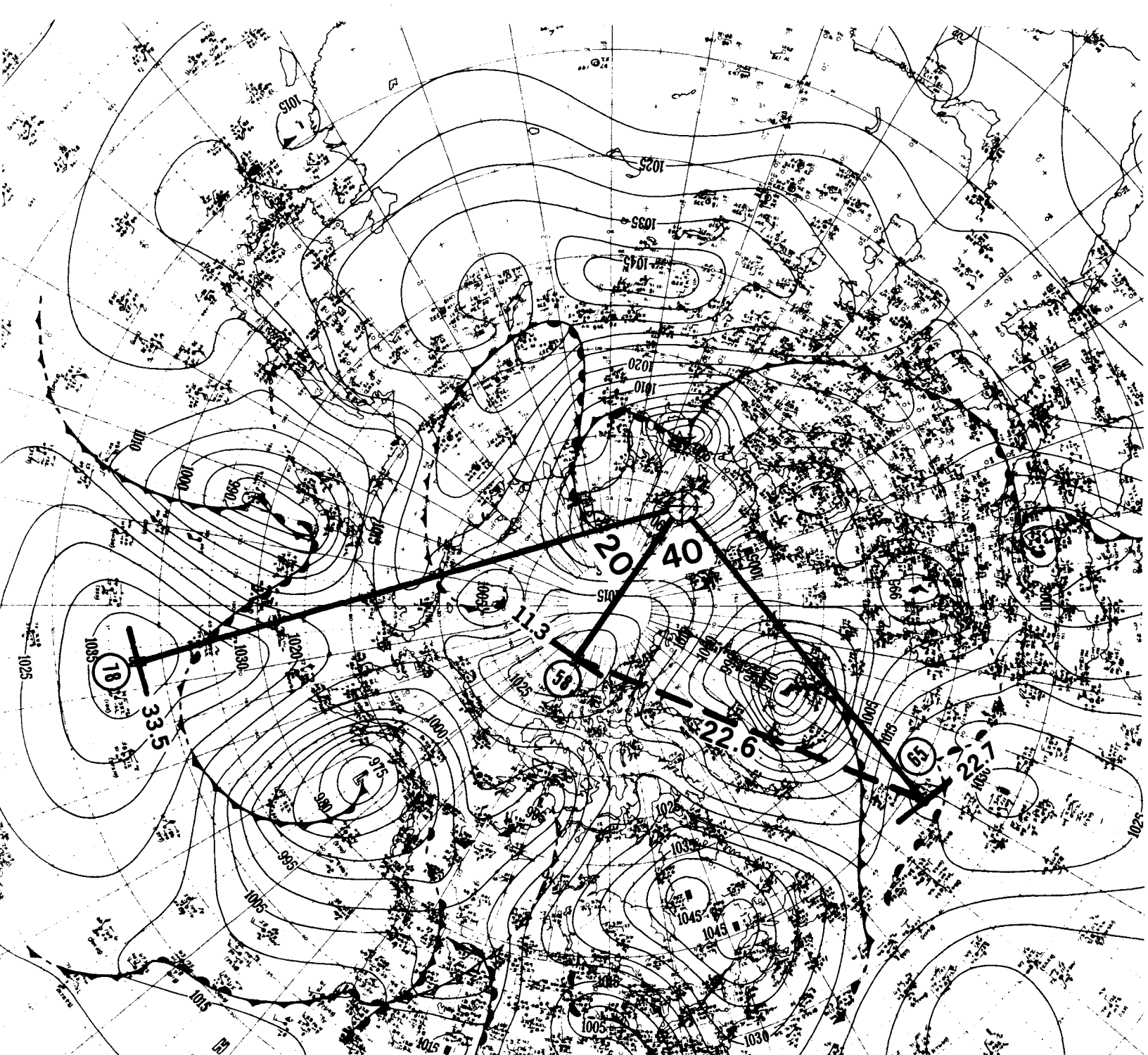


The refreshing feature of this chart is #60 at 12.8 ru, which is doubled by #89 at 25.7 ru, both of which are in a straight line. #76 and #49 at 25.8 ru join with #89 at 25.7 ru, to form a partial ring. #99 at 39 ru (3×13) seems to have taken an LCD that is the average between the 12.8 ru of #60 and the 13.2 ru of #55.

ATIONS
Dsys
M PPP
M t ppo
N WR,
BAN NO

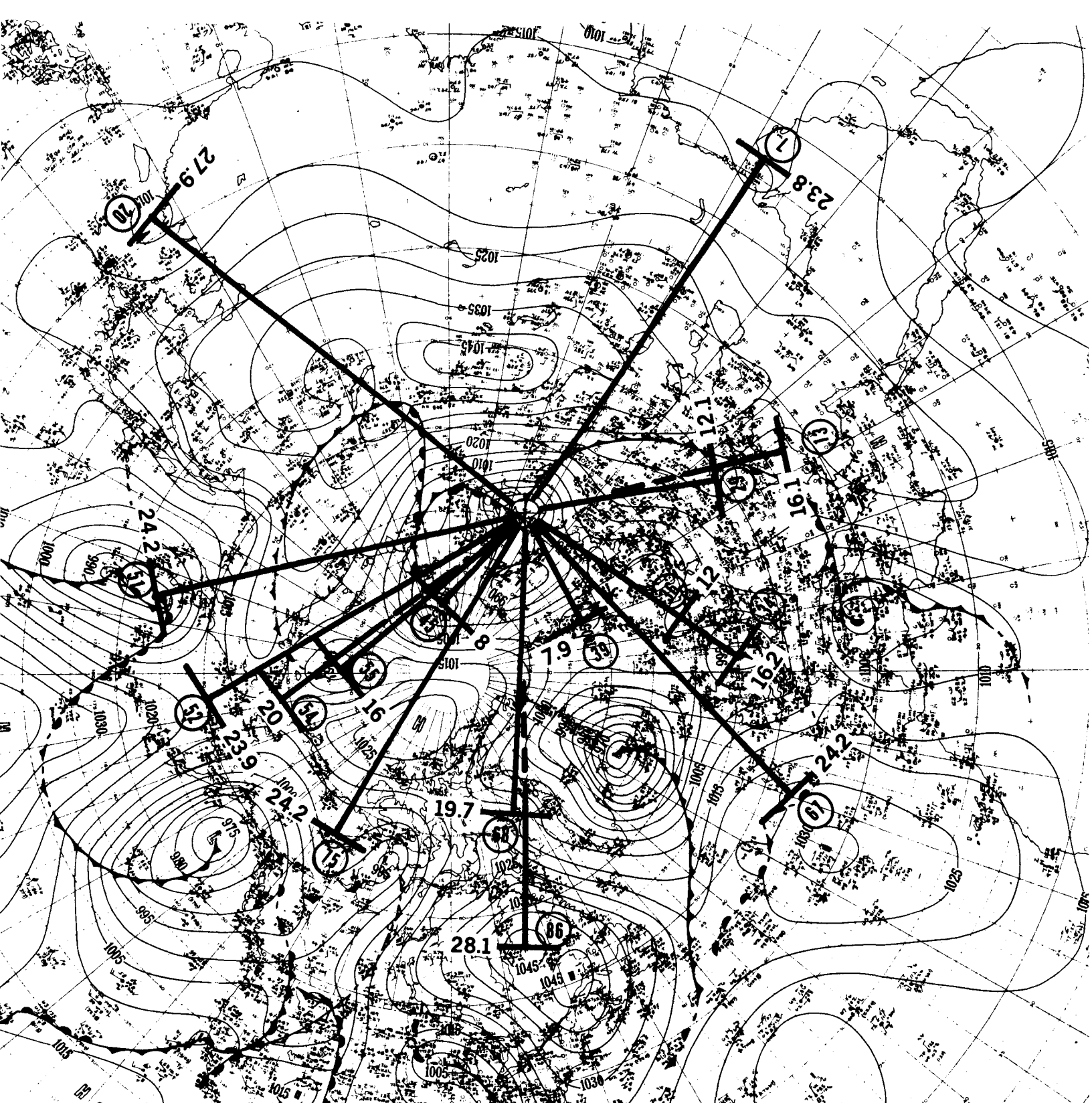


The striking feature of this chart is #56 at 9.9 ru with #77 at exactly 3 times the distance at 29.7 ru. #9 at 39.4 ru ($4 \times 9.9 = 39.6$) is nearly in a straight line with #56. #5 would seem to be unrelated to #77, but the distance between the two points is 44.5 ru ($3 \times 14.8 = 44.4$). 2 times 14.8 ru equals 29.6 ru—so the triangle created by #5, #40 and #77 have sides in the extremely accurate ratio of 2:2:3. #84 at 29.7 ru is out there by itself apparently opposing #5.

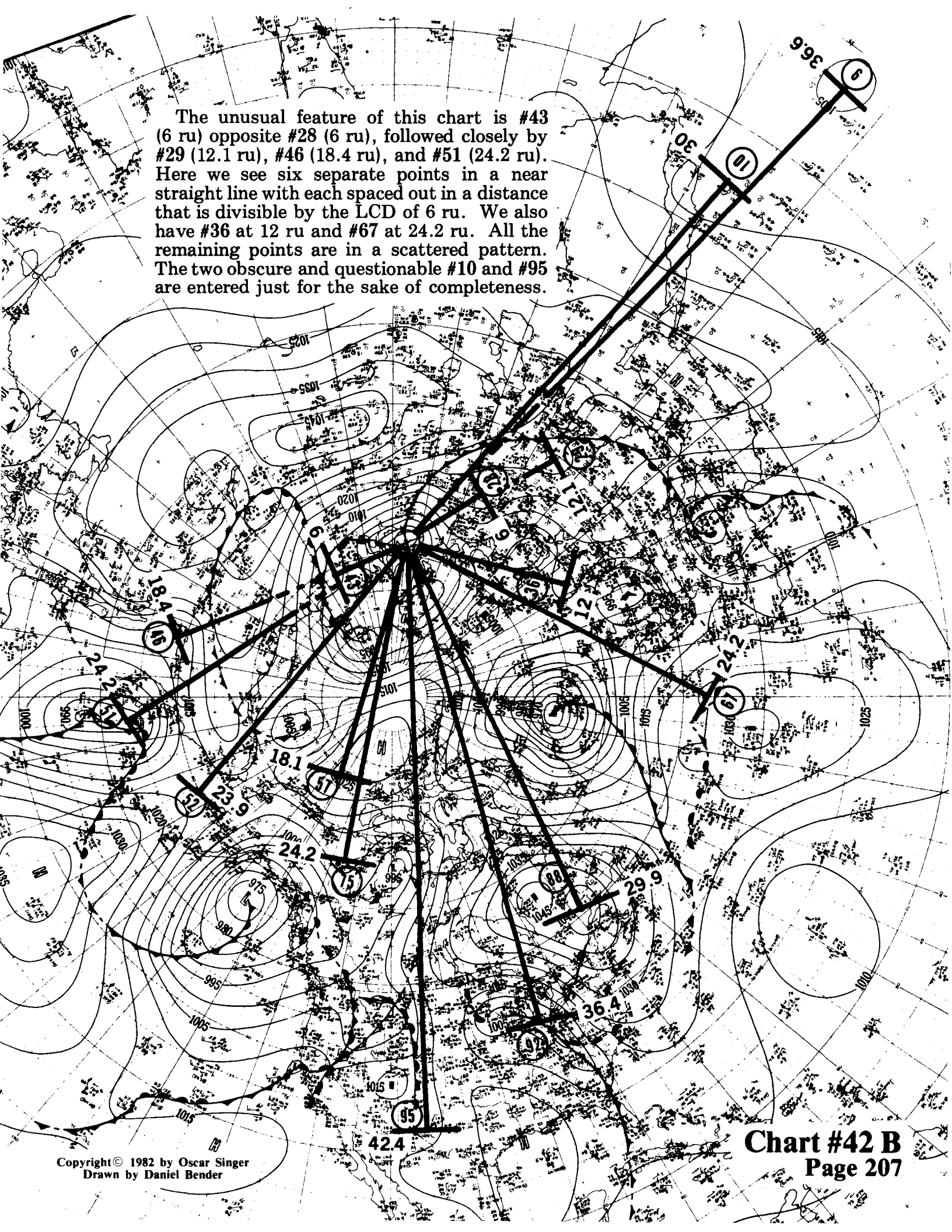


This is a hot one! The three points forming the triangle, #40, #58, and #65, are well defined and relatively close to each other. #58 at 11.3 ru and #65 at 22.7 ru have a distance between them of 22.6 ru, which seems too good to be true. The sides of the triangle form an almost perfect ratio of 2:2:1. To put a cap on this chart, we find that #78 is at an angular separation of 20 cu (compared to 40 cu between the other two points) and is located at a distance of 33.5 ru ($3 \times 11.3 = 33.9$).

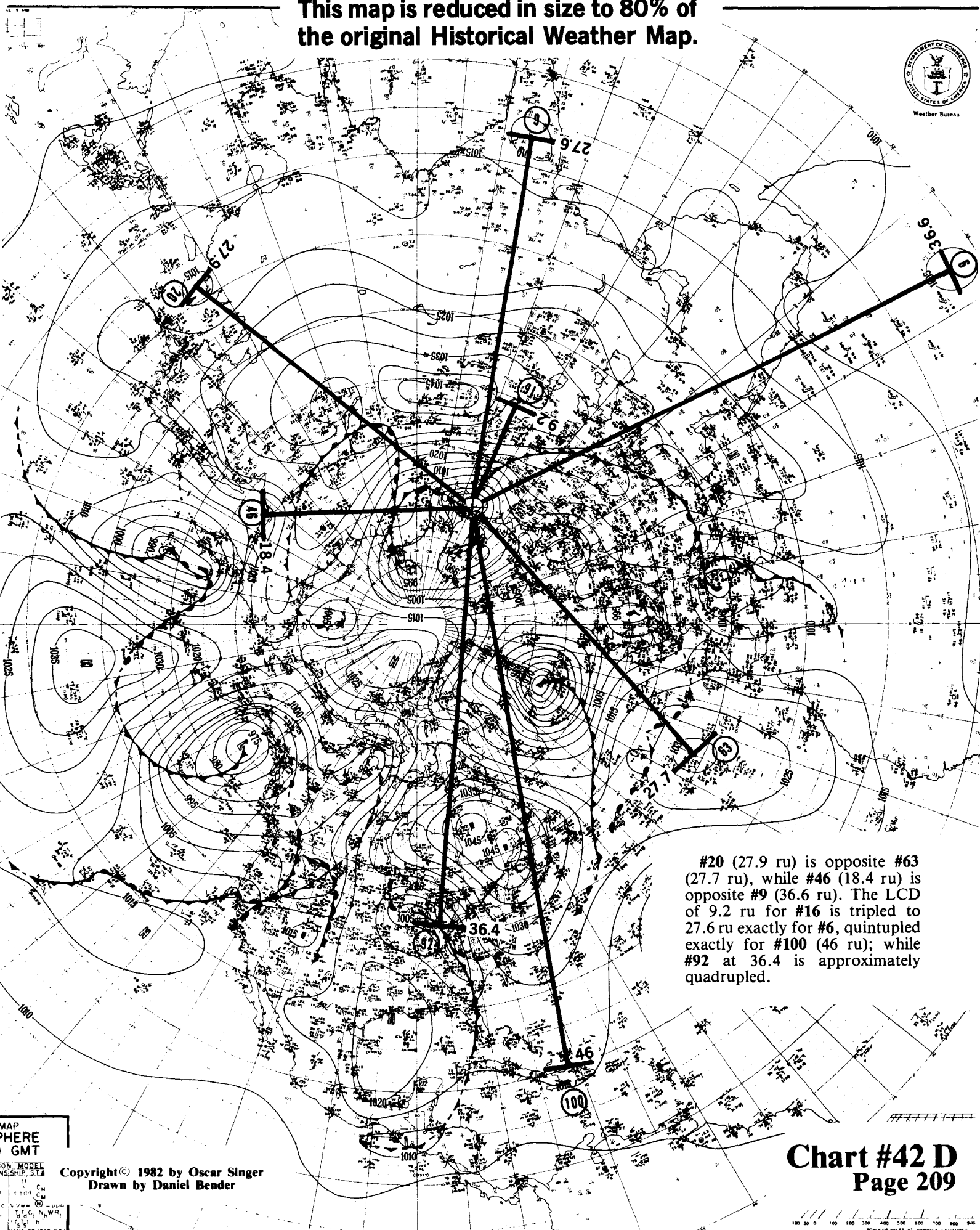
The visual symmetry of this one is pleasant. The LCD, #39 (6.1 ru), is matched very closely in a 1:4 ratio with #30, #87, and #50. #63 (25.1 ru) and #76 (25.8 ru) are not far off.



The unusual feature of this chart is #43 (6 ru) opposite #28 (6 ru), followed closely by #29 (12.1 ru), #46 (18.4 ru), and #51 (24.2 ru). Here we see six separate points in a near straight line with each spaced out in a distance that is divisible by the LCD of 6 ru. We also have #36 at 12 ru and #67 at 24.2 ru. All the remaining points are in a scattered pattern. The two obscure and questionable #10 and #95 are entered just for the sake of completeness.



This map is reduced in size to 80% of the original Historical Weather Map.



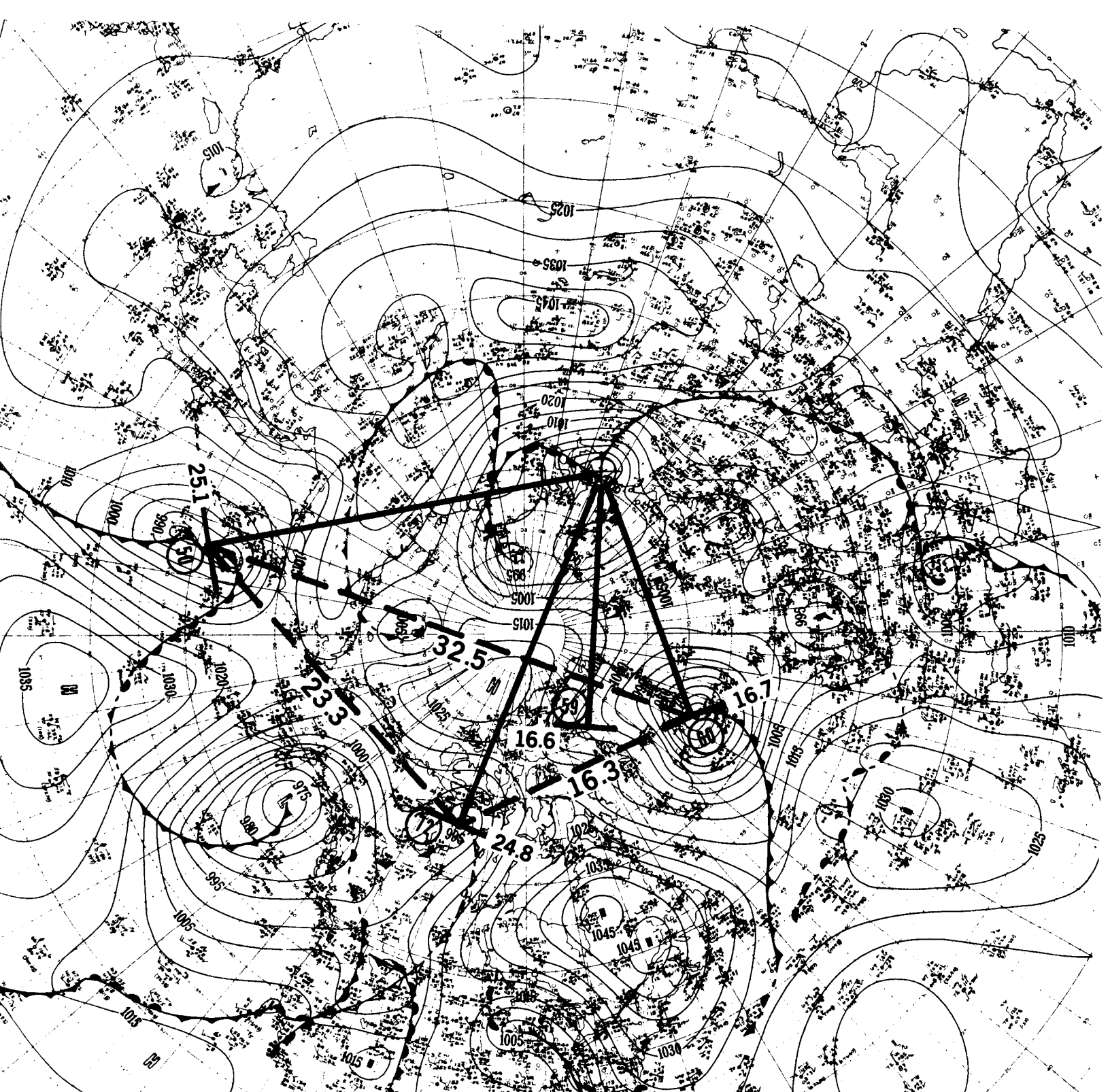
#20 (27.9 ru) is opposite #63 (27.7 ru), while #46 (18.4 ru) is opposite #9 (36.6 ru). The LCD of 9.2 ru for #16 is tripled to 27.6 ru exactly for #6, quintupled exactly for #100 (46 ru); while #92 at 36.4 is approximately quadrupled.

MAP
WHERE
GMT
ON MODEL
SHIP, 27A
CH
© 1982
T.C.N.W.R.
Singer

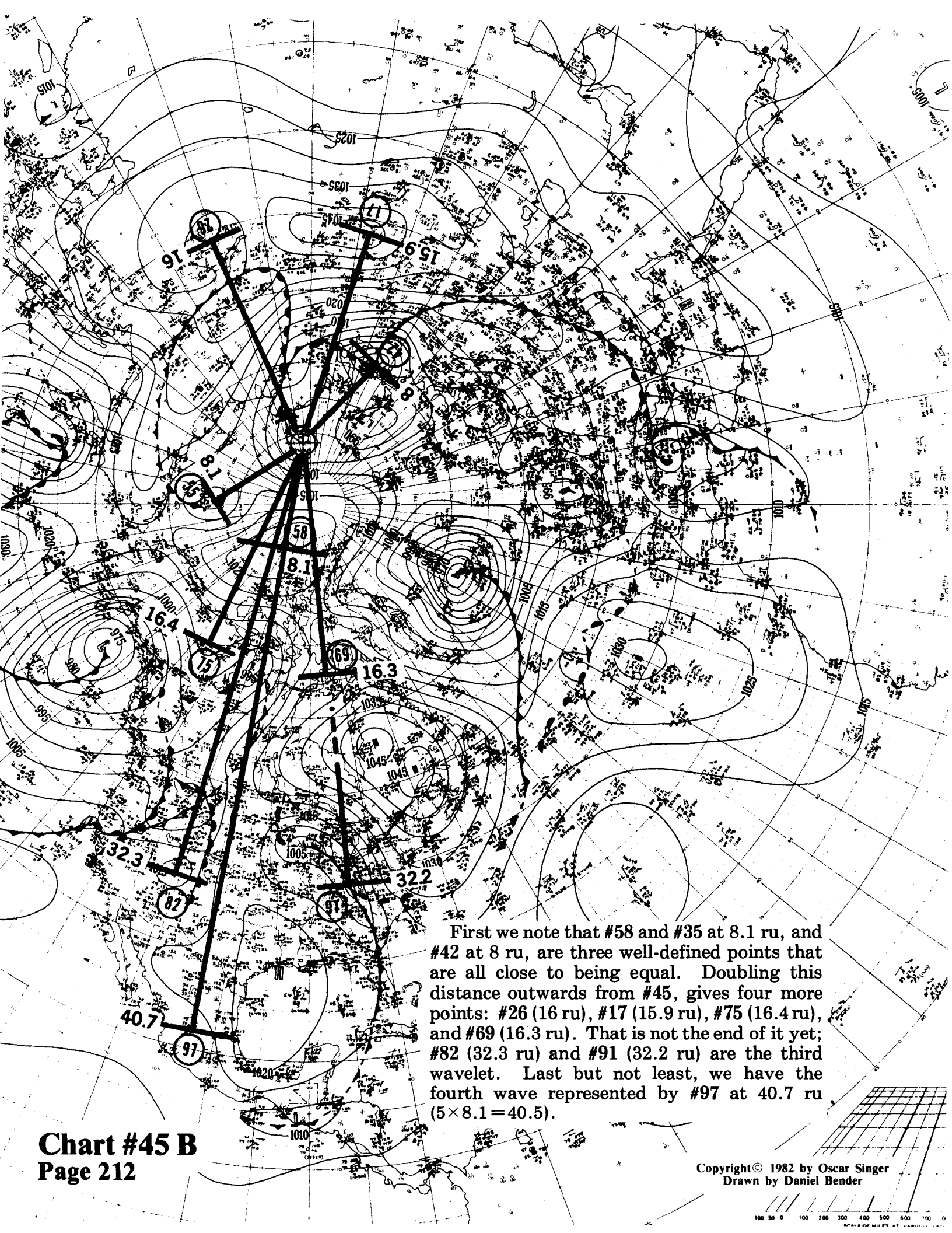
Copyright © 1982 by Oscar Singer
Drawn by Daniel Bender

Chart #42 D
Page 209

100 50 0 100 200 300 400 500 600 700 800 900
SCALE OF MILES AT VARIOUS LATITUDES



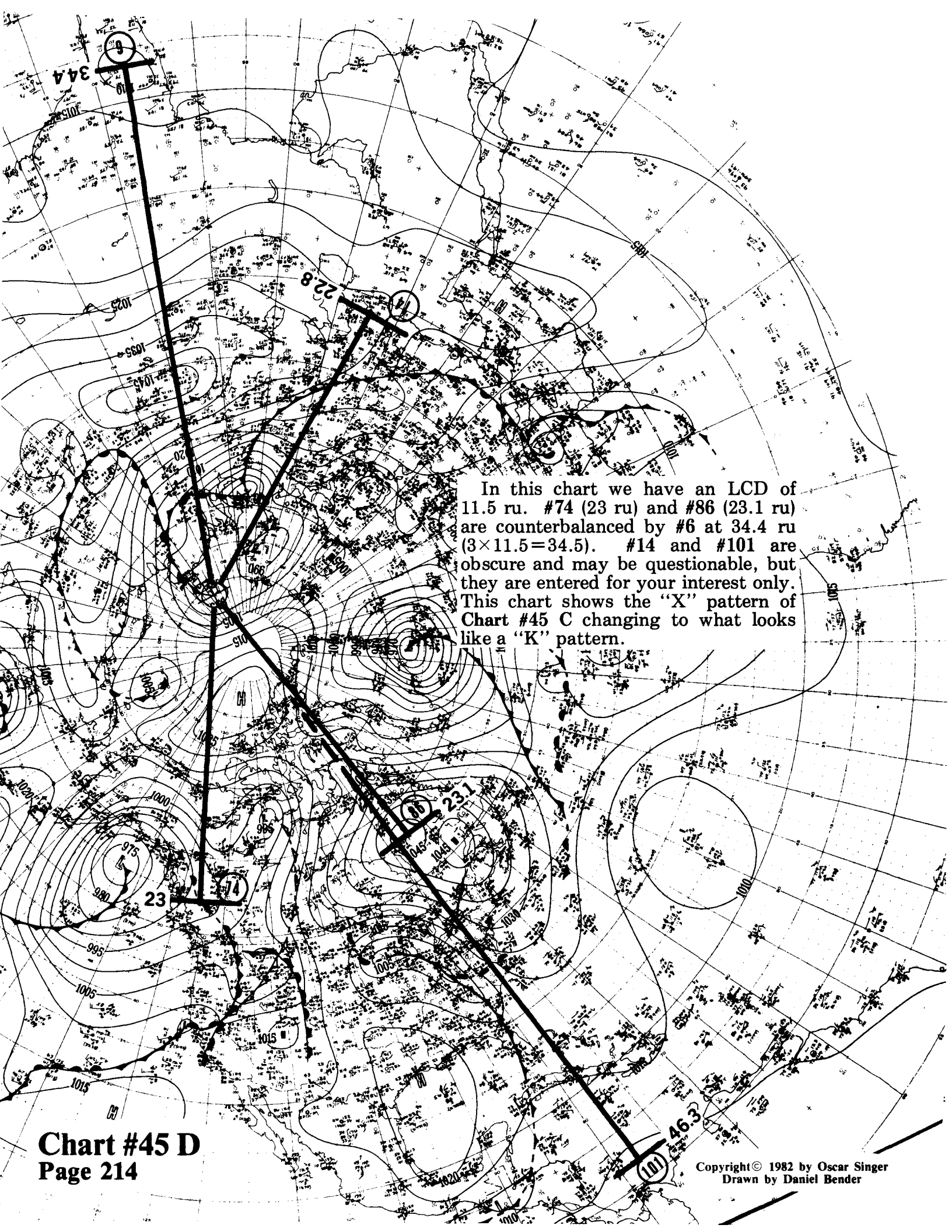
Here we have a triangle formed by #42, #60, and #72, with the length of the sides of the triangle equal to 16.7, 16.3, and 24.8 ru, which is close to a ratio of 1:2:3 if you divide by 8.2 ru. The distance of 32.5 ru from #60 to #50 is cut in half in a symmetrical pattern by the 16.3 ru from #60 to #72, and the 16.7 ru from #60 to #42. The distance of 23.3 ru from #50 to #72 is entered as a matter of interest.



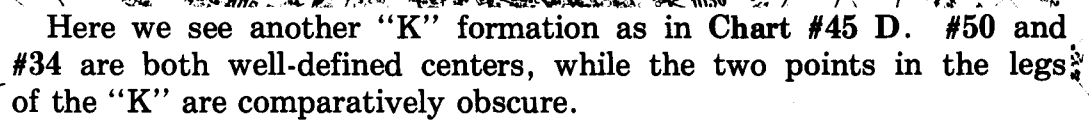
First we note that #58 and #35 at 8.1 ru, and #42 at 8 ru, are three well-defined points that are all close to being equal. Doubling this distance outwards from #45, gives four more points: #26 (16 ru), #17 (15.9 ru), #75 (16.4 ru), and #69 (16.3 ru). That is not the end of it yet; #82 (32.3 ru) and #91 (32.2 ru) are the third wavelet. Last but not least, we have the fourth wave represented by #97 at 40.7 ru ($5 \times 8.1 = 40.5$).

The clear feature of this one is #60 at 15.1 ru, counterbalanced at approximately double the distance, by #21 at 29.8 ru. Likewise, #4 is also at 29.8 ru, and is counterbalanced by #92 at 30.7 ru. Lastly, #103 is 45.2 ru ($3 \times 15.1 = 45.3$).

One additional fact to note at this time is the formation of an "X" type of pattern by the four points: #4, #103, #21, and #60. This "X" formation occurs often.



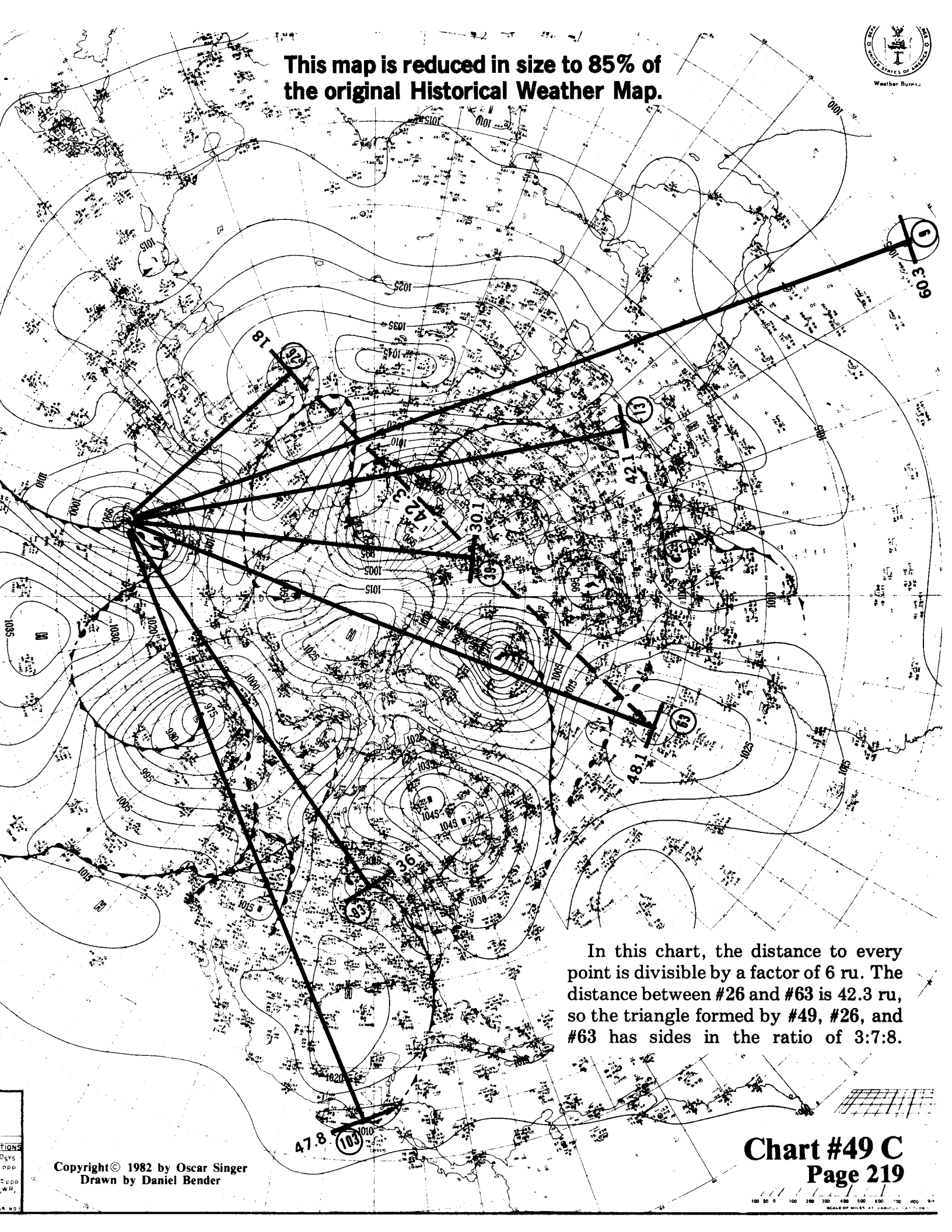
In this chart we have an LCD of 11.5 ru. #74 (23 ru) and #86 (23.1 ru) are counterbalanced by #6 at 34.4 ru ($3 \times 11.5 = 34.5$). #14 and #101 are obscure and may be questionable, but they are entered for your interest only. This chart shows the "X" pattern of Chart #45 C changing to what looks like a "K" pattern.



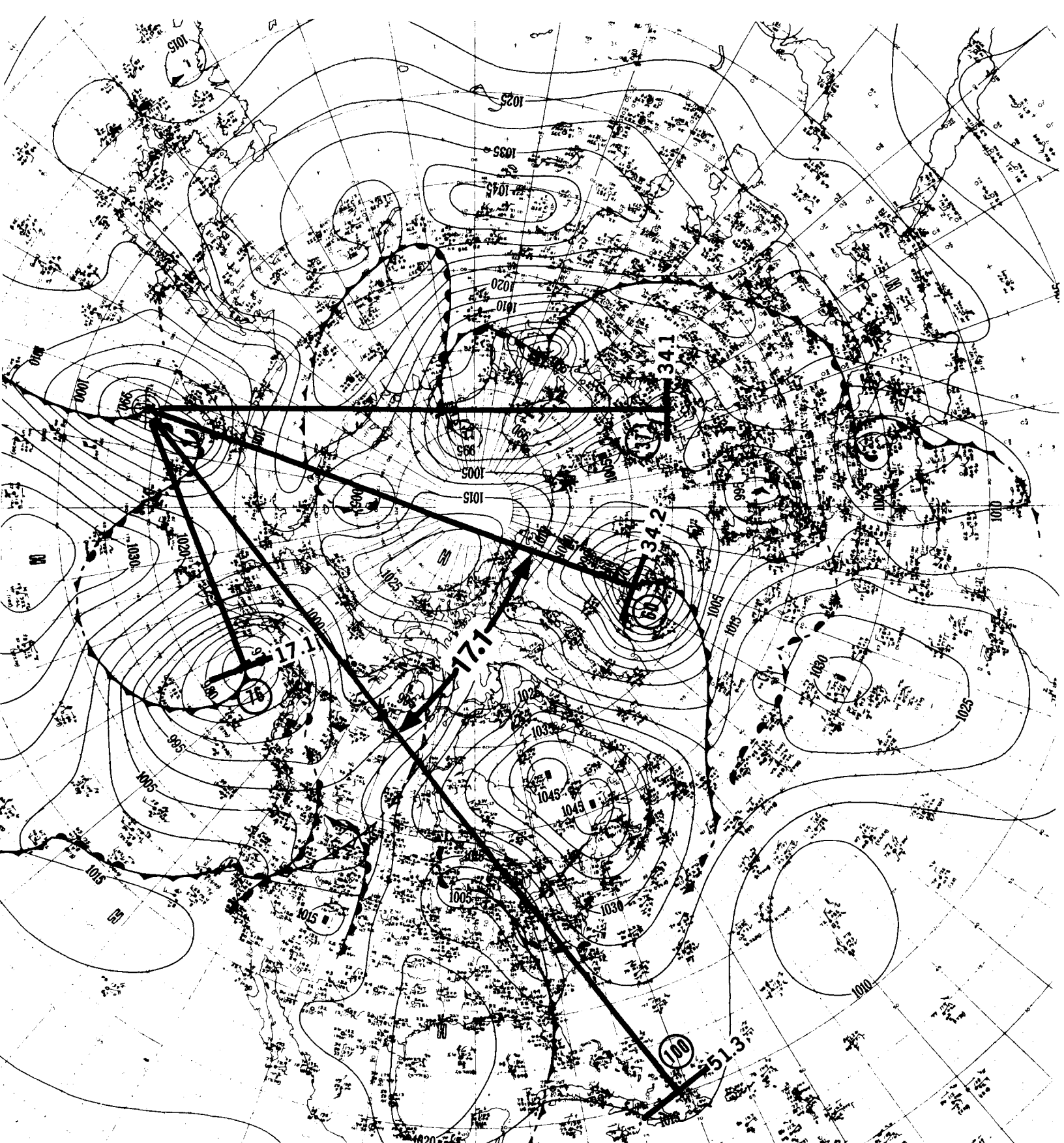
This one is magnificent in its sweep and scope, starting with an LCD of 10 ru established by #53. We find a series of steps in a narrow band: #43 (20.2 ru), #39 (30.1 ru), #34 (40.2 ru), and lastly #30 (50.2 ru). This is neat. The clincher is #6 (40 ru) in central India, counterbalanced by #91 (39.9 ru) in northern Kentucky—with an angular sweep of 27.8 cu and 27.5 cu respectively from the ray to #30 in Algeria.

This chart is the same as the previous one, plus the addition of a few more points and lines. To have entered all the information on one chart would have made too much of a clutter to be digested. The additional points of interest are: the distance between #39 and #91, which is 30.9 ru; the distance between #6 and #14 is 19.8 ru; and #43 at 20.2 ru almost doubles to 39.9 ru at #14, and then triples to 60.3 ru at #9.

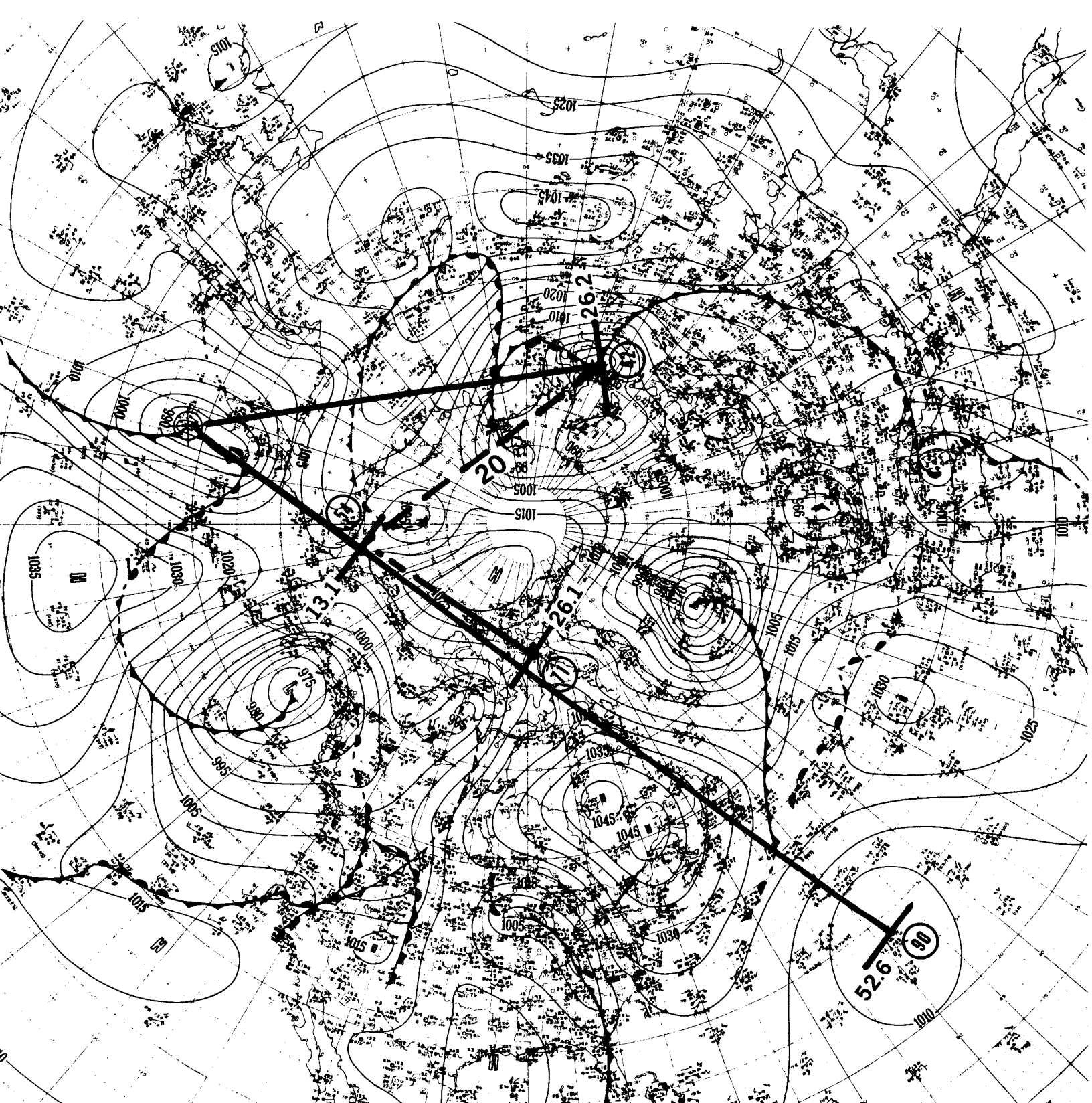
This map is reduced in size to 85% of the original Historical Weather Map.



In this chart, the distance to every point is divisible by a factor of 6 ru. The distance between #26 and #63 is 42.3 ru, so the triangle formed by #49, #26, and #63 has sides in the ratio of 3:7:8.

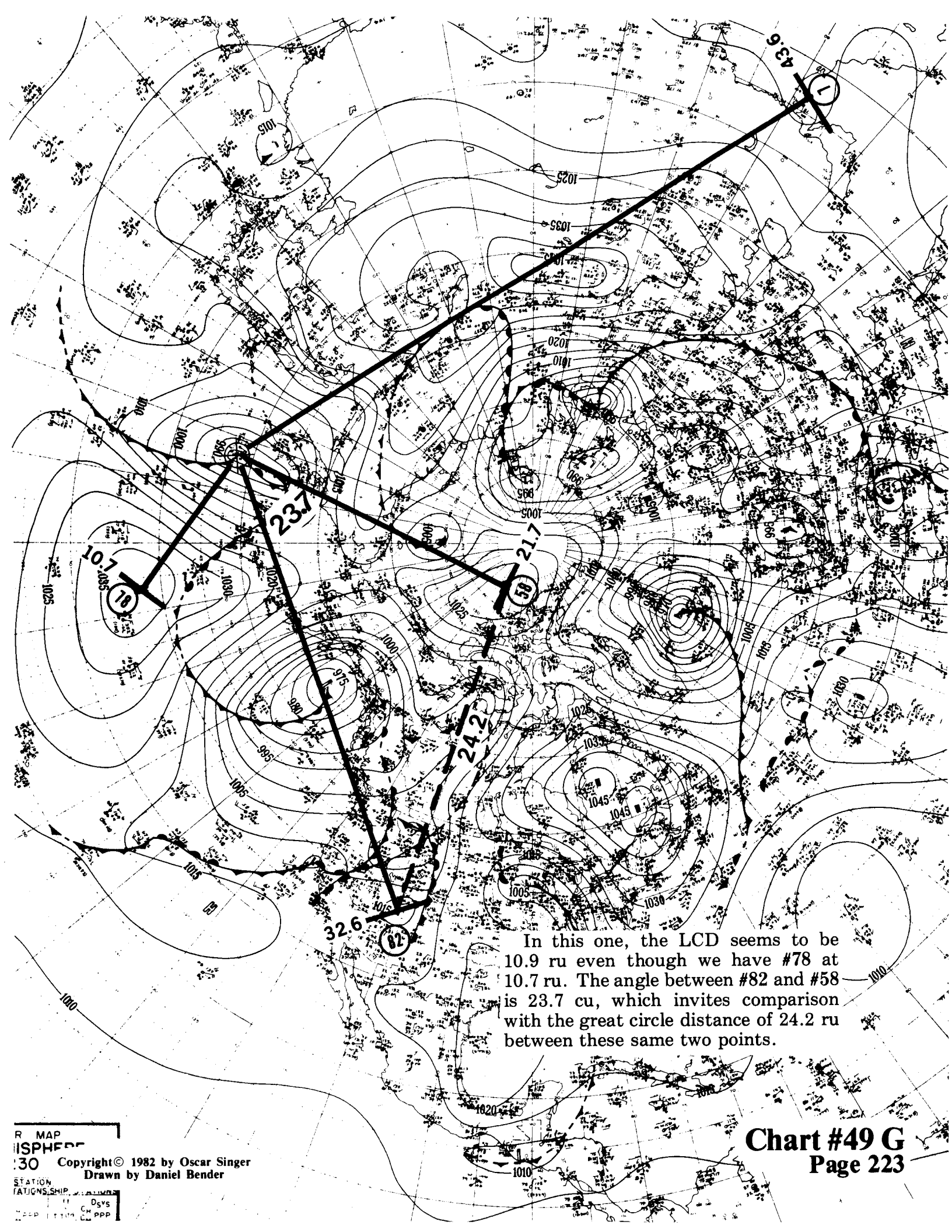


The LCD of 17.1 ru (#76) is tripled exactly at #100 with 51.3 ru. Next, we have an intriguing angle of 17.1 cu between #100 and #60 at 34.2 ru (2×17.1 ru). Lastly, we have a 34.1 ru for #37.



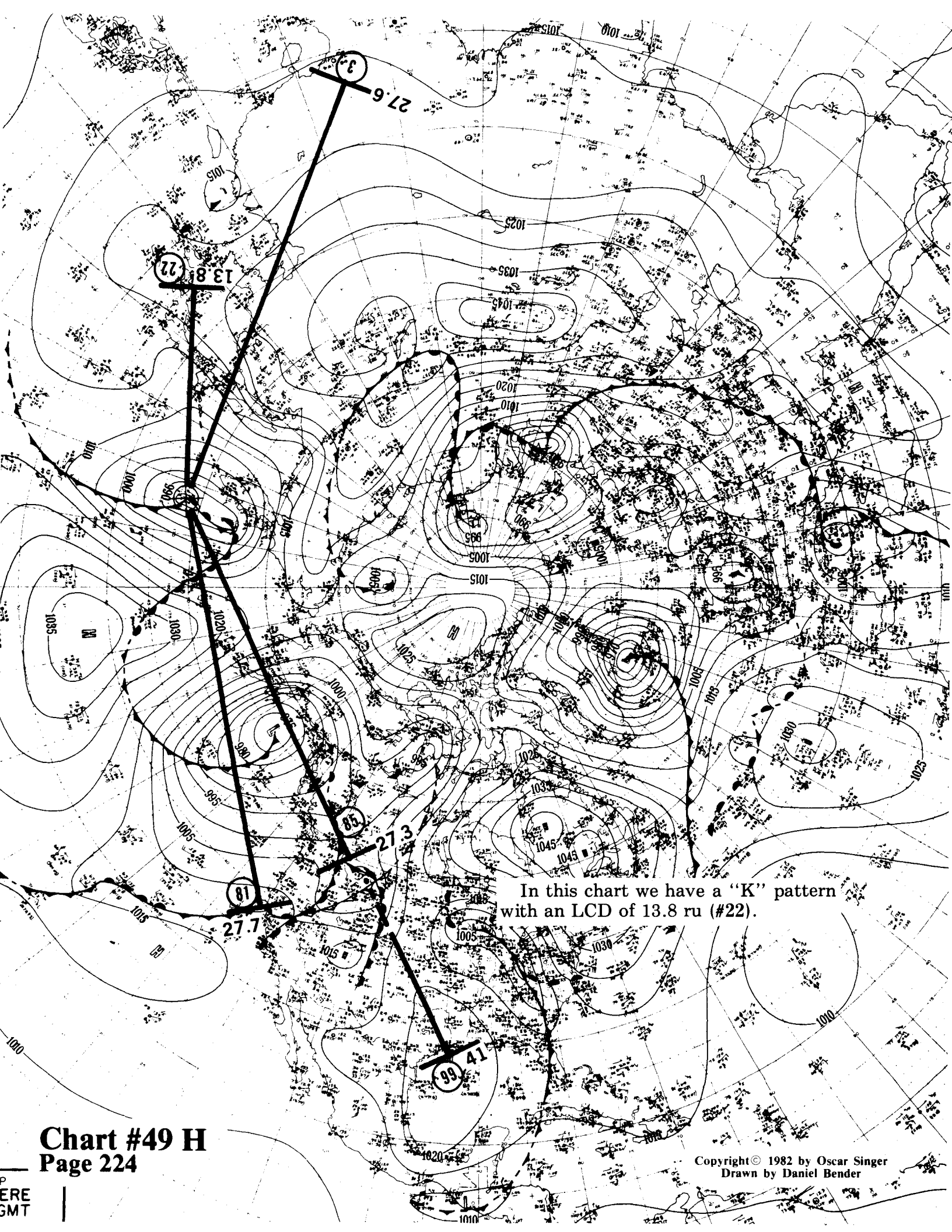
This map is a quiet sparkler. The LCD is 13.1 ru (which equals 2 times 6.55). The LCD is doubled to 26.1 ru at #71, and is quadrupled to 52.6 ru at #90. This indicates that the seemingly innocuous points of #54 and #71, are significantly placed in a nearly straight line direction towards #90. In addition, the distance between #54 and #42 is 20 ru ($3 \times 6.55 = 19.65$).

RE
IT
DEL
STATIONS
DAYS
CH
PPP
C
N
WR
ON (BAR NO.)



In this one, the LCD seems to be 10.9 ru even though we have #78 at 10.7 ru. The angle between #82 and #58 is 23.7 cu, which invites comparison with the great circle distance of 24.2 ru between these same two points.

Chart #49 G
Page 223

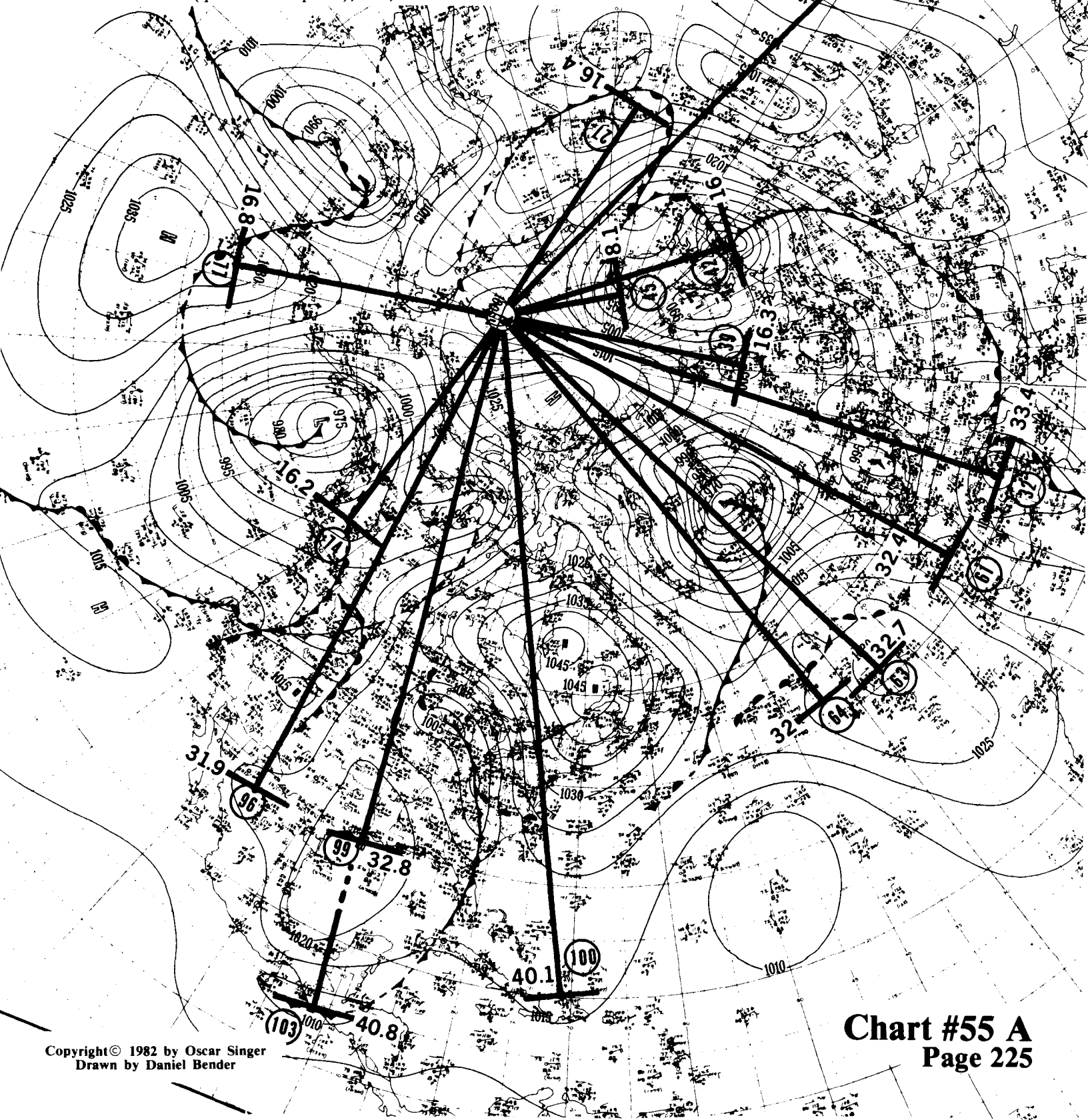


In this chart we have a "K" pattern with an LCD of 13.8 ru (#22).

First we have #77 (16.8 ru) in a nearly straight line with #32 (33.4 ru). This pair looks good together, but they don't really belong in this pattern directly (they have been added since they are close to the value of the others).

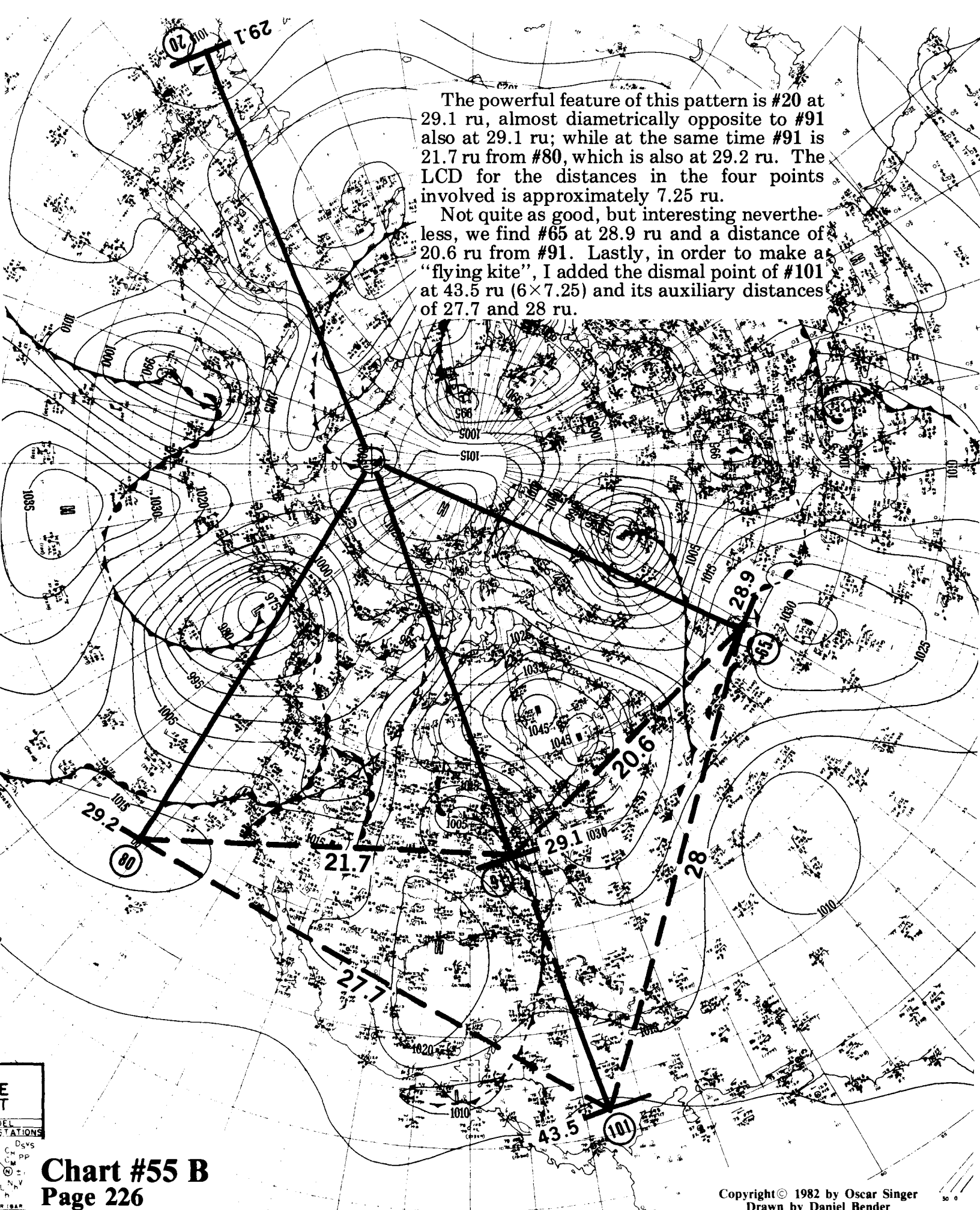
#27 (16.4 ru) is balanced by #74 (16.2 ru), while #45 at 8.1 ru almost doubles to 16 ru at #42. These three pairs are the highlights, while the rest of the points are all divisible by an LCD of 8 to 8.2 ru.

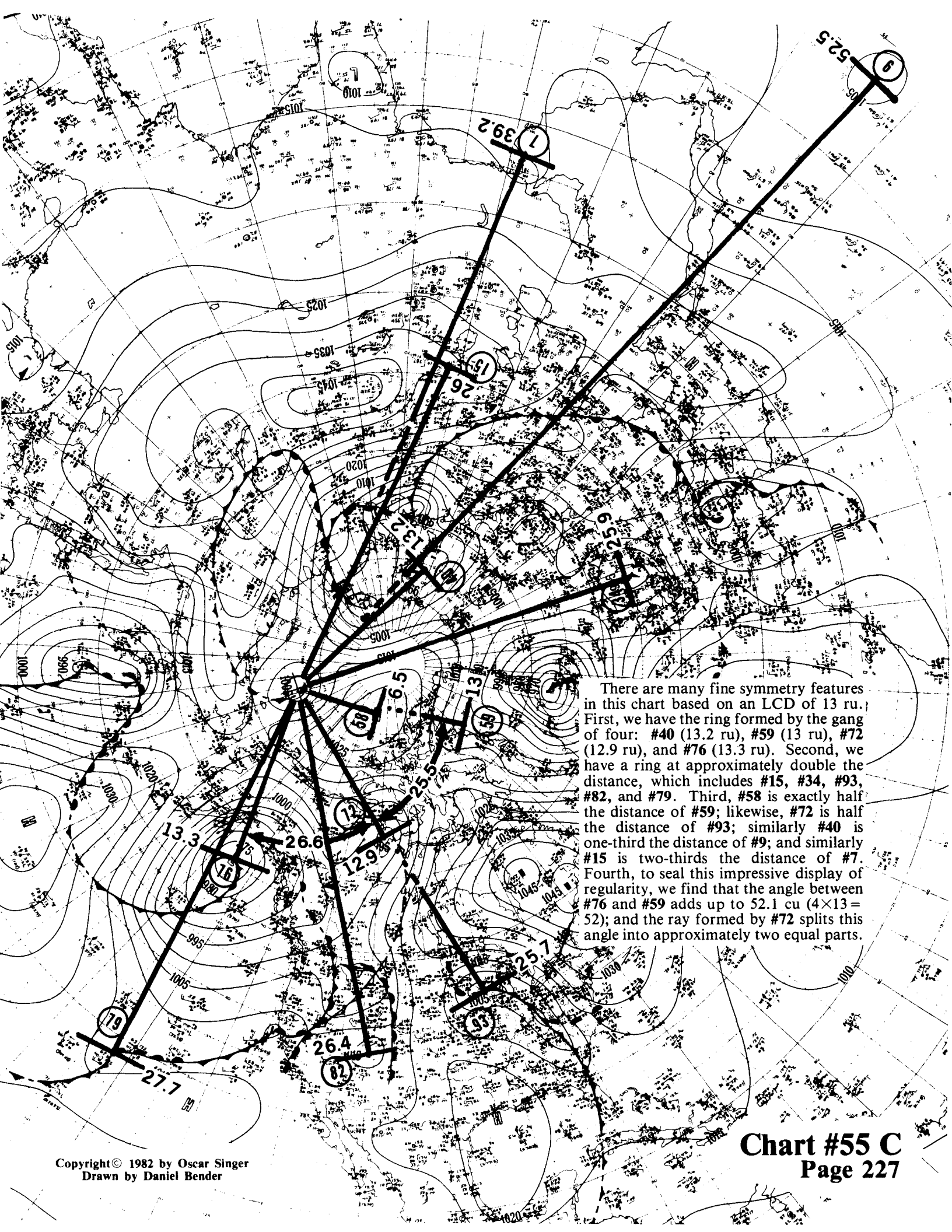
One other feature that should not be overlooked is the existence of two fairly definite rings: the first at approximately 17 ru includes #27, #42, #39, #74, and #77; the second ring at double the distance of approximately 32 ru, includes #32, #61, #63, #64 (questionable point), #99, and #96.



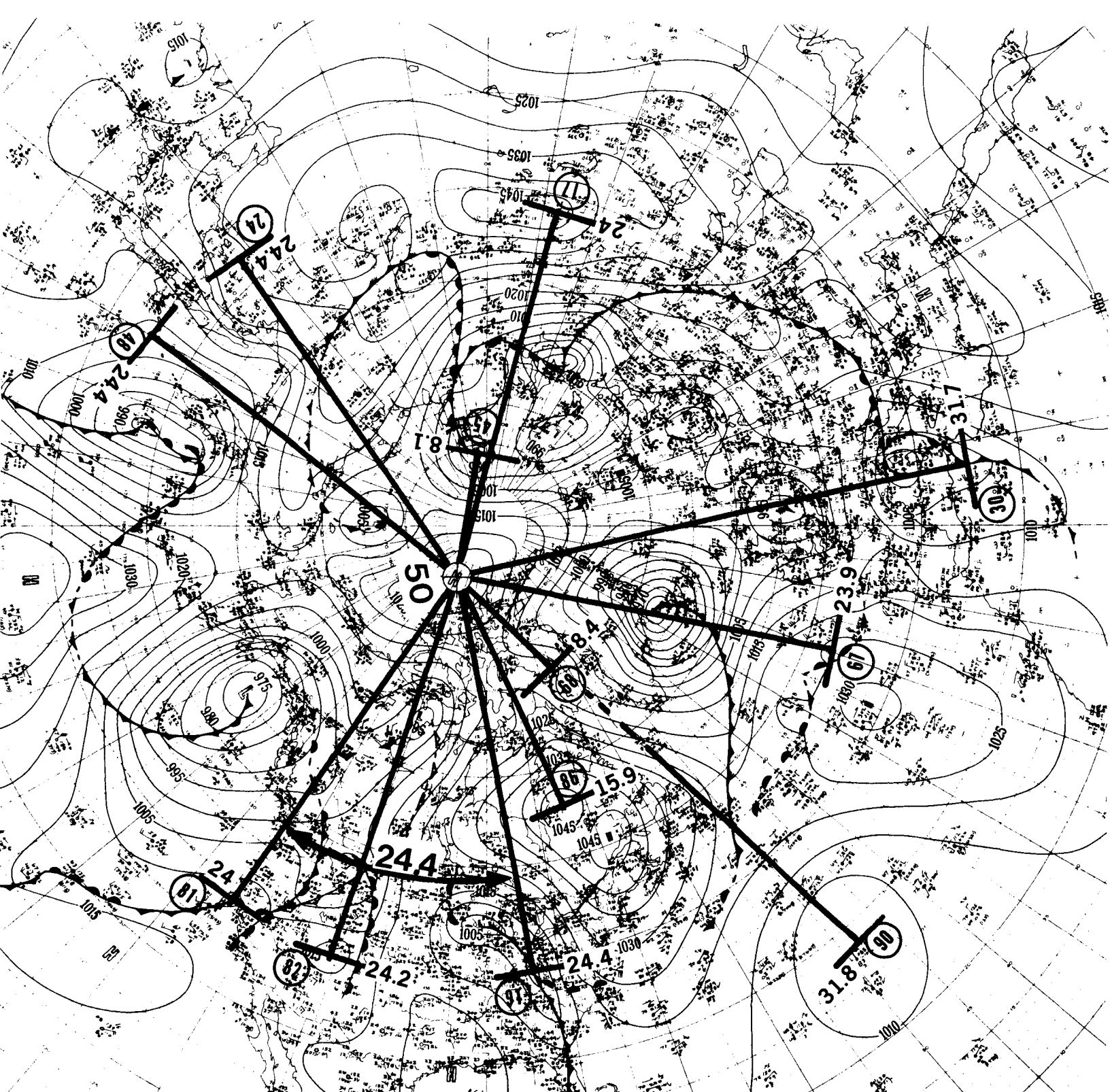
The powerful feature of this pattern is #20 at 29.1 ru, almost diametrically opposite to #91 also at 29.1 ru; while at the same time #91 is 21.7 ru from #80, which is also at 29.2 ru. The LCD for the distances in the four points involved is approximately 7.25 ru.

Not quite as good, but interesting nevertheless, we find #65 at 28.9 ru and a distance of 20.6 ru from #91. Lastly, in order to make a "flying kite", I added the dismal point of #101 at 43.5 ru (6×7.25) and its auxiliary distances of 27.7 and 28 ru.

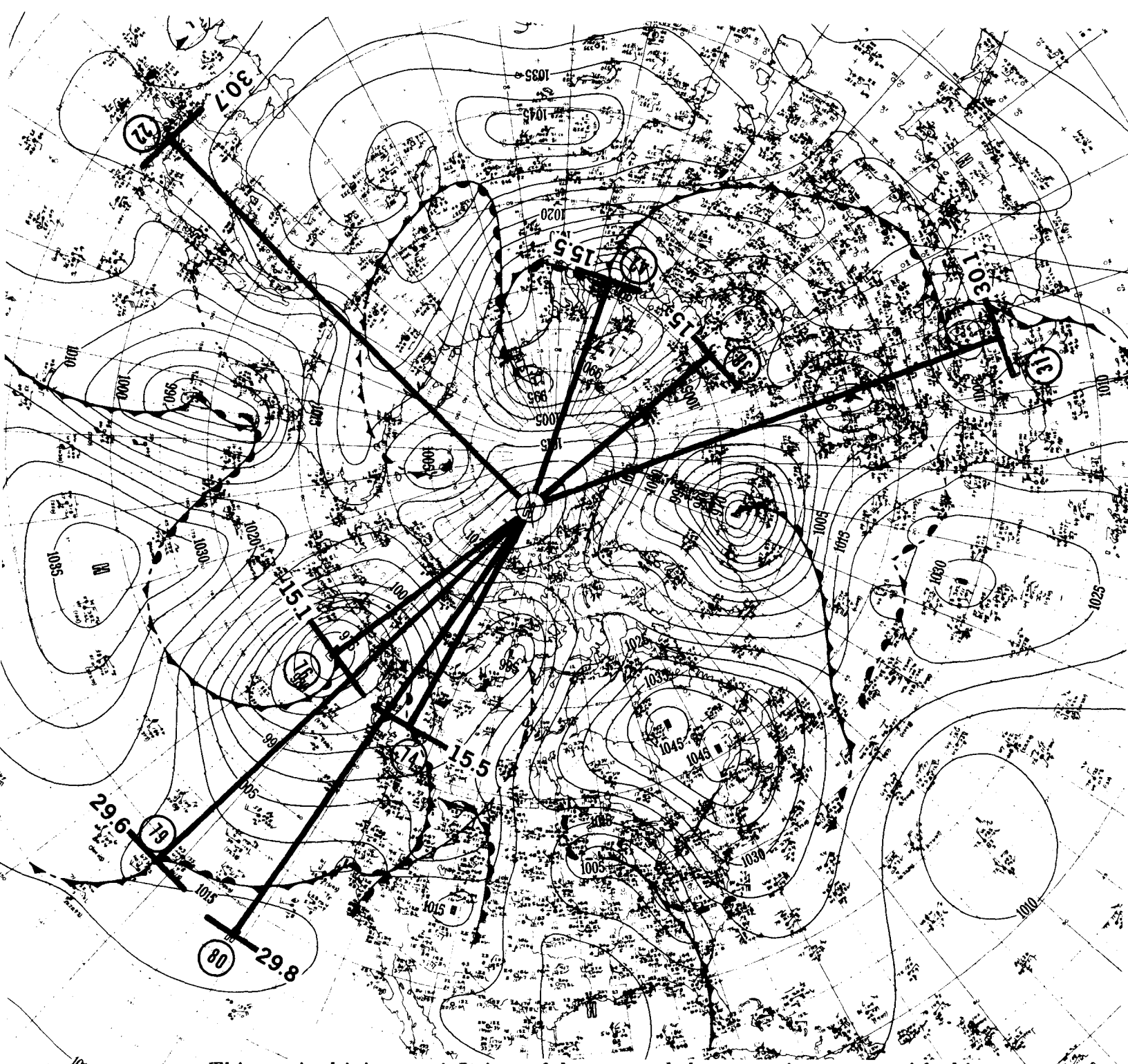




There are many fine symmetry features in this chart based on an LCD of 13 ru. First, we have the ring formed by the gang of four: #40 (13.2 ru), #59 (13 ru), #72 (12.9 ru), and #76 (13.3 ru). Second, we have a ring at approximately double the distance, which includes #15, #34, #93, #82, and #79. Third, #58 is exactly half the distance of #59; likewise, #72 is half the distance of #93; similarly #40 is one-third the distance of #9; and similarly #15 is two-thirds the distance of #7. Fourth, to seal this impressive display of regularity, we find that the angle between #76 and #59 adds up to 52.1 cu ($4 \times 13 = 52$); and the ray formed by #72 splits this angle into approximately two equal parts.

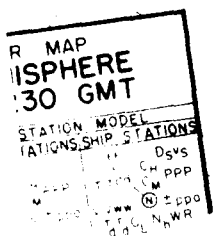


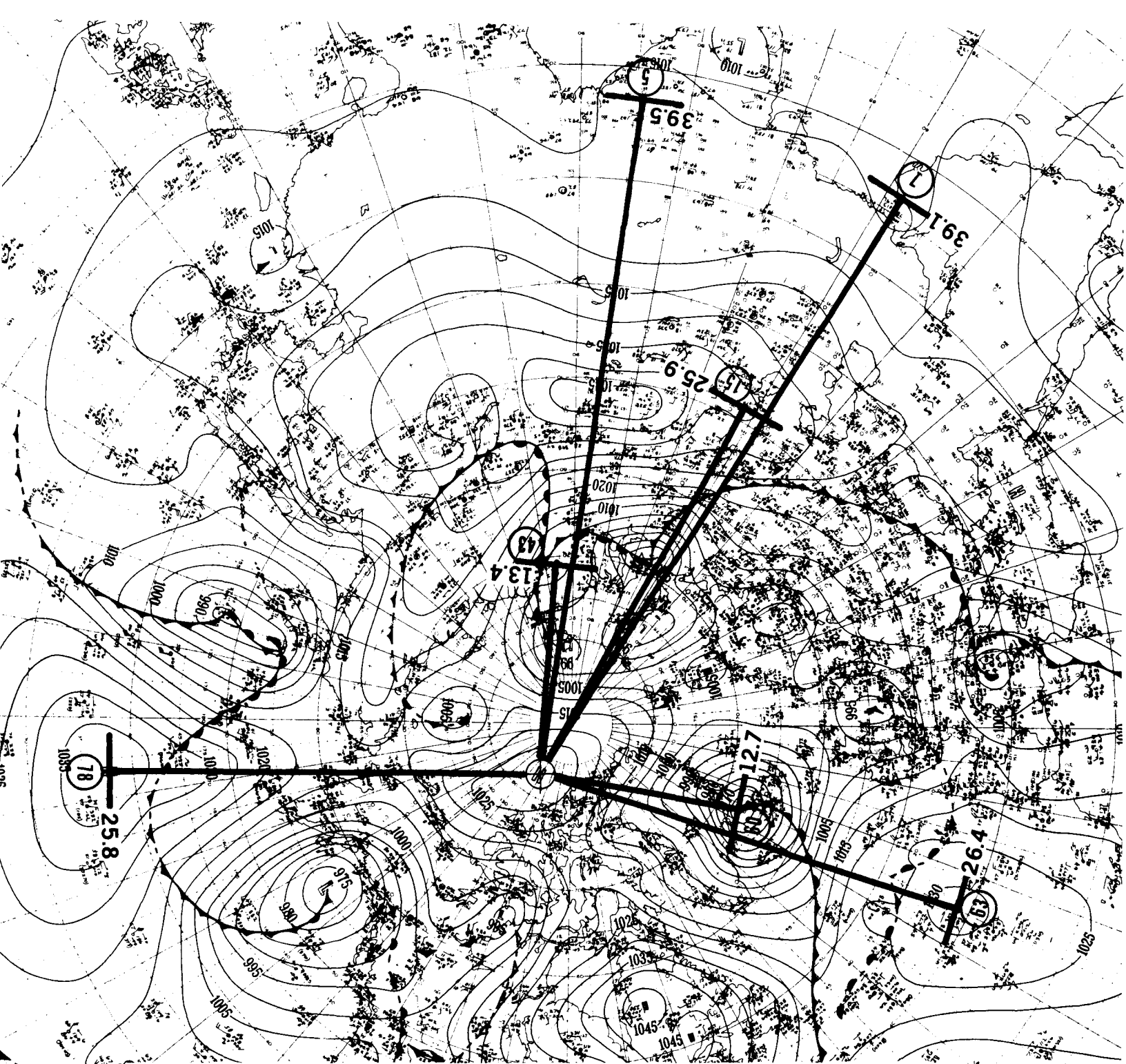
There are four striking features on this chart: first, #82 at 24.2 ru is in a nearly straight line with #17 at 24 ru, while the LCD of 8.1 ru for #45 hugs this line very closely; second, we have a substantial ring involving seven points with about 24 ru (45°); third, there is a secondary ringlet involving #90 and #30 at approximately 32 ru; fourth and last, we have 24.4 cu for the angle between #81 and #91—and 50 cu ($2 \times 24.4 = 48.8$) between #81 and #48.



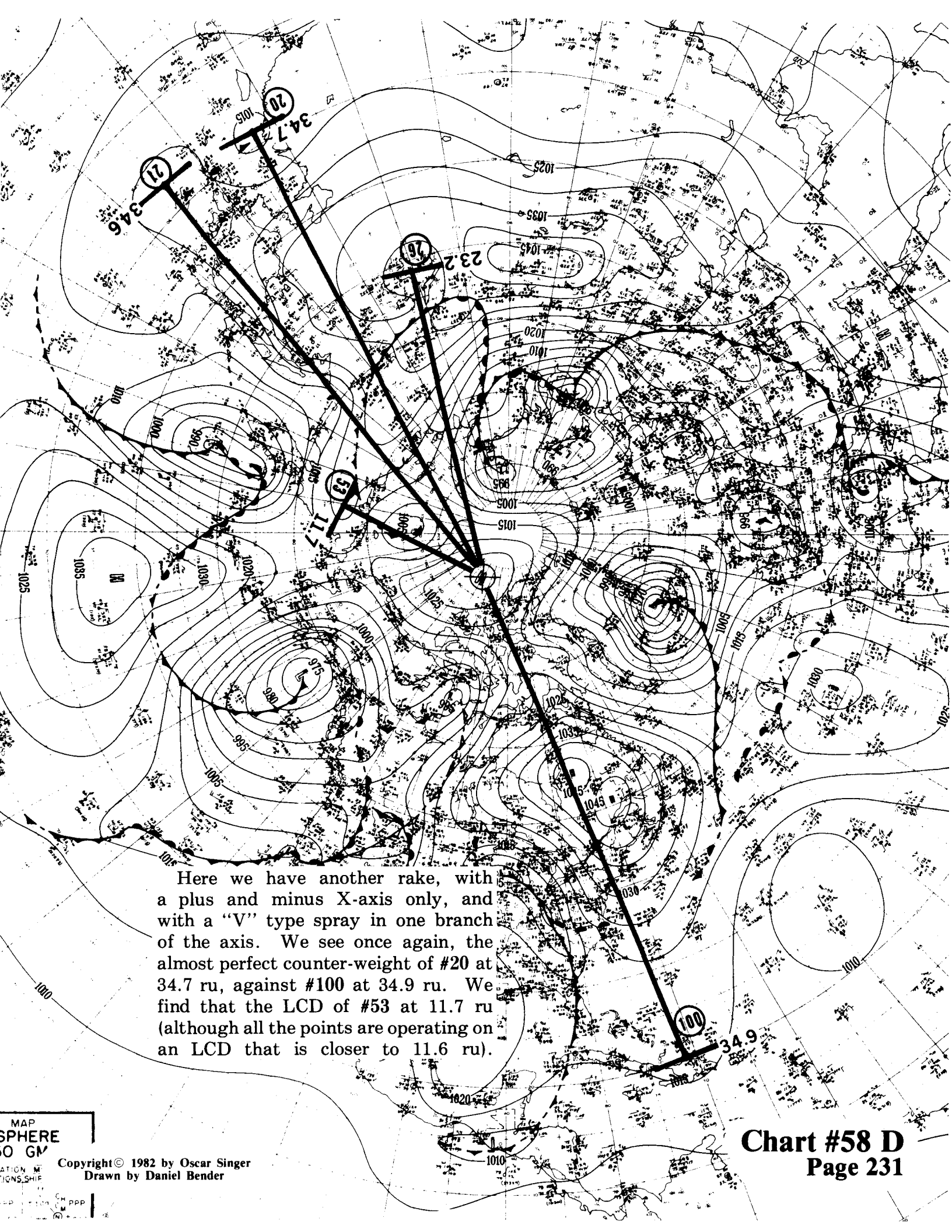
This one is shining star! It is useful to expand the two axis concept with this chart. If we consider the direction from #58 to #38 to be on the positive axis for X, then #79 would lie near the negative axis for X, while #22 would automatically be near the Y axis from #58 as the origin. Looking at this classic pattern, we see two "V" type patterns joining together to form an "X" type pattern. Looking again, we can see two "K" type patterns back to back. We can see that the "K", the "X", and the "V" patterns are actually vestigial portions of this two-axis array.

By inspection, we see essentially two rings—one at approximately 15 ru, and the other at 30 ru.

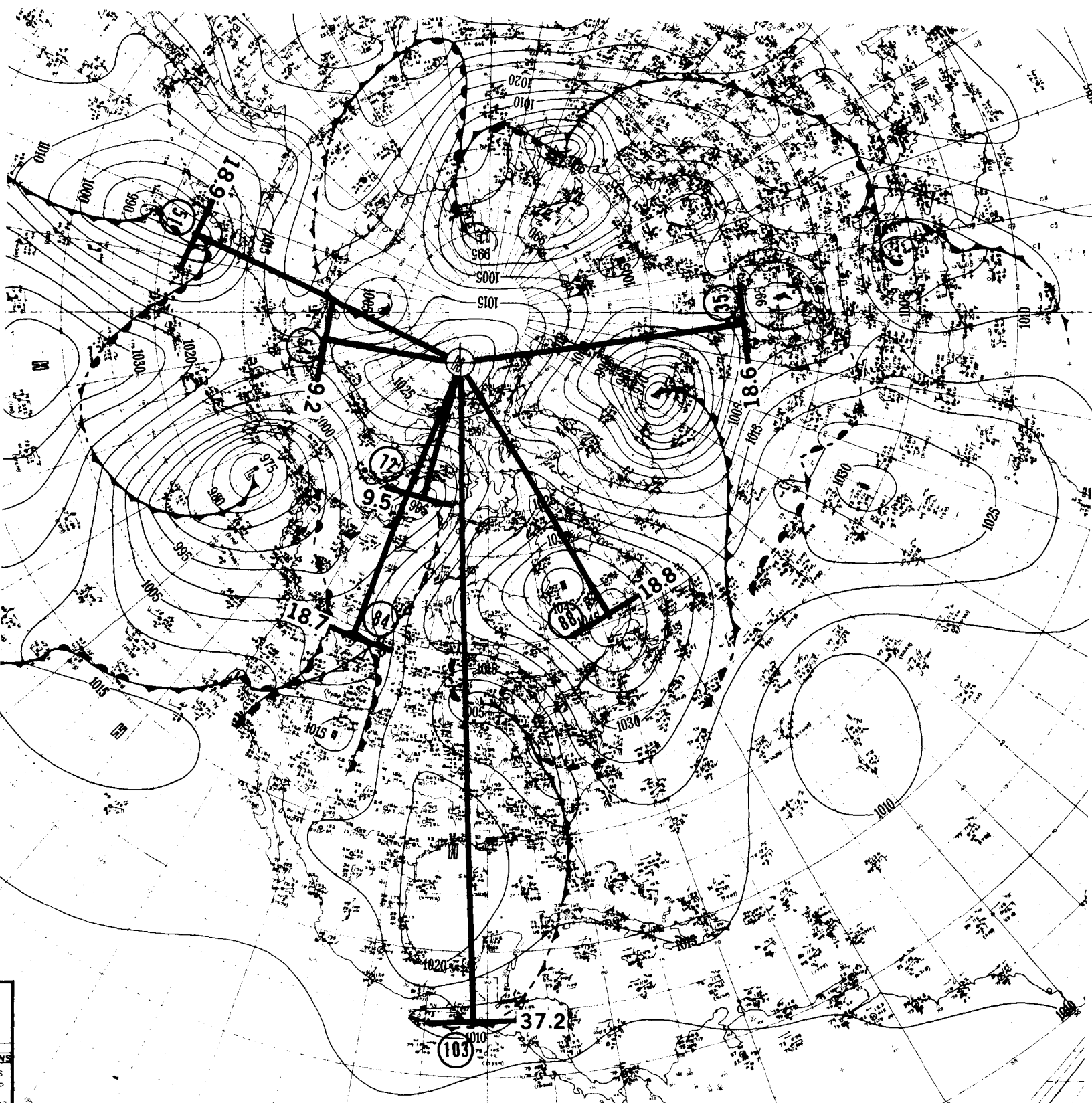




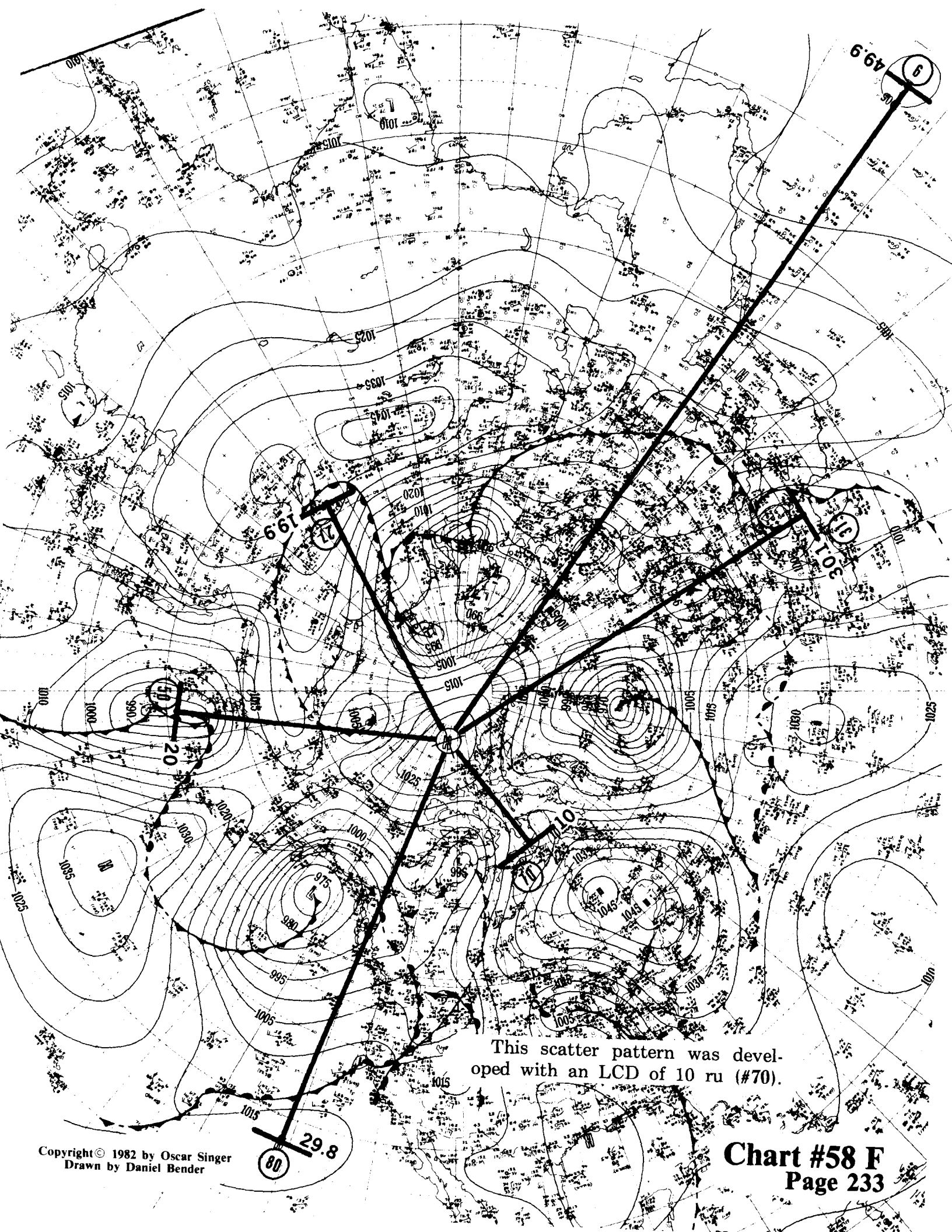
Here we have the two-axis pattern with a "V" type spray in the general direction of the +Y axis, which may be considered as lying along the ray to #5. The LCD is approximately 13 ru. We find that #63 is about twice as far out as #60; that #5 is approximately 3 times as far as #43; and that #15 is two-thirds of the distance of #7. When you take a position at the center of #58 you will see that all the shorter rays are approximately the same angle to the left of the nearest larger ray.



Here we have another rake, with a plus and minus X-axis only, and with a "V" type spray in one branch of the axis. We see once again, the almost perfect counter-weight of #20 at 34.7 ru, against #100 at 34.9 ru. We find that the LCD of #53 at 11.7 ru (although all the points are operating on an LCD that is closer to 11.6 ru).



Another two-axis pattern with a small spray on the -X axis and a wider "V" type spray on the -Y axis. We find an LCD at 9.35 ru, which is the average of 9.2 and 9.5 ru of #54 and #72. With the modified LCD, we get a nice ring at about 18.7 ru.



This scatter pattern was developed with an LCD of 10 ru (#70).

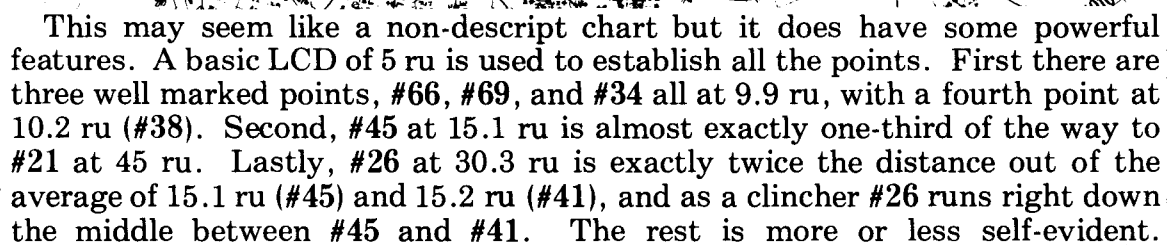
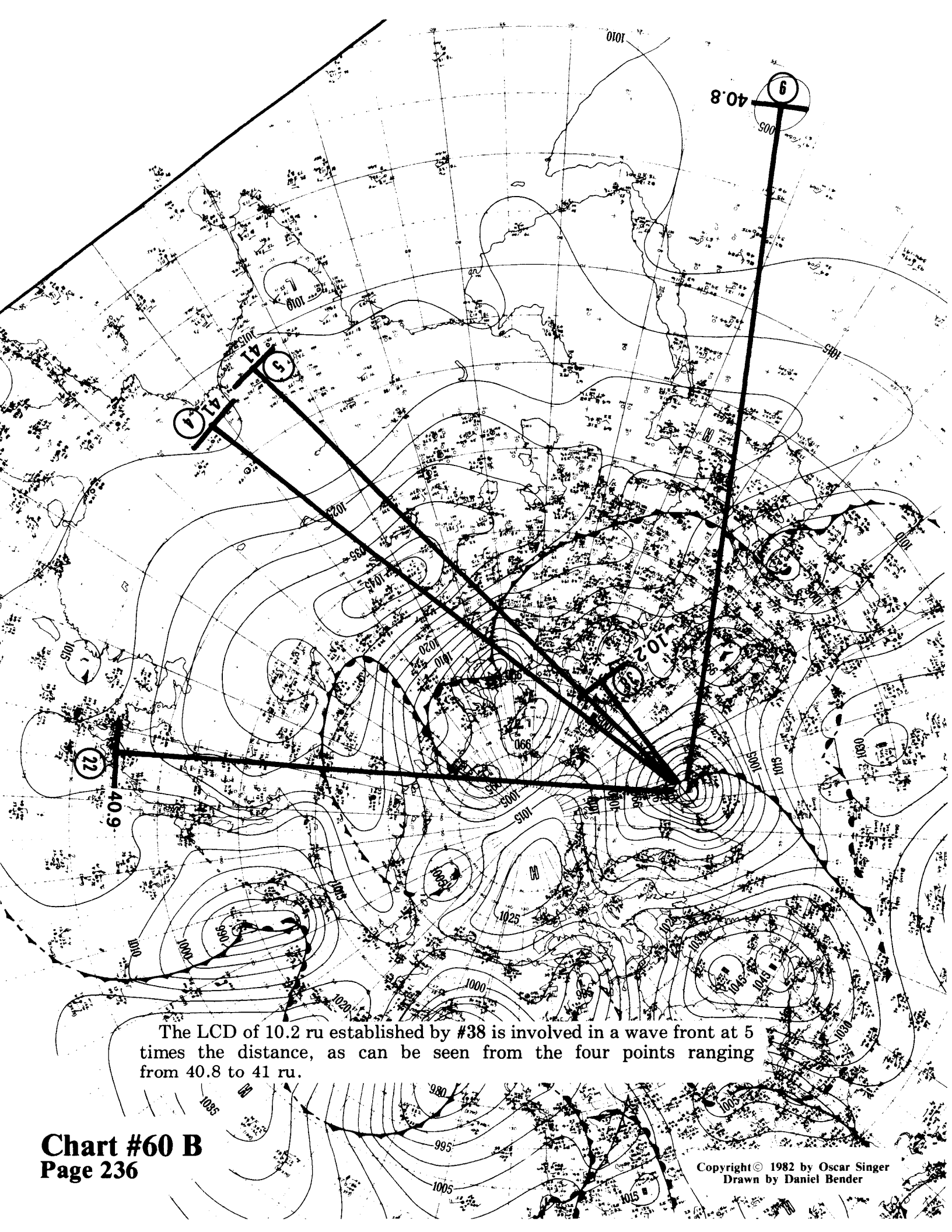
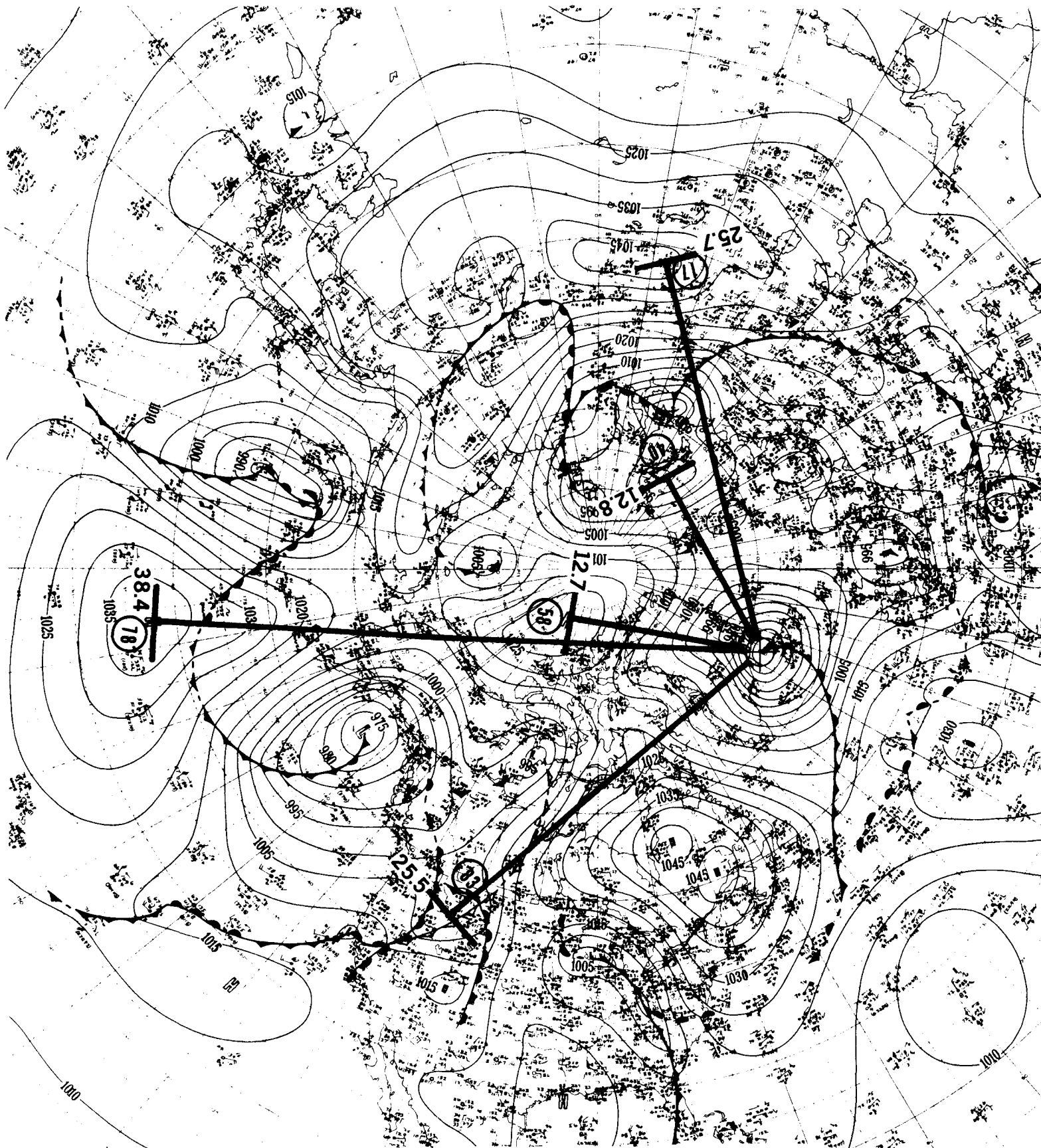


Chart #60 A
Page 235



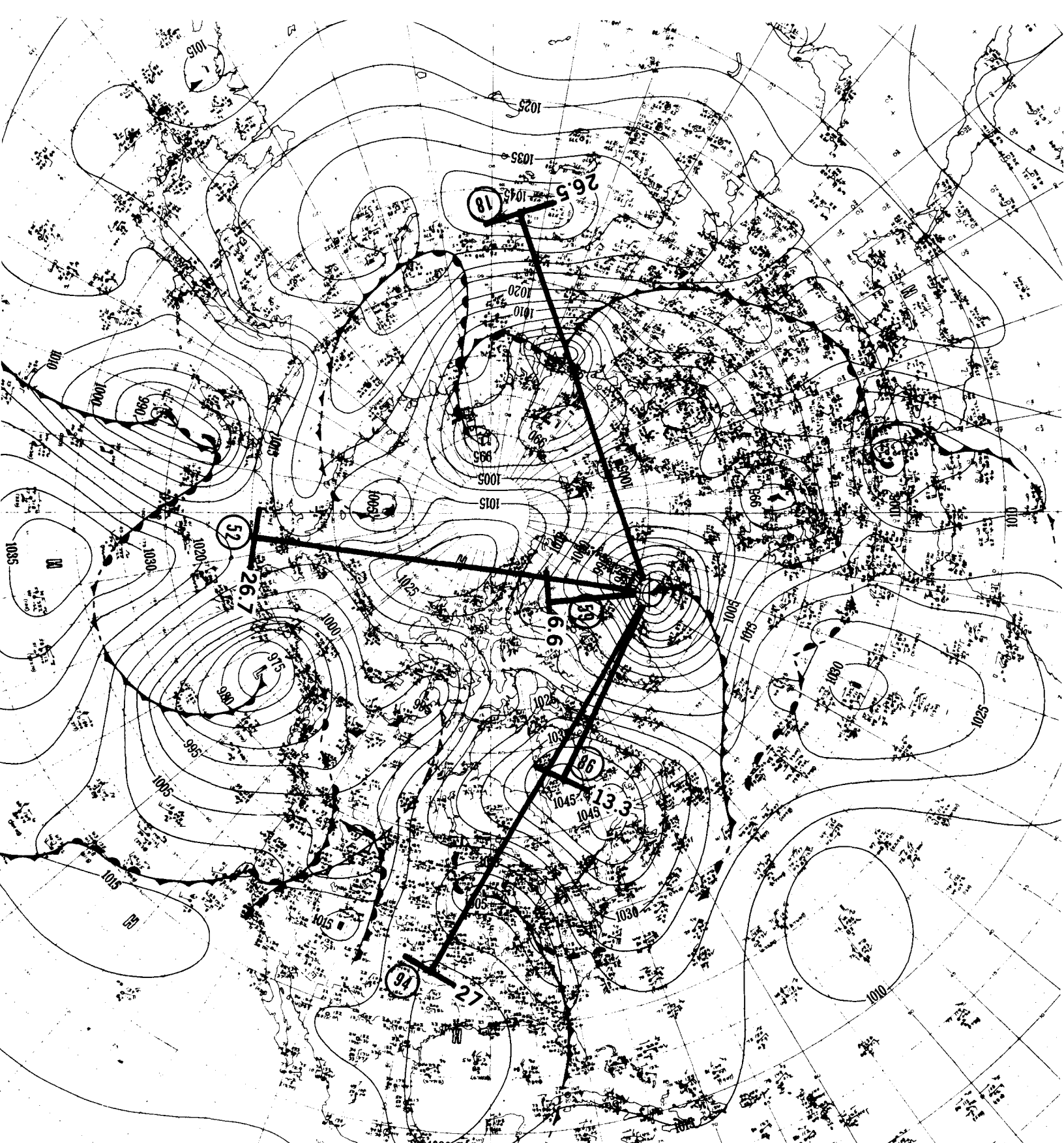


This is a simple pattern operating on an LCD of 12.8 ru.

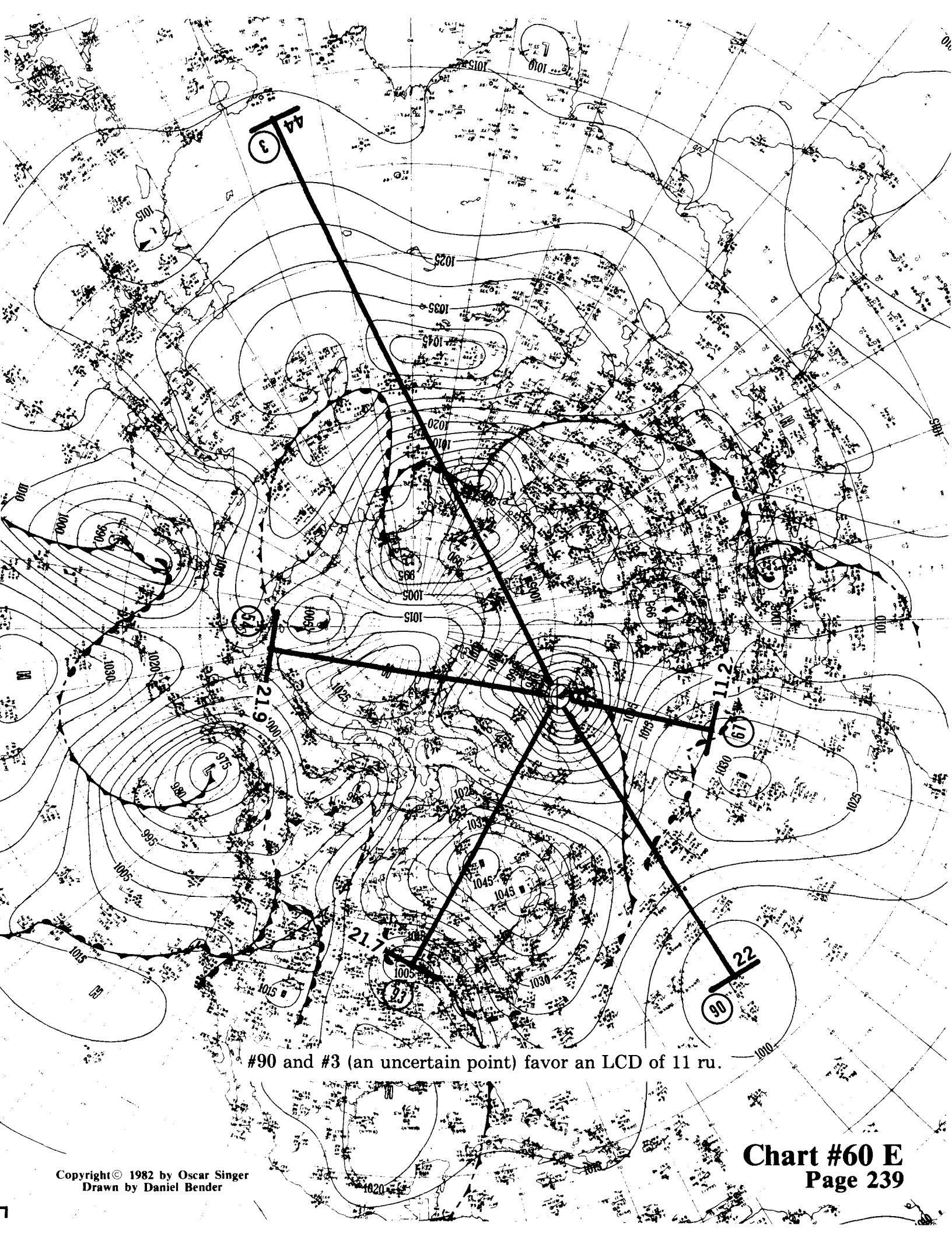
R MAP
ISPHERE
30 GMT

Copyright© 1982 by Oscar Singer
Drawn by Daniel Bender

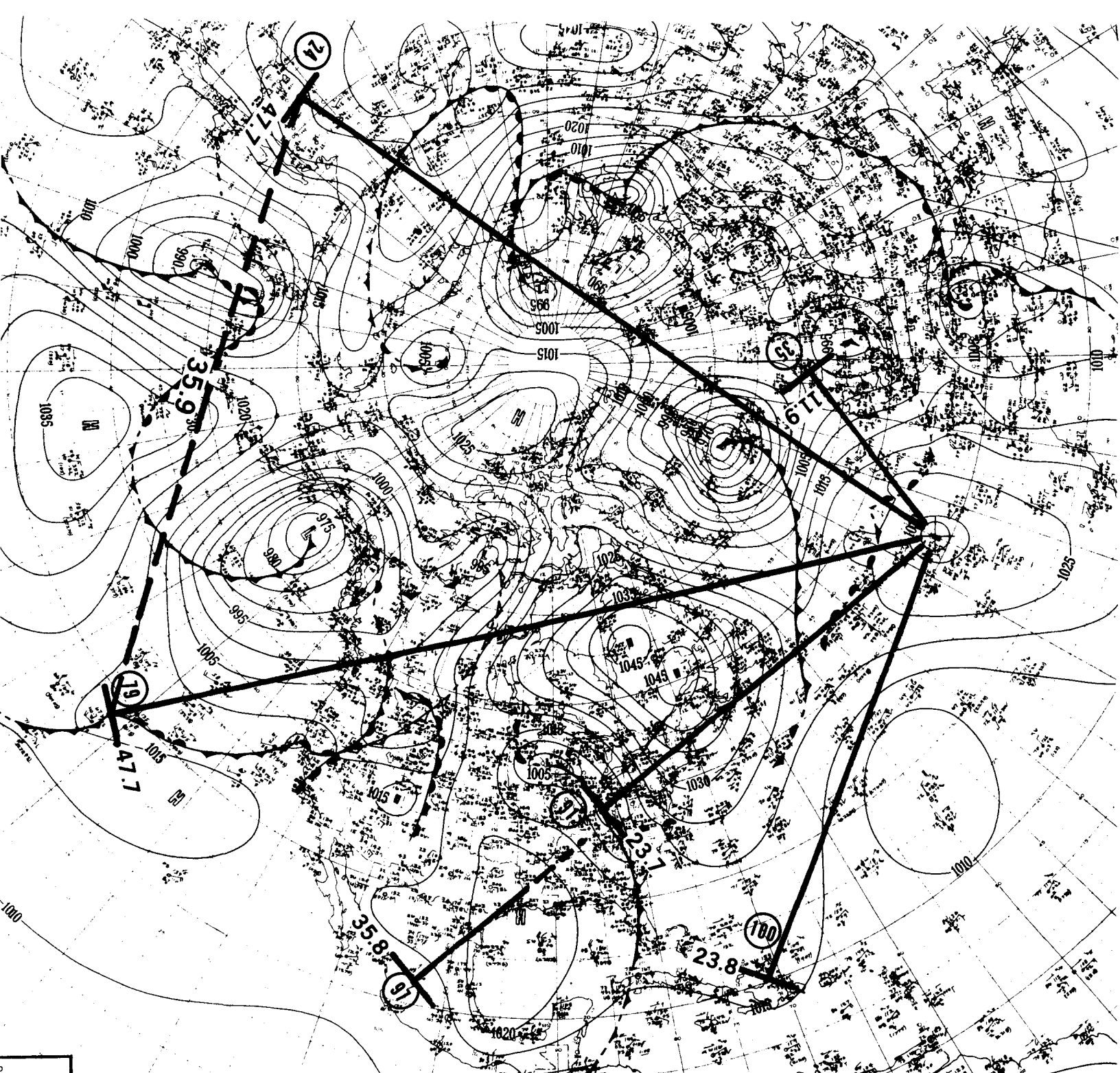
Chart #60 C
Page 237



This chart has good visual symmetry if you believe in the accuracy of #94. All the other points are acceptable with an LCD of 6.6 ru.

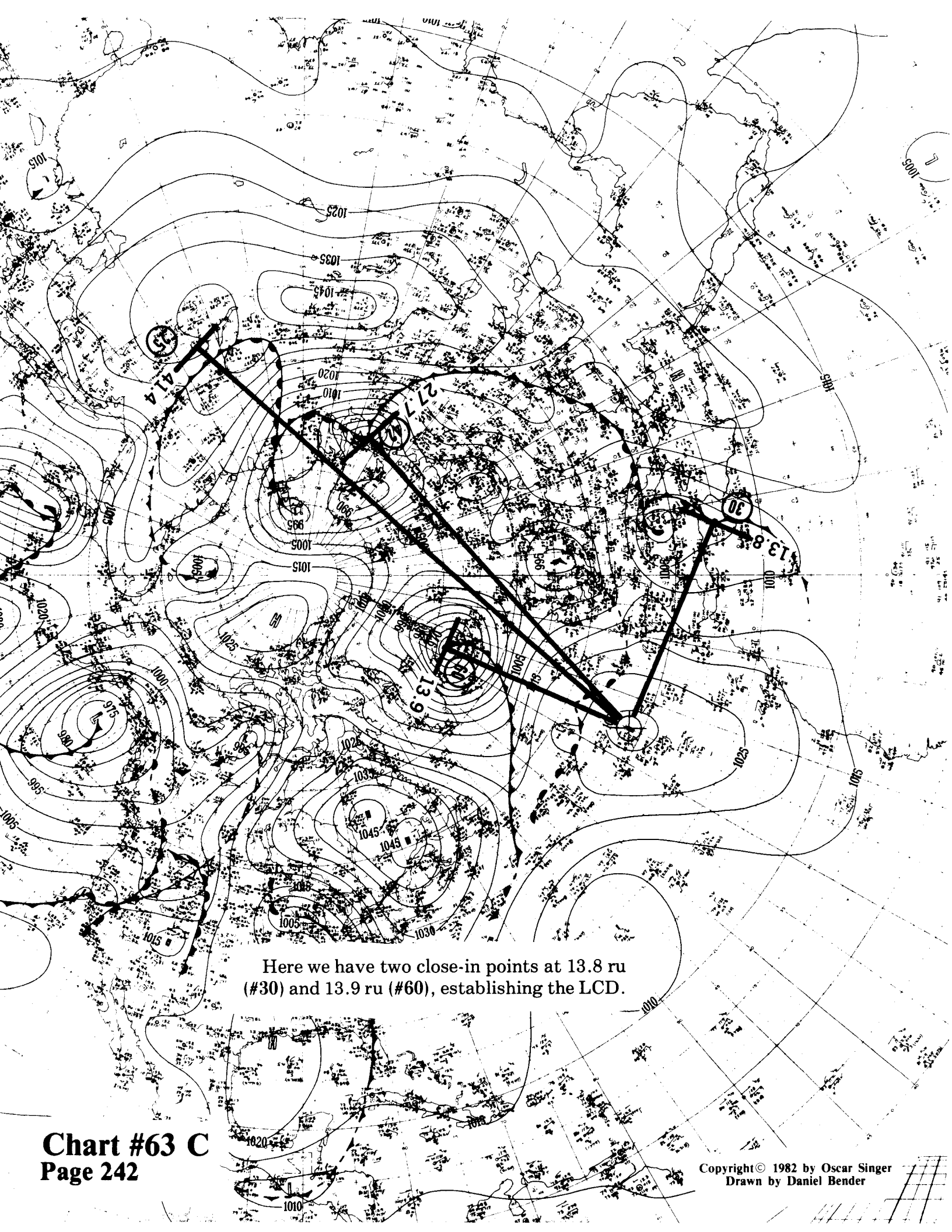


#90 and #3 (an uncertain point) favor an LCD of 11 ru.



HERE
 GMT
 MODEL
 SHIP STATIONS
 DSVS
 CH PPP
 CM
 WW © PPO
 NWR
 SS h
 NAME OR (BAR NO)

In this one we have an accurate LCD of 11.9 ru. We see that #91 (23.7 ru) is two-thirds of the distance of #97 (35.8 ru). The triangle formed by #24, #63, and #79 has sides in the ratio of 4:4:3. The fact that #79 and #24 are separated by 35.9 ru, which is quite closely divisible by the LCD for this pattern, seems to confirm both the existence and the accuracy of the location of the seemingly obscure and questionable #24. Perhaps #24 is not such a dismal choice for a point, since it is associated with a definite bend of the isobars in the immediate vicinity, indicating some disturbance. No incident, whether large or small, can be ignored by the points in the rest of the world—they must accommodate everyone and still conform to the laws of mechanics and symmetry.

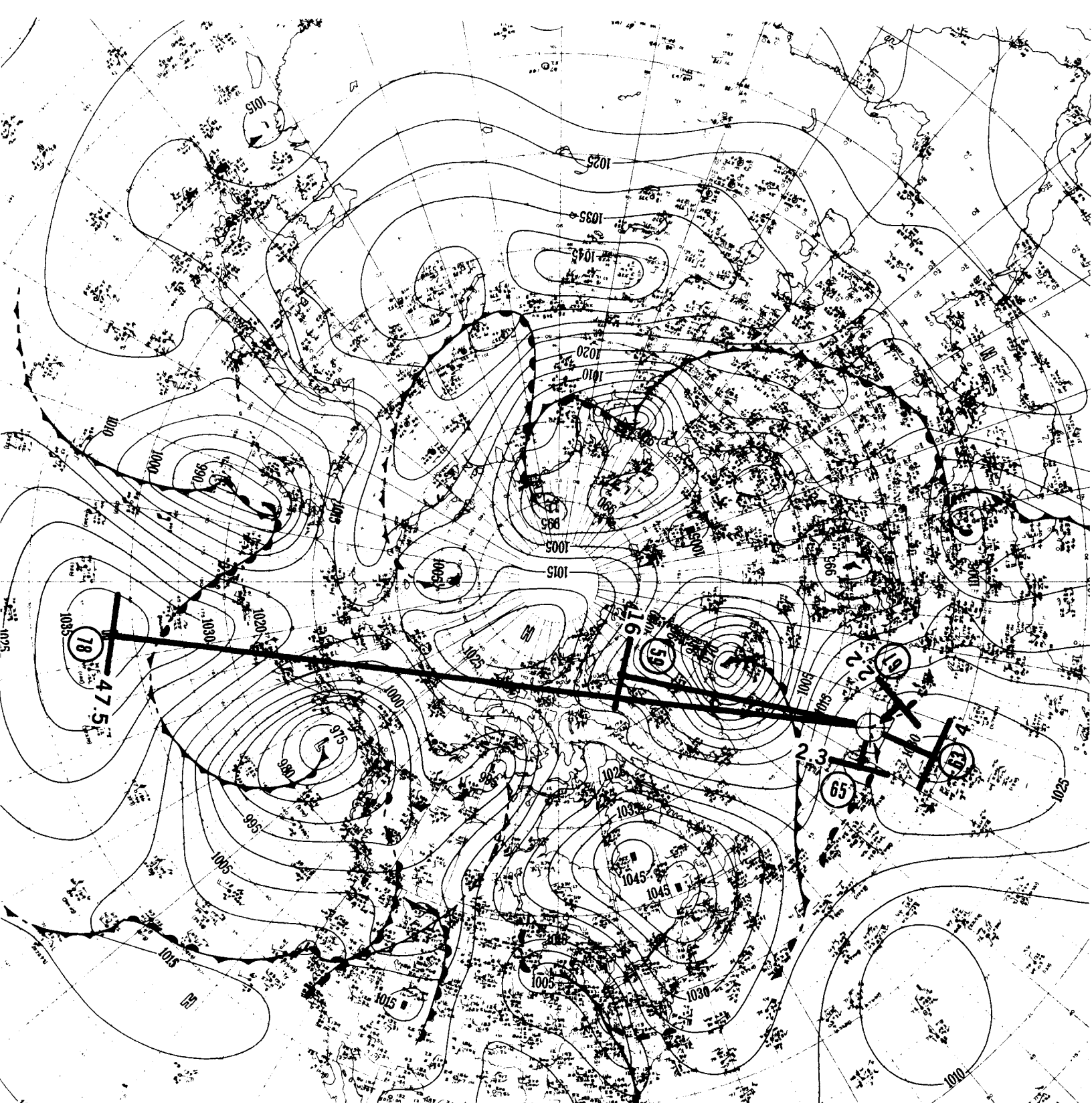


Here we have two close-in points at 13.8 ru (#30) and 13.9 ru (#60), establishing the LCD.

There are three separate patterns (with separate LCDs) on this chart. The first starts with #87 (17.4 ru), which is linked to #96 (35 ru) and #9 (34.6 ru). The second starts with #88 (16.5 ru), which is linked to #82 (33.5 ru). The last one starts with #71 (23 ru), which is linked to #50 (46.4 ru).

9
34.6

Chart #63 D
Page 243



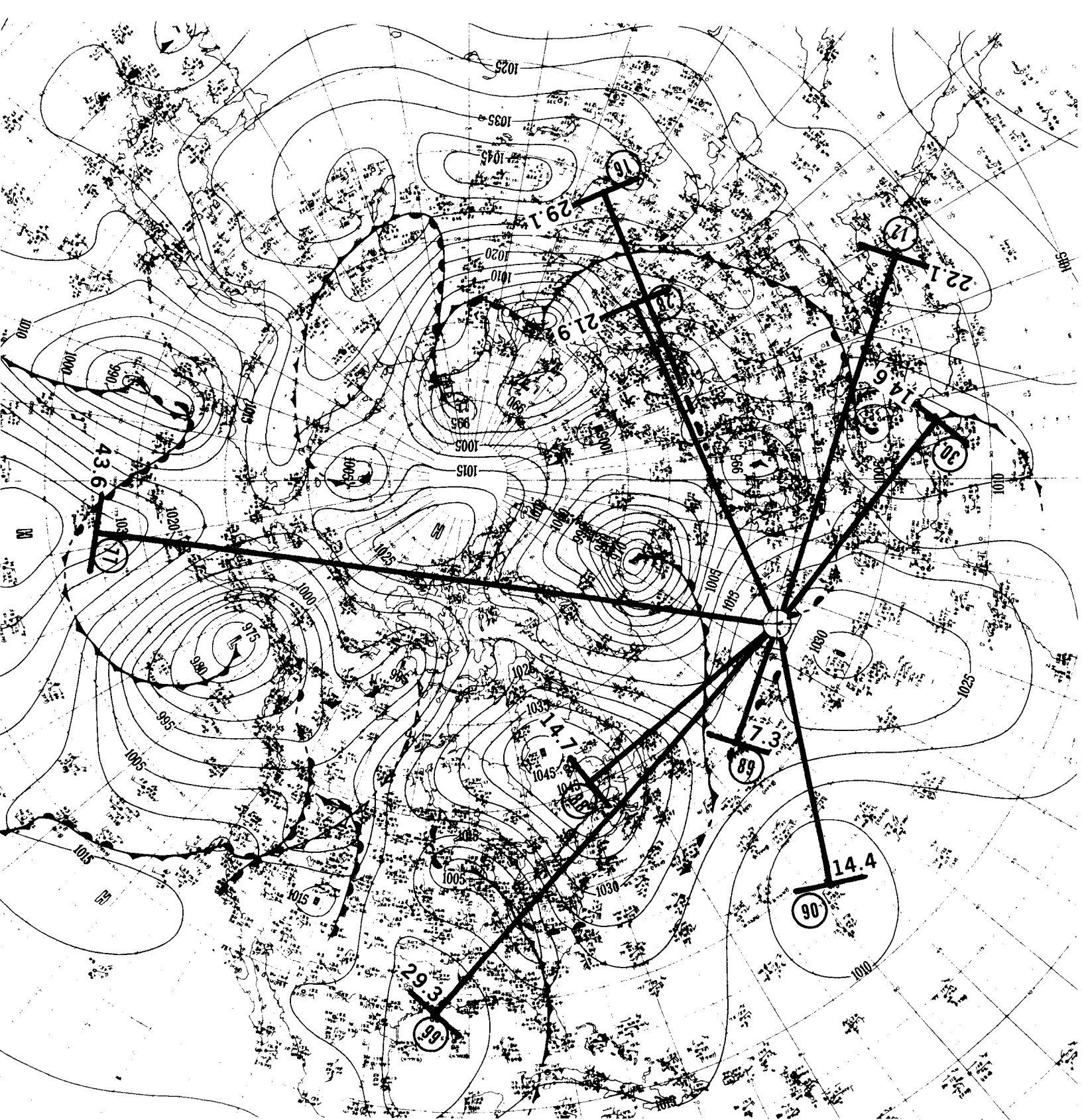
This one has two separate parts. First we have the nearly equal spacing of #65 (2.3 ru) and #67 (2.2 ru). Second, we have #63 at 4 ru with #59 at 16 ru (another seemingly obscure point) at exactly four times the distance, and finally, #78 (47.5 ru) approximately three times 16 ru.

AP
HERE
GMT
N. MOF
SHIP

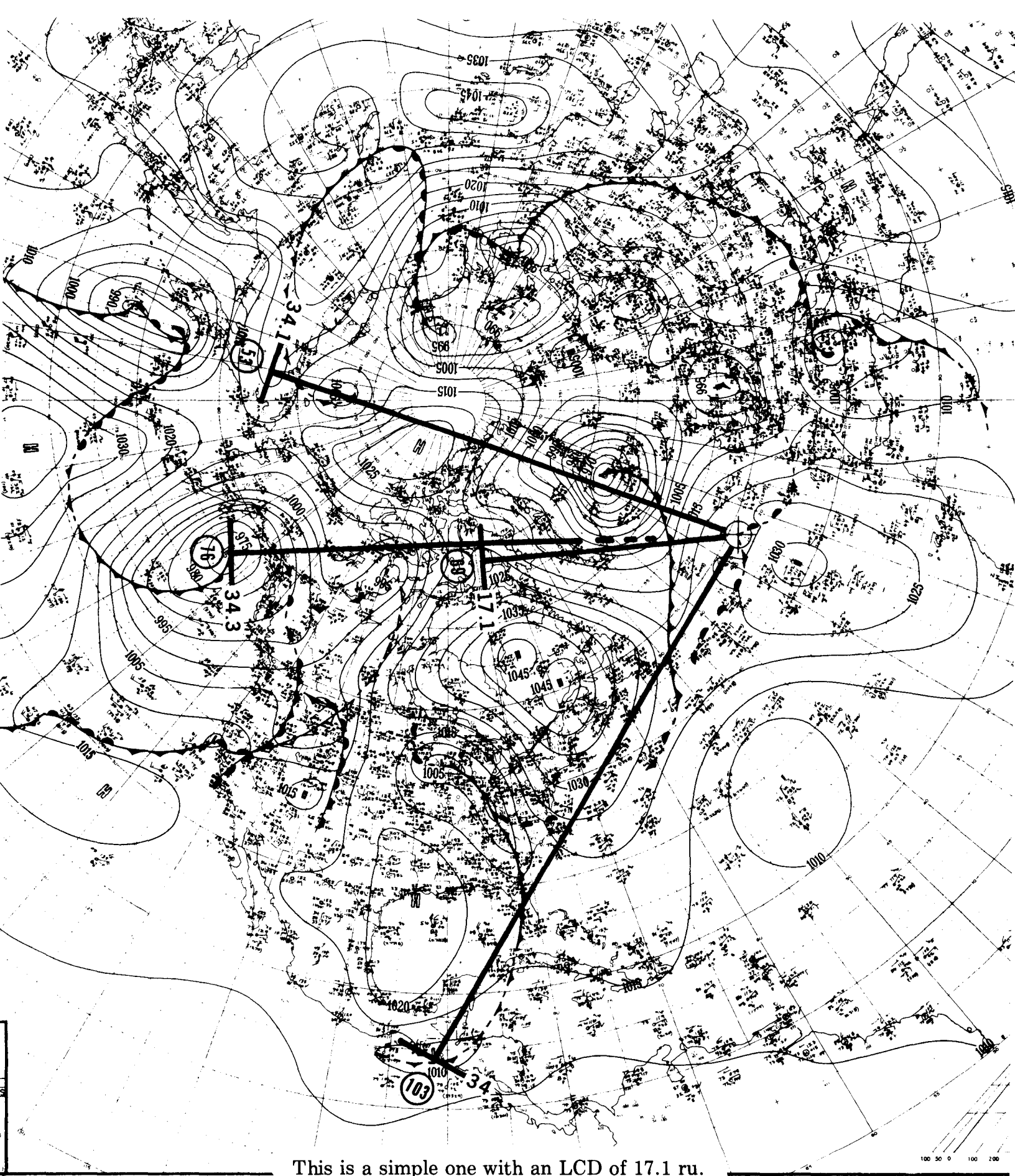
Chart #66 A
Page 244

Copyright © 1982 by Oscar Singer
Drawn by Daniel Bender

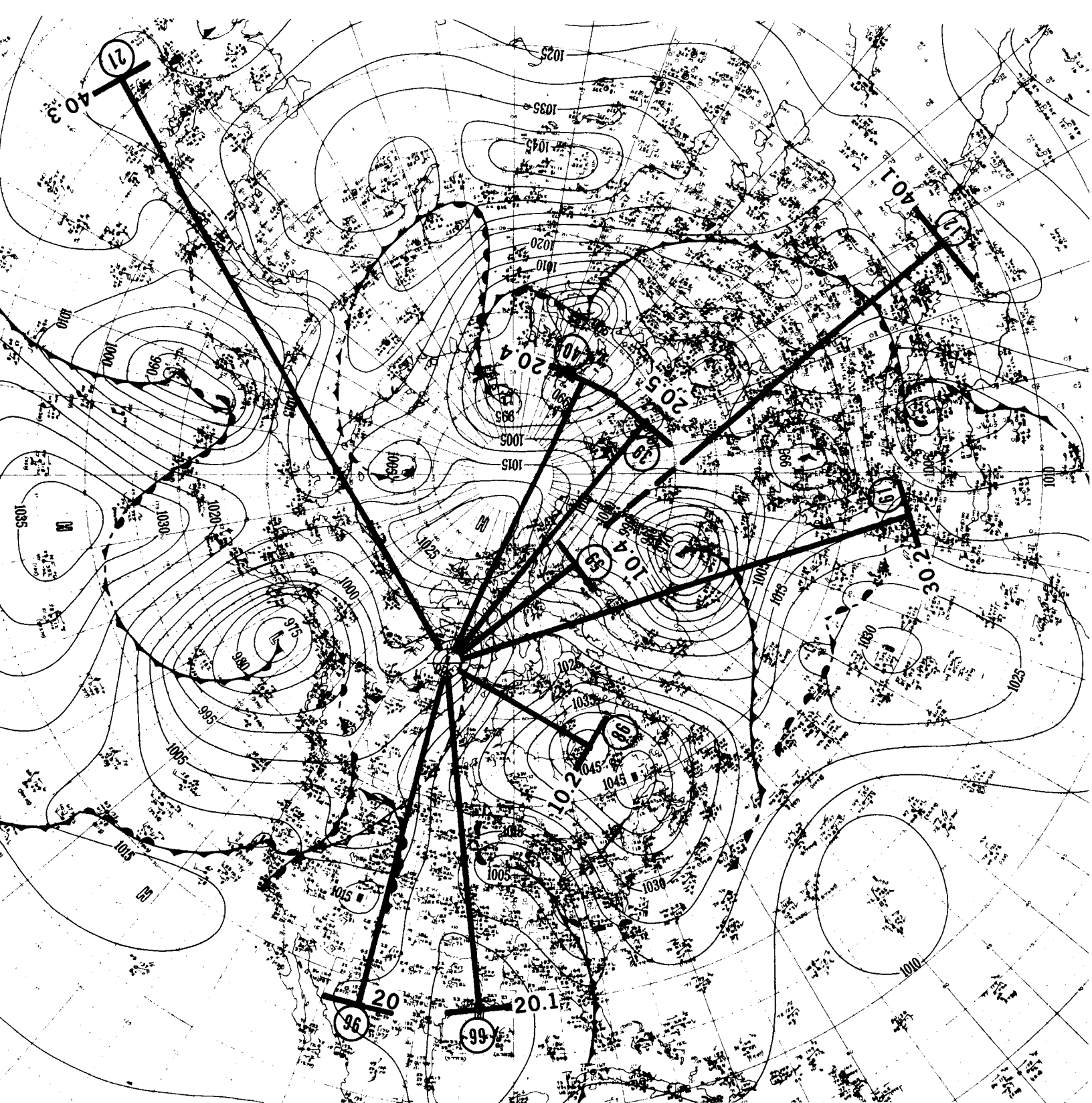
A simple gem. Four points divided into two separate pairs with symmetrical angles between each pair of rays. The distance between #52 and #9 is 60.5 ru, which is approximately divisible by 12 ru (the common LCD).



Here we have another classical two-axis formation with an LCD of 7.3 ru. We can consider the + X axis lying along #12, and the - X axis lying along #89, with #77 at 43.6 ru ($6 \times 7.3 = 43.8$) near the + Y axis. There is an obvious visual symmetry in the rays below the X axis and in a similar manner for the rays above the X axis.

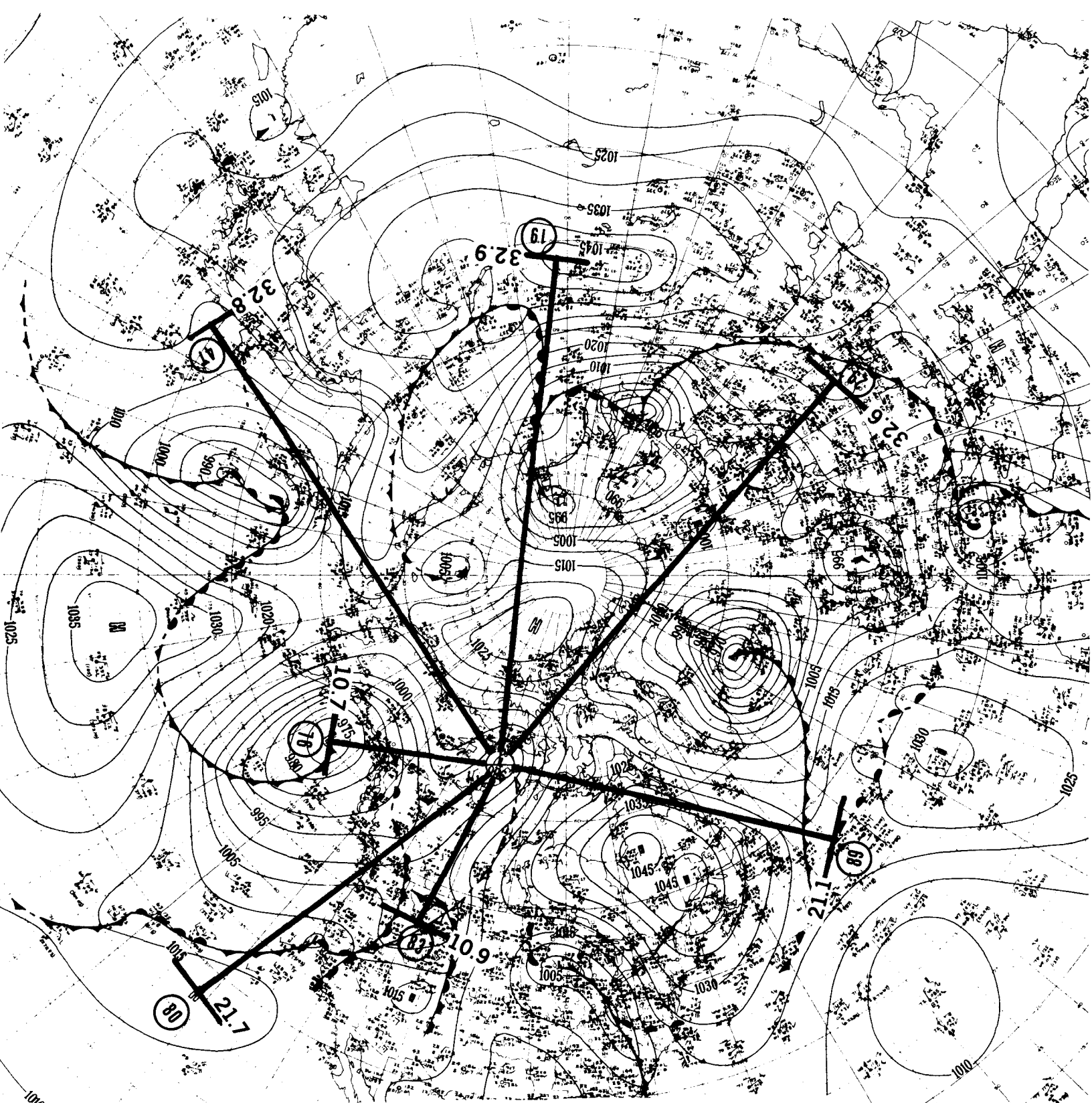


This is a simple one with an LCD of 17.1 ru.



This chart can be interpreted as follows: First, a baseline is established by #40 at 20.4 ru across from #96 at 20 ru. Second, we have #39 at 20.5 ru on one side of the baseline, and #99 symmetrically placed at 20.1 ru on the same side. Lastly, we have #86 at 10.2 ru, which is the approximate LCD for this group. Note that this cluster is fairly close-in and has well-defined locations for the centers of the points. All the other points factor out with an LCD of 10 or 10.1 ru.

ATIONS
Dsys
M ppp
M
D zpp
N, WR,
BAR NO



This one is for general interest only since it has a number of obscure points. The LCD varies between 10.7 and 10.9 ru.

MAP
HERE
GMT
ON MODE
NSHIP 5

Copyright © 1982 by Oscar Singer
Drawn by Daniel Bender

Chart #72 B
Page 249

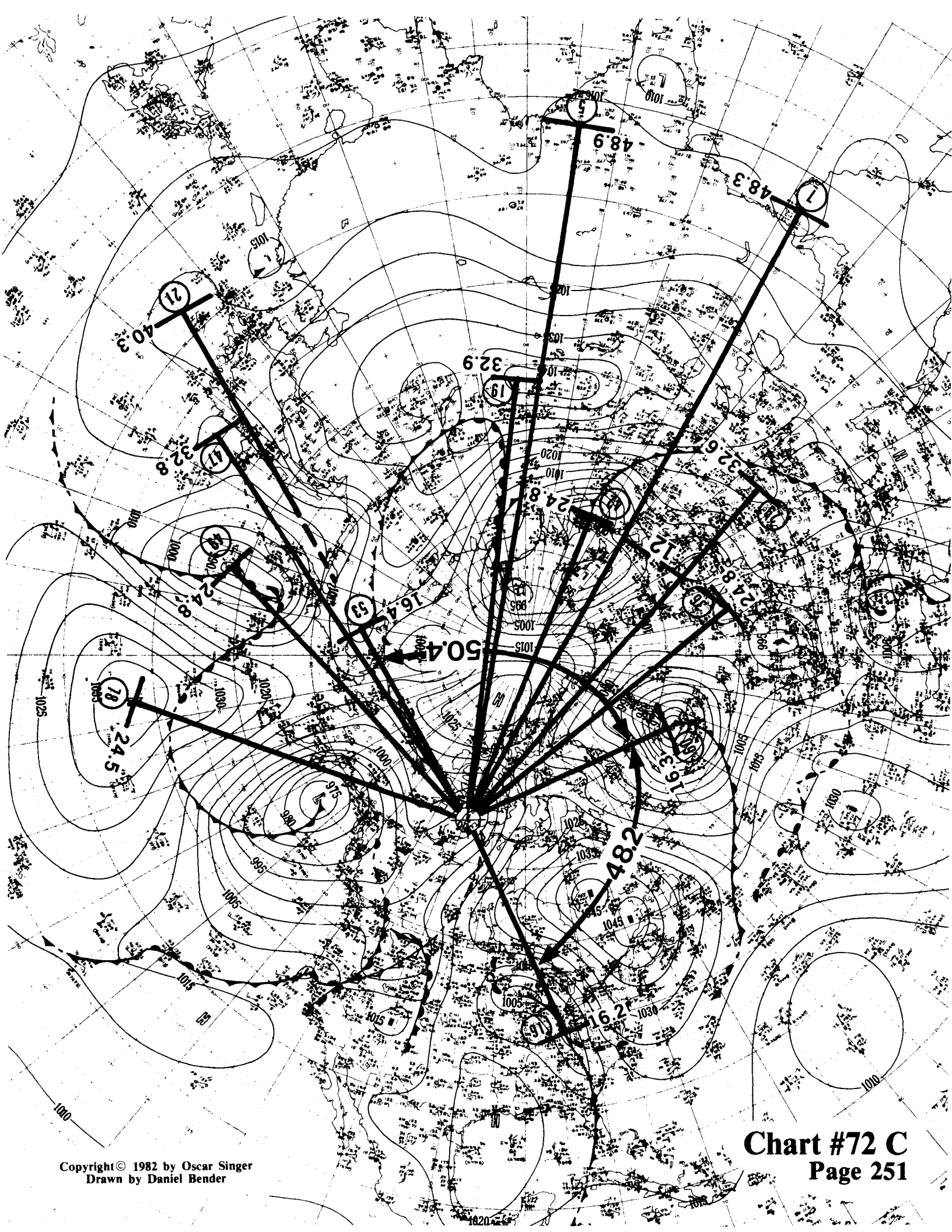
© 1982
WR
S

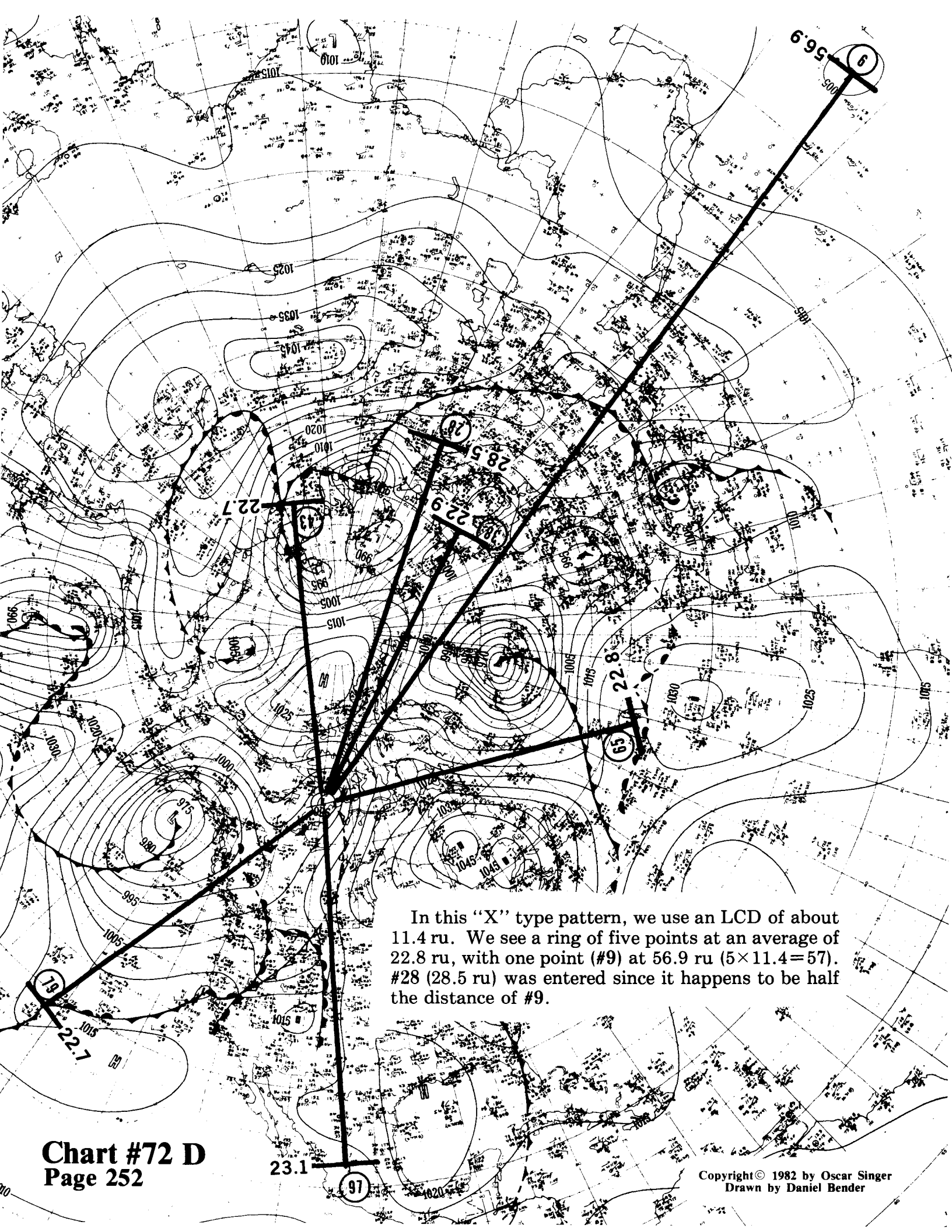
Chart #72 C

This rake is a zinger. Let us consider that #53 (16.4 ru) or #21 (40.3 ru) is close to the -X axis; let #91 (16.2 ru) be the +X axis; and let #60 (16.3 ru) be the +Y axis. Next we see a classical, close in, ring of points at approximately 16.3 ru. We now note (1) the angle of 48.2 cu between #60 and #91 is almost three times their distance from #72, and (2) the great circle distance from #60 to #53 is 24.2 ru (not entered on this chart to reduce clutter).

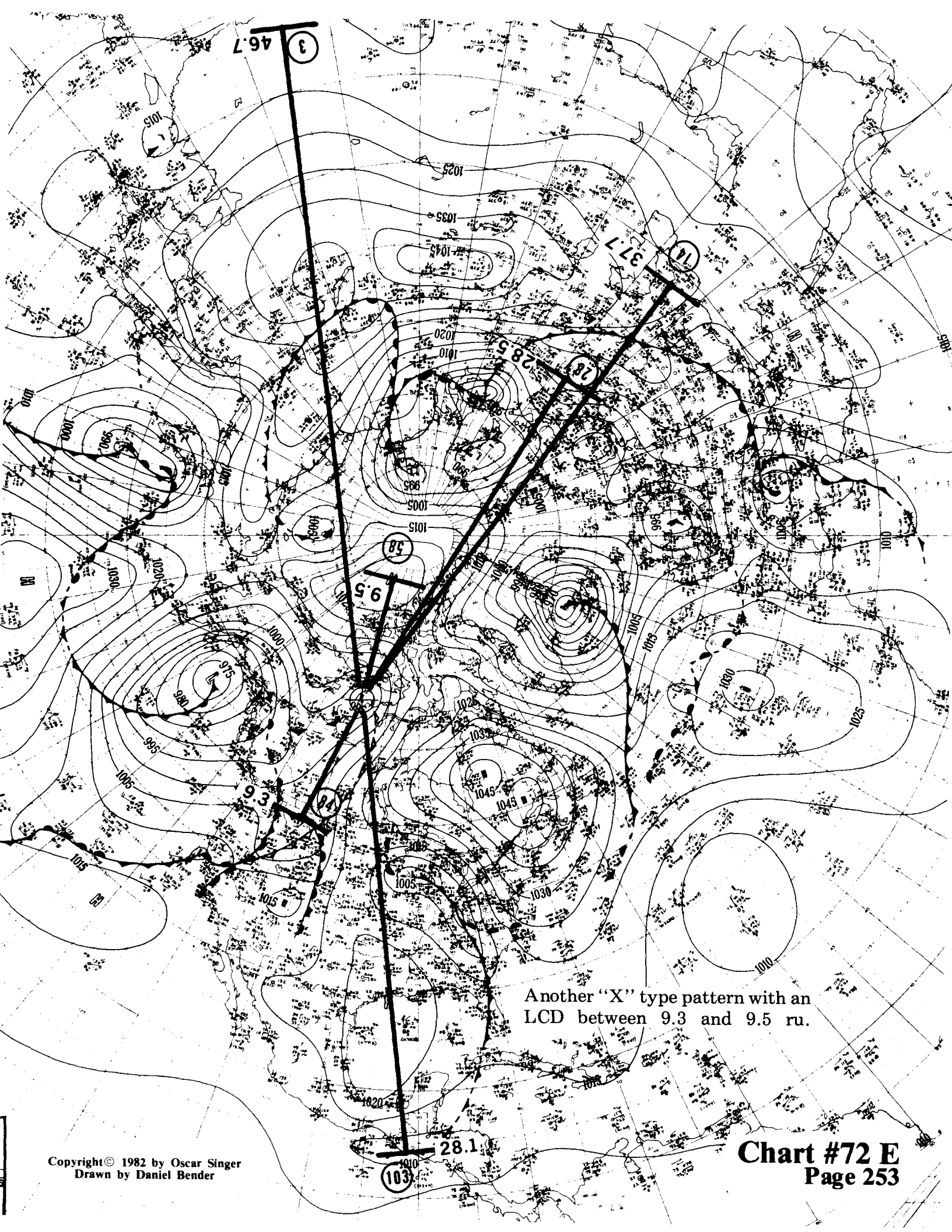
If you haven't guessed by now, we are using an LCD of 8.1 to 8.2 ru. We now move out to the ring or wavefront in the neighborhood of 24 ru. We see three points (#36, #42, and #49) at 24.8 ru and one at 24.5 ru (#78). Upon further inspection, we see that they are grouped into two pairs. #36 of one pair is tilted a certain angle to the left of the +Y axis, and we find that #49 of the second pair is tilted below the -X axis by the same amount. We see, therefore, that this cluster of four points has a rotational symmetry with respect to the axes. In addition, the great circle distance between #42 and #36 is a neat 12 ru.

We now move out a little farther and find three points (#47, #19, and #29), fairly evenly spaced at 32.8, 32.9, and 32.6 ru. Farther still, we find #21 at 40.3 ru. At this time, we run into another point that I have not labeled due to general uncertainty, but there is no doubt that it is there. This point lies along the ray line of #5 and is halfway between #19 and #5. This would give us a value of about 40 ru, which would naturally be another ray at the 40 ru range on this chart. The change in curvature of the isobars and the great spacing between the isobars leave more than enough room for another point. Finally, as far out as we can go on this map, we find the ringlet at 48.3 and 48.9 ru.

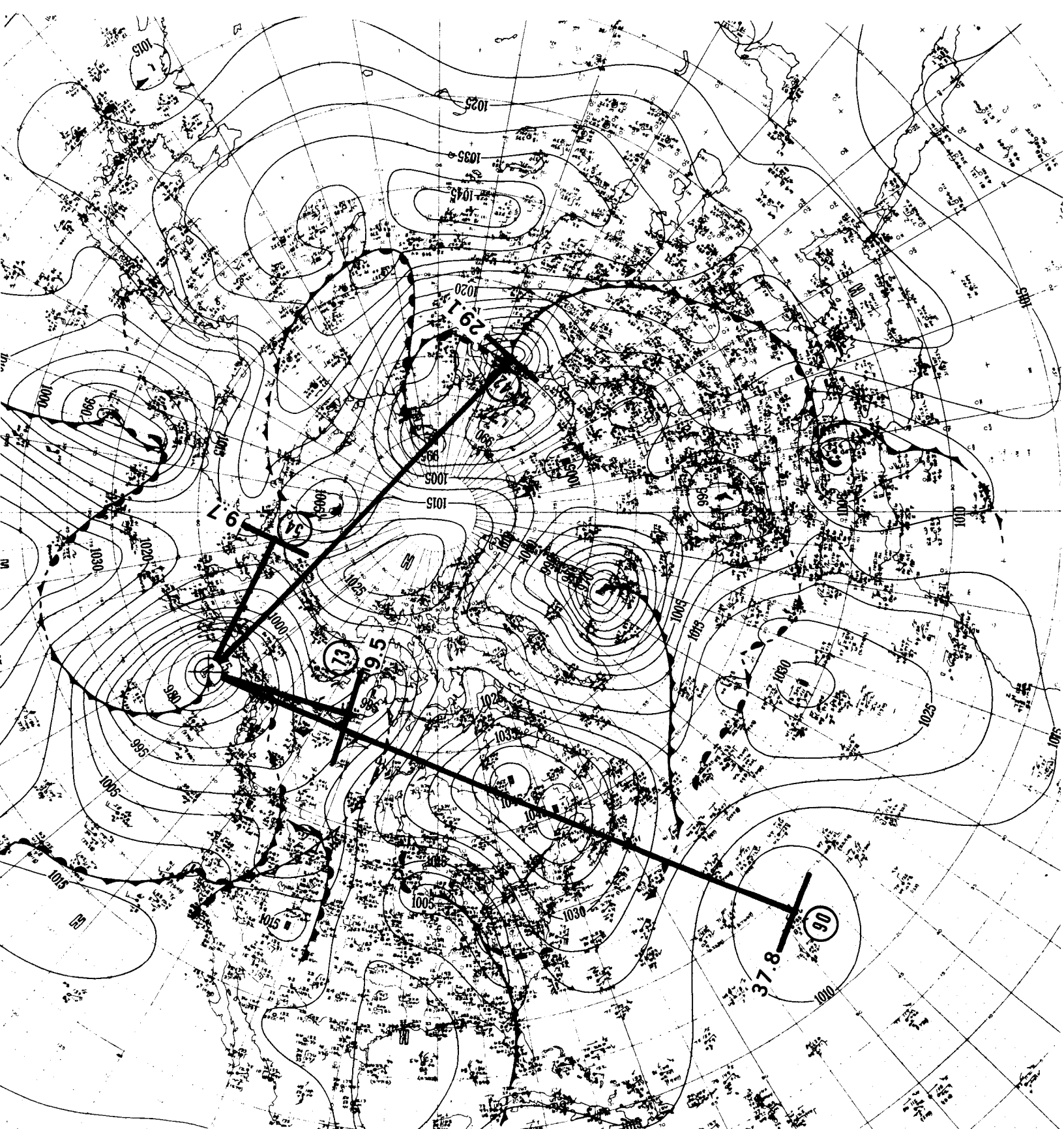




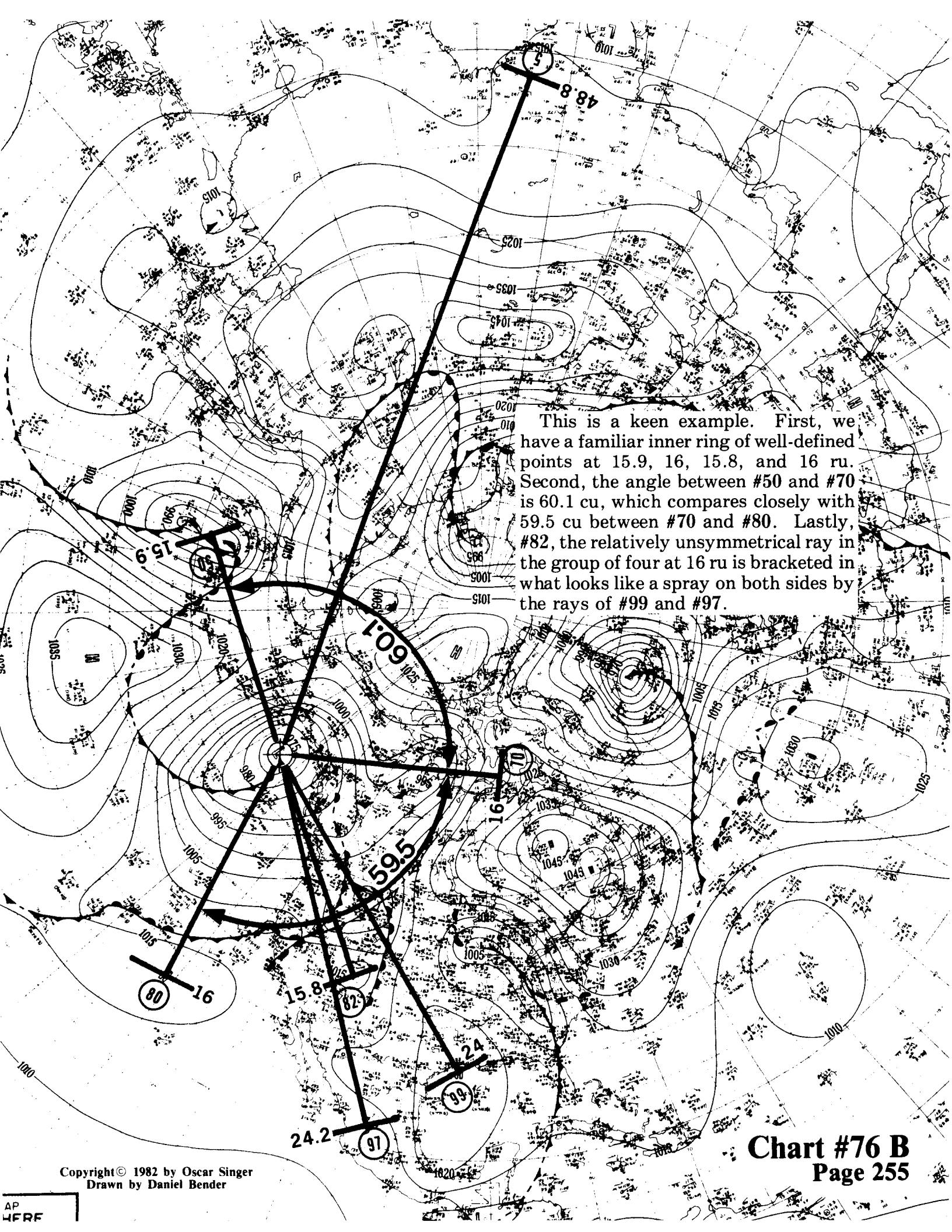
In this "X" type pattern, we use an LCD of about 11.4 ru. We see a ring of five points at an average of 22.8 ru, with one point (#9) at 56.9 ru ($5 \times 11.4 = 57$). #28 (28.5 ru) was entered since it happens to be half the distance of #9.



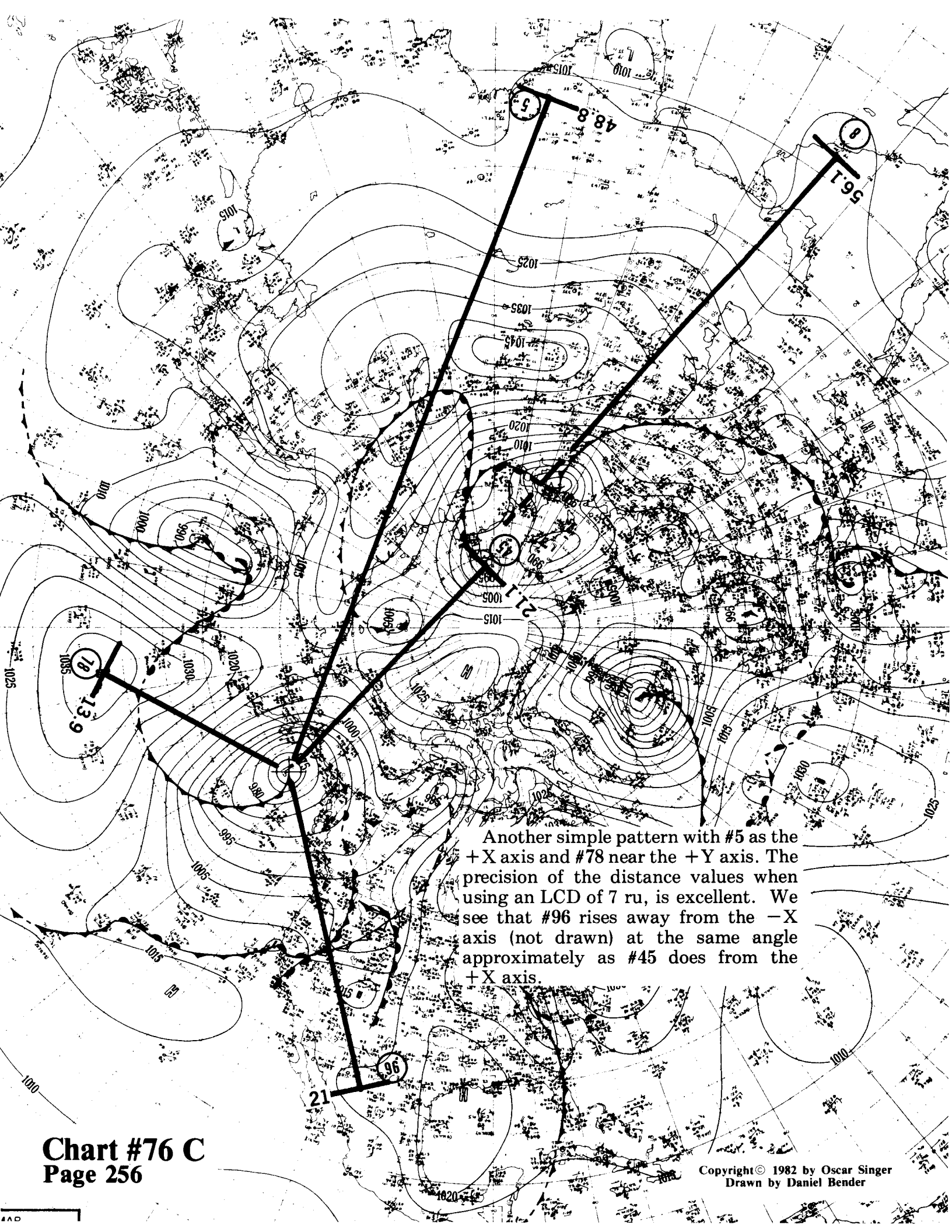
Another "X" type pattern with an LCD between 9.3 and 9.5 ru.



A simple "V" type formation. Here the LCD of 9.7 ru (#54) matches perfectly with #42 at 29.1 ru (3×9.7). On the other leg of "V", the LCD of 9.5 ru at #73 matches closely to #90 at 37.8 ru ($4 \times 9.5 = 38$).



This is a keen example. First, we have a familiar inner ring of well-defined points at 15.9, 16, 15.8, and 16 ru. Second, the angle between #50 and #70 is 60.1 cu, which compares closely with 59.5 cu between #70 and #80. Lastly, #82, the relatively unsymmetrical ray in the group of four at 16 ru is bracketed in what looks like a spray on both sides by the rays of #99 and #97.

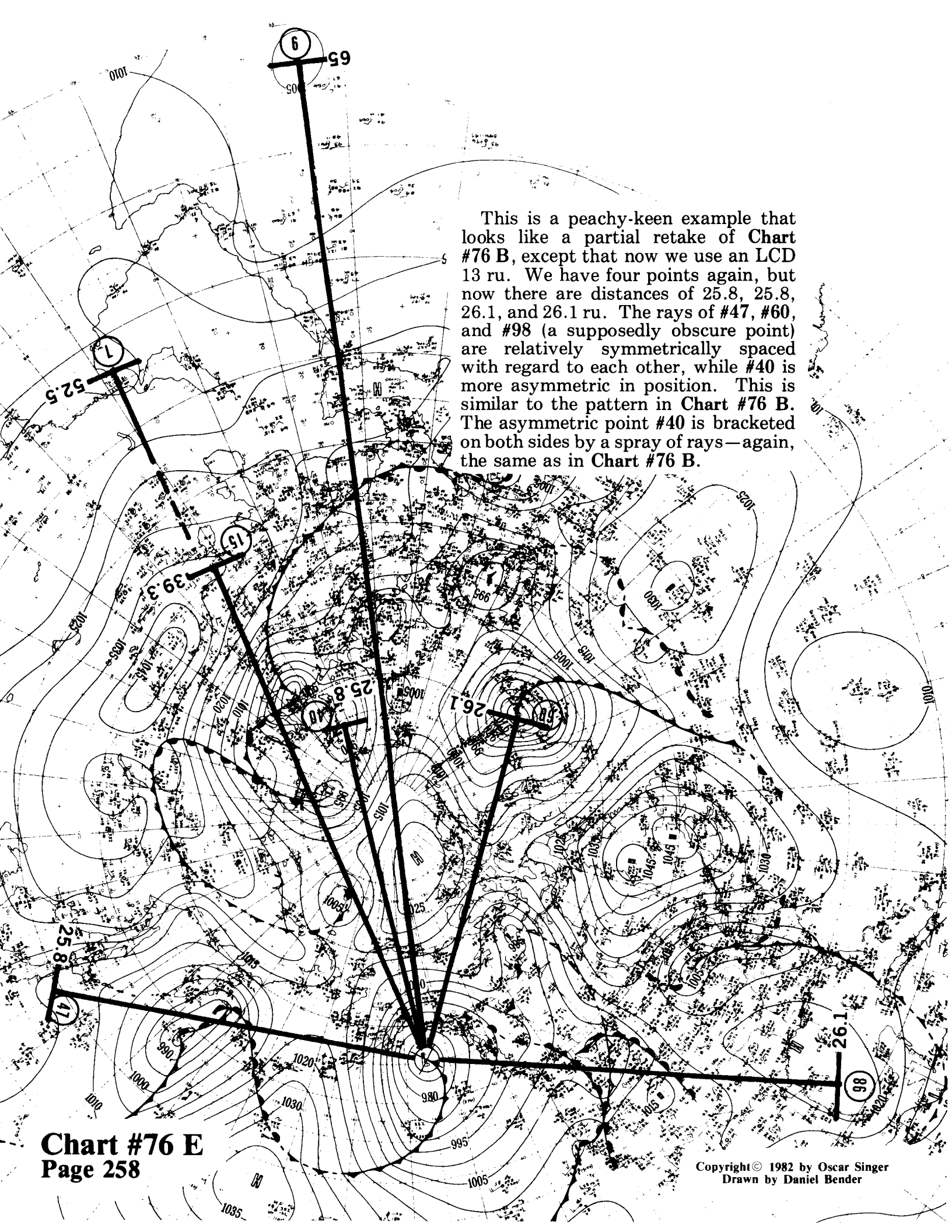


Another simple pattern with #5 as the +X axis and #78 near the +Y axis. The precision of the distance values when using an LCD of 7 ru, is excellent. We see that #96 rises away from the -X axis (not drawn) at the same angle approximately as #45 does from the +X axis.

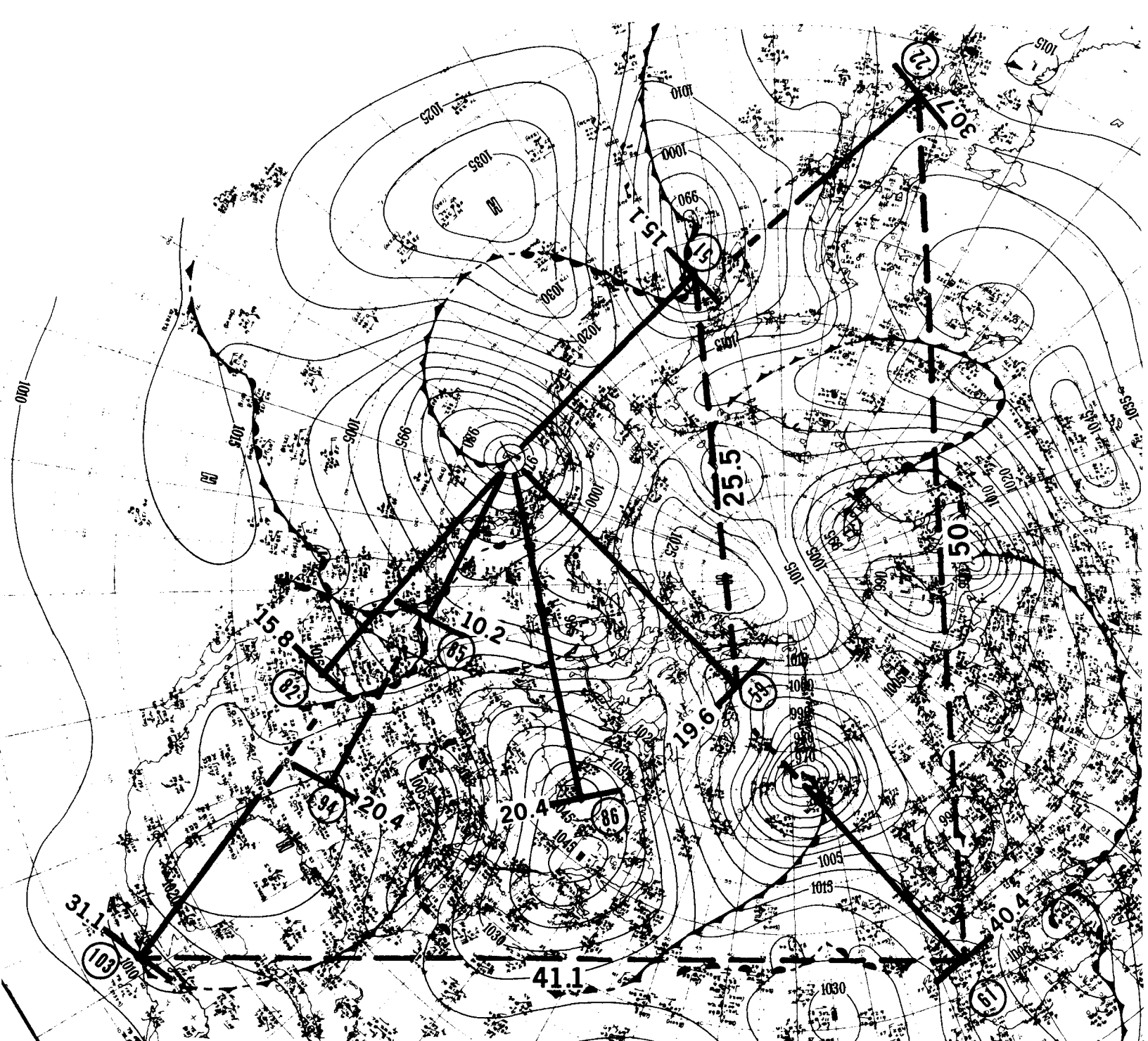
The +X axis is defined by #92 and the -X axis is near #77 while the +Y axis is defined by #45. With an LCD of 10.6 to 10.7 ru, we find that #32 and #6 are generally symmetrical about the +Y axis, while #89 (or #72) and #96 are symmetrical about the +X axis.

Chart #76 D
Page 257

Copyright © 1982 by Oscar Singer
Drawn by Daniel Bender



This is a peachy-keen example that looks like a partial retake of Chart #76 B, except that now we use an LCD 13 ru. We have four points again, but now there are distances of 25.8, 25.8, 26.1, and 26.1 ru. The rays of #47, #60, and #98 (a supposedly obscure point) are relatively symmetrically spaced with regard to each other, while #40 is more asymmetric in position. This is similar to the pattern in Chart #76 B. The asymmetric point #40 is bracketed on both sides by a spray of rays—again, the same as in Chart #76 B.



The -X axis lies along the ray to #51, the +X axis is near the ray to #82, and the +Y axis lies along the ray to #59. An LCD of 10.2 ru is used, except for two points at 15.1 ru and 15.8 ru.

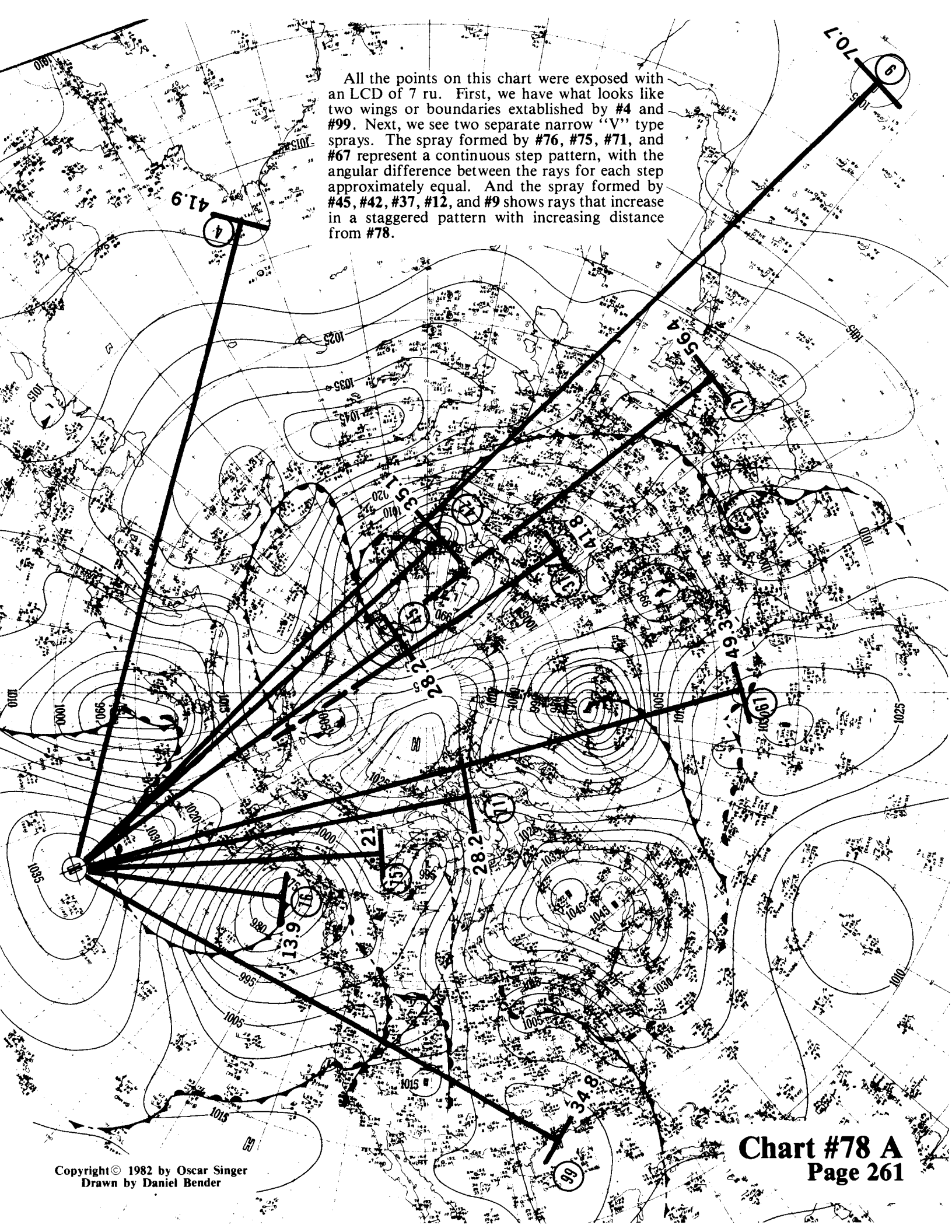
We start along the X axis and find that #51 (15.1 ru) is opposite #82 (15.8 ru). Likewise, #22 (30.7 ru) is balanced by #103 (31.1 ru), while the rays for both points are tilted symmetrically about the same angle above the X axis.

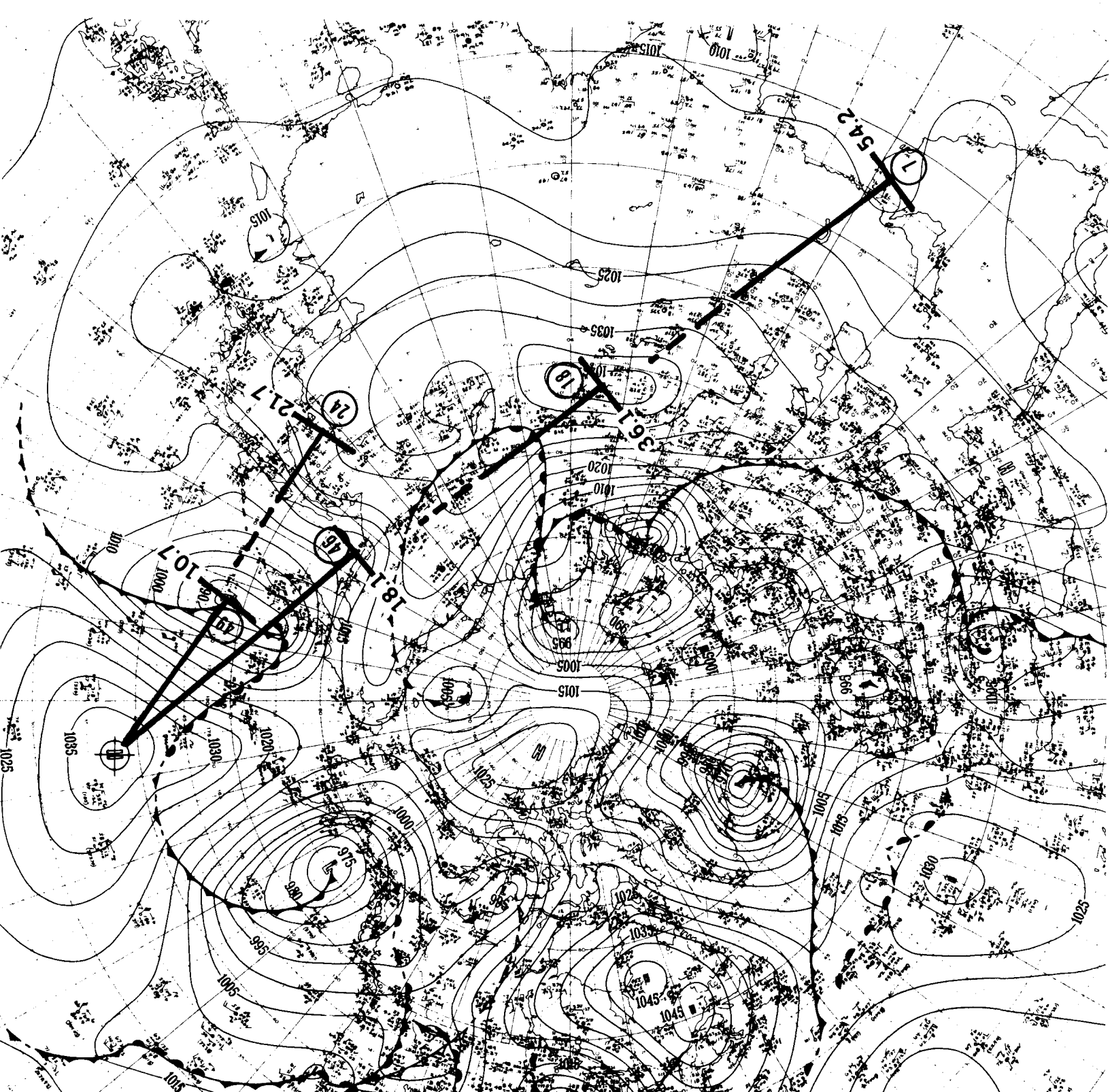
Now we see #85 at 10.2 ru doubling to 20.4 ru at #94, and tripling to 30.7 ru at #22. All these points lie near the X axis. Next, near the Y axis, we see that #61 is 40.4 ru ($4 \times 10.2 = 40.8$).

Now let's come to grips with the unusual feature of this "beast". The distance between #22 and #61 is 50 ru, so a triangle is formed by #76, #61, and #22 with sides of 30.7, 40.4, and 50 ru, which is close to a pythagorean 3:4:5 triangle. Continuing, we see that #59 at 19.6 ru is a little less than half the distance to #61; likewise, #51 at 15.1 ru is also a little less than half the distance to #22. We note that the ray to #59 is tilted slightly to the left of the ray to #61, and the ray to #51 is also tilted slightly left of the ray to #22. The great circle distance between #51 and #59 is 25.5 ru. This gives a second triangle formed by #76, #51, and #59 with sides of 15.1, 19.6, and 25.5 ru, which is close to a ratio of 3:4:5.

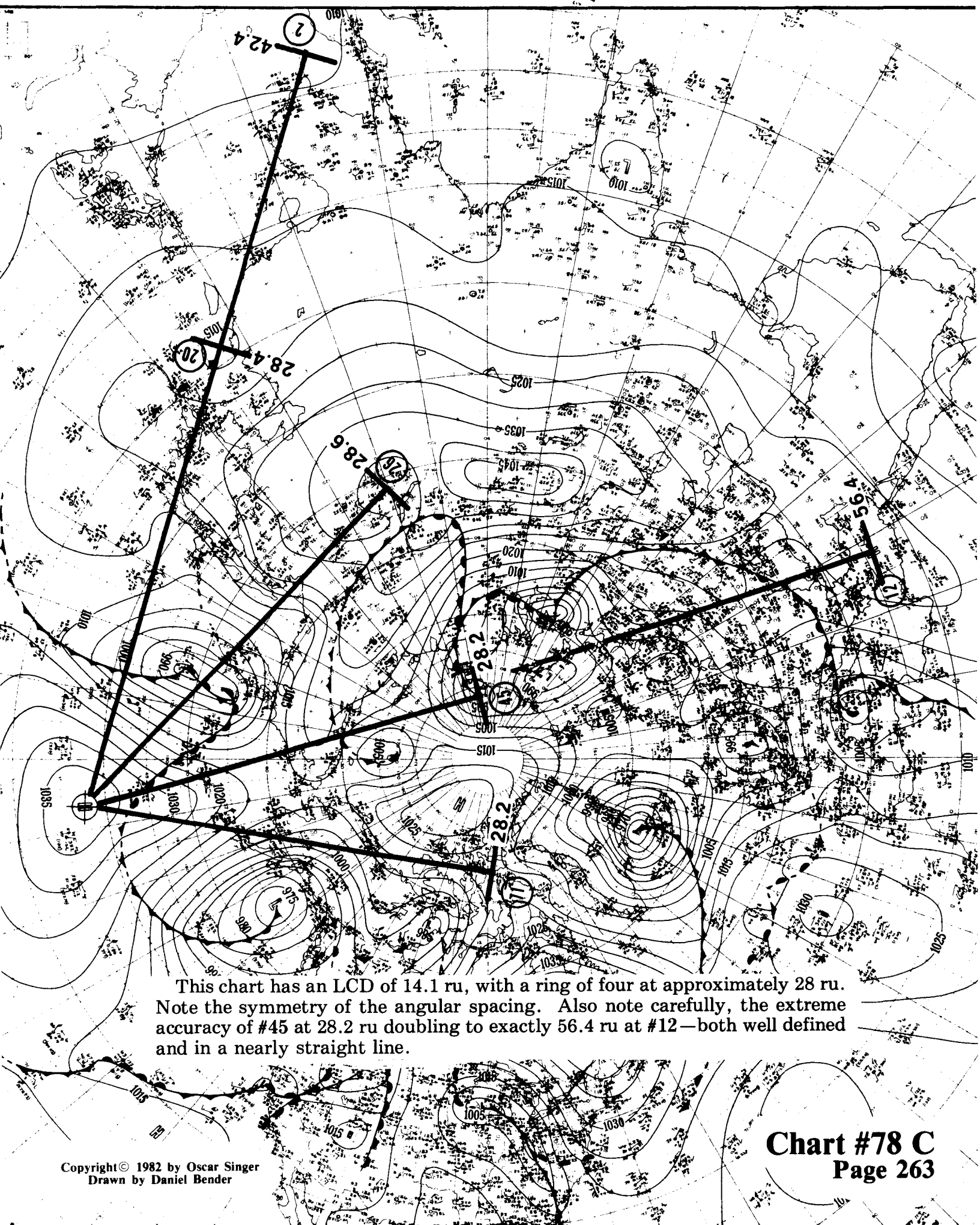
Finally, the triangle formed by #76, #61, and #103 has sides of length 31.1, 40.4, and 41.1 ru, which gives a ratio of 3:4:4 approximately.

All the points on this chart were exposed with an LCD of 7 ru. First, we have what looks like two wings or boundaries established by #4 and #99. Next, we see two separate narrow "V" type sprays. The spray formed by #76, #75, #71, and #67 represent a continuous step pattern, with the angular difference between the rays for each step approximately equal. And the spray formed by #45, #42, #37, #12, and #9 shows rays that increase in a staggered pattern with increasing distance from #78.

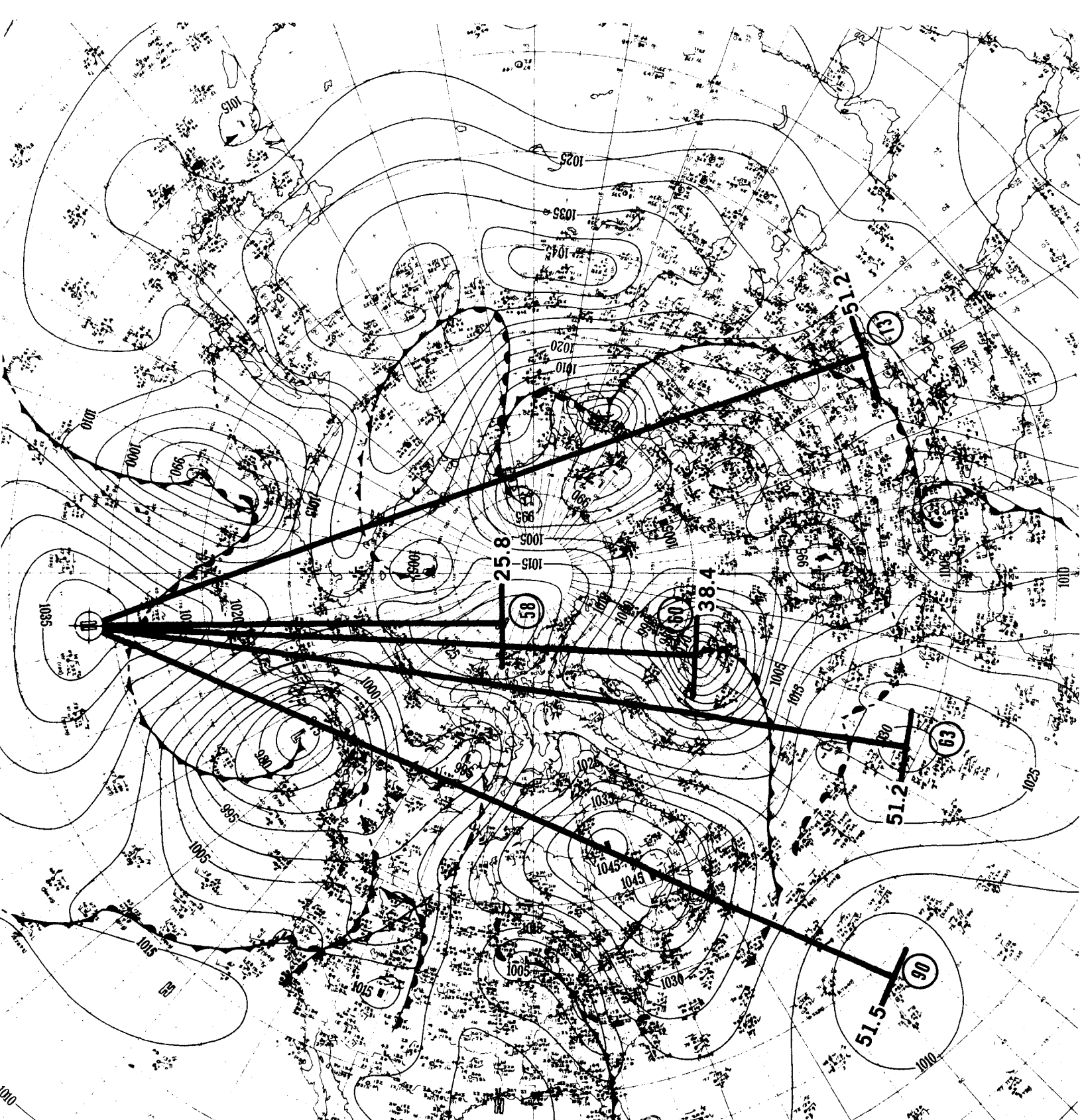




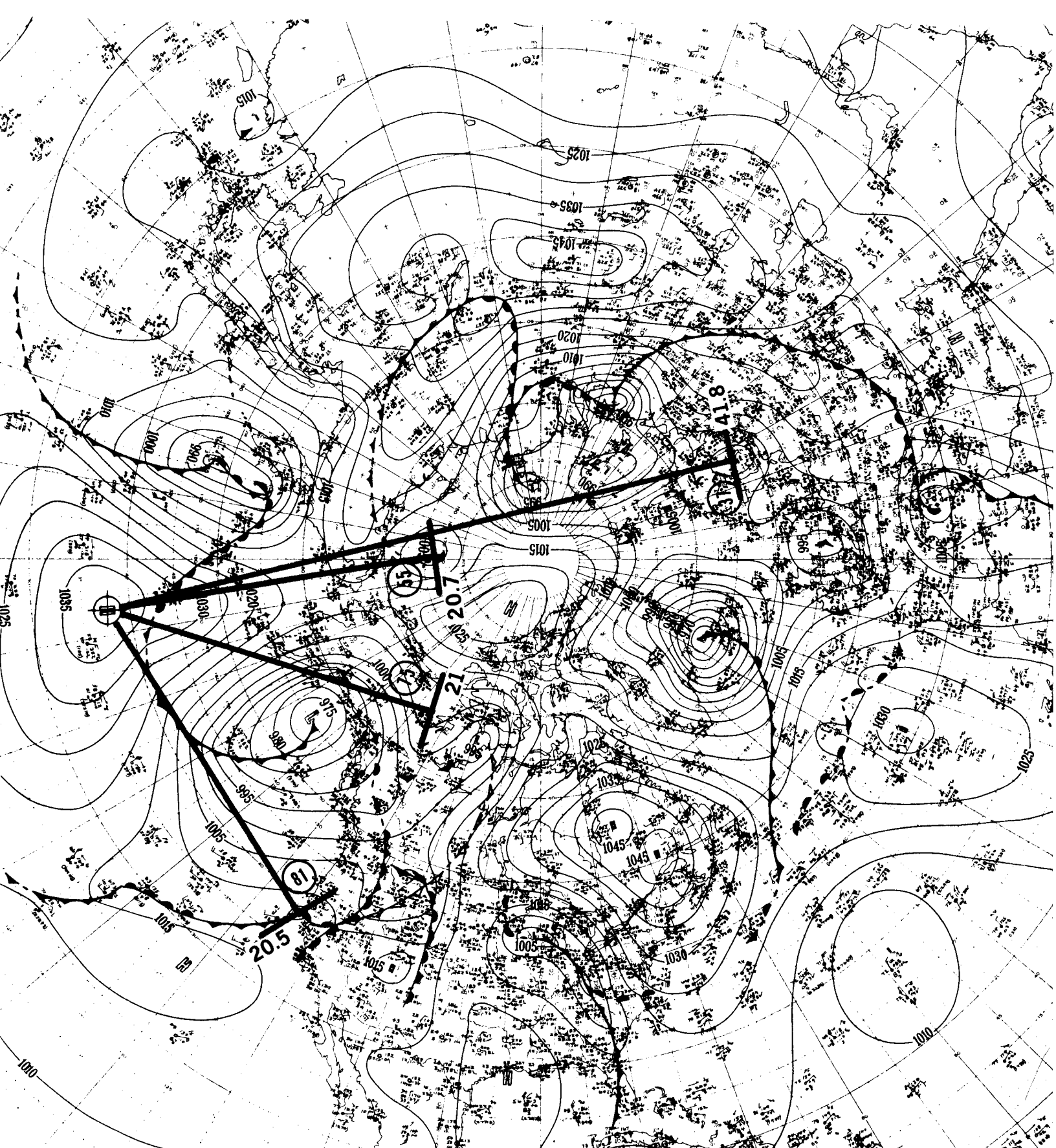
Two separate systems are shown on this chart: first, #49 and #24 have an approximate LCD of 10.7 ru; second, there are three points (#46, #18, and #7) that are in a nearly straight line with an LCD of 18.1 ru.



This chart has an LCD of 14.1 ru, with a ring of four at approximately 28 ru. Note the symmetry of the angular spacing. Also note carefully, the extreme accuracy of #45 at 28.2 ru doubling to exactly 56.4 ru at #12—both well defined and in a nearly straight line.



This is a simple one with an LCD of 25.8 ru (or 12.9 ru) in which we have a step pattern right down the middle between two wings at the outer boundaries.

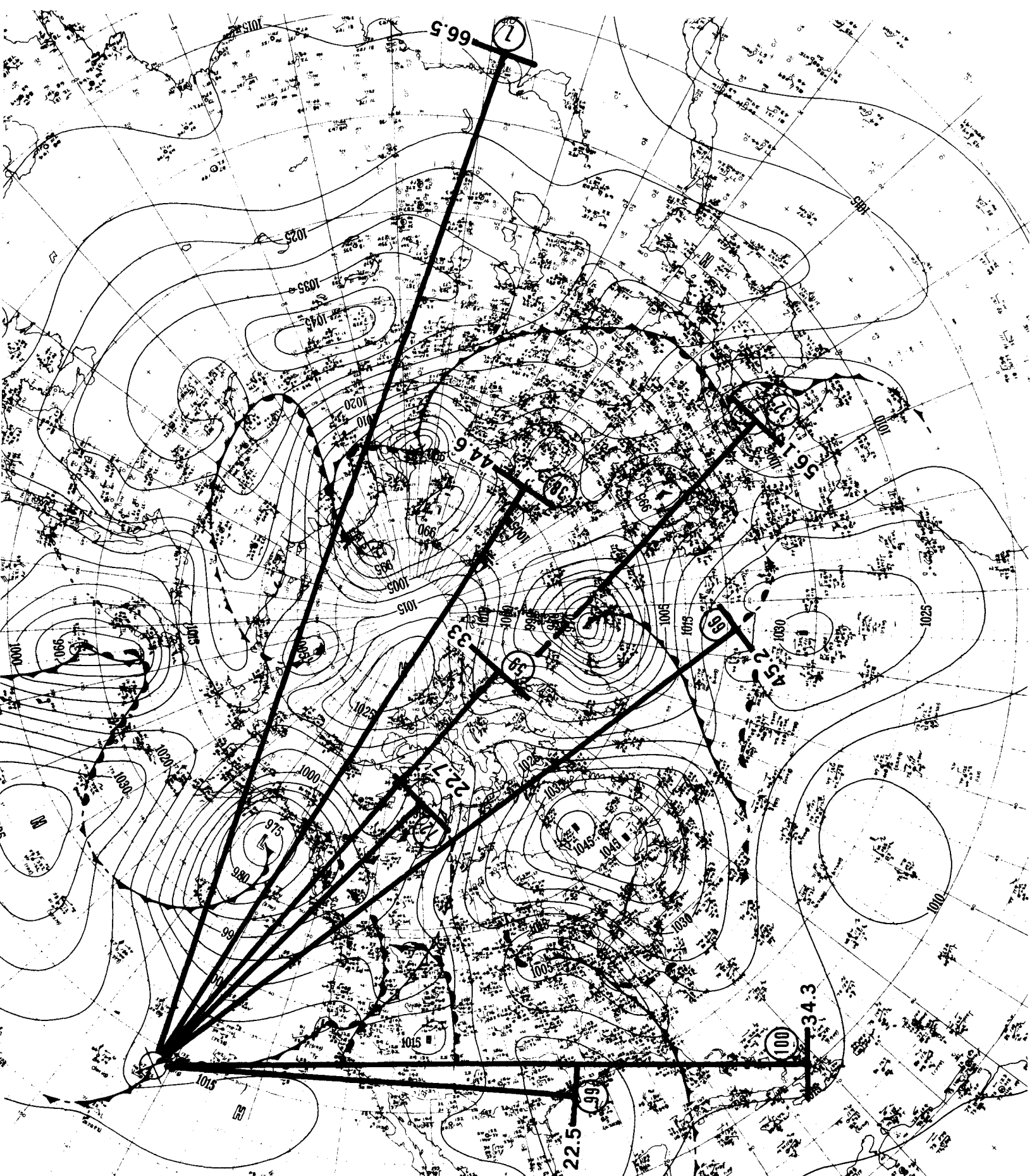


This one shows another ring fairly close in, at approximately 21 ru.

MAP
HERE
GMT
N MODEL
SHIP STA
© 1982
T. L. N. W. R.
S. S. n

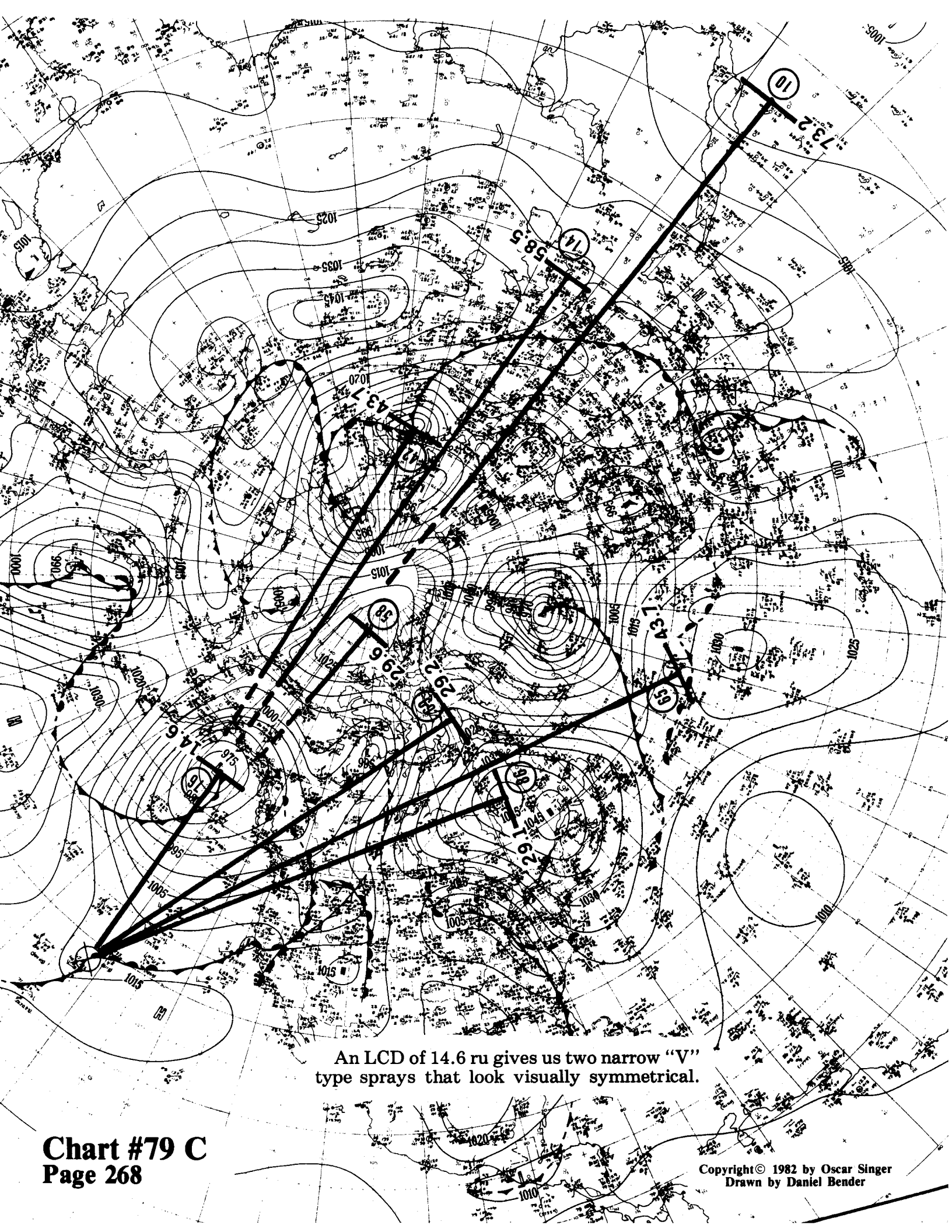
Copyright © 1982 by Oscar Singer
Drawn by Daniel Bender

Chart #78 E
Page 265



This one uses an LCD with a range between 11 and 11.3 ru.

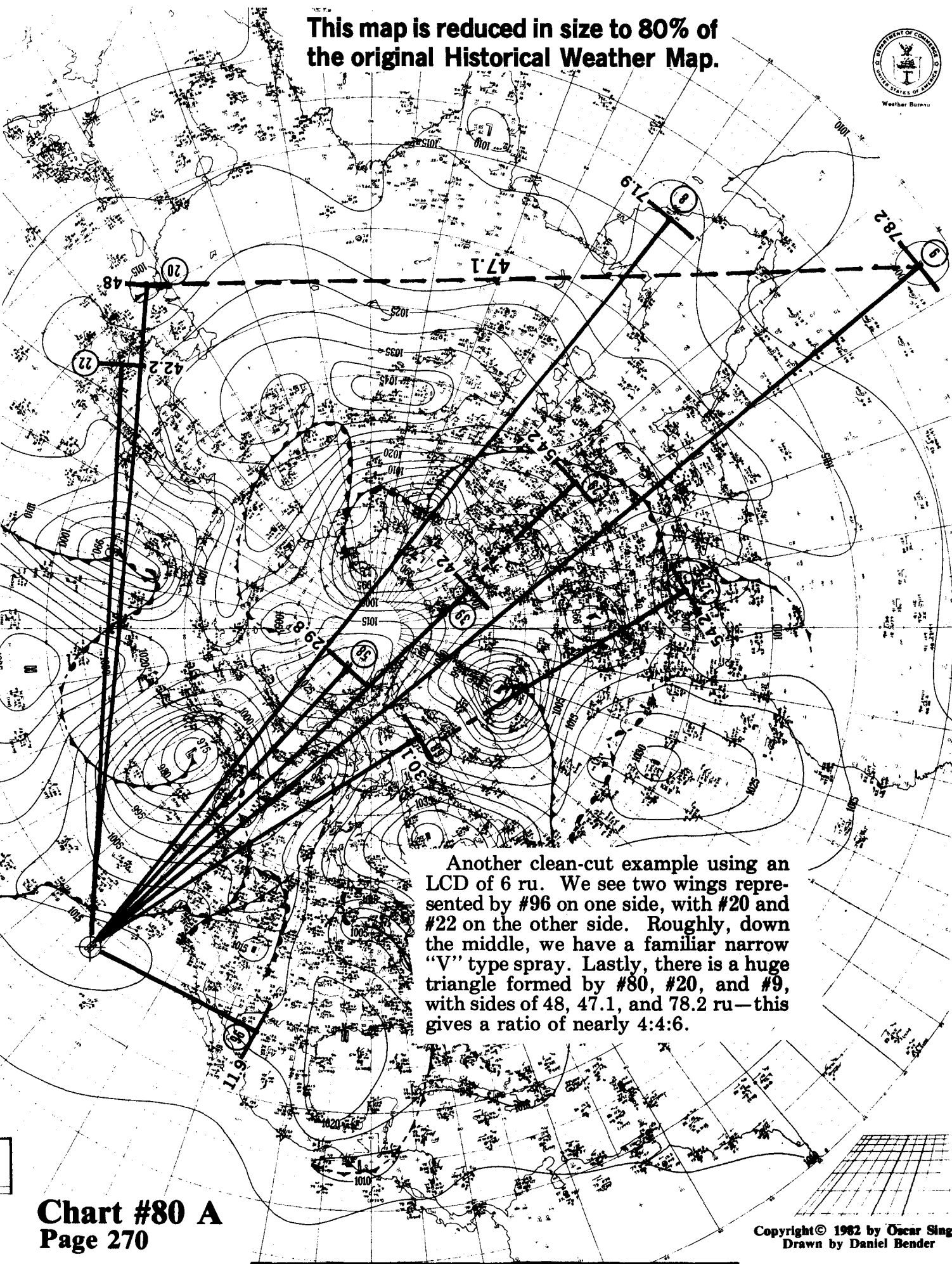
This is a particularly interesting example. There are four separate triangles with the length of all the sides of all the triangles at some multiple of 12 ru. The triangle formed by #79, #63, and #18 has sides of 47.7, 48.1, and 36.3 ru, which gives a ratio of 4:4:3. The triangle formed by #79, #63, and #5 has sides of 47.7, 47.2, and 60 ru, which gives a ratio of 4:4:5. The triangle formed by #79, #63, and #24 has sides of 47.7, 47.6, and 35.9 ru, which gives a ratio of 4:4:3. The triangle formed by the dashed lines between the points of #63, #5, and #24 has sides of 47.7, 47.2 and 24.1 ru, which gives a ratio of 4:4:2.



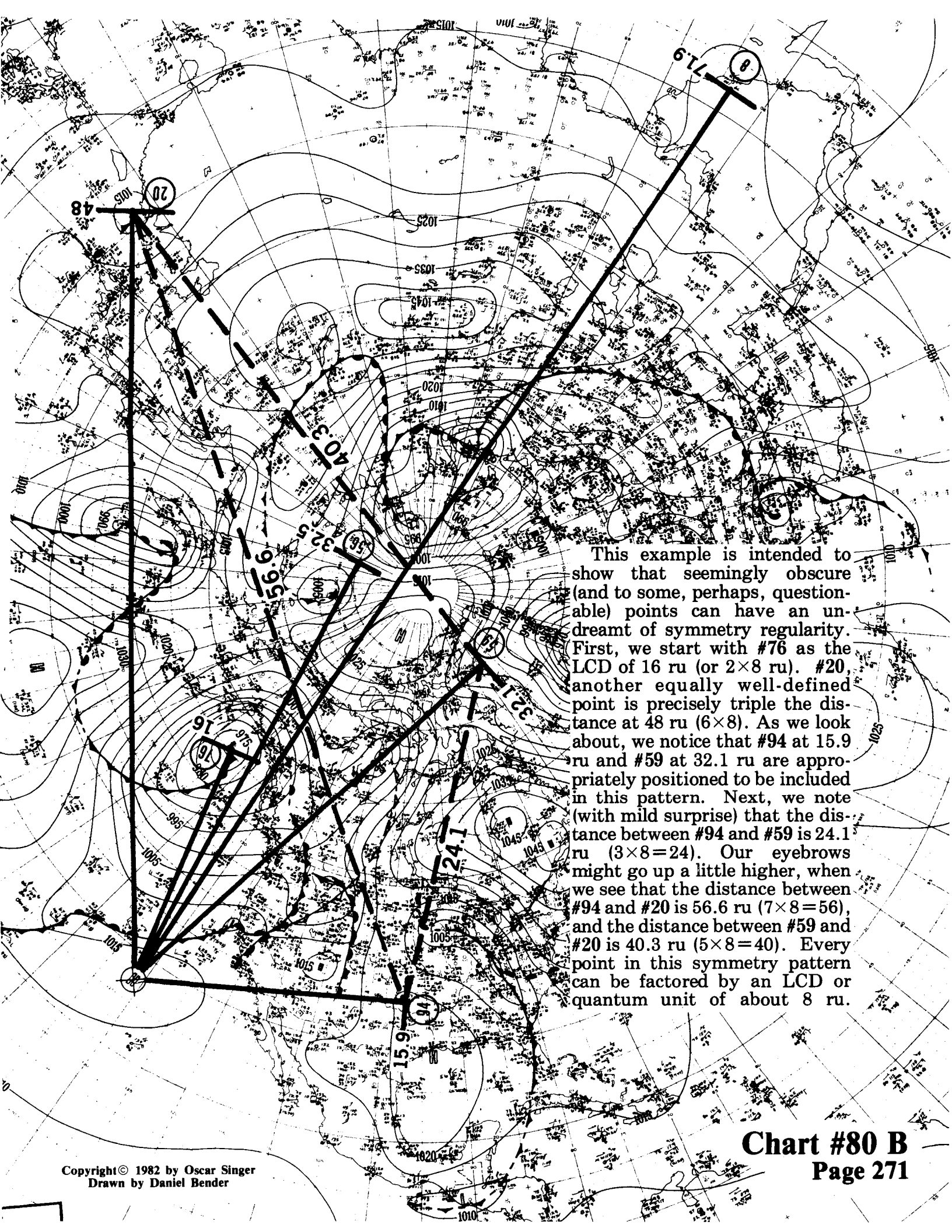
An LCD of 14.6 ru gives us two narrow "V" type sprays that look visually symmetrical.

Another example of a close-in ring at an approximate distance of 15 ru.
Careful inspection will also show elements of visual symmetry.

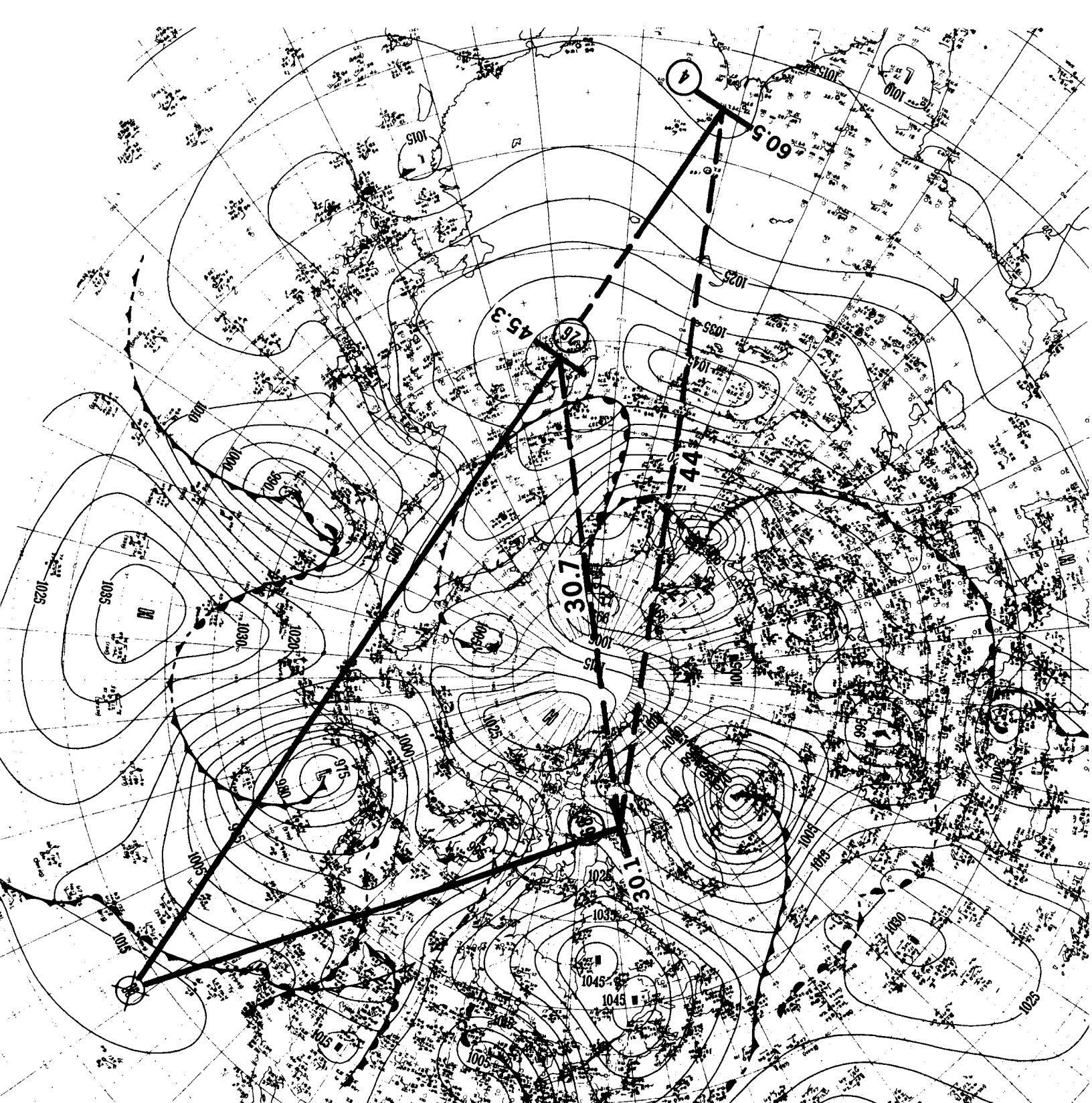
This map is reduced in size to 80% of the original Historical Weather Map.



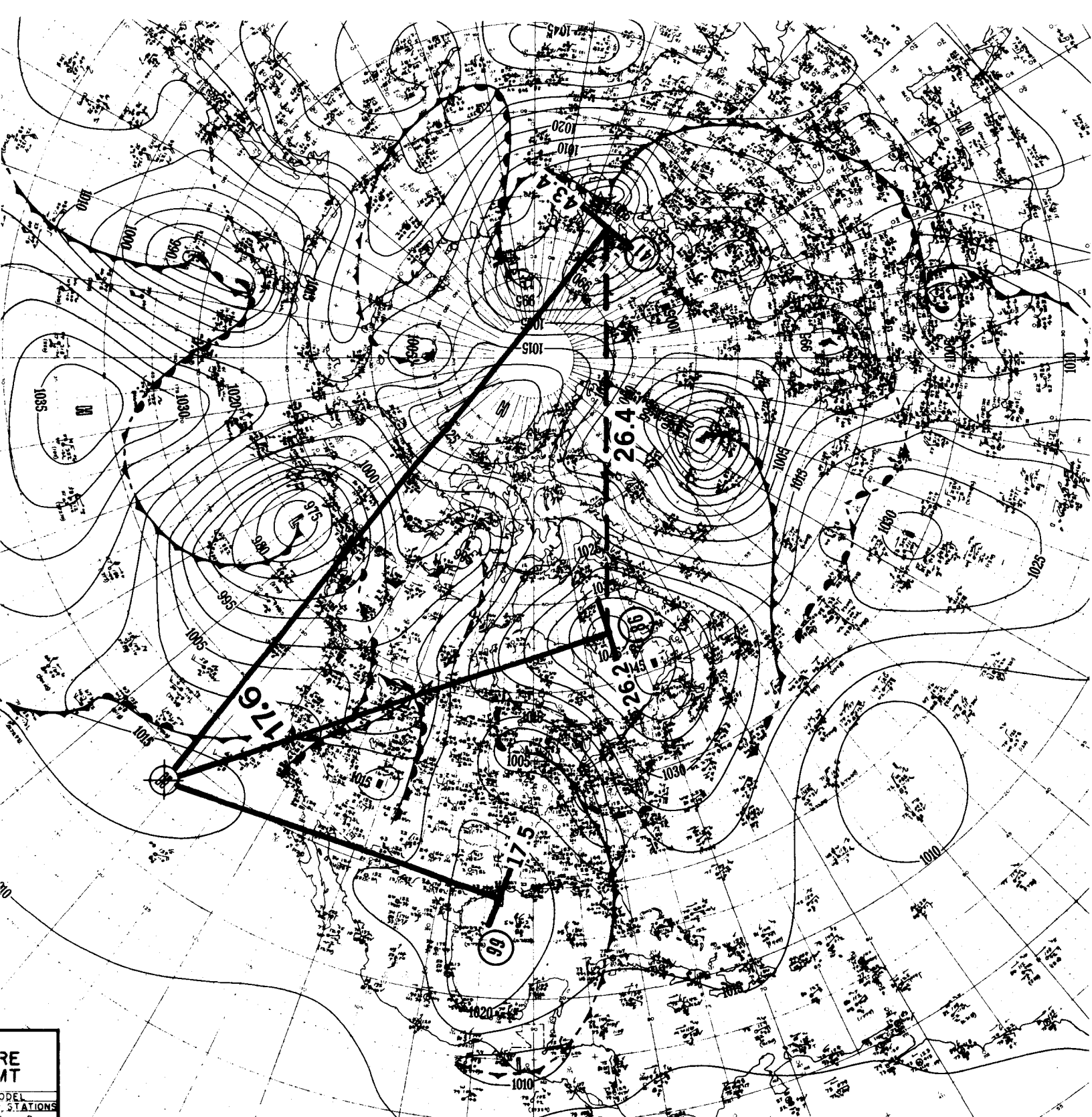
Another clean-cut example using an LCD of 6 ru. We see two wings represented by #96 on one side, with #20 and #22 on the other side. Roughly, down the middle, we have a familiar narrow "V" type spray. Lastly, there is a huge triangle formed by #80, #20, and #9, with sides of 48, 47.1, and 78.2 ru—this gives a ratio of nearly 4:4.6.



This example is intended to show that seemingly obscure (and to some, perhaps, questionable) points can have an undreamt of symmetry regularity. First, we start with #76 as the LCD of 16 ru (or 2×8 ru). #20, another equally well-defined point is precisely triple the distance at 48 ru (6×8). As we look about, we notice that #94 at 15.9 ru and #59 at 32.1 ru are appropriately positioned to be included in this pattern. Next, we note (with mild surprise) that the distance between #94 and #59 is 24.1 ru ($3 \times 8 = 24$). Our eyebrows might go up a little higher, when we see that the distance between #94 and #20 is 56.6 ru ($7 \times 8 = 56$), and the distance between #59 and #20 is 40.3 ru ($5 \times 8 = 40$). Every point in this symmetry pattern can be factored by an LCD or quantum unit of about 8 ru.



Here we have a triangle with an LCD of 15.1 ru formed by #80, #68, and #26; the sides are 30.1, 30.7, and 45.3 ru, which gives an approximate ratio of 2:2:3. There is another triangle, but not quite as good, which is formed by #80, #68, and #4, with sides of 30.1, 44, and 60.5 ru to give an approximate ratio of 2:3:4.



With an LCD of 8.8 ru we get a triangle formed by #80, #86, and #41, with sides of 26.2 ru ($3 \times 8.8 = 26.4$), 26.4 ru (3×8.8), and 43.4 ru ($5 \times 8.8 = 44$), which gives a ratio of 3:3:5. In addition, we find an angle of 17.6 cu (2×8.8) between #86 and #41.

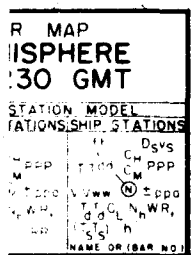
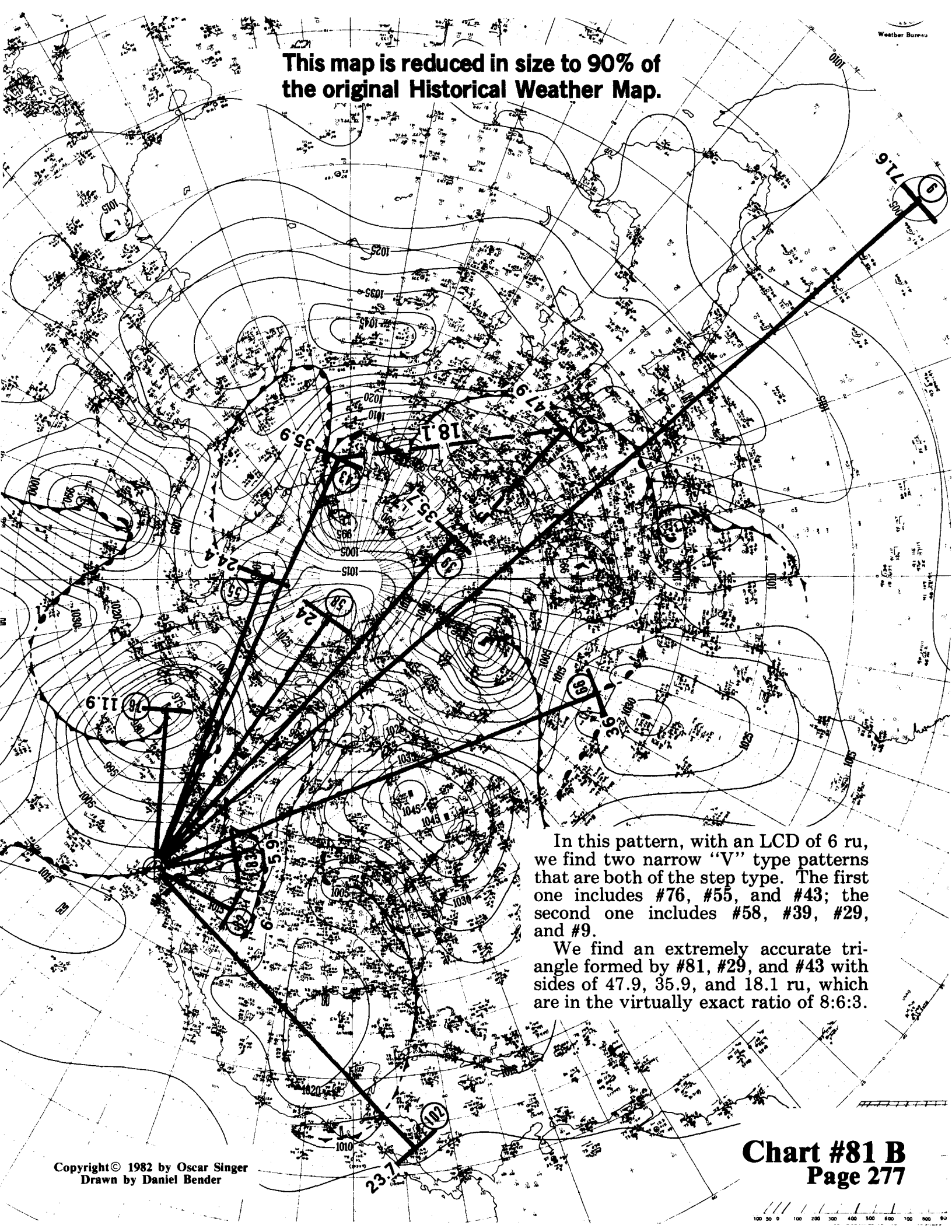


Chart #80 E
Page 274

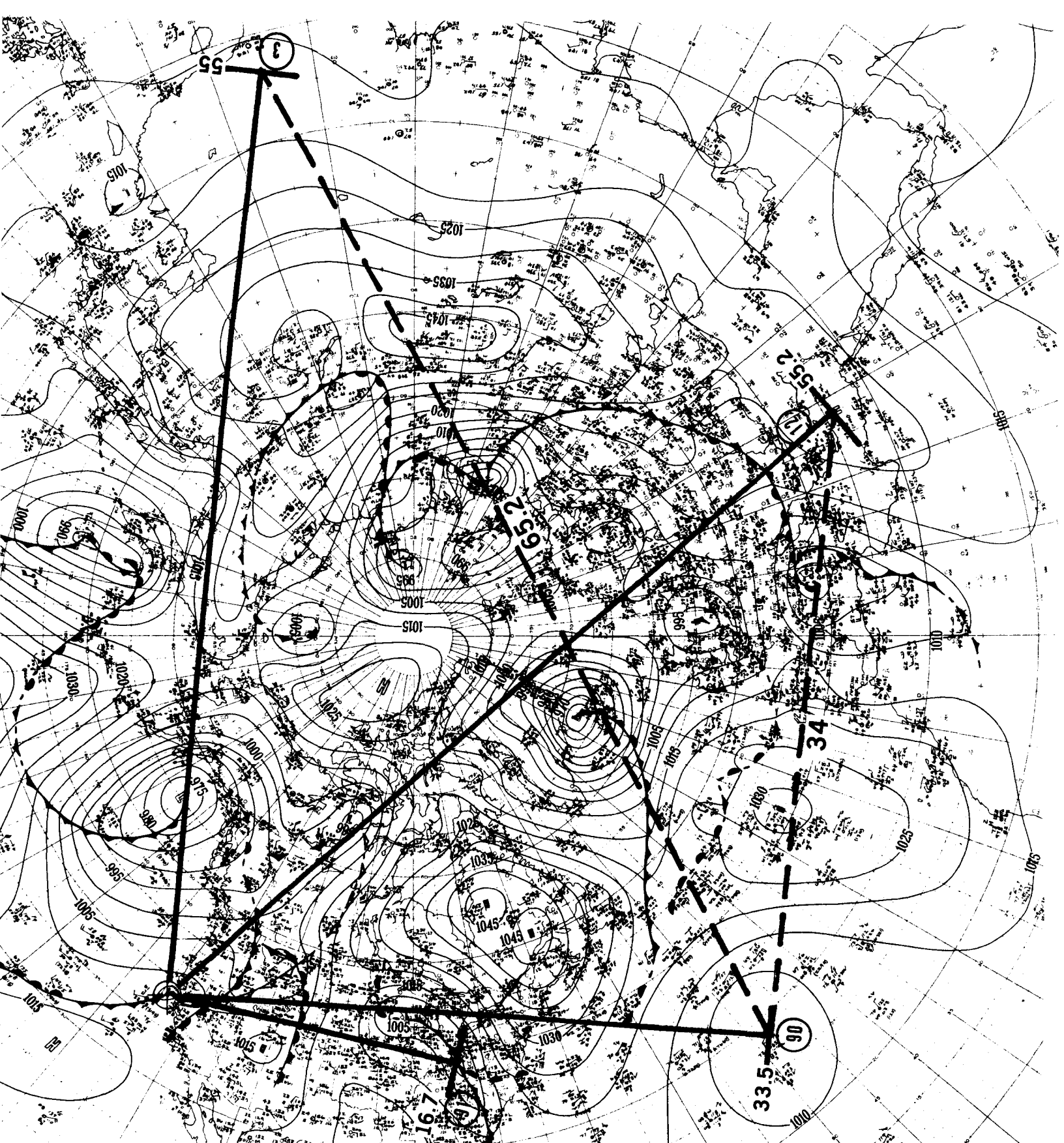
This example is a scatter pattern with a fairly accurate LCD of 9.6 ru.

This map is reduced in size to 90% of
the original Historical Weather Map.

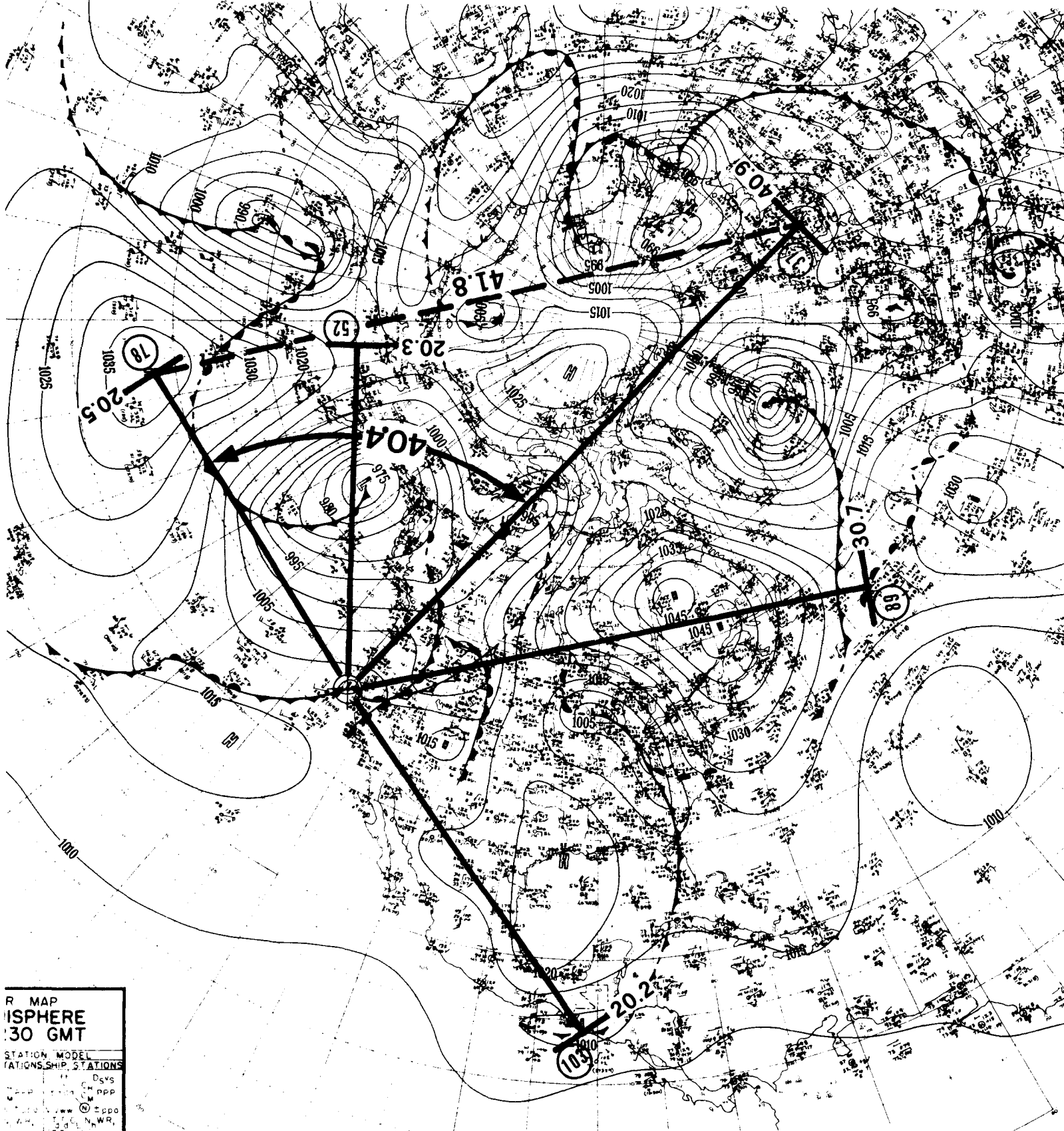


In this pattern, with an LCD of 6 ru, we find two narrow "V" type patterns that are both of the step type. The first one includes #76, #55, and #43; the second one includes #58, #39, #29, and #9.

We find an extremely accurate triangle formed by #81, #29, and #43 with sides of 47.9, 35.9, and 18.1 ru, which are in the virtually exact ratio of 8:6:3.

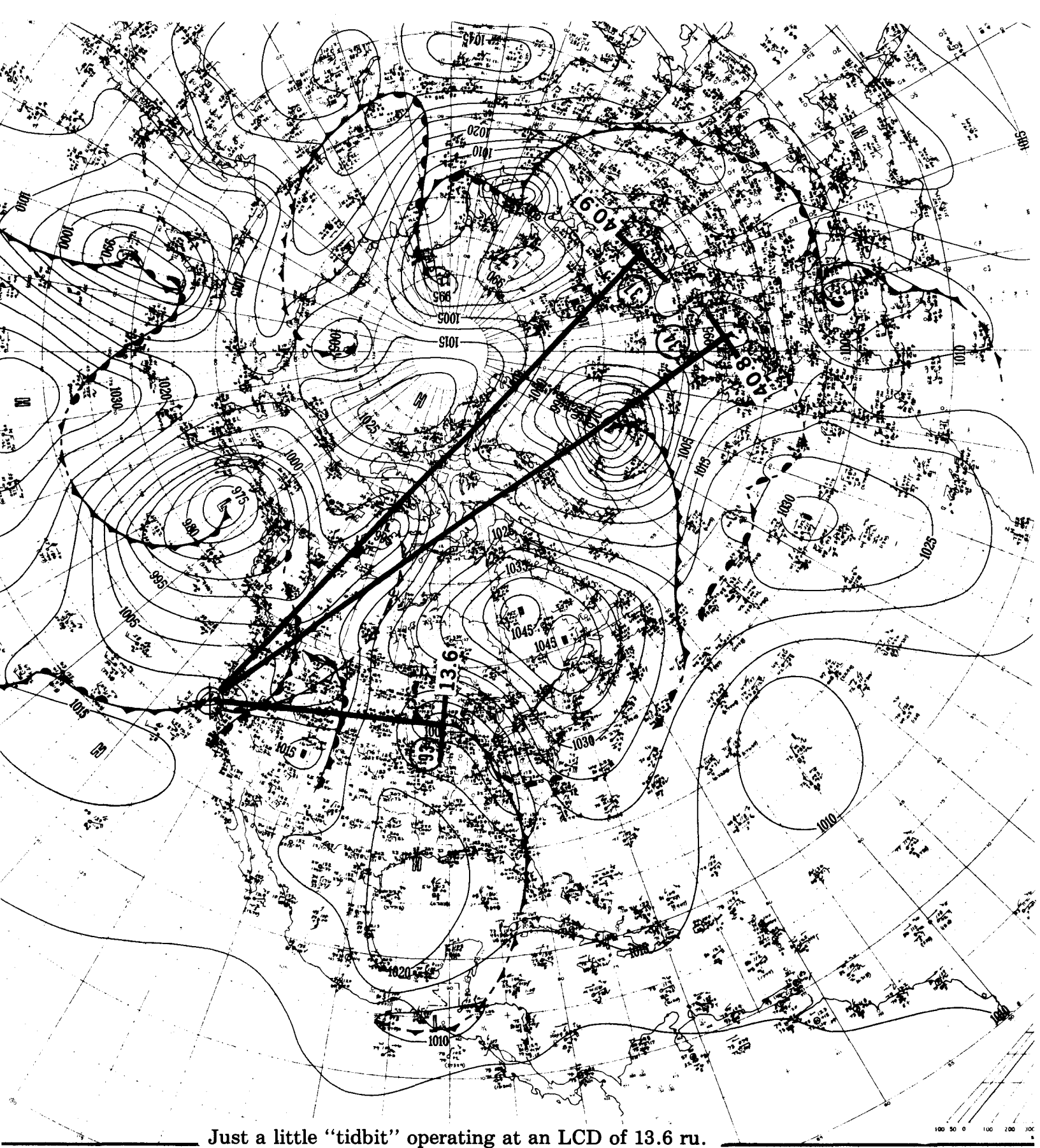


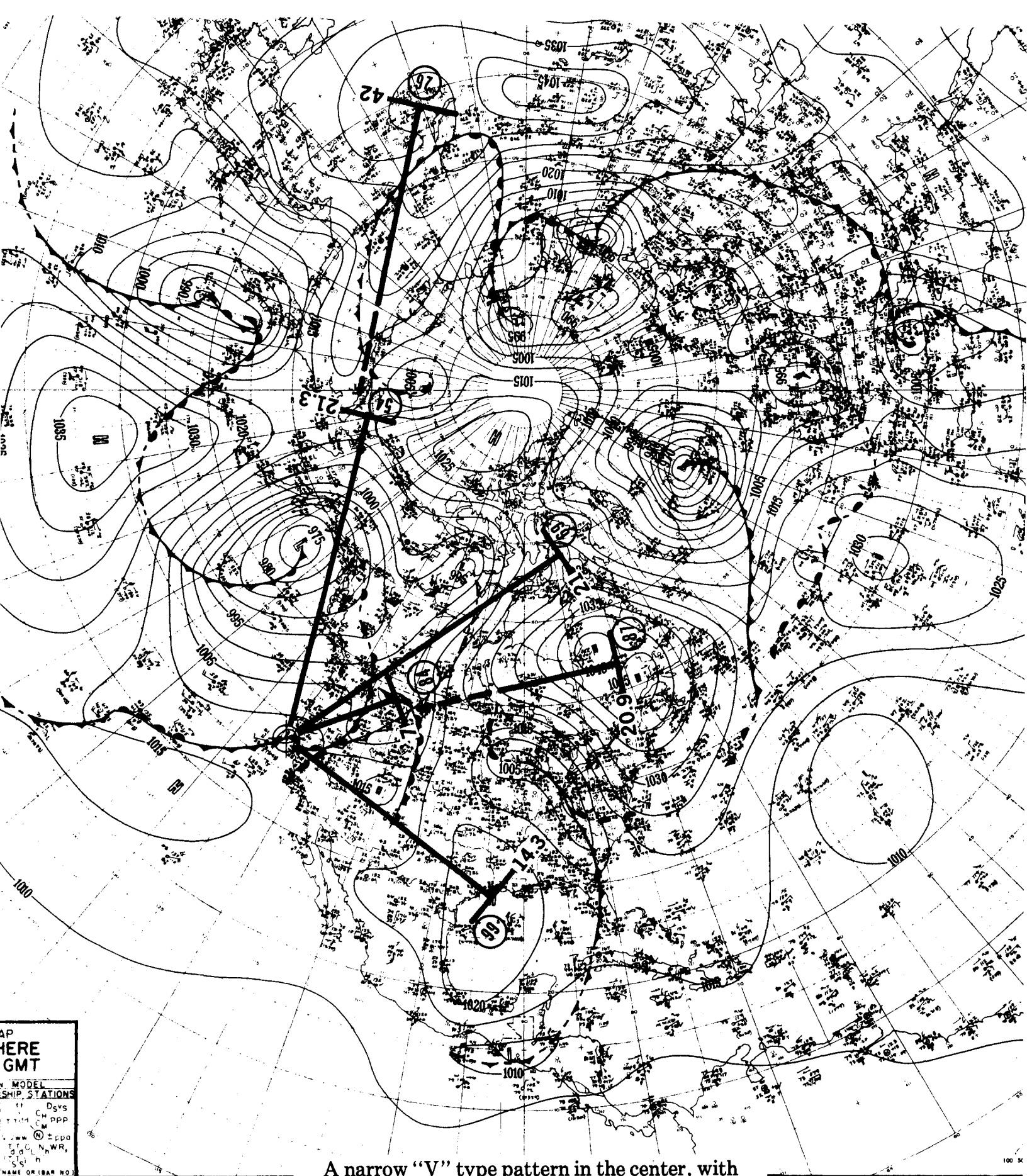
Here we have three points (#3, #12, and #90) at an approximate LCD of 11 ru. We also have #91 shown at one-half the distance of #90 at 16.7 ru. The dashed lines between the points represent distances approximately divisible by the LCD.



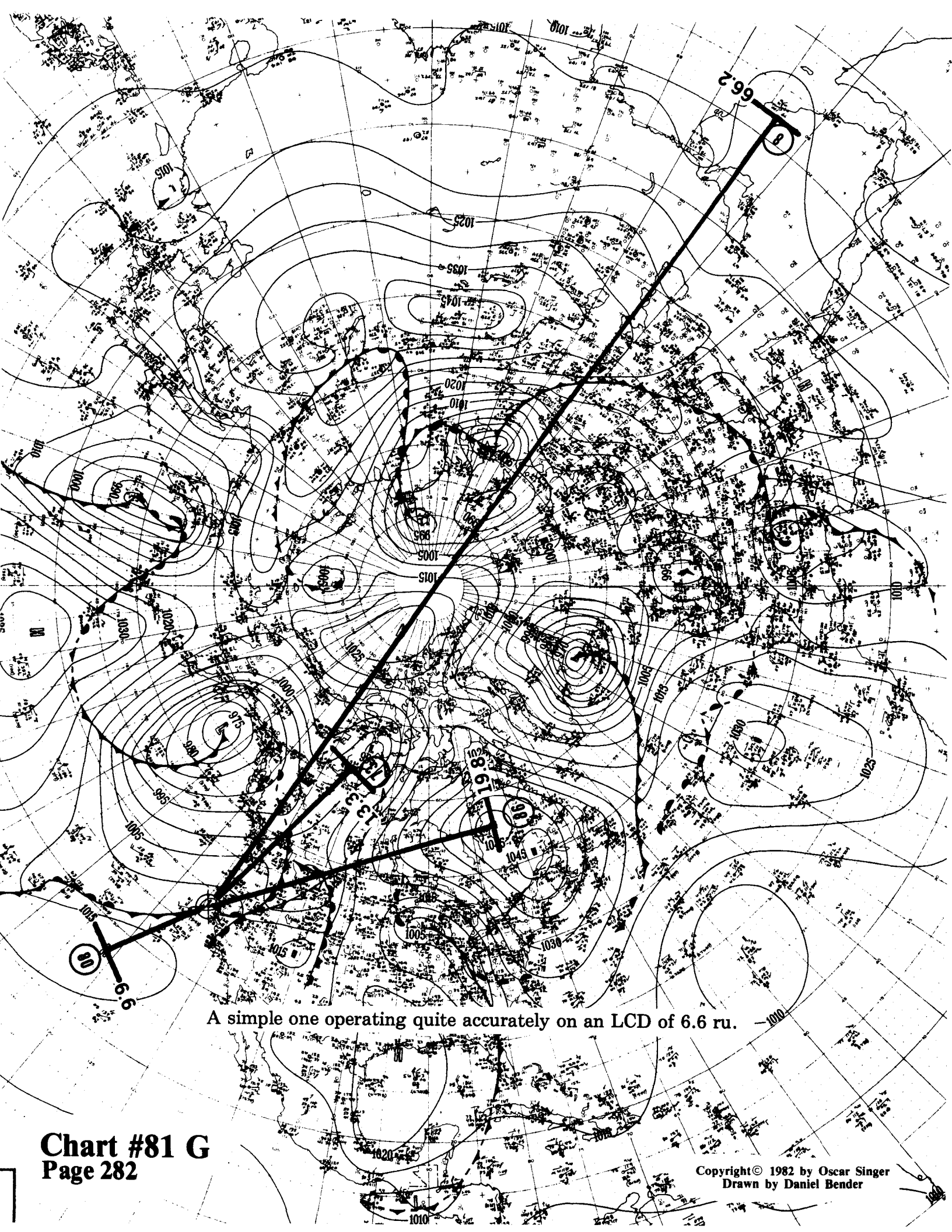
R MAP
 ISPHERE
 30 GMT
 STATION MODEL
 STATIONS SHIP STATIONS
 Dvgs
 Cpp
 @ tppo
 N WR
 h
 NAME OR ISAN NO

With an LCD of 10.2 ru, we find #78 at 20.5 ru as a good counter-balance against #103 at 20.2 ru. The angle between #78 and #37 is 40.4 cu ($4 \times 10.2 = 40.8$), which approximately matches the distance of 41.8 ru between #78 and #37.

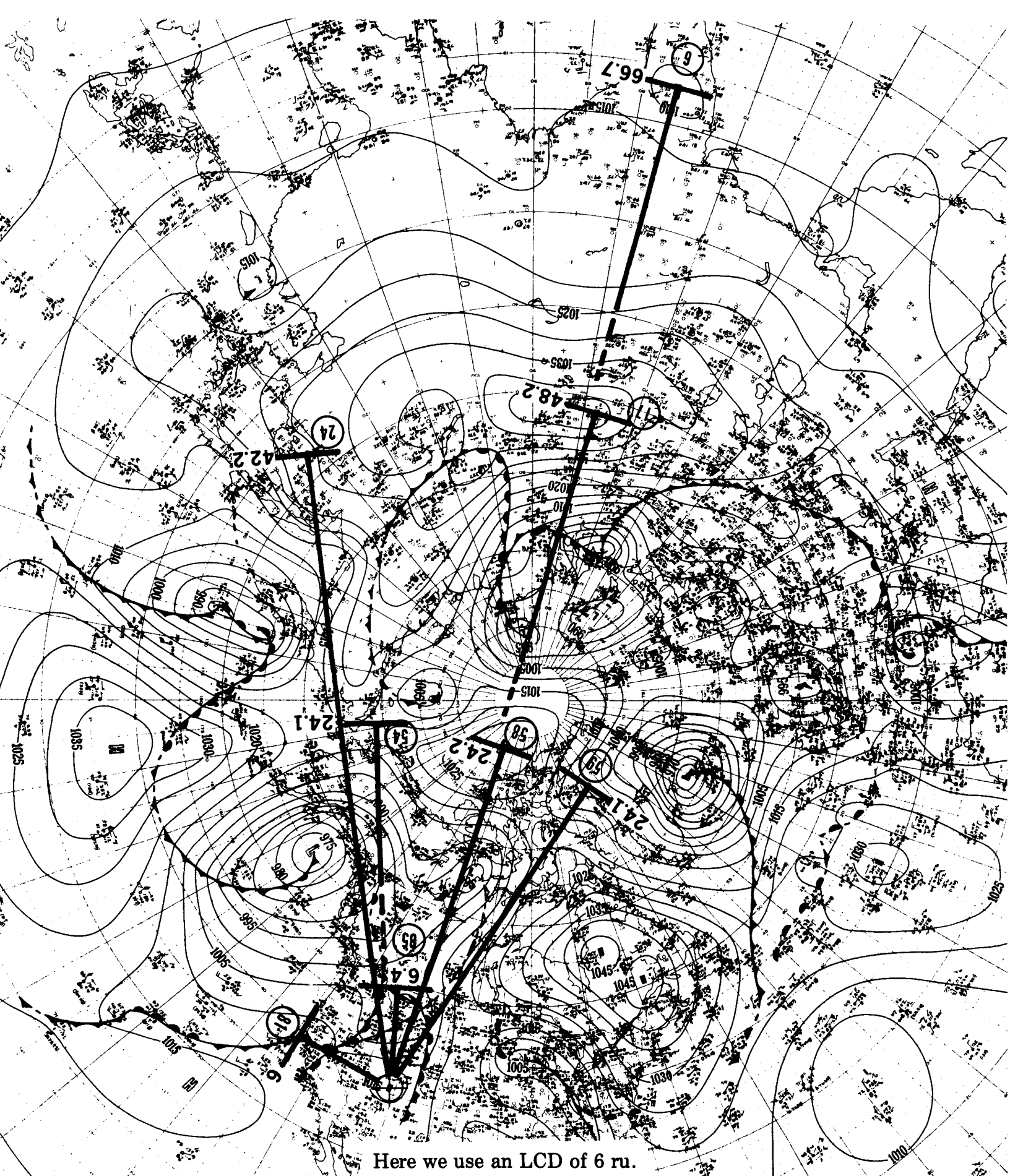




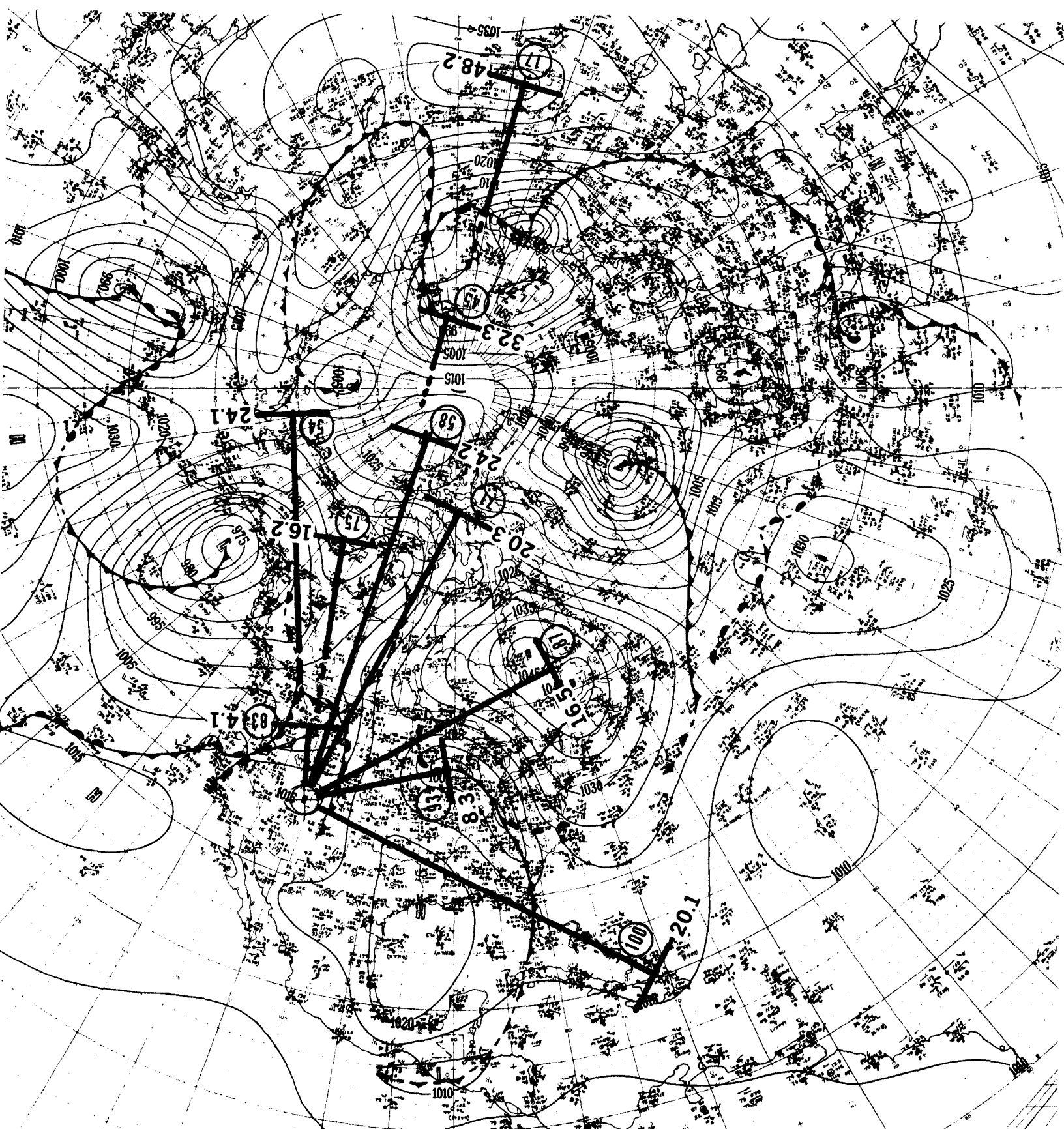
A narrow "V" type pattern in the center, with two wings operating on an LCD of 7 ru.



A simple one operating quite accurately on an LCD of 6.6 ru.



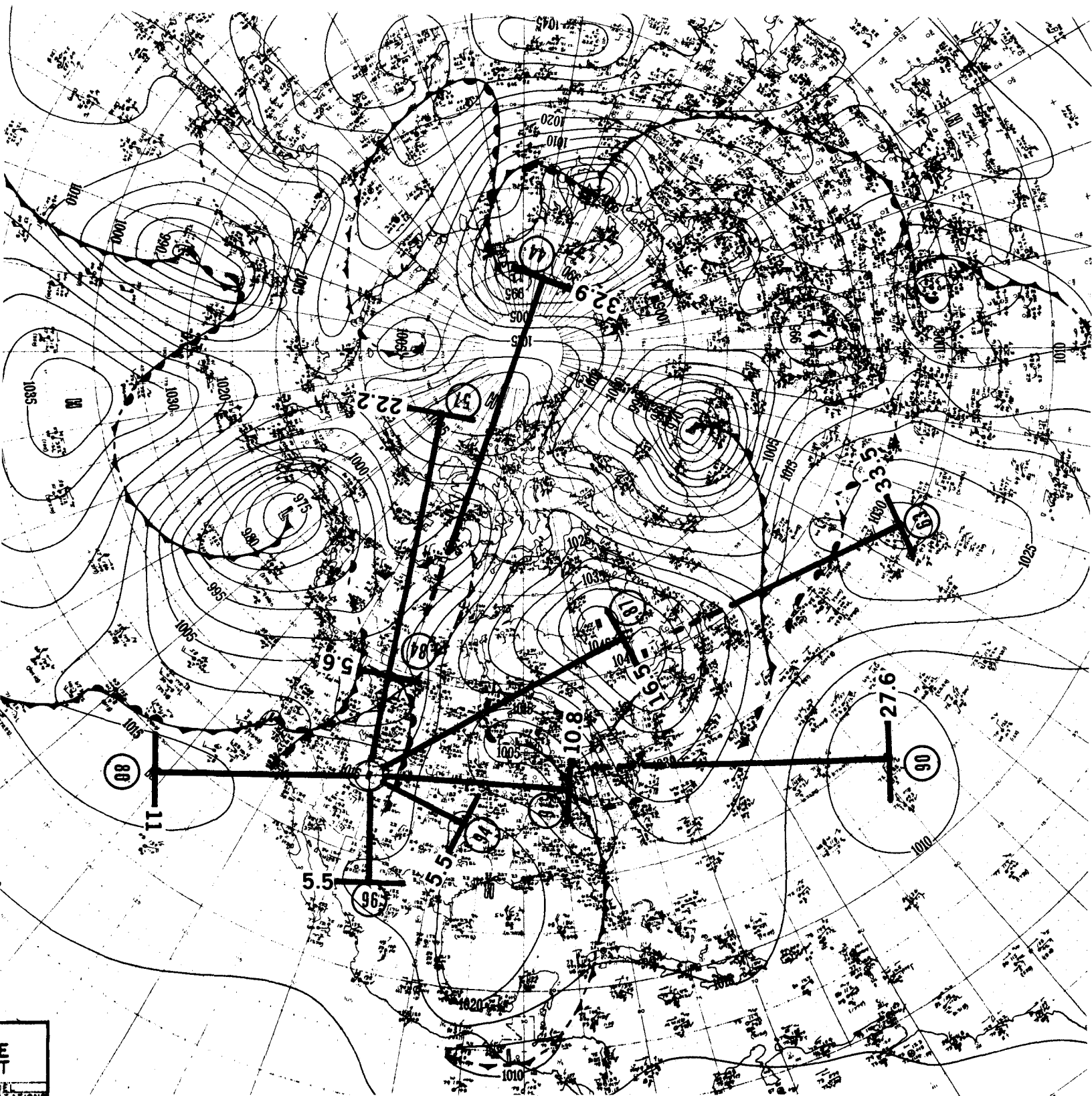
Here we use an LCD of 6 ru.



With an LCD of approximately 4 ru, we find the +X axis is along the ray for #100, and the +Y axis along the ray for #71. There is one "V" type cluster hugging the Y axis and a second narrower V involving #93 and #87.

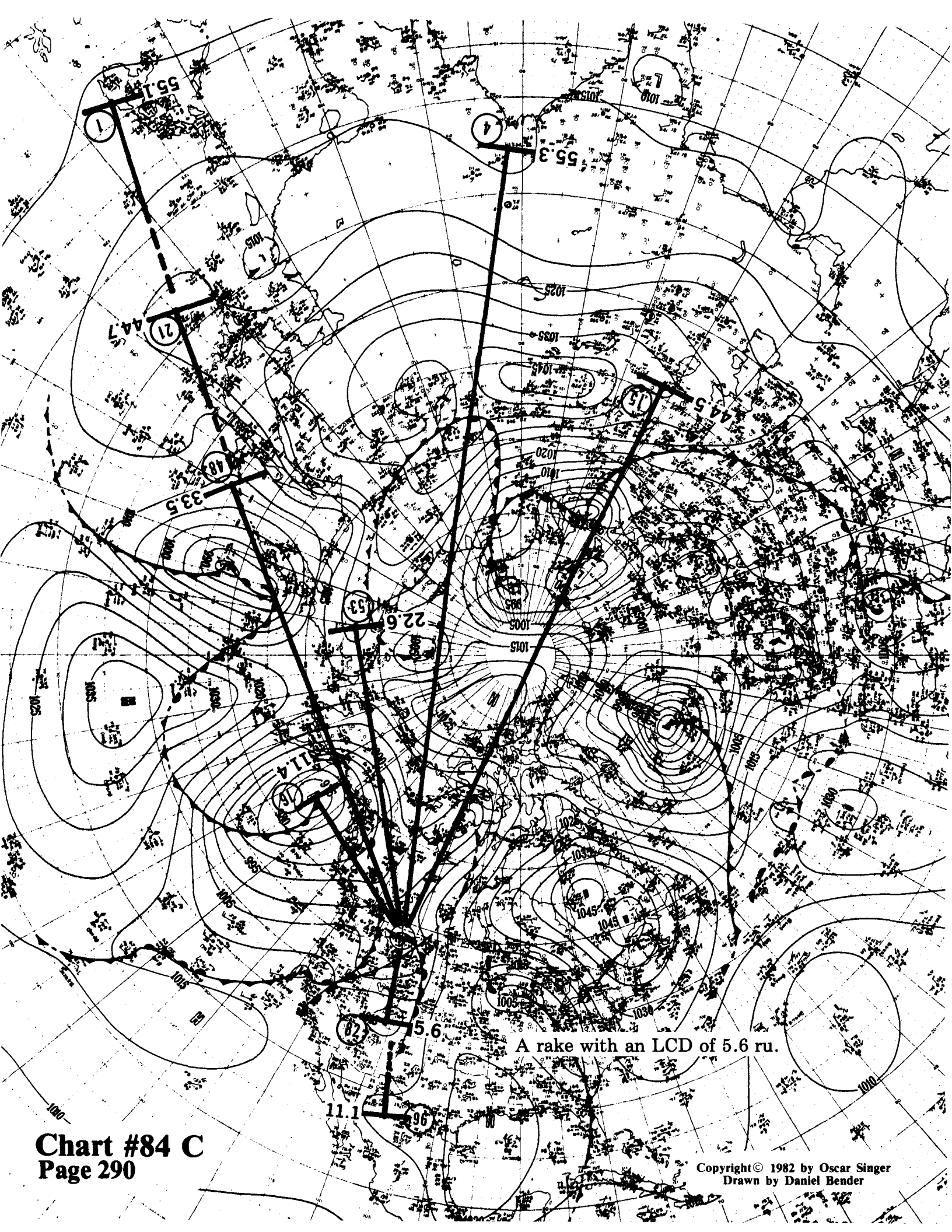
There are two different patterns on this chart which are not directly related. The first is the impressive and accurate straight line relation of #76 at 15.8 ru doubling to 31.5 ru at #50.

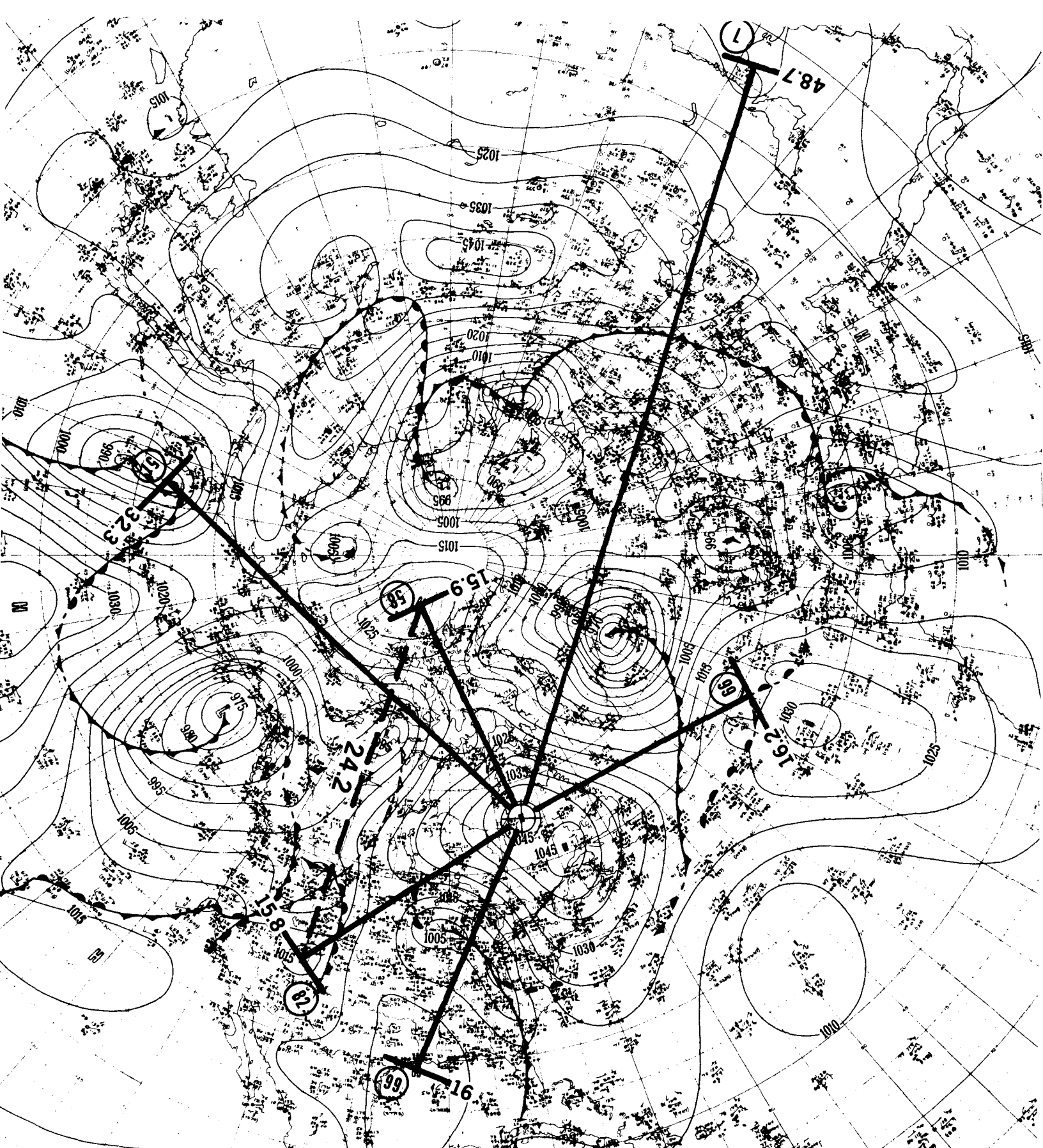
The second cluster, with an LCD of 8.5 ru, has a +X axis along #99 and a +Y axis near #70, with a "V" type spray along the Y axis. The angles between the "V" spray rays look visually symmetrical.



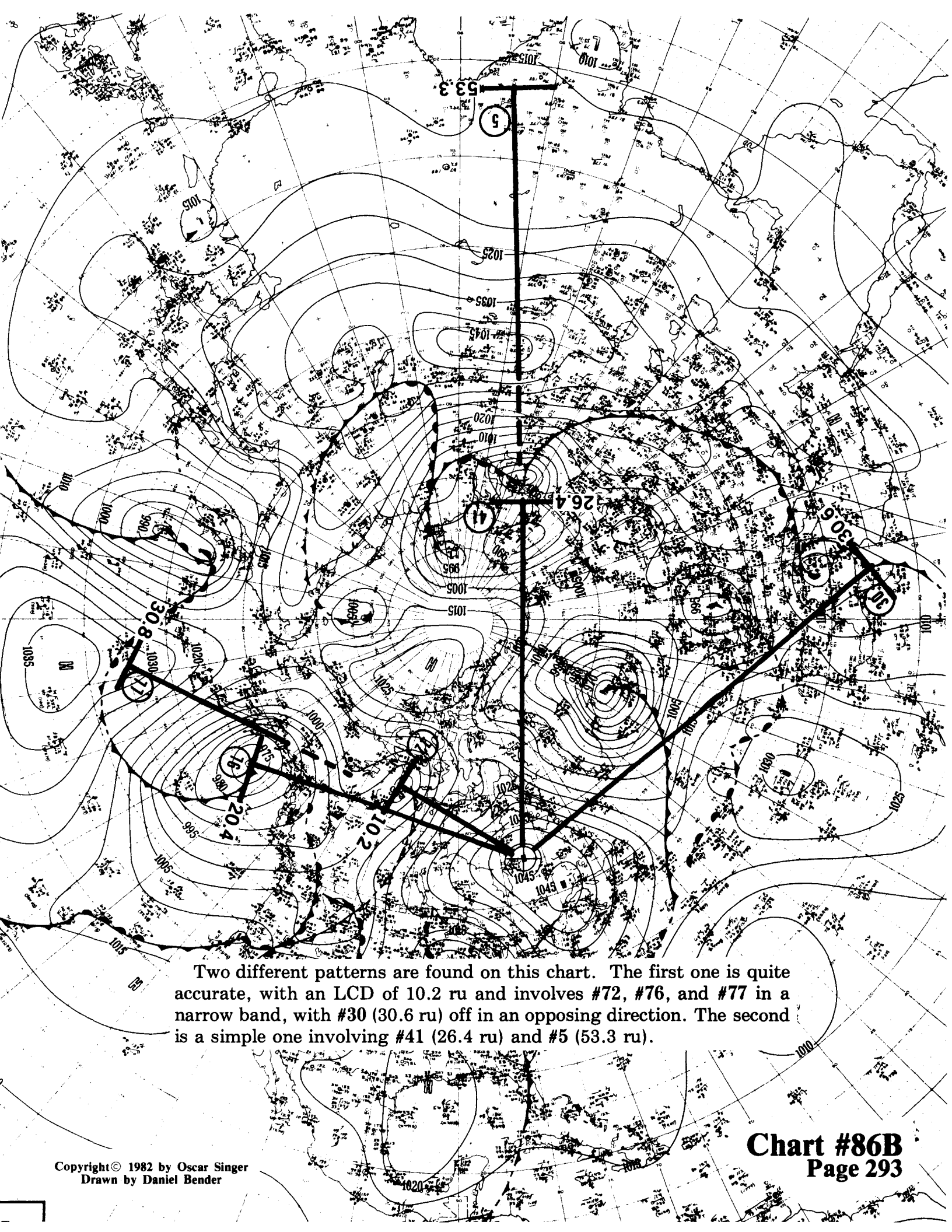
This sample operates on an LCD of 5.5 ru. The hard-core of this pattern is the balancing of #84 (5.6 ru) opposite to #96 (5.5 ru); and the balancing of #80 (11 ru) opposite to #91 (10.8 ru)—all close in to the center. Visual inspection shows #96, #82, #84, #57, and #44 clustering into one narrow beam, while #80, #82, #94, #91, #87, #90, and #63 all clustering into another beam (just not so narrow).

A two-axis formation with an LCD of 12 ru.

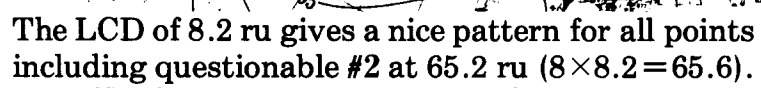


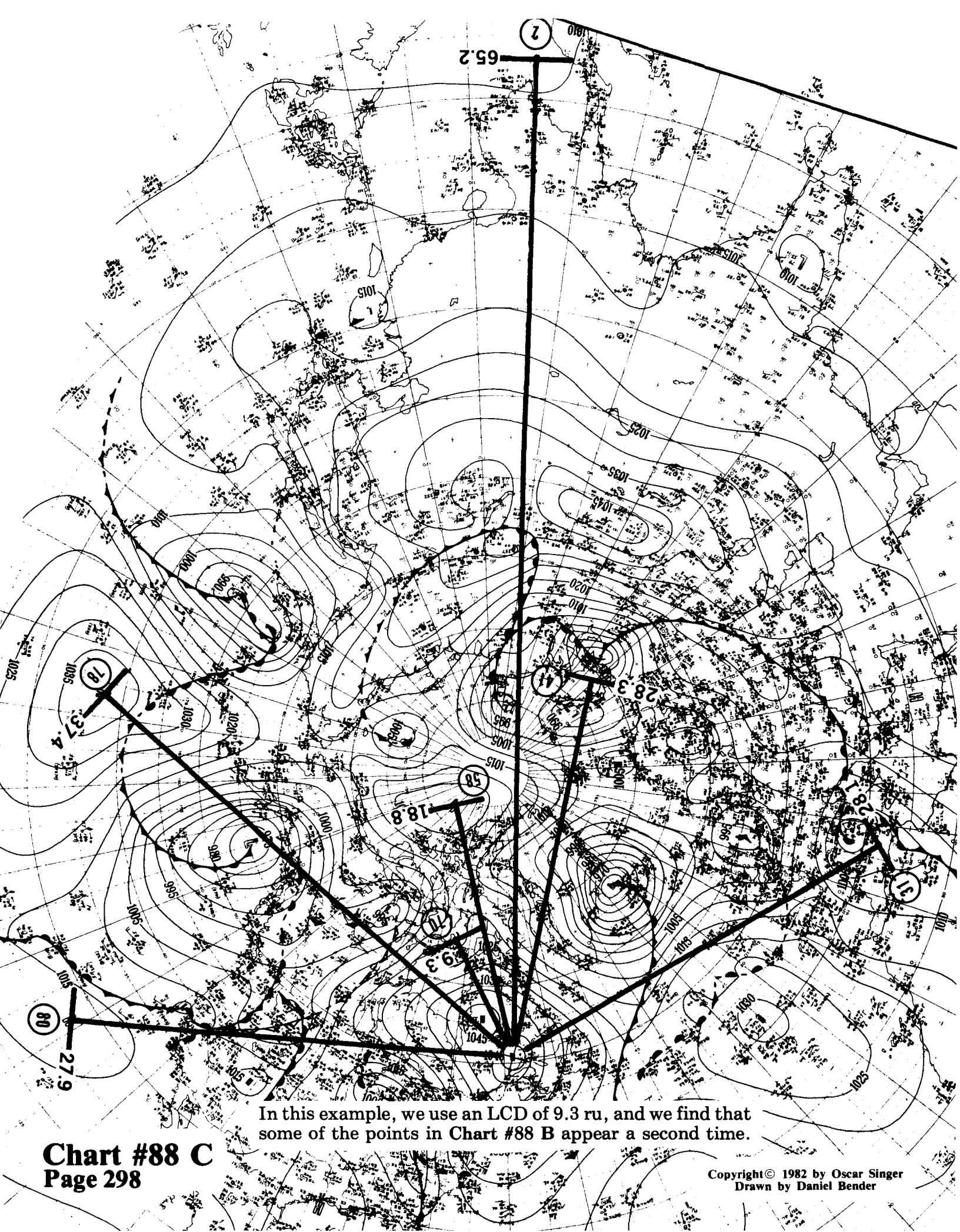


This is a good example with four points at an average of 16 ru. We also have one triangle formed with sides of 15.9, 15.8, and 24.2 ru, which gives a close ratio of 2:2:3.



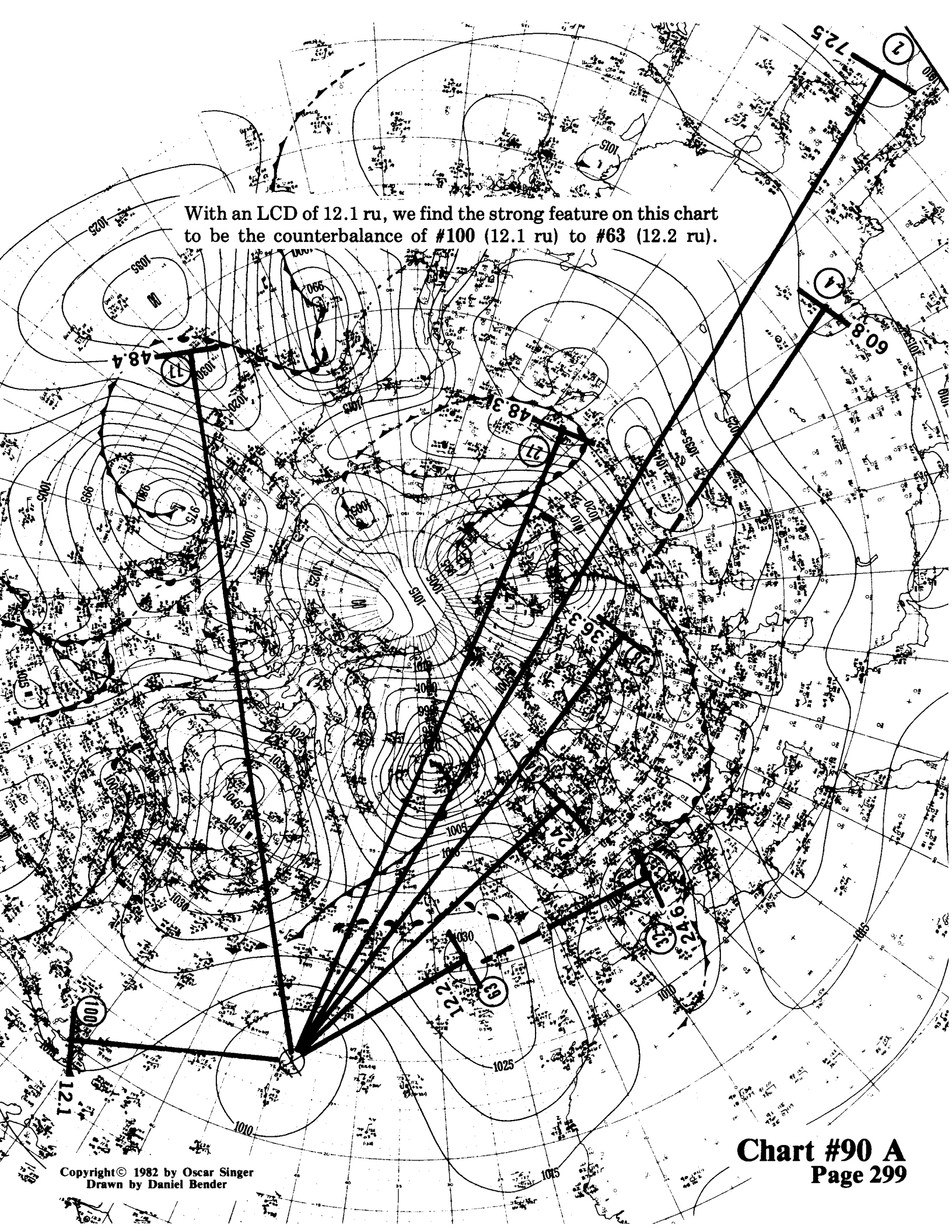
Two different patterns are found on this chart. The first one is quite accurate, with an LCD of 10.2 ru and involves #72, #76, and #77 in a narrow band, with #30 (30.6 ru) off in an opposing direction. The second is a simple one involving #41 (26.4 ru) and #5 (53.3 ru).

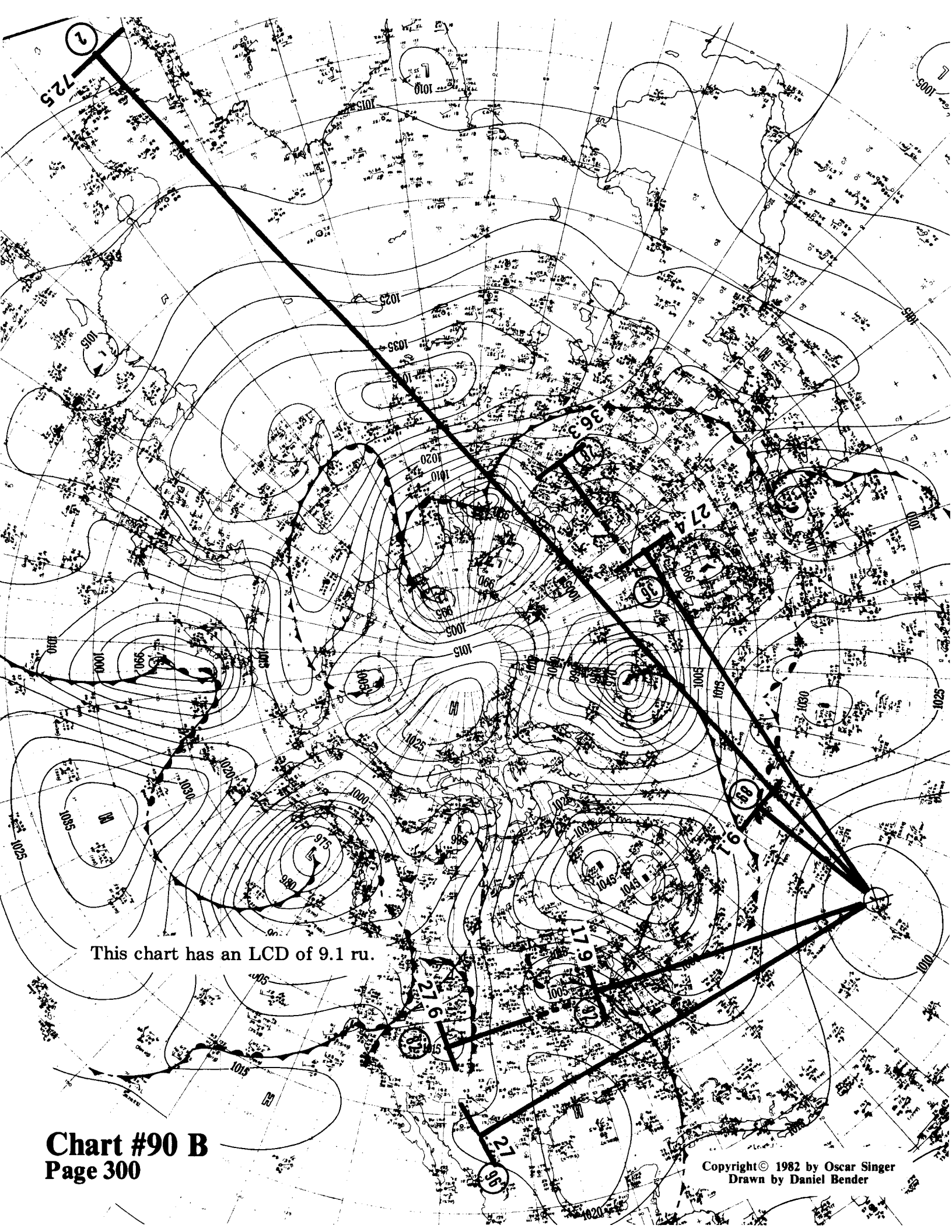




In this example, we use an LCD of 9.3 ru, and we find that some of the points in Chart #88 B appear a second time.

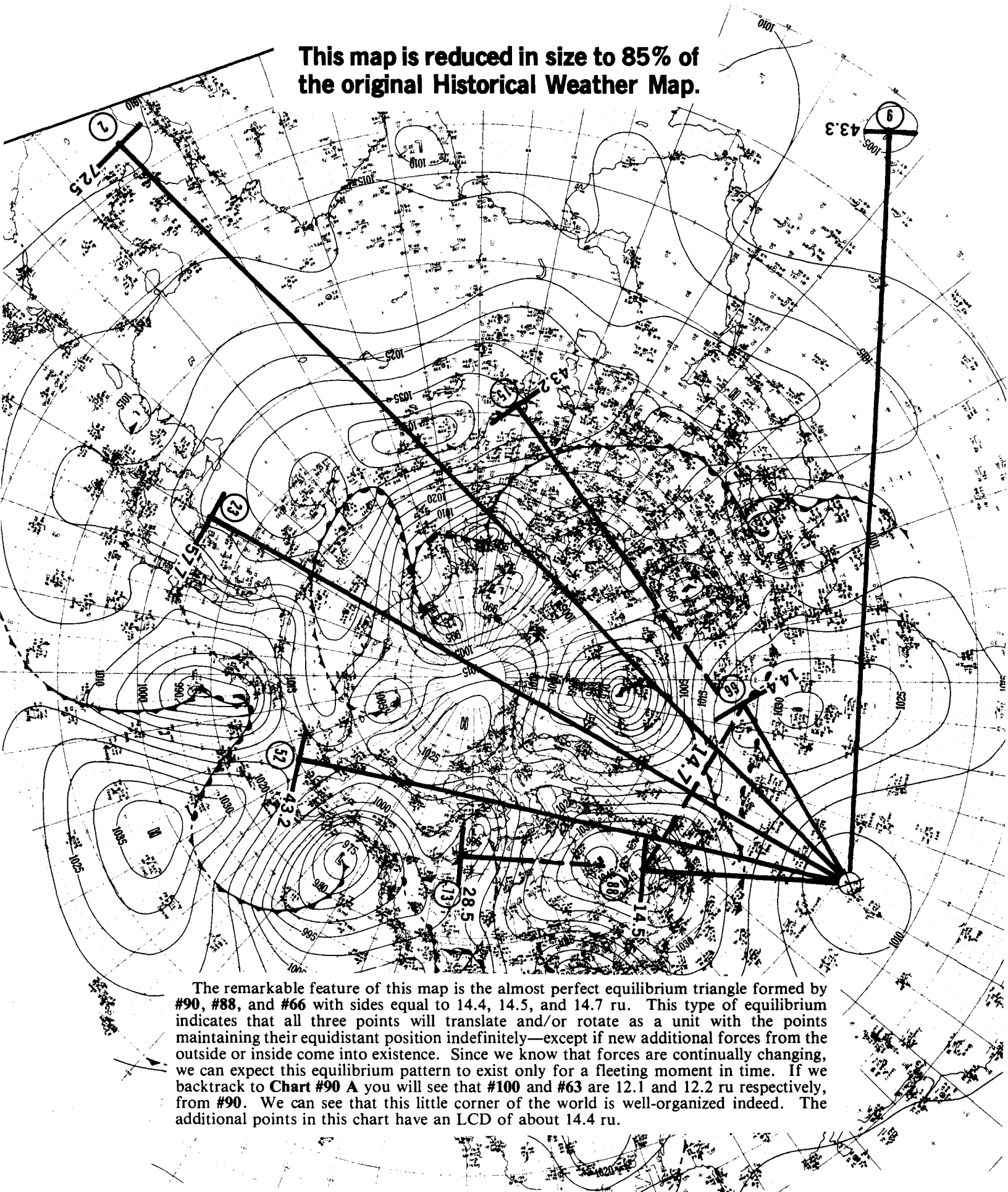
With an LCD of 12.1 ru, we find the strong feature on this chart to be the counterbalance of #100 (12.1 ru) to #63 (12.2 ru).



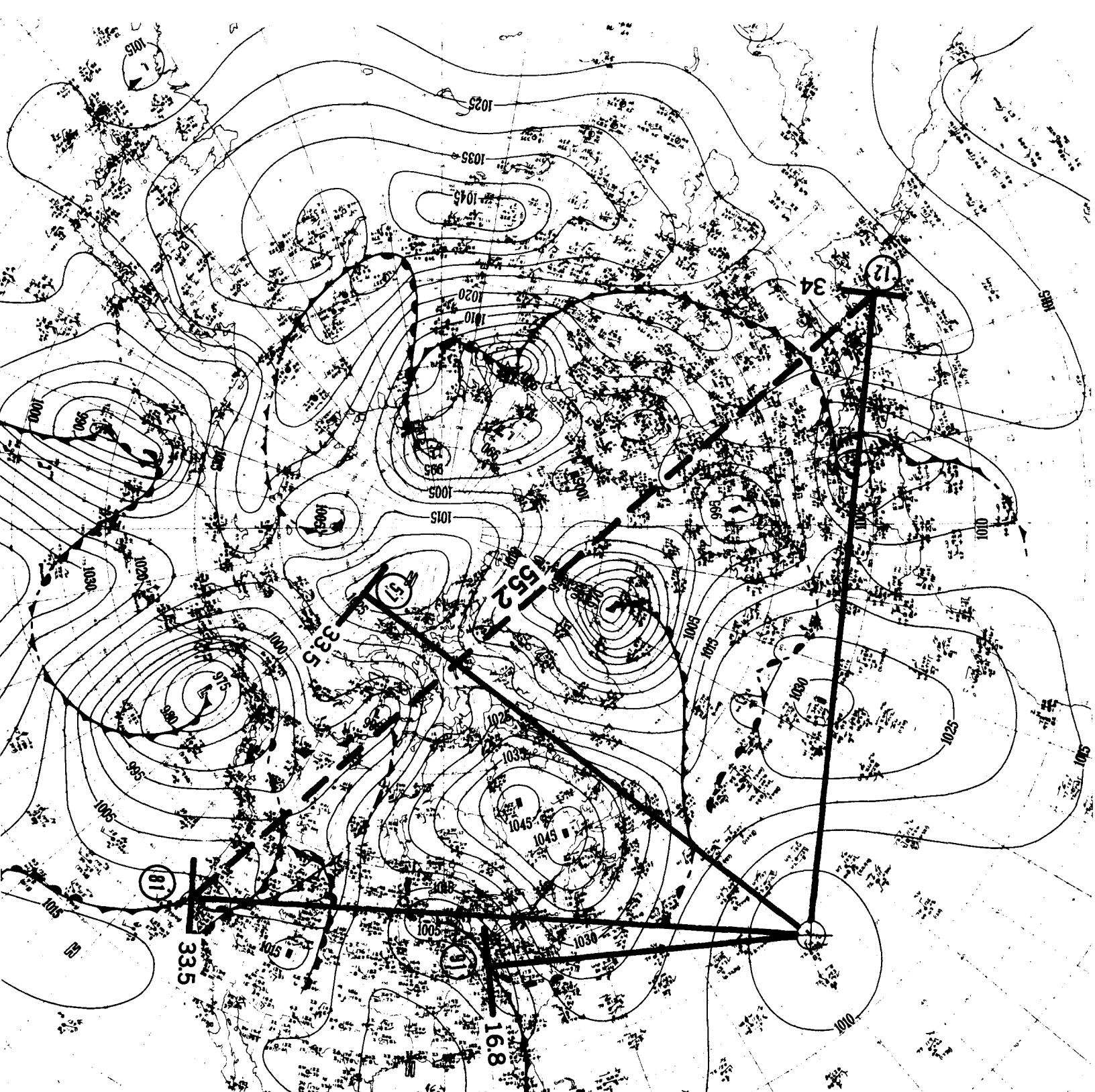


This chart has an LCD of 9.1 ru.

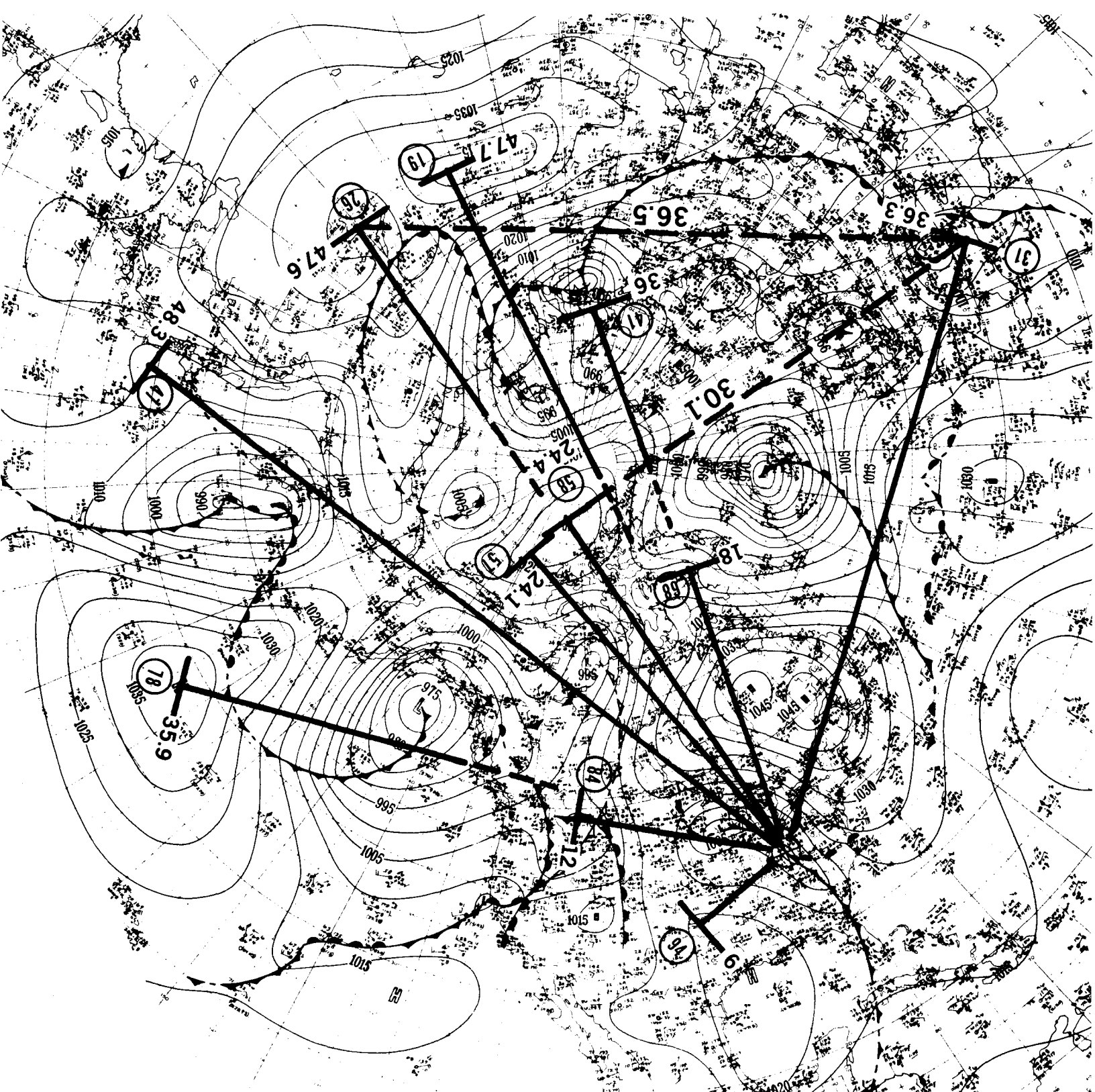
This map is reduced in size to 85% of the original Historical Weather Map.



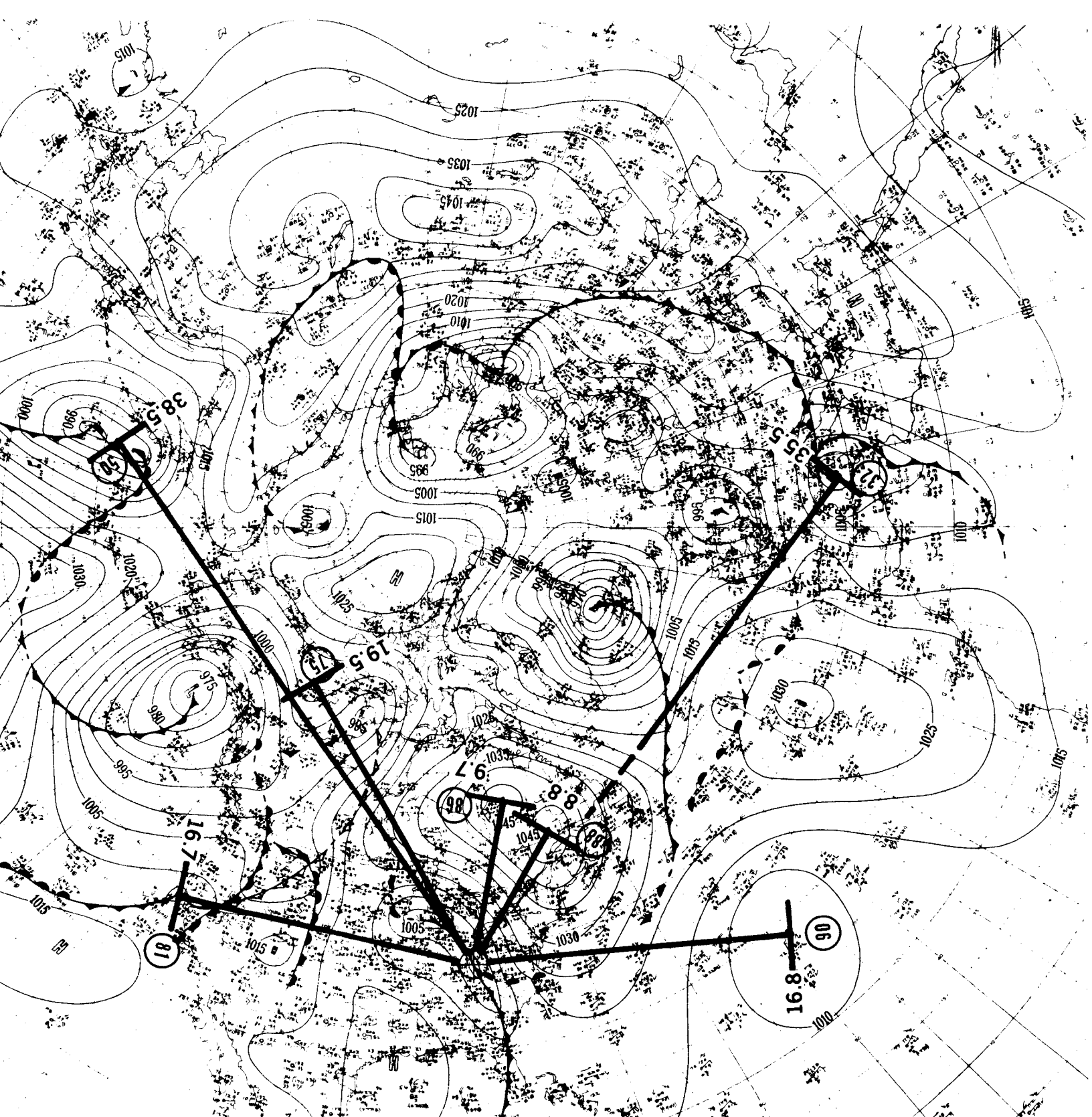
The remarkable feature of this map is the almost perfect equilibrium triangle formed by #90, #88, and #66 with sides equal to 14.4, 14.5, and 14.7 ru. This type of equilibrium indicates that all three points will translate and/or rotate as a unit with the points maintaining their equidistant position indefinitely—except if new additional forces from the outside or inside come into existence. Since we know that forces are continually changing, we can expect this equilibrium pattern to exist only for a fleeting moment in time. If we backtrack to Chart #90 A you will see that #100 and #63 are 12.1 and 12.2 ru respectively, from #90. We can see that this little corner of the world is well-organized indeed. The additional points in this chart have an LCD of about 14.4 ru.



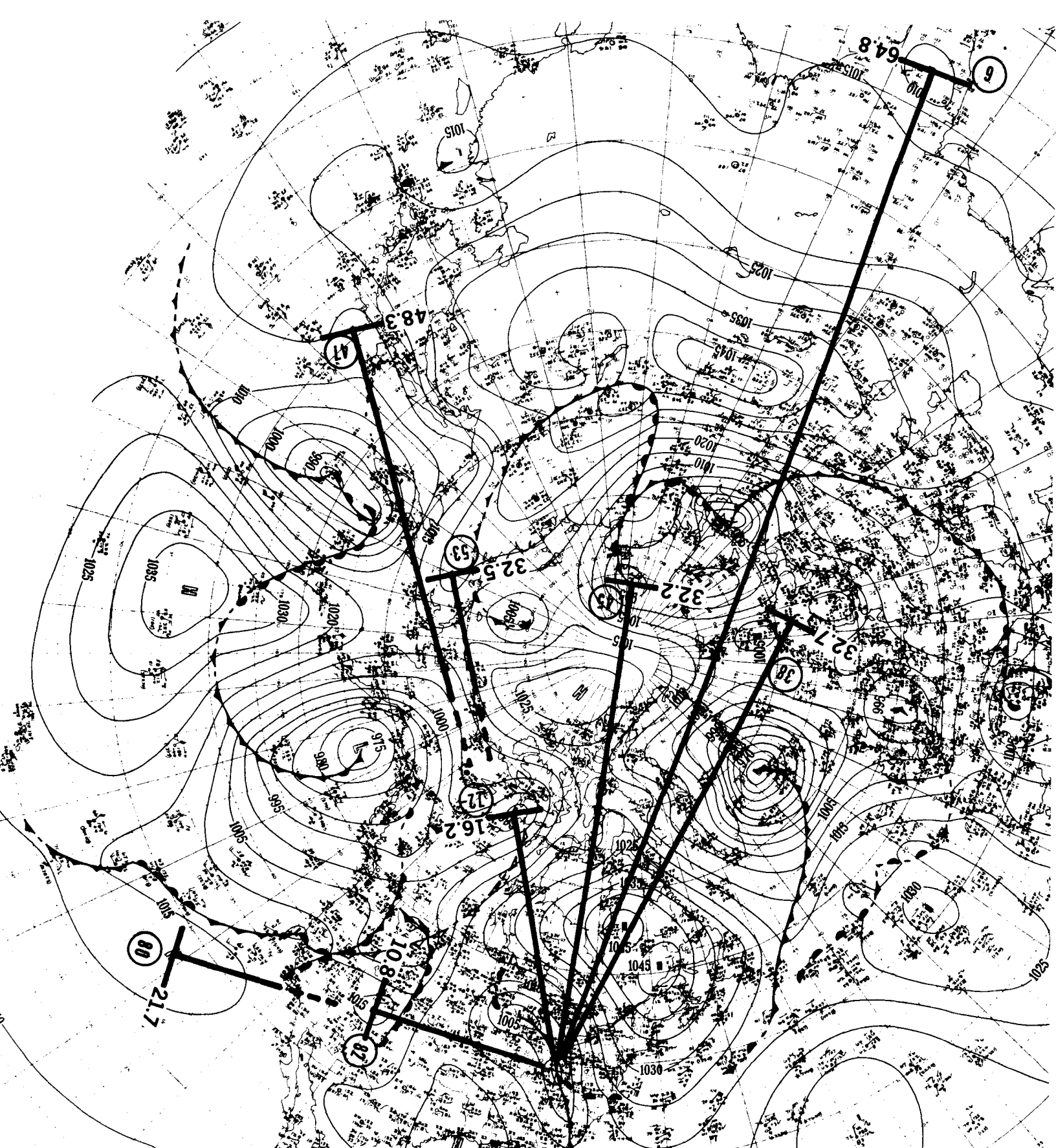
An LCD of 16.8 ru is used to create this chart. The lengths of the sides of the triangle formed by points #90, #81, and #12 are 33.5 ru ($3 \times 11 = 33$), 34 ru ($3 \times 11 = 33$), and 55.2 ru ($5 \times 11 = 55$). In this case a different LCD of 11 ru is used for the sides of the triangle than the one used to create the chart.



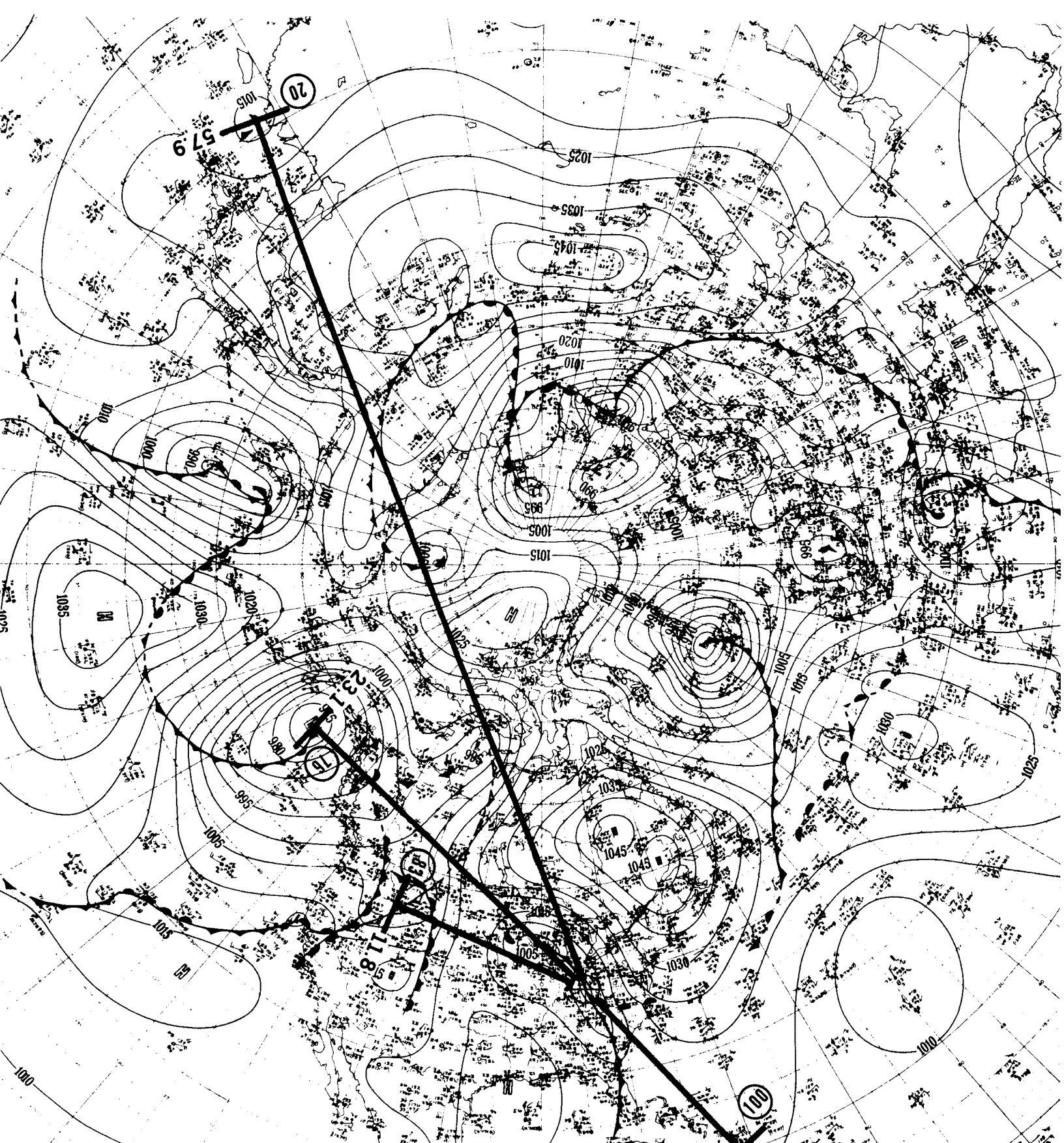
The LCD used in this sample is 6 ru. First, we find that the larger triangle formed by #91, #31, and #26 has sides of 36.3, 36.5 and 46.7 ru, which is in the ratio of 3:3:4. We have another triangle formed by #91, #58, and #31 with sides of 24.1, 30.1, and 36.3 ru, which is in the ratio of 4:5:6. Another strong feature is the well-defined distance of 12 ru (#84) tripling to 35.9 ru (#78).



This chart has three separate LCD numbers, which are not directly related. First, #81 (16.7 ru) balances #90 (16.8 ru)—practically perfect. Second, #88 (8.8 ru) is quadrupled (almost) at #32 (35.5 ru). Third, #86 at 9.7 ru doubles to 19.5 ru at #75, and then quadruples (almost) to 38.5 ru at #50.



An LCD of 10.8 ru (or 5.4 ru) is used in this example. The strongest feature on this chart is #82 at 10.8 ru doubling to 21.7 ru at #80.



In this example, an LCD of 11.5 ru is used.

AP
HERE
GMT

Y. MOD
SHIP. S

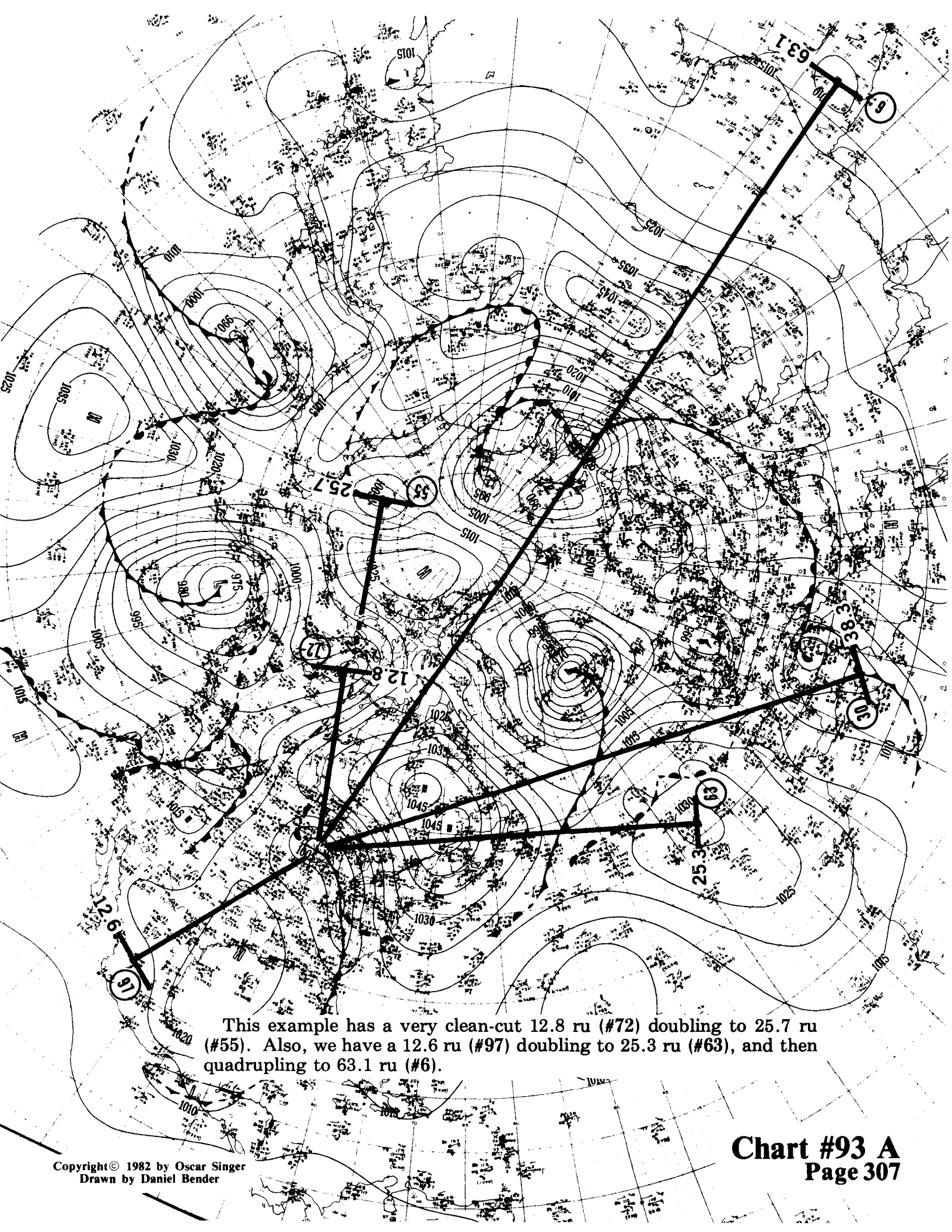
Y. MOD
SHIP. S

Y. MOD
SHIP. S

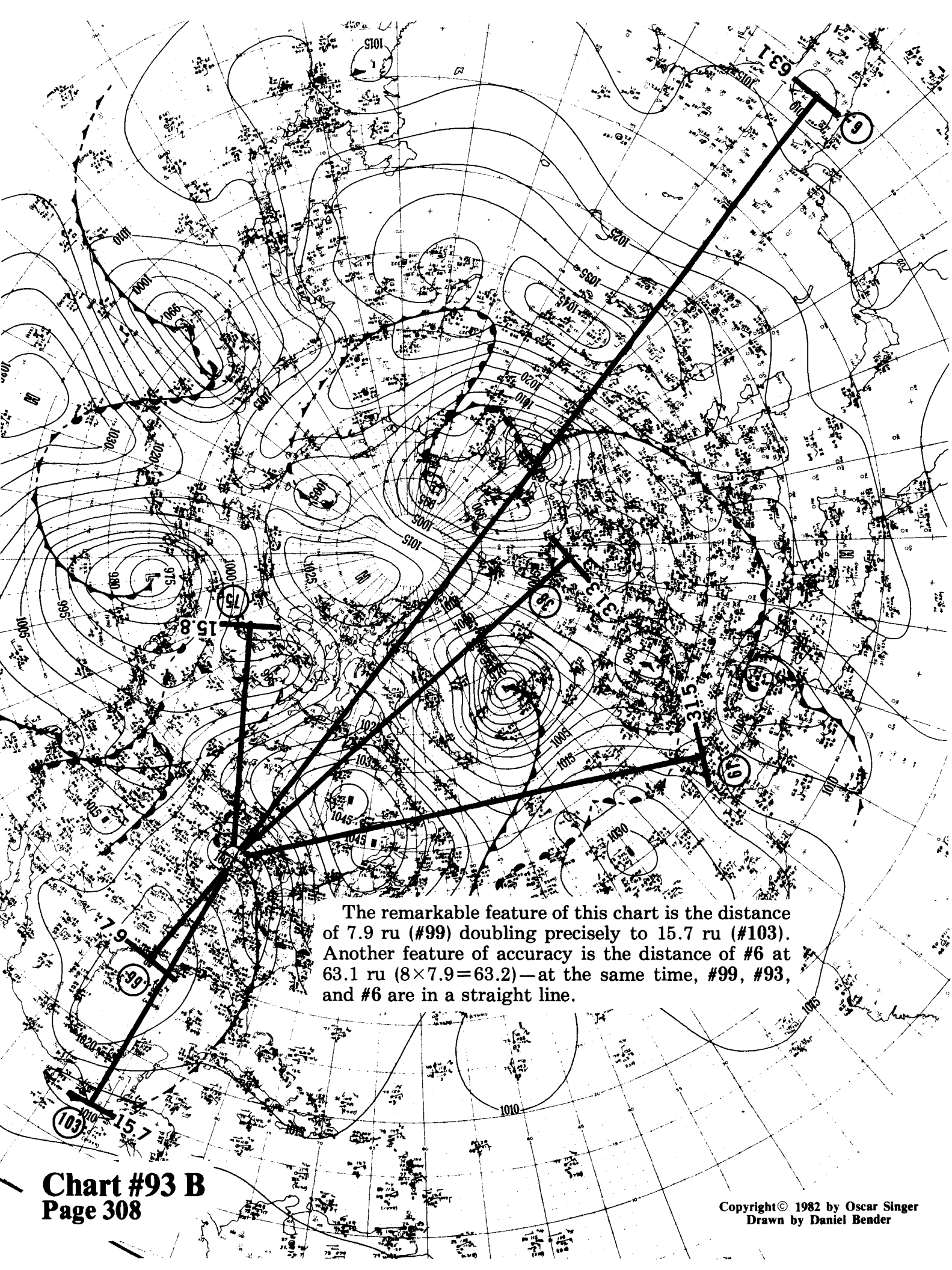
Y. MOD
SHIP. S

Chart #91 D
Page 306

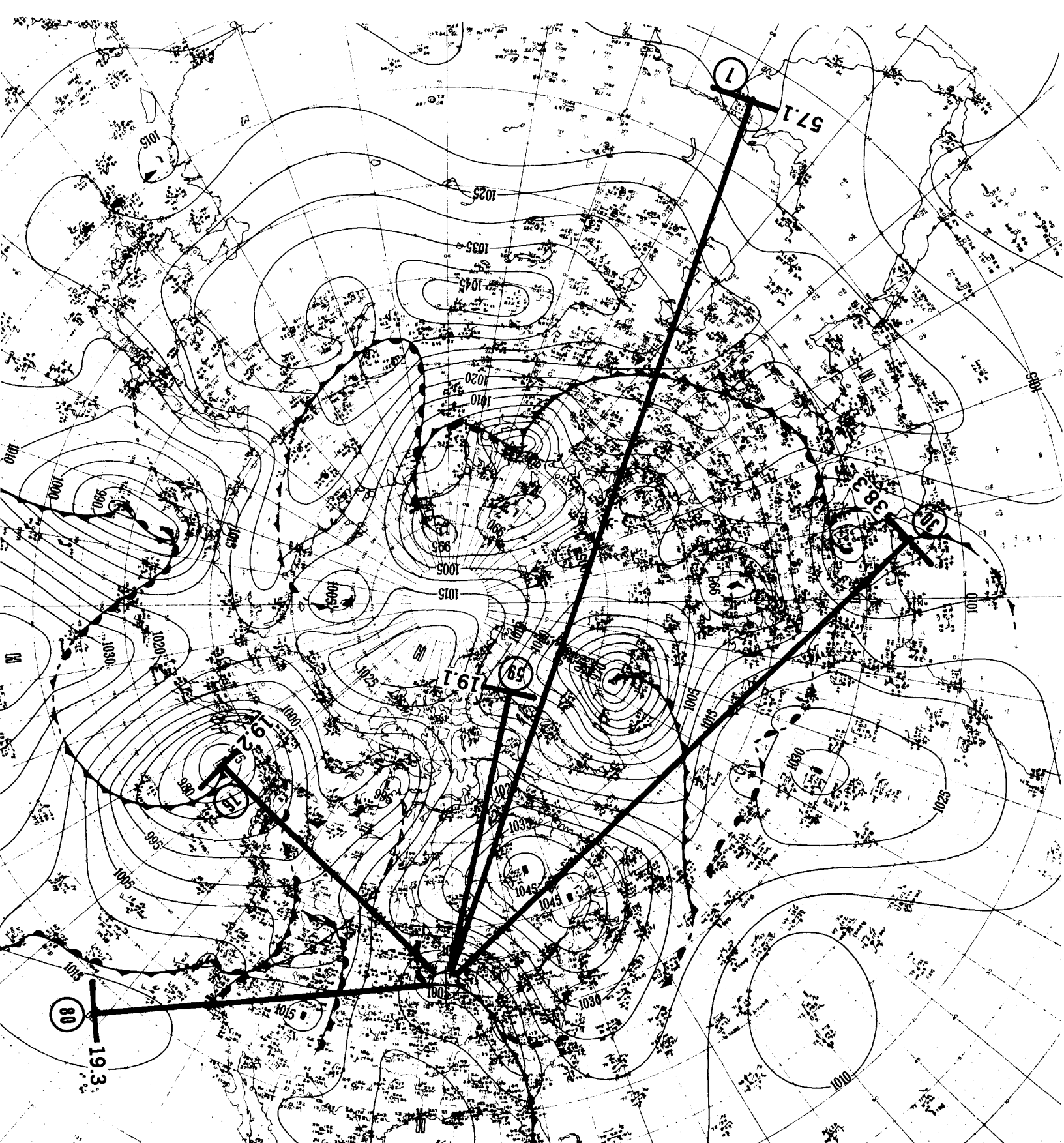
Copyright© 1982 by Oscar Singer
Drawn by Daniel Bender



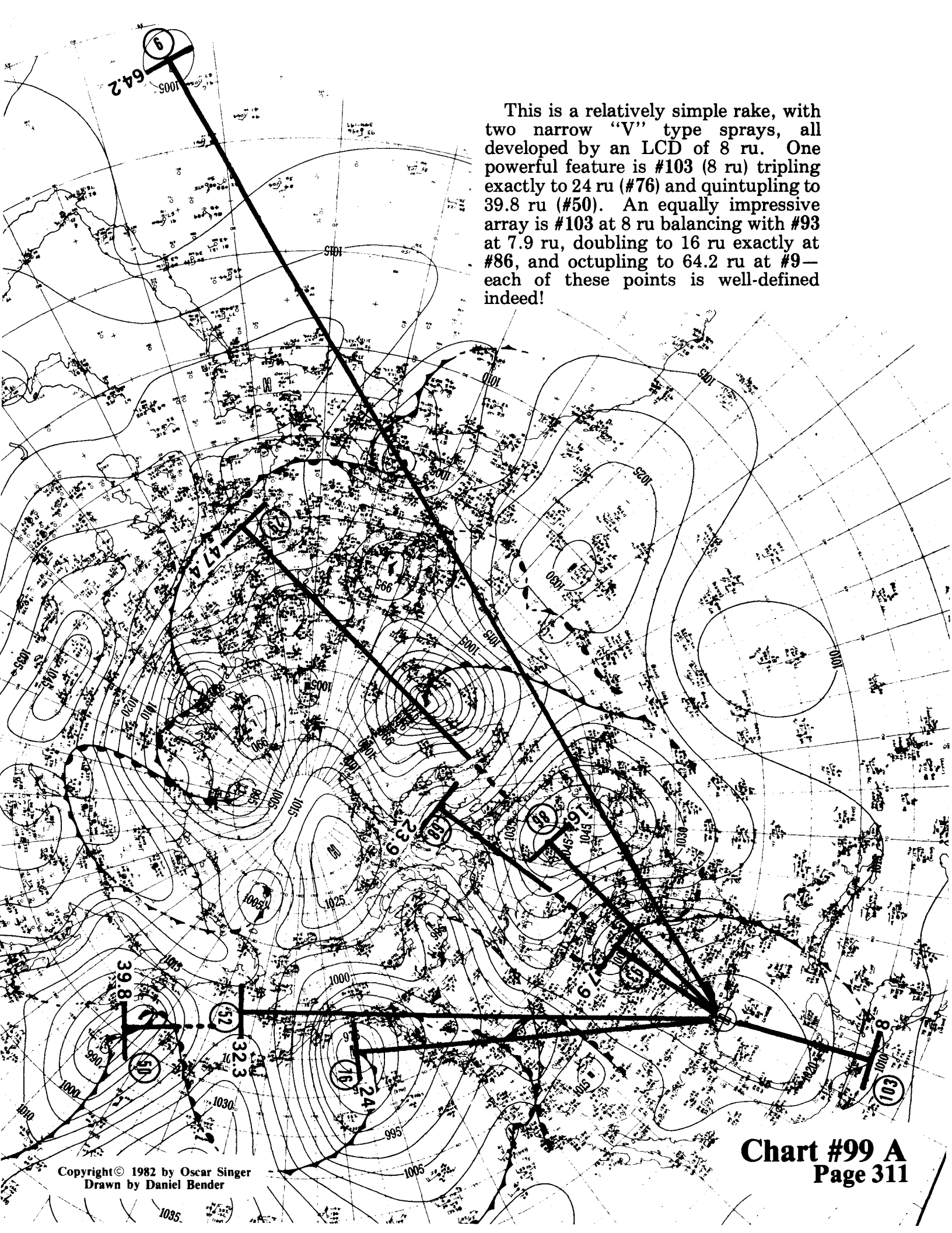
This example has a very clean-cut 12.8 ru (#72) doubling to 25.7 ru (#55). Also, we have a 12.6 ru (#97) doubling to 25.3 ru (#63), and then quadrupling to 63.1 ru (#6).



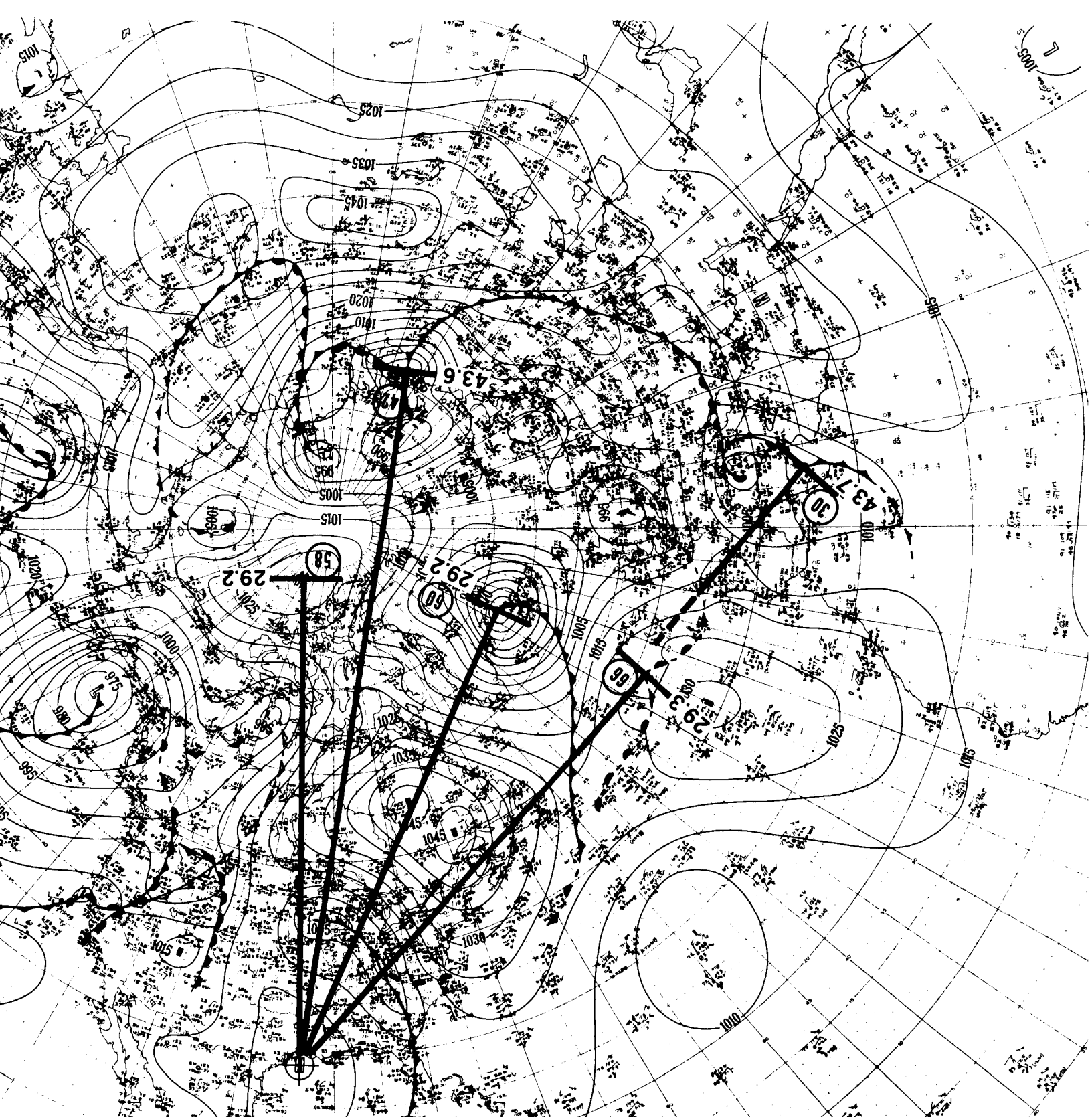
The remarkable feature of this chart is the distance of 7.9 ru (#99) doubling precisely to 15.7 ru (#103). Another feature of accuracy is the distance of #6 at 63.1 ru ($8 \times 7.9 = 63.2$) — at the same time, #99, #93, and #6 are in a straight line.



This example has the recurrent theme of three symmetrically placed points (#80, #76, and #59) around the central point.

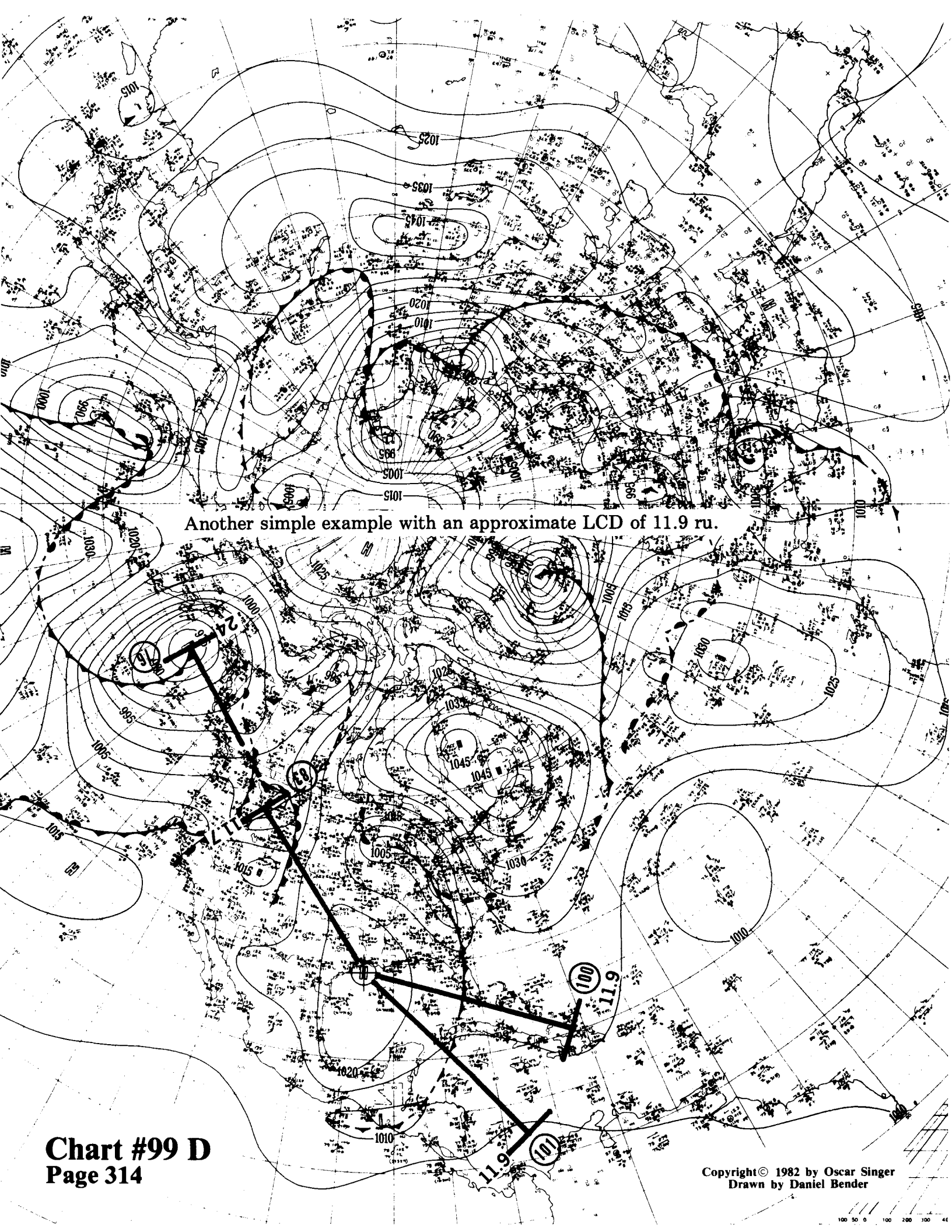


This is a relatively simple rake, with two narrow "V" type sprays, all developed by an LCD of 8 ru. One powerful feature is #103 (8 ru) tripling exactly to 24 ru (#76) and quintupling to 39.8 ru (#50). An equally impressive array is #103 at 8 ru balancing with #93 at 7.9 ru, doubling to 16 ru exactly at #86, and octupling to 64.2 ru at #9—each of these points is well-defined indeed!



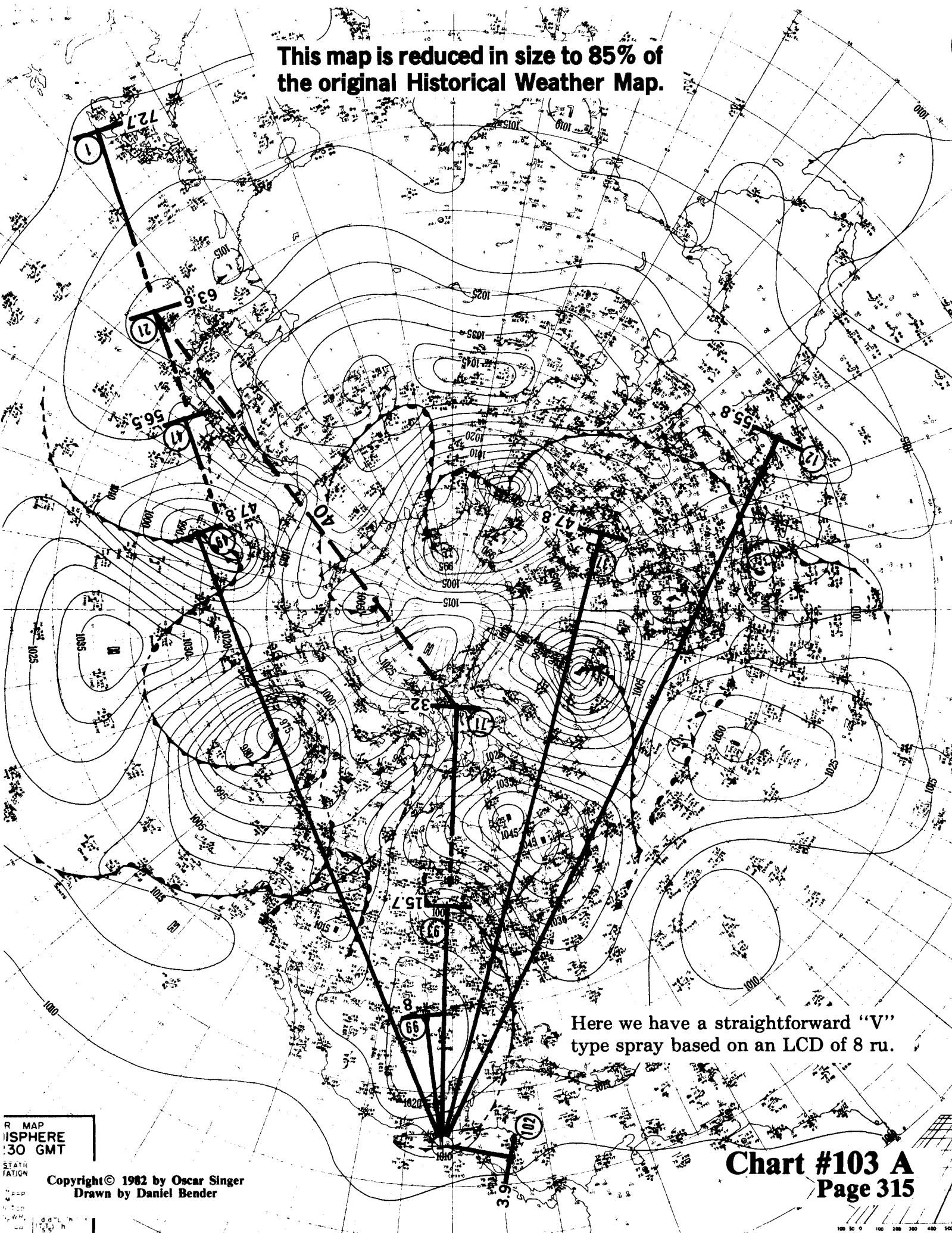
With an LCD of 14.6 ru, we get the familiar pattern of three symmetrically spaced points. The distance out is astonishingly similar—29.2, 29.2, and 29.3 ru. The precision of this pattern carries through to #42 (43.6 ru) and #30 (43.7 ru). This pattern is special because the location of each point is well-defined.

Chart #99 C
Page 313



Another simple example with an approximate LCD of 11.9 ru.

This map is reduced in size to 85% of the original Historical Weather Map.



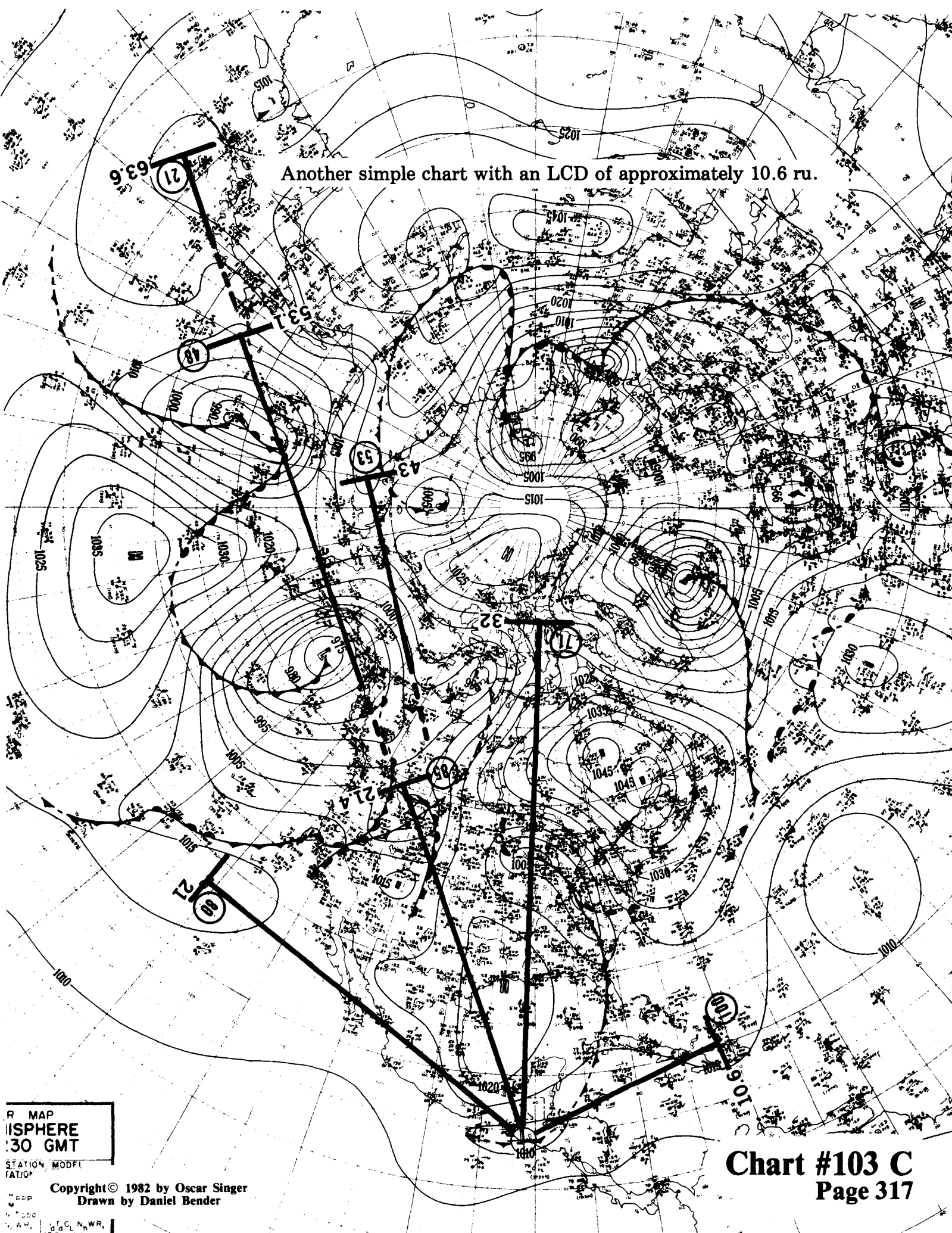
Here we have a straightforward "V" type spray based on an LCD of 8 ru.

R MAP
ISPHERE
30 GMT
STAT
ATION
Copyright © 1982 by Oscar Singer
Drawn by Daniel Bender

Chart #103 A
Page 315

100 30 0 100 200 300 400 500

Another simple chart with an LCD of approximately 10.6 ru.

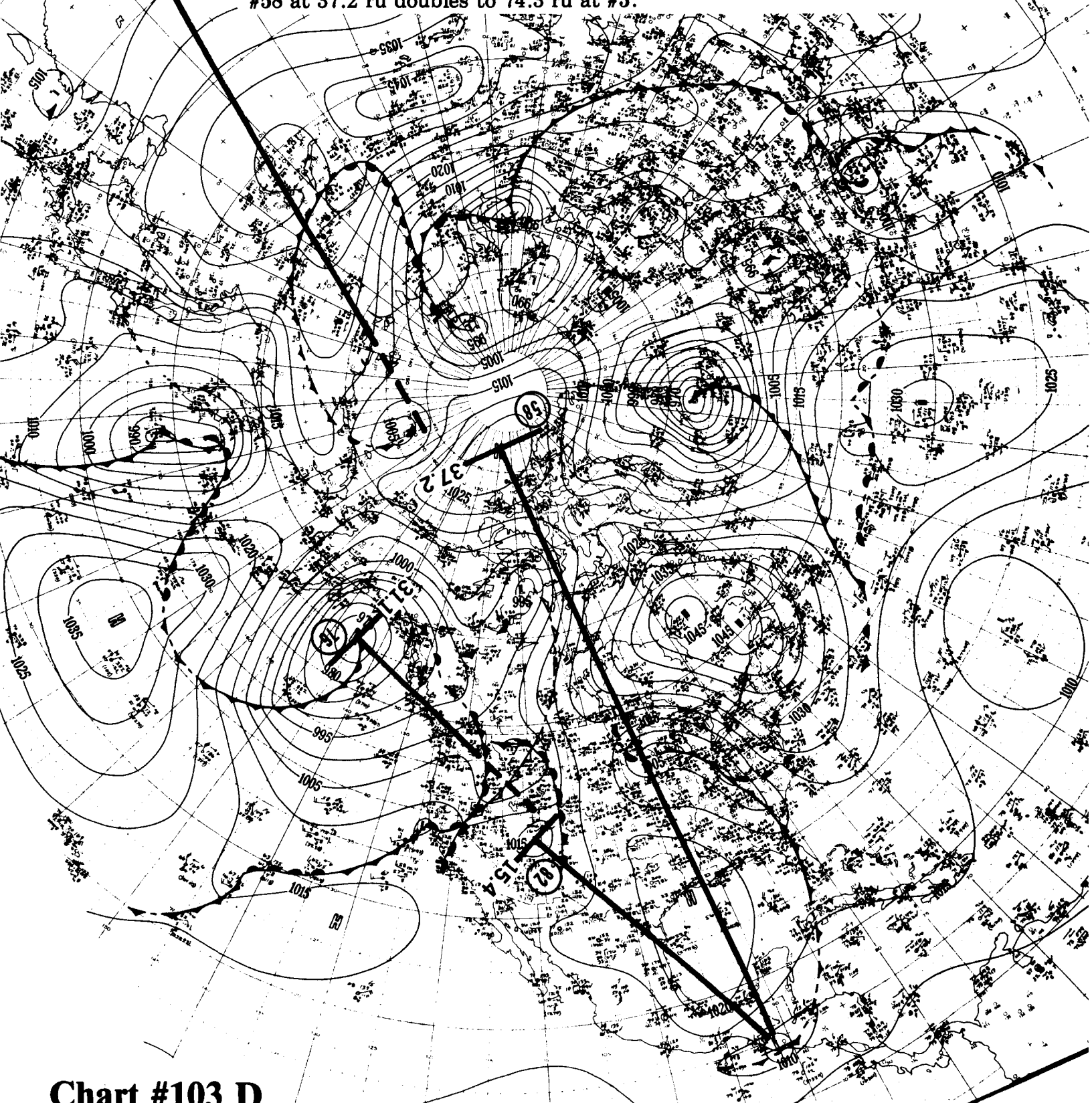


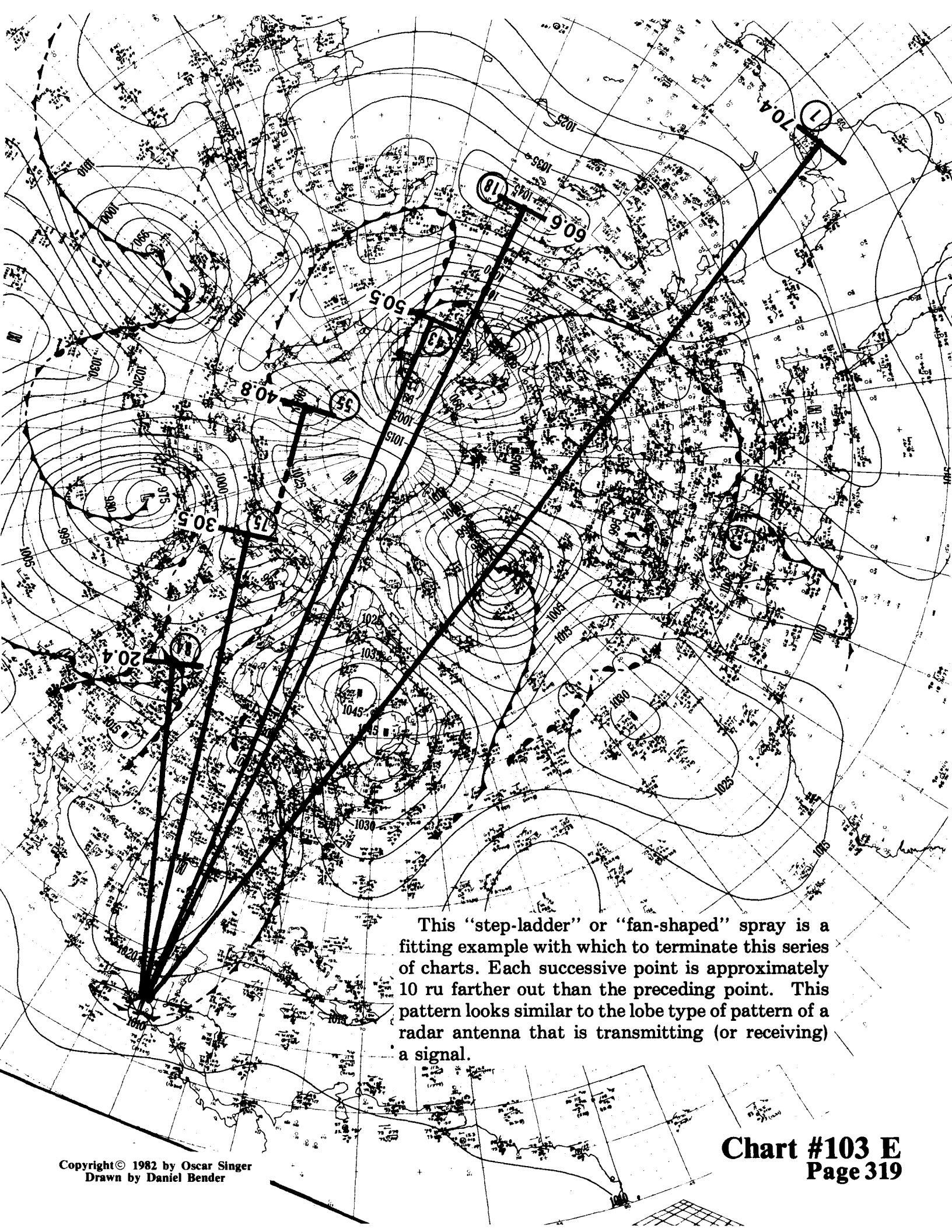
R MAP
SPHERE
30 GMT
STATION, MODFI
SATUR

Copyright © 1982 by Oscar Singer
Drawn by Daniel Bender

Chart #103 C
Page 317

Two separate groups are combined on this chart. First, we have #82 at 15.4 ru becoming slightly more than double at #76 with 31.1 ru. Second, #58 at 37.2 ru doubles to 74.3 ru at #3.





This "step-ladder" or "fan-shaped" spray is a fitting example with which to terminate this series of charts. Each successive point is approximately 10 ru farther out than the preceding point. This pattern looks similar to the lobe type of pattern of a radar antenna that is transmitting (or receiving) a signal.

Chapter 14

June 6, 1944

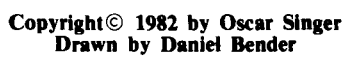
I drew two circumferential patterns for D-day (June 6, 1944), with the nuclear center being the storm that was the focus of attention in the invasion of Europe. Both circumferential patterns are essentially the same, but they highlight different variations of circumferential angular numbers.

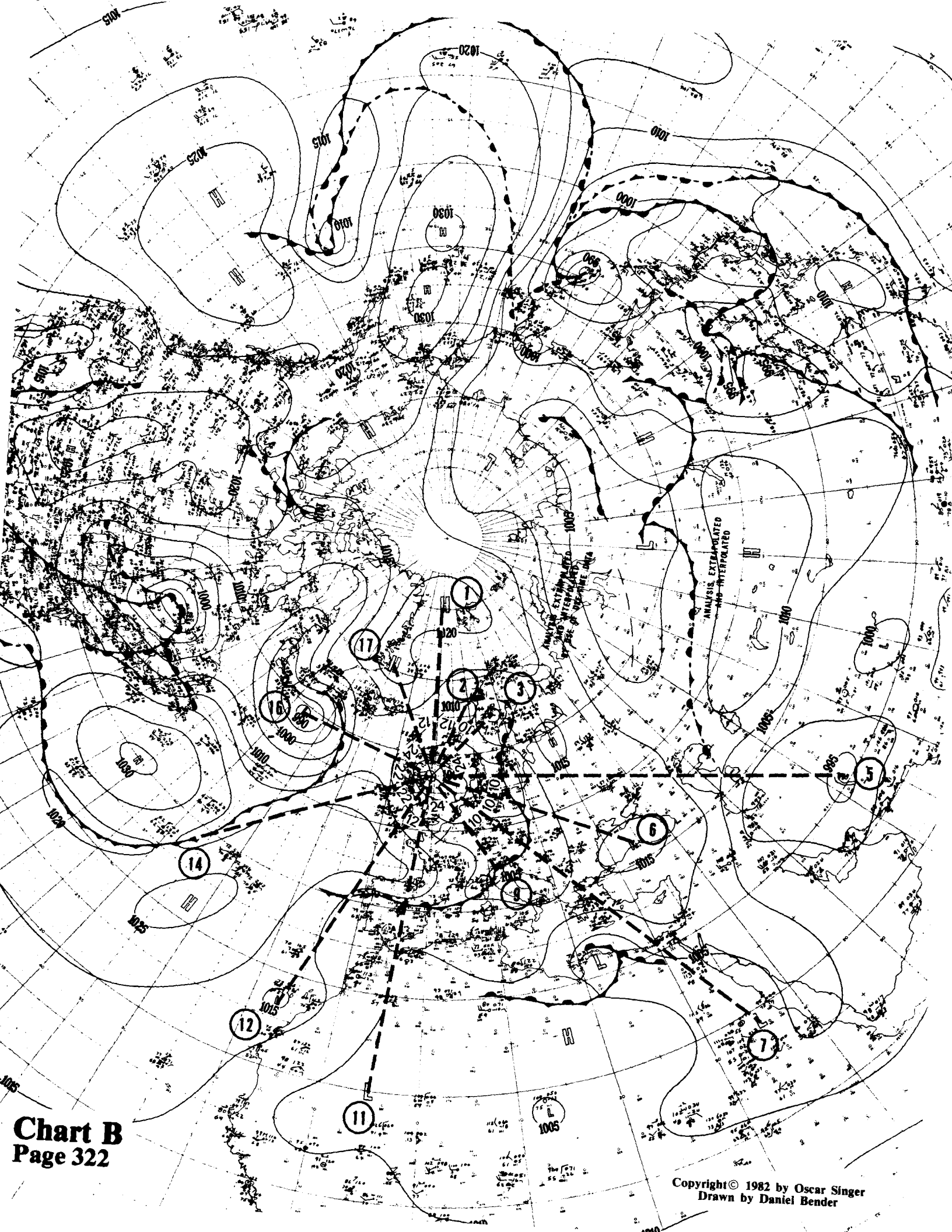
The hard-core and incontrovertible features of these charts are:

1. 12 cu between #15 and #16.
2. 24 cu between #16 and #17.
3. 12 cu between #17 and #1.
4. 12 cu between #1 and #2.
5. 24 cu between #9 and #11.
6. 12 cu between #11 and #12.

The other points on the charts are very good indeed, but the ones listed above are generally close to the nuclear vortex, and have easy to identify centers.

Is it possible that the Allied High Command arranged all these vortexes in a military formation, as indicated above, as an aid in the invasion?





Chapter 15

Some Firsts in Meteorology

I have expressed wavenumber (or wavelength) as angular radial units (ru) or angular circumferential units (cu) throughout the charts in this book. Wavenumber has been used heretofore in meteorology as a rough measure of the type of circulation; for example, strong westerly flow in the mid-latitudes has been thought to represent a low wavenumber (high ru or cu) or long wavelength; weaker westerly flow with a predominance of north-south flow has been thought to be associated with high wavenumber (low ru or cu). Wavenumber is frequently mentioned in the meteorological literature and especially in the laboratory models that use rotating tables to simulate the Bénard experiment (in attempts to duplicate some of the features of the Earth's atmosphere). Wavenumber is used for short and medium-range forecasting through the use of the Rossby equation and its modifications. Changes in wavenumber have been considered important since they result in big changes in hemispheric flow patterns. It has been found that the wavenumber varies when there is a change in the temperature variation from one latitude to another.

The use and description of wavenumbers has been surrounded by limitations, some of which are as follows:

1. It is generally considered as a **statistical average** for a week, a month, a year, etc.
2. It is generally analyzed for the first 50,000 to 60,000 feet.
3. It is often measured at certain fixed latitudes, such as the wavenumber along latitude 30°, 40°, or 50°, etc.

From the above thumb-nail sketch of the history of wavenumber, it is

obvious that the concept of wavenumber is of no surprise in meteorology.

The big surprise is how the concept of wavenumber (described as ru and cu) is used in *Singer's Lock*. The following is a listing of some of the *firsts* in meteorology contained in this book:

1. Straight lines have never been used on a polar stereographic weather map (for the distances I use) in analysis, in forecasting, or in research to merely understand what is happening. Before you can hope to solve the forecast problem in all its details, you must first understand what is happening. An explanation and/or understanding of what is happening or of what has already happened is desirable for its own sake. Moreover, if you understand what is happening, the forecast rules might just be obvious. In addition, the charts in this book represent practical examples on how to actually use straight lines. A similar analysis can be made using only great circles instead of straight lines, but this is immensely more complex since we have to account for spherical excess when measuring spherical angles.

2. Empirical evidence has been given to show that over an entire hemisphere, highs, lows, and cols line up along arcs of small circles on the surface of the Earth. These small circles also line up in relation to each other at significant angles.

3. I do not calculate the wavenumbers as a statistical or average value, but calculate the exact wavenumber at the moment of time represented by the weather map being used.

4. The surface weather map is shown to be a most significant weather map to be used in analysis.

5. Highs and lows are considered as equal points in the procedures used.

6. No wavenumber calculations have ever been made that include obscure points like cols.

7. The calculations are made without any consideration of the size, shape, distance apart of the highs and lows—they are also independent of physical obstructions such as mountains.

8. Wavenumber can be calculated separately for the first time, around each and every high, low and col on the Earth. This includes a separate calculation for the cu and ru numbers.

9. The development of the "diffraction grating" type of tool has

opened the door to a maze of hidden, symmetrically shaped geometric configurations.

10. A significant *first*, is establishing the importance of locating the center of a high, low, or col. Virtually every meteorologist that I have talked to stated flatly to me, that the centers of highs and lows were not particularly significant. Well, the charts that you have seen could not have been produced without the painstaking location of centers as accurately as possible. The use of centers resolved the problem of how to make wavenumber calculations accurately and explain the spacing of all points on the map.

Chapter 16

Problems Following Discoveries

It is the fate of the human race to desperately desire improvements in the way of life, in health, in comfort, and convenience. Yet, when an improvement, of whatever nature, comes along there are quite often a few who are hurt or think that they will be hurt by it, whether true or not. As a consequence, any improvement in any area that is a major advance and not just something minor is confronted with suspicion, prejudice, ignorance, jealousy, ridicule, neglect, apathy, and dishonesty.

This type of situation is common in all phases of life, you name it: business, politics, family . . . It is therefore not surprising that it should also be found in science. However, it does come as a surprise to most people (with science generally considered as a sacred cow), that there should be less than honorable people in positions of leadership.

I will insert at this point a thumb-nail sketch of just a few illustrious moments in the history of science. The discoveries I mention here are only a few of the important ones that helped some of humanity to climb out of the muck and cold of the wilderness to a more comfortable way of life. I am picking a few isolated examples to make the point. I am sure some of my readers can supply more.

A man by the name of *Tartaglia* discovered the general mathematical solution for all forms of cubic equations. According to historical records, he was enticed by *Cardan* to reveal the solution. Cardan promptly published this solution in a book in 1545. Ever since that time it has been called the *Cardan solution of cubic equations*. Should it still be called Cardan's solution in the 20th Century?

The earliest investigator of close packing of objects in space was *Stephen Hales* who used peas. He wrote in his *Vegetable Staticks* in

1727: "I compressed several fresh parcels of Pease in the same Pot with a force equal to 1600, 800, and 400 pounds; in which Experiments, tho' the Pease dilated . . . and thereby formed into pretty regular Dodecahedra". *Buffon*, in 1753, said the same thing in his *Histoire Naturelle* but did not mention Hales. But oops, it is a matter of record that Buffon translated Hales' original work into French in 1735. So, any references to the "peas of Buffon", can be considered as *buffoonery*.

In 1842, *Frankenheim* discovered that there were only 14 different types of space lattices in the shapes of crystals, but he did not rigorously prove it. All he did was to discover something that was never seen or even *thought* of heretofore. A more detailed proof was given by *August Bravais* in 1848 and the 14 lattices are therefore usually called the *Bravais lattices*. This, however, is not the fault of Bravais.

Goldberger discovered the cause and cure of pellagra but was crushed by an "official" investigating team, and unfortunately he died before his experiments were finally verified.

To come into modern times we find a fascinating article on page 673 of *Science* Vol., 205, August 17, 1979, with the title of "Tracing Burt's Descent to Scientific Fraud". A writer of an authorized biography has verified that he engaged in deliberate deception, falsely constructed research data, and also invented nonexistent "colleagues" to confirm his theories about intelligence.

I can go on and on about many other *nefarious* "happenings" in the history of science at many different times and places, but the above is sufficient for now.

I have read any number of times that some major advances in various fields of science have been discovered at about the same time by different people or different groups of people. These supposedly simultaneous discoveries require a little scrutiny in view of the real facts of life.

The main reason for adding this chapter in this first book is to establish for the record that I had attempted to have some of the material in this book published as early as 1976. Some of the evidence of my attempts is discussed in the preface. But I will now quote from a letter dated December 11, 1978, that I received from *Kenneth C. Spengler*, Executive Director of the *American Meteorological Society*, who felt that he closed this matter with his letter. This is entered as a

protection against claims of prior discovery.

"After further review of Dr. Sanders' (Focus on Forecasting Editor's) letter of 10 October, I fully support his decision not to accept your paper for the Bulletin.

So far as I am concerned, this matter has been thoroughly reviewed and this decision is final. I see no reason for any further discussion or correspondence."

There is no incentive for the editors and reviewers of any of the professional scientific magazines to publish anything of real value. They don't get any extra money for doing a good job. Any really good piece of work is a potential threat in that it may draw research funds of which there are never enough. Besides, it is not easy work to read all those papers anyway. So, if the writer of an article is not a favored member of the *team*, then it is much easier to refuse to publish. And as a bonus, they may have picked up a choice piece of information for their own use whenever they or their immediate friends get around to publishing something. At least they get some reward for their time and effort . . . Of course, this type of hanky-panky discourages and acts as a disincentive for further discoveries since the word does get out.

Sometimes, an individual has one or two very good, or brilliant ideas that may be of great value. He just may not have anything additional to add. Once he has submitted his sparkling diamond to an editorial group, and if they proceed to use it without even acknowledging the source, the discoverer has had it, if he has nothing additional.

At this point it is illuminating to look at an article in the **Bulletin of the American Meteorological Society**, Vol. 58, No. 1, January 1977, pg. 84. The article contains a report of some remarks made by *Jerry La Rue*, Meteorologist-in-charge of the National Weather Service's Washington D.C. office. The following is a partial quote as to what he said:

"He went on to discuss technical publications and their lack of appeal and interest to operational weather people. He said that existing professional publications do not deal with the practical techniques or experiences in "doing the job." He contends that operational people experience too much difficulty in getting material published, so they either get frustrated and give up or do not even try. . . ."

I also quote from the book: **The Persecuted Drug: The Story of DMSO** by *Pat McGrady, Sr.*, page 33.

“Journals sometimes refuse to publish articles because the material is too new or too explosively significant. Many of the great scientists have found it difficult or impossible to find an outlet for some of their most challenging papers. The young and relatively unknown, especially, have been denied credit, in this wise, for work that others repeated and reported and sometimes won awards for years later.

It is appropriate to now add some direct quotations of remarks from some *leading meteorologists* (in different conversations with them) about what I had to offer:

“We don’t need it in our procedures . . .”

“We don’t want what you have . . .”

“We won’t use it—whatever it is . . .”

Fortunately, they don’t speak for the rest of us in this country, or elsewhere for that matter. Unfortunately, there is a worldwide spending of over \$300,000,000 for weather research (merely to get a better understanding of how the weather “works”) year, after year, after year . . .

I never received a penny of that money, but this book, nevertheless, is my contribution for fighting inflation. Instead of less of everything at more and more cost, we can have more for less. The defeatist attitude, that our standard of living must lower, is comical in the face of the great developments that are available and not being used or prevented from being used in many areas.

Now here is a kicker. The membership of the **American Meteorological Society** was asked to “vote” on whether to *remove* from the Code of Ethics for members of the society, the following requirements:

“He will not engage in unfair competition . . .”

“He will attempt to secure work on the basis of qualification and performance.”

“He will not unfairly discredit his fellow professionals.”

“He will not take credit knowingly for work done by others, . . .”

Thomas J. Lockhart, CCM, President, Meteorology Research Inc., Pasadena, California, takes offense at the thought that it would be an acceptable standard of behavior to engage in "bribery", "kickbacks", "lying", and/or "stealing" (take credit for someone else's work). You can read more about this in the **Bulletin of the American Meteorological Society.**, Vol. 62, No. 1, January 1981, pg. 90. It is sad that some of the leaders of this society were not *ashamed* to even put this proposal to the membership for a "vote".

Our standard of living and way of life will indeed degenerate if we permit these situations to occur unchallenged. The real truth is that there is a glorious future ahead for all people, if the people will it to be so.

End of Prologue

The best is yet to come . . .

About the Author

Oscar Singer received his baptism in meteorology (and B.S. Degree) as an Aviation Cadet at the University of Chicago when the dynamic Dr. Carl Rossby was Department Head in 1940. He served in the Air Force from that time until 1953 as a Weather Officer. The most significant period from a meteorological standpoint was the time spent in the European theater (1941-1945) where he came to grips with the fundamentals of weather processes. Two other highlights of his tour of duty in the Air Force was a year spent learning about radar and weather electronic equipment, and another year taking graduate training in advanced meteorology at the University of California in Los Angeles, where J. Bjerknes taught in 1950.

Since 1953, he has essentially worked in electronics. It may be amusing to some that what he has to offer, was developed in his spare time, from 1966 to 1982.

About the Assistant

Daniel Bender founded the Monrovia Weather Station in 1978, from which weather observations are sent daily to the National Weather Service Forecast Office in Los Angeles.

He served in public affairs programming and weather reporting for the D.S.A. Community Network, for radio station KROQ FM Pasadena from November 1978 to January 1980. And began helping on this book in January 1980. Since July 1982, he has been working as a cameraman for the Mike Douglas Show on Cable News Network.

References

- (1) J. Bjerknes and H. Solberg, "Life Cycle of Cyclones and the Polar Front Theory of Atmospheric Circulation," *Geof. Pub.*, Vol. 3, No 1, Oslo, 1922.
- (2) Ernst Haeckel, "Art Forms in Nature," originally published by the Verlag des Bibliographischen Instituts, Leipzig and Vienna, in 1904. Republished by Dover Publications, Inc., in 1974.
- (3) Leonhard Euler, "Opera omnia," published in Germany in 1911, which is a summary of his work.
- (4) Conklin, "Embryology of Crepidula," *J. Morph.*, 13 (1897), 203.
- (5) Stéphane Leduc, "Mechanisms of Life," (1911) Chapter 10.
- (6) Henri Bénard, "Les Tourbillons Cellulaires dans une Nappe Liquide Transportant de la Chaleur par Convection en Régime Permanent," *Annales de Chimie et de Physique*, Paris, 7 Série, Tome XXIII, 1901, pp. 62-144.
- (7) E. H. Weber, "Mikroskopische Beobachtungen sehr gesetzmässiger Bewegungen, welche die Bildung von niederschlagen harziger Körper aus Weingeist begleiten," *Annalen der Physik und Chemie*, Leipzig, Band 94, 1855, S. 452.
- (8) Delaunay, "Sur la surface de révolution dont la courbure moyenne est constante," *J. de Math.*, Ed. by J. Liouville, 6 (1841), 309.
- (9) F. Hofmeister, "Lehrbuch von der Pflanzenzelle," pg. 71 (1867).
- (10) Worthington, "Segmentation of a Liquid Annulus," *Proc. Roy. Soc.*, No. 200, 1879.
- (11) Worthington, "The Splash of a Drop and Allied Phenomena," from the *Smithsonian Report* for the year 1894.
- (12) Lord Rayleigh (John William Strutt), "On the Instability of Fluid Surfaces," *Sci. Papers*, 3, pg. 594.

INDEX

- Action, center of, 112
- Alternate interior angle, 25
- American Meteorological Society, 329
- Amplitude, (defined), 60
- Angle, alternate interior, 25; arc, 9; between projected arcs, 26, 27; between two circles, 16; dihedral, 6; phase, 61; polyhedral, 9; spherical, 7, 8; trihedral, 9
- Angles of the hexagon, 48, 49
- Angstrom units, 54
- Angular number, 101, 116, 170; defined, 115
- Antinodes, 64, 65
- Antipodal point, 8
- Apollonius, 83
- Arc angle, 9
- Arc of a circle, 5
- Arc polygon, 10
- Arcs, angle between projections of, 26, 27
- Asymmetric symmetry, 80, 81
- Averages, symmetry of, 76, 77
- Bénard, H., 47, 49, 97, 323
- Bender, Daniel, xv, 331
- Bi-lateral symmetry, 68, 157, 159
- Bjerknes, J., 1, 331
- Bode's Law, 52
- Bohr, Niels, 54, 55, 56
- Bravais, August, 327
- Bravais lattices, 327
- Buffon, (Histoire Naturelle), 327
- Bulletin of the American Meteorological Society, 328, 330
- Burt, 327
- Cardan, 326
- Catenoid, 84, 85
- Center of Action, 112
- Center of Gravity, 112
- Center of Projection, 13
- Central vortex, (nuclear vortex), 101, 102, 115
- Charts, Circumferential, 115-168
- Charts, Radial, 169-319
- Chesterton, Gilbert, 80
- Chladni, Ernst, 91-95
- Chladni Plates, 99, 114, 125, 170
- Chord, 9
- Circle, arc of, 5; equatorial, 22; great, 4, 5, 117, 324; inclination of, 22; nodal, 92; polar distance of, 22; primitive, 22; small, 5, 116, 324
- Circle center, straight line traced by, 85
- Circles, angle of projection between, 16; latitude, errors in projection of, 18-21; projection of center of, 21
- Circumferential Charts, 115-168; #20, 155; #26A, 145; #26B, 146; #32, 147; #34, 138; #37, 132-133; #39, 129; #40, 128; #42, 130, 131; #45A, 123; #45B, 124-127; #49, 156; #55A, 120, 121; #55B, 122; #58, 117-119; #60, 134, 135; #63, 148; #66, 139; #72A, 142, 143; #72B, 144; #76, 136, 137; #78A, 157; #78B, 158; #79, 159; #80, 160; #81, 161; #82, 162; #84, 163; #86, 141; #88, 140; #90A, 164; #90B, 165; #90C, 166; #91A, 149; #91B, 150; #91C, 151; #91D, 152; #93A, 153; #93B, 154; #99, 167; #103, 168
- Circumferential Units, (CU), 116, 323, 324
- Circumferential wavenumber, 92
- Classes of symmetry, (point, line, plane), 67, 68
- Close packing of spheres, 41-46
- Col, defined, 28; 111, 124, 125, 324
- Co-latitude, 18
- Cone, right circular, 83
- Conic section, straight line, 83
- Conic sections, 82-84; Roulette, 84, 85
- Conklin, 45
- Constructive interference, 64
- Crystal, 71, 73; with defects, 81; lattice, 73
- CU (circumferential units), 116, 323, 324
- Curved surface, 5
- Cylinder, surfaces of revolution, 84-89
- Cylindrical structures, 84, 86-88
- D-day (June 6, 1944), 320
- Degrees of freedom, 33
- Delaunay, 84
- Demi-regular patterns, 38-39
- Demi-regular tessellations, 36
- Destructive interference, 64
- Diad, two fold symmetry, 69
- Diameter, nodal, 92
- Dictyocha stapedia, 45
- Diffraction grating, 99, 100, 103, 324
- Dihedral angle, 6; magnitude of, 6
- Dilation symmetry, 71, 73
- Dispersion, 63
- Distigma proteus, 89
- Dodecahedral, 34
- Dodecahedron, 30, 31, 327; regular, 29

- Dynamic, equilibrium, 80
- Edge of two planes, 6
- Einstein, Albert, 79
- Electron wavelength, 55, 56
- Ellipse, straight line, 85; straight line through an, 113
- Elliptical shapes of lows & highs, 112, 113, 118, 164
- Enantiomorphism, 66
- Equatorial circle, 22
- Equatorial plane, 14
- Equilateral triangle, 11, 28, 172, 184
- Equilibrium, 79-81; dynamic, 80; position of, 59, 80; simulated, 80; static, 80; triangle, 301
- Equivalent symmetry points, 76
- Errors in projection of latitude circles, 18-21
- Euler, Leonhard, 44, 48
- Face of plane, 6
- "Fan shape" formation, 319
- Figurate numbers, 42-44; hexagonal, 44
- Fischbeck, Dr. George, xv
- "Flying kite" formation, 226
- Forced oscillation, 59
- Formation, "Fan shaped", 319; "Flying kite", 226; hexagonal, 100, 102; "K", 216, 224, 229; "K", defined, 214; nested, 45; octagonal, 102; pentagonal, 102; square, 28, 45, 100-102, triangular, 100, 101; "V", 229-232, 254, 268, 270, 277, 281, 284, 285, 311, 315, 316; "X", 213, 214, 229, 252, 253; "X", defined, 213; "Y", defined, 203
- Four-fold symmetry, 76
- Fourier analysis, 61-63
- Fourier, J.B., 61, 169
- Frank, Richard A., Administrator of NOAA, xiii
- Frankenheim, 327
- Free oscillation, 59
- Friedrich and Knipping, 100
- Fujiwhara, xiii
- Fundamental harmonic, 62, 63
- Galileo, Galilei, 51
- Glide reflection symmetry, 71, 72
- Goldberger, 327
- Gravity, center of, 112
- Great circle, 4, 5, 117, 324; straight line, 117
- Haeckel, Ernst, 34
- Hales, Stephen, 45, 326, 327
- Harmonic, analysis, 105, 169; fundamental, 1st, 2nd, 3rd, 4th, 5th, resultant, 62, 63; law, 52; motion, simple, 59; movement, 60, 61; vibration, 91-93
- Hexad, six fold symmetry, 69
- Hexagon, angles of, 48, 49; regular, 28, 31
- Hexagonal, compression and elongation, 41; figurate numbers, 44; formations, 100, 102; shapes, 46-49
- Hexahedral, 34
- Hexahedron, 30; regular, 29
- High, elliptical shape of, 112, 113
- Histoire Naturelle (Buffon), 327
- Hofmeister, Wilhelm F., 88
- Icosahedral, 34; pattern, 11
- Icosahedron, 30, 31; regular, 29
- Identification map, 108-110
- Image, mirror, 66, 69
- Inclination of a circle, 22
- Interference, 2, 63-65; constructive, 64; destructive, 64
- Irregular polygon, 28
- Isobars, 111
- June 6, 1944 (D-day), 320-322
- Kepler, Johannes, 51
- Kepler's Law, 51, 52
- "K" formation, 214, 216, 224, 229
- Knipping and Friedrich, 100
- Lagrange, Joseph Louis, 89
- La Rue, Jerry, 328
- Latitude circles, errors in projection of, 18-21
- Latitude, standard, 14
- Lattice, Bravais, 327; crystal, 73
- Laue, Max, 99
- Law, Bode's, 52; Harmonic, 52; Kepler's, 51, 52; Quantum, 54, 55; Roche's, 53, 54; Wolf's, 52, 53
- LCD (Lowest Common Denominator), 170
- Leduc, Stéphane, 46
- Line, classes of symmetry, 67-68; of longitude, 15; of measures, 23; mirror, 69; straight, *see* straight line; symmetry, 67, 68, 92; tangent, 6
- Liverwort, 57
- Lock, definition of, x
- Lockhart, Thomas J., 330
- Longitude, line of, 15
- Longitudinal glide reflection, 124, 155
- Low, elliptical shape of, 112, 113, 118, 164
- Lowest Common Denominator, (LCD), 170
- Lufkin, Daniel, xiii, xiv
- Lune, 8
- Magnitude of dihedral angle, 6
- Map, polar stereographic, 3, 12-27, 71; scale of, 14
- Maximum symmetry, 118
- McGrady, Pat (The Story of DMSO), 329
- Measures, line of, 23
- Menaechmus, 83
- Mirror, image, 69; image equality symmetry, 66; line, 69; plane, 70
- Modes of operation, 60
- National Weather Service, xv
- Natural oscillation, 59
- Nested formation, 45
- Net, parallelogram, 75
- Network of points, symmetry, 71-78
- Newton, Chester, (Editor, Monthly Weather Review), xii
- Nodal, circle, 92; diameter, 92
- Node, 64, 65, 91
- Nodoid, 84, 85
- Nuclear vortex, 101, 102, 115
- Number, angular, 101, 115, 116, 170; significance of, xii
- Numbers, figurate, 42-44; square, 42, 43; triangular, 42, 43
- Octagonal formation, 102
- Octahedral, 34
- Octahedron, 30, 31; regular, 29

INDEX

- Olsen, Harry F., 93
 Operation, modes of, 60; symmetry, 68-71
 Oscillation, defined, 59; forced, 59; free, 59; natural, 59
 Pappus, 46
 Parabolic rate of increase, 136, 261, 264
 Parallelogons, 40
 Parallelogram net, 75
 Patterns, demi-regular, 38, 39; icosahedral, 11; radial, 114, 115; step, 136, 261, 264
 Pentagon, regular, 31
 Pentagonal formation, 102
 Periodic time function, 61
 Phase angle, 61
 Plane, 4; equatorial, 14; face of, 6; mirror, 70; primitive, 14; projection of, 15; surfaces of revolution, 84-89
 Planes, edge of two, 6
 Plateau, Joseph, 84-89; Problem of, 89, 112, 113, 153; Surfaces of revolution, 94
 Point, antipodal, 8; polar distance of, 22; rotation around, symmetry, 69
 Points, crossed by straight lines, 77; polar, 8; network of, symmetry, 71-78
 Polar distance of a circle, 22
 Polar distance of a point, 22
 Polar furrow, 45
 Polar points, 8
 Polar stereographic map, 3, 12-27, 71; distortions of, 17-21; straight line on, 17
 Polar stereographic projection, xii-xiv
 Polygon, 43; arc, 10; irregular, 28; regular, 28; spherical, 9
 Polyhedral angle, 9
 Polyhedron, 28, 29, 32; regular, 29
 Position of equilibrium, 59, 80
 Positions, quantum, 54
 Pournelle, J. E., xii
 Primitive, circle, 22; plane, 14
 Principle of, similitude, 50, 51; superposition, 63, 124
 Problem of Plateau, 89
 Projection, center of, 13; of center of circles, 21; on a plane, 15
 Pyramid, spherical, 7
 Pythagoreans, 28, 29, 42
 Quanta, 48
 Quantum, Law, 54, 55; positions, 54; sized vortex, 97-99; units, 34; units in packages, 96
 Radial Charts, 169-319
 #20A, 170, 171; #20B, 172; #20C, 173; #20D, 174; #20E, 175; #20F, 176
 #20A, 170, 171; #20B, 172; #20C, 173; #20D, 174; #20E, 175; #20F, 176
 #26A, 177; #26B, 178; #26C, 179; #26D, 180; #26E, 181; #26F, 182
 #32A, 183; #32B, 184, 185
 #34A, 186; #34B, 187; #34C, 188; #34D, 189; #34E, 190
 #37A, 191; #37B, 192; #37C, 193
 #39A, 194; #39B, 195; #39C, 196; #39D, 197; #39E, 198
 #40A, 199; #40B, 200; #40C, 201; #40D, 202; #40E, 203; #40F, 204; #40G, 205
 #42A, 206; #42B, 207; #42C, 208; #42D, 209; #42E, 210
 #45A, 211; #45B, 212; #45C, 213; #45D, 214; #45E, 215; #45F, 216
 #49A, 217; #49B, 218; #49C, 219; #49D, 220; #49E, 221; #49F, 222; #49G, 223; #49H, 224
 #55A, 225; #55B, 226; #55C, 227
 #58A, 228; #58B, 229; #58C, 230; #58D, 231; #58E, 232; #58F, 233; #58G, 234
 #60A, 235; #60B, 236; #60C, 237; #60D, 238; #60E, 239
 #63A, 240; #63B, 241; #63C, 242; #63D, 243
 #66A, 244; #66B, 245; #66C, 246; #66D, 247
 #72A, 248; #72B, 249; #72C, 250, 251; #72D, 252; #72E, 253
 #76A, 254; #76B, 255; #76C, 256; #76D, 257; #76E, 258; #76F, 259; #76G, 260
 #78A, 261; #78B, 262; #78C, 263; #78D, 264; #78E, 265
 #79A, 266; #79B, 267; #79C, 268; #79D, 269
 #80A, 270; #80B, 271; #80C, 272; #80D, 273; #80E, 274; #80F, 275
 #81A, 276; #81B, 277; #81C, 278; #81D, 279; #81E, 280; #81F, 281; #81G, 282
 #82A, 283; #82B, 284; #82C, 285; #82D, 286; #82E, 287
 #84A, 288; #84B, 289; #84C, 290; #84D, 291
 #86A, 292; #86B, 293; #86C, 294; #86D, 295
 #88A, 296; #88B, 297; #88C, 298
 #90A, 299; #90B, 300; #90C, 301; #90D, 302
 #91A, 303; #91B, 304; #91C, 305; #91D, 306
 #93A, 307; #93B, 308; #93C, 309; #93D, 310
 #99A, 311; #99B, 312; #99C, 313; #99D, 314
 #103A, 315; #103B, 316; #103C, 317; #103D, 318; #103E, 319
 Radial patterns, 114, 115
 Radial Units, (RU), 117, 323, 324
 Radial wavenumber, 92
 Radiolaria, 44
 Radius, 5
 Rake, 198, 231, 250, 290, 311; defined, 198
 Random time functions, 65
 Rayleigh, Lord, 89
 Referee "B", anonymous editor, xiii
 Referee "C", anonymous editor, xiii
 Reflection line symmetry, 69
 Reflection symmetry, 69, 75
 Regular, dodecahedron, 29; hexagon, 31; hexahedron, 29; icosahedron, 29; octahedron, 29; pentagon, 31; polygon, 28; polyhedron, 29; solid, 29; tessellations, 36; tetrahedron, 29
 Resonance, 60, 105
 Resultant, 62, 63
 Revolution, surfaces of, 84-89
 Ridge, 111
 Right circular cone, 83
 Roche, E., 54
 Roche limit, 54
 Roche's Law, 53, 54
 Rossby, Carl, 323, 331
 Rossby waves, xi

- Rotational symmetry, 69, 75, 250
- Rotation symmetry around a point, 69
- Roulette, conic sections, 84, 85; straight line, 85
- RU (Radial Units), 117, 323, 324
- Sanders, Professor Frederick (Editor, Focus on forecasting, Bulletin of the American Meteorological Society), 328
- Saturn, rings and spokes, 53
- Scale of a map, 14
- Semi-regular tessellations, 36
- Septagon, 30
- Shapes, hexagonal, 46-49
- Similitude, principle of, 50, 51
- Simple harmonic motion, 59
- Simulated Equilibrium, 80
- Sine wave, 61, 62
- Singer's Lock, x, xii, xiv, 1, 8, 76, 124, 130, 169, 170, 324; defined, x
- Six fold symmetry, 69
- Size (of objects), 96
- Small circle, 5, 116, 324
- Solid, regular, 29
- Spengler, Kenneth C., 327
- Spheres, close packing of, 41-46
- Spherical, angle, 7, 8; excess of a triangle, 10; geometry, 4-11; polygon, 9; pyramid, 7; surface, 4; triangle, 7, 9
- Splash of a drop, 89
- Spray, defined, 187
- Square, compression, 41; elongation, 41; formations, 28, 45, 100-102; numbers, 42, 43
- Staggered wavenumber, 57
- Standard latitude, 14
- Standing waves, 64
- Static equilibrium, 80
- Statistics, xi, 2, 49, 50, 68, 105; wavenumber averages, 323, 324
- "Step-ladder" pattern, 319
- "Step" pattern, 261, 264
- Stereographic map, *see* Polar stereographic map
- Straight line, conic section, 83; ellipse, 85, 113; first use in meteorology, 324; great circle, 117; points crossed by, 77; on a polar stereographic map, 17, 21, 33; roulette, 85; symmetry along, 71, 72; through an ellipse, 113; traced by circle center, 85; of vortexes, 95
- Structures, cylindrical, 84, 86-88
- Suitable equality symmetry, 66
- Superposition, principle of, 63, 124
- Surface, curved, 5; spherical, 4
- Surfaces of Revolution, 84-89, 94
- Symmetry, along a straight line, 71, 72; asymmetric, 80, 81; of averages, 76, 77; bi-lateral, 68, 157, 159; classes of, 67, 68; definition of, 66; 67; diad, 69; dilation, 71, 73; elements, 68; four fold, 76; geometrically regular, 66, 67; glide reflection, 71, 72; lines, 67, 68, 92; maximum, 118; mirror image equality, 66; network of points, 71-78; operations, 68-71; patterns, xii; points, equivalent, 76; reflection, 69, 75; reflection line, 69; rotational, 69, 75, 250; rotation around a point, 69; suitable equality, 66; three fold, 69, 76; translational, 70-72; triad, 69, 76; two fold, 69; wall paper pattern, 74
- Tangent line, 6
- Tartaglia, 326
- Tessellations, demi-regular, 36; regular, 36; semi-regular, 36
- Tetrad, four fold symmetry, 69
- Tetrahedral, 34
- Tetrahedron, 30, 31, 34; regular, 29
- Three fold symmetry, 69
- Titius, 52
- Translational symmetry, 70-72
- Triad, three fold symmetry, 69, 76
- Trianea, 88
- Triangle, equilateral, 28; equilibrium, 301; spherical, 7, 9; spherical excess of, 10
- Triangular formations, 100, 101
- Triangular, numbers, 42, 43
- Trihedral angle, 9
- Trough, 111
- Two axis, (x,y), 229, 230-232, 246, 250, 256, 257, 260, 284, 285, 288, 291; defined, 229
- Two fold symmetry, 69
- Unduloid, surfaces of revolution, 84-89
- Units, angstrom, 54; circumferential, 116, 323, 324; quantum, 34; radial, 117, 323, 324
- Vegetable Statics, (by Stephen Hales), 326, 327
- Vertex, 8, 9
- "V" formation, 229-232, 254, 268, 270, 277, 281, 284, 285, 311, 315, 316
- Vibration, 59; harmonic, 91-93
- Vortex, central, 101, 102, 115; nuclear, 101, 102, 115; quantum sized, 97-99
- Vortexes, straight line of, 95
- "Wallpaper" pattern symmetry, 74
- Wave, pulses, 63; sine, 61, 62; standing, 64
- Wavelength, electron, 55, 56; *also see* wavenumber
- Wavenumber, 56, 57, 94, 99, 100, 323-325; circumferential, 92; radial, 92; staggered, 57
- Waves, 58-65
- Weather tool, 102-105
- Weber, E., 48
- Wolf's Law, 52, 53
- Worthington, A. M., 89
- "X" formation, 213, 214, 229, 252, 253; defined, 213
- "Y" formation, defined, 203

Weather Mystery Cracked

This book is a stunning breakthrough in the understanding of weather which takes the field of meteorology out of the "dark ages" into the "main stream" of 20th century science. Nevertheless, it is written at a level that can be understood by most high school science students, since the explanations are based on old, well-established scientific principles.

A common surface weather map for an entire hemisphere is analyzed for a fixed moment in time, in such a manner, as to show in stark simplicity the orderly arrangement and symmetry of storm centers (lows) and their associated centers of fair weather (highs). One hundred and ninety charts are drawn for a single instant of time in order to (1) lead the reader in easy stages through the various ramifications on the weather map and (2) to also present overwhelming proof of the procedures that are used. This book also gives a simplified explanation of **why** these strange configurations are formed and also indicates **how** they can be discovered on any weather map—past, present or future.

Not just another weather book...